IEC/IEEE 62209-1528

Edition 1.0 2020-10

INTERNATIONAL STANDARD

NORME INTERNATIONALE

colour inside

IECNORM.COM : Click to view the full PDF of IEC/IEEE 62209-1528:2020

Measurement procedure for the assessment of specific absorption rate of human exposure to radio frequency fields from hand-held and body-mounted wireless communication devices – Part 1528: Human models, instrumentation, and procedures (Frequency range of 4 MHz to 10 GHz)

Procédure de mesure pour l'évaluation du débit d'absorption spécifique de l'exposition humaine aux champs radiofréquence produits par les dispositifs de communications sans fil tenus à la main ou portés près du corps – Partie 1528: Modèles humains, instrumentation et procédures (Plage de fréquences comprise entre 4 MHz et 10 GHz)



IEC/IEEE 62209-1528:2020-10(en-fr)

THIS PUBLICATION IS COPYRIGHT PROTECTED
Copyright © 2020 IEC, Geneva, Switzerland
Copyright © 2020 IEEE

All rights reserved. Unless otherwise specified, no part of this publication may be reproduced or utilized in any form or by any means, electronic or mechanical, including photocopying and microfilm, without permission in writing being secured. Requests for permission to reproduce should be addressed to either IEC at the address below or IEC's member National Committee in the country of the requester or from IEEE.

IEC Central Office
3, rue de Varembé
CH-1211 Geneva 20
Switzerland
Tel.: +41 22 919 02 11
info@iec.ch
www.iec.ch

Institute of Electrical and Electronics Engineers, Inc.
3 Park Avenue
New York, NY 10016-5997
United States of America
stds.ipr@ieee.org
www.ieee.org

About the IEC
The International Electrotechnical Commission (IEC) is the leading global organization that prepares and publishes International Standards for all electrical, electronic and related technologies.

About IEC publications
The technical content of IEC publications is kept under constant review by the IEC. Please make sure that you have the latest edition, a corrigendum or an amendment might have been published.

IEC publications search - webstore.iec.ch/advsearchform
The advanced search enables to find IEC publications by a variety of criteria (reference number, text, technical committee, …). It also gives information on projects, replaced and withdrawn publications.

IEC Just Published - webstore.iec.ch/justpublished
Stay up to date on all new IEC publications. Just Published details all new publications released. Available online and once a month by email.

IEC Customer Service Centre - webstore.iec.ch/csc
If you wish to give us your feedback on this publication or need further assistance, please contact the Customer Service Centre: sales@iec.ch.

IEC online collection - oc.iec.ch
Discover our powerful search engine and read freely all the publications previews. With a subscription you will always have access to up to date content tailored to your needs.

Electropedia - www.electropedia.org
The world's leading online dictionary on electrotechnology, containing more than 22 000 terminological entries in English and French, with equivalent terms in 18 additional languages. Also known as the International Electrotechnical Vocabulary (IEV) online.

A propos de l'IEC
La Commission Electrotechnique Internationale (IEC) est la première organisation mondiale qui élabore et publie des Normes internationales pour tout ce qui a trait à l'électricité, à l'électronique et aux technologies apparentées.

A propos des publications IEC
Le contenu technique des publications IEC est constamment revu. Veuillez vous assurer que vous possédez l'édition la plus récente, un corrigendum ou amendement peut avoir été publié.

Recherche de publications IEC - webstore.iec.ch/advsearchform
La recherche avancée permet de trouver des publications IEC en utilisant différents critères (numéro de référence, texte, comité d'études, …). Elle donne aussi des informations sur les projets et les publications remplacées ou retirées.

IEC Just Published - webstore.iec.ch/justpublished
Restez informé sur les nouvelles publications IEC. Just Published détaille les nouvelles publications parues. Disponible en ligne et une fois par mois par email.

Service Clients - webstore.iec.ch/csc
Si vous désirez nous donner des commentaires sur cette publication ou si vous avez des questions contactez-nous: sales@iec.ch.

IEC online collection - oc.iec.ch
Découvrez notre puissant moteur de recherche et consultez gratuitement tous les aperçus des publications. Avec un abonnement, vous aurez toujours accès à un contenu à jour adapté à vos besoins.

Electropedia - www.electropedia.org
Le premier dictionnaire d'électrotechnologie en ligne au monde, avec plus de 22 000 articles terminologiques en anglais et en français, ainsi que les termes équivalents dans 16 langues additionnelles. Egalement appelé Vocabulaire Electrotechnique International (IEV) en ligne.

IECNORM.COM : Click to view the full PDF of IEC/IEEE 62209-1528:2020

IEC/IEEE 62209-1528

Edition 1.0 2020-10

INTERNATIONAL STANDARD

NORME INTERNATIONALE

colour inside

IECNORM.COM : Click to view the full PDF of IEC/IEEE 62209-1528:2020

Measurement procedure for the assessment of specific absorption rate of human exposure to radio frequency fields from hand-held and body-mounted wireless communication devices – Part 1528: Human models, instrumentation, and procedures (Frequency range of 4 MHz to 10 GHz)

Procédure de mesure pour l'évaluation du débit d'absorption spécifique de l'exposition humaine aux champs radiofréquence produits par les dispositifs de communications sans fil tenus à la main ou portés près du corps – Partie 1528: Modèles humains, instrumentation et procédures (Plage de fréquences comprise entre 4 MHz et 10 GHz)

INTERNATIONAL ELECTROTECHNICAL COMMISSION

COMMISSION ELECTROTECHNIQUE INTERNATIONALE

ICS 17.220.20

ISBN 978-2-8322-9562-5

Warning! Make sure that you obtained this publication from an authorized distributor.
Attention! Veuillez vous assurer que vous avez obtenu cette publication via un distributeur agréé.

® Registered trademark of the International Electrotechnical Commission
Marque déposée de la Commission Electrotechnique Internationale

CONTENTS

FOREWORD 14
INTRODUCTION 17
1 Scope 18
2 Normative references 18
3 Terms and definitions 18
4 Symbols and abbreviated terms 26
4.1 Physical quantities 26
4.2 Constants 26
4.3 Abbreviated terms 27
5 Quick start guide and evaluation plan checklist 28
6 Measurement system specifications 30
6.1 General requirements for full SAR testing 30
6.2 Phantom specifications 31
6.2.1 General 31
6.2.2 Basic phantom parameters 31
6.2.3 Head phantom 33
6.2.4 Flat phantom 34
6.2.5 Device-specific phantoms 35
6.3 Influence of hand on SAR in head 35
6.4 Scanning system requirements 36
6.5 Device holder specifications 36
6.6 Characteristics of the readout electronics 37
7 Protocol for SAR assessment 37
7.1 General 37
7.2 Measurement preparation 37
7.2.1 Preparation of tissue-equivalent medium and system check 37
7.2.2 Preparation of the wireless communication DUT 38
7.2.3 DUT operating mode requirements 38
7.2.4 Positioning of the DUT relative to the phantom 40
7.2.5 Antenna configurations 57
7.2.6 Options and accessories 57
7.2.7 DUTs with alternative form factor 57
7.2.8 Test frequencies for DUTs 58
7.3 Tests to be performed for DUTs 58
7.3.1 General 58
7.3.2 Basic approach for DUT testing 59
7.4 Measurement procedure 60
7.4.1 General 60
7.4.2 Full SAR testing procedure 60
7.4.3 Drift 64
7.4.4 SAR measurements of DUTs with multiple antennas or multiple transmitters 66
7.5 Post-processing of SAR measurement data 72
7.5.1 Interpolation 72
7.5.2 Extrapolation 72
7.5.3 Definition of the averaging volume 72

IECNORM.COM : Click to view the full PDF of IEC/IEEE 62209-1528:2020

7.5.4 Searching for the maxima 73
7.6 Time-period averaged SAR considerations 73
7.6.1 General 73
7.6.2 RF conducted power 73
7.6.3 Time-period averaged SAR measurement settings for SAR measurement methods 73
7.6.4 Exposure condition and test position considerations 74
7.6.5 Time-period averaged SAR for simultaneous transmission 74
7.6.6 TX factor assessment 74
7.6.7 SAR measurements 75
7.6.8 Uncertainty in TPAS evaluations 75
7.7 Proximity sensors considerations 76
7.7.1 General 76
7.7.2 Procedures for determining proximity sensor triggering distances 77
7.7.3 Procedure for determining proximity sensor coverage area 80
7.7.4 SAR measurement procedure involving proximity sensors 81
7.8 SAR correction for deviations of complex permittivity from targets 81
7.8.1 General 81
7.8.2 SAR correction formula 82
7.8.3 Uncertainty of the correction formula 83
7.9 Minimization of testing time 83
7.9.1 General 83
7.9.2 Fast SAR testing 84
7.9.3 SAR test reductions 89
8 Measurement uncertainty estimation 100
8.1 General 100
8.2 Requirements on the uncertainty evaluation 101
8.3 Description of uncertainty models 102
8.3.1 General 102
8.3.2 SAR measurement of a DUT 102
8.3.3 System validation and system check measurement 102
8.3.4 System check repeatability and reproducibility 102
8.3.5 Fast SAR testing (relative measurement) 102
8.4 Parameters contributing to uncertainty 104
8.4.1 Measurement system errors 104
8.4.2 Phantom and device (DUT or validation antenna) errors 105
8.4.3 Corrections to the SAR result (if applied) 107
9 Measurement report 108
9.1 General 108
9.2 Items to be recorded in the measurement report 108
Annex A (normative) SAR measurement system verification 112
A.1 Overview 112
A.2 System check 112
A.2.1 Purpose 112
A.2.2 Phantom set-up 113
A.2.3 System check antenna 113
A.2.4 System check antenna input power measurement 114
A.2.5 System check procedure 115
A.2.6 System check acceptance criteria 116

IECNORM.COM : Click to view the full PDF of IEC/IEEE 62209-1528:2020

A.3 System validation 116
A.3.1 Purpose 116
A.3.2 Phantom set-up 116
A.3.3 System validation antennas 116
A.3.4 Input power measurement 117
A.3.5 System validation procedure 117
A.4 Fast SAR testing system validation and system check 119
A.4.1 General 119
A.4.2 Fast SAR testing system validation 119
A.4.3 Fast SAR testing system check 120
Annex B (informative) SAR test reduction supporting information 122
B.1 General 122
B.2 Test reduction based on characteristics of DUT design 122
B.2.1 General 122
B.2.2 Statistical analysis overview 122
B.2.3 Analysis results 123
B.2.4 Conclusions 126
B.2.5 Expansion to multi-transmission antennas 126
B.3 Test reduction based on analysis of SAR results on other signal modulations 126
B.3.1 General 126
B.3.2 Analysis results 127
B.4 Test reduction based on SAR level analysis 128
B.4.1 General 128
B.4.2 Statistical analysis 129
B.4.3 Test reduction applicability example 132
B.5 Other statistical approaches to search for the high SAR test configurations 134
B.5.1 General 134
B.5.2 Test reductions based on a DOE 134
B.5.3 One factor at a time (OFAT) search 134
B.5.4 Analysis of unstructured data 134
Annex C (informative) Measurement uncertainty of results obtained from specific fast SAR testing methods 135
C.1 General 135
C.2 Measurement uncertainty evaluation – contributing parameters 135
C.2.1 General 135
C.2.2 Probe calibration and system calibration drift 136
C.2.3 Isotropy 136
C.2.4 Probe positioning 137
C.2.5 Mutual sensor coupling 138
C.2.6 Scattering within the probe array 139
C.2.7 Sampling error 139
C.2.8 Array boundaries 139
C.2.9 Probe or probe array coupling with the DUT 139
C.2.10 Measurement system immunity / secondary reception 139
C.2.11 Deviations in phantom shape 140
C.2.12 Spatial variation in dielectric properties 140
C.2.13 Reconstruction 140
C.3 Uncertainty budget 140
Annex D (normative) SAR system validation antennas 143

IECNORM.COM : Click to view the full PDF of IEC/IEEE 62209-1528:2020

D.1 General antenna requirements 143
D.2 Standard dipole antenna 143
D.2.1 Mechanical description 143
D.2.2 Numerical target SAR values 146
D.3 Standard waveguide 148
D.3.1 Mechanical description 148
D.3.2 Numerical target SAR values 149
D.4 System validation antennas for below 150 MHz 149
D.4.1 General 149
D.4.2 Confined loop antenna 150
D.4.3 Meander dipole antenna 152
D.5 Orthogonal E-field source – VPIFA 153
D.5.1 Mechanical description 153
D.5.2 Numerical target SAR values 156
Annex E (normative) Calibration and characterization of dosimetric (SAR) probes 157
E.1 Introductory remarks 157
E.2 Linearity 158
E.3 Assessment of the sensitivity of the dipole sensors 158
E.3.1 General 158
E.3.2 Two-step calibration procedures 158
E.3.3 One-step calibration procedure – reference antenna method 164
E.3.4 One-step calibration procedure – coaxial calorimeter method 168
E.4 Isotropy 170
E.4.1 Axial isotropy 170
E.4.2 Hemispherical isotropy 170
E.5 Lower detection limit 175
E.6 Boundary effect 176
E.7 Response time 176
Annex F (informative) Example recipes for phantom tissue-equivalent media 177
F.1 General 177
F.2 Ingredients 177
F.3 Tissue-equivalent medium liquid formulas (permittivity/conductivity) 178
Annex G (normative) Phantom specifications 180
G.1 Rationale for the phantom characteristics 180
G.1.1 General 180
G.1.2 Rationale for the SAM phantom 180
G.1.3 Rationale for the flat phantom 180
G.2 SAM phantom specifications 181
G.2.1 General SAM phantom specifications 181
G.2.2 SAM phantom shell specification 185
G.3 Flat phantom specifications 187
G.4 Justification of flat phantom dimensions 188
G.5 Rationale for tissue-equivalent media 191
G.6 Definition of a phantom coordinate system and a DUT coordinate system 193
Annex H (informative) Measurement of the dielectric properties of tissue-equivalent media and uncertainty estimation 195
H.1 Overview 195
H.2 Measurement techniques 195
H.2.1 General 195

IECNORM.COM : Click to view the full PDF of IEC/IEEE 62209-1528:2020

H.2.2 Instrumentation 195
H.2.3 General principles 195
H.3 Slotted coaxial transmission line 196
H.3.1 General 196
H.3.2 Equipment set-up 196
H.3.3 Measurement procedure 197
H.4 Contact coaxial probe 197
H.4.1 General 197
H.4.2 Equipment set-up 198
H.4.3 Measurement procedure 199
H.5 TEM transmission line 199
H.5.1 General 199
H.5.2 Equipment set-up 200
H.5.3 Measurement procedure 200
H.6 Dielectric properties of reference liquids 201
Annex I (informative) Studies for potential hand effects on head SAR 204
I.1 Overview 204
I.2 Background 204
I.2.1 General 204
I.2.2 Hand phantoms 205
I.3 Summary of experimental studies 205
I.3.1 Experimental studies using fully compliant SAR measurement systems 205
I.3.2 Experimental studies using other SAR measurement systems 205
I.4 Summary of computational studies 206
I.5 Conclusions 206
Annex J (informative) Skin enhancement factor 207
J.1 Background 207
J.2 Rationale 208
J.3 Simulations 208
J.4 Recommendation 209
Annex K (normative) Application-specific phantoms 211
K.1 General 211
K.2 Phantom basic requirements 211
K.3 Examples of specific alternative phantoms 211
K.3.1 Face-down SAM phantom 211
K.3.2 Head-stand SAM phantom 212
K.3.3 Wrist phantom 212
K.4 Scanning and evaluation requirements 213
K.5 Uncertainty assessment 213
K.6 Reporting 213
Annex L (normative) Fast compliance evaluations using a flat-bottom phantom with a curved corner (Uniphantom) 214
L.1 General 214
L.2 Uniphantom 214
L.3 Device positions for compliance testing and definitions of handset shapes 214
L.3.1 General 214
L.3.2 Handsets with a straight form factor 215
L.3.3 Handsets with a clamshell form factor 215
L.4 Testing procedure 215

IECNORM.COM : Click to view the full PDF of IEC/IEEE 62209-1528:2020

L.4.1 General 215
L.4.2 Handsets with straight form factors 215
L.4.3 Handsets with clamshell form factors 216
L.5 Uncertainty of SAR measurement results using Uniphantom 217
Annex M (informative) Wired hands-free headset testing 218
M.1 Concept 218
M.2 Example results 219
M.3 Discussion 220
Annex N (informative) Applying the head SAR test procedures 221
Annex O (normative) Uncertainty analysis for measurement system manufacturers and calibration laboratories 224
O.1 Probe linearity and detection limits 224
O.2 Broadband signal uncertainty 225
O.3 Boundary effect 225
O.4 Field-probe readout electronics uncertainty 226
O.5 Signal step-response time uncertainty 226
O.6 Probe integration-time uncertainty 227
O.6.1 General 227
O.6.2 Probe integration-time uncertainty for periodic pulsed signals 227
O.6.3 Probe integration-time uncertainty for non-periodic signals 228
O.7 Contribution of mechanical constraints 228
O.7.1 Mechanical tolerances of the probe positioner (directions parallel to phantom surface) 228
O.7.2 Probe positioning with respect to phantom shell surface 228
O.7.3 First-order approximation of exponential decay 229
O.8 Contribution of post-processing 229
O.8.1 General 229
O.8.2 Evaluation test functions 230
O.8.3 Data-processing algorithm uncertainty evaluations 232
O.9 Tissue-equivalent medium properties uncertainty 235
O.9.1 General 235
O.9.2 Medium density 235
O.9.3 Medium conductivity uncertainty 235
O.9.4 Medium permittivity uncertainty 235
O.9.5 Assessment of dielectric properties measurement uncertainties 235
O.9.6 Medium temperature uncertainty 237
Annex P (normative) Post-processing techniques 239
P.1 Extrapolation and interpolation schemes 239
P.1.1 General 239
P.1.2 Extrapolation schemes 239
P.1.3 Interpolation schemes 239
P.2 Averaging scheme and maximum finding 239
P.2.1 Volume average schemes 239
P.2.2 Finding the psSAR and estimating the uncertainty 240
Annex Q (informative) Rationale for time-period averaged SAR test procedure 241
Annex R (normative) Measurement uncertainty analysis for testing laboratories 242
R.1 RF ambient conditions 242
R.2 Device positioning and holder uncertainties 242
R.2.1 General 242

IECNORM.COM : Click to view the full PDF of IEC/IEEE 62209-1528:2020

R.2.2 Device holder perturbation uncertainty 243
R.2.3 DUT positioning uncertainty with a specific test device holder: Type A 244
R.3 Probe modulation response 244
R.4 Time-period averaged SAR 245
R.4.1 General 245
R.4.2 TX factor uncertainty 245
R.5 Measured SAR drift 246
R.5.1 General 246
R.5.2 Accounting for drift 246
R.6 SAR scaling uncertainty 247
Annex S (normative) Validation antenna SAR measurement uncertainty 248
S.1 Deviation of experimental antennas 248
S.2 Other uncertainty contributions when using system validation antennas 248
Annex T (normative) Interlaboratory comparisons 250
T.1 Purpose 250
T.2 Phantom set-up 250
T.3 Reference devices 250
T.4 Power set-up 250
T.5 Interlaboratory comparison – procedure 251
Annex U (informative) Determination of the margin for compliance evaluation using the Uniphantom 252
U.1 General 252
U.2 Deviation of the psSAR measured using the Uniphantom from the psSAR measured using the SAM phantom 252
U.3 Determination of margin based on 95 % confidence interval 253
U.4 Examples of the determination of the margin factor 253
U.4.1 Margin for handsets with straight form factors at flat-bottom position 253
U.4.2 Margin for handsets with straight form factors (except smart phones at flat-bottom position) 255
U.4.3 Margin for smart phones at flat-bottom position 257
U.4.4 Margin for smart phones at corner position 259
U.4.5 Margin for handsets with clamshell form factors at corner position 261
Annex V (informative) Automatic input power level control for system validation 264
V.1 General 264
V.2 Operational mechanism of AIPLC 264
Annex W (informative) LTE test configurations supporting information 266
W.1 General 266
W.2 Study 1 266
W.3 Study 2 268
W.4 Justifications of relative standard deviations 269
Bibliography 271

Figure 1 – Quick start guide 29
Figure 2 – Dimensions of the elliptical phantom 35
Figure 3 – Mounting of the DUT in the device holder using low-permittivity and low-loss foam to avoid changes of DUT performance by the holder material 37
Figure 4 – Designation of DUT reference points 41

IECNORM.COM : Click to view the full PDF of IEC/IEEE 62209-1528:2020

Figure 5 – Measurements performed by shifting a large device over the efficient measurement area of the system including overlapping areas – in this case: six tests performed 42
Figure 6 – Test positions for body-worn devices 43
Figure 7 – Device with swivel antenna 44
Figure 8 – Test positions for body supported devices 45
Figure 9 – Test positions for desktop devices 47
Figure 10 – Test positions for front-of-face devices 48
Figure 11 – Test position for hand-held devices, not used at the head or torso 49
Figure 12 – Test position for limb-worn devices 49
Figure 13 – Test position for clothing-integrated wireless communication devices 50
Figure 14 – Possible test positions for a generic device 51
Figure 15 – Vertical and horizontal reference lines and reference points A and B on two example device types: a full touch-screen smart phone (left) and a DUT with a keypad (right) 53
Figure 16 – Cheek position of the DUT on the left side of SAM where the device position shall be maintained for the phantom test set-up 56
Figure 17 – Tilt position of the DUT on the left side of SAM 56
Figure 18 – An alternative form factor DUT with reference points and reference lines 57
Figure 19 – Block diagram of the tests to be performed 60
Figure 20 – Orientation of the probe with respect to the line normal to the phantom surface, for head and flat phantoms, shown at two different locations 64
Figure 21 – Measurement procedure for different types of correlated signals 72
Figure 22 – Positioning of the surfaces and edges of the DUT for determining the proximity sensor triggering distance 79
Figure 23 – Positioning of the edges of the DUT to determine proximity sensor triggering distance variations with the edge positioned at different angles from the perpendicular position 80
Figure 24 – Fast SAR Procedure A 87
Figure 25 – Fast SAR Procedure B 89
Figure 26 – Modified chart of Figure 19 93
Figure 27 – Use of conducted power for LTE mode selection, for Band 1 (1 920 MHz to 1 980 MHz) (MPR values are in dB) 97
Figure 28 – Use of conducted power for LTE mode selection, for Band 17 (704 MHz to 716 MHz) (MPR values are in dB) 98
Figure A.1 – Test set-up for the system check 114
Figure B.1 – Distribution of Tilt/Cheek 124
Figure B.2 – SAR relative to SAR in position with maximum SAR in GSM mode 128
Figure B.3 – Two points identifying the minimum distance between the position of the interpolated maximum SAR and the points at 0,6 × SAR_{max} 130
Figure B.4 – Histogram for D_{min} in the case of GSM 900 and iso-level at 0,6 × SAR_{max} 130
Figure B.5 – Histogram for random variable $Factor_{1g,1800}$ 132
Figure D.1 – Mechanical details of the standard dipoles 145
Figure D.2 – Standard waveguide (dimensions are according to Table D.3) 148
Figure D.3 – Drawing of the CLA that corresponds to a resonant loop integrated in a metallic structure to isolate the resonant structure from the environment 150
Figure D.4 – Mechanical details of the meander dipoles for 150 MHz 152

IECNORM.COM : Click to view the full PDF of IEC/IEEE 62209-1528:2020

Figure D.5 – VPIFA validation antenna 155
Figure D.6 – Mask for positioning VPIFAs 155
Figure E.1 – Experimental set-up for assessment of the sensitivity (conversion factor) using a vertically-oriented rectangular waveguide 162
Figure E.2 – Illustration of the antenna gain evaluation set-up 165
Figure E.3 – Schematic of the coaxial calorimeter system 169
Figure E.4 – Set-up to assess hemispherical isotropy deviation in tissue-equivalent medium 171
Figure E.5 – Alternative set-up to assess hemispherical isotropy deviation in tissue-equivalent medium 172
Figure E.6 – Experimental set-up for the hemispherical isotropy assessment 173
Figure E.7 – Conventions for dipole position (ξ) and polarization (θ) 174
Figure E.8 – Measurement of hemispherical isotropy with reference antenna 175
Figure G.1 – Illustration of dimensions in Table G.1 and Table G.2 182
Figure G.2 – Close up side view of phantom showing the ear region 184
Figure G.3 – Side view of the phantom showing relevant markings 185
Figure G.4 – Sagittally bisected phantom with extended perimeter (shown placed on its side as used for device SAR tests) 186
Figure G.5 – Picture of the phantom showing the central strip 186
Figure G.6 – Cross-sectional view of SAM at the reference plane 187
Figure G.7 – Dimensions of the flat phantom set-up used for deriving the minimal phantom dimensions for W and L for a given phantom depth D 189
Figure G.8 – FDTD predicted error in the 10 g psSAR as a function of the dimensions of the flat phantom compared with an infinite flat phantom at 800 MHz 190
Figure G.9 – Complex permittivity of human tissues compared to the phantom target properties 193
Figure G.10 – Example reference coordinate system for the left-ear ERP of the SAM phantom 194
Figure G.11 – Example coordinate system on a DUT 194
Figure H.1 – Slotted line set-up 196
Figure H.2 – An open-ended coaxial probe with inner and outer radii a and b, respectively 198
Figure H.3 – TEM line dielectric properties test set-up [85] 200
Figure J.1 – SAR and temperature increase (ΔT) distributions simulated for a three-layer (skin, fat, muscle) planar torso model 207
Figure J.2 – Statistical approach to protect 90 % of the population 209
Figure J.3 – psSAR skin enhancement factors 210
Figure K.1 – SAM face-down phantom 212
Figure K.2 – SAM head-stand phantom 212
Figure K.3 – Wrist phantom 213
Figure L.1 – Cross section of the unified phantom (Uniphantom) with its dimensions 214
Figure L.2 – Measurement positions of handsets with straight and clamshell form factors 215
Figure L.3 – Flow chart of testing procedure for handsets with straight form factors 216
Figure L.4 – Flow chart of testing procedure for handsets with clamshell form factors 217
Figure M.1 – Configuration of a personal wired hands-free headset 218

IECNORM.COM : Click to view the full PDF of IEC/IEEE 62209-1528:2020

Figure M.2 – Configuration without a personal wired hands-free headset 219
Figure O.1 – Orientation and surface of averaging volume relative to phantom surface 235
Figure U.1 – Categories (classes) for comparison of the measured psSAR between the Uniphantom (SAR_{uni}) and the SAM phantom (SAR_{SAM}) 252
Figure U.2 – Histogram of the deviation of the 10 g psSAR of 45 handsets with straight form factors positioned at the flat bottom of the Uniphantom 254
Figure U.3 – Histogram of the deviation of the 1 g psSAR of 40 handsets with straight form factors positioned at the flat bottom of the Uniphantom 255
Figure U.4 – Histogram of the deviation of the 10 g psSAR of 25 handsets with straight form factors positioned at the flat bottom of the Uniphantom 256
Figure U.5 – Histogram of the deviation of the 1 g psSAR from 20 handsets with straight form factors positioned at the flat bottom of the Uniphantom 257
Figure U.6 – Histogram of the deviation of the 10 g psSAR of 20 handsets with straight form factors or smart phones positioned at the flat bottom of the Uniphantom 258
Figure U.7 – Histogram of the deviation of the 1 g psSAR of 20 handsets with straight form factors or smart phones positioned at the flat bottom of the Uniphantom 259
Figure U.8 – Histogram of the deviation of the 10 g psSAR of 20 handsets with straight form factors or smart phones positioned at the corner of the Uniphantom 260
Figure U.9 – Histogram of the deviation of the 1 g psSAR of 19 handsets with straight form factors or smart phones positioned at the corner of the Uniphantom 261
Figure U.10 – Histogram of the deviation of the 10 g psSAR of 20 handsets with clamshell form factors at the corner of the Uniphantom 262
Figure U.11 – Histogram of the deviation of the 1 g psSAR of 19 handsets with clamshell form factors at the corner of the Uniphantom 263
Figure V.1 – Generated RF input power variations to operation time without and with application of AIPLC 264
Figure V.2 – The system block diagram of the AIPLC 265
Figure V.3 – Power variation characteristics by adjusting the amplifier or signal generator outputs 265
Figure W.1 – Low, middle, and high channels at 2 GHz band (Band 1) 267
Figure W.2 – RF conducted power versus 10 g psSAR 268
Figure W.3 – 1 g SAR as a function of RF conducted power in various test conditions 269

Table 1 – Evaluation plan checklist 28
Table 2 – Dielectric properties of the tissue-equivalent medium 32
Table 3 – Area scan parameters 63
Table 4 – Zoom scan parameters 63
Table 5 – Example method to determine the combined SAR value using Alternative 1 70
Table 6 – Root-mean-squared error SAR correction formula as a function of the maximum change in permittivity or conductivity [28] 83
Table 7 – Threshold values $TH(f)$ used in this proposed test reduction protocol 93
Table 8 – Divisors for common probability density functions (PDFs) 101
Table 9 – Uncertainty budget template for evaluating the uncertainty in the measured value of 1 g or 10 g psSAR from a DUT or validation antenna (N = normal, R = rectangular) 103
Table 10 – Uncertainty of Formula (8) (see 7.8.2) as a function of the maximum change in permittivity or conductivity 107
Table B.1 – The number of DUTs used for the statistical study 123

IECNORM.COM : Click to view the full PDF of IEC/IEEE 62209-1528:2020

Table B.2 – Statistical analysis results of P(Tilt/Cheek > x) for various x values 124
Table B.3 – Statistical analysis results of P(Tilt/Cheek > x) for 1 g and 10 g psSAR 124
Table B.4 – Statistical analysis results of P(Tilt/Cheek > x) for various antenna locations 125
Table B.5 – Statistical analysis results of P(Tilt/Cheek > x) for various frequency bands 125
Table B.6 – Statistical analysis results of P(Tilt/Cheek > x) for various device types 126
Table B.7 – Distance D^{*}_{min} for various “iso-level” values 130
Table B.8 – Experimental thresholds to have a 95 % probability that the maximum measured SAR value from the area scan will also have a psSAR 132
Table B.9 – SAR values from the area scan (GSM 900 band): Example 1 133
Table B.10 – SAR values from the area scan (GSM 900 band): Example 2 133
Table C.1 – Measurement uncertainty budget for relative SAR measurements using Class 2 fast SAR testing, for tests performed within one frequency band and modulation 141
Table C.2 – Measurement uncertainty budget for system check using Class 2 fast SAR testing 142
Table D.1 – Mechanical dimensions of the reference dipoles 146
Table D.2 – Numerical target SAR values (W/kg) for standard dipole and flat phantom 147
Table D.3 – Mechanical dimensions of the standard waveguide 148
Table D.4 – Numerical target SAR values for waveguides 149
Table D.5 – Numerical target SAR values for CLAs 151
Table D.6 – Mechanical dimensions of the reference meander dipole 152
Table D.7 – Numerical target SAR value (W/kg) for meander dipole 153
Table D.8 – Dimensions for VPIFA antennas at different frequencies 154
Table D.9 – Electric properties for the dielectric layers for VPIFA antennas 155
Table D.10 – Numerical target SAR values for VPIFAs on the flat phantom 156
Table E.1 – Uncertainty analysis for transfer calibration using temperature probes 160
Table E.2 – Guidelines for designing calibration waveguides 163
Table E.3 – Uncertainty analysis of the probe calibration in waveguide 164
Table E.4 – Uncertainty template for evaluation of reference antenna gain 166
Table E.5 – Uncertainty template for calibration using reference antenna 167
Table E.6 – Uncertainty components for probe calibration using thermal methods 170
Table F.1 – Suggested recipes for achieving target dielectric properties, 30 MHz to 900 MHz 178
Table F.2 – Suggested recipes for achieving target dielectric properties, 1 800 MHz to 10 000 MHz 179
Table G.1 – Dimensions used in deriving SAM phantom from the ARMY 90th percentile male head data (Gordon et al. [61]) 183
Table G.2 – Additional SAM dimensions compared with selected dimensions from the ARMY 90th percentile male head data (Gordon et al. [61]) – specialist head measurement section 183
Table G.3 – Parameters used for calculation of reference SAR values in Table D.2 190
Table H.1 – Parameters for calculating the dielectric properties of various reference liquids 202
Table H.2 – Dielectric properties of reference liquids at 20 °C 203
Table J.1 –psSAR correction factors 209

IECNORM.COM : Click to view the full PDF of IEC/IEEE 62209-1528:2020

Table N.1 – SAR results tables for example test results in GSM 850 band 221
Table N.2 – SAR results tables for example test results in GSM 900 band 222
Table N.3 – SAR results tables for example test results in GSM 1800 band 222
Table N.4 – SAR results tables for example test results in GSM 1900 band 223
Table O.1 – Parameters for the reference function f_1 in Formula (O.12) 231
Table O.2 – Reference SAR values from the distribution functions f_1, f_2, and f_3 232
Table O.3 – Example uncertainty template and example numerical values for permittivity (ε_r') and conductivity (σ) measurement 237
Table S.1 – Uncertainties relating to the deviations of the parameters of the standard waveguide from theory 248
Table S.2 – Other uncertainty contributions relating to the dipole antennas specified in Annex D 249
Table S.3 – Other uncertainty contributions relating to the standard waveguides specified in Annex D 249
Table U.1 – Summary of information to determine the margin for handsets with straight form factors positioned at the flat bottom of the Uniphantom 254
Table U.2 – Summary of information to determine the margin for handsets with straight form factors, including slide-type and bar handsets (except smart phones), positioned at the flat bottom of the Uniphantom 256
Table U.3 – Summary of information to determine the margin for the smart phones positioned at the flat bottom of the Uniphantom 258
Table U.4 – Summary of information to determine the margin for smart phones positioned at the corner of the Uniphantom 260
Table U.5 – Statistical analysis results of P(Tilt/Cheek > x) for various device types 261
Table U.6 – Summary of information to determine the margin for handsets with clamshell form factors positioned at the corner of the Uniphantom 262
Table W.1 – Relative standard deviation of α found in Study 1 (without MPR) 267
Table W.2 – Maximum relative standard deviation of α found in Study 2 (with MPR) 269

IECNORM.COM : Click to view the full PDF of IEC/IEEE 62209-1528:2020

INTERNATIONAL ELECTROTECHNICAL COMMISSION

_____

MEASUREMENT PROCEDURE FOR THE ASSESSMENT OF SPECIFIC ABSORPTION RATE OF HUMAN EXPOSURE TO RADIO FREQUENCY FIELDS FROM HAND-HELD AND BODY-MOUNTED WIRELESS COMMUNICATION DEVICES –

Part 1528: Human models, instrumentation, and procedures (Frequency range of 4 MHz to 10 GHz)

FOREWORD

1) The International Electrotechnical Commission (IEC) is a worldwide organization for standardization comprising all national electrotechnical committees (IEC National Committees). The object of IEC is to promote international co-operation on all questions concerning standardization in the electrical and electronic fields. To this end and in addition to other activities, IEC publishes International Standards, Technical Specifications, Technical Reports, Publicly Available Specifications (PAS) and Guides (hereafter referred to as "IEC Publication(s)"). Their preparation is entrusted to technical committees; any IEC National Committee interested in the subject dealt with may participate in this preparatory work. International, governmental and non-governmental organizations liaising with the IEC also participate in this preparation.

   IEEE Standards documents are developed within IEEE Societies and Standards Coordinating Committees of the IEEE Standards Association (IEEE SA) Standards Board. IEEE develops its standards through a consensus development process, approved by the American National Standards Institute, which brings together volunteers representing varied viewpoints and interests to achieve the final product. Volunteers are not necessarily members of IEEE and serve without compensation. While IEEE administers the process and establishes rules to promote fairness in the consensus development process, IEEE does not independently evaluate, test, or verify the accuracy of any of the information contained in its standards. Use of IEEE Standards documents is wholly voluntary. *IEEE documents are made available for use subject to important notices and legal disclaimers (see* http://standards.ieee.org/IPR/disclaimers.html *for more information).*

   IEC collaborates closely with IEEE in accordance with conditions determined by agreement between the two organizations. This Dual Logo International Standard was jointly developed by the IEC and IEEE under the terms of that agreement.

2) The formal decisions of IEC on technical matters express, as nearly as possible, an international consensus of opinion on the relevant subjects since each technical committee has representation from all interested IEC National Committees. The formal decisions of IEEE on technical matters, once consensus within IEEE Societies and Standards Coordinating Committees has been reached, is determined by a balanced ballot of materially interested parties who indicate interest in reviewing the proposed standard. Final approval of the IEEE standards document is given by the IEEE Standards Association (IEEE SA) Standards Board.

3) IEC/IEEE Publications have the form of recommendations for international use and are accepted by IEC National Committees/IEEE Societies in that sense. While all reasonable efforts are made to ensure that the technical content of IEC/IEEE Publications is accurate, IEC or IEEE cannot be held responsible for the way in which they are used or for any misinterpretation by any end user.

4) In order to promote international uniformity, IEC National Committees undertake to apply IEC Publications (including IEC/IEEE Publications) transparently to the maximum extent possible in their national and regional publications. Any divergence between any IEC/IEEE Publication and the corresponding national or regional publication shall be clearly indicated in the latter.

5) IEC and IEEE do not provide any attestation of conformity. Independent certification bodies provide conformity assessment services and, in some areas, access to IEC marks of conformity. IEC and IEEE are not responsible for any services carried out by independent certification bodies.

6) All users should ensure that they have the latest edition of this publication.

7) No liability shall attach to IEC or IEEE or their directors, employees, servants or agents including individual experts and members of technical committees and IEC National Committees, or volunteers of IEEE Societies and the Standards Coordinating Committees of the IEEE Standards Association (IEEE SA) Standards Board, for any personal injury, property damage or other damage of any nature whatsoever, whether direct or indirect, or for costs (including legal fees) and expenses arising out of the publication, use of, or reliance upon, this IEC/IEEE Publication or any other IEC or IEEE Publications.

8) Attention is drawn to the normative references cited in this publication. Use of the referenced publications is indispensable for the correct application of this publication.

IECNORM.COM : Click to view the full PDF of IEC/IEEE 62209-1528:2020

9) Attention is drawn to the possibility that implementation of this IEC/IEEE Publication may require use of material covered by patent rights. By publication of this standard, no position is taken with respect to the existence or validity of any patent rights in connection therewith. IEC or IEEE shall not be held responsible for identifying Essential Patent Claims for which a license may be required, for conducting inquiries into the legal validity or scope of Patent Claims or determining whether any licensing terms or conditions provided in connection with submission of a Letter of Assurance, if any, or in any licensing agreements are reasonable or non-discriminatory. Users of this standard are expressly advised that determination of the validity of any patent rights, and the risk of infringement of such rights, is entirely their own responsibility.

International Standard IEC/IEEE 62209-1528 has been prepared by IEC technical committee 106: Methods for the assessment of electric, magnetic and electromagnetic fields associated with human exposure, in cooperation with the International Committee on Electromagnetic Safety of the IEEE Standards Association, under the IEC/IEEE Dual Logo Agreement.

This first edition of IEC/IEEE 62209-1528 cancels and replaces IEC 62209-1:2016, IEC 62209-2:2010, IEC 62209-2:2010/AMD1:2019 and IEEE Std 1528-2013. This edition constitutes a technical revision.

This edition includes the following significant technical changes with respect to the previous edition:

a) extension of the frequency range down to 4 MHz and up to 10 GHz;
b) testing of devices with proximity sensors;
c) application specific phantoms;
d) device holder specifications;
e) fast SAR testing procedures;
f) test reduction procedures;
g) LTE assessment procedure;
h) revision of validation clause, including validation antennas;
i) revision of SAR assessment procedure;
j) time-average SAR measurement procedure;
k) uncertainty analysis;

This publication is published as an IEC/IEEE Dual Logo standard.

This publication contains attached files in the form of the Fast SAR Wizard described in 7.9.2.2 as well as CAD files for the SAM phantom. These files are available at:

http://www.iec.ch/dyn/www/f?p=103:227:0::::FSP_ORG_ID,FSP_LANG_ID:1303,25.

These files are intended to be used as a complement and do not form an integral part of the publication.

The text of this standard is based on the following IEC documents:

FDIS	Report on voting
106/514/FDIS	106/520/RVD

Full information on the voting for the approval of this standard can be found in the report on voting indicated in the above table.

International Standards are drafted in accordance with the rules given in the ISO/IEC Directives, Part 2.

IECNORM.COM : Click to view the full PDF of IEC/IEEE 62209-1528:2020

The IEC Technical Committee and IEEE Technical Committee have decided that the contents of this publication will remain unchanged until the stability date indicated on the IEC web site under "http://webstore.iec.ch" in the data related to the specific publication. At this date, the publication will be

- reconfirmed,
- withdrawn,
- replaced by a revised edition, or
- amended.

IMPORTANT – The 'colour inside' logo on the cover page of this publication indicates that it contains colours which are considered to be useful for the correct understanding of its contents. Users should therefore print this document using a colour printer.

IECNORM.COM : Click to view the full PDF of IEC/IEEE 62209-1528:2020

INTRODUCTION

The objective of this document is to provide procedures for measuring the human exposure from devices intended to be used at a position near the human head or body. It was developed to provide procedures to evaluate electromagnetic field (EMF) exposures due to radio frequency (RF) transmitting devices used next to the ear, in front of the face, mounted on the body, operating in conjunction with other RF-transmitting and non-transmitting devices or accessories (e.g. belt-clips), or embedded in garments. The types of devices dealt with include but are not limited to mobile telephones, cordless telephones, cordless microphones, and radio transmitters in personal computers. The applicable frequency range is from 4 MHz to 10 GHz. The document defines:

– measurement system requirements (Clause 6),
– SAR measurement protocols (Clause 7),
– SAR measurement uncertainty evaluation (Clause 8), and
– reporting requirements (Clause 9).

At the time this document was developed, two computational and measurement joint IEC/IEEE projects dealing with millimetre-wave power density assessment were under development, covering the frequency range from 6 GHz to 300 GHz. Hence there is an overlap of frequency between this document, which deals with SAR, and the other joint IEC/IEEE projects dealing with power density from 6 GHz to 10 GHz. The IEC/IEEE joint working group was aware of this fact and believed that it would give the flexibility of using whatever metrics suitable for the considered case of compliance assessment.

IECNORM.COM : Click to view the full PDF of IEC/IEEE 62209-1528:2020

MEASUREMENT PROCEDURE FOR THE ASSESSMENT OF SPECIFIC ABSORPTION RATE OF HUMAN EXPOSURE TO RADIO FREQUENCY FIELDS FROM HAND-HELD AND BODY-MOUNTED WIRELESS COMMUNICATION DEVICES –

Part 1528: Human models, instrumentation, and procedures (Frequency range of 4 MHz to 10 GHz)

IECNORM.COM : Click to view the full PDF of IEC/IEEE 62209-1528:2020

1 Scope

This document specifies protocols and test procedures for the reproducible and repeatable measurement of the conservative exposure peak spatial average SAR (psSAR) induced inside a simplified model of the head and the body by radio-frequency (RF) transmitting devices, with a defined measurement uncertainty. These protocols and procedures apply to a significant majority of the population, including children, during the use of hand-held and body-worn wireless communication devices. These devices include single or multiple transmitters or antennas, and are operated with their radiating structure(s) at distances up to 200 mm from a human head or body. This document is employed to evaluate SAR compliance of different types of wireless communication devices used next to the ear, in front of the face, mounted on the body, operating in conjunction with other RF-transmitting, non-transmitting devices or accessories (e.g. belt-clips), or embedded in garments. The applicable frequency range is from 4 MHz to 10 GHz. Devices operating in the applicable frequency range can be tested using the phantoms and other requirements defined in this document.

The device categories covered include, but are not limited to, mobile telephones, cordless microphones, and radio transmitters in personal, desktop and laptop computers, for multi-band operations using single or multiple antennas, including push-to-talk devices. This document can also be applied for wireless power transfer devices operating above 4 MHz.

This document does not apply to implanted medical devices.

2 Normative references

The following documents are referred to in the text in such a way that some or all of their content constitutes requirements of this document. For dated references, only the edition cited applies. For undated references, the latest edition of the referenced document (including any amendments) applies.

IEC 62209-3:2019, *Measurement procedure for the assessment of specific absorption rate of human exposure to radio frequency fields from hand-held and body-mounted wireless communication devices – Part 3: Vector measurement-based systems (Frequency range of 600 MHz to 6 GHz.*

ISO/IEC Guide 98-3:2008, *Uncertainty of measurement – Part 3: Guide to the expression of uncertainty in measurement (GUM:1995)*

3 Terms and definitions

For the purposes of this document, the following terms and definitions apply.

ISO, IEC, and IEEE maintain terminological databases for use in standardization at the following addresses:

- IEC Electropedia: available at http://www.electropedia.org/
- ISO Online browsing platform: available at http://www.iso.org/obp
- IEEE Dictionary Online: available at http://dictionary.ieee.org

3.1
accessory
optional component or attachment that can be used in conjunction with the device under test (DUT)

EXAMPLE 1 Accessories for holding, affixing, or otherwise carrying, wearing or attaching the device, as well as providing a specific use condition on the body of the user (e.g. a belt-clip, wrist-strap or any other body strap, or lanyard for wearing the device using a necklace).

EXAMPLE 2 Electronic accessories for performing specialized tasks or which provide additional features (e.g. GPS modules, outboard printers, MP3 players, cameras or viewing devices).

EXAMPLE 3 Electronic accessories providing audio or video input or output (e.g. headsets, microphones, cameras).

EXAMPLE 4 Accessories providing enhanced RF capability to the device (e.g. original, replacement, or auxiliary antennas).

EXAMPLE 5 Batteries and related DC power components.

EXAMPLE 6 Combinations of accessories, where two or more of the above are combined within one component.

3.2
axial isotropy
maximum deviation of the SAR measured when rotating the probe around its major axis while it is exposed to a wave impinging from a direction coinciding with its major axis

3.3
basic restriction
human exposure limits for compliance with time-varying electric, magnetic, and electromagnetic fields measured inside the body that are based on established adverse health effects

Note 1 to entry: Within the scope of this document, the physical quantity used as a basic restriction is the specific absorption rate (SAR).

3.4
body-worn device
device containing one or more wireless transmitters or transceivers which is positioned in close proximity to a person's torso or limbs (excluding the head) by means of a carrying accessory to support intended use operations

Note 1 to entry: This document uses the term body-worn synonymously for the term body-mounted, which was employed in earlier versions.

3.5
body-supported device
device containing one or more wireless transmitters or transceivers, with intended use that includes transmitting with any portion of the device being held directly against a user's body

3.6
boundary effect
change in the sensitivity of an electric-field probe when the probe tip is located close (less than one probe-tip diameter) to media boundaries

Note 1 to entry: This effect is caused by distortion of the scattered field at the probe tip due to the nearby phantom dielectric surface. This effect can be compensated if the probe orientation with respect to the phantom surface is known.

IECNORM.COM : Click to view the full PDF of IEC/IEEE 62209-1528:2020

3.7
cable
wire that is necessary for the device functionality in the intended operational configuration

3.8
channel
RF channel
specific sub-division of the transmit frequency range according to the operating parameters of a particular wireless technology

Note 1 to entry: The number of RF channels and the corresponding channel bandwidth can vary among individual wireless technologies. For the purpose of this document, SAR measurements are performed at specific channels; for example, the high, middle, and low channels of the transmission band.

3.9
conducted power
power delivered by the power amplifier of the device to a matched load

3.10
conservative exposure
estimate of the psSAR, including uncertainties as specified in this document, representative of and slightly higher than that expected to occur in the head or body of a significant majority of the human population during intended use of a wireless transmitting device

3.11
constant-envelope mode
transmission mode where the signal amplitude does not vary with time

3.12
correlated signals
electromagnetic fields, associated to distinct signal waveforms, yielding non-zero time-domain correlation integral at some time instant

Note 1 to entry: Details are specified in IEC TR 62630 [1].

3.13
desktop device
device placed or mounted on a desk, table, or similar supporting structure, with antennas that are intended to be operated at or closer than 200 mm from the human body

3.14
device holder
fixture constructed of low-loss dielectric material that is used to hold the device under test in the required test position during SAR measurement

3.15
device under test
DUT
device containing one or more wireless transmitters or transceivers that is tested according to the methods of this document

Note 1 to entry: A device under test may be further categorized as a body-worn, body-supported, desktop, front-of-face, hand-held, limb-worn, clothing-integrated, or generic device.

3.16
duty factor
proportion of time that a transmitter transmits over a specified period

IECNORM.COM : Click to view the full PDF of IEC/IEEE 62209-1528:2020

3.17
fast SAR testing
usage of special techniques, methods, or algorithms to decrease the SAR measurement time compared to full SAR testing

Note 1 to entry: Class 1 fast SAR testing uses hardware that complies with all of the requirements of this document for full SAR testing. However, it uses faster testing procedures than those that comply with full SAR testing procedures.

Note 2 to entry: Class 2 fast SAR testing uses hardware and testing procedures that do not comply with the requirements of this document for full SAR testing.

3.18
frequency band
transmitting frequency range associated with a specific wireless operating mode

Note 1 to entry: The frequency band is usually referred to using rounded figures, however the actual frequency allocation can be slightly different; e.g. the GSM 850 MHz band actually uses 824 MHz to 849 MHz and 869 MHz to 894 MHz, and the GSM 900 MHz band actually uses 880 MHz to 915 MHz and 925 MHz to 960 MHz. In other cases, the official 3GPP nomenclature might be used, for instance LTE Band 12 (uplink 699 MHz to 716 MHz; downlink 729 MHz to 746 MHz).

3.19
front-of-face device
hand-held device containing one or more wireless transmitters or transceivers operated in close proximity to the face

Note 1 to entry: Front-of-face device types include PTT devices, two-way radios, and devices equipped with an optical camera.

3.20
full SAR testing
usage of methods, procedures and specific hardware which fully comply with all of the normative requirements in this document, except those specified in 7.9.2

3.21
generic device
device that cannot be categorized as belonging to any of the specific device categories

3.22
hand-held device
portable device which is operated in a user's hand at a distance of over 200 mm from the head or torso during its intended use

3.23
handset
wireless communication device intended to be held in the hand and operated next to the ear, consisting of an acoustic output or earphone and an acoustic input or microphone, and containing a radio transmitter and receiver

Note 1 to entry: For synonymous terms such as "mobile phone", the terms "mobile" and "portable" have specific but generic meanings in IEC 60050 – mobile: capable of operating while being moved (IEC 60050-151:2001, 151-16-46); portable: capable to be carried by one person (IEC 60050 151:2001, 151-16-47). The term "portable" often implies the ability to operate when carried on the user. These definitions are used interchangeably in various wireless regulations and industry specifications, in some cases referring to types of wireless communication devices and in other cases to intended use.

3.24
head-mounted device
device containing one or more wireless transmitters or transceivers that is positioned in close proximity to a person's head or neck by means of an accessory, if necessary, to support its intended use operation

Note 1 to entry: This definition excludes hand-held devices.

IECNORM.COM : Click to view the full PDF of IEC/IEEE 62209-1528:2020

3.25
hemispherical isotropy
maximum deviation of the measured SAR when rotating the probe around its major axis with the probe exposed to reference waves impinging from the half space in front of the probe tip, at varying incidence angles relative to the axis of the probe

3.26
host
equipment that needs to be operated with a wireless device or module during testing to provide transmitting functionality according to its intended use

3.27
intended use
use conditions for which a product is intended according to the full range of available functions, in accordance with the specifications, instructions, and information provided by the manufacturer in the user documentation

3.28
limb-worn device
device containing one or more wireless transmitters or transceivers, with intended use that includes being strapped onto the arm or leg of the user while transmitting

Note 1 to entry: Limb-worn device types include wrist-worn, ankle-worn, and forearm-worn devices. Some regulatory jurisdictions specify different requirements for devices worn on limbs away from the wrists or ankles.

3.29
linearity error
maximum deviation of a measured quantity from the expected linear dependency over the measurement range

3.30
measurement drift
continuous or incremental change in the measured quantity over time, due to changes in metrological properties of a measuring instrument

3.31
measurement uncertainty

3.31.1
uncertainty evaluation
<Type A> evaluation of uncertainty by the statistical analysis of series of observations (measurements)

3.31.2
uncertainty evaluation
<Type B> evaluation of uncertainty by means other than the statistical analysis of series of observations (measurements)

3.31.3
standard uncertainty
estimated standard deviation of a measurement result, equal to the positive square root of the estimated variance

3.31.4
combined uncertainty
estimated standard deviation of the measurement result obtained by combining the individual standard uncertainties of both Type A and Type B evaluations using the usual “root-sum-squares” method of combining standard deviations that were obtained by taking the positive square root of the estimated variances

IECNORM.COM : Click to view the full PDF of IEC/IEEE 62209-1528:2020

3.31.5
expanded uncertainty
quantity defining an interval about the result of a measurement that is expected to encompass a distribution of values within a specified confidence interval that could reasonably be attributed to the measured quantity

3.32
multi-band
<wireless communication device> capable of operating in more than one frequency band

3.33
operating mode
wireless protocol or standard used by a device to communicate with another terminal or device over the wireless network

Note 1 to entry: The operating mode includes all parameters to establish the communication over the wireless network. The specific operating mode parameters include, but are not limited to, communication standard, frequency band, channel, signal modulation, communications protocol, data rate, bandwidth, number and positions of time slots, and number and positions of resource blocks. Some operating modes do not have some of these parameters.

Note 2 to entry: Modern terminals can have multiple operating modes for individual or simultaneous transmission. Examples of operating modes include wireless protocols such as GSM, EDGE, EVDO, GPRS, CDMA, WCDMA, LTE, 5G NR, Bluetooth®[1], and Wi-Fi®[2]. Multiple operating modes can transmit in one or more frequency bands, e.g. a DUT could support both multiple wireless technologies in a frequency band, and also allow multiple wireless transmission modes within a wireless technology, such as GSM, GPRS, EDGE, or WCDMA and HSPA, or 5G NR.

3.34
output power
power at the output of the RF transmitter when the antenna, or a load with the same input impedance as the antenna, is connected to it

3.35
primary peak SAR value
largest interpolated local SAR value determined in an area scan measurement

3.36
secondary peak SAR value
in an area scan measurement, interpolated local SAR maximum that is smaller than the primary peak SAR value

3.37
peak spatial-average SAR
psSAR
maximum SAR averaged within a local region based on a specific averaging mass, e.g. any 1 g or 10 g of tissue in the shape of a cube

Note 1 to entry: In this document, the terms psSAR (over 1 g or 10 g) and the terms 1 g SAR and 10 g SAR are used interchangeably.

3.38
penetration depth
depth at which the SAR of an associated incident plane wave, penetrating into a homogeneous lossy medium, is reduced to $1/e^2$ of its value just beneath the surface of the medium

IECNORM.COM : Click to view the full PDF of IEC/IEEE 62209-1528:2020

---

1 Bluetooth® is a trademark of the Bluetooth Special Interest Group (SIG). This information is given for the convenience of users of this document and does not constitute an endorsement by IEC.

2 Wi-Fi® is a trademark of the Wi-Fi Alliance. This information is given for the convenience of users of this document and does not constitute an endorsement by IEC.

Note 1 to entry: For a plane-wave incident normally on a planar half-space, the E-field penetration depth δ is given as:

$$\delta = \frac{1}{\omega}\left[\frac{\mu_0 \varepsilon'_r \varepsilon_0}{2}\left(\sqrt{1+\left(\frac{\sigma}{\omega \varepsilon'_r \varepsilon_0}\right)^2}-1\right)\right]^{-\frac{1}{2}}$$

where

ω is the angular frequency;

μ_0 is the magnetic permeability of vacuum, in henry per metre;

ε_0 is the dielectric permittivity of vacuum, in farad per metre;

ε'_r is the relative dielectric permittivity of the lossy medium, unitless;

σ is the electrical conductivity of the lossy medium, in siemens per metre.

3.39
phantom
physical model with an equivalent human anatomy and comprised of a tissue-equivalent medium with dielectric properties specified in this document

3.40
pinna
auricle
cartilaginous projecting portion of the outer ear, consisting of the helix, lobule, and anti-helix

3.41
power control algorithm
protocol of the DUT to set and adjust the maximum output power of the transmitter over a specified averaging period

3.42
production variation
range in output power among DUT production samples when set to transmit at the maximum level

3.43
push-to-talk device
hand-held radio transceiver that enables a user to operate a mechanical switch to toggle between radio transmission and reception (simplex operating mode)

EXAMPLE Two-way radio.

3.44
probe isotropy
property pertaining to the degree to which the response of an electric field probe or magnetic field probe is independent of the polarization and direction of propagation of the incident wave

Note 1 to entry: See also axial isotropy (3.2) and hemispherical isotropy (3.25).

3.45
proximity sensor
capacitive sensor or combination of sensors in the DUT utilized for the detection of user proximity for the purpose of limiting transmitter power in order to ensure compliance with RF exposure limits

IECNORM.COM : Click to view the full PDF of IEC/IEEE 62209-1528:2020

3.46
readout electronics
measurement system component that connects to the E-field probe and provides an analog-to-digital conversion of the measured values to the post-processor of the measurement system

3.47
response time
time required by the measuring equipment to reach 90 % of its final value after a step variation of the input signal

3.48
scanning system
automatic positioning system capable of placing the measurement probe at specified positions according to requirements of this document

3.49
sensitivity
ratio of the magnitude of the system response (e.g. voltage) to the magnitude of the quantity being measured (e.g. electric field strength squared)

3.50
separation distance
distance between the device under test and the outside surface of the phantom

Note 1 to entry: The separation distance represents the distance during intended use.

3.51
specific absorption rate
SAR
measure of the rate at which energy is absorbed by the human body when exposed to a radio frequency electromagnetic field

Note 1 to entry: The SAR in the tissue-equivalent medium can be determined by the rate of temperature increase or by E-field measurements, according to the following formulas:

$$SAR = \frac{\sigma E^2}{\rho}$$

$$SAR = c_h \left.\frac{\partial T}{\partial t}\right|_{t=0}$$

where:

SAR is the specific absorption rate in watts per kilogram;

E is the RMS value of the electric field strength in the tissue-equivalent medium in volts per metre;

σ is the electrical conductivity of the tissue-equivalent medium in siemens per metre;

ρ is the mass density of the tissue-equivalent medium in kilograms per cubic metre;

c_h is the specific heat capacity of the tissue-equivalent medium in joules per kilogram per kelvin;

$\left.\frac{\partial T}{\partial t}\right|_{t=0}$ is the initial time derivative of temperature in the tissue-equivalent medium in kelvin per second.

3.52
test configuration
set of DUT parameters applicable to the SAR measurement, consisting of the position of the DUT on the applicable phantom, the DUT use configuration (e.g. antenna position), and operating mode

IECNORM.COM : Click to view the full PDF of IEC/IEEE 62209-1528:2020

3.53
time-period averaged SAR
TPAS
SAR averaged over a specified averaging period when a power control algorithm is applied

3.54
time-averaged SAR
SAR measured over a sufficiently long integration time to ensure a stable result over the duty factor and other characteristics of the modulated signal

3.55
tune-up specification
output power tolerance when setting a sample of the DUT to transmit at the maximum output power level

3.56
TX factor
ratio of the average output power to the peak output power of the DUT over a specified time-averaging period

4 Symbols and abbreviated terms

4.1 Physical quantities

The International System of Units (SI) is used throughout this document.

Symbol	Quantity	Unit	Dimensions
α	Attenuation coefficient	reciprocal metre	1/m
P	Average (temporal) absorbed power	watt	W
J	Current density	ampere per square metre	A/m^2
σ	Electric conductivity	siemens per metre	S/m
E	Electric field strength	volt per metre	V/m
f	Frequency	hertz	Hz
ρ	Mass density	kilogram per cubic metre	kg/m^3
δ	Penetration depth	metre	m
μ	Permeability	henry per metre	H/m
c_h	Specific heat capacity	joule per kilogram per kelvin	J/(kg K)
ε	Permittivity	farad per metre	F/m
SAR	Specific absorption rate	watt per kilogram	W/kg
T	Temperature	kelvin	K
λ	Wavelength	metre	m

NOTE In this document, temperature is quantified in degrees Celsius, as determined by: T(°C) = T(K) – 273,15 K.

4.2 Constants

Symbol	Physical constant	Magnitude
c_0	Speed of light in vacuum	$2{,}998 \times 10^8$ m/s
ε_0	Permittivity of free space	$8{,}854 \times 10^{-12}$ F/m
μ_0	Permeability of free space	$4\pi \times 10^{-7}$ H/m

IECNORM.COM : Click to view the full PDF of IEC/IEEE 62209-1528:2020

4.3 Abbreviated terms

5G NR	Fifth generation new radio
AIPLC	Automatic input power level control
APS	Absolute psSAR
CAD	Computer aided design
CDMA	Code division multiple access
CLA	Confined-loop antenna
CW	Continuous Wave
DCS	Digital Cellular Service
DOE	Design of experiments
DUT	Device under test
EDGE	Enhanced Data rates for GSM Evolution
E-field	Electric field strength
ERP	Ear reference point
FDTD	Finite-difference time-domain
GPRS	General Packet Radio Service
GSM	Global System for Mobile Communications
H-field	Magnetic field strength
ICES	International Committee on Electromagnetic Safety
ICNIRP	International Commission on Non-Ionizing Radiation Protection
LE	Left ear
LTE	Long Term Evolution
MIMO	Multiple input multiple output
MPR	Maximum power reduction
OFAT	One-factor-at-a-time
OFDM	Orthogonal frequency-division multiplexing
OFDMA	Orthogonal frequency-division multiple access
PCS	Personal Communications Service
PDF	Probability density function
psSAR	Peak spatial-average SAR
PTT	Push-to-talk
RE	Right ear
RF	Radio frequency
RMS	Root mean square
RSS	Root sum square
SAM	Specific anthropomorphic mannequin
SAR	Specific absorption rate
STBC	Space-time block coding
TDMA	Time division multiple access
TX	Transmission
UMTS	Universal Mobile Telecommunications System
VPIFA	Vertical Planar Inverted F-Antenna
WCDMA	Wideband code division multiple access
WiMax	Worldwide Interoperability for Microwave Access

IECNORM.COM : Click to view the full PDF of IEC/IEEE 62209-1528:2020

WLAN	Wireless local area network

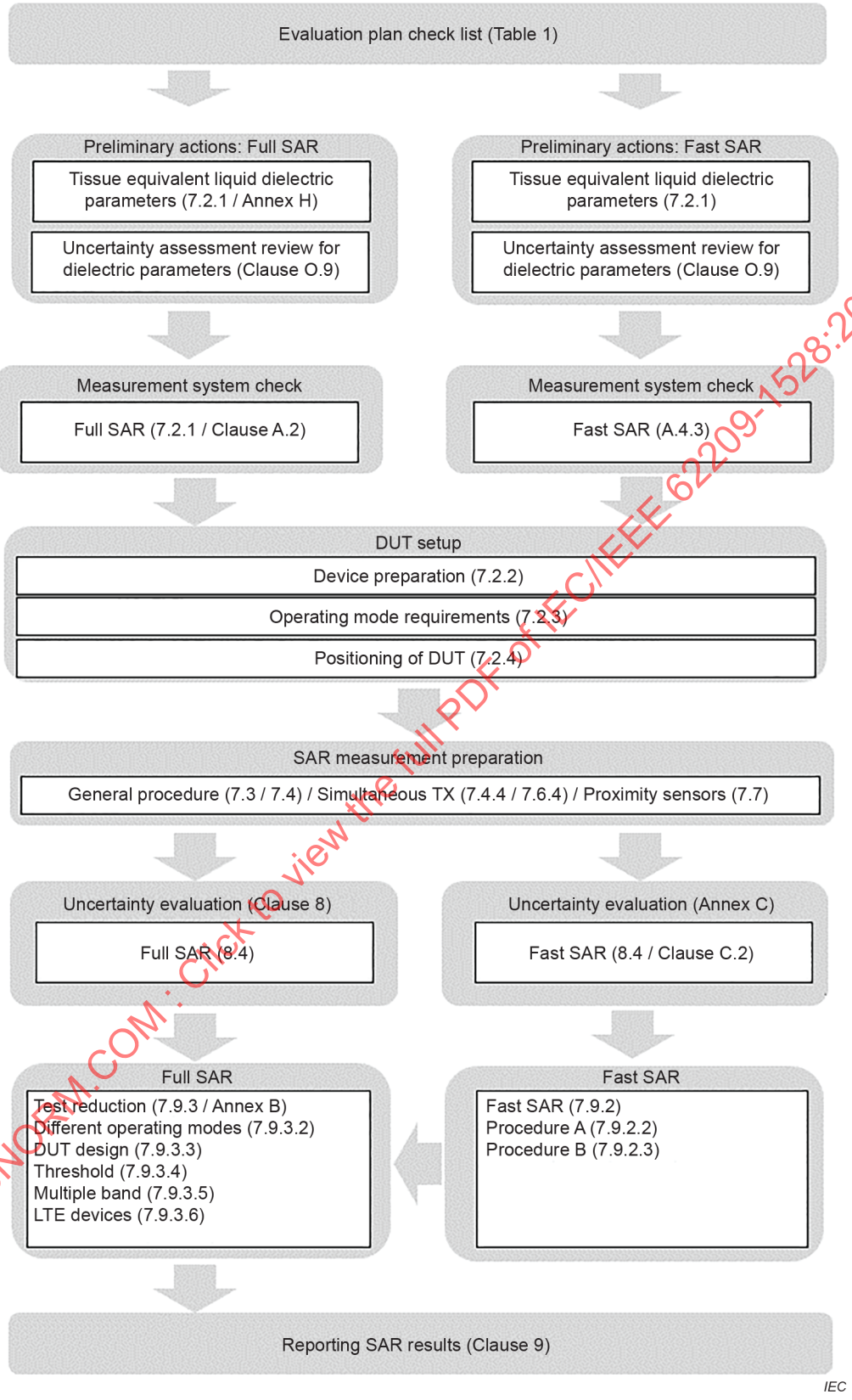
5 Quick start guide and evaluation plan checklist

The quick start guide shown in Figure 1 and the evaluation plan checklist shown in Table 1 provide a high level overview of the SAR measurement procedures of this document. For the details of each step, refer to the relevant clause specified in Figure 1 and Table 1.

Table 1 – Evaluation plan checklist

Stage	Evaluation steps	Action
Evaluation plan checklist Planning of the measurement configurations	– What type of device is being evaluated? – Review of antennas and supported wireless technologies, single or multiple combinations. – What are the test positions applicable? – Working under laboratory conditions and following good laboratory practice and documentation, prepare to conduct the necessary evaluation.	Complete checklist based on evaluation plan.
Preliminary actions and measurement system check	– A liquid dielectric properties measurement shall be performed and recorded. **For array systems, this is typically provided by the manufacturer* – System check needs to be performed to verify that the system components are working correctly.	Should be conducted before starting a project and repeated.
DUT set-up	The protocol for SAR assessment defines all the permutations of operational conditions that should be tested. The essential steps include: – Preparing the DUT by establishing a connection to a base station simulator. – Configuring the DUT to operate on the appropriate test frequencies. – Positioning the DUT in relation to the phantom.	Ensure the DUT is configured in the correct way and radiating appropriately when positioned against the phantom.
Uncertainty evaluation	– Guidelines and approximation formulas are provided, enabling the estimation of each individual uncertainty component. – The uncertainty budget shall cover the appropriate frequency range with regards to equipment used in the SAR system.	Determine uncertainty and complete the uncertainty table.
SAR measurements procedures	– This stage is the actual procedure for the measurement of SAR. – The procedure is iterative to ensure that the highest value of the psSAR of a DUT is captured. – This is done by a systematic process looking at all device positions, configurations and operating modes in all frequency bands accordingly. – Measurement systems can incorporate a single probe or array probes. Either fast SAR testing or test reduction techniques may be used. Some accepted techniques may be used to either reduce or accelerate the measurement process.	Determining highest SAR. Ensure the rationale for test reduction or fast SAR testing is recorded and reported if used.
Reporting SAR results	– The final report describes the results of the evaluations, provides enough technical details to allow for repeatability of the evaluations performed, and reports the results by comparison with the relevant limit. – The measurement report shall contain enough details and information for demonstrating compliance to the requirements of this document.	Prepare the final measurement report along with addressing the requirements.

IECNORM.COM : Click to view the full PDF of IEC/IEEE 62209-1528:2020



IECNORM.COM : Click to view the full PDF of IEC/IEEE 62209-1528:2020

Figure 1 – Quick start guide

6 Measurement system specifications

6.1 General requirements for full SAR testing

A SAR measurement system consists of the phantom (a SAM phantom representing the human head, or a flat phantom representing the human body, or both) filled with tissue-equivalent medium, electronic measurement instrumentation, a scanning system, and a DUT holder. Procedures for full SAR testing are described in 7.4. SAR tests performed in accordance with this document shall conform to the following requirements.

a) SAR shall be measured using a probe that is automatically positioned to measure the internal E-field distribution in the phantom. From the measured E-field values, the SAR distribution and the psSAR value shall be calculated.

b) The phantom shall be filled with the required tissue-equivalent medium, representing the dielectric properties of tissues in the human head or body.

c) The tissue-equivalent medium shall be a liquid of low viscosity to allow free movement of the probe within it.

d) For the tissue-equivalent media, a density ρ of 1000 kg/m^3 shall be used.

e) At least three reference points shall be defined on the phantom by the phantom manufacturer to be used when aligning the scanning system with the phantom. These points shall be visible to the user, enclosing at least 80 % of the phantom top surface and each point shall be at least 20 cm from any other point.

f) Both the ambient temperature and tissue-equivalent medium temperature shall be in the range of 18 °C to 25 °C, inclusive; see O.9.6 to determine the temperature uncertainty.

g) Prior to the measurements of tissue-equivalent medium dielectric properties and SAR, the DUT, test equipment, medium, and phantom shall have been kept in the laboratory long enough for their temperatures to have stabilized (i.e. they shall not have been recently moved from another area with a different ambient temperature, such as a refrigerator or storage area).

NOTE Depending on the shape, size, volume, and initial temperature of the medium and the container, 24 hours or more might be required for temperature stabilization.

h) The temperature of the tissue-equivalent medium during the SAR measurements shall be within 2 °C (or a temperature difference corresponding to a 5 % change in either permittivity or conductivity, if this is smaller) of the temperature at which the dielectric properties were measured. If the temperature change exceeds this tolerance, the dielectric properties shall be re-measured.

i) The effect of reflections from cables, test equipment, or other reflectors shall be determined by the SAR system check procedure described in Clause A.2, by comparing the SAR measured with and without the reflectors present, or where necessary with the judicious placement of absorbing materials and/or the use of ferrite beads on cables.

j) SAR measurements of DUTs shall only be performed when the effects of reflections, secondary RF transmitters, etc., result in a psSAR (for 1 g or 10 g mass, whichever is applicable to the test) less than 0,012 W/kg by measuring the psSAR at (approximately) 0,4 W/kg (used to establish the 3 % low detection limit, see 8.4.1.7). When the effect of cables and reflectors is more than 0,012 W/kg, ferrite beads, RF absorbers, and other mitigation techniques shall be applied to reduce the SAR error.

If the preceding limit cannot be achieved, a value higher than 3 % (0,012 W/kg) may be considered in the uncertainty budget in the “RF ambient conditions–reflections” row of the applicable tables in Annex C, provided it can be demonstrated that the SAR contribution due to reflections determined by the system check procedure is less than 10 % of the SAR measured for the DUT.

k) The requirement on reflections shall be verified at least every year, or whenever the system check shows unexpected results.

l) During testing, the DUT shall not be connected to any wireless network, except a base station simulator in the laboratory.

IECNORM.COM : Click to view the full PDF of IEC/IEEE 62209-1528:2020

m) System validation according to the protocol specified in Clause A.3 shall be done at least once per year, and additionally when a new measurement system is put into operation, and whenever modifications have been made to the measurement system (such as a new software version, different type or version of readout electronics, or different probes). The transmit sources used for system validation shall be designed and validated to meet the requirements specified in Annex D. Additional transmit sources of dipole and waveguide types at specific frequencies not presently included in Table D.1, Table D.2, Table D.3, Table D.4, Table D.5, Table D.6, Table D.7, Table D.8, Table D.9, and Table D.10 may be used as sources provided they meet the requirements specified in Annex D. In this document, flat phantoms shall be used for system check and system validation.

n) The measurement system shall be validated as a complete system.

o) The probe shall be calibrated in a tissue-equivalent medium required for the calibration frequency and temperature range, according to the methodology specified in Annex E. Calibration of the probe separately from the measurement system is allowed, provided that the same electrical interface characteristics specified for the probe and readout electronics are used during measurements. The probe(s) shall be calibrated together with an identical amplifier, measurement device, and data acquisition system.

p) The lower detection limit shall be at most 0,01 W/kg, and the maximum detection limit shall be at least 100 W/kg.

q) The probe isotropy shall be less than the expanded uncertainty for the axial isotropy component using the procedures of Table 9 and 8.4.1.5, or ±0,2 dB (±5 %), whichever is less, as determined in the tissue-equivalent medium.

r) The outermost diameter of the probe tip shall not exceed 8 mm in the vicinity of the measurement elements, for frequencies up to and including 2 GHz.

s) For frequencies above 2 GHz, the probe tip diameter shall not exceed $\lambda/3$, where λ is the wavelength in the medium. The probe tip diameter may be larger if it can be demonstrated that the E-field from any potential field distribution can be measured with an uncertainty of less than ±15 % (k = 2) at the distances from the surface of the phantom as listed in Table 3 and Table 4, or at the distances recommended by the SAR measurement system manufacturer (whichever is less).

t) The system linearity shall be within ±0,5 dB over the SAR range from 0,12 W/kg to 100 W/kg.

u) Where this document explicitly specifies performance characteristics for the measurement system or a part of the measurement system, the manufacturer of the system or sub-system, or the system integrator, shall document the conformity with the provisions of this document.

6.2 Phantom specifications

6.2.1 General

Subclause 6.2 specifies phantoms to be used for psSAR measurements of the DUT. Subclause 6.2.3 defines the head phantom to be used for evaluating exposure in the head, next to the ear. Subclause 6.2.4 defines the flat phantom to be used for evaluating exposure in the torso or other body regions. If the standard head or flat phantoms are not applicable, due to physical constraints of the scanning system or intended use conditions of the DUT, the specific phantoms described in 6.2.5 may be used.

6.2.2 Basic phantom parameters

The phantom shell material shall be resistant to damage or reaction with the chemicals used in the tissue-equivalent medium. The phantom shell shall be made of low-loss and low-permittivity material, having loss tangent $\tan\delta \leq 0{,}05$ and relative permittivity:

- $\varepsilon_r' \leq 5$, for $f \leq 3$ GHz
- $3 \leq \varepsilon_r' \leq 5$, for $f > 3$ GHz

IECNORM.COM : Click to view the full PDF of IEC/IEEE 62209-1528:2020

Target dielectric properties of the tissue-equivalent medium in the phantom are specified in Table 2 for discrete frequencies ranging between 4 MHz and 10 GHz. For other frequencies within this range, the nominal dielectric properties shall be obtained by linear interpolation between the higher and lower tabulated figures. Example recipes for preparing tissue-equivalent media designed to produce the dielectric properties at some of the frequencies in the 4 MHz to 10 GHz range are provided in Annex F. The rationale for the medium dielectric properties is given in Clause G.5. The liquid temperature specifications are given in 6.1.

NOTE 1 Nominal values are target dielectric properties with a specific tolerance requirement.

To minimize reflections from the upper surface of the tissue-equivalent medium, the depth of the medium should be at least 15 cm. Medium depth of less than 15 cm may be used only if it is demonstrated (e.g. using numerical simulations) that the effect on psSAR is less than 1 % during system validation (see Annex A). If it is more than 1 % but less than 3 %, uncertainty for the highest value from the system validation shall be added to the uncertainty budget.

The dielectric properties shall be measured and compared with the values given in Table 2 using linear interpolation. This measurement can be performed using the equipment and procedures specified in Annex H. The measured dielectric properties, not the values of Table 2, shall be used in the SAR calculations.

NOTE 2 The dielectric properties (permittivity and conductivity) of the medium have been specified to result in conservative exposure (see Clause G.5 for the rationale used to derive the medium dielectric properties).

NOTE 3 See 7.2.1 for the allowable variations between the measured and the target dielectric properties specified in Table 2.

Table 2 – Dielectric properties of the tissue-equivalent medium

Frequency MHz	**Real part of the complex relative permittivity,** ε_r'	**Conductivity,** σ S/m	**Penetration depth (E-field),** δ mm
4	*55,0*	*0,75*	293,0
13	*55,0*	*0,75*	165,5
30	55,0	0,75	112,8
150	52,3	0,76	62,0
300	45,3	0,87	46,1
450	43,5	0,87	43,0
750	*41,9*	*0,89*	39,8
835	41,5	0,90	39,0
900	41,5	0,97	36,2
1 450	40,5	1,20	28,6
1 800	40,0	1,40	24,3
1 900	40,0	1,40	24,3
1 950	40,0	1,40	24,3
2 000	40,0	1,40	24,3
2 100	*39,8*	*1,49*	22,8
2 450	39,2	1,80	18,7
2 600	*39,0*	*1,96*	17,2
3 000	38,5	2,40	14,0
3 500	*37,9*	*2,91*	11,4
4 000	*37,4*	*3,43*	10,0
4 500	*36,8*	*3,94*	9,7

IECNORM.COM : Click to view the full PDF of IEC/IEEE 62209-1528:2020

Frequency MHz	Real part of the complex relative permittivity, ε_r'	Conductivity, σ S/m	Penetration depth (E-field), δ mm
5 000	*36,2*	*4,45*	1,5
5 200	*36,0*	*4,66*	8,4
5 400	*35,8*	*4,86*	8,1
5 600	*35,5*	*5,07*	7,5
5 800	35,3	5,27	7,3
6 000	*35,1*	*5,48*	7,0
6 500	*34,5*	*6,07*	6,7
7 000	*33,9*	*6,65*	6,4
7 500	*33,3*	*7,24*	6,1
8 000	*32,7*	*7,84*	5,9
8 500	*32,1*	*8,46*	5,3
9 000	*31,6*	*9,08*	4,8
9 500	*31,0*	*9,71*	4,4
10 000	*30,4*	*10,40*	4,0

NOTE For convenience, permittivity and conductivity values are linearly interpolated for frequencies that are not a part of the original data from Drossos et al. [2]. They are shown in italics in Table 2. The italicized values are linearly interpolated (below 5800 MHz) or extrapolated (above 5800 MHz) from the non-italicized values that are immediately above and below these values.

6.2.3 Head phantom

The specific anthropomorphic mannequin (SAM) phantom shall be used for evaluating exposure in the head. The rationale for choosing the specific head phantom model (i.e. SAM) for this document is based on the following criteria.

a) The psSAR shall provide conservative exposure.

b) The test results shall not unnecessarily overestimate the maximum SAR expected in actual users.

c) The phantom shall allow stable and repeatable device positioning for psSAR measurements, and be effective for verifying measurement repeatability according to system check procedures, and measurement reproducibility through inter-laboratory comparisons.

d) The phantom shall be practical for routine SAR evaluation use.

e) The phantom shall support these criteria for contemporary and future wireless device designs, and be unbiased with respect to any particular design or shape.

f) Based on the presently available science, literature, and experience, the design of the SAM phantom that meets the above criteria is a function of at least the following parameters:

   1) size and shape of the head phantom shell;

   2) dielectric properties and material homogeneity of the tissue-equivalent media and the phantom shell;

   3) ear pinna size, shape, location, and material properties;

   4) exclusion of the hand for measuring SAR in the head (Annex I, 6.3).

IECNORM.COM : Click to view the full PDF of IEC/IEEE 62209-1528:2020

6.2.4 Flat phantom

a) For evaluating exposure in the body, the following requirements apply.

   1) The flat phantom shall be used.

   2) Its shell shall be constructed in the form of an open-top container with a flat bottom.

   3) Any flat phantoms used shall be large enough to allow the measurement of SAR in 1 g and 10 g volumes with an influence from the container shape of less than 1 % (Clause G.4).

b) The flat phantom shall have the following shape and dimensions (Figure 2).

   1) Except as specified in b) 2), the phantom flat bottom wall shall have the shape of an ellipse with a length of 600 mm and a width of 400 mm.

   2) For frequencies above 150 MHz, and for separation distances less than or equal to 25 mm from the outer surface of the bottom of the phantom shell, phantoms with other shapes and smaller dimensions are allowed as follows:

      i) between 150 MHz and 800 MHz, the phantom flat bottom wall may have any shape that encompasses an ellipse with length of 0,6 λ_0 and width of 0,4 λ_0, where λ_0 is the wavelength in air;

      ii) between 800 MHz and 10 GHz, the phantom may have any shape flat bottom wall that encompasses an ellipse with length of 225 mm and width of 150 mm.

c) The thickness of the bottom-wall of the flat phantom shall be 2,0 mm, with a tolerance of ±0,2 mm. When filled with the required depth of medium, any sagging of the bottom surface of the phantom within the projection of the DUT shall be determined and considered in the uncertainty budget (see 8.4.2.4). If the preceding dimensional requirements are met, the effect of the shape and thickness on the repeatability of SAR measurement results is less than 1 % (see Clause G.4). Effects on the SAR due to the influence of the deviation from the required shell parameters and thickness shall be included in the uncertainty estimation (see 8.4.2.3).

NOTE Use of a flat phantom as a standard phantom for SAR evaluations of body-worn and body-supported devices is intended to represent maximum coupling between the DUT and the human body. Such coupling to the phantom, while maintaining prescribed distances, is likely to produce conservative exposure. Annex J provides more details about this topic.

IECNORM.COM : Click to view the full PDF of IEC/IEEE 62209-1528:2020

Dimensions in millimetres

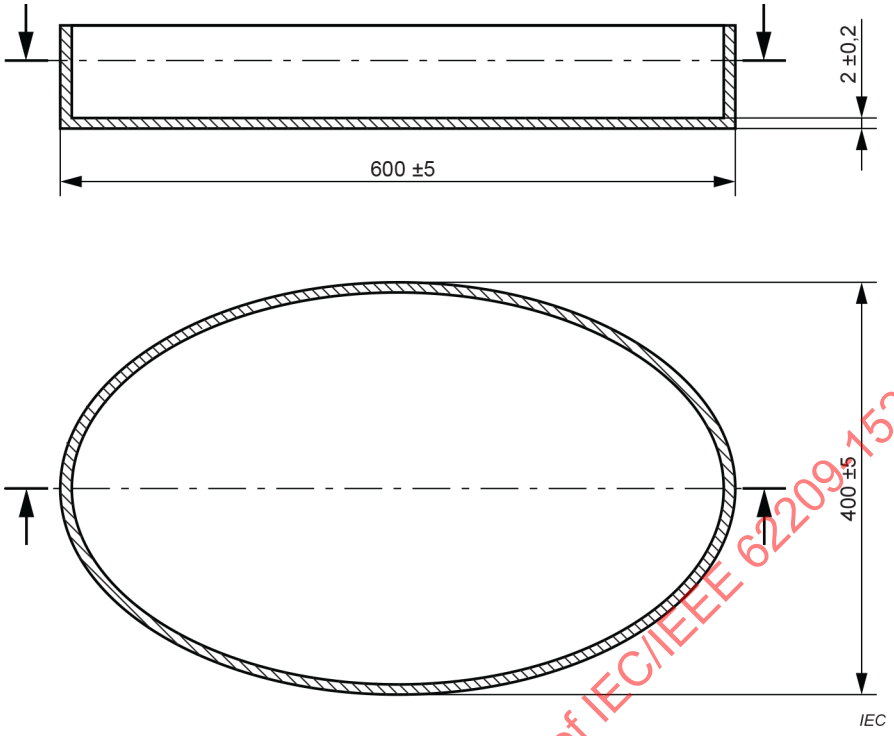


Figure 2 – Dimensions of the elliptical phantom

6.2.5 Device-specific phantoms

Device specific phantoms, alternative to those specified in 6.2.3 or 6.2.4, may be used if the flat phantom or SAM does not support the exposure conditions, or if either of the following applies:

a) the device is intended for operation on different parts of the body other than the head or torso (e.g. the wrist);

b) the physical constraints imposed on the scanning system by the phantom do not allow psSAR for the DUT to be determined with the required accuracy.

Examples of alternative device-specific phantoms are specified in Annex K and Annex L. The scientific or technical rationale and specifications of these phantoms are provided in the aforementioned annexes. Alternative device positioning procedures can also be required. These, and the rationale for using alternative specific phantoms, shall be reported.

6.3 Influence of hand on SAR in head

During normal operation, the head and hand are in the near-field of the DUT when used next to the ear, and hence both absorb energy. For extremities such as the hand, a higher SAR limit is allowed (e.g. 4 W/kg averaged over 10 g of tissue in ICNIRP RF exposure guidelines [3] and IEEE Std C95.1-2019 [4]). Numerical and experimental studies have shown that the SAR in the hand at the power levels used by typical DUTs is not expected to exceed those limits (Francavilla et al. [5], Gandhi et al. [6], Jensen and Rahmat-Samii [7], [8], Kuster et al. [9], Watanabe et al. [10]). Furthermore, a practical phantom for SAR measurement in the hand is currently unavailable. Therefore, SAR measurement in the hand is not addressed in this document.

IECNORM.COM : Click to view the full PDF of IEC/IEEE 62209-1528:2020

The influence of a hand holding a DUT to the head during SAR measurements was considered in IEEE Std 1528-2013 [11]. Earlier work by Balzano et al. [12] and Kuster et al. [9] reported that the presence of the hand either decreased or had no significant effect on the head SAR; however numerical results by Meyer et al. [13] showed one case with 7 % increase in head SAR due to the hand. These deviations in head SAR were concluded to be within the conservativeness provided by the SAM phantom. Based on these studies, the exclusion of the hand from test procedures would lead to head SAR overestimation in the majority of situations, as confirmed by more recent research results [14], [15], [16] on DUT SAR levels. For these reasons, hand models are not considered in this document.

The state of dosimetric research on the effect of the hand on head SAR produced by DUTs is specified in Annex I. This research shows that there are cases when the SAR produced by DUTs in the SAM phantom can increase as well as decrease significantly due to the hand holding the DUT, for specific DUT designs, operating bands, and hand grips. These initial findings have shown that the SAM phantom alone can still overestimate head SAR in a statistically significant number of cases, compared to when the hand is present for the measurement. Nevertheless this deserves further investigations, which may potentially warrant future changes in this document.

6.4 Scanning system requirements

The SAR probe scanning system shall be able to scan the required measurement regions of the phantom that are within the projections of a DUT in order to evaluate the area and zoom scans. The tolerance of the probe tip positioning at a measurement point in the phantom shall be ≤ 0,2 mm. Accuracy of the probe positioning system in relation to the phantom shall be verified according to the phantom reference points defined by the phantom manufacturer. The mechanical structure of the scanning system shall not interfere with the SAR measurements. The scanning range shall cover at least 90 % of the phantom dimensions in all directions.

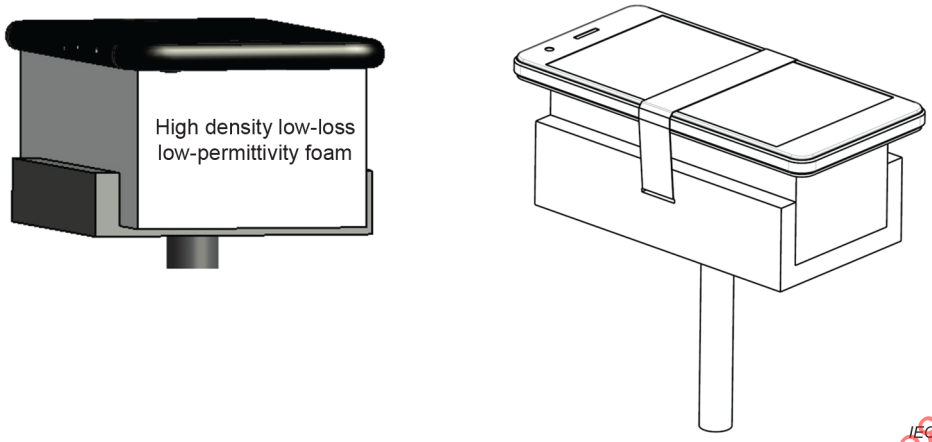
6.5 Device holder specifications

The device holder shall permit the DUT to be positioned according to the definitions given in 7.2.4. It shall be made of low loss and low permittivity material(s): loss tangent ≤ 0,05, and relative permittivity ≤ 5.

The DUT is preferably mounted on a piece of low relative permittivity (< 1,2) and low loss foam before being mounted into the device holder, to avoid any direct contact between the device holder and the DUT (Figure 3). If this is not possible, the device holder shall provide the minimum amount of contact to the DUT to give a secure hold and maintain the required position during the measurement. In cases where a default relative positioning cannot be achieved, e.g. due to the device holder interaction with buttons and sensors on the DUT, then minimal position offsets in a predefined direction should be applied to achieve the required DUT test position. The details shall be provided in the measurement report.

The device holder shall ensure precise and repeatable positioning of the DUT for SAR measurement. The positioning uncertainties shall be estimated following the procedures specified in 8.4.2.5 and 8.4.2.6. If the highest psSAR is determined according to step 3 of the test protocol in 7.3.2, then the device holder uncertainty effect on the reported SAR value is considered to be negligible.

IECNORM.COM : Click to view the full PDF of IEC/IEEE 62209-1528:2020



NOTE The DUT may be fixed on top of the foam (left), or held down using a thin strap (right).

Figure 3 – Mounting of the DUT in the device holder using low-permittivity and low-loss foam to avoid changes of DUT performance by the holder material

6.6 Characteristics of the readout electronics

The probe output is processed by the readout electronics and associated instrumentation that combines the voltages from the probe's sensors to provide an output that is proportional to the amplitude-squared of the E-field incident on the sensors. Detector diodes at the dipole feed-point are used to rectify the sensor voltages. The rectified signals are transmitted through resistive (RF-transparent) lines to the readout electronics system. For a continuous-wave signal at low field strength levels, the probe output is proportional to the square of the amplitude of the incident E-field; at higher signal levels (above the diode compression point), the output is not linearly proportional to $|E|^2$, but becomes proportional to $|E|$. This signal compression will lead to an underestimation of the actual SAR at high field strength conditions if it is not compensated correctly through probe calibration. Also, amplifiers in the readout electronics can deviate from an ideal linear response and introduce additional uncertainty. For uncertainties associated with the probe readout electronics, see 8.4.1.6.

7 Protocol for SAR assessment

7.1 General

All measurements should be carried out following good laboratory practice, e.g. in accordance with ISO/IEC 17025 [17], and any other national requirements for device certification. This document does not contain methods to verify the parameters of the DUT operating mode (e.g. modulation, data rate, time slots, resource blocks; see 3.33).

7.2 Measurement preparation

7.2.1 Preparation of tissue-equivalent medium and system check

a) The measured dielectric properties of the tissue-equivalent media shall be applied in the SAR evaluation. The dielectric properties shall be measured within 24 hours before the SAR measurements, and for every 48 hours of continuous use. However, in the situation where a laboratory documents compliance with Table 2 and the requirements of 6.2.2 using measurement intervals of up to a maximum of one week, less frequent dielectric properties measurements are acceptable. When the test series takes longer than 48 hours, the medium properties shall also be measured at the end of the test series.

IECNORM.COM : Click to view the full PDF of IEC/IEEE 62209-1528:2020

b) Tissue-equivalent media shall yield measured relative permittivity and conductivity values within ±5 % of the target values at frequencies at which the SAR is measured. When the method of 7.8 is used to correct the measured SAR for the deviations in permittivity and conductivity, the tolerance may be relaxed to a maximum of ±10 % from the targets. When out-of-tolerance dielectric properties measurements are made during a measurement interval longer than 48 hours, all SAR data measured since the last dielectric properties measurement shall be discarded.

c) For fast SAR testing systems that are hermetically sealed, the manufacturer shall provide either a procedure for the accurate measurement of the dielectric properties, or documentation of the dielectric properties of the medium (with corresponding medium temperature and ambient temperature) that were measured for the specific phantom when it was manufactured, or during system recalibration.

d) The temperature of the tissue-equivalent medium shall be measured and recorded at the time of the dielectric properties measurement, and prior to the system check and SAR measurements.

e) The system check shall be performed at each frequency band to be tested, in order to detect possible drift over short time periods and other measurement errors in the system. A system check according to the procedures of Clause A.2 shall be completed within 24 hours before performing SAR measurements for a DUT.

f) The system check procedure shall be performed on the same SAR measurement system, with the same SAR probe(s) and same tissue-equivalent medium required by the SAR evaluation of the device for each frequency band tested. To limit power drift during the system check, automatic input power level control may be implemented, as specified in Annex V.

7.2.2 Preparation of the wireless communication DUT

a) Any radiating element(s), battery, and accessories shall be those specified by the manufacturer, and documented in the measurement report. The battery shall be fully charged before each measurement, and the DUT positioned without external connections or cables that are not required for normal operation.

b) The RF output power and frequency (channel) shall be controlled by a wireless link to a base station or network simulator for supported operating modes. When a wireless link cannot be established with a base station simulator, test software and internal test codes may be used.

NOTE 1 Some national regulatory agencies might require that verification be undertaken by the device manufacturer for tests performed on prototypes, to ensure that the commercial version has the exact same mechanical and electrical characteristics as the tested prototype.

c) The DUT shall be set to transmit at the highest time-averaged output power level, within the range of the product's tune-up specifications and production variations.

For testing of wireless power transfer devices, other preparation procedures should be applied, as specified in IEC TR 62905 [18].

NOTE 2 For devices that can monitor and control their transmit power to maintain the time-average SAR below the applicable SAR limit, see 7.6.

7.2.3 DUT operating mode requirements

7.2.3.1 Requirements on DUT output power and signal parameters

The objectives of 7.2.3.1 are as follows.

- To determine that SAR of the DUT is evaluated at its maximum power level, taking into consideration device maximum output power tolerance and production variations.
- To correctly apply probe linearity compensation for time-varying signals, and to ensure that the signal is sampled correctly.

IECNORM.COM : Click to view the full PDF of IEC/IEEE 62209-1528:2020

The power requirements are as follows.

a) The maximum time-averaged power levels of the DUT shall be verified by the device manufacturer, e.g. by conducted power tests with a fully charged battery, to support SAR scaling.

b) All applicable operating modes shall be considered for testing, although testing of some operating modes might not be required (7.9.3).

c) A DUT operating in constant-envelope modes shall be tested at the maximum output power of its CW-equivalent (carrier) signal.

d) A DUT operating in pulsed-envelope modes shall be tested using the same pulse characteristics (duty factor, pulse period). If the DUT is capable of transmitting several modes by varying the pulse characteristics (e.g. transmission in multiple slots) in a wireless technology, the signal with the highest time-average output power per frequency band shall be tested, after considering the maximum output power of the DUT for each mode.

e) If the pulsed-envelope mode has a long pulse period such that the lowest frequency component of the signal envelope is below the low-pass filter cutoff frequency of the SAR measurement acquisition sub-system, the integration time and/or sample acquisition period shall be chosen to accurately measure the RMS of the signal, e.g. by using an integral number of pulse periods to avoid aliasing.

f) A DUT in operating modes where the envelope of the signal varies randomly with time (e.g. CDMA, OFDM) shall be tested in the mode resulting in the maximum time-averaged output power transmitted by the device for each wireless technology. The probe shall be calibrated over its dynamic range, and the probe output shall include probe linearity compensation. The linearity compensation in general depends on the operating mode, as reported by Di Nallo and Faraone [19] and by Nadakuduti et.al [20].

g) If the DUT cannot operate for the duration of the SAR measurement at its highest time-averaged output power level, within the range of the product's tune-up specifications and production variations, the following shall be applied.

   1) The DUT may be operated at a lower output power or lower duty factor, and the SAR shall be scaled to the required highest time-averaged output power level. However, the time-average output power shall be within the tolerance range specified for the device.

   2) The SAR of the device shall be shown to increase linearly with conducted power.

   3) Devices that operate with dual-output amplifiers, where both amplifiers are not required when operating at low power levels, or those that are designed to operate intermittently at very low duty factors, might require additional considerations to ensure SAR can be scaled linearly.

NOTE Some regulatory authorities might impose additional requirements on the maximum time-averaged output power reduction allowed for device SAR testing.

The procedure for power scaling is given in 7.2.3.2.

7.2.3.2 SAR scaling procedure for DUT power or signal variations

SAR scaling is the extrapolation of the SAR of a DUT determined with a tested operating mode (mod_X) to a SAR of the same device in the same exposure test position and frequency channel with a different operating mode (mod_Y). The difference can be in the power level, operating mode, or both. The time-averaged RF output power ratio of mod_X and mod_Y shall both be determined either by measuring the average power, or by numerical integration of the power envelope if the signals are sufficiently well known. SAR scaling is possible if:

a) the same RF amplifier stage is used for mod_X and mod_Y;

b) the same antenna is used for mod_X and mod_Y, and MIMO or other antenna diversity techniques are not applied;

c) the probe modulation response uncertainty has been evaluated for the modulated signal mod_X (8.4.2.7), and the SAR has been determined for mod_X;

IECNORM.COM : Click to view the full PDF of IEC/IEEE 62209-1528:2020

d) the time-averaged RF output power ratio (R_p) of mod_X and mod_Y after the RF amplifier stage is known, according to Formula (1):

$$R_p = \frac{P_{max,\,mod\,Y}}{P_{mod\,X}} \quad (1)$$

where $P_{max,modY}$ corresponds to the highest time-averaged output power setting. If the two signals differ in operating mode, then the test signal will be set at maximum time-averaged output power: $P_{modX} = P_{max,modX}$.

The factor R_p shall be determined by experimental means (e.g. measurement using an average power meter).

e) the RF carrier frequency of mod_X is the same as for mod_Y;

f) the RF signal bandwidth ratio R_m of mod_X and mod_Y satisfies Formula (2):

$$R_m = \left| \frac{BW_{mod\,Y}}{BW_{mod\,X}} - 1 \right| \times 100 \le 30\,\% \quad (2)$$

g) the channel bandwidths of mod_X and mod_Y are each within 5 % of the carrier frequency.

If the preceding requirements are fulfilled, a scaling of the SAR from mod_X and mod_Y shall be performed according to Formula (3), and scaling uncertainty shall be determined as specified in 8.4.3.2:

$$SAR_{mod\,Y} = R_m \cdot SAR_{mod\,X} \quad (3)$$

When the approach in 7.2.3.2 is used, it shall be stated in the measurement report that points a) through g) are satisfied.

For devices supporting PTT modes or other technology specific TDD operations, the maximum duty factor shall be assessed.

7.2.4 Positioning of the DUT relative to the phantom

7.2.4.1 Test distance and positioning relative to the flat phantom

7.2.4.1.1 General

Subclause 7.2.4.1 describes how the DUT, with or without accessories, shall be positioned, oriented, and configured relative to the phantom for SAR measurement. The specified test position(s) is (are) applicable for device-to-phantom surface separations up to and including 200 mm.

Subclause 7.2.4.1 describes positioning procedures for the following device types:

– devices that are large relative to phantom surface area (7.2.4.1.4);
– devices used with body-worn accessories (7.2.4.1.5);
– devices with hinged or swivel antenna (7.2.4.1.6);
– devices used next to or against the body without an accessory (7.2.4.1.7);
– desktop device (7.2.4.1.8);
– front-of-face device (7.2.4.1.9);
– hand-held usage of the device, not at the head or torso (7.2.4.1.10);
– limb-worn device (7.2.4.1.11);
– clothing-integrated device (7.2.4.1.12);

IECNORM.COM : Click to view the full PDF of IEC/IEEE 62209-1528:2020

– generic device (7.2.4.1.13);

NOTE The figures provided in 7.2.4.1 are for illustration purposes only, and are not to scale or representative of the areas that need SAR measurement.

7.2.4.1.2 DUT-to-phantom separation distance

When performing measurements against the flat phantom, the DUT-to-phantom separation distance may be set according to the following hierarchy.

a) Regulatory requirement: When there is a national regulatory requirement that specifies the DUT separation distance to the phantom, the DUT shall be positioned according to this requirement.

b) "Intended use distance" specified by the manufacturer: When there is no regulatory requirement, the intended use condition or distance specified by the manufacturer shall be used. This information shall be acquired from the user documentation accompanying the DUT.

c) Default separation distance: When there is neither a regulatory requirement nor an intended use distance specified by the manufacturer, the DUT shall be measured with each accessible face in direct contact with the surface of the phantom (see also 7.2.4.1.13 generic device).

The stated separation distance may be determined with the carry accessory attached to the DUT, when such condition is tested; see 7.2.4.1.5.

Care should be taken to ensure precise positioning at the applicable separation distances, for example using calibrated gauge blocks or similar means to ensure repeatability.

7.2.4.1.3 DUT reference points

General guidance to identify the orientation of a DUT, or when placed in a carry accessory for positioning to the flat phantom, is as follows. P1, P2, P3, and P4 are defined as the midpoint on each edge of the surface facing the phantom as shown in Figure 4. Line P1-P2 and Line P3-P4 shall be parallel to the phantom surface such that the distance between P1 and the phantom surface is equal to the distance between P2 and the phantom surface. Similarly, the distance between P3 and the phantom surface shall be equal to the distance between P4 and the phantom surface. The separation distance is specified as the distance between the phantom shell and the closest point on the DUT when positioned as specified in the preceding sentences. This general guidance may need to be adapted for specific designs, such as devices or carry accessories with curved surfaces, that require the device to be positioned differently for testing. Clear details of the actual test positions used shall be fully documented in the measurement report.

IECNORM.COM : Click to view the full PDF of IEC/IEEE 62209-1528:2020

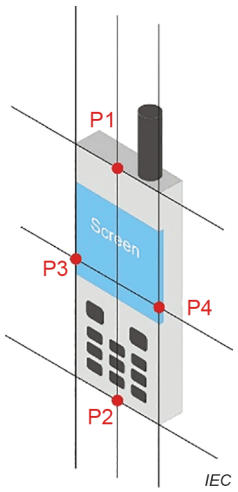


Figure 4 – Designation of DUT reference points

7.2.4.1.4 Positioning for devices that are large relative to phantom surface area

If the DUT is larger than the measurable region of the flat phantom specified in 6.2.4, the following applies.

a) The DUT shall be shifted such that the SAR distribution of the DUT can be covered by multiple area scans. When the DUT is shifted, the RF coupling between the DUT and phantom could change, resulting in a different SAR distribution compared to that using a larger phantom. A larger phantom, however, might not be representative of the significant majority of exposure situations involving people (see NOTE in 6.2.4).

b) To limit differences in the measured SAR due to coupling variations, two successive scans shall have an overlapping area of at least one third the size of the combined area, as shown in Figure 5.

c) In the overlapping area, the SAR distribution shall be similar such that the SAR difference at any point relative to the DUT geometry is less than the expanded uncertainty for repeatability. Otherwise, the DUT shall be shifted by a smaller amount such that the SAR difference is within the uncertainty.

Shifting is not needed if the radiating structures are small compared to the DUT and the phantom and/or the first area scan shows that the SAR distribution is entirely captured within the scanning area. In the situation where shifting was omitted, the rationale shall be clearly documented in the measurement report.

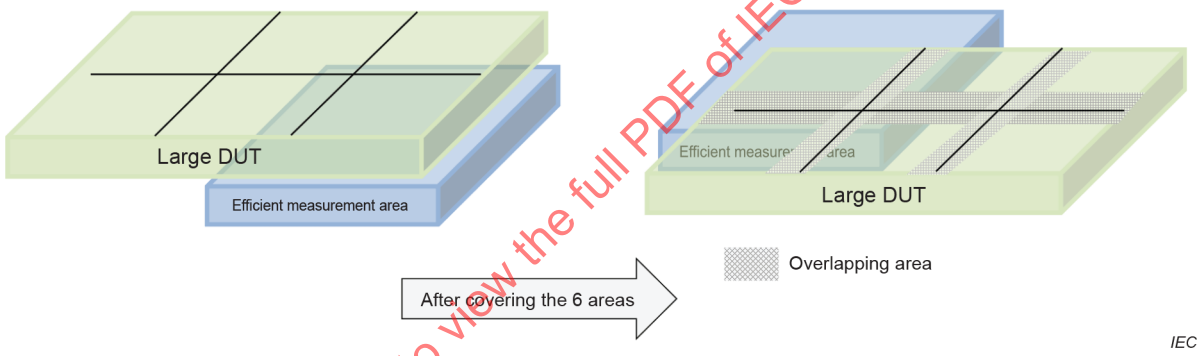


Figure 5 – Measurements performed by shifting a large device over the efficient measurement area of the system including overlapping areas – in this case: six tests performed

7.2.4.1.5 Devices used with body-worn accessories

A device within the scope of this document intended for use with a body-worn accessory approved or specified by the device manufacturer shall be assessed according to the following requirements.

a) If the user instructions provided by the manufacturer specify the intended use with a carry accessory (belt-clip, holster, carry-case or similar), the device shall be placed in that carry accessory and positioned in the intended use conditions against the flat phantom.

b) For carry accessories constructed from non-conductive materials that are capable of holding the DUT at varying distances to the phantom, the carry accessory providing the closest separation distance is expected to produce the highest SAR; therefore, testing of a carry accessory providing larger separation distances is not necessary unless the carry accessory contains conductive materials.

c) If there are multiple carry accessories that hold the DUT at the same distance, at least one carry accessory should be tested. Note that all carry accessories containing conductive materials shall be tested.

IECNORM.COM : Click to view the full PDF of IEC/IEEE 62209-1528:2020

d) For carry accessories that do not contain conductive materials (e.g. no metal parts), it is acceptable to substitute the carry accessory with an air-gap that keeps the DUT at a distance from the phantom surface no greater than the distance provided by the carry accessory.

e) The device shall be positioned in the intended use configuration with the body-worn accessory where the distance to the outer surface of the phantom is established by the specific accessory (Figure 6).

f) When evaluating devices that are not supplied with body-worn accessories but users can acquire body-worn accessories on their own, body-worn accessory SAR shall be measured with a separation distance according to the conditions of 7.2.4.1.2.

g) The surface of the device pointing towards the flat phantom should be positioned at the surface of the phantom according to 7.2.4.1.3; however, not all devices have a flat surface. Therefore, the details of the device position, e.g. the definition of the distance and the physical relationship between the device and the phantom according to the body-worn accessories, shall be documented in the measurement report.

h) When it is unclear if multiple surfaces can operate in a body-worn accessory facing the user, the DUT shall be tested with all applicable surfaces placed at the most conservative separation distance from the flat phantom. The details of the device position, attached to the accessory, shall be documented in the measurement report. If testing of some (but not all) surfaces is not required, this shall be documented with an associated rationale in the measurement report.

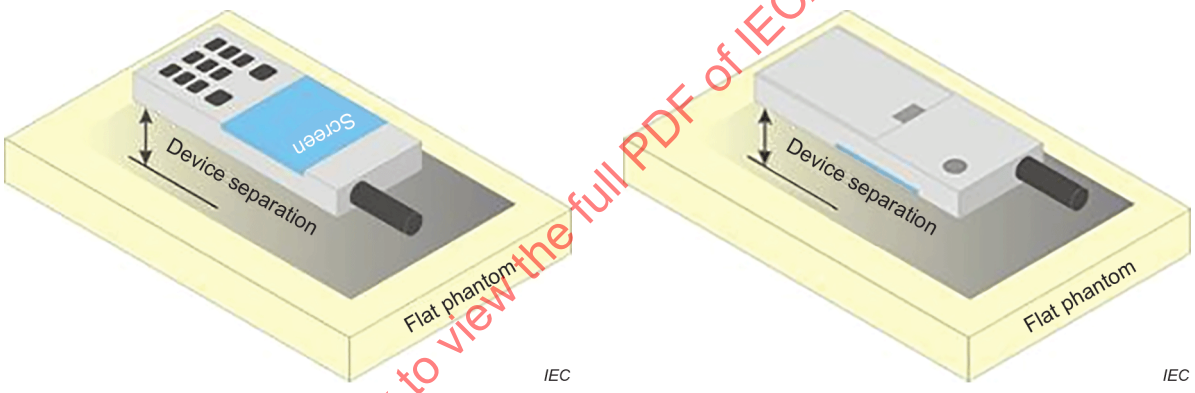


Figure 6 – Test positions for body-worn devices

IECNORM.COM : Click to view the full PDF of IEC/IEEE 62209-1528:2020

7.2.4.1.6 Devices with hinged or swivel antenna(s)

For devices that employ one or more external antennas with variable positions (e.g. antenna extended, retracted, rotated), the following applies.

a) The DUT shall be positioned in accordance with 7.2.4.1.2 and 7.2.4.1.3.

b) When it is unclear if certain antenna positions are applicable, tests shall be performed for the antenna positions and polarizations that are expected to be used by the users (Figure 7); for example with the antenna extended and retracted such as to obtain the highest exposure condition.

c) For antennas that can be rotated through one or two planes, a preliminary investigation across rotation ranges should be made and documented in the measurement report, to determine the highest exposure scenario(s) so that only that position(s) need(s) to be tested.

d) For devices with multiple detachable antennas, each antenna should be considered separately to determine SAR test requirements; for example, if the antennas are substantially similar (equivalent), certain test reduction considerations may be applied (7.9.3.3).

Subclause 7.2.4.1.6 may be applied in conjunction with test configurations specified in other subclauses, as appropriate for the device.

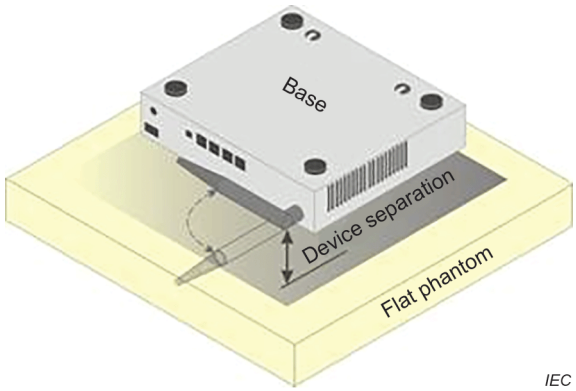


Figure 7 – Device with swivel antenna

7.2.4.1.7 Devices used next to or against the body without an accessory

A typical example of a device used next to the body is a wireless enabled laptop or a tablet device containing a peripheral plug-in radio transmitter that can be supported on the user's body. Other devices that fall into this category include tablets of equivalent sizes or larger than a netbook computer (> 20 cm diagonal display), credit card transaction authorization terminals, and point-of-sale and/or inventory terminals. The example in Figure 8 a) shows a tablet form factor portable computer for which SAR should be separately assessed with each surface and edge containing an antenna positioned against the flat phantom in accordance with the conditions of 7.2.4.1.2. Some tablets might limit display orientations so that the edges with antennas are not used next to the user; therefore, such edges might not need testing.

To assess these types of use conditions, the following applies.

a) The DUT shall be positioned with its base (bottom surface) and applicable edges against the flat phantom. The orientations and other use positions can be host device specific. Therefore, these should be determined according to the transmitter and antenna locations on the host device.

NOTE 1 RF transmitters that can operate in different hosts might require additional consideration.

b) For antennas incorporated in the display screen of a laptop, notebook or netbook computers, tests shall be performed with the display screen open at a 90° angle as seen in Figure 8 b) (left side), or at a more conservative angle allowing the antennas to be closer to the phantom for assessing the user exposure conditions.

c) Devices in the scope of 7.2.4.1.7 with a display screen that should be open during normal operation generally do not need to be tested, provided the antenna(s) on the screen is sufficiently far away from the user's body according to the maximum output power of the antenna.

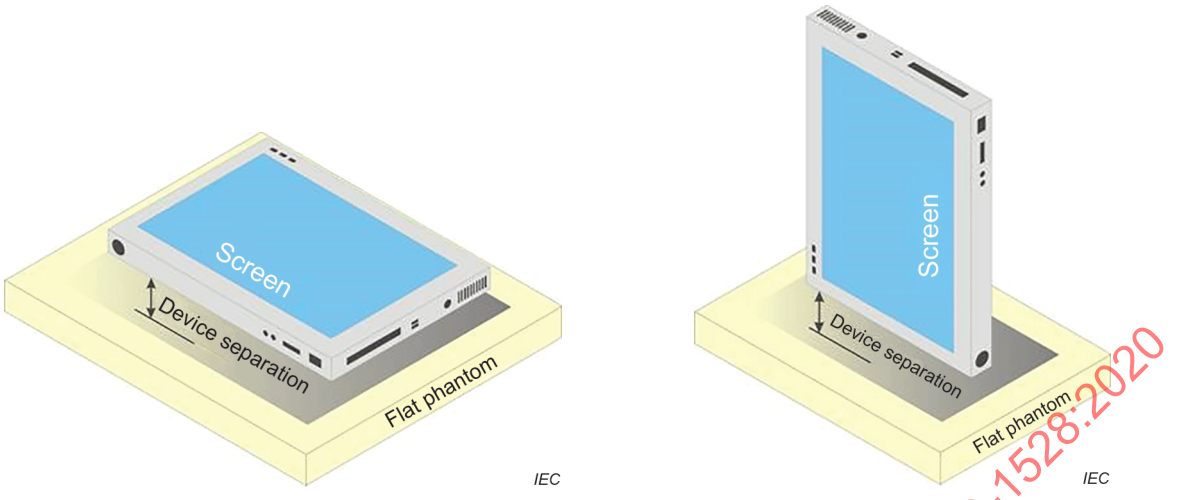
d) Where a screen mounted antenna is present, the SAR measurement for bystander exposure shall be performed with the screen positioned parallel to the flat phantom as shown in Figure 8 b) (right side).

NOTE 2 A separation distance of 2,5 cm is considered to be conservative for covering a wide range of expected bystander exposure conditions.

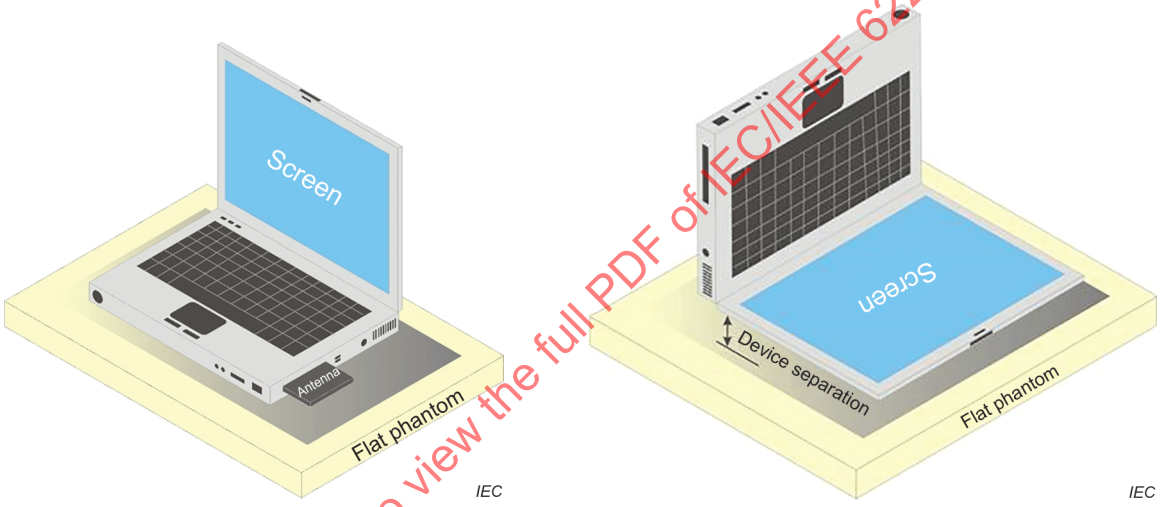
e) Body-supported devices with an external power supply (e.g. AC adapter) supplemental to the battery shall be tested with and without the external power supply attached.

f) For devices that employ an external antenna with variable positions, the procedures for swivel and detachable antenna should be used; see 7.2.4.1.6 and Figure 7.

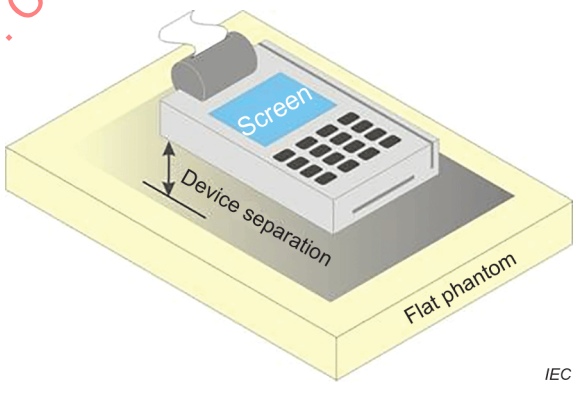
IECNORM.COM : Click to view the full PDF of IEC/IEEE 62209-1528:2020



a) Tablet form factor portable computer



b) Portable computer with external-antenna plug-in radio card (left side) or with internal antenna located in screen section (right side)



c) Wireless credit card transaction authorization terminal

Figure 8 – Test positions for body supported devices

7.2.4.1.8 Desktop device

A typical example of a desktop device is a wireless enabled desktop computer placed on a table or desk at closer than 200 mm to users while being used.

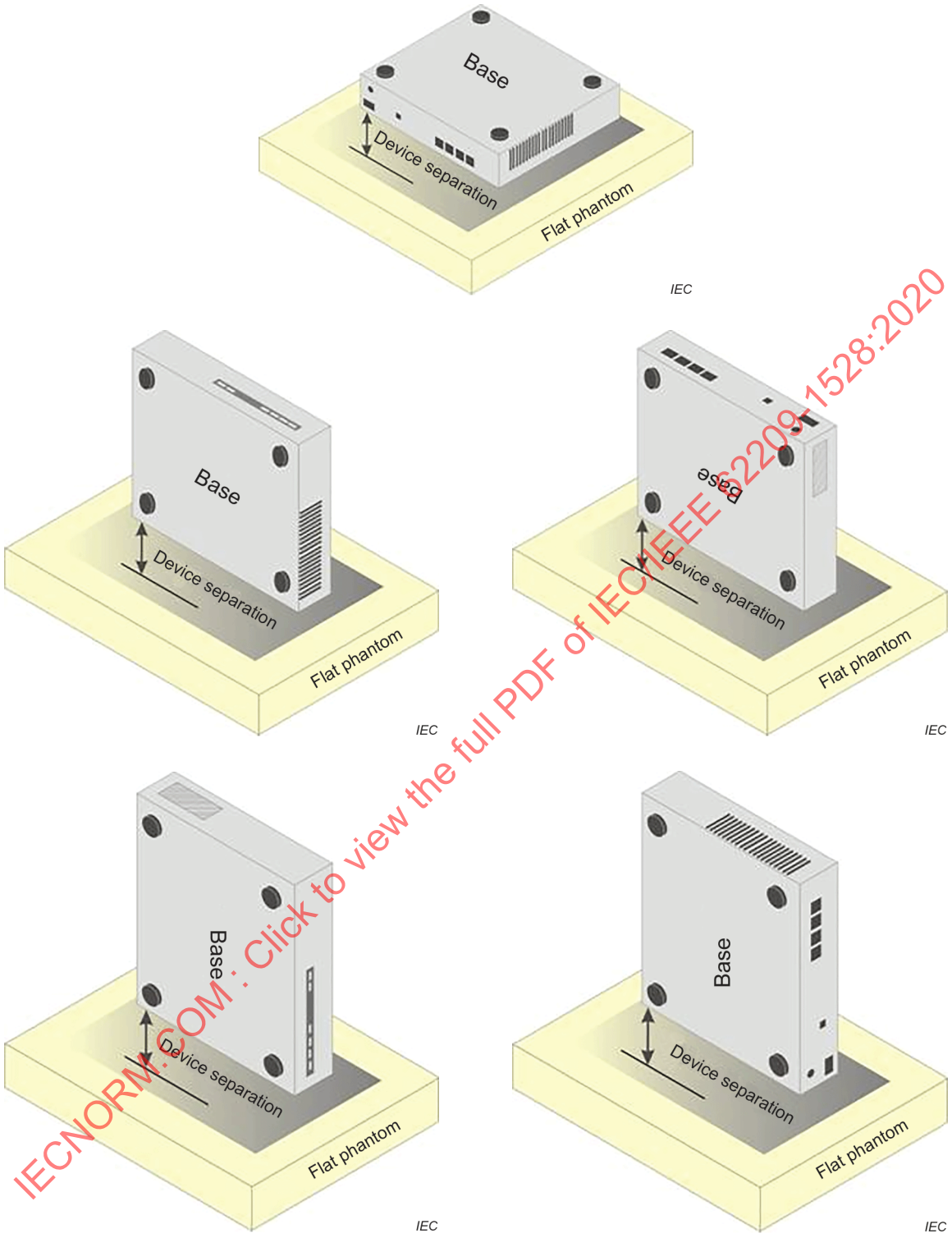
IECNORM.COM : Click to view the full PDF of IEC/IEEE 62209-1528:2020

To assess this type of device the following applies.

- The DUT shall be positioned against the flat phantom in accordance with the conditions of 7.2.4.1.2.
- For devices that employ an external antenna with variable positions, tests shall be performed for all antenna positions specified. Figure 7 and Figure 9 illustrate the SAR test positions for desktop device.

Due to the physical design, some device surfaces might not require testing, e.g. the base of a desk standing device.

IECNORM.COM : Click to view the full PDF of IEC/IEEE 62209-1528:2020



IECNORM.COM : Click to view the full PDF of IEC/IEEE 62209-1528:2020

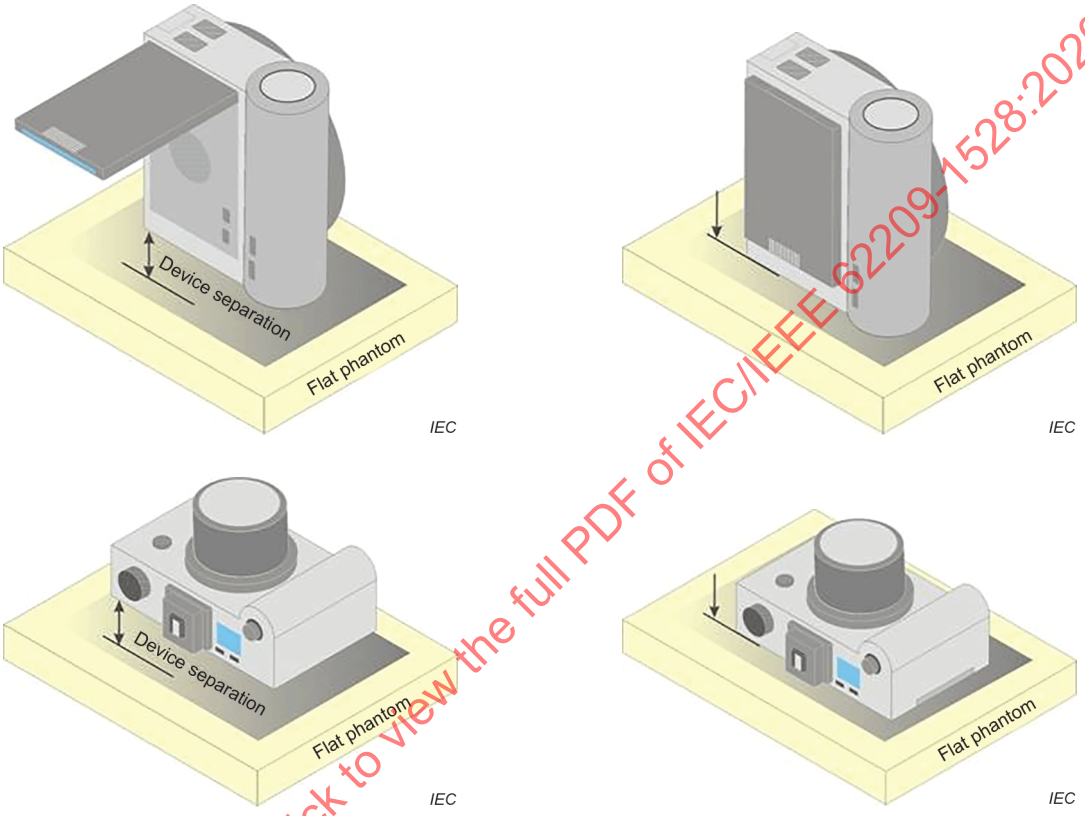
Figure 9 – Test positions for desktop devices

7.2.4.1.9 Front-of-face device

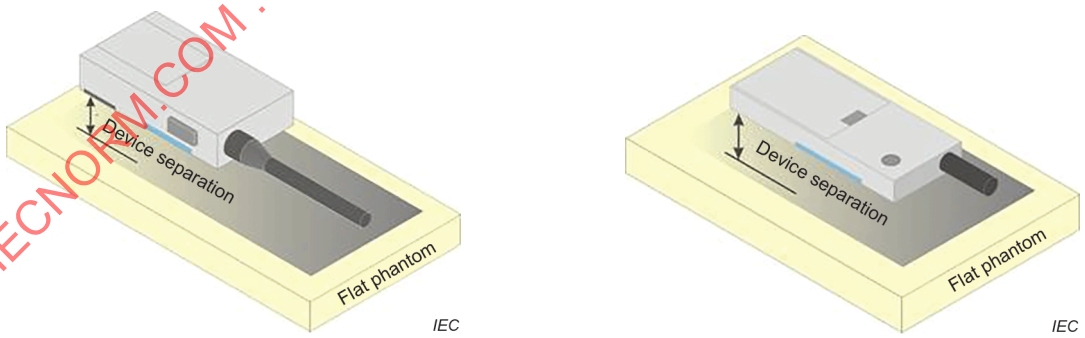
A typical example of a front-of-face device is a two-way radio that is held at a close distance from the face of the user while transmitting. Other devices that fall into this category include wireless-enabled still cameras and video cameras capable of sending data to a network or other device (Figure 10 a)).

To assess this type of device, the following apply:

- The DUT shall be positioned at a test separation distance to the phantom surface in accordance with the conditions of 7.2.4.1.2.
- For a device with intended use that requires contact with the user's face (e.g. device with an optical viewfinder), such a device shall be placed directly against the phantom (Figure 10 a), right side).



a) Still cameras and video cameras



b) Two-way radios

Figure 10 – Test positions for front-of-face devices

IECNORM.COM : Click to view the full PDF of IEC/IEEE 62209-1528:2020

7.2.4.1.10 Hand-held usage of the device, not at the head or torso

When SAR measurement is necessary for hand-held devices that do not transmit while at the head or torso, a flat phantom may be used. To assess this type of device, the device shall be placed directly against the flat phantom as shown in Figure 11, for the sides of the device that are in contact with the hand for the intended use.

NOTE Concerning a measurement phantom representing the hand, there are practical difficulties in specifying a unique hand holding position that is applicable to all devices. Additional studies are needed for devising a representative method for evaluating SAR in the hand of hand-held devices (whether or not they are hand-operated devices). Future versions of this document are intended to contain a test method based on scientific data and rationale.

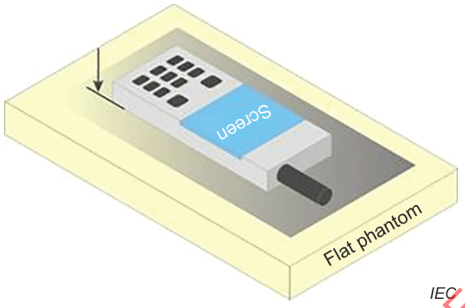


Figure 11 – Test position for hand-held devices, not used at the head or torso

7.2.4.1.11 Limb-worn device

Limb-worn devices are strapped to the arm or leg of the user while transmitting. These are similar to a body-worn device.

To assess this type of device, the following applies.

- The test positions of 7.2.4.1.5 shall be applied.
- The device shall be placed against the phantom such that the measured SAR is a conservative exposure (e.g. by opening or removing the strap as shown in Figure 12, if applicable).
- When the flat phantom or a curved section of the SAM phantom is not applicable, specific phantoms may be considered (e.g. see Annex K and Annex L).

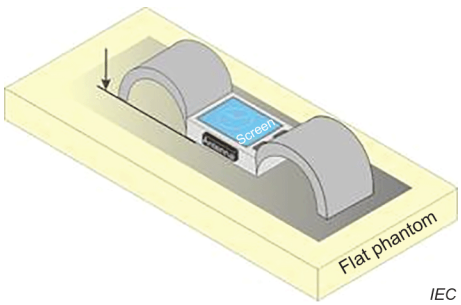


Figure 12 – Test position for limb-worn devices

7.2.4.1.12 Clothing-integrated device

A typical example of a clothing-integrated device is a wireless communication device integrated into a jacket to provide voice communications through an embedded speaker and microphone. This category also includes head-mounted devices with integrated wireless communication devices.

IECNORM.COM : Click to view the full PDF of IEC/IEEE 62209-1528:2020

To assess this type of device, the following applies.

- All wireless or RF transmitting components shall be positioned against the flat phantom (or specific phantoms, see Annex K and Annex L) that correspond to the intended use conditions when they are integrated into the clothing (Figure 13).
- Devices integrated in head-mounted devices may be tested using the SAM phantom (if appropriate) or specific phantoms (6.2.3 or 6.2.5).

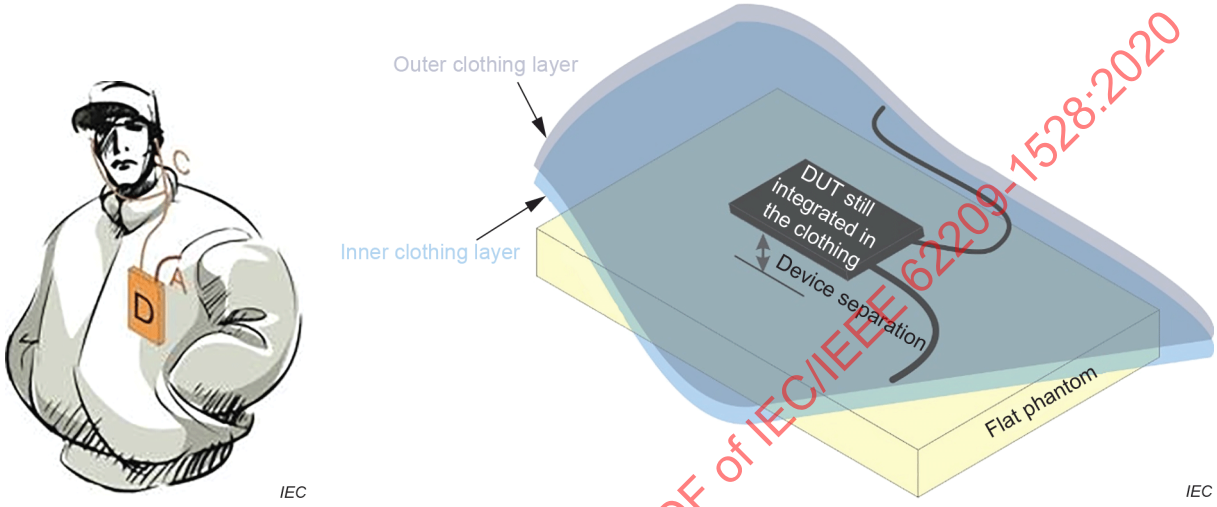


Figure 13 – Test position for clothing-integrated wireless communication devices

7.2.4.1.13 Generic device

A device that cannot be categorized as any of the device types in 7.2.4.1.5 through 7.2.4.1.12 is considered a generic device; i.e. it is represented by a closed box incorporating at least one internal RF transmitter and antenna. The generic device principle may be applied to any device. In situations when a transmitter is added to the host device so that the host and transmitter operate as a single device, the generic category may be considered only if the provisions of 7.2.4.1.5 to 7.2.4.1.12 are not applicable. When the antenna or the attached RF transmitter is external to the host and the positioning of the antenna or attached RF transmitter is independent of positioning of the host (e.g. transmitter or antenna is attached by a cable and 7.2.4.1.6 does not apply), it shall be assessed using the generic device procedures.

The DUT distance hierarchy specified in 7.2.4.1.2 shall be used to assess generic devices.

Testing of all six faces of the DUT (see Figure 14) might not be required; justification shall be provided when omitting testing of some faces. The surface of the generic device pointing towards the flat phantom shall be according to 7.2.4.1.3.

IECNORM.COM : Click to view the full PDF of IEC/IEEE 62209-1528:2020

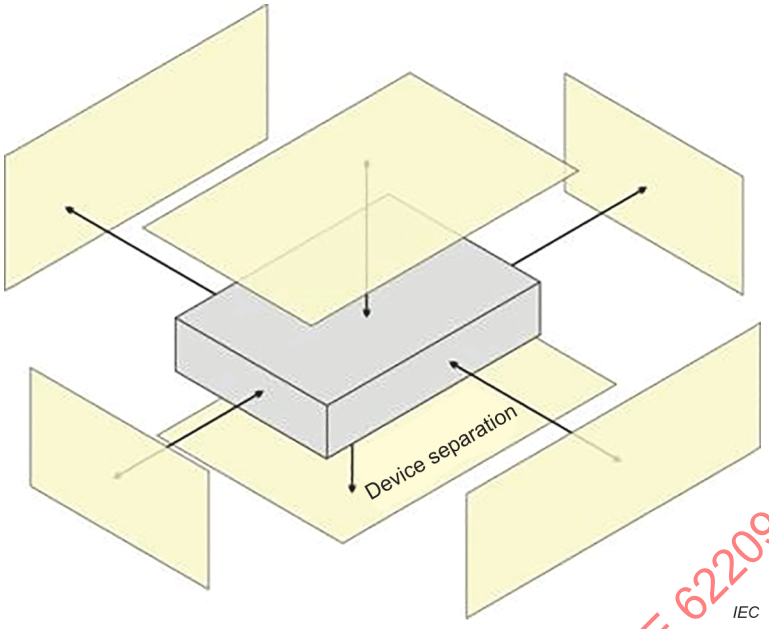


Figure 14 – Possible test positions for a generic device

7.2.4.2 Positioning relative to the head phantom

7.2.4.2.1 General

This document specifies two DUT test positions against the head phantom – the “cheek” position and the “tilt” position. These two test positions are specified in 7.2.4.2.2 and 7.2.4.2.3. The DUT shall be tested in both of these positions, on the left and right sides of the SAM phantom.

In some cases, such as asymmetric DUTs or other form factors, the DUT positioning procedures of 7.2.4.2.2 and 7.2.4.2.3 cannot be used. In these cases, adapted alignment procedures may be applied. The resulting test positions shall replicate the intended use conditions as closely as possible.

Clear details of the actual test positions used, including adapted alignment procedures (where needed), shall be fully documented in the measurement report.

7.2.4.2.2 Definition of the cheek position

The cheek position is established using steps a) to j) as follows.

a) Configure the DUT for voice operation, if necessary. For example, for a DUT with a flip, swivel, or slide cover piece, open the cover if this is consistent with voice operation. If the DUT can also be used with the cover closed, both configurations shall be tested.

b) Define two imaginary lines on the DUT, the vertical centreline and the horizontal line, relative to the DUT in vertical orientation as shown in Figure 15.

c) The vertical centreline passes through two points on the front side of the DUT: the midpoint of the width w_t of the DUT at the level of the acoustic output (Point A in Figure 15), and the midpoint of the width w_b at the bottom of the DUT (Point B). The horizontal line is perpendicular to the vertical centerline, and passes through the centre of the acoustic output (Figure 15). The two lines intersect at Point A. Note that for many DUTs, Point A coincides with the centre of the acoustic output. However, the acoustic output could be located elsewhere on the horizontal line. Also note that the vertical centreline is not necessarily parallel to the front face of the DUT, especially for clamshell DUTs, DUTs with flip cover pieces, and other irregularly shaped DUTs.

IECNORM.COM : Click to view the full PDF of IEC/IEEE 62209-1528:2020

d) Position the DUT close to the surface of the phantom such that Point A is on the (virtual) extension of the line passing through points RE (right-ear ear reference point) and LE (left-ear ear reference point) on the phantom (see Figure 16a) and Figure 16b)). The plane determined by the vertical centreline and the horizontal line of the DUT shall be parallel to the sagittal plane of the phantom.

e) Translate the DUT towards the phantom along the line passing through RE and LE until the DUT touches the ear (see Figure 16c)).

f) Rotate the DUT around the (virtual) LE-RE Line until the DUT vertical centreline is in the reference plane (see Figure 16d)).

g) Rotate the DUT around its vertical centreline until the plane established by the DUT vertical centreline and horizontal line is parallel to the N-F line (see Annex G), and then translate the DUT towards the phantom along the LE-RE line until DUT Point A touches the ear at the ERP (ear reference point) (see Figure 16e)).

h) While keeping Point A on the line passing through RE and LE and maintaining the DUT in contact with the pinna, rotate the DUT about the N-F line until any point on the DUT is in contact with a phantom point below the pinna (cheek) (see Figure 16f)). The physical angles of rotation shall be documented.

i) While keeping DUT Point A in contact with the ERP, rotate the DUT around a line perpendicular to the plane established by the DUT vertical centreline and horizontal line and passing through DUT Point A, until the DUT vertical centreline is in the reference plane (see Figure 16g)).

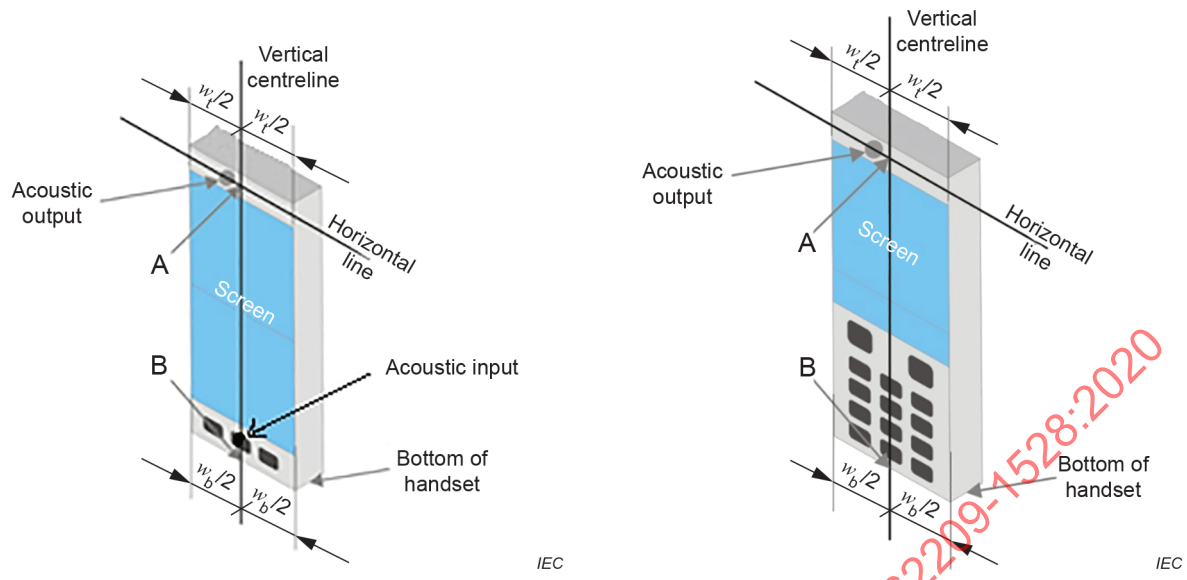
j) Verify that the cheek position is correct as follows:

   1) the N-F line is in the plane established by the DUT vertical centreline and horizontal line;

   2) DUT Point A touches the pinna at the ERP;

   3) the DUT vertical centreline is in the reference plane.

IECNORM.COM : Click to view the full PDF of IEC/IEEE 62209-1528:2020



Key

w_t Width of the DUT at the level of the acoustic output

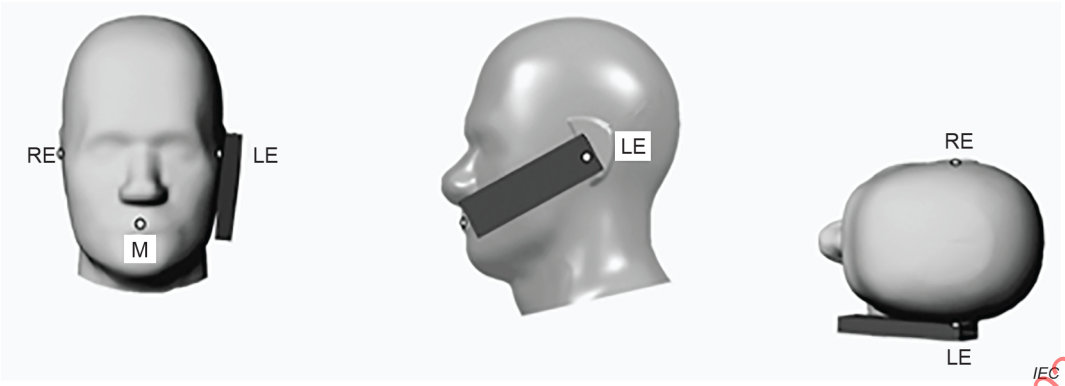
w_b Width of the bottom of the DUT

A Midpoint of the width w_t of the DUT at the level of the acoustic output

B Midpoint of the width w_b of the bottom of the DUT

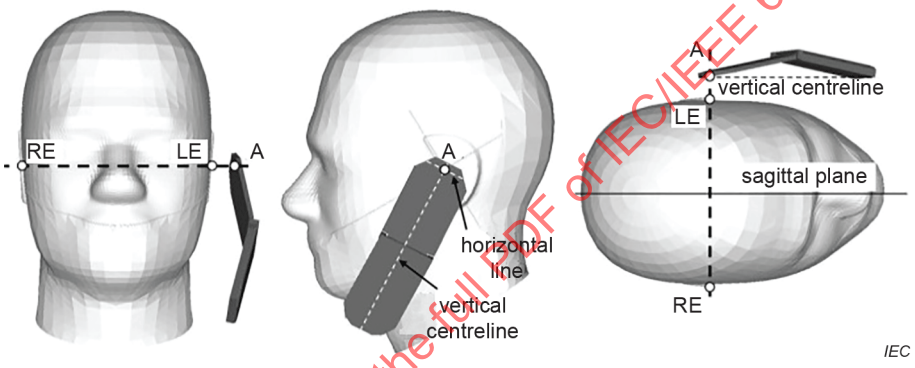
Figure 15 – Vertical and horizontal reference lines and reference points A and B on two example device types: a full touch-screen smart phone (left) and a DUT with a keypad (right)

IECNORM.COM : Click to view the full PDF of IEC/IEEE 62209-1528:2020

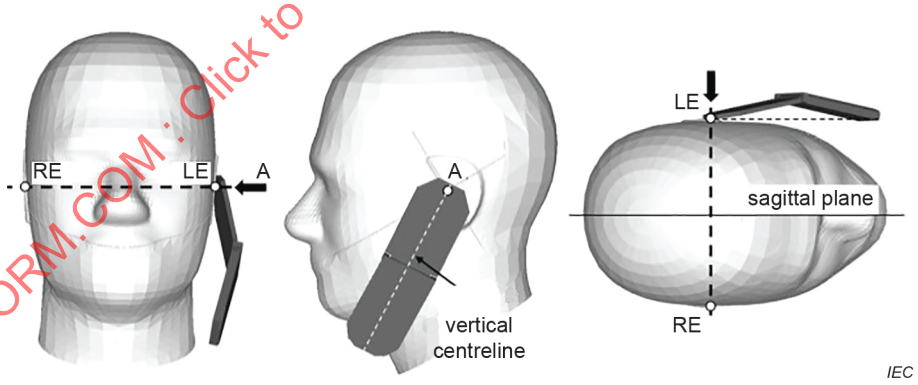


NOTE The reference points for the right-ear ear reference point (RE), left-ear ear reference point (LE), and mouth (M), which establish the reference plane for DUT positioning, are indicated. This device position shall be maintained for the sagittal phantom test set-up shown in Figure G.4.

a) Phone position 1 – cheek position



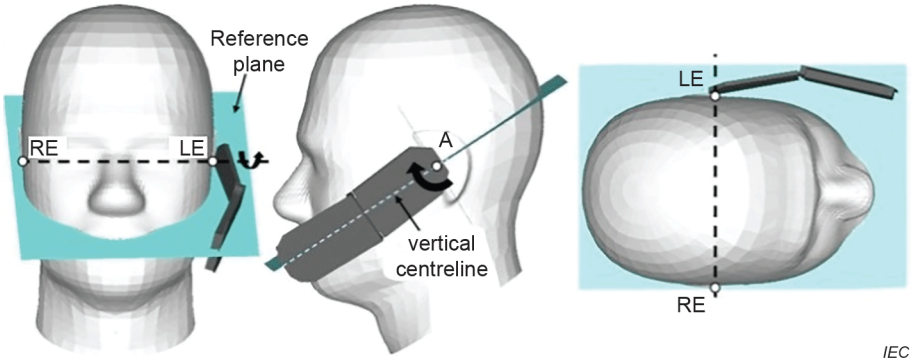
b) One possible DUT position against the head after applying 7.2.4.2.2 c)



NOTE The black arrows show the direction of translation of the DUT for 7.2.4.2.2 d).

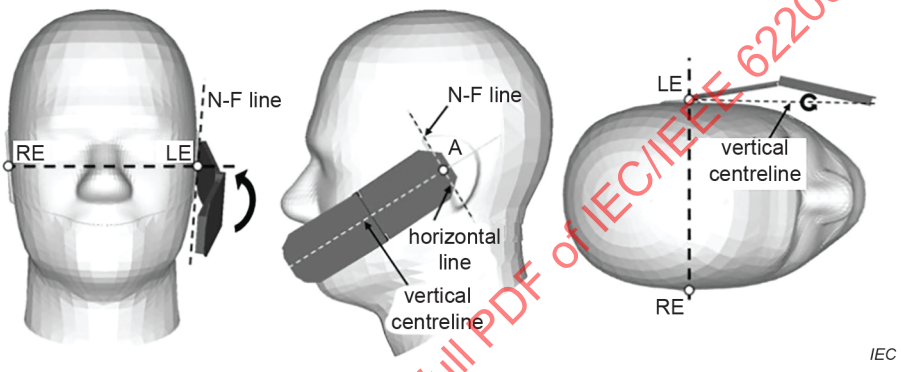
c) DUT position after applying 7.2.4.2.2 d)

IECNORM.COM : Click to view the full PDF of IEC/IEEE 62209-1528:2020



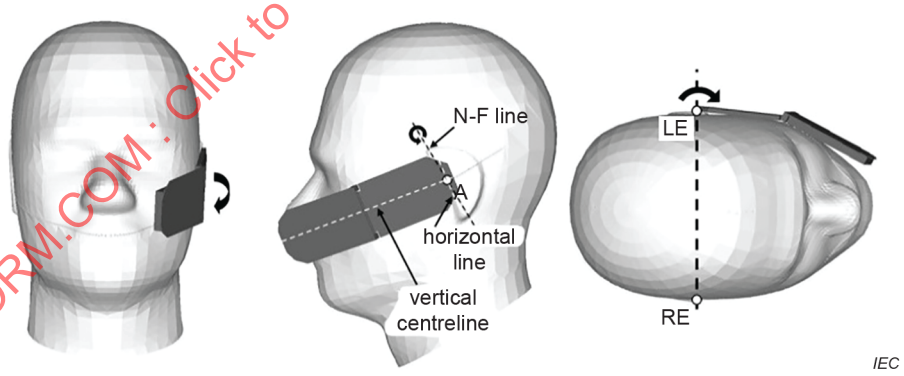
NOTE The curved black arrows show the direction of rotation of the DUT for 7.2.4.2.2 e).

d) DUT position after applying 7.2.4.2.2 e)



NOTE The curved black arrows show the direction of rotation of the DUT for 7.2.4.2.2 f).

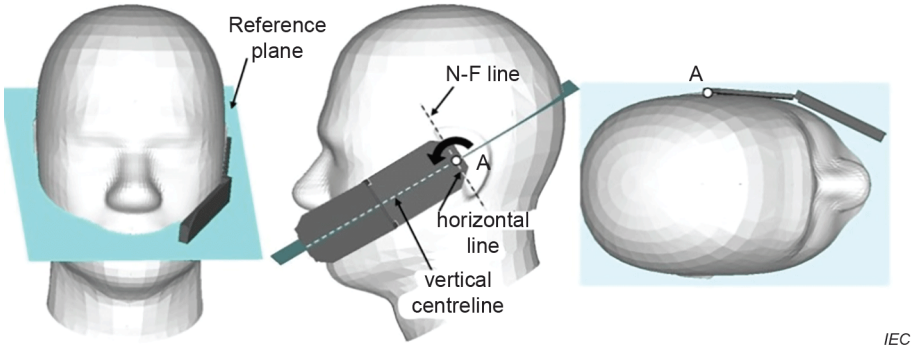
e) DUT position after applying 7.2.4.2.2 f)



NOTE The curved black arrows show the direction of rotation of the DUT for 7.2.4.2.2 g)

f) DUT position after applying 7.2.4.2.2 g)

IECNORM.COM : Click to view the full PDF of IEC/IEEE 62209-1528:2020



NOTE The curved black arrows show the direction of rotation of the DUT for 7.2.4.2.2 h).

g) DUT position after applying 7.2.4.2.2 h)

Figure 16 – Cheek position of the DUT on the left side of SAM where the device position shall be maintained for the phantom test set-up

7.2.4.2.3 Definition of the tilt position

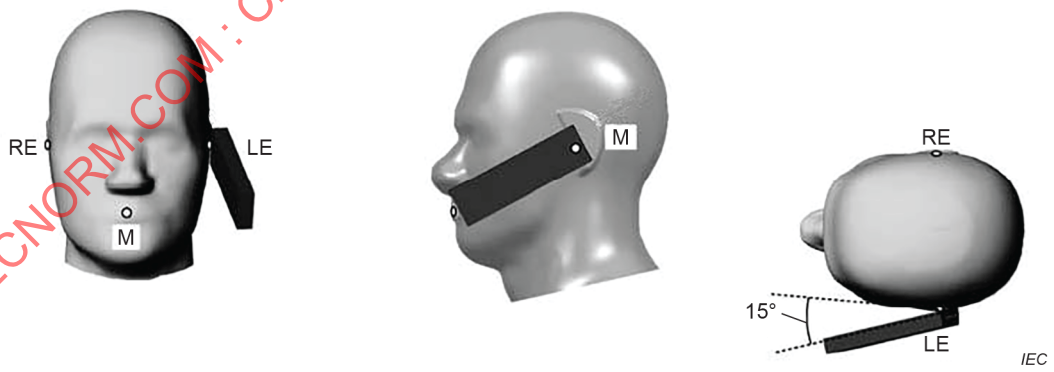
The tilt position is established using steps a) through d) as follows.

a) Repeat steps a) through j) of 7.2.4.2.2 to place the DUT in the cheek position (see Figure 16).

b) While maintaining the orientation of the DUT, move the DUT away from the pinna along the line passing through RE and LE far enough to allow a rotation of the DUT away from the cheek by 15°.

c) Rotate the DUT around the horizontal line by 15° (see Figure 17).

d) While maintaining the orientation of the DUT, move the DUT towards the phantom on a line passing through RE and LE until any part of the DUT touches the ear. The tilt position is obtained when the contact is on the pinna. If the contact is at any location other than the pinna, e.g. an extended antenna in contact with the back of the head phantom, the angle of the DUT shall be reduced. In this case, the tilt position is obtained if any part of the DUT is in contact with the pinna and a second point on the DUT is in contact with the phantom, e.g. the antenna in contact with the back of the head.



Key

M Mouth reference point

LE Left-ear ear reference point

RE Right-ear ear reference point

This device position shall be maintained for the phantom test set-up.

Figure 17 – Tilt position of the DUT on the left side of SAM

IECNORM.COM : Click to view the full PDF of IEC/IEEE 62209-1528:2020

7.2.5 Antenna configurations

For devices that employ one or more external antennas with variable positions (e.g. extended, retracted, or rotated antennas), these shall be positioned in accordance with the user instructions provided by the manufacturer. If no intended antenna position is specified, tests shall be performed with the antenna(s) oriented to obtain the highest exposure condition while maintaining the device in the positions of 7.2.4. For antennas that can be extended, testing shall be performed with the antenna fully extended and fully retracted. The antenna configurations shall be documented in the measurement report. Transmit diversity antennas shall be tested independently for SAR.

7.2.6 Options and accessories

Other accessories that affect the RF output power or RF current distribution of the DUT when used next to a person shall be tested according to the intended use conditions specified by the manufacturer; see 7.2.4.1.5 for next to body positioning and 7.2.4.2 for next to head positioning. For example, a) optional antennas, b) optional battery packs that change the wireless communication device performance or SAR, etc., and c) wires connected during intended use. Low-power NFC or receive-only wireless power transfer accessories generally do not require SAR measurement, but their influence on the SAR of other transmitters shall be considered.

7.2.7 DUTs with alternative form factor

The basic principles identified and specified in 7.2.4 may be applied to devices with similar form factors. Wireless headsets (e.g. connected by Bluetooth) are examples of head-mounted devices that may be evaluated by applying these principles.

The geometry and coordinate mapping system shown in Figure 18 is applicable. Point A, being the acoustic output, is located at the mid-point of the width, and point B, being the primary microphone, is located at the bottom of the device (the end closest to the mouth). Note that for the purpose of applying the positioning procedures, the DUT is considered to be a conventional bar type (rectangular, cuboid) form factor.

Prior to using 7.2.7, consideration shall be made of the available operating modes and the maximum operating power levels, because some devices might not require testing.

All details relating to alternative form factor DUTs shall be fully documented in the measurement report, including diagrams or photographs. Sound engineering practice shall be applied to implement the mapping of an alternate form factor device.

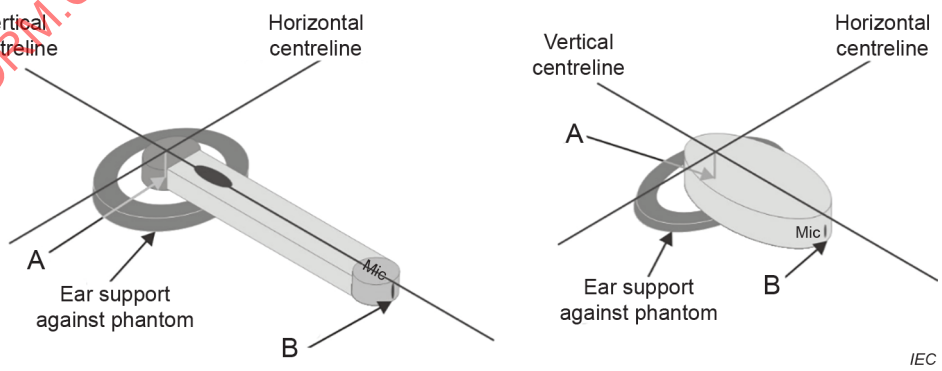


Figure 18 – An alternative form factor DUT with reference points and reference lines

IECNORM.COM : Click to view the full PDF of IEC/IEEE 62209-1528:2020

7.2.8 Test frequencies for DUTs

A DUT shall be compliant with applicable exposure standards at all transmitting frequencies. However, testing at every channel is impractical and unnecessary. The purpose of 7.2.8 is to define a practical subset of channels where SAR measurements are to be performed. This subset of channels is chosen to give a characterization of a DUT for comparison with applicable exposure standards.

Before performing testing using the specific channels required by this document, the maximum output power of the channels shall be verified to determine that the selected channels are producing the highest rated output of the device. The process used to establish the channels for testing purposes shall be documented in the measurement report.

For each operating mode of a wireless technology used by the DUT:

a) tests shall be performed at the channel producing the highest rated output power;

b) when the width of the transmit frequency band ($\Delta f = f_{high} - f_{low}$) exceeds 1 % of its centre frequency f_c, the channels at the lowest and highest frequencies of the transmit band shall also be tested;

c) when the width of the transmit frequency band exceeds 10 % of its centre frequency, Formula (4) shall be used to determine the number of channels, N_c, to be tested:

$$N_c = 2 \times \text{roundup}\left[10 \times \left(f_{high} - f_{low}\right) / f_c\right] + 1 \quad (4)$$

where

f_c is the centre frequency channel of the transmission band in Hz;

f_{high} is the highest frequency channel of the transmission band in Hz;

f_{low} is the lowest frequency channel of the transmission band in Hz;

N_c is the number of channels.

NOTE 1 The function roundup(x) rounds its argument x to the next highest integer. Thus, the number of channels, N_c, will always be an odd number.

NOTE 2 National regulatory agencies might have different requirements on the number of channels to be tested per transmission band, according to frequency allocations and other wireless technology requirements. One example is given in Formula (5):

$$N_c = \text{round}\left[\sqrt{\frac{100\left(f_{high} - f_{low}\right)}{f_c}} \left(\frac{f_c}{100}\right)^{0,2}\right] \quad (5)$$

The number of channels, N_c, should be equally spaced and shall meet the preceding requirements.

Probe calibrations shall be valid for all test frequencies and medium dielectric properties at those frequencies. Multiple probe calibration points and different tissue-equivalent media to cover the entire frequency band can be required for devices with substantially large transmission bands.

7.3 Tests to be performed for DUTs

7.3.1 General

The DUT test procedure encompasses the following two main processes:

– the selection of the test configurations to be measured using the test reduction techniques discussed in 7.9.3 (optional), and

IECNORM.COM : Click to view the full PDF of IEC/IEEE 62209-1528:2020

– the SAR evaluation of these test configurations using the full SAR testing procedure discussed in 7.4.2; optionally, fast SAR testing conforming to the requirements set forth in 7.9.2 may be employed.

In all cases where test reductions (7.9.3) have been applied, the device including accessory combinations that are excluded from SAR measurement and the rationale for test reduction shall be clearly documented in the measurement report.

7.3.2 Basic approach for DUT testing

In order to determine the highest psSAR of a DUT, all required device test positions, configurations and operating modes shall be tested for each frequency band according to the following steps 1 through 3. For devices capable of simultaneous transmission, apply the appropriate procedure specified in 7.4.4; the test process is shown in Figure 19. Application examples are given in Annex N.

For LTE modes, the procedure of 7.9.3.6.3 shall be used, rather than 7.3.2.

Step 1: The measurement procedure specified in 7.4 shall be performed at the channel producing the highest rated output power for each transmit antenna used:

a) for all device test positions (as specified in 7.2.4),

b) for all use configurations for each device position in a), e.g. with device slide or cover open and closed, or antenna extended and retracted, and

c) for all operating modes (see 3.33), for each device position in a) and for each configuration in b), in each frequency band.

Step 2: For the test configuration providing the highest psSAR determined in step 1, and for each test in a), b) and c), perform all tests specified in 7.4 at the other applicable test frequency channels, e.g. lowest and highest channels (7.2.8). In addition, for each device position, configuration, and operating mode where the psSAR value determined in steps 1 a), b), and c) is greater than or equal to half of the applicable SAR limit, testing of all channels of 7.2.8 is required; otherwise it is not required.

Step 3: If the highest psSAR from steps 1 and 2 is larger than the applicable SAR limit reduced by the expanded measurement uncertainty; and if, for this test configuration, the DUT was in direct contact with parts of the device holder having relative permittivity greater than 1,2, this test configuration shall be tested again after mounting the device on a piece of foam, as specified in 6.5 and Figure 3. Both values shall be reported.

Step 4: Examine all data and report the measured psSAR from step 1, step 2, and step 3 according to regulatory requirements.

IECNORM.COM : Click to view the full PDF of IEC/IEEE 62209-1528:2020

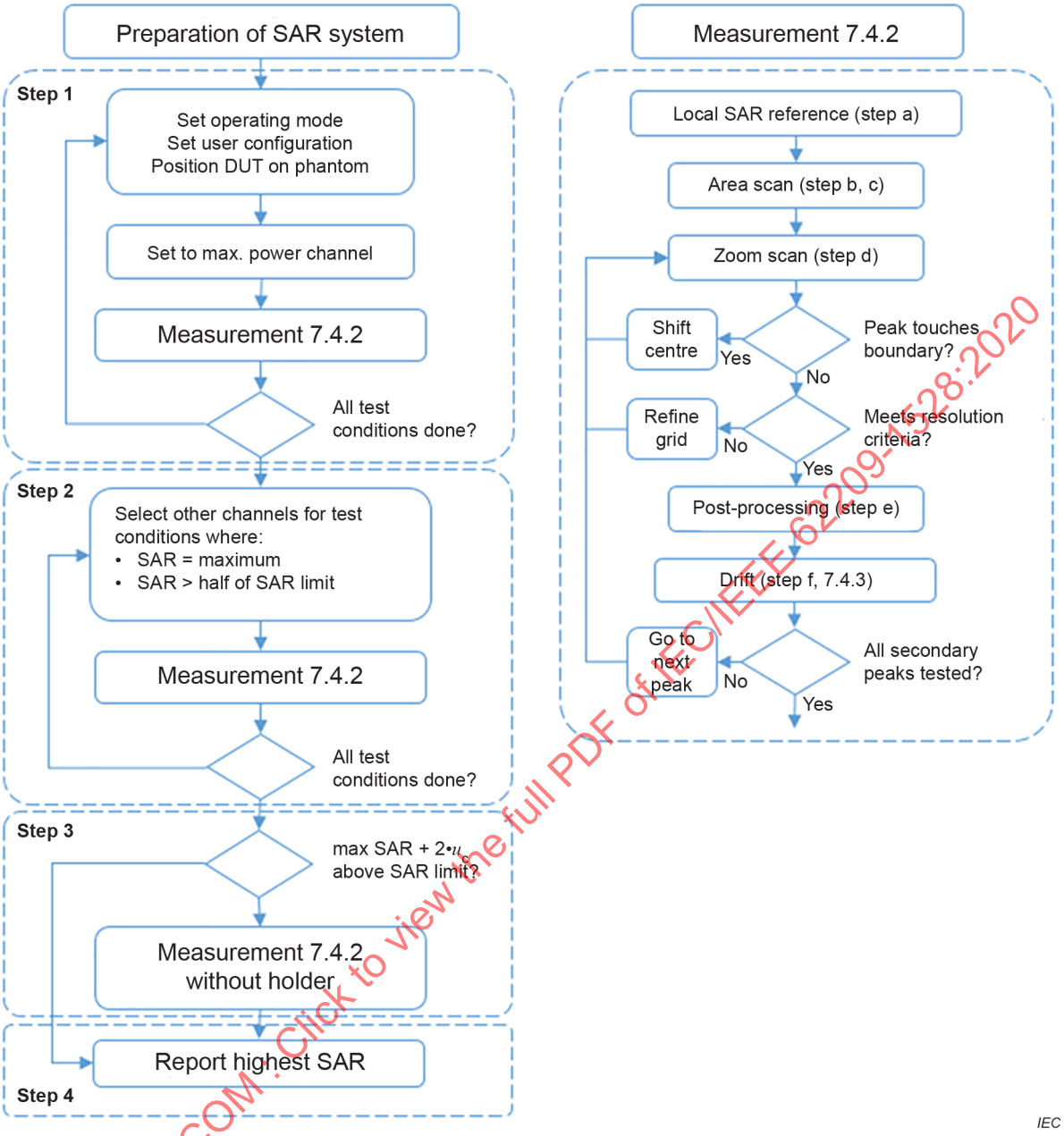


Figure 19 – Block diagram of the tests to be performed

IECNORM.COM : Click to view the full PDF of IEC/IEEE 62209-1528:2020

7.4 Measurement procedure

7.4.1 General

Subclause 7.4 describes the procedure for evaluating the psSAR of the DUT, including the minimum number of drift measurements to be performed. If the drift is high for a particular operating mode and frequency channel, more drift measurements can be necessary, as specified in 7.4.3.

7.4.2 Full SAR testing procedure

The following procedure shall be performed for each test configuration (Figure 19) specified in 7.3. Table 3 provides the measurement parameters used in the area scan, and Table 4 for the zoom scan.

a) Measure the local SAR at a test point within 5 mm of the inner surface of the phantom where the measured local SAR exceeds the lower detection limit of the measurement system. Preferably, the test point will be near the expected peak SAR location, and still within the said distance from the phantom surface. As explained in step f), a comparative measurement shall be made by the system at the same point after completion of the SAR measurement.

b) Measure the two-dimensional SAR distribution within the phantom (i.e. the area scan). Table 3 provides the measurement parameters required for the area scan.

   1) The area over which the SAR measurement is performed shall cover at least an area larger than the projection of the DUT, including its antenna. For some DUTs, the area projected onto the phantom can be relatively large, such that the probe might not reach all points. In this case, rotated phantoms may be used, and the area may be assessed by multiple overlapping area scans. The measurement resolution and spatial resolution for interpolation shall be selected to allow identification of the local peak locations to within one-half of the linear dimension of the corresponding side of the zoom-scan volume.

   2) For the flat phantom, the boundary of the measurement area shall not be closer than 20 mm from the phantom side walls.

c) From the area-scan SAR distribution, identify the position of the maximum SAR value. In addition, identify the positions of any local maxima with SAR values within 2 dB of the maximum value, and that will not be within the zoom scan of other peaks. Additional zoom scans shall be measured for such peaks only when the primary peak is within 2 dB of the SAR compliance limit (e.g. 1 W/kg for 1,6 W/kg 1 g limit, or 1,26 W/kg for 2 W/kg 10 g limit).

d) Measure the three-dimensional SAR distribution at each of the local maxima locations identified in step c) (i.e. the zoom scan).

   1) For frequencies at or below 3 GHz, the following procedure shall be applied (see Table 4).

      i) The minimum size of the zoom scan volume shall be 30 mm by 30 mm by 30 mm.

      ii) The horizontal grid step shall be 8 mm or less.

      iii) The grid step in the vertical direction shall be 5 mm, or less if uniform spacing is used.

      iv) If variable spacing is used in the vertical direction, the maximum spacing between the two closest measured points to the phantom shell (M1 and M2, see Figure 20) shall be 4 mm or less, and the spacing between the farther points shall increase by a factor of 1,5 or less.

      v) For other parameters, see Table 4 and Figure 20.

   2) For frequencies above 3 GHz, the following procedure shall be applied.

      i) the minimum size of the zoom scan volume may be reduced to 22 mm by 22 mm by 22 mm.

      ii) The horizontal grid step shall be $(24/f[\text{GHz}])$ mm or less.

      iii) If uniform spacing in the vertical direction is used, the grid step in the vertical direction shall be $(10/(f[\text{GHz}] - 1))$ mm or less.

      iv) If variable spacing is used in the vertical direction, the maximum spacing between the two measured points closest to the phantom shell shall be $(12/f[\text{GHz}])$ mm or less, and the spacing between farther points shall increase by a factor of 1,5 or less.

      v) For other parameters, see Table 4 and Figure 20.

   3) If the highest SAR 1 g or 10 g cube is touching the boundary of a zoom-scan volume, the entire zoom scan shall be repeated with the new centre located at the maximum psSAR location indicated by the preceding zoom scan measurement. It is also acceptable to expand the zoom scan during measurement until the 1 g or 10 g cube is no longer touching the boundary of the zoom-scan volume.

IECNORM.COM : Click to view the full PDF of IEC/IEEE 62209-1528:2020

4) If the zoom scan measured as specified in the preceding paragraphs complies with both i) and ii), or if the psSAR is below 0,1 W/kg, no additional measurements are needed.

   i) The smallest horizontal distance from the local SAR peaks to all points 3 dB below the SAR peak shall be larger than the horizontal grid steps in both x- and y-directions (Δx, Δy). This shall be checked for the measured zoom scan plane conformal to the phantom at the distance z_{M1}. The minimum distance shall be recorded in the SAR test report.

   ii) The ratio of the SAR at the second measured point (M2) to the SAR at the closest measured point (M1) at the x-y location of the measured maximum SAR value shall be at least 30 % (Figure 20). This ratio (in %) shall be recorded in the SAR test report.

   NOTE 1 The evaluation of the zoom scan is typically done by the post-processor, interpolation and extrapolation, and without reconstruction of the field. More focused induced SAR distributions (e.g. for more localized sources such as capacitively-coupled sources) require a denser grid, such that the same integration and extrapolation algorithms can be used for the same assessment uncertainty.

   NOTE 2 The minimum ratio of 30 % is derived from the plane wave penetration depth at 6 GHz.

5) If one or both of step d) 4) i) and ii) are not met, the zoom scan measurement shall be repeated using a finer resolution while keeping the other zoom scan parameters compatible with Table 4. New horizontal and vertical grid steps shall be determined from the measured SAR distribution so that d) 4) i) and ii) are met. Compliance with d) 4) i) and ii) shall be demonstrated for the new measured zoom scan. The size of the higher-resolution zoom scan and the other parameters of Table 4 shall apply. The closest point to the phantom shell shall be 2 mm or less for graded grids, and the grading factor shall be 1,5 or less.

6) Uncertainties due to field distortion between the media boundary and the dielectric enclosure of the probe should also be minimized, which is achieved if the distance between the phantom surface and physical tip of the probe is larger than the probe tip diameter. Other methods may utilize correction procedures to compensate for boundary effects, which can enable high precision measurements at closer than half the probe tip diameter [22]. For all measurement points, the angle of the probe normal to the phantom surface shall be less than 5° for flat phantoms, and less than 30° for head phantoms. If these angles cannot be achieved, additional uncertainty evaluation is required (see Clause O.3).

e) Use the post-processing (i.e. interpolation and extrapolation) procedures specified in 7.5 to determine psSAR values.

f) Measure the local SAR at exactly the same test point location as in step a). The SAR drift of the DUT may be estimated by the difference between the two measured local SAR values from steps a) and f). See 7.4.3 for more information on addressing SAR measurement drift.

IECNORM.COM : Click to view the full PDF of IEC/IEEE 62209-1528:2020

Table 3 – Area scan parameters

Parameter	DUT transmit frequency being tested	
	$f \leq 3$ GHz	3 GHz < $f \leq 10$ GHz
Maximum distance between the measured points (geometric centre of the sensors) and the inner phantom surface (z_{M1} in Figure 20 in mm)	5 ± 1	$\delta \ln(2)/2 \pm 0{,}5$ [a]
Maximum spacing between adjacent measured points in mm (see O.8.3.1)[b]	20, or half of the corresponding zoom scan length, whichever is smaller	$60/f$, or half of the corresponding zoom scan length, whichever is smaller
Maximum angle between the probe axis and the phantom surface normal (α in Figure 20)[c]	5° (flat phantom only) 30° (other phantoms)	5° (flat phantom only) 20° (other phantoms)
Tolerance in the probe angle	1°	1°

[a] δ is the penetration depth for a plane-wave incident normally on a planar half-space.

[b] See Clause O.8 on how Δx and Δy may be selected for individual area scan requirements.

[c] The probe angle relative to the phantom surface normal is restricted due to the degradation in the measurement accuracy in fields with steep spatial gradients. The measurement accuracy decreases with increasing probe angle and increasing frequency. This is the reason for the tighter probe angle restriction at frequencies above 3 GHz.

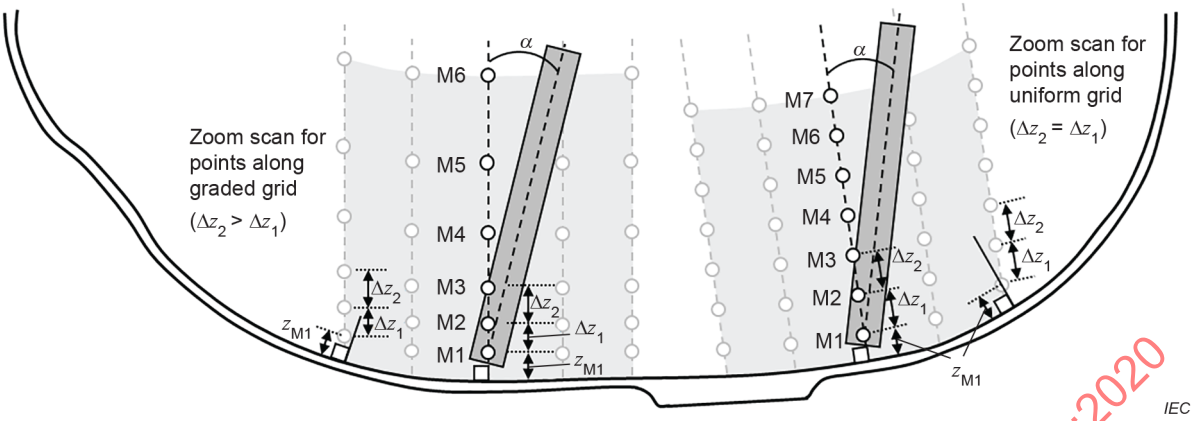
Table 4 – Zoom scan parameters

Parameter	DUT transmit frequency being tested	
	$f \leq 3$ GHz	3 GHz < $f \leq 10$ GHz
Maximum distance between the closest measured points and the phantom surface (z_{M1} in Figure 20 and Table 3, in mm)	5	$\delta \ln(2)/2$ [a]
Maximum angle between the probe axis and the phantom surface normal (α in Figure 20)	5° (flat phantom only) 30° (other phantoms)	5° (flat phantom only) 20° (other phantoms)
Maximum spacing between measured points in the x- and y-directions (Δx and Δy, in mm)	8	$24/f$ [b]
For uniform grids: Maximum spacing between measured points in the direction normal to the phantom shell (Δz_1 in Figure 20, in mm)	5	$10/(f - 1)$
For graded grids: Maximum spacing between the two closest measured points in the direction normal to the phantom shell (Δz_1 in Figure 20, in mm)	4	$12/f$
For graded grids: Maximum incremental increase in the spacing between measured points in the direction normal to the phantom shell ($R_z = \Delta z_2/\Delta z_1$ in Figure 20)	1,5	1,5
Minimum edge length of the zoom scan volume in the x- and y-directions (L_z in O.8.3.2, in mm)	30	22
Minimum edge length of the zoom scan volume in the direction normal to the phantom shell (L_h in O.8.3.2 in mm)	30	22
Tolerance in the probe angle	1°	1°

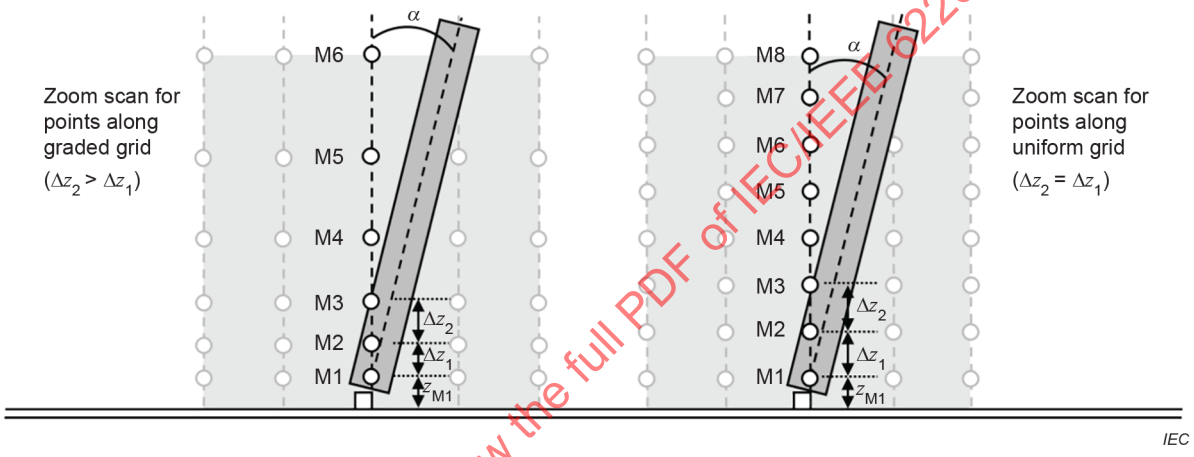
[a] δ is the penetration depth for a plane-wave incident normally on a planar half-space.

[b] This is the maximum spacing allowed, which might not work for all circumstances.

IECNORM.COM : Click to view the full PDF of IEC/IEEE 62209-1528:2020



a) Head phantom



b) Flat phantom

NOTE M1 to M8 are example measurement points used for extrapolation to the surface. The maximum of the angle α between the evaluation axis and the surface normal line is given in Table 3 and Table 4. The distance z_{M1} is from the phantom shell to the first measurement point M1, and its maximum value is given in Table 3 and Table 4. The distances Δz_i (i = 1, 2, 3, …) are the distances from measurement points M_i to M_{i+1}. For uniform grids, all Δz_i are equal. For graded grids, $\Delta z_{i+1} > \Delta z_i$. The term $R_z = \Delta z_{i+1}/\Delta z_i$ is a ratio with a maximum value given in Table 4. The z-direction corresponds to the vertical direction, the x-direction is horizontal and the y-direction is horizontal into the page.

Figure 20 – Orientation of the probe with respect to the line normal to the phantom surface, for head and flat phantoms, shown at two different locations

IECNORM.COM : Click to view the full PDF of IEC/IEEE 62209-1528:2020

7.4.3 Drift

a) The SAR measurement drift of the DUT is accounted for by the first and last step of the measurement process specified in 7.4.2 by using the following two methods.

1) As the preferred method, local SAR measurements are made by the SAR measurement system prior to performing the area scan. A second measurement is made by the system at the same point after completion of the SAR measurement. The measurement is done within the tissue-equivalent medium at a reference point where the SAR values for the first and second measurements shall exceed the lower detection limit of the measurement system. The distance from the reference point to the inner phantom surface, in the normal direction from the inner phantom surface, shall be less than or equal to 5 mm.

2) Alternatively, and if the preferred method in a) is not sensitive enough, conducted power measurements may be made on the device at the antenna port using equipment capable of measuring RF power, prior to device placement for SAR test. A second RF power measurement shall be made after the SAR test has completed.

b) For either of case a) 1) or a) 2), the drift is recorded as the percentage difference of the second reference measurement, $Ref_{\text{secondary}}$ (SAR or conducted power), from the first reference measurement, Ref_{primary}, as described in Formula (6):

$$drift = 100\ \% \times \frac{Ref_{\text{secondary}} - Ref_{\text{primary}}}{Ref_{\text{primary}}} \tag{6}$$

The SAR drift during the measurement of the wireless device shall be within ±5 %. Some devices could have significant fluctuations in output power that are a characteristic of the normal operating behaviour of the device, and therefore are not classified as undesirable power drift. In this case, other methods such as SAR scaling shall be considered to ensure that an accurate and conservative exposure is obtained.

c) When the SAR drift cannot meet the 5 % threshold while performing the SAR testing in accordance with 7.4.2, a drift measurement for the longest intended measurement evaluation time shall be performed without recharging the battery. This is done by performing a measurement in accordance with a) 1) or a) 2) continuously over the evaluation time (at least once every 5 s). This time sweep measurement shall be performed at each frequency band for the operating mode having the highest time-averaged output power. When the difference between the maximum and minimum in the time sweep is less than 5 % of the average value, or when the difference is less than 10 % and the SAR primarily decreases during the time sweep (it does not increase by more than 2 % at any time during the time sweep), it is sufficient to perform reference measurements at the beginning of the area scan and at end of the last zoom scan, as specified in 7.4.2 a) and f). Otherwise, additional reference measurements shall be taken during the zoom scan, and the zoom scan measurements shall be corrected prior to performing extrapolation, integration, and averaging.

d) Linear interpolation between the reference measurements is performed prior to the correction. The SAR values measured during the zoom scan shall be corrected by the difference between the interpolated values and the first reference value measured before the area scan. The time between reference measurements during the zoom scan shall be sufficiently small such that correction of the time sweep curve specified in the preceding paragraph is conservative for all points.

e) When the SAR drift is within 5 %, it can be treated either as an uncertainty (i.e. random error) or a systematic offset. When the drift is larger than 5 %, the measurement drift shall be considered a systematic offset rather than an uncertainty. If treated as an uncertainty, the absolute value of the drift is recorded in the uncertainty table; also, the drift is not added to the assessed SAR value. The uncertainty value reported in the uncertainty budget shall either be the value corresponding to the highest SAR measurement drift reported, or the maximum allowed (i.e. 5 %). If treated as a systematic offset, apply compensation to the measured SAR; i.e. add the absolute difference to the determined SAR value if the drift is either negative or positive, as described in Formula (7):

$$SAR_{\text{compensated}} = SAR_{\text{measured}} \times \left(1 + \left|drift\right| / 100\ \%\right) \tag{7}$$

In this case, it is not necessary to record the drift in the uncertainty budget (i.e. u_i = 0 %). To maintain a conservative exposure, drifts are not subtracted from the assessed SAR. If different assessed operating modes of the device exhibit different drift ratios, all the corresponding measured SAR values can be compensated by the same ratio, provided that the applied drift ratio is the largest one detected during the SAR testing over all operating modes of the device. The uncertainty shall be estimated assuming a rectangular probability distribution

IECNORM.COM : Click to view the full PDF of IEC/IEEE 62209-1528:2020

7.4.4 SAR measurements of DUTs with multiple antennas or multiple transmitters

7.4.4.1 General

DUTs with multiple antennas or multiple transmitters (with single or multiple antennas) transmitting simultaneously require special test considerations. The methods to combine the fields in order to determine the combined SAR distribution differ depending on whether the corresponding RF transmitters emit waveforms that are correlated or uncorrelated in time. The field summation method and the associated measurement instrumentation requirements for correlated signal waveforms are different from those for uncorrelated signals (see IEC TR 62630 [1]).

A procedure that is suitable for assessing the SAR in the head from a wired personal hands-free headset is described in Annex M.

7.4.4.2 SAR measurements for non-correlated signals

7.4.4.2.1 General

The following procedures are applicable to devices incorporating multiple operating modes that are intended to operate simultaneously.

a) For multiple frequencies (f_1, f_2, etc.) that are separated by more than the valid frequency range of the probe calibration or the tissue-equivalent medium, whichever is the smallest, the SAR cannot normally be assessed simultaneously using the same probe and medium. The valid frequency range of probe calibration is typically narrow (e.g. ±50 MHz to ±100 MHz) for electric field probes in most systems currently in use. Also, because electric field probes used in present systems typically have a DC voltage at the output, the probe cannot distinguish between signals at different frequencies. The valid frequency range of the tissue-equivalent medium refers to the frequency range over which the dielectric properties are within tolerance of the target values (see Table 2 and [2]). Due to these limitations, the SAR values shall first be assessed separately, then combined arithmetically.

b) In the case of multiple antennas transmitting different operating modes at the same frequency, measurements can be made with both signals transmitting simultaneously. However, this is not necessary when the psSAR is measured separately for each operating mode then summed as specified in Alternative 1 (see 7.4.4.2.2), because that method provides a conservative exposure for the combined SAR. For the case of multiple antennas transmitting correlated signals (e.g. certain MIMO configurations), see 7.4.4.3.

c) In 7.4.4.2, a test combination is designated as a particular combination of device positions (left cheek, right tilt, etc.), device configurations (e.g. antenna position), and device accessories (battery). Subclauses 7.4.4.2.2 through 7.4.4.2.5 specify alternative evaluation procedures for simultaneous transmission in different frequency bands. The procedures also apply to simultaneous transmission in the same frequency band, when required by device test set-up conditions or test mode software configurations. The following prerequisites apply for the alternative methods.

   1) The area scan, zoom scan and psSAR are evaluated separately at each frequency (in accordance with 7.4.2) with the transmission at that frequency turned on, and transmission at the other frequencies turned off.

   2) The SAR data from different frequencies or antennas are combined only when the test combination is the same for those frequency bands or antennas, and the test combination is intended for simultaneous operation.

d) Different alternative methods may be used for different test combinations. The alternatives are summarized as follows:

   1) Alternative 1: Summation of psSAR values – simplest, but most conservative method to find an upper bound; always applicable (7.4.4.2.2).

   2) Alternative 2: Selection of the highest assessed psSAR value – simple method; applicable when SAR distributions have little to no overlap (7.4.4.2.3).

IECNORM.COM : Click to view the full PDF of IEC/IEEE 62209-1528:2020

3) Alternative 3: Calculation of combined volumetric SAR from existing area and/or zoom scans – accurate and fast method; always applicable (7.4.4.2.4).

4) Alternative 4: Volumetric scanning – most accurate method; always applicable (7.4.4.2.5).

e) The DUT measurement is deemed to fully comply with the requirements of this document when it meets the requirements of one of these alternative evaluation procedures.

f) The uncertainty according to Clause 8 shall be assessed, and documented in the measurement report.

Alternative 1 is the most conservative and computationally simple, and it requires no additional SAR measurement. Alternatives 2 and 3 successively reduce the degree of over-estimation; however, they require greater computation and test analysis. Alternative 4 provides the least overestimation, and requires the most effort.

7.4.4.2.2 Alternative 1: Evaluation by summation of psSAR values

This procedure is applied to determine an upper bound for the combined SAR in a conservative manner when the same maximum output power of each transmitter or antenna is used for both standalone and simultaneous transmission. Note that the different psSAR values being summed can be at different spatial locations. This procedure is always applicable, and note that it will overestimate the combined SAR. The following procedures shall be applied using full SAR testing that complies with all of the normative requirements of this document. Fast SAR testing may be used to identify the highest SAR test configurations for each frequency band, as specified in 7.9.2.

a) For a test combination where simultaneous operation is intended, add the psSAR values for each antenna and frequency band where simultaneous operation is intended (see NOTE 1, NOTE 2, and NOTE 3).

b) Check if the maximum summed SAR value is within 3 dB of the applicable SAR limit. If so, ensure that all the required test frequency channels in 7.2.8 have been measured in all frequency bands and for all antennas at which simultaneous operation is intended. Repeat steps a) and b) to determine simultaneous transmission psSAR values.

c) The maximum summed SAR value in steps a) and b) is the combined-SAR.

NOTE 1 The SAR value at each frequency band corresponds to the frequency channel tested in that band at which the measured psSAR is the highest. In 7.2.8 the appropriate subset of frequencies to be measured for each frequency band is specified, and procedures for measuring at fewer frequencies than this subset are provided in 7.3. For example, if the SAR has been measured at the lowest, middle, and highest channels in a band, and the highest SAR is at the lowest frequency channel, the psSAR at the lowest frequency channel is used as the SAR value for that frequency band. If only the SAR at the middle frequency channel has been measured, in accordance with the procedures in 7.3, then the psSAR at the middle frequency channel is used as the SAR value for that frequency band.

NOTE 2 An acceptable variation of 7.4.4.2.2 a) is to add the highest psSAR values applicable to all simultaneous transmission combinations, regardless of the test configuration. To do so, the highest psSAR for one frequency band (among all test configurations at that frequency band) is added to the highest psSAR value at the other frequency band (among all test configurations), and so on for the other frequency bands where simultaneous operation is intended. Each of the test combinations that is considered using this method is then evaluated in 7.4.4.2.2 b) and c). This method is more conservative than the method of 7.4.4.2.2 a).

NOTE 3 Having identified the maximum SAR test combination, it is acceptable to perform volumetric scanning on that test combination, according to 7.4.4.2.5, to obtain a more realistic estimate of the maximum combined SAR. The volumetric scan can be used if the test position and device configuration are the same for the different frequency bands or antennas.

IECNORM.COM : Click to view the full PDF of IEC/IEEE 62209-1528:2020

7.4.4.2.3 Alternative 2: Evaluation by selection of highest assessed maximum psSAR values

This procedure gives an estimate of the combined SAR when the separately measured zoom scan SAR distributions have little or no overlap. The maxima are then separated to such an extent that the maximum psSAR value of each distribution will not increase by more than 5 % when the SAR distributions from all the other simultaneous operating modes are added. This alternative is only applicable if the highest psSAR is less than 70 % of the compliance limit, as calculated from the zoom scans at each frequency. This procedure shall be applied using full SAR testing that complies with all normative requirements of this document.

a) Measure the psSAR at each frequency separately according to 7.4.2. The area scans shall be performed in the same plane at each frequency. The distance z_{M1} for all area scans shall be less than or equal to the smallest z_{M1} value specified in Table 4 for the frequencies of interest. The probe tip diameter shall comply with the requirements of 6.1 r) at all of the frequencies of interest, and probe calibration shall comply with the requirements in this document.

b) The separate area scans shall be interpolated such that the overlapping area has the same grid. The resolution of the interpolated grid shall be 1 mm or better. Find the peak value in each of the area scans.

c) The overlapping area shall contain all SAR peaks.

d) For all measured area scans, create a new SAR distribution by adding the interpolated area scans spatially, i.e. point-by-point, within the overlapping area.

e) When the peak value in the new SAR distribution created in step c) does not exceed the highest of the separate maximum peak SAR values found in step b) by more than 5 %, the combined SAR is selected as the highest of the separate psSAR values calculated from the zoom scan, as calculated in step a).

7.4.4.2.4 Alternative 3: Evaluation by calculated volumetric SAR data

This procedure uses existing area scans and zoom scans, in combination with interpolation and extrapolation, for generation of volumetric SAR data, and it is a quick way of obtaining the combined SAR. Different algorithms to accomplish this have been presented in [23], [24], [25], [26], and [27]. The uncertainty of the method used shall be well documented according to the procedures in Clause 8, and shall be recorded. This method is always applicable. This procedure shall be applied using full SAR testing that complies with all of the normative requirements of this document.

a) For a test combination where simultaneous operation is intended, calculate the volumetric SAR distribution over a region corresponding to the area scan for each frequency band where simultaneous operation is intended.

b) Add the volumetric SAR distributions of all frequency bands spatially, using interpolation according to 7.5.1. For each frequency band where simultaneous operation is intended, this step shall be performed for each measured frequency channel, according to the requirements of 7.2.8 and the procedures of 7.3 (see NOTE 1 of 7.4.4.2.2).

c) Use post-processing procedures specified in 7.5 and Annex P to determine the psSAR values from the SAR distributions of step b).

d) Check if the maximum psSAR value is within 3 dB of the compliance limit. If so, ensure that all of the required test frequency channels in 7.2.8 have been measured in all frequency bands at which simultaneous operation is intended, and repeat steps a) to c).

7.4.4.2.5 Alternative 4: Evaluation by volumetric scanning

This procedure is the most accurate way of assessing the combined SAR, and it is always applicable. The SAR data are combined for each test configuration (see 3.52) where simultaneous transmission is intended. This procedure shall be applied using full SAR testing that complies with all of the normative requirements of this document.

IECNORM.COM : Click to view the full PDF of IEC/IEEE 62209-1528:2020

a) For a test combination where simultaneous operation is intended, ensure that the zoom scan has been measured according to 7.4.2 at all test frequency channels specified in 7.2.8, for each frequency band at which simultaneous operation is intended.

b) Determine a volumetric grid that encompasses the zoom scans at the test frequencies determined in step a) over all the frequency bands at which simultaneous operation is intended. If the zoom scans at frequencies f_1, f_2, etc., are so far apart that the volumetric grid is very large, resulting in very long measurement times, an acceptable variation of this is to identify all zoom scan locations for each frequency channel in step a) then apply the alternative procedure in step c).

c) At each frequency channel determined in step a), measure the volumetric grid found in step b). This volumetric grid measurement adheres to all of the requirements of 7.4.2 steps c) and d), except that the volumetric grid is larger than the zoom scan. When it was decided in step b) to use zoom scan locations instead of volumetric grid, at each frequency channel determined in step a), measure the zoom scan for the other frequencies at exactly the same locations as for each previously measured zoom scan in step a). The measurement is performed with the operating mode at that frequency turned on, and the operating modes at the other frequencies turned off.

d) Add the SAR distributions obtained in step c) spatially to obtain a summed SAR distribution. Calculate the maximum combined SAR from the summed distribution, using the post-processing procedures (interpolation, extrapolation, and averaging) specified in 7.5 to determine the psSAR. When volumetric scans are performed for each frequency, these shall be summed, and the maximum peak is determined based on the total distribution. In case only zoom scans are performed in step c), the zoom scans at each peak location in each frequency band are combined, and the highest one is identified to compute psSAR.

The DUT should be fixed on the phantom when the equivalent media are changed so that the summation of the SAR distributions is as accurate as possible. If the battery of the device needs to be recharged, the charger cable shall be attached to the DUT while it remains positioned on the phantom. The cable shall only be attached when the battery is being charged between SAR measurements, and shall be detached during testing.

7.4.4.2.6 Example calculation of the combined SAR using Alternative 1

Subclause 7.4.4.2.6 describes an example of the application of the summation of psSAR values method (Alternative 1). It is for illustrative purposes only. Table 5 shows an example of a DUT having two antennas and four operating modes, where 10 g psSAR values from single-band measurements are shown in the third column and third row for the four operating modes and antennas. The SAR values are shown in the third row for Antenna 1, and in the third column for Antenna 2. The cells to the bottom and right of these values show the combined SAR values. In this example, the cells that are not marked with "–" will be the only ones to be evaluated. The four operating modes consist of two voice modes and two data modes, each in two frequency bands. The 10 g psSAR values have all been measured at the centre channel of the respective frequency bands for single-band operation (one operating mode and antenna is transmitting, while the other band and antenna are switched off). The combined SAR values are computed using Alternative 1 (i.e. simple summation of the 10 g psSAR values in row 3 and column 3). For this example, the DUT supports only one voice mode at a time, and one data mode at a time, and it supports simultaneous transmission of voice and data. Therefore, a voice mode is not combined with another voice mode, for example. Also, SAR measurements on the left side of the head are not combined with SAR measurements on the right side. However, it is intended for this example that the two antennas could transmit simultaneously.

IECNORM.COM : Click to view the full PDF of IEC/IEEE 62209-1528:2020

Table 5 – Example method to determine the combined SAR value using Alternative 1

Antenna 2			Antenna 1							
			Voice Band 1		Voice Band 2		Data Band 1		Data Band 2	
			Left	Right	Left	Right	Left	Right	Left	Right
			0,285	0,250	0,333	0,315	0,512	0,489	0,593	0,574
Voice Band 1	Left	0,141	–	–	–	–	0,653	–	0,734	–
	Right	0,120	–	–	–	–	–	0,609	–	0,694
Voice Band 2	Left	0,131	–	–	–	–	0,643		0,724	–
	Right	0,130	–	–	–	–	–	0,619	–	0,704
Data Band 1	Left	0,220	0,505	–	0,553	–	–	–	–	–
	Right	0,213	–	0,463	–	0,528	–	–	–	–
Data Band 2	Left	0,225	0,510	–	0,558	–	–	–	–	–
	Right	0,216	–	0,466	–	0,531	–	–	–	–

7.4.4.3 SAR measurements for correlated signals

DUTs with multiple antennas transmitting correlated signals simultaneously represent a particular case of devices, such as MIMO transmitters with digital beam-forming capabilities, and require special test considerations. Signals of such DUTs can be classified based on the change of relative phases in a typical communication session. In general, there are two types of signals that can be found in most recent generation multi-antenna transmitters.

The first are signals with relative phases unchanged for a relatively long duration compared with symbol duration; these are denoted as Type 1 signals for the purposes of this document. Type 1 signals are used in phased array antenna systems, where the relative phases of signals fed to the antennas are controlled to form the radiation pattern of the array antenna toward a specific direction. In different operating environments, the relative phases can be changed to obtain different desired radiation patterns. As soon as the transmitting direction is determined and the pattern is formed, the relative phases will be fixed for a specific duration, and will only change when the radiation pattern is configured to another form. The duration that the relative phases are kept unchanged is usually relatively long compared with the duration of a symbol in typical communication sessions.

On the other hand, the second type of signals are those with relative phases that vary quickly over a relatively short period; these are denoted as Type 2 signals for the purposes of this document. Type 2 signals can be found in systems utilizing MIMO techniques. The relative phases of the signals will be changed from symbol to symbol, using the function of space-time block coding (STBC) in MIMO schemes. The relative phases of signals are changed from symbol to symbol according to the STBC, but beam-forming is not used during typical communication sessions.

IECNORM.COM : Click to view the full PDF of IEC/IEEE 62209-1528:2020

As explained in IEC TR 62630 [1], correlated signals are those that can only be transmitted at the same carrier frequency, and SAR depends on the relative phase(s) between the signals. Therefore the psSAR cannot be precisely evaluated using scalar E-field probes from a single measurement with the multiple transmitters set to fixed relative phase conditions if those phases are subject to change during the normal operations of the device. Instead, for precise SAR evaluation, repeated measurements corresponding to all phase combinations between the transmitters are needed. This is a rather time consuming evaluation, and might not be practical unless SAR systems that enable fast SAR testing are used, combined with software control of the DUT to cycle through all possible phase combinations of the signals transmitted simultaneously at their highest time-averaged output powers. In general, it is also possible to accurately evaluate psSAR of each individual transmitter transmitting separately at the highest time-averaged output power using single SAR measurements; however this approach requires complex vector E-field measurements (i.e. measurements of magnitude and phase of all three E-field components), and is therefore less practical.

The alternative method utilizing conventional SAR systems is based on SAR measurements for each transmitter transmitting separately at the highest time-averaged output power, then combining the individual SAR results as described in IEC TR 62630 [1]. This approach leads to much faster SAR measurement times, but provides only an upper bound of the SAR, thus potentially overestimating the results. IEC TR 62630 [1] describes two methods of combining the SAR from individual measurements using conventional scalar E-field probes.

The two methods described in IEC TR 62630 [1] can be implemented using conventional SAR measurement systems, and require only a limited number of SAR scans equal to the number of transmitters. The first method is based on combining the magnitudes of the E-field values, and the second is based on magnitudes of the individual E-field components. Especially for the Type 1 signals or unspecified signals, the second approach based on combining the individual E-field components should be used, because it leads to lower potential SAR overestimation, and many available SAR systems readily provide the required input data for the post-processing described in [1]. The measurement procedure for the two types of correlated signals is described in Figure 21. For Type 2 signals, the approach of time-averaged SAR measurements (see NOTE) should be used, which requires only use of the measurement procedure specified in 7.4, with conventional scalar probes.

NOTE Another method is to measure time-averaged SAR in a specific averaging period using conventional scalar SAR measurement systems. This method can only be applicable to the devices generating Type 2 correlated signals. A signal property is assumed such that the combination of relative phases that produces the maximum SAR occurs only infrequently, and when it does occur it is in a very short time before being dominated by other phase combinations that produce lower SAR. Because SAR is determined by electromagnetic (EM) energy absorbed in the exposed tissue-equivalent medium, introducing time-averaging procedure is suitable for the evaluation of SAR with such rapidly fluctuating EM fields. To evaluate the time-averaged SAR from such devices, all transmitting antennas are turned on as they are during normal communications at the same time, and instantaneous SAR values are measured at each measurement point within a sampling-time interval, then averaged over a time-duration appropriate for capturing the signal characteristics.

This method has the benefit of using conventional scalar SAR probes, and furthermore, provides measured SAR that is close to actual SAR. Also the method requires only a single time-averaging measurement at each measurement point in accordance with the procedure of 7.4, regardless of the number of transmitting antennas. The averaging time for a multi-antenna system, however, is longer than that for conventional single-transmitting antenna measurements. Also, when the number of antennas increases, the averaging time would be slightly longer to obtain converged SAR results, because the time-fluctuation of the instantaneous SAR increases along with the increase in the number of antennas. The averaging time also depends on the probe sampling rates of the SAR measurement systems. The averaging time is reduced as the sampling rate is increased, and vice versa. For example, with a SAR measurement system having a measurement rate of 1 250 samples per second, the averaging time of 1 s provides a standard deviation of the instantaneous SAR values due to multiple transmitting antennas that is kept under 2 %. In such a case, total measurement uncertainty evaluated by using typical values and the uncertainty budget in Clause 8, the uncertainty for multiple transmitting antennas results is of the same level compared with that of single antenna cases (typically at 8,7 %).

IECNORM.COM : Click to view the full PDF of IEC/IEEE 62209-1528:2020

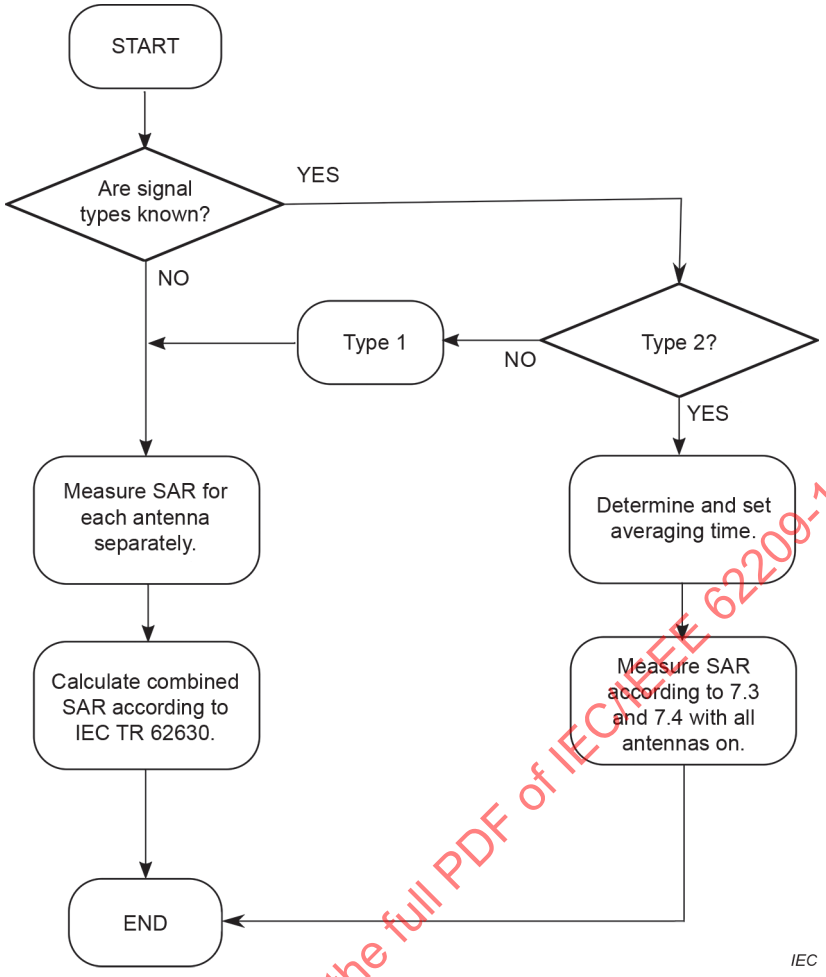


Figure 21 – Measurement procedure for different types of correlated signals

7.5 Post-processing of SAR measurement data

7.5.1 Interpolation

The resolution of the measurement grid is not as fine as what is required by the interpolation requirements for the area and zoom scan to compute the psSAR. Interpolation shall be applied to the measurement points. Examples of interpolation schemes are given in Annex P.

7.5.2 Extrapolation

The electric field probes used to measure SAR usually contain three orthogonal dipoles in close proximity and embedded in a protective cover/case. The measurement (calibration) point is situated a few millimetres from the tip of the probe and this offset shall be taken into account when identifying the position of the measured SAR. Because of probe boundary effect errors and probe sensor offset, SAR is not measured at the surface of the phantom. The measured points closest to the surface are extrapolated to estimate the highest SAR at the phantom surface. Examples of extrapolation schemes are given in Annex P.

7.5.3 Definition of the averaging volume

The averaging volume shall be in the shape of a cube with side dimension that establishes a 1 g or 10 g mass. The side length of the 1 g cube shall be 10 mm, and the side length of the 10 g cube shall be 21,5 mm. The orientation of the cubical volume is given in Annex P.

IECNORM.COM : Click to view the full PDF of IEC/IEEE 62209-1528:2020

7.5.4 Searching for the maxima

The cubical averaging volume shall be shifted throughout the interpolated and extrapolated zoom-scan volume at the inner surface of the phantom in the vicinity of the local maximum SAR, using considerations such as those given in Annex P. The cube with the highest psSAR shall not be at the edge/perimeter of the zoom-scan volume. In case it is, the zoom-scan volume shall be shifted and the measurements shall be repeated.

7.6 Time-period averaged SAR considerations

7.6.1 General

Subclause 7.6 specifies the test procedures for assessing the time-period averaged SAR (TPAS) when the DUT uses time-period power control. The applicable time-averaging period is specified in international guidelines (e.g. ICNIRP) or national regulations. This test procedure differs from the general SAR test procedures specified in 7.4 that are applicable for DUTs that do not have power control algorithms. The rationale for assessment of TPAS is given in Annex Q.

NOTE Some national SAR regulations might have varying definitions of time averaging requirements for their SAR limit.

A procedure and its requirements for assessing the TPAS are provided in 7.6.3 to 7.6.7. The procedure may be applied if the following requirements are met.

a) The power control algorithms in the DUT shall not be alterable or accessible by the user.

b) The DUT manufacturer shall provide sufficient documentation about the power control algorithms and their implementation such that the measurements result in a conservative exposure.

If the preceding requirements are not met, the SAR shall be assessed at the maximum output power level as described in 7.4.

Alternative procedures to 7.6.2 to 7.6.7 may be applied if justified and documented.

7.6.2 RF conducted power

RF conducted power measurements may be used to determine TX factors.

The power detection, integration time, and sample averaging settings of the power meter ensure that the uncertainty component for TPAS is within the assessed value in 7.6.8. Conducted power measurements shall also be accurate for the respective operating mode. Linear (e.g. milliwatt) readings shall be used.

7.6.3 Time-period averaged SAR measurement settings for SAR measurement methods

7.6.3.1 General

Subclause 7.6.3 provides requirements for TPAS measurement, and for calculation of the TX factor for periods up to six minutes.

7.6.3.2 Array SAR systems

For Class 2 fast SAR testing (see 7.9.2), the measurement of $SAR_{\text{time-average}}$ shall be performed over the averaging period, and the measurement of $SAR_{\text{full-power}}$ shall be performed over a time period long enough that the measurement is stable. Neither the DUT nor the sensors shall be moved during the averaging period. The sampling rate of the measurement shall be enough to ensure that the uncertainty component for TPAS is within the assessed value in 7.6.8.

IECNORM.COM : Click to view the full PDF of IEC/IEEE 62209-1528:2020

7.6.3.3 Scanning SAR systems

For scanning probe SAR systems, including single probe SAR systems and Class 1 fast SAR testing systems (see 7.9.2), the following apply.

a) Both $SAR_{\text{full-power}}$ and $SAR_{\text{time-average}}$ are local SAR measurements.

b) The probe shall be positioned at the location of the peak SAR from an area scan performed in accordance with the requirements of 7.4.2.

c) The SAR level at this location shall be above the noise level.

d) The probe or probe array shall be in the same position for both the $SAR_{\text{full-power}}$ and $SAR_{\text{time-average}}$ measurements.

e) $SAR_{\text{time-average}}$ shall be measured over the defined time period.

f) $SAR_{\text{full-power}}$ shall be measured over a time period long enough that the measurement is stable.

g) The sampling rate of the measurement shall be enough to ensure that the uncertainty component for TPAS is within the assessed value in 7.6.8.

7.6.4 Exposure condition and test position considerations

TPAS shall be assessed separately for each frequency band and operating mode, except when it can be demonstrated that the same TX factor can be applied to multiple frequency bands and/or wireless operating modes. Two approaches are considered, depending on whether the device is capable of detecting and distinguishing its usage position reliably (e.g. detecting head and body-worn positions according to audio routing to the earpiece of a device during a voice call).

a) If the different usage positions are not detected and distinguished by the device, the maximum TPAS among all applicable test/use positions and conditions, including all head, body-worn, and other positions, are used to determine compliance. This is the most conservative and simple approach that applies to all use conditions.

b) Otherwise, the SAR test positions may be grouped as follows.

   1) Head test positions: The maximum TPAS among all head test positions (left cheek, left tilt, right cheek, and right tilt), corresponding to voice calls via the earpiece, is used to determine head exposure SAR compliance.

   2) Body-worn and other test positions: The maximum TPAS among all applicable body-worn and other test positions, based on the applicable separation distances for the corresponding use positions, when there is no voice call via the earpiece, is used to determine non-head SAR compliance.

7.6.5 Time-period averaged SAR for simultaneous transmission

Due to the complexity of combining simultaneous transmission with TPAS, the following requirements apply to determine the highest psSAR:

a) the TX factor assessment in 7.6.6 shall be applied to a maximum of one of the simultaneous transmissions;

b) all simultaneous transmissions aside from the one in a) shall be assessed at the maximum output power;

c) the combined SAR of all simultaneous transmitters shall be assessed according to 7.4.4.

7.6.6 TX factor assessment

The TX factor is used to scale the measured SAR at the maximum output power (see 7.6.7) down to the time-period averaged SAR. It is separately applied for each operating mode (e.g. GSM, WCDMA, LTE, 5G NR), and for each applicable frequency band, except when it can be demonstrated that the same TX factor can be applied to multiple frequency bands and/or wireless operating modes.

IECNORM.COM : Click to view the full PDF of IEC/IEEE 62209-1528:2020

The following steps shall be performed to determine TX factors.

a) The power control algorithm shall be initially disabled.

b) The DUT shall be under the control of a radio communication test set (call-box).

c) The radio communication test set shall be set to request maximum TX power and duty factor from the DUT according to wireless technology requirements.

d) When using a SAR measurement system for TX factor assessment, the DUT shall be positioned in accordance with 7.6.4.

e) Measure the conducted power (see 7.6.2) or local SAR. The conducted power or SAR data shall be recorded and documented in the measurement report. This value shall be noted as $P_{\text{full-power}}$ or $SAR_{\text{full-power}}$, respectively for power or SAR measurement.

f) Enable the power control algorithm. Ensure that the DUT position against the phantom is maintained during this step.

g) Measure the conducted power or local SAR over at least the time-averaging period. Record the average conducted power or SAR over the time-averaging period. This value shall be noted as $P_{\text{time-average}}$ or $SAR_{\text{time-average}}$.

h) The TX factor is $P_{\text{time-average}}$ / $P_{\text{full-power}}$ or $SAR_{\text{time-average}}$ / $SAR_{\text{full-power}}$.

7.6.7 SAR measurements

SAR measurement shall be performed for all required test positions and conditions as specified in 7.2.4. The power control algorithms in the DUT shall be disabled during these SAR measurements.

There are two options for performing the SAR measurements.

– Option 1: During the SAR measurements, transmit power shall be at the maximum specified for the DUT (7.2.3.1). The TX factors obtained in step h) of 7.6.6 shall be applied to the maximum full power SAR results obtained, i.e. be multiplied by the TX factor. These calculated TPAS results are compared directly against the applicable SAR limit to determine compliance.

– Option 2: Transmit power shall be limited to the time-period averaged power level $P_{\text{time-average}}$, determined in step h) of 7.6.6, in order that the measured SAR corresponds to the TX factor. When TX factors are determined using local SAR measurement in step h) of 7.6.6, and it is demonstrated that SAR and power are linearly scalable for the wireless configuration used in the DUT (7.2.3.2), the time-period averaged power level $P_{\text{time-average}}$ is determined by scaling the maximum power (7.2.3.1) used to establish the TX factor. These TPAS results are compared directly against the applicable SAR limit to determine compliance.

7.6.8 Uncertainty in TPAS evaluations

The uncertainty related to TPAS calculation shall be assessed according to general guidance given in Clause 8, and documented in the measurement report.

The additional uncertainty related to TPAS assessment is due to the sampling rate of the measurement. The TPAS uncertainty can be neglected depending on method selected to determine the TX factor (i.e. using either 7.6.3 SAR measurements or 7.6.2 conducted power measurements).

The TPAS uncertainty is different from signal modulation uncertainty (MOD) and data acquisition errors (DAE) specified in 8.4.

IECNORM.COM : Click to view the full PDF of IEC/IEEE 62209-1528:2020

If the combined uncertainty of the SAR measurement method and the time-averaged calculation (either SAR based or conducted-power based) exceeds the upper uncertainty limit specified in this document, a scaling factor ($U_{TPAS} - U_{SAR}$) shall be applied to the measurement result, where U_{TPAS} is uncertainty for TPAS assessment, and U_{SAR} is the uncertainty for SAR measurements at full power and maximum duty cycle. The measurement system manufacturer shall be consulted for details of the uncertainty calculation.

7.7 Proximity sensors considerations

7.7.1 General

Proximity sensors are used to reduce the output power of the DUT based on the distance to users and nearby objects. When the device is operating at closer than the triggering distance of the proximity sensor, the maximum output power of a DUT is reduced to ensure SAR compliance. At distances larger than the sensor triggering distance, the proximity sensor is disabled and the maximum output power is restored. Depending on the antenna dimension and its location, a DUT could incorporate one or more proximity sensors to ensure sensor coverage.

The procedure specified in 7.7 only applies to proximity sensors designed to cover a single transmitting antenna. The procedures apply to a single sensor or to multiple sensors where the sensor responses are combined to provide a single unique and unconditional triggering. The procedure is not intended for multiple sensors that trigger more than one antenna. However, the procedure may be applied separately to multiple antennas, provided each antenna is triggered independently.

NOTE 1 The procedure is not intended for conditional triggering for different use conditions. Neither does the procedure cover simultaneous transmission.

NOTE 2 The procedure specified in 7.7 only applies to single-step power reduction with one proximity sensor triggering distance. If multi-step power reduction is applied using multiple separation distances, regulatory authorities can be consulted to determine the testing procedures and requirements.

NOTE 3 The procedure specified in 7.7 has been established for devices used next to the body, where the flat phantom is applicable for SAR testing. The procedure does not consider test cases on the head or application-specific phantoms described in Annex K, where changes in body contours would require more complex test considerations to validate proximity sensor operating characteristics.

NOTE 4 DUTs typically ensure that if the proximity sensor is not functional then they will default to reduced output power.

Subclause 7.7 shall be used to determine the triggering distance and coverage area of proximity sensors to ensure that:

a) power reduction is triggered consistently and reliably at the specified distance from the DUT to the user (7.7.2);

b) the proximity sensor covers a sufficient area or region surrounding the peak SAR location to ensure consistent triggering from all applicable DUT orientations with respect to the user (7.7.3);

c) the test separation distance for SAR testing at full power is determined. This distance is the smaller of the triggering distance for perpendicular DUT orientation (7.7.2.2) and the triggering distance for tilted DUT orientation (7.7.2.3) minus 1 mm. The minus 1 mm spacing is generally required to ensure all production units are compliant. If more production variation in triggering distance is expected, it shall be taken into account accordingly.

d) any hysteresis effects in the triggering distance are accounted for.

The procedures shall be conducted separately for all antennas implementing proximity sensor-based power reduction. Each implemented proximity sensor sensitivity setting shall be tested once using one of the corresponding operating mode and frequency band combinations. If the implemented proximity sensor sensitivity settings are not known, the procedures shall be performed for all operating mode and frequency band combinations.

IECNORM.COM : Click to view the full PDF of IEC/IEEE 62209-1528:2020

Capacitive sensors are typically used for proximity sensing. The presence of approaching nearby objects in the vicinity of the sensor can be detected by changes in sensor capacitance. Depending on the antenna dimension and extent of the SAR distribution, one or more sensors could be required to ensure adequate sensor coverage for the corresponding SAR distribution. The procedures for determining sensor coverage are specified in 7.7.3.

NOTE 5 Proximity sensors can use techniques other than capacitive sensing. The procedures in 7.7 have been written for capacitive sensors only, which will require adaptation or might not be suitable for testing other sensing technologies. As appropriate, the regulatory authorities can be consulted to determine the testing and validation requirements for other sensing techniques.

7.7.2 Procedures for determining proximity sensor triggering distances

7.7.2.1 General

Proximity sensors are typically incorporated on the flat surfaces or along edges of a device where the antenna is located so that the triggering of output power reduction can appropriately limit the SAR. The procedures in 7.7.2 are used to meet the following requirements.

a) The minimum triggering distance shall be determined and used to establish a test separation distance for the SAR compliance measurements at full power, when power reduction is inactive.

b) The minimum triggering distance shall account for variations due to hysteresis and variations across production units due to implementation tolerances.

c) For sensors that are located along the edge of a device, the minimum triggering distance shall cover the various angles and orientations that the edge can be positioned relative to the user to determine the test separation distance for SAR measurement.

d) All proximity sensors in the DUT shall be tested in actual use conditions as if the device was normally operated by the user, including multiple proximity sensors used to cover an extended SAR distribution of an antenna. Any interactions between the proximity sensors shall be taken into account during the testing.

e) When proximity sensors are required to cover different use conditions – for example, sensors that wrap around the edge of a device to support both edge and surface detection – all applicable use conditions shall be tested.

f) Each antenna that is triggered to lower its output power shall be tested separately. Procedures shall be conducted for all operating mode and frequency band combinations that apply to the antenna.

g) The phantoms and tissue-equivalent media specified in this document shall be used to determine the minimum triggering distance of the sensor. The dielectric properties of the tissue-equivalent medium shall be within the tolerances specified in Table 2 at the frequency band of interest for each proximity sensor test.

h) The full and reduced maximum output power corresponding to triggering disabled and enabled conditions shall be verified. This may be done either by using built-in test software, by measuring the conducted power, or by measuring the radiated power. When test software is used to identify triggering, conducted or radiated power measurement shall be performed separately to verify the actual power levels. Conducted power measurement is preferred over radiated power measurements.

i) When conducted power measurement is used, the losses of the RF cables shall be accounted for in order to verify the maximum power required for SAR measurement in the corresponding triggering states.

j) When radiated power measurement is used, the maximum output power levels for the triggering conditions shall be identified unambiguously by taking into account the effects of RF propagation and environmental perturbation. Local SAR at the peak SAR location may be recorded to identify the change in triggering condition associated with the step change in device output power. The measured local SAR can be correlated with that at the same location in the 1 g or 10 g SAR compliance measurement.

IECNORM.COM : Click to view the full PDF of IEC/IEEE 62209-1528:2020

k) Any cables and connectors used for the conducted power measurement shall be configured and positioned such that neither the sensing characteristics of the proximity detection nor the SAR levels and distributions (for local SAR) are perturbed compared to without such cables and connectors.

l) The SAR test report shall include tabulated data of the measured output power and sensor states versus distance of the DUT to the phantom.

7.7.2.2 Triggering distance for perpendicular DUT orientation

The procedure for determining the triggering distance of proximity sensors (e.g. single proximity sensor or combination of proximity sensors as specified in 7.7.2.1) incorporated on the flat surface or edge of a device, approaching the phantom (user) perpendicularly is covered in 7.7.2.2. The variation in triggering distance due to tilted orientations of the DUT is covered in 7.7.2.3.

For normal approach of the DUT to the phantom, the procedure is as follows.

a) Each antenna within the DUT that requires proximity sensing shall be tested in the applicable frequency bands using a flat phantom specified in 6.2.4.

b) The surface or edge of the DUT that contains the sensor shall be positioned perpendicularly to the flat phantom, at an initial distance that is at least 10 mm beyond the distance where the proximity sensor is triggered.

NOTE This triggering distance procedure is only applicable to SAR measurements in a flat phantom. This generally does not apply to the SAM phantom or other hand-held use conditions.

c) The surface or edge of the DUT shall be moved toward the phantom in step sizes of 5 mm until the maximum output power is reduced.

d) The surface or edge of the DUT shall be moved away from the phantom by at least 5 mm and until the maximum output power is returned to the higher level.

e) The surface or edge of the DUT shall again be moved toward the phantom, but in 1 mm steps until it is at least 5 mm past the triggering point or touching the phantom.

f) If the DUT is not touching the phantom, it shall be moved in step sizes of 3 mm until it is touching the phantom to confirm that the sensor remains triggered and maximum power stays reduced.

g) The DUT shall be moved away from the phantom, using the same step sizes as those in steps c) to f), to determine the distance when triggering is released. The movement should continue until it is at least 50 mm beyond the point that triggers the return of normal maximum power.

h) The smallest separation distance determined by the sensor triggering procedure for movements to and from the phantom shall be the minimum triggering distance for perpendicular movement of the corresponding surface or edge towards the user.

IECNORM.COM : Click to view the full PDF of IEC/IEEE 62209-1528:2020

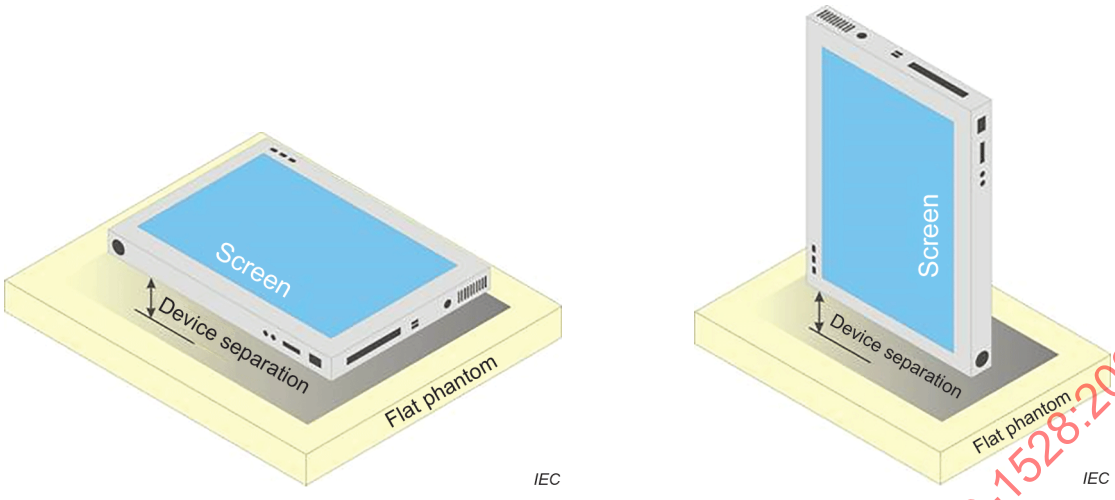


Figure 22 – Positioning of the surfaces and edges of the DUT for determining the proximity sensor triggering distance

7.7.2.3 Triggering distance for tilted DUT orientation

For sensors located on the edge of a device, in addition to perpendicular triggering, influence of the DUT edge to the triggering distance shall also be evaluated with the device edge positioned at different angles from normal to the phantom (Figure 22). The procedure to determine triggering variations due to the edge of a device oriented at various angles to the phantom is as follows.

a) Position the DUT edge at the minimum triggering distance determined in 7.7.2.2.

b) Ensure that the proximity sensor is triggered when the DUT is in the perpendicular orientation specified in 7.7.2.2.

c) Rotate the DUT as shown in Figure 23. The angle shall vary by ±40° from the perpendicular orientation in increments of 10°. At each of these angles, ensure that the proximity sensor is still triggered.

d) Reduce the edge distance to the phantom by 1 mm and go back to step b) if sensor triggering is released or normal maximum output power is restored in step c).

e) The smallest separation distance determined in steps a) and b) is the sensor triggering distance for non-perpendicular edge triggering conditions.

f) The smallest triggering distance determined for the edge in perpendicular and rotated conditions shall be the minimum triggering distance for that edge.

IECNORM.COM : Click to view the full PDF of IEC/IEEE 62209-1528:2020

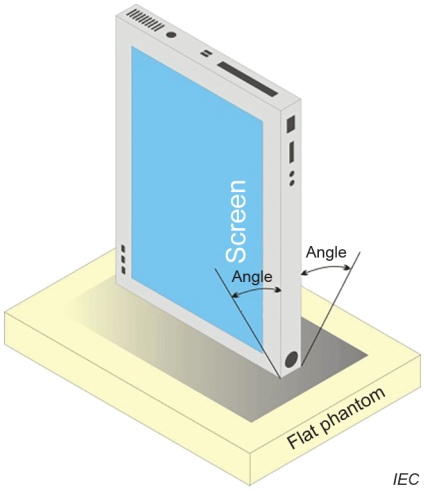


Figure 23 – Positioning of the edges of the DUT to determine proximity sensor triggering distance variations with the edge positioned at different angles from the perpendicular position

7.7.3 Procedure for determining proximity sensor coverage area

This procedure verifies that the coverage area of the proximity sensors contains the applicable psSAR cube. This ensures that the sensor provides adequate triggering relevant to the recorded SAR at the reduced power level.

Proximity sensors cover an area or region surrounding the peak SAR location associated with the SAR distribution of an antenna. Depending on the implementation, the sensor can be co-located or spatially offset from the antenna.

The surface(s) or edge(s) where the sensor coverage area test is applied are determined as follows.

– All surfaces and edges that require proximity sensing to trigger power reduction shall be tested, except when the antenna and sensor are both co-located with the psSAR cube.

– Two edges of the DUT shall be tested if the sensor or applicable antenna is located within 50 mm of the corner of the two adjacent edges and testing of both edges is required in 7.2.4.1.

NOTE 50 mm is considered sufficiently far away from the corner so that the antenna/sensor is not influenced by the adjacent edge; 50 mm also corresponds to the typical size of the significant portions of the SAR distribution for antennas in devices for which the procedure outlined in 7.7.3 has been developed.

If the procedure to determine sensor coverage area is amended (i.e. the procedure is inadequate due to concerns relating to antenna placement, extent of the SAR distribution or sensor offset), any amendment shall be documented.

Depending on the SAR distribution of the antenna and sensor offset, if reducing the triggering distance extends the coverage area to include the peak SAR location, the smaller triggering distance may be considered to avoid sensor coverage problems.

The test of the coverage area of the proximity sensor is as follows.

a) Orient the DUT such that the applicable surface or edge (determined above) is in contact with the flat phantom. Align the long axis of the DUT surface or edge with the long axis of the phantom.

b) Move the DUT away from the phantom by the minimum triggering distance determined in 7.7.2.2. The surface or edge shall be maintained parallel to the flat phantom shell.

IECNORM.COM : Click to view the full PDF of IEC/IEEE 62209-1528:2020

c) Establish the initial DUT position by moving the DUT lateral to the phantom until both the antenna and proximity sensor are outside the perimeter of the phantom. The surface or edge shall be maintained parallel to the flat phantom shell. If the precise location of the antenna or proximity sensor is not known, ensure that the entire surface or edge is outside the perimeter of the phantom.

d) Ensure that the proximity sensor is not triggered in the initial DUT position. If it is, check the set-up to ensure that other objects in the vicinity are not triggering the proximity sensor.

e) Move the DUT lateral to the phantom until the proximity sensor is triggered. The surface or edge shall be maintained parallel to the flat phantom shell. Record this DUT location with respect to the phantom edge.

f) Rotate the DUT 90°. The axis of rotation is normal to the flat phantom surface.

g) Move the DUT back to the initial position in step c).

h) Repeat steps d) and e). Record the location of the DUT where the proximity sensor is triggered.

i) Repeat steps f), g), and h) so that the triggering is tested at 0°, 90°, 180°, and 270° orientations of the applicable surface or edge. Four DUT locations (one for each orientation) are recorded.

j) Determine the coverage area as the region between the four DUT locations recorded above.

k) Determine the location of the psSAR with respect to the DUT surface or edge.

   Ensure that the psSAR cube is fully contained within the coverage area. If this is not the case, the reduced power SAR test in 7.7.4 shall not be applied without additional justification.

7.7.4 SAR measurement procedure involving proximity sensors

Two different maximum output power levels are applied according to the triggering conditions of the proximity sensor. SAR measurements shall be performed for the two different maximum output power state and test distance combinations.

a) Full power: SAR tests shall be performed at the test separation distance corresponding to the minimum sensor triggering distance among all triggering and coverage tests of 7.7, minus 1 mm, as specified in 7.7.2 and 7.7.3.

b) Reduced power: SAR tests shall be performed at the closest intended use distance or at the closest distance required by the regulator.

SAR measurements at these two power and distance combinations are enough to ensure compliance for the use conditions requiring proximity sensing and power reduction at the applicable device to user distance.

The test set-up photos, required power measurement, and triggering distance results, for supporting sensor triggering and sensor coverage, shall be documented in the measurement report.

IECNORM.COM : Click to view the full PDF of IEC/IEEE 62209-1528:2020

7.8 SAR correction for deviations of complex permittivity from targets

7.8.1 General

In this document, dielectric properties of the tissue-equivalent medium used for SAR measurement are selected to give conservative exposure. Deviations of the dielectric properties from the target values can lead to measurement uncertainty. One way to reduce measurement uncertainty is to keep the dielectric properties of the tissue-equivalent media within a tight tolerance of the targets (e.g. within ±5 %). However, it can be difficult to find suitable and stable recipes with dielectric properties that are close to the targets, particularly at frequencies above 2 GHz. There are three solutions to this problem:

a) modify the target dielectric properties to match those of available recipes;

b) widen the tolerance (without correcting the SAR for the deviation in dielectric properties);

c) allow a wider tolerance, and correct the SAR for the deviation of the measured dielectric properties from the target values.

The third solution is the best, because changing the targets restricts the applicability of the document to particular recipes, and simply widening the tolerance increases the measurement uncertainty.

The methodology used to determine the SAR correction is specified in 7.8.2. The methodology was conducted over a frequency range of 4 MHz to 10 GHz. The methodology was also studied for permittivity and conductivity ranges of ±20 % from the target values in Table 2, but ranges of ±10 % have been selected for this document, as specified below. Given that the change in dielectric properties influences the conversion factor of the probe, this influence will be small if a ±10 % range is used.

7.8.2 SAR correction formula

From Douglas et al. ([28], [29]), a linear relationship was found between the percentage change in SAR (denoted ΔSAR) and the percentage change in the permittivity and conductivity from the target values in Table 2 (denoted $\Delta\varepsilon_r$ and $\Delta\sigma$, respectively). This linear relationship agrees with the results of Kuster and Balzano [30] and Bit-Babik et al. [31]. The relationship is given by:

$$\Delta SAR = c_\varepsilon \Delta\varepsilon_r + c_\sigma \Delta\sigma \tag{8}$$

where

c_ε = $\partial(\Delta SAR)/\partial(\Delta\varepsilon)$ is the coefficient representing the sensitivity of SAR to permittivity where SAR is normalized to output power;

c_σ = $\partial(\Delta SAR)/\partial(\Delta\sigma)$ is the coefficient representing the sensitivity of SAR to conductivity, where SAR is normalized to output power.

The values of c_ε and c_σ have a simple relationship with frequency that can be described using polynomial equations. For dipole antennas at frequencies from 4 MHz to 6 GHz, the 1 g averaged SAR c_ε and c_σ are given by

$$c_\varepsilon = -7{,}854\times10^{-4} f^3 + 9{,}402\times10^{-3} f^2 - 2{,}742\times10^{-2} f - 0{,}202\,6 \tag{9}$$

$$c_\sigma = 9{,}804\times10^{-3} f^3 - 8{,}661\times10^{-2} f^2 + 2{,}981\times10^{-2} f + 0{,}782\,9 \tag{10}$$

where f is the frequency in GHz. Above 6 GHz, the sensitivity is non-varying with frequency due to the small penetration depth; the values of c_ε = −0,198 and c_σ = 0 shall be used.

For frequencies from 4 MHz to 6 GHz, the 10 g averaged SAR c_ε and c_σ are given by:

$$c_\varepsilon = 3{,}456\times10^{-3} f^3 - 3{,}531\times10^{-2} f^2 + 7{,}675\times10^{-2} f - 0{,}186\,0 \tag{11}$$

$$c_\sigma = 4{,}479\times10^{-3} f^3 - 1{,}586\times10^{-2} f^2 - 0{,}197\,2 f + 0{,}771\,7 \tag{12}$$

IECNORM.COM : Click to view the full PDF of IEC/IEEE 62209-1528:2020

where f is the frequency in GHz. Above 6 GHz, the sensitivity is non-varying with frequency due to the small penetration depth; the values of c_ε = −0,250 and c_σ = 0 shall be used. For specific antennas and frequencies, the procedure of O.9.5 may be applied to determine the sensitivity coefficients, as appropriate.

7.8.3 Uncertainty of the correction formula

The mean power uncertainty of the formulas in 7.8.2, specified in Douglas et al. [28] as the RMS error between the SAR deviation predicted by the formulas and the simulated deviation over 440 analysed cases, is shown in Table 6 for the 1 g psSAR and 10 g psSAR. Table 6 shows how the mean power error increases as the maximum allowable value of $\Delta\varepsilon_r$ and $\Delta\sigma$ increases. It has also been shown in [28] that these corrections are valid for realistic DUT models.

Using this approach, the measurement uncertainty is lower, because this correction eliminates the need for uncertainty items that account for the deviation of the dielectric properties from the targets. Instead, there is an uncertainty item which accounts for the error of the correction formula. The value of this uncertainty item is given in Table 6. For ±10 % deviation in permittivity and conductivity, enter 1,9 % and 1,6 % in the uncertainty budget for 1 g and 10 g psSAR, respectively. These uncertainty values should be entered into the appropriate row of Table 9 where a normal probability distribution is assumed.

Table 6 – Root-mean-squared error SAR correction formula as a function of the maximum change in permittivity or conductivity [28]

Max. change in ε_r or σ	RMS uncertainty for SAR_{1g} %	RMS uncertainty for SAR_{10g} %
±5 %	1,2	0,97
±10 %	1,9	1,6

7.9 Minimization of testing time

7.9.1 General

Subclause 7.9 gives methods for minimizing the test time to identify a subset of the highest SAR conditions for a DUT. Full SAR testing, i.e. testing that is fully compliant with the requirements of 7.4 of this document, shall be performed for the subset of device configurations identified as having the highest SAR values from these tests. One of two methods for reducing the overall test time for a DUT may be used:

a) test reduction methods in which a set of rules are applied to reduce the total number of device configurations that require testing specified in 7.9.3;

b) fast SAR testing that reduces the measurement time for each device configuration as specified in 7.9.2.

Test reduction methods shall not be used in conjunction with fast SAR testing.

NOTE Studies are ongoing for a future revision of this document to check whether test reduction methods and fast SAR testing may be used in conjunction with each other, while still providing that the reported SAR is conservative.

IECNORM.COM : Click to view the full PDF of IEC/IEEE 62209-1528:2020

7.9.2 Fast SAR testing

7.9.2.1 General

Full SAR testing uses measurement systems and procedures that fully comply with all the requirements of this document are referred to herein as "full SAR" systems (see also 3.20). The procedures specified in 7.9.2 apply to fast SAR testing. Fast SAR testing differs from full SAR testing in that it uses special techniques, methods, algorithms, or different measurement equipment that do not comply with all the normative requirements of this document, but decreases the measurement time (see also 3.17).

Fast SAR testing may be used together with full SAR testing to reduce the overall measurement time needed to evaluate a wireless communication device. Fast SAR testing may be used to identify the highest SAR test configurations, and is therefore used to evaluate relative SAR levels. Full SAR testing shall be used to assess the absolute SAR levels. Full SAR testing shall be performed on at least the highest SAR test configuration, and those within the confidence levels given in the procedures specified in 7.9.2.2 and 7.9.2.3.

NOTE 1 These testing alternatives are not mandatory; the user of this document remains free to apply the full SAR testing procedure specified in 7.1 through 7.5 for all testing.

Fast SAR testing does not fall in the category of test reduction methods (see 7.9.3). Fast SAR testing generally aims at decreasing the time spent to perform a measurement, whereas test reduction methods aim to reduce the total number of measurements to be performed.

Due to the decreased time needed to perform fast SAR testing, it can be anticipated that multiple fast SAR testing methods may be performed using a single battery charge when testing a device. The requirements of 7.4.3 shall be satisfied regarding the power drift remaining within ±5 % from the average value throughout the measurement interval.

The following procedures do not address all forms of multiple transmitter SAR evaluations. Additional full SAR testing can be necessary to meet the requirements outlined in 7.4.4.

Two classes of fast SAR testing are designated for the purposes of this document.

a) Class 1: These are fast SAR testing methods based on measurements made using equipment that conforms with all of the normative clauses of this document but where special techniques are applied to improve the measurement speed; for example by measuring reduced numbers of points then using additional post-processing. Class 1 fast SAR testing is based on scanning and post-processing requirements of the individual fast SAR testing method used to reduce measurement time, but with less accuracy or higher measurement uncertainty than for full SAR testing. The measurement uncertainty shall be determined according to Clause 8 and Annex C, and shall be documented. Each individual fast SAR testing method shall be fully validated to determine its applicability for testing different wireless communication devices, as specified in A.4.2. The valid ranges of frequencies, SAR distributions, and SAR levels applicable to the fast SAR testing method shall be documented, as specified in A.4.2. The users of a fast SAR testing method shall perform a system check to demonstrate the reliability and consistency of the method, as specified in A.4.3.

IECNORM.COM : Click to view the full PDF of IEC/IEEE 62209-1528:2020

b) Class 2: These are fast SAR testing methods based on measurements made using equipment that does not conform with all of the normative clauses of this document. Scanning systems or array systems that employ field-reconstruction algorithms fall into this class. Class 2 fast SAR testing systems shall meet the SAR measurement system verification and validation requirements of IEC 62209-3, with the exception that the measurement uncertainty is not limited to a threshold of 30 %, and the validation as well as the system verification may also be reduced to the ranges of operating modes and frequencies tested. When used in conjunction with the fast SAR measurement Procedure A (see 7.9.2.3), Class 2 fast SAR testing can effectively identify the highest SAR test configurations that shall subsequently be measured with full SAR testing to assess the maximum peak-spatial SAR that would occur in the head or body (e.g. for compliance demonstration purposes). Like with Class 1 fast SAR testing, Class 2 fast SAR testing systems shall be calibrated and fully validated to determine their applicability for testing different wireless communication devices for the specific communication technologies, exposure conditions, and device configurations being assessed for SAR. The measurement uncertainty shall be determined and documented (see Annex C).

Requirements for vector measurement-based systems are given in IEC 62209-3. It is recommended to apply its requirements to this document.

NOTE 2 Field reconstruction techniques are specified in IEC 62209-3.

7.9.2.2 Fast SAR testing Procedure A

Procedure A may be applied to determine the maximum SAR of a DUT for all the required test configurations, or a subset thereof. Class 1 fast SAR testing and Class 2 fast SAR testing may use Procedure A. This procedure shall be applied separately for head and body phantom types. For the head phantom type, the left head and right head data can be considered as one data set. For the body phantom type, all body phantom configurations (e.g. if multiple phantom sizes were used) can be considered as one data set.

NOTE 1 An extensive inter-laboratory study was carried out to assess the robustness of fast SAR testing Procedure A. In this study, supported by IEC TC 106 and organized by Innovation, Science and Economic Development (ISED) Canada, 10 laboratories performed over 7 500 measurements using full SAR testing and Class 1 and Class 2 fast SAR testing. One outcome of the study was a revision of Procedure A to improve its success rate. Results obtained from this study showed that both Class 1 and Class 2 methods can be used in conjunction with fast SAR testing Procedure A with a very high level of confidence while considerably reducing the amount of time and effort necessary to complete the compliance evaluation of a DUT.

Figure 24 is a simplified workflow depicting the steps detailed in Procedure A.

In order to substantially increase the user-friendliness of this procedure as well as to ensure that the steps of Procedure A are consistently being followed correctly, a tool called the Fast SAR Wizard has been developed. The Fast SAR Wizard can be downloaded from:

http://www.iec.ch/dyn/www/f?p=103:227:0::::FSP_ORG_ID,FSP_LANG_ID:1303,25

Procedure A has the following steps:

a) Use fast SAR testing to perform measurements on a chosen set of test configurations (see 3.52). The test configurations shall be grouped separately into N frequency band and operating mode combinations, each having M_i test configurations. These fast SAR testing values are denoted $SAR_{\text{fast},(i,j)}$ (i = 1 to N and j = 1 to M_i). When a Class 1 fast SAR testing system is used, it is sufficient to include the centre channel for each test configuration. When a Class 2 fast SAR testing is used, all required channels specified in 7.2.8 shall be tested for each test configuration.

b) Use full SAR testing to measure the highest SAR test configuration from each of the N groups. These N fast SAR testing values are denoted $SAR_{\text{max,fast},i}$ (i = 1 to N). Select the maximum fast SAR testing value $SAR_{\text{max,fast}}$ = max($SAR_{\text{max,fast},i}$).

IECNORM.COM : Click to view the full PDF of IEC/IEEE 62209-1528:2020

With Class 1 fast SAR testing, it is not necessary to repeat the entire area scan during full SAR testing when the number of SAR peaks is already known from fast SAR testing. The full SAR testing method used in this step may use a reduced area, where all of the requirements of 7.4.2 b) and Table 3 apply, except that the area may be smaller than the projection of the DUT and antenna. The reduced area scan shall include at least the grid point at each SAR peak found in step a), and the eight adjacent points surrounding each SAR peak. The resulting area scan is valid if it also identifies the same SAR peaks and peak locations found in step a), within positioning tolerance.

c) Use full SAR testing to measure all other test configurations (i,j), at the channel giving highest fast SAR testing result, where the condition of Formula (13) is met. The second paragraph of step b) applies.

$$SAR_{\text{fast},(i,j)} \geq SAR_{\text{max,fast}} \times \left(B_{\text{fast},i} - \sqrt{B_{\text{fast},i}^2 - 1} \right) \tag{13}$$

$B_{\text{fast},i}$ is calculated according to Formula (14).

$$B_{\text{fast},i} = \frac{1}{1 - \left(1{,}64\, U_{\text{fast},i}\right)^2} \tag{14}$$

$U_{\text{fast},i}$ in Formula (14) is the standard measurement uncertainty (k = 1) of fast SAR testing results at the i-th frequency band and operating mode combination.

When using Class 2 system for fast SAR testing, $U_{\text{fast},i}$ shall be set to the standard uncertainty or 35 % / 2 = 17,5 %, whichever is greater. The 35 % figure is based on analysis of a fast SAR testing interlaboratory comparison study completed in 2017.

NOTE Formula (13) and Formula (14) are derived for a 95 % confidence interval where

$$SAR_{\text{fast},(i,j)} \leq SAR_{\text{max,fast},i}$$

This confidence interval is given as:

$$\left(SAR_{\text{max,fast}} - SAR_{\text{fast},(i,j)}\right) - 1{,}64 U_{\text{fast},i} \sqrt{S_{\text{max,fast}}^2 + S_{\text{fast},(i,j)}^2} \leq 0 \,.$$

Solving for $SAR_{\text{fast},(i,j)}$ results in Formula (13) and Formula (14), where $U_{\text{fast},i}$ is the standard uncertainty and has a Gaussian distribution. The value of 1,64 is the factor for a one-sided 95 % confidence interval of a Gaussian distributed random variable.

d) Use full SAR testing to measure all other test configurations where the condition of Formula (15) is met. The second paragraph of step b) and the last paragraph of step c) apply.

$$SAR_{\text{fast},(i,j)} \geq SAR_{\text{limit}} \times \left(B_{\text{fast},i} - \sqrt{B_{\text{fast},i}^2 - 1} \right) \tag{15}$$

e) Use full SAR testing to measure all required channels specified in 7.2.8 across the frequency band for the test configuration that resulted in the highest psSAR, $SAR_{\text{highest,full}}$ = max($SAR_{\text{full},(i,j)}$), if this has not already been done. The reduced area scan requirements outlined in step b) for Class 1 methods apply.

f) Use full SAR testing in accordance with 7.3 to measure any other test configurations that have not been tested by fast SAR testing in step a) and are not excluded from testing by this document or by applicable regulations.

IECNORM.COM : Click to view the full PDF of IEC/IEEE 62209-1528:2020

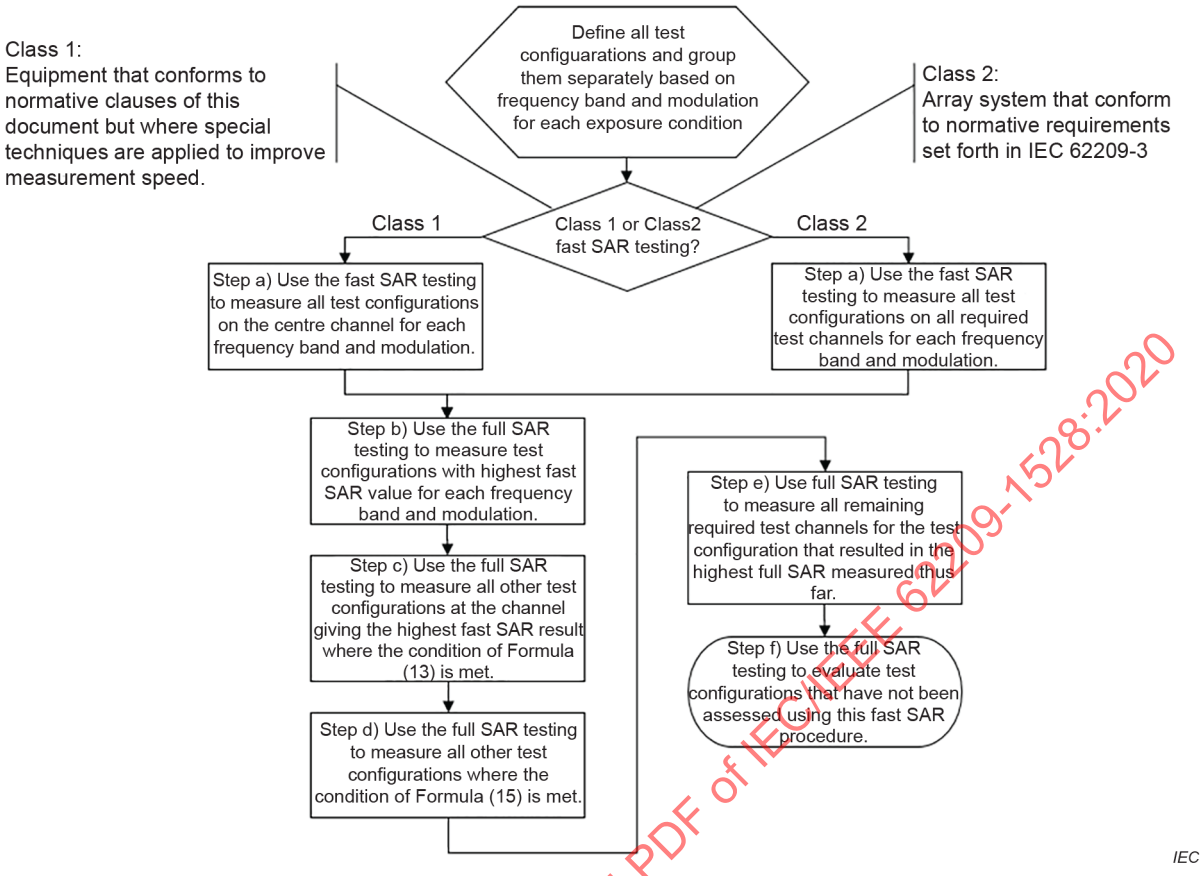


Figure 24 – Fast SAR Procedure A

7.9.2.3 Fast SAR testing Procedure B

Procedure B may be applied to determine the maximum SAR of a DUT for all the required test configurations, or a subset thereof. Only Class 1 fast SAR testing may use Procedure B. This procedure shall be applied separately for head and body phantom types. For the head phantom type, the left head and right head data can be grouped together. For the body phantom type, all body phantoms (e.g. if multiple phantom sizes were used) can be grouped together.

Figure 25 shows a simplified workflow depicting the steps detailed in Procedure B.

Procedure B has the following steps:

a) Use fast SAR testing to perform measurements on a chosen set of test configurations (see 3.52). The test configurations shall be grouped separately into N frequency band and operating mode combinations, each having M_i test configurations. These fast SAR testing values are denoted $SAR_{\text{fast},(i,j)}$ (i = 1 to N and j = 1 to M_i). It is sufficient to include the centre channel for each test configuration, but measurement of other required test channels shall also be done for the configuration giving highest SAR for each of the N groups.

b) Use full SAR testing to measure the highest SAR test configuration from each of the N groups.

c) Use full SAR testing to measure all other test configurations (i,j), at the channel giving highest fast SAR testing result, where the condition of Formula (15) is met. These values in steps b) and c) are denoted $SAR_{\text{full},(i,j)}$.

IECNORM.COM : Click to view the full PDF of IEC/IEEE 62209-1528:2020

Full SAR testing can be limited to the channel giving highest fast SAR testing result only when relative SAR distributions between channels are identical. Otherwise, full SAR testing is required for all channels. In some specific cases (e.g. narrowband signals), a visual comparison of SAR measurement plots for different channels can be applied to determine that the SAR distributions are identical.

d) For all the full SAR testing values in steps b) and c), calculate and record the $R_{i,j}$ according to Formula (16):

$$R_{i,j} = \frac{SAR_{\text{fast},(i,j)} - SAR_{\text{full},(i,j)}}{SAR_{\text{full},(i,j)}} \tag{16}$$

Use full SAR testing to measure all other test configurations, for all groups N where $R_{i,j} \geq U_{\text{fast},i}$ and highest $SAR_{\text{fast},(i,j)}$ and $SAR_{\text{full},(i,j)}$ are at least 6 dB above their stated noise thresholds. This testing is done at the channel having the highest fast SAR testing result.

Some test configurations could have only a single fast SAR testing result available, which shall be interpreted as the highest result.

e) Use full SAR testing to measure all required channels specified in 7.2.8 across the frequency band for the test configuration that resulted in the highest psSAR, $SAR_{\text{highest,full}} = \max[SAR_{\text{full},(i,j)}]$, if this has not already been done.

f) Use full SAR testing in accordance with 7.3 to measure any other test configurations that have not been tested by the fast SAR testing method in steps a) and e) and are not excluded from testing by this document or by applicable regulations.

IECNORM.COM : Click to view the full PDF of IEC/IEEE 62209-1528:2020

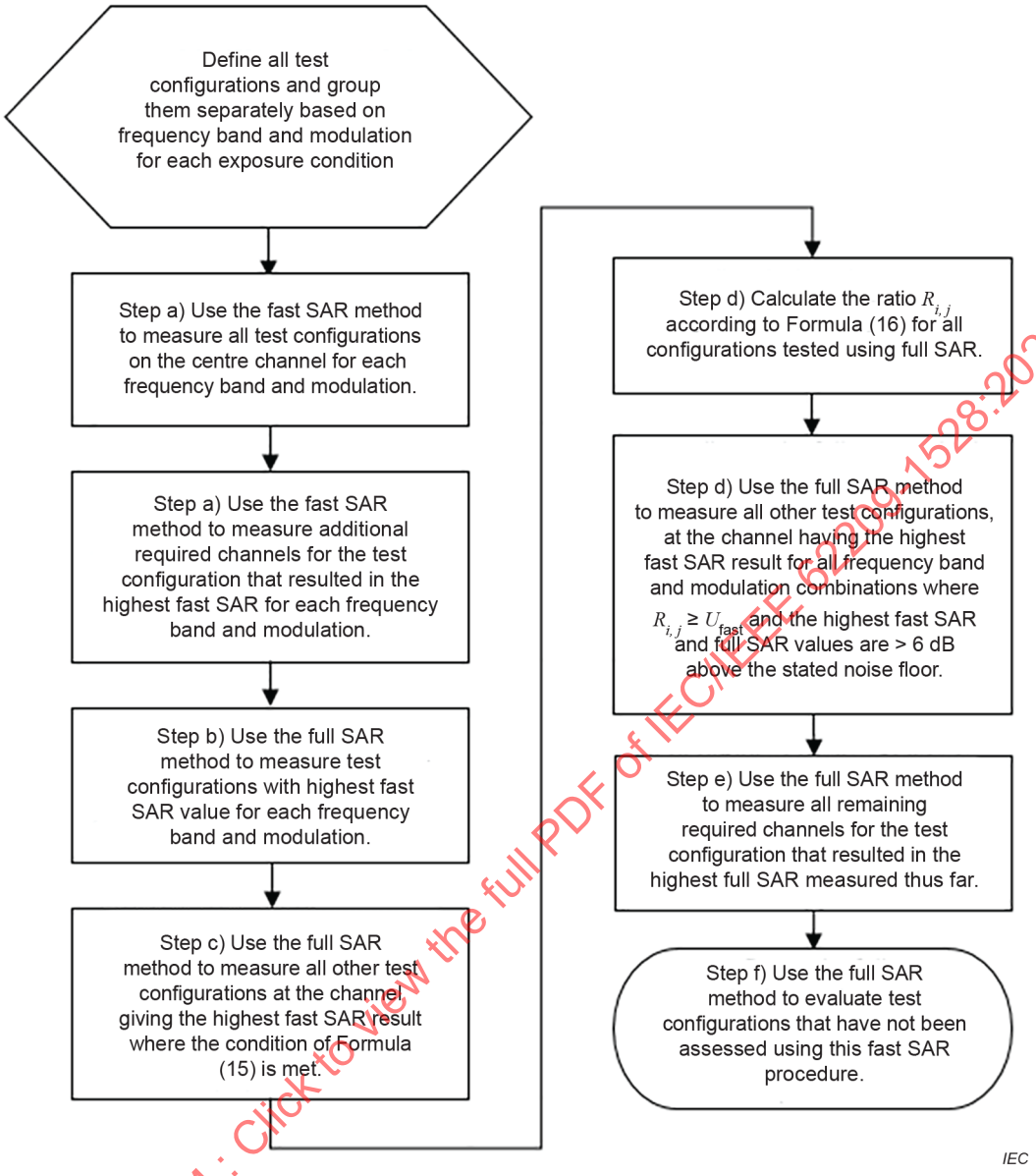


Figure 25 – Fast SAR Procedure B

IECNORM.COM : Click to view the full PDF of IEC/IEEE 62209-1528:2020

7.9.3 SAR test reductions

7.9.3.1 General

The number of SAR tests required to identify the configuration giving the maximum psSAR can be large for a DUT capable of transmitting in multiple frequency bands and with different usage configurations. This is also the case if the DUT can be used with different accessories. The total measurement time required to test a personal wireless communication device can be reduced by using fast measurement techniques that decrease the measurement time for each series of tests (per 7.9.2), or by directly reducing the number of tests to be performed (in accordance with 7.9.3). Combining test reduction techniques with fast SAR testing requires further investigation, which will be considered in subsequent revisions of this document. SAR test reduction methods applied during testing shall be reported as specified in 9.2 f).

Alternative approaches for reducing the number of tests are presented in 7.9.3. These approaches are:

a) test reduction for different operating modes at the same test frequency band using the same wireless technology;

b) test reduction based on characteristics of the DUT design;

c) test reduction based on peak SAR level analysis;

d) test reduction based on simultaneous multi-band transmission considerations.

NOTE 1 For example, GSM, GPRS, and EDGE (all using GMSK modulation) are considered to be the same wireless technology, but GSM and UMTS are not considered the same wireless technology.

NOTE 2 The SAR test reduction procedures specified in 7.9.3 allow users of this document to save time required for testing. These testing alternatives are not mandatory.

Supporting information on SAR test reduction can be found in Annex B.

7.9.3.2 Test reduction for lower power operating modes in the same frequency band using the same wireless technology

When different operating modes (mod_X, mod_Y, etc.) work in the same frequency band, procedures may be employed in some cases to reduce the number of measurements for the lower power operating modes (mod_Y, etc.) without compromising the stringency of the tests for assessing the conservative exposure psSAR. The procedures may be applied if the following conditions are met.

a) The same RF amplifier stage is used for mod_X and mod_Y.

b) The same antenna is used for mod_X and mod_Y.

c) No MIMO (multiple-input and multiple-output) techniques are applied for both mod_X and mod_Y.

d) The same wireless technology is used for mod_X and mod_Y.

e) Either the same signal modulation is used and this modulation has constant amplitude, or the time-averaged output power of mod_Y is at least 2 dB below the output power of mod_X.

f) The SAR probe calibration is valid for both mod_X and mod_Y (i.e. the probe calibration certificate specifies the validity and uncertainty of the calibration applicable to both mod_X and mod_Y).

g) The same SAR measurement system (probe, phantom, tissue-equivalent medium, and electronics) is used for testing all operating modes.

h) The RF carrier frequency of mod_X is the same as for mod_Y.

i) The channel bandwidth ratio (R_m) of mod_X and mod_Y satisfies Formula (17):

$$R_m = \left| \frac{BW_{modY}}{BW_{modX}} - 1 \right| \leq 0{,}3 \qquad (17)$$

To reduce the number of tests required, the following procedure may be applied if all of the preceding conditions are met:

Step 1 Test all operating modes (mod_X, mod_Y etc.) in any one of the standard test configurations (e.g. left-ear touch position).

Step 2 Fully test in all standard test configurations the operating mode that had the highest SAR value in step 1.

Step 3 Fully test in all standard test configurations all other operating modes evaluated in step 1 for which both of the following conditions apply:

- if the SAR value measured in step 1 for the operating mode under consideration is within 15 % of the SAR value measured in step 1 of the highest SAR operating mode (i.e. the operating mode chosen for use in step 2), and
- if the highest SAR value measured in step 2 is within 15 % of the applicable SAR limit.

IECNORM.COM : Click to view the full PDF of IEC/IEEE 62209-1528:2020

The 15 % margin corresponds approximately to half the maximum expanded measurement uncertainty of 30 %.

NOTE Both GSM and GPRS use GMSK, which is a constant amplitude modulation; therefore, the maximum time-averaged output power with respect to the maximum number of time slots used in each operating mode can be used to determine the most conservative operating mode for SAR testing. Similarly, EGPRS (which uses GMSK and 8PSK) can be included with GSM and GPRS in this determination of the most conservative operating mode for SAR testing, due to its innate similarities to GSM and GPRS. On the other hand, WiMAX uses OFDMA with high peak-to-average power ratio, where the SAR measurement error is expected to vary with power.

7.9.3.3 Test reduction based on characteristics of DUT design

There is a wide range of different designs of handsets on the market. The SAR data analysis in Clause B.2 has shown that the following test reduction and exclusion principles can be applied for handsets used at the side of the head with internally mounted antennas and operating frequencies between 800 MHz and 2 GHz. These criteria are based on the antenna locations within a DUT and the variations in DUT styles. An extension above 2 GHz could be considered if further supporting data becomes available.

The following requirements related to multiple operating modes within the same wireless technology and frequency bands shall be satisfied to apply the 7.9.3.3 test reduction procedure.

a) The same RF circuitry shall be used (transmitter, antenna feed-point, matching components etc.).

b) The same antenna and antenna grounding shall be used.

c) No MIMO (multiple-input and multiple-output) techniques shall be applied.

d) The same SAR measurement system (probe, phantom, tissue-equivalent medium, and electronics) shall be used.

For a DUT with a bottom-mounted internal antenna (i.e. an internal antenna mounted in the bottom half of the DUT) that is fully embedded within 2,5 cm from the bottom of the device, when the highest cheek position psSAR for a frequency band and operating mode is at least 3 dB from the SAR limit, testing in the tilt position is not required. For other antenna locations, when SAR measured in tilt position using the highest SAR channel tested for the cheek position is at least 3 dB from the SAR limit, testing of the other required channels for the tilt position is not required.

To apply additional test reduction for the DUT using the same bottom-mounted internal antenna for multiple operating modes within the same wireless technology and frequency bands, select the communications system with the highest maximum time-averaged output power then perform the full SAR testing procedure, including all configurations and test positions specified in 7.3. Testing at tilt positions for other operating modes within this same frequency band is not required regardless of the SAR level in cheek position(s), if both of the following two conditions listed below are met.

- The cheek position has the highest psSAR value for a frequency band.
- The psSAR values for the configurations in the tilt position are at least 30 % below the SAR limit.

The SAR measurement report shall include drawings or photos illustrating the layout as well as the locations of the antennas in the DUT, and describing the wireless operating modes applicable to each antenna, to support the considered test reduction and exclusion. When the test reduction related to devices with the same bottom-mounted internal antenna for multiple operating modes within same frequency band is to be applied, the antenna and the RF and antenna matching circuitry shall be described for each operating mode in the SAR measurement report.

Clause B.2 provides the rationale and supporting information for the analysis performed to support these test reduction and exclusion principles.

IECNORM.COM : Click to view the full PDF of IEC/IEEE 62209-1528:2020

7.9.3.4 Test reduction based on SAR level analysis

The purpose of this test reduction approach is to eliminate the “zoom scan” session for each single measurement (7.4.2 d)) when the measured peak SAR from the “area scan” is below a threshold, by assuring that the maximum psSAR value will be:

- correctly assessed and not underestimated, especially when it could generate a psSAR close to the applicable compliance limit;
- correctly identified, even if the “zoom scan” session is not executed.

NOTE This test reduction procedure is different from the fast SAR testing procedure specified in 7.9.2. In this test reduction protocol, the decision to apply the full SAR testing procedure is taken after looking at values measured from the area scan (not the final psSAR). Moreover, a threshold value is necessary since the goal is to avoid the zoom scan for some particular measurement configurations and not depend on a particular fast SAR fast SAR testing algorithm to estimate the psSAR.

The rationale and studies supporting this test reduction approach are reported in Clause B.4.

When applying the protocol specified below, it is necessary:

– to adjust the “area scan” parameters specified in the Table 3 to use grid spacing not larger than 10 mm;

– to perform the area scans at a fixed 4 mm maximum distance between the measured points (geometric centre of the sensors) and the phantom inner surface.

The single band test reduction protocol (valid for each operating mode supported by the DUT) is specified as follows.

a) Measure the local SAR as specified in 7.4.2 a).

b) Perform the area scan procedure for one of the positions specified in 7.4.2, at the channel of the considered band having the highest rated output power, as indicated in the complete measurement scheme specified in 7.4.2.

c) Determine the peak local SAR of the area scan; this is designated as the Absolute psSAR (APS).

d) Perform the zoom scan, as indicated in the complete measurement scheme specified in 7.4.2.

e) Perform post-processing to determine the psSAR as in 7.4.2 e).

f) Measure the local SAR and evaluate the measurement drift as specified in 7.4.2 f).

g) For all the other positions and frequency channels to be tested, repeat the following steps 1) through 5).

   1) Measure the local SAR as specified in 7.4.2 a).

   2) Perform the area scan procedure as indicated in the complete measurement scheme specified in 7.4.2 b).

   3) Evaluate the peak local SAR of the area scan; if the peak local SAR of the area scan is greater than APS, then APS shall be assigned to the peak SAR of the area scan, after completing step 4).

   4) Perform the zoom scan required by 7.4.2 if the area scan peak SAR is not less than 1,3 W/kg (80 % of 1,6 W/kg) or if the peak SAR is greater than or equal to $TH(f) \times APS$, where the frequency dependent threshold value $TH(f)$ is specified in Table 7 and APS is the Absolute psSAR. If multiple peaks (as in 7.4.2 c)) are required to be measured, apply this step to all the peaks.

   5) Perform post-processing to determine the psSAR as in 7.4.2 e).

   6) Evaluate the measurement drift as indicated in 7.4.2 f). If the drift is higher than 5 %, the drift shall be addressed according to 7.4.2 f).

h) Step g) shall be performed sequentially for all applicable bands. The frequency dependent threshold values used in step g) 4) are summarized in Table 7.

IECNORM.COM : Click to view the full PDF of IEC/IEEE 62209-1528:2020

i) When the 7.9.3.4 test reduction procedure is followed:

1) The block diagram on the left of Figure 19 shall be applied.

2) The block diagram on the right of Figure 19 shall be applied only for the first SAR measurement. Subsequent SAR measurements shall be performed according to Figure 26, which is a modification of the procedure specified in Figure 19.

Clause B.4 provides the rationale for the threshold levels used in this test reduction protocol, based on SAR spatial gradient analysis.

Table 7 – Threshold values $TH(f)$ used in this proposed test reduction protocol

Operating mode	$TH(f)$
GSM900	0,75
UMTS VI [a]	0,75
DCS1800	0,60
UMTS IX [a]	0,60
UMTS I	0,60

[a] 3GPP UMTS-FDD Band VI and Band IX have uplink frequencies very close to GSM900 and DCS1800, respectively. Even if only devices operating in GSM900, DCS1800 and UMTS I bands were considered in Clause B.2, the thresholds in this table shall be applied for UMTS-FDD Band VI and for UMTS-FDD Band IX.

IECNORM.COM : Click to view the full PDF of IEC/IEEE 62209-1528:2020

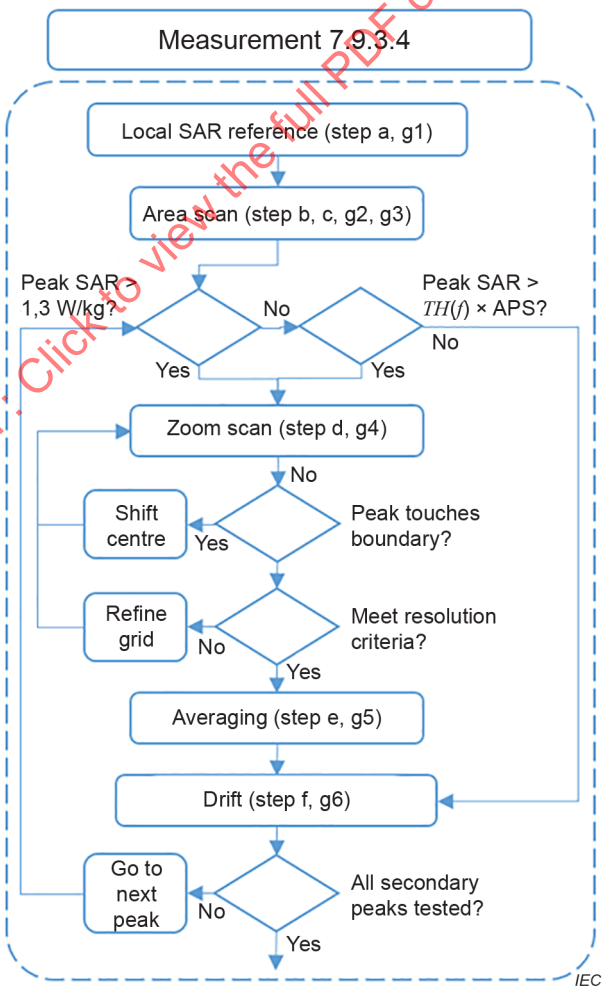


Figure 26 – Modified chart of Figure 19

7.9.3.5 Test reduction based on simultaneous multi-band transmission considerations

Simultaneous multi-band transmission means that the device can transmit in multiple frequency bands at the same time, e.g. a Wideband Code Division Multiple Access (WCDMA) transmission at 2 GHz and a Wireless Local Area Network (WLAN) transmission at 2,45 GHz. The time-averaged output power of a secondary transmitter (i.e. the lower power transmitter, e.g. Bluetooth, WLAN) can be much lower than that of the primary transmitter (i.e. the higher power transmitter, e.g. WCDMA). In some cases, the secondary transmitter can be excluded from SAR testing when used alone. However, when the primary and secondary transmitters are used together (simultaneous transmission), the SAR limit could still be exceeded. A means of determining the threshold power for the secondary transmitter that allows it to be excluded from SAR testing is required.

One way of determining the threshold power level for the secondary transmitter ($P_{\text{available}}$) is to calculate it from the measured psSAR of the primary transmitter (SAR_1) according to Formula (18):

$$P_{\text{available}} = P_{\text{max},m} \times (SAR_{\text{lim}} - SAR_1) / SAR_{\text{lim}} \quad (18)$$

where $P_{\text{max},m}$ is the maximum threshold exclusion power level, which is calculated by $SAR_{\text{lim}} \times m$, and m is an averaging mass.

For example, an exposure limit of SAR_{lim} = 2,0 W/kg and an averaging mass of m = 10 g gives total transmitting power of $P_{\text{max},m}$ = 20 mW.

For example, an exposure limit of SAR_{lim} = 1,6 W/kg and an averaging mass of m = 1 g gives total transmitting power of $P_{\text{max},m}$ = 1,6 mW.

Formula (18) can be easily generalized to the case where more than two transmitters are transmitting simultaneously. If there are N simultaneous transmitters and the psSAR of the first $N - 1$ transmitters are known (SAR_i), then the threshold power level for the Nth transmitter can be found from Formula (19):

$$P_{\text{available}} = P_{\text{max},m} \times (SAR_{\text{lim}} - \sum_{i=1}^{N-1} SAR_i) / SAR_{\text{lim}} \quad (19)$$

NOTE The applicability of power thresholds as specified in Annex B of IEC 62479:2010 [32] requires investigation, to replace $P_{\text{max},m}$ in the case where: i) the DUT is measured at the SAM ear, and ii) the radiating parts of the DUT are closer than 5 mm to the phantom surface. The definition of new power thresholds for such configuration is needed.

7.9.3.6 SAR measurements and test reductions for LTE devices

7.9.3.6.1 General LTE SAR testing considerations

LTE technology shows an added complexity over previously available radio schemes. In order to configure and test LTE devices, many signal parameters are taken into account: frequency band, channel bandwidth (e.g. from 1,4 MHz to 20 MHz), modulation (e.g. QPSK and 16-QAM and higher-order QAM), number of resource blocks (RBs) allocated, offset of the resource blocks within the channel bandwidth, as well as maximum power reduction (MPR). The combinations of parameters in a given frequency band can result in hundreds of LTE modes and SAR test configurations. In order to address this, a specific protocol is necessary for SAR assessment of LTE devices. The main purpose of this protocol is to support demonstration of DUT compliance with applicable limits based on a reasonable number of SAR evaluations.

NOTE 1 National regulatory agencies might have different requirements on test configurations for LTE devices.

IECNORM.COM : Click to view the full PDF of IEC/IEEE 62209-1528:2020

For a given LTE mode and device position, the psSAR is related to the maximum RF output power. As a consequence, RF conducted power measurements can be used to quickly identify high SAR LTE modes. SAR and RF conducted power are however not directly proportional because:

a) RF conducted power is measured with a 50 Ω load impedance;

b) the antenna impedance of a DUT is generally not 50 Ω and varies over frequency;

c) the antenna impedance can be affected by device position and phantom coupling conditions.

Because of this, a single SAR measurement using the LTE mode with the highest measured maximum conducted output power in a frequency band might not be sufficient to demonstrate compliance, unless the SAR value is significantly lower than the applicable compliance limit. The required test conditions are established by applying the protocol in 7.9.3.6.3.

NOTE 2 The power measurement procedures are applicable to the LTE modes in a frequency band. SAR is measured for the highest measured power condition in a frequency band for all device test positions according to LTE conditions.

The LTE test configurations are measured according to the SAR measurement protocols in this document. This document only specifies the procedures to identify the LTE test configurations that will most likely result in SAR levels closest to the highest, and conservative exposure can be obtained according to procedures in 7.9.3.6.2.

For the preceding reasons, studies on the relationship between RF conducted power and SAR were conducted by IEC TC 106 using DUTs operating in 3GPP LTE bands 1, 4, and 17. The results in Annex W show the following.

– QPSK modulation with 1 RB allocation generally produces the highest psSAR; MPR (maximum power reduction) does not apply in this case.

– psSAR has good correlation with the measured RF conducted output power. The relationship deviates from proportionality by less than 25 % (k = 2).

– For LTE modes with maximum conducted power lower than 85 % of P_{max}, where P_{max} is the highest measured maximum RF conducted output power across all LTE modes in the frequency band, it is highly unlikely that highest SAR results would be expected.

7.9.3.6.2 Description of LTE mode selection

Conducted power shall be measured for the largest channel bandwidth supported by the LTE modes in each frequency band, using QPSK modulation with 1 RB allocation. The required test channels shall be determined according to 7.2.8.

– When the number of required channels is one, the 1 RB shall be allocated at offset = centre.

– When the number of required channels is three, the 1 RB shall be allocated at: i) offset = 0, ii) centre, and iii) maximum within the channel bandwidth.

– When the number of required channels is five, the 1 RB shall be allocated at: i) offset = 0, ii) below centre, iii) centre, iv) above centre, and v) maximum within the channel bandwidth, respectively, for channels from lowest to highest.

Other LTE modes besides “QPSK modulation with 1 RB allocation” shall also be measured for the different channel bandwidth configurations using the modulations and RB allocations specified by 3GPP for conformance testing. MPR settings are found in the appropriate 3GPP documentation.

Conducted maximum output power shall be measured using the following test channel and RB offset configurations.

a) When MPR does not apply, the configurations in Clause W.2 are measured for the low and middle channels with RB offset = 0, and RB offset = maximum for the high channel.

IECNORM.COM : Click to view the full PDF of IEC/IEEE 62209-1528:2020

b) When MPR applies, the configurations in Clause W.3 are measured

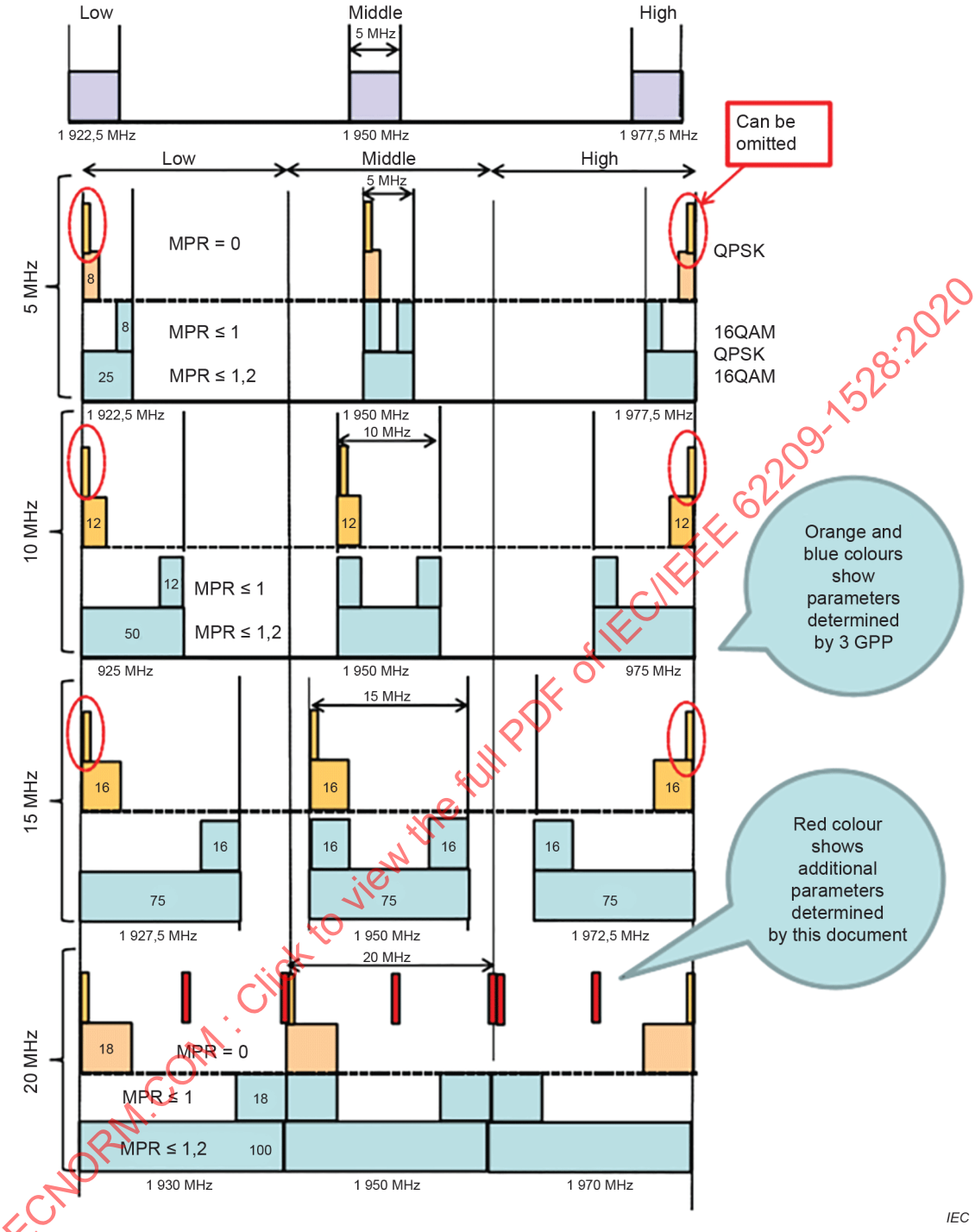
1) for the low channel with RB offset = maximum,
2) for middle channel with RB offset = 0 and maximum,
3) for high channel with RB offset = 0.

For “QPSK modulation with 1 RB allocation” in smaller channel bandwidth configurations, when the same RB offset has already been measured in the highest channel bandwidth, such RB offset configurations may be omitted. These correspond to RBs allocated next to the channel edges; for example, offset = 0 for the low channel and maximum for the high channel, for 5 MHz, 10 MHz, 15 MHz channel bandwidths in Band 1, may be omitted.

The conducted maximum output power measurement conditions are illustrated in Figure 27 for 5 MHz, 10 MHz, 15 MHz, and 20 MHz channel bandwidths in Band 1 (1 920 MHz to 1 980 MHz), and in Figure 28 for 5 MHz and 10 MHz channel bandwidths in Band 17 (704 MHz to 716 MHz). The orange and blue colour RBs correspond to test conditions that are specified by 3GPP for conformance testing. The red colour RBs are the additional configurations required for QPSK and 1 RB allocation in the largest channel bandwidth configuration, not specified for 3GPP conformance testing. The required channels are determined according to 7.2.8.

Conducted power testing for additional LTE modes is allowed, when the results form a superset of the above requirements (e.g. conducted power testing according to FCC requirements). When such a conducted power superset is reported, all results shall be taken into account in the following SAR test procedures.

IECNORM.COM : Click to view the full PDF of IEC/IEEE 62209-1528:2020



IECNORM.COM : Click to view the full PDF of IEC/IEEE 62209-1528:2020

Figure 27 – Use of conducted power for LTE mode selection, for Band 1 (1 920 MHz to 1 980 MHz) (MPR values are in dB)

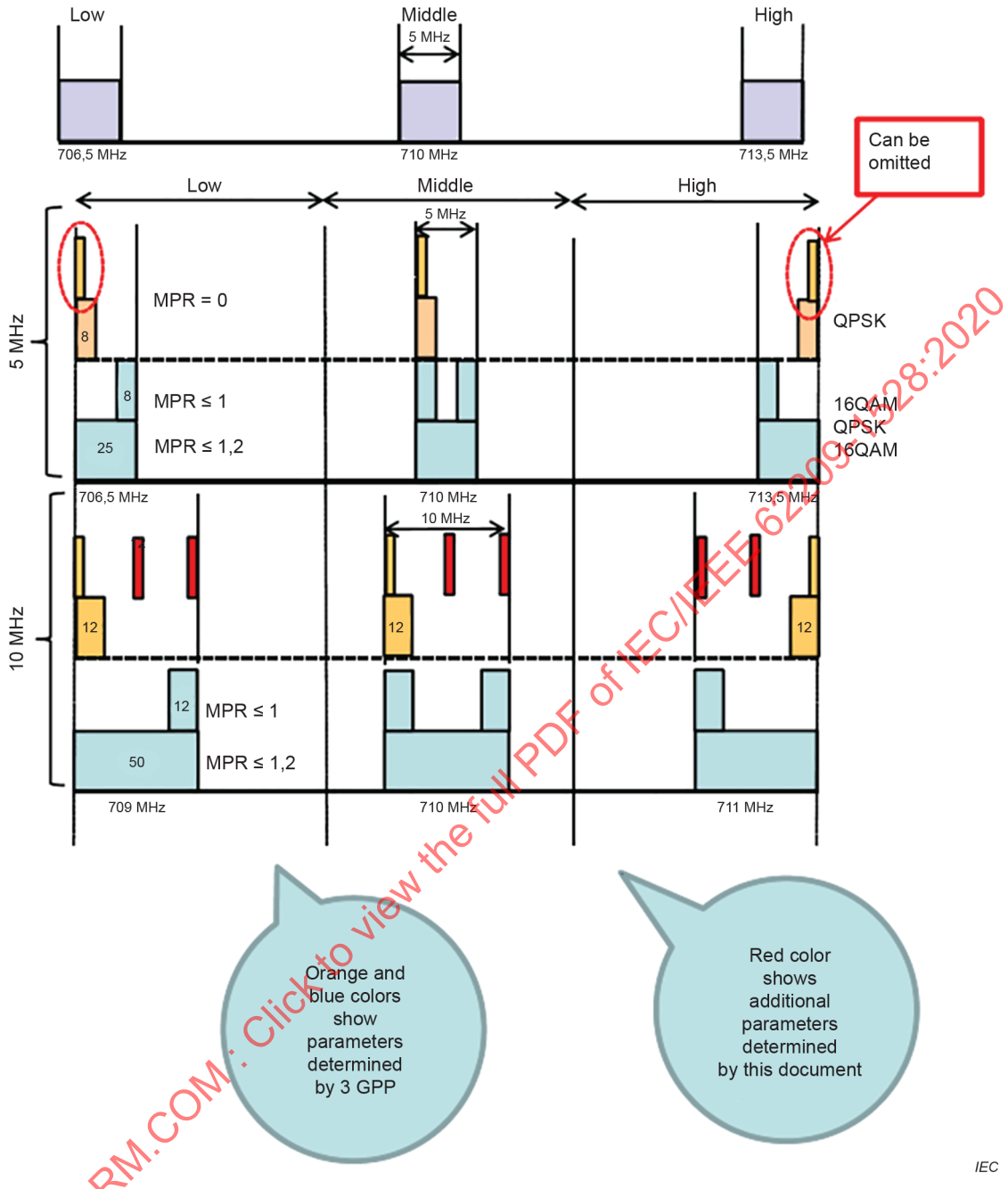


Figure 28 – Use of conducted power for LTE mode selection, for Band 17 (704 MHz to 716 MHz) (MPR values are in dB)

IECNORM.COM : Click to view the full PDF of IEC/IEEE 62209-1528:2020

7.9.3.6.3 Power and SAR measurement protocol

SAR is tested at the highest conducted output power LTE mode for all device positions in each frequency band, as determined by the power measurement procedures in 7.9.3.6.1. The number of subsequent SAR tests is minimized according to the three alternative approaches described in step 3.

The following measurement protocol is the same in principle as the protocol of 7.3, except that it commences with the LTE mode with the highest conducted power, rather than the centre of the transmit frequency band. The protocol applies if the DUT has the same maximum output power settings regardless of the use condition (e.g. body worn versus voice mode).

a) Step 1 – RF conducted power measurement.

1) RF conducted power measurement shall be performed for all LTE modes specified in 7.9.3.6.2, where $P(m)$ are the measured power for the m LTE modes. The measurement protocol for RF conducted output power is specified in 7.9.3.6.4.

2) The LTE mode with the highest measured maximum conducted output power in each frequency band is identified as P_{max}.

3) The subset of LTE modes in a frequency band with measured power greater than or equal to 85 % of P_{max} is identified as S.

b) Step 2 – SAR measurement for the LTE mode generating maximum RF conducted power (P_{max}) and device position causing maximum SAR.

SAR measurement shall be performed for all device positions for the LTE mode with maximum RF conducted power (P_{max}) to determine the device position with the highest psSAR, identified as SAR_{step2}.

c) Step 3 – The following three approaches can be applied to determine the highest psSAR.

1) Approach 1 (AP1) – Select the SAR measurement at device position causing maximum SAR for step 2.

– For the test position corresponding to SAR_{step2}, multiply by α_{95} to yield the scaled highest psSAR, identified as AP1 SAR_{step3}. The factor of α_{95} is the 95th percentile value (mean plus two standard deviations) of the ratio $\alpha(m)$ between SAR and conducted power (Formula (W.1)). A value of α_{95} = 1,35 has been derived in the two studies as described in Annex W. Other factors of α_{95} may be used if justification is given in the test report.

– Approach 1 is a fast method yielding conservative exposure. If maximum SAR results obtained using this approach are above the SAR limit, Approach 2 can be used to obtain more accurate maximum SAR results.

2) Approach 2 (AP2) – SAR measurement at device position causing maximum SAR for LTE modes included in subset S.

– For the test position corresponding to SAR_{step2}, perform SAR measurements in this test position for the other LTE modes included in the subset S. The highest psSAR is identified as AP2 SAR_{step3}.

– Approach 2 is the more accurate method, but requires testing of the LTE modes in each subset S.

3) Approach 3 (AP3) – Limited SAR measurements at device position causing maximum SAR for LTE modes included in subset S.

– For the test position corresponding to SAR_{step2}, perform SAR measurements in this test position for another LTE mode having the highest conducted power among all the untested LTE modes included in the subset S.

– Multiply the measured psSAR by α_{95} to yield the new scaled psSAR, identified as AP3 SAR_{scaled}.

– If AP3 SAR_{scaled} is not below the SAR limit, repeat SAR measurement for the next LTE mode as specified above in this step, otherwise select the highest value among all the measured psSAR results and the last scaled value AP3 SAR_{scaled} and identify it as AP3 SAR_{step3}.

4) SAR_{step3} from AP1, AP2, or AP3 shall be reported as maximum SAR for the LTE frequency band.

NOTE When assessing simultaneous multi-transmission SAR (e.g. LTE + WLAN), the maximum LTE SAR value for each test position obtained using the preceding approaches AP1, AP2, or AP3, or combination of those, are applied according to the simultaneous transmission SAR procedures in this document for this assessment.

IECNORM.COM : Click to view the full PDF of IEC/IEEE 62209-1528:2020

7.9.3.6.4 RF conducted output power measurement for LTE modes

As explained in 7.9.3.6.1, RF conducted output power measurements are used to identify test configurations that are unlikely to produce the highest SAR values for the LTE modes in a frequency band. It is essential to define guidelines for ensuring repeatable and precise RF conducted power measurements for LTE devices. Studies performed by IEC TC 106 [32] showed that the results of such measurements can be affected by the presence or absence of the device charger, and the number of data frames (10 ms for LTE) used for RMS power averaging.

Hence, the following requirements apply to the measurement of conducted output power.

a) The device RF output port shall be connected to the measurement instrument (e.g. power meter) and the cable shall not move during assessment of conducted power for a given frequency band.

b) The device shall be battery powered and no charger shall be connected to the device. Battery shall be fully charged for all power measurements.

c) The same subframe allocation shall be used for power measurements of all LTE modes in a given frequency channel. As an example, measurements for all LTE modes in band 17 could be carried out with the following scheme: only subframe #0 is actively transmitting in each data frame with the remaining nine subframes inactive.

d) The measured RF conducted output power shall be averaged over at least 20 frames.

Conducted power measurement results shall be documented, and measurement uncertainty shall be taken into account. For a given frequency channel and a given LTE mode m, $U[P(m)]$ denotes the relative standard deviation of conducted power measurement results of mode m obtained over at least five repeated measurements. The relative standard deviation is the standard deviation divided by the average $\overline{P}(m)$ across the five measurements.

Conducted output power $P(m)$ for a given LTE mode m at a specified frequency channel is defined as $\overline{P}(m)$. The maximum output conducted power across the m LTE modes is designated as $\max_{m=1:M}\left\{\overline{P}(m)_{\max}\right\}$. $U(P,\ k\ =\ 2)$ denotes the k = 2 uncertainty of conducted power assessment, designated as $\max_{m=1:M}\left\{U\left[P(m)\right]\right\}$. The notation $P(m)$ and $P_{\max}$ is used for simplicity.

8 Measurement uncertainty estimation

8.1 General

The uncertainty budget is applicable to head and body SAR measurement results. The estimate of the measurement repeatability, as verified by the system check procedure, is obtained by omitting the Type B contributions from the uncertainty budget. Table 9 (see 8.3) is an example uncertainty budget for 1 g or 10 g SAR measurement of a DUT or a validation antenna.

Each input quantity is described together with an example of how the associated standard uncertainty is evaluated. These are general examples that might not be applicable to all measuring systems, and additional quantities not addressed in this document can be required in specific cases.

Further information on assessing the uncertainty contributions for system manufacturers and calibration laboratories is given in 8.4.1.1 through 8.4.1.6, 8.4.1.8, 8.4.1.9, and 8.4.2.1.

IECNORM.COM : Click to view the full PDF of IEC/IEEE 62209-1528:2020

The expanded measurement uncertainty is calculated from Formula (20):

$$U = k \cdot u_c(y) \tag{20}$$

A coverage factor of k = 2 is used in this document, corresponding to a 95 % confidence interval. The combined standard uncertainty, $u_c(y)$, is calculated from Formula (21):

$$u_c(y) = \sqrt{\sum_{i=1}^{N} c_i^2 \cdot \left[a(x_i)/q_i\right]^2} = \sqrt{\sum_{i=1}^{N} c_i^2 \cdot u^2(x_i)} = \sqrt{\sum_{i=1}^{N} u_i^2(y)} \tag{21}$$

where

x_i is the estimated value of the i-th input quantity X_i that influences the uncertainty;

y is the value of the output quantity Y that corresponds to the combined uncertainty;

$a(x_i)$ is the uncertainty value of x_i having a probability density function PDF_i;

q_i is the divisor corresponding to the probability density function PDF_i of x_i;

$u(x_i)$ = $a(x_i)$ / q_i is the standard uncertainty of x_i, corresponding to a normal distribution;

c_i is the sensitivity coefficient associated with x_i. It describes how y varies with small changes in x_i. It is calculated as the partial derivative of the model function f with respect to x_i as described in Formula (22):

$$c_i = \partial f / \partial x_i \tag{22}$$

$u_i(y) = c_i \cdot u(x_i)$ is the standard uncertainty of y, corresponding to a normal distribution.

The divisors q_i shall be applied according to the probability density function PDF_i as specified in ISO/IEC Guide 98-3. Table 8 gives divisors for common PDFs.

Table 8 – Divisors for common probability density functions (PDFs)

PDF	Normal	Rectangular	Triangular	U-shape
Divisor q	k	√3	√6	√2

8.2 Requirements on the uncertainty evaluation

The expanded measurement uncertainty, U, is the result of the uncertainty evaluation, specific details of which are recorded in an uncertainty budget. Separate uncertainty budgets shall be evaluated for SAR measurements according to the following.

a) The expanded uncertainty in the measured value of psSAR (1 g or 10 g) shall be assessed in accordance with the guidance and explanations given in ISO/IEC Guide 98-3.

b) The frequency range and measurement conditions for which the uncertainty analysis is valid shall be specified.

c) The reported uncertainty shall represent the maximum expanded uncertainty within this range.

d) The expanded uncertainty in the system check and system validation measurements shall also be evaluated. The uncertainty shall be quoted at the 95 % confidence level, and the expanded uncertainty shall not exceed 30 % of the psSAR value in the range 0,4 W/kg to 10 W/kg. For psSAR values below 0,4 W/kg, the expanded uncertainty shall not exceed 0,12 W/kg (30 % of 0,4 W/kg).

e) Where acceptable by national requirements, if the expanded uncertainty is greater than 30 %, the reported data needs to take into account the percentage difference between the actual uncertainty and the 30 % target value – e.g. see method of [34].

IECNORM.COM : Click to view the full PDF of IEC/IEEE 62209-1528:2020

8.3 Description of uncertainty models

8.3.1 General

The uncertainty models in 8.3 are described in the format of Formula (23):

$$Y = X_1 + X_1 + \cdots + X_N \tag{23}$$

$Y = \Delta SAR$ is the output quantity corresponding to the combined SAR assessment uncertainty. The input quantities X_i are described by the symbols in 8.4. Formula (21) (see 8.1) shall be used to calculate combined standard uncertainty $u_c(y)$.

With reference to the guidelines for uncertainty assessment in ISO/IEC Guide 98-1 [35] and ISO/IEC Guide 98-3, the uncertainty models for the following processes are specified using the symbols described in 8.4.

8.3.2 SAR measurement of a DUT

The measurement uncertainty model formula (model equation) for results of DUT SAR measurements is given by Formula (24).

$$\begin{aligned}\Delta SAR = {} & CF + CF_{\text{drift}} + LIN + BBS + ISO + DAE + AMB + \frac{2}{\delta}\Delta_{xyz} + DAT + LIQ(\sigma) \\ & + LIQ(T_c) + 0{,}25EPS + 2DIS + D_{xyz} + H + MOD + TAS + RF_{\text{drift}} + C(\varepsilon', \sigma) + C(R)\end{aligned} \tag{24}$$

Table 9 shows the uncertainty budget template for DUT psSAR measurement results, as well as descriptions of the symbols used in Formula (24).

8.3.3 System validation and system check measurement

The measurement uncertainty model formula for results of system validation and system check SAR measurements is given by Formula (25).

$$\begin{aligned}\Delta SAR = {} & CF + CF_{\text{drift}} + LIN + ISO + DAE + AMB + \frac{2}{\delta}\Delta_{xyz} + DAT + LIQ(\sigma) \\ & + LIQ(T_c) + 0{,}25EPS + 2DIS + RF_{\text{drift}} + P_{\text{in}} + VAL + C(\varepsilon', \sigma)\end{aligned} \tag{25}$$

Table 9 shows the uncertainty budget template for system validation psSAR measurement results, as well as descriptions of the symbols used in Formula (25).

8.3.4 System check repeatability and reproducibility

The measurement uncertainty model formula for results of system check repeatability and reproducibility SAR measurements is given by Formula (26); symbols are as described in Table 9.

$$\Delta SAR = CF_{\text{drift}} + \frac{2}{\delta}\Delta_{xyz} + LIQ(\sigma) + LIQ(T_c) + 0{,}25EPS + 2DIS + RF_{\text{drift}} + P_{\text{in}} + C(\varepsilon', \sigma) \tag{26}$$

8.3.5 Fast SAR testing (relative measurement)

The measurement uncertainty model formula for results of fast SAR (relative) measurements is given by Formula (27); symbols are as described in Table 9.

IECNORM.COM : Click to view the full PDF of IEC/IEEE 62209-1528:2020

$$\Delta SAR = LIN + ISO + DAE + AMB + \frac{2}{\delta}\Delta_{xyz} + DAT + 2DIS + H + D_{xyz} + MOD + RF_{\text{drift}} \quad (27)$$

Table 9 – Uncertainty budget template for evaluating the uncertainty in the measured value of 1 g or 10 g psSAR from a DUT or validation antenna (N = normal, R = rectangular)

Symbol	Input quantity X_i (source of uncertainty)	Ref.	Prob. Dist.[a] PDF_i	Unc. $a(x_i)$	Div.[a] q_i	$u(x_i) = a(x_i)/q_i$	c_i	$u(y) = c_i \cdot u(x_i)$	v_i
Measurement system errors									
CF	Probe calibration	8.4.1.1	N (k = 2)		2		1		∞
CF_{drift}	Probe calibration drift	8.4.1.2	R		√3		1		∞
LIN	Probe linearity and detection limit	8.4.1.3	R		√3		1		∞
BBS	Broadband signal	8.4.1.4	R		√3		1		∞
ISO	Probe isotropy	8.4.1.5	R		√3		1		∞
DAE	Other probe and data acquisition errors	8.4.1.6	N		1		1		∞
AMB	RF ambient and noise	8.4.1.7	N		1		1		∞
Δ_{xyz}	Probe positioning errors	8.4.1.8	N		1		$2/\delta$		
DAT	Data processing errors	8.4.1.9	N		1		1		∞
Phantom and device (DUT or validation antenna) errors									
$LIQ(\sigma)$	Measurement of phantom conductivity(σ)	8.4.2.1	N		1		c_ε, c_σ		∞
$LIQ(T_c)$	Temperature effects (medium)	8.4.2.2	R		√3		c_ε, c_σ		∞
EPS	Shell permittivity	8.4.2.3	R		√3		see 8.4.2.3		∞
DIS	Distance between the radiating element of the DUT and the phantom medium	8.4.2.4	N		1		2		∞
D_{xyz}	Repeatability of positioning the DUT or source against the phantom	8.4.2.5	N		1		1		5
H	Device holder effects	8.4.2.6	N		1		1		
MOD	Effect of operating mode on probe sensitivity	8.4.2.7	R		√3		1		∞
TAS	Time-average SAR	8.4.2.8	R		√3		1		∞
RF_{drift}	Variation in SAR due to drift in output of DUT	8.4.2.9	N		1		1		
VAL	Validation antenna uncertainty (validation measurement only)	8.4.2.10	N		1		1		
P_{in}	Uncertainty in accepted power (validation measurement only)	8.4.2.11	N		1		1		
Corrections to the SAR result (if applied)									
$C(\varepsilon',\sigma)$	Phantom deviation from target (ε',σ)	8.4.3.1	N		1		1		
$C(R)$	SAR scaling	8.4.3.2	R		√3		1		
$u(\Delta SAR)$	Combined uncertainty								
U	Expanded uncertainty and effective degrees of freedom						U =		v_{eff} =

[a] Other probability distributions and divisors may be used if they better represent available knowledge of the quantities concerned.

IECNORM.COM : Click to view the full PDF of IEC/IEEE 62209-1528:2020

8.4 Parameters contributing to uncertainty

8.4.1 Measurement system errors

8.4.1.1 Probe calibration

CF – Calibration uncertainty for the sensitivity of the SAR probe in the phantom, obtained from the calibration certificate. A protocol for the evaluation of the SAR probe calibration coefficients and the uncertainty estimation is given in Annex E.

8.4.1.2 Probe calibration drift

CF_{drift} – Drift in *CF* during the calibration interval, estimated from the probe calibration history, knowledge of similar probes, or manufacturer's specifications.

8.4.1.3 Probe linearity and detection limit

LIN – Change in probe sensitivity as a function of applied SAR for CW signals between the measured SAR and the level at which the probe was calibrated. The probe linearity and detection limit errors, measured according to Clause O.1 over the range of at least 0,12 W/kg to 100 W/kg, are given in the probe calibration certificate or manufacturer's specifications.

8.4.1.4 Broadband signal

BBS – Uncertainty due to the variable response of the probe as a function of frequency. This term is negligible for measurement of narrowband signals. Otherwise, it shall be calculated as specified in Clause O.2.

8.4.1.5 Probe isotropy

ISO – Change in sensitivity of the SAR probe due its rotation and inclination relative to the field vector being measured. It is usually given in the calibration certificate, or from manufacturer's specifications as axial isotropy (change in sensitivity as the probe is rotated about its axis) and hemispherical isotropy (change in sensitivity as the probe is rotated about its axis and inclined with respect of the field vector). The isotropy of the probe shall be measured according to the protocol specified in Clause E.4. During the measurements, the probe axis is maintained within a specified angle to the normal of the phantom surface, in order to limit the isotopy errors (Table 3 and Table 4). An empirical approximation for the total isotropy error for this case is given by Formula (28):

$$ISO = \sqrt{0{,}5\mu_{\text{axial}}^2 + 0{,}5\mu_{\text{hemispherical}}^2} \tag{28}$$

and a rectangular probability distribution shall be used.

8.4.1.6 Other probe and data acquisition errors

DAE – Other probe and data acquisition errors, including spatial resolution (fast SAR testing), sensor offset distance, probe integration-time and response-time (Clause O.6), boundary effects and corrections (Clause O.3), and data acquisition errors (Clause O.4), which are given in manufacturer's specifications.

8.4.1.7 RF ambient noise and reflections

AMB – The effects of ambient RF signal and system noise levels as well as reflections are assessed by performing a SAR measurement without the DUT transmitting. This document specifies that the results shall be less than or equal to 0,012 W/kg (i.e. 3 % of 0,4 W/kg). It is not necessary to check RF ambient noise prior to each SAR test, provided the laboratory can demonstrate that there are no new RF sources. The procedure to evaluate the contributions of the ambient noise and reflections to the uncertainty is given in Clause R.1.

IECNORM.COM : Click to view the full PDF of IEC/IEEE 62209-1528:2020

8.4.1.8 Probe positioning errors

Δ_{xyz} – Error in the position of the probe tip relative to the surface of phantom shell over the volume used for the calculation of 1 g or 10 g SAR. The uncertainty is obtained from manufacturer's specifications, or by measuring the probe tip position and separation from the phantom shell at several points within the scan volume and comparing these to the requested positions. In the case of the flat phantom, this assessment shall include the effect of sag of the bottom of the tank. The positional tolerance shall be ≤ 0,2 mm. Because the SAR decays with distance from the phantom surface as $e^{-2x/\delta}$, the sensitivity coefficient c_i is approximately $2/\delta$, where δ is the penetration depth in the phantom in mm. Details are given in Clause O.7. Since $N \geq 96$ measurement positions are used to determine the 1 g or 10 g SAR, the Type A contributions associated with the scanning system repeatability will be reduced by $\sqrt{N}$.

8.4.1.9 Data processing errors

DAT – Error resulting from calculation and data processing algorithms used in the measurement software for the 1 g or 10 g averaged SAR calculated from a limited number of spatial samples. The errors include those due to extrapolation and interpolation. The error magnitude is assessed by the manufacturer or software supplier using a set of test functions. Details are given in Clause O.8.

8.4.2 Phantom and device (DUT or validation antenna) errors

8.4.2.1 Measurement of phantom conductivity

$LIQ(\sigma)$ – Error in the measurement of phantom conductivity using the dielectric properties measurement techniques specified in Annex H, normally obtained from the system vendor. The procedure is specified and an example uncertainty table is given in Clause O.9.

8.4.2.2 Temperature effects

$LIQ(T_c)$ – Error due to a temperature variation ΔT of the phantom between the dielectric properties measurement and the SAR measurement.

For each phantom recipe, the temperature coefficient T_c (°C) of ε' and σ at the frequency of interest should be estimated from measurements with the tissue-equivalent medium at different temperatures from 18 °C to 25 °C, and measured to an accuracy of 0,1 °C.

The error due to the temperature variation of ΔT is then calculated from Formula (29):

$$LIQ(T_c) = \Delta T \times \left\{0{,}25\left|T_c(\varepsilon')\right| + 0{,}75\left|T_c(\sigma)\right|\right\} \tag{29}$$

where the weighting factors are obtained from consideration of the correction formulas of O.9.6. The value of ΔT shall not exceed 2 °C.

8.4.2.3 Shell permittivity

EPS – Tolerance in the real relative permittivity of the shell relative to $\varepsilon' = 4$ is calculated from Formula (30):

$$EPS = \frac{\Delta\varepsilon'}{\varepsilon'} = \frac{\left|\varepsilon' - 3{,}5\right|}{3{,}5} \tag{30}$$

IECNORM.COM : Click to view the full PDF of IEC/IEEE 62209-1528:2020

The actual relative permittivity shall lie in the range 2 to 5 for head phantoms, and 3 to 5 for body phantoms. Within this range, and for frequencies greater than 3 GHz, a 25 % change in ε' yields an approximately 5 % change in 1 g or 10 g averaged SAR, so a sensitivity coefficient c_i = 0,25 shall be used. For frequencies up to 10 GHz, the change in psSAR increases to 10 %. For frequencies of 3 GHz and below, the error due to the shell permittivity is negligible. For the uncertainty of the psSAR due to the shell permittivity, the following sensitivity coefficient c_i shall be applied as described in Formula (31):

$$c_i = \begin{cases} 0 & f \le 3\ \text{GHz} \\ 0{,}25 & 3\ \text{GHz} < f \le 6\ \text{GHz} \\ 0{,}5 & 6\ \text{GHz} < f \le 10\ \text{GHz} \end{cases} \tag{31}$$

Further information can be found in [36].

8.4.2.4 Distance between DUT and tissue-equivalent medium

DIS – Uncertainty in the separation distance between the radiating element within the DUT and the tissue-equivalent medium. The separation d of the current source to the phantom is the sum of the spacer thickness, the shell thickness, the sag, and the 5 mm default distance from the radiating element to the surface of the DUT. This distance can be changed to reflect the actual distance if available.

The sag in the bottom of the flat phantom when filled with the required depth of tissue-equivalent medium (sag) can be assessed by placing a straight edge such as a metal ruler under the shell. For the head phantom, the sag is usually insignificant and can be assumed to be zero.

The resulting distance error, DIS, is then calculated from Formula (32):

$$DIS = \frac{\Delta d}{d} = \frac{1}{d}\sqrt{\left(\Delta_{\text{spacer}}\right)^2 + \left(\Delta_{\text{thickness}}\right)^2 + \left(sag\right)^2} \tag{32}$$

where $\Delta_{\text{thickness}}$ is obtained from the manufacturer's specifications for the tolerance of the shell thickness, and shall be less than 0,2 mm. Because the SAR in the phantom decays as approximately d^2, a sensitivity coefficient of 2 shall be applied.

8.4.2.5 Positioning repeatability

D_{xyz} – Error in SAR measurements due to the deviation of the DUT position from the nominal position. It is assessed by performing at least five repeated 1 g or 10 g SAR measurements while repositioning the DUT in the holder after each measurement. This error may be assessed for a group of DUTs having very similar shape (form factors), dimensions, and SAR distributions, provided that at least six different devices are tested and each is repositioned five times with half the measurements being in the cheek position and half being in the tilt position. Where a database of such tests is maintained for a particular device holder, it is recommended that this is updated yearly in order to account for DUT design changes. Details are given in Clause R.2.

8.4.2.6 Device holder effects

H – Change in the 1 g or 10 g SAR caused by the device holder. This depends on the DUT. The error shall be assessed by performing 1 g or 10 g SAR measurements with the DUT in contact with the phantom: a) with the DUT in the device holder, and b) with the DUT supported by a polystyrene block. A device holder uncertainty can be attributed to a generic device type provided that the variability between a sample of at least six of these devices is assessed, and an additional Type A uncertainty term is added to account for this variability. Details are given in Clause R.2.

IECNORM.COM : Click to view the full PDF of IEC/IEEE 62209-1528:2020

8.4.2.7 Signal modulation

MOD – Probe measurement error due to the operating mode of the DUT. This occurs when the probe detectors do not yield the RMS value of the modulated signal emitted by the DUT. Where the uncertainty for a particular modulation scheme is not provided by the probe manufacturer, this shall be assessed in accordance with the procedure given in Clause R.3.

8.4.2.8 Time-average SAR

TAS – The uncertainty related to time-period averaged SAR assessment is due to the sampling rate of the measurement. A fast sampling rate will allow the SAR measurement system to accurately capture fast changes in the signal amplitude or duty cycle over the averaging time, allowing accurate calculation of the TX factor (details are given in Clause R.4).

8.4.2.9 Variation of SAR due to drift

RF_{drift} – Change in the SAR at a fixed position within the phantom due to drift in the RF output of the DUT during the SAR measurement sequence (7.2.4). Where the drift is greater than 5 %, additional stability measurements of the DUT shall be made (Clause R.5), and corrections may be applied to the SAR measurement data to compensate for this variation. If such corrections are applied, RF_{drift} may be omitted from the uncertainty analysis.

8.4.2.10 Validation antenna uncertainty

VAL – Error arising from deviation of the physical validation antenna from that used to derive the reference values, including the accepted power, power losses and dimensions (Annex S).

8.4.2.11 Uncertainty in accepted power

P_{in} – Error in the power accepted by the validation antenna.

8.4.3 Corrections to the SAR result (if applied)

8.4.3.1 Phantom deviation from target dielectric properties

$C(\varepsilon',\sigma)$ – Correction given in 7.8 is applied to the 1 g or 10 g SAR to correct for deviations of the phantom target properties from those specified in this document. The mean tolerance of this correction, specified as the square root of the mean of the squared differences between the SAR deviation predicted by the formulas and the simulated deviations, is shown in Table 10 for the 1 g psSAR and the 10 g psSAR. Table 10 shows how the uncertainty increases as the maximum allowable values of $\Delta\varepsilon'$ and $\Delta\sigma$ increase. It has also been shown that these corrections are valid for realistic DUT models [28], [29].

Table 10 – Uncertainty of Formula (8) (see 7.8.2) as a function of the maximum change in permittivity or conductivity

Max. tolerance for ε or σ	Standard uncertainty for 1 g SAR, %	Standard uncertainty for 10 g SAR, %
±5 %	1,2	0,97
±10 %	1,9	1,6

8.4.3.2 SAR scaling

$C(R)$ – Error in the power ratio R used to determine the SAR from a DUT based on measurements made with the device transmitting a different mode and or power (7.2.3.2). If the signal envelopes of the two operating modes are the same, this error corresponds to the linearity of the power measurement device used. Where the envelopes are different, the effect on the sensitivity of the power meter shall also be included. The error should not exceed 5 %.

IECNORM.COM : Click to view the full PDF of IEC/IEEE 62209-1528:2020

The uncertainty may be evaluated by measuring the SAR from the DUT at the location of the psSAR in both modes/power levels and comparing the ratio obtained with R. In this case a rectangular probability distribution should be used. Details are specified in Clause R.6.

9 Measurement report

9.1 General

All test results shall be recorded in a measurement report and shall include all the information necessary for the interpretation of the DUT configurations tested, calibration performed and all information required by the method and instrumentation used.

A measurement report, compliant with ISO/IEC 17025 [17] and including as a minimum the items listed below, shall be used demonstrate compliance with the requirements of this document.

9.2 Items to be recorded in the measurement report

All of the information needed for performing repeatable tests, calculations, and measurements giving results within the required calibration and uncertainty limits, shall be recorded. The measurement report shall include the following items.

a) General introduction
   1) Identification of the test laboratory.
   2) Identification of the DUT including hardware and software revision numbers, serial number, e.g. IMEI (international mobile equipment identity).
   3) Compliance requirements, e.g. test standards, guidelines, recommendations, etc.
   4) Exposure limits applicable, e.g. ICNIRP, IEEE/ICES, etc.
   5) A list of any accreditations provided by national or international bodies to perform testing in accordance with the standards listed in a) 3). This shall include the date of expiry.

b) Measurement system (for SAR measurement, and fast SAR testing if used)
   1) Measurement system main components descriptions, including positioner, tissue-equivalent medium, readout electronics, device holder, phantom(s), and any other relevant components.

      For the probe(s) used, include dimensions, isotropy, spatial resolutions, dynamic range, and linearity.
   2) Calibration data for relevant components, including fast SAR testing system critical components, e.g. probe calibration certificates, shall be provided in the measurement report.
   3) Description of the interpolation and extrapolation algorithms used in the area scans and/or zoom scans shall be documented in the measurement report.
   4) Tissue-equivalent media and materials used and characteristics.

      For each tissue-equivalent medium or material used, include:

      i) dielectric properties for each frequency band;
      ii) deviation from target value;
      iii) tissue-equivalent medium temperature;
      iv) composition summary of the tissue-equivalent media.
   5) Results of system check:

      i) measurement results for each frequency band;
      ii) deviation from the SAR target value;
      iii) radiating source description.

IECNORM.COM : Click to view the full PDF of IEC/IEEE 62209-1528:2020

c) Uncertainty estimation (system check for SAR measurement, system validation, and fast SAR testing if used)

1) To include measurement uncertainty values from Clause 8 and Annex C.

2) Any other relevant items.

d) Device and test details

1) Description of the form factor of the DUT and a brief description of its intended function.

2) Description of the positions and orientations tested, including photos, and rationale for any test reductions. If any offset in the DUT position (in accordance with 6.5), then this shall also be documented.

3) Description of the available and tested antenna(s) and accessories, including batteries.

4) Description of the available and tested operating modes, power levels, and frequency bands; and rationale for any test reductions.

5) Testing environmental condition, e.g. temperature.

6) Results of all tests performed (psSAR value for each test, and graphical representation of the coarse scans with respect to the device for the maximum SAR value of each operating mode) and details on scaling of the results.

e) The measurement report shall include the following information relevant to the validation of the SAR measurement method.

1) Description of the validation procedure(s).

2) Results of the computations, measurements, and/or other assessments performed by the method developer (e.g. system manufacturer) in order to validate the SAR measurement method.

3) Additional analyses or conditions imposed by the method developer and applied by the user to satisfy the SAR measurement method if applicable.

4) Radiating source description and SAR distribution for each frequency band.

5) Operating frequencies, operating modes, device operating configurations, DUT position on the phantom, and SAR distributions for each frequency band specific to the method.

6) SAR results measurement uncertainty.

7) In the case of fast SAR testing, details of any modifications to post-processing algorithms from those implemented for full SAR testing.

f) SAR test reduction reporting

When test reduction procedures are applied during the SAR measurements of a DUT, the measurement report shall include additional information related to the following test reduction alternatives.

1) Test reduction for different operating modes at the same frequency (see 7.9.3.2). The measurement report shall provide a detailed description on how the conditions of 7.9.3.2 have been met.

2) Test reduction based on characteristics of the DUT design (see 7.9.3.3). The measurement report shall include drawings or photographs illustrating the layout and locations of antennas in a DUT, and describing the wireless operating modes applicable to each antenna, to support the test reduction and test exclusion considered.

3) Test reduction based on peak SAR level analysis (see 7.9.3.4). The measurement report shall include a systematic description on how the test reduction protocol 7.9.3.4 was applied for the measurements of the DUT.

4) Test reduction based on simultaneous multi-band transmission considerations (see 7.9.3.5). The measurement report shall include the measured time-averaged output power, and how it meets the threshold power level available, in accordance with Formula (18) and Formula (19).

IECNORM.COM : Click to view the full PDF of IEC/IEEE 62209-1528:2020

g) Measurement report summary (for all fast SAR testing and full SAR testing data)

1) Frequency bands and configurations:

i) list of all operating modes tested;

ii) list of all test configurations assessed.

2) Tabulated SAR values over the testing positions, bands, operating modes, and device configurations.

3) Tabular and graphical results for the highest fast SAR testing value for each operating mode.

4) Results of all full SAR tests performed as a result of 7.4 and 7.5, which include the psSAR value for each required test, and graphical representation of the scans with respect to the device.

5) The values related to the conditions of Formula (13) through Formula (19) shall be documented in the measurement report.

6) A systematic rationale based on 7.9.2 and 7.9.3 for excluding full SAR testing shall be provided.

7) Reference to exposure limits and a statement of compliance, or otherwise a list of the exposure limits and a compliance statement.

h) Proximity sensors reporting

For a DUT requiring SAR testing with active proximity sensor(s), the measurement report shall include all reporting requirements of 7.7. In addition, the measurement report shall include the following.

1) Description of the proximity sensor(s), location(s) in the DUT, the tissue-equivalent media used in the triggering procedures, and any other relevant information.

2) Description of the test set-up for the conducted power measurements (or radiated power measurements, if applicable).

3) Test set-up photos.

4) Tabulated results of sensor triggering distance, sensor coverage, and sensor sensitivity (capacitance/mm as specified by the sensor manufacturer). The triggering points shall also be documented graphically, with the antenna and sensor clearly identified, along with all relevant dimensions.

5) The test set-up that establishes the 1 mm movement related to the triggering distance shall be explained in the measurement report (see 7.7.4).

6) The measured output power or sensor state determined by the test software, within ±5 mm of the triggering points, or until the DUT is touching the phantom, for movements to and from the phantom, shall be tabulated in the report (see 7.7.4). The output power (or sensor state in case of test software usage) versus the DUT to phantom spacing shall also be plotted.

7) The default power level for sensor failure and malfunctioning, including all compliance concerns, shall be fully documented in the report.

8) If the triggering procedures applied varied from the procedures outlined in 7.7, the measurement report shall include the product-specific triggering procedures. It shall also include a description of the proximity sensor triggering conditions in the normal operating mode of the DUT, location of each proximity sensor, applicable transmission mode, and frequency range of the antenna(s) covered by each proximity sensor, and any other information that is required for regulatory approval or deemed relevant for testing the device.

9) If additional SAR tests were required because the measured peak SAR location for the antenna was not within the triggering coverage area, the test configurations for the additional testing shall be clearly described and justified in the measurement report.

i) Time-averaged SAR

1) Description/specifications of the SAR measurement system ability to measure and capture the time-averaging algorithm results, including the minimum response time.

IECNORM.COM : Click to view the full PDF of IEC/IEEE 62209-1528:2020

2) Description of the time-averaging implementation, including the accuracy of the averaging algorithm(s), and minimum response time necessary to properly assess the TX factor.

3) Detailed description of the applicable test mode software, including version number, required to obtain worst case TX factor, if required.

4) Signal characteristics that are controlled/modified by the time-averaging algorithm (e.g. output power, duty factor, modulation, bit rate, etc.).

5) Applicable frequency bands and operating modes.

6) Applicable exposure conditions, test positions, and associated test separation distances.

7) Maximum psSAR evaluation for all applicable modes of operation.

8) TX factor assessment, including output power/SAR measurement plots used to determine the TX factor.

9) Simultaneous transmitter SAR considerations.

10) Repeated TX factor assessment for the worst-case test condition. If more than one time-averaging algorithm implementation is being used by the device for different chipsets (e.g. one for WLAN and one for WWAN), the TX factor assessment shall be repeated for each chipset for the worst-case tested configuration.

11) Mechanism(s) that are in place to prevent the power control algorithm(s) from being altered or accessed by the user.

12) Time-averaged SAR results measurement uncertainty evaluation.

13) Results of the computations, and/or measurements performed in order to validate the measurement system's capability to perform TX factor assessment.

IECNORM.COM : Click to view the full PDF of IEC/IEEE 62209-1528:2020

Annex A
(normative)

SAR measurement system verification

A.1 Overview

Procedures are specified for two levels of SAR measurement system verification:

– system check;
– system validation.

System check provides a fast and reliable test method that can be applied routinely to verify SAR system measurement accuracy. The objective is to ascertain that the SAR system and tissue-equivalent media are acceptable for testing at the operating frequencies of the DUT. The system check test requires a flat phantom (see A.2.2) and a radiating antenna (see A.2.3).

System validation provides a means of system-level validation against the specifications of the SAR system and its components. The test set-up consists of a flat phantom and a system validation antenna (Annex D). This test is performed annually (e.g. after probe calibration), before measurements related to interlaboratory comparison (Annex T), and every time modifications have been made to the system, such as new probes, software changes, or adding different readout electronics or probes.

Since a flat phantom is used, both system check and system validation do not address measurement uncertainty relating to the anthropomorphic SAM phantom (when applicable) and test device positioning variability.

NOTE For measurements made using the anthropomorphic SAM phantom, interlaboratory comparisons (see Annex T) enable SAR measurement reproducibility to be quantified using a reference DUT. The measurements address both data scattering due to the SAM phantom and device positioning uncertainty, which are not included in system check and system validation. The tests can also be used to establish the expected measurement accuracy and uncertainty across various laboratories.

A.2 System check

A.2.1 Purpose

The purpose of the system check is to verify that the measurement system operates within its specifications at the device test frequencies. The system check verifies the measurement accuracy and repeatability of a SAR system before compliance testing; the system check is not a validation of all system specifications. The latter is not required for testing a device, but is mandatory before the system is deployed. The system check detects possible short-term drift and unacceptable measurement errors or uncertainties in the system, such as:

a) incorrect tissue-equivalent medium parameters, or changes in the medium parameters;
b) test system component failures;
c) test system component drift;
d) operator errors in measurement set-up or software parameters;
e) other possible adverse conditions in the system configuration, e.g. RF interference.

IECNORM.COM : Click to view the full PDF of IEC/IEEE 62209-1528:2020

The system check is a complete 1 g or 10 g psSAR measurement in a simplified set-up with a system check antenna (see A.2.3). The system components, software settings, and other procedures in the system check shall be the same as those used for the compliance tests. The system check shall be performed using the same tissue-equivalent medium and probe calibration frequency point as in the compliance tests, and within the valid frequency range of the probe calibration, tissue-equivalent medium dielectric properties, and antenna return loss required for the SAR measurements. The system check shall be performed at a chosen fixed frequency that is within the validity of the calibration conversion factors, and within ±10 % or ±100 MHz of the compliance test mid-band frequency, whichever is greater. Above 6 GHz, the system check test frequency shall be within ±1 GHz of the compliance test mid-band frequency. The environmental requirements for system check tests are specified in 6.1.

The system check shall be performed within 24 hours before the DUT SAR evaluation, and on the same SAR measurement system that is used for the SAR evaluation of the DUT.

The system check acceptance criteria are provided in A.2.6.

A.2.2 Phantom set-up

A flat phantom shall be used with the recommended tissue-equivalent medium for system check and system validation. The specifications for the flat phantom are given in Clause G.3.

For dipole antennas, the feed-point shall be positioned below the centre of the flat phantom (dimensions given in 6.2.4), and the dipole arms shall be aligned with the major or long axis of the phantom (see D.2.1 for dipole specifications). For waveguides, the longer side of the waveguide shall be aligned with the major axis of the phantom. For confined loop antennas (CLA), the device shall be centred below the middle of the flat phantom. For meander dipole antennas, the feed-point shall be positioned below the centre of the flat phantom. For VPIFAs, the feed-point shall be positioned below the centre of the flat phantom, and the ground plane (see Figure D.5) shall be aligned with the major or long axis of the phantom.

A.2.3 System check antenna

The phantom shall be irradiated using an antenna for the required frequency, e.g. a half-wave dipole, CLA, VPIFA, meander dipole, patch antenna, or open-ended waveguide. The system validation antennas (see Annex D) are typically, but not necessarily, used for the system check. A system check antenna shall have good positioning repeatability, mechanical stability, and impedance matching. In the following positioning instructions, a half-wave dipole is used as an example to illustrate system check antenna positioning requirements. Similar instructions shall be applied for other antennas.

A half-wave dipole shall be positioned below the bottom of the phantom and centred with its axis parallel to the longest dimension of the phantom, within ±2°. The distance between the inner surface of the phantom and the dipole feed-point, s, is specified for each test frequency.

For the reference dipoles specified in Clause D.2, a dielectric spacer is used to provide the distance s and spacer mechanical tolerance, as given by the following:

a) s = 15 mm ± 0,2 mm, for 150 MHz ≤ f ≤ 1 000 MHz

b) s = 10 mm ± 0,2 mm, for 1 000 MHz < f ≤ 6 000 MHz

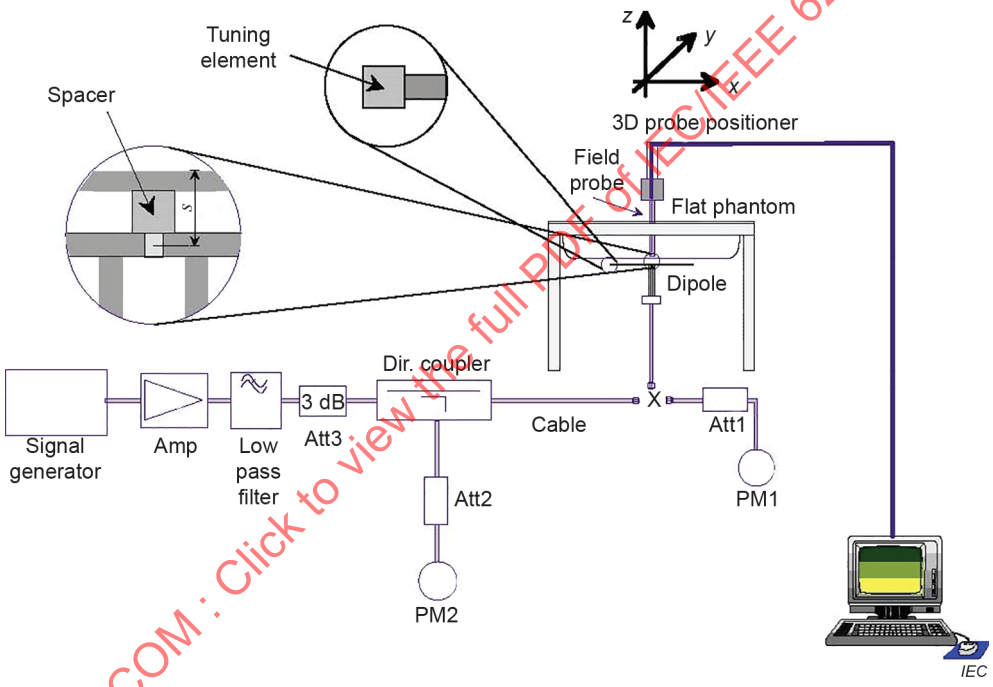
c) s = 5 mm ± 0,1 mm, for 6 000 MHz < f ≤ 10 000 MHz

IECNORM.COM : Click to view the full PDF of IEC/IEEE 62209-1528:2020

A spacer with low loss (loss tangent < 0,05) and low permittivity (relative permittivity < 5) shall be used to establish the correct distance between the top surface of the dipole and the bottom surface of the phantom. Below 3 GHz, the spacer shall not change the measured 1 g and 10 g psSAR by more than 1 %, compared to the no-spacer condition. Above 3 GHz, the spacer could affect the SAR target value of a dipole, and shall be accounted for through additional experimental validation (see NOTE 3 in D.2.2, Table D.2). The dipole shall have a return loss better than 20 dB at the system check test frequency, which shall be measured annually during system validation using a network analyser, to ensure SAR measurement uncertainty due to power reflection remains low.

A.2.4 System check antenna input power measurement

The uncertainty of the power delivered to the antenna shall be as low as possible. This document requires the use of a test set-up with directional couplers and power meters during the system check. The recommended set-up is shown in Figure A.1 (which uses a half-wave dipole as an example of a system check antenna). To limit the power drift during the measurement, automatic input power level control may be implemented, as specified in Annex V.



NOTE This set-up uses a dipole antenna as an example to illustrate system check antenna and measurement configurations. Same or equivalent set-up applies to other antennas.

Figure A.1 – Test set-up for the system check

The input return loss of the system check antenna shall be checked using a network analyser (e.g. during annual performance characterization intervals) to ensure that the return loss is greater than 20 dB. If a different antenna or a waveguide is used where a greater mismatch is inherent to its design (e.g. waveguide specified in Clause D.3), a lower return loss is acceptable only if it has been fully characterized to be stable. The specified return loss shall be determined at the frequency at which the system check is performed.

IECNORM.COM : Click to view the full PDF of IEC/IEEE 62209-1528:2020

The component and instrumentation requirements are as follows.

a) The signal generator and amplifier power outputs shall be stable to within 2 % (after warm-up) of the desired output value. The forward power supplied to the system check antenna shall produce a psSAR of at least 0,4 W/kg. The 1 g or 10 g psSAR range is 0,4 W/kg to 10 W/kg. If the signal generator can deliver 15 dBm or more, an amplifier is generally not necessary if it is connected to the system check antenna with a low loss cable. Some high power amplifiers shall not be operated at a level far below their maximum output power, e.g. a 100 W power amplifier operated at 250 mW output power can be too noisy. An attenuator between the signal generator and amplifier is recommended to protect the amplifier input.

b) The low pass filter inserted after the amplifier reduces the effect of harmonics and noise from the amplifier. For most amplifiers in normal operating ranges, the filter is not necessary.

c) The attenuator after the amplifier improves the matching and the accuracy of the power sensor (consult the power meter manual).

d) The directional coupler (recommended −20 dB coupling coefficient) is used to monitor the forward power for making adjustments to the signal generator output to maintain constant forward power at PM2. The coupler shall have a return loss greater than 25 dB at the input and output ports. A dual directional coupler shall be used when both forward and reflected power need to be measured (e.g. when waveguides are used).

e) The power meter PM2 shall have low drift and a resolution of 0,01 dB; otherwise, the absolute accuracy has negligible impact on the power setting to the system check antenna (absolute calibration is not required).

f) The power meter PM1 and attenuator Att1 shall be high-quality components. These shall be calibrated, preferably together. The attenuator (10 dB) improves the accuracy of the power reading (some high-power heads come with a built-in calibrated attenuator). The exact attenuation of the attenuator at the test frequency shall be known – for some attenuators this can vary by more than ±0,2 dB from the specified value across the frequency band of operation.

g) A fixed power level setting shall be used for PM1 and PM2 to avoid linearity and range switching uncertainties in the power measurements. If power level is adjusted, the same power level setting shall be used for PM1 and PM2.

h) The system check antenna shall be connected directly to the cable at location X. If the power meter has a different connector type, high-quality adapters shall be used.

i) The insertion loss of cables, especially the cable that connects the directional coupler to the antenna, shall be checked periodically to ensure the insertion loss is stable across frequencies. It should be considered that a cable that works well at one frequency (e.g. 900 MHz) might not perform equivalently at a different frequency (e.g. 5 GHz). During system check measurements, all cable movements shall be avoided as this could cause changes to cable loss characteristics and introduce SAR errors.

A.2.5 System check procedure

System check is a complete 1 g and/or 10 g psSAR measurement performed in accordance with the requirements in A.2.1 to A.2.4.

System check antennas may have two pairs of target values:

a) Numerical targets $SAR_{1g,num}$ and $SAR_{10g,num}$ – If the antennas of Annex D are used, the numerical targets provided in Annex D shall be used. Otherwise, the numerical targets shall be determined in accordance with the requirements ofClause D.1.

b) Experimental targets $SAR_{1g,sys}$ and $SAR_{10g,sys}$ – These are measured SAR values of specific system check antennas. They are determined using a system check test set-up (see A.2.4) with calibrated equipment. The experimental targets shall be determined by the calibration laboratory within two weeks of the antenna calibration. $SAR_{1g,sys}$ and $SAR_{10g,sys}$ shall be provided to the user. The values of $SAR_{1g,sys}$ and $SAR_{10g,sys}$ shall not deviate from the numerical targets $SAR_{1g,num}$ and $SAR_{10g,num}$ by more than ±10 %.

IECNORM.COM : Click to view the full PDF of IEC/IEEE 62209-1528:2020

A.2.6 System check acceptance criteria

The measured 1 g and/or 10 g psSAR shall be normalized to 1 W by the input power of the system check antenna (forward power for dipoles, meander dipole, VPIFAs, and CLA, and net power for waveguides). The normalized SAR values, $SAR_{1g,meas}$ and $SAR_{10g,meas}$, are compared against the targets. The following requirements apply.

a) The measured psSAR values shall not deviate from the numerical targets by more than the expanded measurement uncertainty for the system check antennas, $2u_s$, or ±15 %, whichever is less, as described in Formula (A.1) and Formula (A.2).

$$\left|SAR_{1g,meas} - SAR_{1g,num}\right| / SAR_{1g,num} \leq 2 \cdot u_{s,1g} \quad \text{(A.1)}$$

$$\left|SAR_{10g,meas} - SAR_{10g,num}\right| / SAR_{10g,num} \leq 2 \cdot u_{s,10g} \quad \text{(A.2)}$$

b) The measured psSAR values shall not deviate from the experimental targets by more than ±10 %, as described in Formula (A.3) and Formula (A.4).

$$\left|SAR_{1g,meas} - SAR_{1g,sys}\right| / SAR_{1g,sys} \leq 10\ \% \quad \text{(A.3)}$$

$$\left|SAR_{10g,meas} - SAR_{10g,sys}\right| / SAR_{10g,sys} \leq 10\ \% \quad \text{(A.4)}$$

A.3 System validation

A.3.1 Purpose

The system validation procedure tests the SAR system using system validation antennas to verify the measurement accuracy and performance of probe, readout electronics, and system software. It is a validation of the system with respect to all performance specifications. This set-up utilizes a flat phantom, and a system validation antenna as specified in Annex D. Thus, this validation process does not include data scattering and device positioning uncertainty. System validation shall be performed at least annually, when a new system is put into operation, or whenever modifications have been made to the system, such as software updates, using different readout electronics or probes, and after probe calibration. System validation shall be done with a calibrated probe.

The objective of Clause A.3 is to provide a methodology for SAR measurement system validation. Since SAR measurement equipment, calibration techniques, phantoms, and tissue-equivalent media can vary among laboratories, a validation methodology is needed to ascertain that uniform results are obtained within reasonable measurement uncertainties. Numerically calculated reference SAR values for the system validation antennas specified in A.3.3 are listed in Table D.2, Table D.4, Table D.5, Table D.7, and Table D.10. These numerical values have also been validated experimentally. The environmental requirements for system validation tests are as specified in 6.1.

A.3.2 Phantom set-up

The flat phantom set-up specified for the system check (see A.2.2 and Figure A.1) is also used for the system validation tests. The system validation shall be performed using tissue-equivalent media having dielectric properties as specified in Table 2 (see 6.2.2).

A.3.3 System validation antennas

System validation antennas are specified in Annex D.

IECNORM.COM : Click to view the full PDF of IEC/IEEE 62209-1528:2020

A.3.4 Input power measurement

The input power measurement set-up specified for the system check (A.2.4) is also used for system validation tests.

A.3.5 System validation procedure

System validation is used to verify the measurement accuracy of a complete SAR system, including the software algorithms. Test device positioning and phantom shape uncertainties are not considered during system validation. The forward power shall be limited so that the measured SAR values are within the dynamic range of the probe, to avoid probe damage.

The system validation procedure consists of up to seven steps, i.e. the following steps a) to g). Step a) shall be done for each combination of the probe, readout electronics, and measurement and post-processing system version, every time that system validation is required. Tests b) to f) shall be done every time that system components have been modified (e.g. new software release, new readout electronics, new probe or calibrations). Step g) may be omitted if sufficient information is provided by the system manufacturer to the user that the uncertainty budget is valid for capacitively-coupled sources. The system validation procedure is as follows.

a) SAR evaluation: A complete 1 g and/or 10 g psSAR measurement is performed using a system validation antenna as specified in Annex D. The input power of the system validation antenna is adjusted to produce a 1 g and/or 10 g psSAR value within the range of 0,4 W/kg to 10 W/kg. The 1 g and/or 10 g psSAR is measured at the frequencies in Table D.2, Table D.4, Table D.5, Table D.7 and Table D.10. The psSAR results are normalized as specified in Table D.2 (dipole antennas), Table D.4 (waveguides), Table D.5 (CLAs), Table D.7 (meander dipole), or Table D.10 (VPIFAs) and compared with the normalized numerical SAR values The differences between the measured values and the numerical target values shall be less than the expanded uncertainty for the system validation using the procedures of Table 9 but not more than 10 %.

b) Extrapolation routine: Local SAR values are measured along a vertical axis directly above the centre of the system validation antenna (i.e. dipole, meander antenna or VPIFA feed-point, centreline of waveguide, or centre of the CLA) using the same test grid-point spacing as used for the zoom scan of the DUT SAR evaluations. The measured values are extrapolated to the phantom surface and compared to the appropriate numerical target value given in Table D.2 (column 5), Table D.4 (column 5 with d = 0), Table D.5 (column 5), Table D.7 (column 5) and Table D.10 (column 5). If the dipole antenna, meander dipole or VPIFA is used, this measurement is repeated along another vertical axis with a 2 cm transverse offset (y-direction of Figure A.1) from the feed-point. SAR values are extrapolated to the phantom surface and compared with the normalized numerical values given in column 6 of Table D.2, column 6 of Table D.5 and column 6 of Table D.10. The difference between the extrapolated values and the numerical target values given in Table D.2 (or values for the specific antenna used) shall be less than the expanded uncertainty for the system validation using the procedures of Table 9 or 15 %, whichever is less. Note that step b) may be performed at the same time as step a) if an enlarged zoom scan is used in step a) to provide the extrapolated SAR values.

c) Probe linearity for CW equivalent signals: The measurements in step a) are repeated using different input power levels. The power levels are selected for each frequency to produce 1 g or 10 g psSAR values of approximately 10 W/kg, 2 W/kg, 0,4 W/kg and 0,12 W/kg. The measured psSAR values are normalized as specified in the appropriate tables (see step a)) and compared with the normalized measured results in step a). The difference between these values shall be less than the expanded uncertainty for the linearity component using the procedures of Table 9 and 8.4.1.3 or 10 %, whichever is less.

IECNORM.COM : Click to view the full PDF of IEC/IEEE 62209-1528:2020

d) Probe linearity for periodic pulsed signals: This step shall be conducted after step c) requirements are satisfied. The measurements in step a) are repeated with pulse-modulated signals having a duty factor of 0,1 and pulse repetition rate of 10 Hz. The power is adjusted to produce a 1 g or 10 g psSAR of approximately 8 W/kg with the periodic pulse modulated signal or a peak SAR of approximately 80 W/kg. The measured SAR values are scaled to a duty factor of 1, then normalized as specified in the appropriate tables (see step a) and compared with the normalized measured results in step a). The difference between these values shall be less than the expanded uncertainty for system validation using the procedures of Table 9 or 10 %, whichever is less.

e) Probe linearity for non-pulsed signals (e.g. CDMA and OFDM signals): The measurements in step a) are repeated with the specific operating modes that will be tested by the laboratory. This test may be done at just one frequency per operating mode. The power is adjusted to produce a 1 g psSAR of approximately 8 W/kg. If the peak-to-average power ratio of the operating mode is high enough such that the peak local SAR exceeds the dynamic range of the system, the input power should be reduced to produce a 1 g psSAR lower than 8 W/kg but still as high as possible. The measured SAR values are scaled to a duty factor of 1, then normalized as specified in the appropriate tables (see step a) and compared with the normalized measured results in step a). The difference between these values shall be less than the expanded uncertainty for system validation using the procedures of Table 9 or 10 %, whichever is less.

NOTE 1 A more detailed procedure to validate the system for all operating modes is planned for a future revision of this document through an amendment, revision, or accompanying Technical Report. The procedure will include steps to ensure that the bandwidth of the validation source is sufficient to cover the channel bandwidth and any carrier aggregation modes.

f) Probe axial isotropy: The geometric centre of the sensors of the probe is placed directly above the centre of the system validation antenna at a measurement distance of approximately one probe tip diameter from the inner phantom surface. The probe is rotated around its axis ±180° in steps no larger than 15°. The maximum and minimum SAR readings are recorded. The difference between these values shall be less than the expanded uncertainty for the axial isotropy component using the procedures of Table 9 and 8.4.1.5 or 5 %, whichever is less.

g) SAR evaluation for E-field component normal to the phantom surface: A complete 1 g and/or 10 g psSAR measurement is performed using the VPIFAs specified in Clause D.5. The zoom scan for frequencies above 3 GHz specified in 7.4.2 should be used, regardless of the operating frequency of the VPIFA. The results are normalized to 1 W forward power and compared against the numerical reference values in Clause D.5. The purpose of this validation is to test the accuracy of the measurement system using antennas with a dominant normal E-field component. This step tests the system implementation and the probe design for suitability for capacitively coupled fields and can be performed by the manufacturer of the measurement system and need not be repeated by the test laboratory as long the appropriate documentation from the manufacturer is available. The differences between the measured values and the numerical target values shall be less than the expanded uncertainty for the system validation but not more than 10 %.

NOTE 2 The system validation procedure is neither an alternative to probe calibration nor to the uncertainty estimation of Clause 8. The probe and readout electronics are calibrated regularly according to the procedures given in Annex E. Probe hemispherical isotropy is not considered in the protocol for system validation.

For frequencies below 300 MHz, appropriate validation antennas specified in Annex D shall be used to perform system validation procedure.

IECNORM.COM : Click to view the full PDF of IEC/IEEE 62209-1528:2020

A.4 Fast SAR testing system validation and system check

A.4.1 General

Class 1 and Class 2 fast SAR testing methods specified in 7.9.2 are based on assumptions or approximations that are typical of each fast SAR method and that deviate from the standard measurement procedure. For a given SAR measurement system, since fast SAR testing is based on simplifications and approximations specific to each approach, system check and system validation methods required for full SAR testing have been considered insufficient for dealing with 7.9.2 fast SAR methods. New system check and system validation methods are hence introduced.

Subclause A.4.2 describes the system validation that shall be done by the method developer. It defines a set of minimal requirements or principles to be followed by the fast SAR method developer to validate that the method has been implemented correctly. These requirements are also minimum requirements applicable to fast SAR methods specified in Annex C. The developer shall clearly document the computations, measurements and other assessments performed to validate the fast SAR method for users to determine how to apply the specific method for SAR evaluation. Any additional analyses or conditions the user shall satisfy to apply the fast SAR method shall be clearly specified.

Subclause A.4.3 describes the fast SAR method system check the user shall perform. For a given SAR measurement system, a single system check antenna may be used for both full SAR testing and fast SAR testing using the procedures in Clause A.2 and A.4.3.

A.4.2 Fast SAR testing system validation

Fast SAR testing system validation is a way to quantify the validity and reliability of the method. Since the validation and the measurement uncertainty are both determined by the developer of the fast SAR testing method, the system validation serves also as to confirm the uncertainty budget. The following principles are applied for system validation of a Class 2 fast SAR method.

a) Multiple radiators with SAR distributions suitable for validating the method shall be used. The radiators may be wireless DUTs or other antennas or waveguides that comply with the requirements of Clause A.4. Multiple samples (e.g. one sample for each band) can be used for fast SAR testing system validation. The developer shall demonstrate that the fast SAR testing method is not biased by the selected radiators or SAR distributions in validating or calibrating the method to such radiators.

b) The system validation shall be performed over the full range of operating frequencies, operating modes, power levels (e.g. 10 g psSAR between 0,1 W/kg and 10 W/kg), device operating configurations, exposure conditions, and SAR distributions that are specified with the method and used for device evaluation.

c) The radiators chosen shall cover the range of SAR distributions (e.g. distributions with a SAR which is larger than −3 dB of a local maximum within a radius ranging from 5 mm to 50 mm; dominant polarization both normal and parallel to the phantom surface; locations within the measurement area specified for the fast SAR testing method; and number of SAR peaks), supported by the fast SAR testing method. The fast SAR testing method developer shall specify the radiators used to validate the particular fast SAR testing method and provide the necessary validation details to ensure users can apply the method correctly.

d) The radiators shall be chosen so that the measurement uncertainty during system validation is not strongly dependent on or dominated by the radiator (e.g. positioning, uncertainty, or the validation antenna), and phantom configurations.

e) A minimum of 10 configurations shall be tested, per frequency band, so that there is high confidence in the system validation. This could be achieved, for example, by using two radiators at five different distances or orientations.

IECNORM.COM : Click to view the full PDF of IEC/IEEE 62209-1528:2020

System validation protocols and procedures, and validation antennas, for use with vector measurement-based systems are given in IEC 62209-3. The validation guidance in IEC 62209-3 shall be applied for the purposes of testing in accordance with Annex A.

SAR uncertainty for fast SAR testing system validation is determined by comparing the psSAR determined with the fast SAR testing method, $SAR_{\text{fast},i}$ with the target SAR of full SAR testing, $SAR_{\text{full},i}$, for the i-th test configuration (radiator, frequency, SAR distribution). The standard deviation of the difference between the two methods is determined according to Formula (A.5), Formula (A.6), and Formula (A.7):

$$SAR_{\text{tol}}[\%] = \sqrt{\frac{1}{N}\sum_{i=1}^{N}(\Delta_i - \mu)^2} \tag{A.5}$$

$$\Delta_i[\%] = 100 \times \left(\frac{SAR_{\text{fast},i} - SAR_{\text{full},i}}{SAR_{\text{full},i}} \right) \tag{A.6}$$

$$\mu = \frac{1}{N}\sum_{i=1}^{N}\Delta_i \tag{A.7}$$

The system validation shall be applied separately for each frequency band and operating mode supported by the fast SAR testing method, and as used for device evaluation.

The standard deviation of Formula (A.6) shall be within the standard uncertainty of the fast SAR testing method (Table 9 and Annex C). Otherwise, the developer of the fast SAR testing method shall either revise the combined uncertainty of the fast SAR testing method in accordance with the system validation results, or consider whether the fast SAR testing method is applicable.

The fast SAR testing system validation shall be performed when modifications to the fast SAR testing or post-processing algorithms are made. A summary of the developer's system validation methods and results shall be described in the SAR report, to support the test results.

A.4.3 Fast SAR testing system check

A.4.3.1 General

SAR system check is an easy way for laboratories to verify the reliability and consistency of fast SAR testing implemented in a SAR system. The fast SAR testing system check requirements are similar to the system check of full SAR testing, as specified in Clause A.2. The following principles apply for SAR system check.

a) It is applied separately for each frequency band in which components of the system (e.g. probe, tissue-equivalent medium) are different.

b) It shall be performed within 24 hours before fast SAR testing of the DUT.

c) It shall be performed on the same measurement system that is used for the fast SAR testing of the DUT.

d) It is performed using a single system check antenna (either the dipole antennas or waveguides and the set-up specified in Clause A.2, or another well characterized radiator). The fast SAR testing reference value for the radiator shall be determined for the fast SAR testing system check set-up, and a measurement uncertainty budget for the system check shall be provided.

IECNORM.COM : Click to view the full PDF of IEC/IEEE 62209-1528:2020

A.4.3.2 Acceptance criteria for fast SAR testing system check

The fast SAR testing system check measurement result is compared to the fast SAR testing reference value for the same radiator and frequency band. The acceptance criteria are the same as those for the full SAR system check.

a) Measured values, $SAR_{1g,meas}$ and $SAR_{10g,meas}$, are compared to the numerical targets $SAR_{1g,num}$ and/or $SAR_{10g,num}$. The difference is within two standard deviations of the fast SAR method system standard uncertainty u_s as described in Formula (A.8) and Formula (A.9) :

$$\left|SAR_{1g,meas} - SAR_{1g,num}\right| \Big/ SAR_{1g,num} \leq 2 \cdot u_{s,1g} \tag{A.8}$$

$$\left|SAR_{10g,meas} - SAR_{10g,num}\right| \Big/ SAR_{10g,num} \leq 2 \cdot u_{s,10g} \tag{A.9}$$

b) All measured values are within ±10 % of the relative targets $SAR_{1g,sys}$ and $SAR_{10g,sys}$ for that fast SAR testing method measurement system using the system check antenna, and same system or system type as described in Formula (A.10) and Formula (A.11):

$$\left|SAR_{1g,meas} - SAR_{1g,sys}\right| \Big/ SAR_{1g,sys} \leq 10\ \% \tag{A.10}$$

$$\left|SAR_{10g,meas} - SAR_{10g,sys}\right| \Big/ SAR_{10g,sys} \leq 10\ \% \tag{A.11}$$

Otherwise, the fast SAR testing system shall not be used for compliance testing purposes.

IECNORM.COM : Click to view the full PDF of IEC/IEEE 62209-1528:2020

Annex B
(informative)

SAR test reduction supporting information

B.1 General

Annex B provides useful supporting information related to the test reduction procedures described in 7.9.3.

Clause B.2 is related to the test reduction procedure based on characteristics of DUT design, while Clause B.4 deals with the test reduction procedure based on SAR level analysis. Finally, Clause B.5 describes other possible statistical approaches to identify high SAR test configurations. Clause B.5 provides general information rather than detailed procedures. For this reason, the approaches specified in Clause B.5 generally require considerable user input to determine which test configurations could be effectively excluded. In conclusion, it is strongly recommended not to use the statistical approaches specified in Clause B.5 for compliance testing purposes. In principle, they can however be used for early investigation purposes (e.g. pre-compliance during research and development stages).

B.2 Test reduction based on characteristics of DUT design

B.2.1 General

When the first editions of IEEE Std 1528 and IEC 62209 were developed, there were many DUTs with extendable antennas. It was considered that the tilt position could induce a higher SAR in the head in comparison to the touch or cheek position, because tilting the DUT could decrease the separation distance between the extendable antenna and the head. However, the vast majority of the latest DUT designs contain internal antennas. When the antenna is located at the bottom of the DUT, in contrast the tilt position will increase the separation distance between the antenna and the head. In addition, the contributions to the SAR in the head from RF currents that flow on the surface of the DUT will be decreased when the phone is in the tilt position, again because of the increased separation.

B.2.2 Statistical analysis overview

B.2.2.1 Aims and hypothesis

After years of testing, experience has shown that for internal antennas the SAR value in the tilt position is generally lower than the SAR value at cheek in the same test configuration. The aim of the supporting investigation was to conduct a probability analysis of the relationship between the SAR measured in the tilt position versus the cheek position for the same test configurations to ascertain if, and under what conditions, testing in the tilt position could be eliminated.

The hypothesis for this study was that there is a very low probability that the SAR value in the tilt position could exceed the SAR in the cheek position by more than a factor of two, and therefore, the SAR in the tilt position could not exceed the applicable SAR limit, and the device is expected to be compliant with the SAR regulation if the SAR in the cheek position is 3 dB below the applicable SAR limit.

IECNORM.COM : Click to view the full PDF of IEC/IEEE 62209-1528:2020

B.2.2.2 DUTs under analysis

The analysis was undertaken with 139 DUTs from two manufacturers (which were predominantly year 2009 models). The analysis included DUTs with various antenna locations, device types and multiple operating frequency bands. In most cases, both 1 g and 10 g psSAR values were measured, and therefore the total number of SAR measurements used for the analysis was actually larger than the number of DUTs (139). Table B.1 shows the basic characteristics of the DUTs used for the study.

Table B.1 – The number of DUTs used for the statistical study

DUT type	Manufacturer A	Manufacturer B	Total
Total	112	27	139
Top antenna	30	14	44
Bottom antenna	82	13	95
Slider, slide open	29	4	33
Slider, slide closed	58	8	66
Clamshell	23	4	27
Bar	60	19	79

B.2.3 Analysis results

B.2.3.1 Overall analysis results

Subclause B.2.3 shows the result of the statistical analysis with 270 test results including 1 g and 10 g psSAR values of all test devices regardless of DUT types, antenna locations, and manufacturers. Figure B.1 shows the distribution of 'Tilt/Cheek' values for the test devices. The mean and standard deviation values are 0,52 and 0,19, respectively.

Table B.2 shows the probability that the SAR in the tilt position over the SAR in the cheek position is higher than certain values (x) analysed by using normal distribution and cumulative probability analysis, based on mean and standard deviation identified with sample data shown in Figure B.1. While the actual distribution was close to a gamma distribution, the analysis has been undertaken assuming a normal distribution, because this gives an upper bound for the probability function and simplifies the calculation significantly.

The analysis result shows that the probability that the SAR at tilt is higher than twice the SAR at cheek is $4{,}330 \times 10^{-15}$, which can be considered as zero probability. Even the probability that the SAR at tilt is higher than the SAR at cheek is $6{,}057 \times 10^{-3}$, which is still very low probability.

IECNORM.COM : Click to view the full PDF of IEC/IEEE 62209-1528:2020

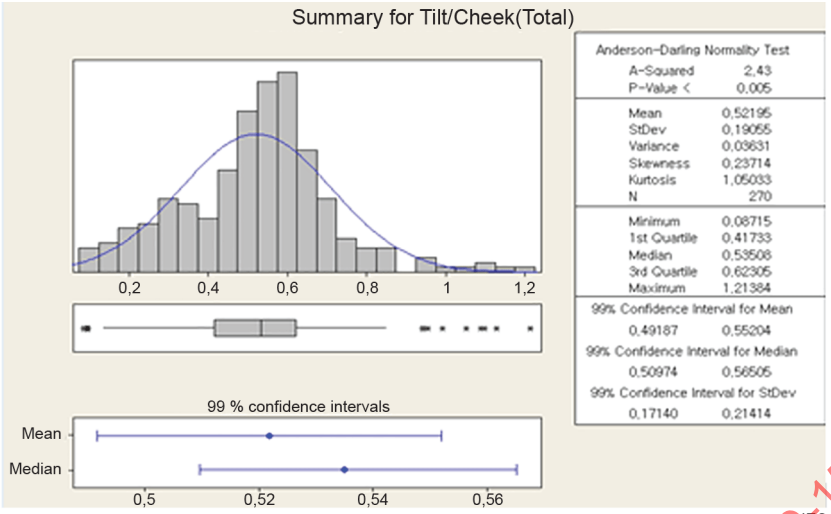


Figure B.1 – Distribution of Tilt/Cheek

Table B.2 – Statistical analysis results of *P*(Tilt/Cheek > *x*) for various *x* values

x	*P*(Tilt/Cheek > *x*)
1,0	$6{,}057 \times 10^{-3}$
1,1	$1{,}208 \times 10^{-3}$
1,2	$1{,}866 \times 10^{-4}$
1,3	$2{,}221 \times 10^{-5}$
2,0	$4{,}330 \times 10^{-15}$

B.2.3.2 Comparison between 10 g and 1 g psSAR

Table B.3 is the analysis result showing the differences between 1 g psSAR and 10 g average SAR. It shows even for 1 g average SAR, the probability that the SAR at tilt is higher than twice the SAR at cheek is $6{,}428 \times 10^{-14}$.

Table B.3 – Statistical analysis results of *P*(Tilt/Cheek > *x*) for 1 g and 10 g psSAR

x	*P*(Tilt/Cheek > *x*)	
	10 g psSAR	1 g psSAR
1,0	$4{,}307 \times 10^{-3}$	$4{,}307 \times 10^{-3}$
1,1	$7{,}122 \times 10^{-4}$	$7{,}122 \times 10^{-4}$
1,2	$8{,}759 \times 10^{-5}$	$8{,}759 \times 10^{-5}$
1,3	$7{,}978 \times 10^{-6}$	$7{,}978 \times 10^{-6}$
2,0	$1{,}110 \times 10^{-16}$	$1{,}110 \times 10^{-16}$

IECNORM.COM : Click to view the full PDF of IEC/IEEE 62209-1528:2020

B.2.3.3 Comparison between DUTs with bottom antenna and top antenna

Table B.4 is the analysis result showing the differences between DUTs with bottom antennas and with top antennas. It shows the probability that the SAR at tilt is higher than twice the SAR at cheek is $5{,}217 \times 10^{-9}$ even for devices with top antennas, which have been considered before to introduce higher SAR value at tilt than at cheek for DUTs with extendable antennas.

Table B.4 – Statistical analysis results of P(Tilt/Cheek > x) for various antenna locations

x	P(Tilt/Cheek > x)	
	Bottom antenna	Top antenna
1,0	$1{,}718 \times 10^{-3}$	$3{,}725 \times 10^{-2}$
1,1	$2{,}095 \times 10^{-4}$	$1{,}472 \times 10^{-2}$
1,2	$1{,}815 \times 10^{-5}$	$5{,}062 \times 10^{-3}$
1,3	$1{,}112 \times 10^{-6}$	$1{,}511 \times 10^{-3}$
2,0	0,0 [a]	$5{,}217 \times 10^{-9}$

[a] This number is below the numerical precision of the computer used to perform statistical analysis.

B.2.3.4 Comparison among frequency bands

Table B.5 is the analysis result showing the differences among operating frequency bands. It shows the probability that the SAR at tilt is higher than twice the SAR at cheek is $3{,}492 \times 10^{-7}$ even for higher frequency bands.

Table B.5 – Statistical analysis results of P(Tilt/Cheek > x) for various frequency bands

x	P(Tilt/Cheek > x)			
	850 MHz	900 MHz	1 800 MHz	1 900 MHz
1,0	$7{,}638 \times 10^{-3}$	$4{,}578 \times 10^{-3}$	$6{,}536 \times 10^{-2}$	$1{,}920 \times 10^{-2}$
1,1	$1{,}526 \times 10^{-3}$	$6{,}350 \times 10^{-4}$	$3{,}170 \times 10^{-2}$	$7{,}076 \times 10^{-3}$
1,2	$2{,}334 \times 10^{-4}$	$6{,}172 \times 10^{-5}$	$1{,}385 \times 10^{-2}$	$2{,}283 \times 10^{-3}$
1,3	$2{,}721 \times 10^{-5}$	$4{,}180 \times 10^{-6}$	$5{,}442 \times 10^{-3}$	$6{,}435 \times 10^{-4}$
2,0	$3{,}331 \times 10^{-15}$	$0{,}000 \times 10^{0}$	$3{,}492 \times 10^{-7}$	$1{,}839 \times 10^{-9}$

B.2.3.5 Comparison among device types

Table B.6 is the analysis result showing the differences among device types. It shows the probability that the SAR at tilt is higher than twice the SAR at cheek is very low, regardless of device types.

IECNORM.COM : Click to view the full PDF of IEC/IEEE 62209-1528:2020

Table B.6 – Statistical analysis results of P(Tilt/Cheek > x) for various device types

x	P(Tilt/Cheek > x)			
	Bar	Clamshell	Slide (open)	Slide (closed)
1,0	$6{,}853 \times 10^{-3}$	$2{,}992 \times 10^{-8}$	$5{,}441 \times 10^{-4}$	$1{,}771 \times 10^{-3}$
1,1	$1{,}334 \times 10^{-3}$	$3{,}769 \times 10^{-10}$	$2{,}138 \times 10^{-5}$	$1{,}739 \times 10^{-4}$
1,2	$1{,}982 \times 10^{-4}$	$2{,}801 \times 10^{-12}$	$4{,}385 \times 10^{-7}$	$1{,}131 \times 10^{-5}$
1,3	$2{,}240 \times 10^{-5}$	$1{,}221 \times 10^{-14}$	$4{,}658 \times 10^{-9}$	$4{,}844 \times 10^{-7}$
2,0	$1{,}998 \times 10^{-15}$	$0{,}000 \times 10^{0}$	$0{,}000 \times 10^{0}$	$0{,}000 \times 10^{0}$

B.2.4 Conclusions

As a result of statistical analysis with the latest DUT designs and models (i.e. as of 2009), the probability that the SAR at tilt is higher than the SAR at cheek is very low and very close to zero, which means the SAR at tilt is most likely never higher than the applicable SAR limit if the SAR at cheek is 3 dB lower than the SAR limit. This approach will ensure that the handsets are within the respective SAR limits, but does not ensure that the maximum SAR will be measured. Therefore if the main goal is to show compliance with the respective SAR limit, the requirement for the testing of DUTs in the tilt position can be excluded under the conditions reported in 7.9.3.3.

B.2.5 Expansion to multi-transmission antennas

The analysis for this study has used hand-held devices with a single transmitting antenna. However the conclusion can also be applied to hand-held devices with multiple transmitting antennas. SAR measurement method applicable to DUTs with multiple transmitting antennas is based on summation of SAR distributions from each transmitting antenna. Therefore, it can be concluded that the SAR at tilt even with multiple transmitting antennas is not higher than twice of SAR at cheek with the same antennas, where the SAR at tilt or cheek is calculated by summing SAR distributions from multiple transmitting antennas.

B.3 Test reduction based on analysis of SAR results on other signal modulations

B.3.1 General

When the first editions of IEEE Std 1528 and IEC 62209 were developed, DUTs typically used only one operating mode per frequency band. The standardized test procedure required each operating mode for a given frequency band to be fully tested. Current generation DUTs now have several operating modes in use for a given frequency band, e.g. GSM/GPRS, CDMA, WCDMA (3G), LTE (4G) and 5G NR. Therefore, the amount of testing for each frequency band has increased considerably. It is expected that this trend will continue for future DUTs, unless test reduction procedures can be applied.

Generally, signal modulation will have little effect on the SAR distribution if all signals are transmitted using the same antenna, antenna feed-point, and matching circuit (see full list of requirements in at the end of B.3.1). This is also true concerning the currents on the body of the transmitting device, because the same antenna excites the same currents regardless of the signal modulation used.

It is usually enough to fully measure one signal modulation, mod_X, in all positions/configurations, then the other signal modulations mod_Y, mod_Z, etc., in the position/configuration giving highest psSAR result for the signal modulation mod_X. The preceding consideration applies if the following parameters are the same for all the transmitted signal modulations:

IECNORM.COM : Click to view the full PDF of IEC/IEEE 62209-1528:2020

- frequency band;
- frequencies of the required test channels;
- antenna radiating element;
- antenna feed-point;
- antenna grounding;
- antenna matching circuitry (if any);
- antenna tuner and tuner settings (if any).

If the design of the phone is not sufficiently known, i.e. it is not known if the preceding conditions are met, then test reductions cannot be applied and full SAR testing should be performed for all signal modulations.

B.3.2 Analysis results

Studies described in B.3.2 and [37] provide the rationale for performing the SAR measurement for other signal modulations mod_Y, mod_Z, etc., at the same position/configuration yielding the maximum psSAR level for signal modulation mod_X. For example, if the left cheek position yields the highest psSAR value for GSM transmission, the left cheek position will typically generate the highest psSAR value for other modulations such as WCDMA and LTE operating within the same frequency band.

Minor deviations from this rule can be explained by the measurement uncertainties associated with testing. For instance, a shift in the maximum SAR value from the left cheek position to the right cheek position when the SAR distribution is highly symmetrical along the phone's vertical axis will be dependent on the positioning accuracy. Deviations are often seen in cases where the SAR levels for both cheek and tilt positions are very low (less than 0,4 W/kg). This is due to decreasing sensitivity of the measurement system, which introduces noise to the measurement results.

To decrease the possibility of not obtaining the maximum psSAR value of a DUT, a psSAR value threshold was included in the test reduction procedure (7.9.3.4) of this document. Namely, if the maximum psSAR values were obtained at the cheek positions and the psSAR values for the tilt positions are at least 30 % below the applicable SAR limit for the signal modulation mod_X, measurements for the tilt positions are not required for other signal modulations within the same frequency band.

The analysed data consist of a total of 181 DUT and frequency band combinations. The DUT models with multiple operating modes within the same frequency band were selected from different manufacturers. The data consisted of a total of 115 DUTs and frequency band combinations operating below 1 GHz, and 66 DUT and frequency band combinations operating above 1 GHz, altogether representing a total of 181 cases.

The data were divided into two categories, because handsets operating below 1 GHz have higher electromagnetic fields from RF currents flowing along the chassis of the device, while for handsets operating above 1 GHz the currents are concentrated close to the antenna element and chassis. Based on current antenna design trends in multimode handsets, the devices were assumed to have bottom antennas (as specified in 7.9.3.3 of this document) fulfilling all the conditions listed in B.3.1. Frequency bands that had at least two different operating modes were analysed. Each frequency band generally had two or three different operating modes. Results for the 850 MHz, 900 MHz, 1 700 MHz, 1 800 MHz, 1 900 MHz, and 1 950 MHz frequency bands were analysed.

The 1 g or 10 g psSAR results for all test positions (left cheek, left tilt, right cheek, and right tilt) were collected. The averaging volume was the same for each phone and frequency band combination.

IECNORM.COM : Click to view the full PDF of IEC/IEEE 62209-1528:2020

For each frequency band and operating mode, all psSAR values were divided by the maximum psSAR value found for the GSM mode. The GSM mode was chosen as the baseline, because it was available in all the analysed test cases. This means that if any relative SAR values for other operating modes (e.g. WCDMA or LTE) were greater than 1, the maximum SAR for that operating mode was measured in a different test configuration than for GSM.

In Figure B.2, the x-axis represents all results with the maximum absolute SAR value of each measurement, and the y-axis represents the SAR value relative to maximum SAR value for the GSM mode. The results are divided by cheek and tilt position below 1 GHz and above 1 GHz. Figure B.2 shows that the majority of the results are below 1, i.e. the maximum SAR was found in same position for example for LTE as it was found for GSM.

Among the 181 test cases, the maximum psSAR was found in a different position than for GSM in one of the other operating modes for only 19 cases. In all 19 cases, the maximum psSAR values were less than 0,4 W/kg for both GSM and the other operating modes. Of these 19 cases, only three cases occurred for tilt positions, with a ratio less than 1,2. In the remaining 162 cases where the psSAR values were greater than 0,4 W/kg, the maximum SAR test configuration was correctly identified based on GSM tests.

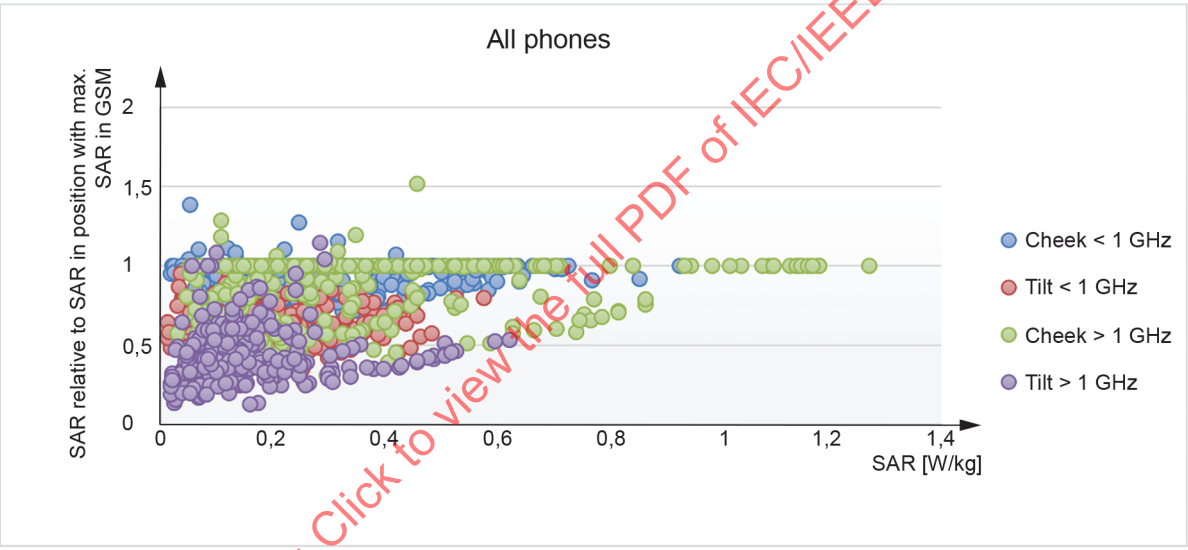


Figure B.2 – SAR relative to SAR in position with maximum SAR in GSM mode

B.4 Test reduction based on SAR level analysis

B.4.1 General

In the SAR measurement procedure specified in 7.4, the results from only a single zoom scan are used to obtain psSAR to be compared with basic restrictions. Consequently, a considerable number of zoom scans could be avoided, saving measurement time, if there is a criterion able to forecast that the psSAR for a test configuration will be lower than the highest value of psSAR among all test configurations. By extending this concept to multi-band and multi configuration devices, the measurement time can be further reduced by defining a SAR measurement session not limited by the single band operational mode, but extended to all the operational bands and configurations supported by the device and included in the scope of the present test reduction method. The basic idea is to avoid performing the zoom scan session for each single test (i.e. 7.4.2 d)) if the maximum measured SAR value of the area scan is below a threshold. The threshold is chosen so that the highest psSAR value will be:

IECNORM.COM : Click to view the full PDF of IEC/IEEE 62209-1528:2020

- correctly assessed and not underestimated, especially when it could generate a psSAR close to the basic restriction limit;
- correctly identified, even if not executing the zoom scan session.

In order to specify the value of the threshold satisfying the first requirement, the psSAR from the zoom scan measurement has been correlated to the maximum measured SAR value found in the corresponding area scan [38]. It was observed that if the maximum measured SAR value in the area scan is lower than a threshold, then the basic limit for the psSAR is never exceeded; in particular there was a good correlation between the maximum measured SAR of the area scan and the 1 g psSAR. In [38], choosing a threshold of 1,3 W/kg (80 % of basic 1 g limit of 1,6 W/kg) gives a high probability that the limit for the psSAR is never exceeded. The same threshold can be used also for the evaluation of the 10 g psSAR.

The statistical analysis described in B.4.2 has been performed to address the question of correct identification of the highest peak spatial average SAR [39].

B.4.2 Statistical analysis

The statistical analysis presented here considers DUTs operating in the GSM 900 / DCS 1800 and UMTS I bands. The area scan grid spacing parameters used in this analysis were both (x and y) set to 10 mm, so they fit the requirements of this document, and area scans were performed at a specified fixed distance (4 mm spacing between sensors and SAM surface in this case) from the SAM internal surface.

Because the maximum SAR value could not be exactly identified from the area scan, due to the fact that it could be located (in x and y) inside a square region having 10 mm size, it is recommended to first experimentally evaluate the spatial gradient in order to estimate the magnitude of the peak SAR value that could be missed in applying only the area scan. To do this, 420 SAR distributions in the GSM 900 band, 420 distributions in the DCS 1800 band, and 300 distributions in the UMTS I band have been considered. The distributions are relevant to mobile phones marketed between 2007 and 2010. All handset form factors, including clamshell and slider, have been considered in this study. The first step was to identify the "iso-level" as the set of points having a fixed SAR value, and then compute the minimum distance D_{min} between the "iso-level" at a fixed SAR level and the position of the interpolated maximum SAR (SAR_{max}, the distance between the two points marked with an X in Figure B.3).

Figure B.4 shows the histogram related to the random variable D_{min} in the case of GSM 900 band and the 0,6 × SAR_{max} level. The red curve shows a normal probability density function (PDF) fitted to data using a maximum likelihood estimation procedure.

Even if in some cases data fail the normality hypothesis test (e.g. Jarque-Bera normality test) and data can be more efficiently fitted by using other PDF (e.g. hyperbolic PDF), for the purpose of this analysis only normal fits have been considered in this work. Considering normal PDF, the value D^{*}_{min} represents the value for which the probability to have D_{min} less than D^{*}_{min} is 5 %.

Table B.7 summarizes all the analysis performed, for each frequency band considered in this study. In this table the iso-level is expressed as a percentage, so a value of 90 % means the iso-level at 0,9 × SAR_{max}.

IECNORM.COM : Click to view the full PDF of IEC/IEEE 62209-1528:2020

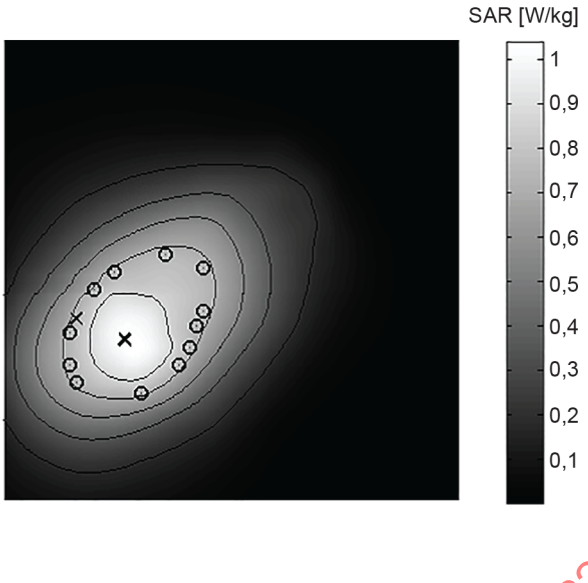


Figure B.3 – Two points identifying the minimum distance between the position of the interpolated maximum SAR and the points at 0,6 × SAR_{max}

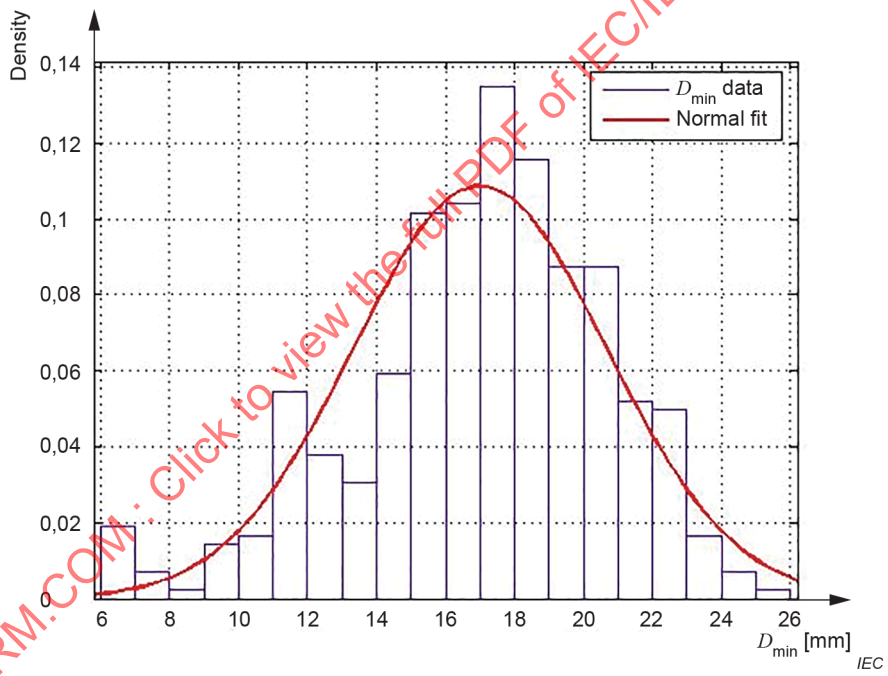


Figure B.4 – Histogram for D_{min} in the case of GSM 900 and iso-level at 0,6 × SAR_{max}

Table B.7 – Distance D^*_{min} for various "iso-level" values

GSM 900		DCS 1800		UMTS I	
Iso-level (%)	D^*_{min}	Iso-level (%)	D^*_{min}	Iso-level (%)	D^*_{min}
90	4,23	90	3,04	90	1,82
80	6,74	80	4,82	80	4,63
75	**7,86**	70	6,19	70	6,10
70	8,90	65	6,92	65	6,81
60	10,96	**60**	**7,54**	**60**	**7,48**
50	13,15	50	9,06	50	8,88

IECNORM.COM : Click to view the full PDF of IEC/IEEE 62209-1528:2020

To summarize the results of this analysis, considering for example the GSM 900 band, it can be concluded that is improbable to find SAR values having the value 0,75 × SAR_{max} if a distance of 7,86 mm from the SAR_{max} point is considered. In particular, the values shown in bold in Table B.7 have D^{*}_{min} values higher than 7 mm, which is the value in the middle of the 10 mm chosen grids. In other words, still considering GSM 900 as an example, it is improbable to miss a SAR value inside a 10 mm area scan grid that is higher than 0,75 times the maximum SAR value measured during the area scan.

To conclude the statistical analysis, the correlation between the measured maximum measured SAR value of the area scan and the psSAR values found after zoom scans has been investigated. To do this, a database of 100 handsets operating in the GSM 900 and DCS 1800 bands, and 50 DUTs operating in the UMTS I band, have been considered.

For each handset the maximum measured SAR value of the area scan, the 1 g psSAR and the 10 g psSAR, as measured after the complete measurement procedure were collected. Figure B.5 shows the histogram, as well as the normal PDF fit for the random variable $Factor_{1g,1800}$, designated as the ratio between the psSAR for 1 g mass and the maximum measured SAR value of the area scan in case of DCS 1800 band.

In this particular case, it can be shown that the 95 % probability is achieved to find $Factor_{1g,1800}$ in the interval [0,859, 1,015]. In this particular case, it can be concluded that if there are two area scans with two different measured peak SAR values (not the interpolated one), and they differ from a factor of 0,859/1,015 = 0,84, then it is improbable that the distribution having the higher maximum SAR value measured during the area scan will have the lower 1 g psSAR. In this particular case, 0,84 can be assumed as an experimental threshold: if two different area scans are considered and the measured peak SAR values measured for each one differ by a factor lower than the threshold, then there is a 95 % probability that the area scan with the higher SAR will yield the higher psSAR.

Similar conclusions can be obtained analysing the other bands, as well as the 10 g psSAR. Table B.8 summarizes the overall results.

In conclusion, the same thresholds found in Table B.7 (75 % for GSM 900, 60 % for DCS 1800 and UMTS I) are sufficient also to determine (with a 95 % probability value) the fact that the psSAR will be correctly identified even without performing a zoom scan.

IECNORM.COM : Click to view the full PDF of IEC/IEEE 62209-1528:2020

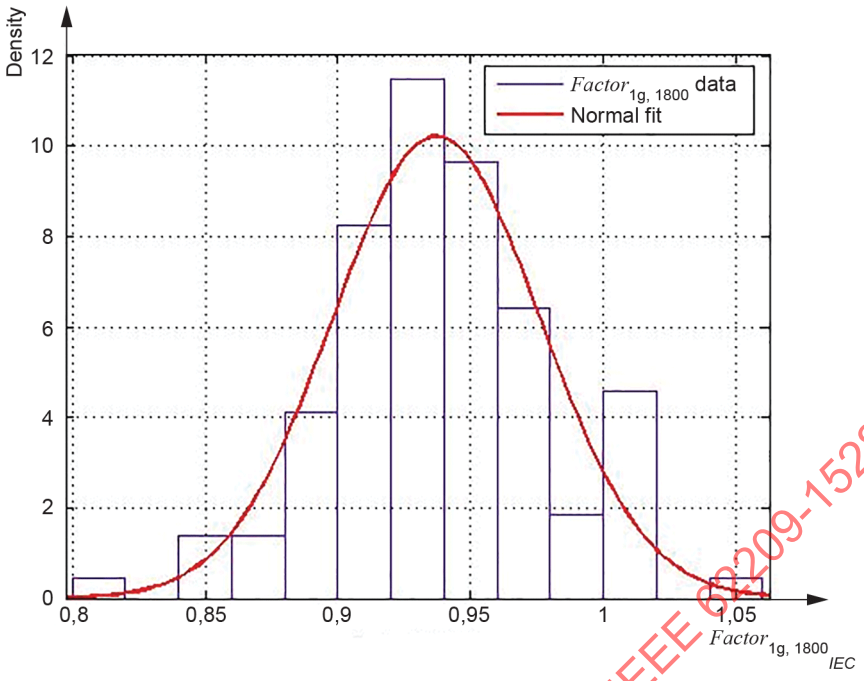


Figure B.5 – Histogram for random variable $Factor_{1g,1800}$

Table B.8 – Experimental thresholds to have a 95 % probability that the maximum measured SAR value from the area scan will also have a psSAR

GSM 900		DCS 1800		UMTS I	
Threshold 1 g	Threshold 10 g	Threshold 1 g	Threshold 10 g	Threshold 1 g	Threshold 10 g
0,86	0,76	0,84	0,63	0,74	0,62

B.4.3 Test reduction applicability example

Two examples of application of the procedures introduced in B.4.2 are described in the following paragraphs. In the first, the test reduction method is applied to a single operational mode (i.e. GSM 900), while in the second a dual mode (GSM 900/DCS 1800 and UMTS I) DUT is considered.

Table B.9 and Table B.10 show the reported SAR values, which are the maximum measured SAR values from the area scan (GSM 900 band).

Because this example is related to GSM 900, a threshold of 0,75 should apply. For the first position (left cheek, middle uplink frequency) the zoom scan is needed because the maximum SAR value is 1,3 W/kg (80 % of 1,6 W/kg), while for the left tilt 0,6 W/kg is lower than 0,75 × 1,3, so the zoom scan is not needed. Then in the right cheek position the zoom scan is needed, and the new absolute peak SAR (APS) becomes 1,5 W/kg. This new APS precludes the need to perform the zoom scan for right tilt (middle frequency) and right cheek (lower frequency), while it is not high enough to exclude the last zoom scan (right cheek, higher frequency).

For the second example, GSM 900 band is tested before DCS 1800 and UMTS I, but in general the order in which the bands are tested may be different.

IECNORM.COM : Click to view the full PDF of IEC/IEEE 62209-1528:2020

In this second example, the procedure applied in GSM 900 is repeated considering all the other tests and previous APS found. For each band the user should choose an appropriate threshold (B.4.2). For the first measurement in a different band, the user will use, for the comparison with the maximum measured peak SAR value from the area scan, the previous APS found and the threshold related to the new band. As an example, the first area scan measurement of DCS 1800 has a peak maximum SAR value of 0,9 W/kg that is equal to 60 % (the threshold of DCS 1800) of 1,5 W/kg (the previous APS), so in this case zoom scan is needed.

As can be seen in this example, nine measurements (50 %) do not require a zoom scan to be performed (i.e. bold rows in Table B.10). The number of zoom scans that can be precluded depends on maximum measured peak SAR values from the area scans.

Table B.9 – SAR values from the area scan (GSM 900 band): Example 1

Frequency	Position	Maximum SAR value [W/kg] [a]
Middle	Cheek left	1,3
Middle	**Tilt left**	**0,6**
Middle	Cheek right	1,5
Middle	**Tilt right**	**0,8**
Lower	**Cheek right**	**1,0**
Higher	Cheek right	1,3

[a] For bold rows, according to the proposed test reduction procedure, a zoom scan is not required.

Table B.10 – SAR values from the area scan (GSM 900 band): Example 2

Frequency	Position	Maximum SAR value [W/kg] [a]
Middle (GSM 900)	Cheek left	1,3
Middle (GSM 900)	**Tilt left**	**0,6**
Middle (GSM 900)	Cheek right	1,5
Middle (GSM 900)	**Tilt right**	**0,8**
Lower (GSM 900)	**Cheek right**	**1,0**
Higher (GSM 900)	Cheek right	1,3
Middle (DCS 1800)	Cheek left	0,9
Middle (DCS 1800)	**Tilt left**	**0,6**
Middle (DCS 1800)	**Cheek right**	**0,8**
Middle (DCS 1800)	**Tilt right**	**0,7**
Lower (DCS 1800)	Cheek right	1,1
Higher (DCS 1800)	**Cheek right**	**0,8**
Middle (UMTS I)	Cheek left	1,1
Middle (UMTS I)	**Tilt left**	**0,7**
Middle (UMTS I)	Cheek right	1,4
Middle (UMTS I)	**Tilt right**	**0,6**
Lower (UMTS I)	Cheek right	1,2
Higher (UMTS I)	Cheek right	1,4

[a] For bold rows, according to the proposed test reduction procedure, a zoom scan is not required.

IECNORM.COM : Click to view the full PDF of IEC/IEEE 62209-1528:2020

B.5 Other statistical approaches to search for the high SAR test configurations

B.5.1 General

A device could operate in different transmission modes and could be usable with several antenna options, battery options and other accessories, and the number of possible combinations can be very large. Methods are therefore needed to streamline the measurement process, so that the highest SAR test configurations can be quickly identified. For example, a device with two antenna configurations (antenna extended and retracted) and four battery types testing all possible combinations would result in a considerable number of tests. It is unnecessary to test all possible combinations; statistical techniques can be used to show trends from a smaller set of data and determine which device-accessory combinations result in higher SAR values.

Three traditional methods of experimentation are described in B.5.3 and B.5.4. These methods have drawbacks compared to the design-of-experiments (DOE) approach specified in B.5.2.

B.5.2 Test reductions based on a DOE

Analysis of SAR data, e.g. statistical analysis based on a DOE approach, may be used to develop scientific or engineering rationales for the test reduction of certain SAR tests. For example, if devices are available with optional faceplates with paint coatings of varying metal content, statistical analysis of SAR data may be used to justify excluding the testing of faceplates with less than a certain amount of metal content. The application of the test reduction should be limited to products that are sufficiently similar to the original product for which the test reduction was determined.

Using a design of experiments (DOE) is the preferred statistical method of achieving test reductions. A DOE is a structured, organized method for analysing the influence of factors and the interactions between factors on the output of a process. The DOE approach is extensively covered in the literature [40].

B.5.3 One factor at a time (OFAT) search

With this method, the experimenter starts with a baseline test configuration, and then successively varies one factor at a time while holding all other factors constant. For example, this could be achieved by first varying antenna configurations, then battery types, then carry accessory types, then audio accessory types. At the end of each step, the factor giving the highest SAR is selected for the next steps. The main drawback of this approach is that it does not consider any interactions between the different accessory types (e.g. the interaction of the battery and the antenna on SAR, which is not explained by the influences of each factor independently). If interactions exist, the OFAT approach might not find the optimum (i.e. highest SAR) solution.

B.5.4 Analysis of unstructured data

A common source of unstructured data is historical data. This data typically was collected without any specific objective in mind, or it could have been collected for different purposes than the current experimental objective. This data may be useful in spotting trends, but it might be very difficult to have high confidence in the findings.

For this reason, any findings from the analysis of unstructured data should be verified (e.g. using a DOE).

IECNORM.COM : Click to view the full PDF of IEC/IEEE 62209-1528:2020

Annex C
(informative)

Measurement uncertainty of results obtained from specific fast SAR testing methods

C.1 General

Among the existing and known fast SAR testing methods, many of them focus on reducing probe movements, especially by using scanning techniques or a probe array, and employing field reconstruction techniques to determine the spatial distribution of the SAR and the psSAR. Probes of various types may be used (e.g. probes measuring only two tangential field components, or thermal probes). Some of the systems also use specific probe technologies and electronics allowing measurement of the phase of the electric field in a given plane. Different types of dedicated post-processing algorithms can then be used to reconstruct the volumetric SAR distribution inside the phantom.

NOTE Field reconstruction techniques are described in IEC 62209-3.

The dielectric properties of the tissue-equivalent medium used for fast SAR testing should comply with the requirements of Annex G. The tissue-equivalent medium may be liquid, gel, or solid. If the tissue-equivalent medium of the fast SAR testing system is accessible and replaceable by the user, the dielectric properties should be characterized as specified in 7.2.1. If the tissue-equivalent medium is inaccessible or not replaceable by the user, the system manufacturer should demonstrate and document compliance of the dielectric properties with the requirements of Annex G, including any effects of spatial variations of the dielectric properties (C.2.11) or aging of the material.

The fast SAR testing methods that are specified in Annex C use the SAR measurement procedure specified in 7.9.2. They also use the system validation and system check specified in Clause A.4. The full range of sensor locations should also be considered for the type of fast SAR testing systems specified in Annex C. These ranges should be provided with the system validation results. Annex C is informative because the system validation requirements have not yet been fully determined for the type of fast SAR system that is specified herein.

Because this class of fast SAR testing methods uses specific hardware and software that do not conform to those used for full SAR testing required by this document, the information in Clause 8 might not be sufficient to determine the measurement uncertainty. Additional uncertainty components that are specific to the measurement system and the method under consideration can be needed. Clause C.2 gives general guidance for determining the measurement uncertainty of results obtained using this class of fast SAR testing methods.

C.2 Measurement uncertainty evaluation – contributing parameters

C.2.1 General

General guidance is provided to determine the relative measurement uncertainty of a Class 2 fast SAR testing method. For Class 1 fast SAR testing systems, the uncertainty analysis is the same as that specified in Clause 8, except that additional sampling error uncertainty is added as specified in C.2.7.

Uncertainty assessment methods for SAR results obtained using vector measurement-based systems are given in IEC 62209-3. The uncertainty assessment guidance in IEC 62209-3 shall be applied for the purposes of this document.

IECNORM.COM : Click to view the full PDF of IEC/IEEE 62209-1528:2020

For a specific fast SAR testing method, rigorous uncertainty analysis should be applied for all applicable uncertainty terms, including any terms that are not specified in Clause C.2. The relative uncertainty is required, so uncertainty contributions that represent fixed offsets for a set of test configurations are not considered in the uncertainty budget. This includes fixed offsets due to system calibration, dielectric properties that do not change significantly during the tests (tissue-equivalent medium temperature variations between tested configurations fulfil the requirements in 6.1), uncertainties in phantom construction that are fixed for a given system, and other offsets. Uncertainty terms that result in variations in the measured values from their nominal values for a given set of measurements should be considered in the relative uncertainty budget. This includes noise in the electronics, variations due to device positioning and measurement errors, and other items.

For Class 2 fast SAR testing, two uncertainty budgets are presented in Annex C.

a) Table C.1 (see Clause C.3) is the uncertainty budget to be used when fast SAR testing is applied for several test configurations within the same frequency band and modulation (e.g. GSM in the 824 MHz to 849 MHz frequency band). Fixed offsets that apply when relative assessments are conducted are not included in the uncertainty. Also, fixed offsets that are specific to frequency and operating mode (e.g. offsets due to calibration uncertainty and modulation) are not included.

b) Table C.2 (see Clause C.3) is the uncertainty budget for the system check for Class 2 fast SAR testing. This uncertainty budget is very similar to the uncertainty budget of Clause 8.

All uncertainty contributions should be computed in a rigorous way, using appropriate statistical techniques. A description of the procedures used in the evaluations of uncertainty contributions, if different from those reported in this document, should be included in the measurement report.

C.2.2 Probe calibration and system calibration drift

If the fast SAR testing method uses one probe, then the same method specified in 8.4.1.1 should be used, where appropriate. If the Class 2 fast SAR testing method uses several probes, then the calibration should be applied over the number of sensors used by the system, where appropriate. The system calibration uncertainty should be documented and appropriate to the calibration method applied.

The probe calibration drift over time is an estimate for the change in calibration values of the system over the calibration interval within a specific calibration laboratory, and is based on the calibration history of the system. It is determined by Type A evaluation (8.4.1.2). For example, the calibration laboratory may have a specific system that it uses for regular re-calibration. In this case, the calibration drift should be specified as the standard deviation of the re-calibrations, relative to the mean value. It is recommended that the system calibration measurements that are used to determine this uncertainty are made over a period that is longer than the calibration period of the other equipment (e.g. power meters) used during calibration. This ensures that the calibration drift uncertainty includes variations due to the re-calibration of this equipment. Where a calibration history is not available, the manufacturer's estimate for the stability of the system over the calibration interval should be used. If the calibration drift uncertainty is not available, the full calibration uncertainty should be used instead.

C.2.3 Isotropy

Probe isotropy uncertainty specified in 8.4.1.5 is applicable to probes that can be positioned in a range of angles with respect to the phantom shell according to the specifications of Table 3 and Table 4 (see 7.4.2).

IECNORM.COM : Click to view the full PDF of IEC/IEEE 62209-1528:2020

If the probes of the fast SAR testing system are positioned in a similar way as for Class 1 fast SAR testing, then the probe isotropy uncertainty procedure specified in 8.4.1.5 should be used, where appropriate. If the probe angles with respect to the phantom shell do not comply with the probe angles specified in Table 3 and Table 4, then additional uncertainty evaluation can be needed. If the probe angles are limited to a narrower range, the isotropy uncertainty can be performed over that range. The isotropy assessment should be applicable to the measurement system used. If algorithms are applied to compensate for the deviation from isotropic response, then the SAR uncertainty shall be determined with the same evaluation hardware and software as is used for performing the SAR measurements.

For Class 2 fast SAR testing, technology-specific considerations shall be taken into account. The manufacturer shall evaluate this contribution during the calibration. If algorithms are applied to compensate for the deviation from isotropic response, then the SAR uncertainty shall be determined with the same evaluation hardware and software as is used for performing the SAR measurements. To evaluate the isotropy, the SAR measurement system shall be exposed to reference fields containing waves with varying angles of incidences with respect to the line normal to the phantom surface. The SAR gradients in the direction normal to the phantom shell shall be low enough that probe positioning tolerance does not significantly influence the isotropy assessment. The isotropy shall be characterized for at least one frequency in each frequency band of interest to the communication system of the DUT. The assessed tolerance valid at the sensor location needs to be translated to the uncertainty for the psSAR and filled into Table C.1. The translation is a function of the actual implemented 3D reconstruction and can only be performed by the manufacturer. All steps shall be documented.

C.2.4 Probe positioning

There is some uncertainty of the exact location of the sensor(s) used by the fast SAR testing method. If the fast SAR testing system uses one or more moveable sensors, then the uncertainty is due to uncertainties in the positioning of the sensors. If the fast SAR testing system uses one or more fixed sensors, the uncertainty is due to mechanical uncertainties in the sensor location during manufacturing.

The uncertainty is evaluated using the set of reference distributions in O.8.2. The procedure is as follows.

a) For each reference distribution, the field is sampled at points and in polarizations which correspond to the measurement grid applied by the physical system.

b) From these original sampled data, the psSAR is computed using the same processing as used for measurements with this particular system. In this process, step a) gives the reference SAR, $SAR_{\text{ref},i}$, for each field distribution case i (several i distributions are assumed per frequency).

c) The known tolerance on probe positioning is used to generate measurement scan grids G_j (j = 1 to J) affected by mechanical errors. The manufacturer shall make a model to represent such mechanical errors. For example, each tolerance may have a rectangular or triangular distribution if the manufacturer defines maximum acceptable deviations from nominal locations. In the case of moving probes, the repeatability uncertainty of the probe positioning shall be included in the mechanical error. J sampled distributions of each reference vector field are then created by using the G_j sampling grids.

d) For each reference distribution i and each grid j, the reconstruction algorithms of the measurement system are applied to compute the psSAR, $SAR_{i,j}$. The software shall assume ideal positions of the points in the grid. Consequently, the algorithms are used as if sampled field values were obtained from a probe or probe-array with perfectly known position, whereas the probe or probe-array is actually sampling the field on a grid which deviates from the targeted locations.

e) For each (i, j) pair, the relative difference $\Delta SAR_{i,j}$ = $(SAR_{i,j} - SAR_{\text{ref},i})$ / $SAR_{\text{ref},i}$ is computed.

IECNORM.COM : Click to view the full PDF of IEC/IEEE 62209-1528:2020

U_i is then calculated for each reference field configuration i as the 95th percentile of the absolute value of $\Delta SAR_{i,j}$ for all J probe or probe-array grid locations. The uncertainty is then estimated as the RMS value of U_i across the applicable frequency range for all I exposure conditions. This value is calculated on $I \times J$ cases with $I \times J - 1$ degrees of freedom. A normal distribution (k = 2) is assumed.

The assessed tolerance valid at the sensor location needs to be translated to the uncertainty for the psSAR and filled into Table C.1. The translation is a function of the actual implemented 3D reconstruction and can only be performed by the manufacturer. All steps shall be documented.

C.2.5 Mutual sensor coupling

For systems using more than one probe, coupling between the probe sensors might exist, due to imperfect isolation of the sensors. This uncertainty term is caused by port-to-port coupling, where the readout at a given sensor port is influenced by the voltage and/or current at another sensor port. Mutual sensor coupling may be evaluated and compensated during calibration. However, this coupling is in principle dependent on the polarization, distribution, and angle of incidence of the impinging field, and is therefore difficult to remove completely during calibration.

The assessed tolerance valid at the sensor location needs to be translated to the uncertainty for the psSAR and filled into Table C.1. The translation is a function of the actual implemented 3D reconstruction and can only be performed by the manufacturer. All steps shall be documented.

In order to isolate this uncertainty contribution from other components:

a) the probe or probe-array shall be immersed in tissue-equivalent medium complying with the requirements of this document;

b) the reference antennas used shall have a polarization purity of more than 10 dB. Polarization purity is the ratio of the field strength of the dominant field component to the field strength of the two orthogonal field components. It is specified at the location of the psSAR. It is assessed from numerical simulations of the reference antenna;

c) the reference antennas shall be far enough from the phantom so that the interaction with the probe or probe-array can be neglected;

d) the field levels shall be sufficiently above the noise floor.

In the case of probe arrays with probes that are calibrated independently prior to assembly, or in the case of probe arrays that are calibrated together in the final operating condition without compensation for mutual coupling, the mutual sensor coupling uncertainty shall be evaluated by computing the difference between the single point SAR measured using one probe in isolation and the SAR measured by the same probe surrounded by the other probes. Several source antennas with different polarizations and angles of incidence are required. The antennas are moved to the required positions so that each sensor is actually exposed to a field strength compatible with the dynamic range of the measurement system. For each test condition, the calibration coefficients and post-processing are applied on the measured data to evaluate the vector field distribution over the measurement surface. It shall be documented how the error propagates and how the uncertainty is coupled to other uncertainty terms.

For probe-arrays where the probes are calibrated together in the final operating condition and the mutual coupling between the sensors is characterized as a scattering matrix then compensated (e.g. during the probe-array calibration), mutual coupling will be reduced. However, the remaining mutual sensor coupling error shall be assessed. Also, the uncertainty of the compensation is taken into account as an additional contribution to the measurement system calibration uncertainty. It shall be documented how the error propagates and how the uncertainty is coupled to other uncertainty terms.

IECNORM.COM : Click to view the full PDF of IEC/IEEE 62209-1528:2020

C.2.6 Scattering within the probe array

Scattering of the electromagnetic fields in the phantom due to the presence of the probe array causes distortion of the impinging field distribution captured by the sensors. These reflections are strongly dependent on the distribution, polarization, and angle of incidence of the incident fields; therefore, they cannot be fully calibrated out. This uncertainty term is correlated with the uncertainty due to mutual coupling between the sensors.

It is also possible to assess together the isotropy (C.2.3), mutual sensor coupling (C.2.5), and scattering within the array (C.2.6) uncertainty components.

C.2.7 Sampling error

The measured SAR distribution is estimated from the direct sampling of the field at a set of discrete points. If the sampling resolution is coarse compared to the gradients of the induced SAR distribution, the psSAR can be inaccurate. The uncertainty is evaluated using the set of reference distributions in O.8.2.

The evaluation of this uncertainty may be combined with the evaluation of the uncertainty of reconstruction algorithms.

C.2.8 Array boundaries

In addition to SAR errors due to the spatial resolution and the locations of the sensors, there are errors at the boundary of the measurement area due to truncation of the measured field distribution and extrapolation of the measured field distribution beyond the measurement area.

This uncertainty may be evaluated together with the uncertainty of reconstruction algorithms.

The uncertainty is evaluated using the reference distributions of O.8.2. The reference distributions are applied close to the boundary of the measurement area. If the measurement system provides warnings or error messages to the user about the measurement error at locations near the boundary, the evaluation shall be performed inside of these locations. Compare the resulting 1 g and 10 g psSAR with the target values.

C.2.9 Probe or probe array coupling with the DUT

In addition to the coupling specified in C.2.5, there can be coupling between the sensors and the DUT that also contribute to measurement uncertainty. To assess the uncertainty, several radiating devices and test positions should be assessed, as appropriate for the measurement system, using both fast SAR testing and full SAR testing.

C.2.10 Measurement system immunity / secondary reception

As with full SAR testing systems, fast SAR testing systems should be designed in such a way as to mitigate any noise or offsets in the measurements due to signal pickup that is not measured at the sensor(s). Incident electric fields on high impedance transmission lines can be picked up by the lines, causing interference (secondary reception) with the signal picked up by the sensor(s). For full SAR testing, this effect is minimized by using high impedance lines along the probe axis. For fast SAR testing systems using different sensor arrangements, the immunity to these secondary signals should be measured. This should be accomplished by performing a single point measurement of one probe of the fast SAR testing system using the system validation set-up specified in Annex A, then comparing the measured value against the value using a probe used for full SAR testing. To ensure that potential coupling between the sensors and the DUT (C.2.5 and C.2.9) is not included, the radiating source should be kept away from the fast SAR testing system by a minimum of one quarter of a wavelength in air.

IECNORM.COM : Click to view the full PDF of IEC/IEEE 62209-1528:2020

NOTE It is sufficient to test this uncertainty term using the densest probe spacing of the probe array if the probe array has variable spacing.

C.2.11 Deviations in phantom shape

This uncertainty term takes into account measurement variations due to the phantom shape, if the phantom shape deviates from the standardized phantom specified in Annex G. This term should be determined from the difference between the SAR in the phantom shape used by the fast SAR testing method and the SAR in the standardized phantom. It is recommended to perform the measurements in both phantoms using full SAR testing, so as not to include the sensor coupling with the DUT (C.2.9) in the uncertainty analysis. Different sources and source positions with respect to the phantom should be applied, as appropriate, to evaluate the influence of the phantom shape on different SAR distributions.

C.2.12 Spatial variation in dielectric properties

The dielectric properties of the tissue-equivalent medium can vary spatially. The spatial variation in the dielectric properties can be assessed on a production sample of the material by making dielectric properties measurements at multiple regions (at least 10, including different locations in x-, y- and z-directions in the volume surrounding the sensor locations) in a dielectric sample across the frequency range of interest. If the tissue-equivalent medium is inaccessible to the user, this measurement should be performed by the system manufacturer. The methods of Annex H can be used to measure the dielectric properties, if appropriate. The dielectric properties measurement methods should be appropriate to the material being tested. The uncertainty term is calculated from the highest percentage difference in each of the permittivity and conductivity from the average value, and a rectangular distribution is assumed.

C.2.13 Reconstruction

The method to evaluate the uncertainty contribution due to reconstruction algorithms, excluding psSAR averaging, is as follows.

a) Sample reference analytical field distributions at grid points and using polarizations corresponding to the measurement scan performed by the actual system.

b) Process the sampled data by utilizing system reconstruction and peak spatial-averaging algorithms.

c) For each distribution, compute the relative difference between the psSAR obtained in step b) and the reference SAR targets for the provided analytical functions.

NOTE Analytical field distributions are described in IEC 62209-3.

C.3 Uncertainty budget

The measurement uncertainty budget specified in Table C.1 is the uncertainty of the measured SAR value for one test configuration compared to the measured SAR of the other test configurations that have been measured using the same fast SAR testing system at the same frequency band and modulation.

The relative uncertainty budget for the system check performed for a fast SAR testing method is shown in Table C.2. This uncertainty budget is similar to the repeatability uncertainty budget for system check. The uncertainty terms that can be neglected have weighting coefficients of c_i = 0.

IECNORM.COM : Click to view the full PDF of IEC/IEEE 62209-1528:2020

Table C.1 – Measurement uncertainty budget for relative SAR measurements using Class 2 fast SAR testing, for tests performed within one frequency band and modulation

Input quantity X_i (source of uncertainty)	Ref.	Prob. Dist. PDF_i	Unc. $a(x_i)$	Div. q_i	$u(x_i) = a(x_i)/q_i$	c_i (1 g, 10 g)	$u(y) = c_i \cdot u(x_i)$	v_i or v_{eff}
Measurement system								
System calibration	C.2.2	N		1		0		∞
Isotropy	C.2.3	R		√3		1		∞
Boundary effect	8.4.1.6	R		√3		1		∞
Linearity	8.4.1.3	R		√3		1		∞
System detection limits	8.4.1.3	R		√3		1		∞
Modulation response	8.4.2.7	R		√3		1		∞
Readout electronics	8.4.1.6	N		1		0		∞
Response time	8.4.1.6	R		√3		0		∞
Integration time	8.4.1.6	R		√3		1		∞
RF ambient conditions – noise	8.4.1.7	R		√3		1		∞
RF ambient conditions – reflections	8.4.1.7	R		√3		0		∞
Probe positioning	C.2.4	R		√3		1		∞
Mutual sensor coupling	C.2.5	R		√3		1		∞
Scattering within the array	C.2.6	R		√3		1		∞
Sampling error	C.2.7	R		√3		1		∞
Array boundaries	C.2.8	R		√3		1		∞
Probe or probe array coupling with DUT	C.2.9	R		√3		1		∞
Measurement system immunity	C.2.10	R		√3		1		∞
Post-processing of measurement data	8.4.1.9	R		√3		1		$N-1$
Spatial variation in dielectric properties	C.2.12	R		√3		1		∞
Reconstruction	C.2.13	R		√3		1		∞
Test sample related								
Test sample positioning	8.4.2.5	N		1		1		∞
Device holder uncertainty	8.4.2.6	N		1		1		∞
Output power variation – SAR drift measurement	8.4.2.9	R		√3		1		∞
SAR scaling	8.4.3.2	R		√3		0		∞
Phantom and tissue parameters								
Deviations in phantom shape	C.2.11	R		√3		1		∞
Uncertainty in SAR correction for deviations in permittivity and conductivity	8.4.3.1	N		1		0		∞
Medium conductivity measurement	8.4.2.1	N		1		0		M
Medium permittivity measurement	8.4.2.1	N		1		0		M
Medium conductivity – temperature uncertainty	8.4.2.2	R		√3		0		∞
Medium permittivity – temperature uncertainty	8.4.2.2	R		√3		0		∞
Combined standard uncertainty, $u(\Delta SAR)$		RSS						v_{eff}
Expanded uncertainty, U		k = 2						

IECNORM.COM : Click to view the full PDF of IEC/IEEE 62209-1528:2020

Table C.2 – Measurement uncertainty budget for system check using Class 2 fast SAR testing

Input quantity X_i (source of uncertainty)	Ref.	Prob. Dist. PDF_i	Unc. $a(x_i)$	Div. q_i	$u(x_i) = a(x_i)/q_i$	c_i (1 g; 10 g)	$u(y) = c_i \cdot u(x_i)$	v_i or v_{eff}
Measurement system								
System calibration drift	C.2.2	N		1		1		∞
Isotropy	C.2.3	R		√3		0		∞
Boundary effect	8.4.1.6	R		√3		0		∞
Linearity	8.4.1.3	R		√3		0		∞
System detection limits	8.4.1.3	R		√3		0		∞
Modulation response	8.4.2.7	R		√3		0		∞
Readout electronics	8.4.1.6	N		1		0		∞
Response time	8.4.1.6	R		√3		0		∞
Integration time	8.4.1.6	R		√3		0		∞
RF ambient conditions – noise	8.4.1.7	R		√3		0		∞
RF ambient conditions – reflections	8.4.1.7	R		√3		0		∞
Probe positioning	C.2.4	R		√3		1		∞
Mutual sensor coupling	C.2.5	R		√3		1		∞
Scattering within the array	C.2.9	R		√3		0		∞
Sampling error	C.2.7	R		√3		1		∞
Array boundaries	C.2.8	R		√3		0		∞
Probe or probe array coupling with DUT	C.2.6	R		√3		0		∞
Measurement system immunity	C.2.10	R		√3		1		∞
Post-processing of measurement data	8.4.1.9	R		√3		0		$N-1$
Spatial variation in dielectric properties	C.2.12	R		√3		0		∞
Reconstruction	C.2.13	R		√3		1		∞
Test sample related								
Test sample positioning	8.4.2.5	N		1		0		∞
Device holder uncertainty	8.4.2.6	N		1		0		∞
Output power variation – SAR drift measurement	8.4.2.9	R		√3		0		∞
SAR scaling	8.4.3.2	R		√3		0		∞
Phantom and tissue parameters								
Deviations in phantom shape	C.2.11	R		√3		1		∞
Uncertainty in SAR correction for deviations in permittivity and conductivity	8.4.3.1	N		1		*1;0,84*		∞
Medium conductivity measurement	8.4.2.1	N		1		*0,78;0,71*		M
Medium permittivity measurement	8.4.2.1	N		1		*0,23;0,26*		M
Medium conductivity – temperature uncertainty	8.4.2.2	R		√3		*0,78;0,71*		∞
Medium permittivity – temperature uncertainty	8.4.2.2	R		√3		*0,23;0,26*		∞
Combined standard uncertainty		RSS						v_{eff}
Expanded uncertainty, U		k = 2						

IECNORM.COM : Click to view the full PDF of IEC/IEEE 62209-1528:2020

Annex D
(normative)

SAR system validation antennas

D.1 General antenna requirements

Annex D describes antennas that are used to validate SAR measurement systems that conform to the normative requirements of this document. Antennas other than those specified in the subclauses of Annex D may be considered for system validation. The following are minimum requirements for any system validation antenna.

a) Justification shall be provided for the inclusion of an antenna and how its use strengthens the validation protocol.

b) The test configurations (e.g. frequencies, locations on the phantom, distance, rotation angle) shall be provided.

c) Detailed drawings, including all dimensions and tolerances, shall be provided. CAD files of the antennas shall be made available with enough detail of the construction and parameters so that the numerical targets can be independently verified.

d) Numerical target SAR values shall be determined from numerical simulations of the CAD file of the antenna. The numerical simulations shall conform to the requirements of IEC/IEEE 62704-1 [41].

e) Numerical target SAR values shall be available for all specified test configurations on the phantoms.

f) Physical antennas shall be measured using a SAR measurement system that has an accredited calibration (e.g. ISO/IEC 17025 [17]) to validate the numeric target values and generate a certificate of traceability.

NOTE Regulatory acceptance of alternative antenna designs might involve additional requirements other than those described above.

Various antennas that meet the preceding requirements are specified in Clauses D.2 to D.5.

D.2 Standard dipole antenna

D.2.1 Mechanical description

The standard dipole antennas of Figure D.1 with mechanical dimensions given in Table D.1 will produce the SAR values given in Table D.2 when the system validation test of A.3.5 is followed. If dipole antennas are used that have different dimensions than those given in Table D.1, or if dipole antennas are used at frequencies other than those listed in Table D.1, the reference SAR values for those antennas shall be documented and independently verified using procedures that are consistent with the methodologies specified in this document.

The reference dipole shall be positioned below the flat phantom and centred with its axis parallel to the longest side of the phantom. A low loss (loss tangent < 0,05) and low permittivity (relative permittivity < 5) spacer should be used to establish the correct distance between the top surface of the reference dipole and the bottom surface of the phantom. Below 3 GHz, the spacer shall not change the measured 1 g and 10 g psSAR values by more than 1 %, compared to the no-spacer condition. Above 3 GHz, the spacer could affect the measured SAR and introduce deviations from the numerical target values in Table D.2; therefore, experimentally validated SAR targets with specific spacers shall be used (see Table D.2). The reference dipole shall have a return loss better than 20 dB at the test frequency to reduce power reflection and SAR measurement uncertainty.

IECNORM.COM : Click to view the full PDF of IEC/IEEE 62209-1528:2020

For the reference dipoles, a dielectric spacer is used to provide the distance s and spacer mechanical tolerance as given by the following:

s = 15 mm ± 0,2 mm, for 300 MHz ≤ f ≤ 1 000 MHz
s = 10 mm ± 0,2 mm, for 1 000 MHz < f ≤ 6 000 MHz
s = 5 mm ± 0,1 mm, for 6 000 MHz < f ≤ 10 000 MHz

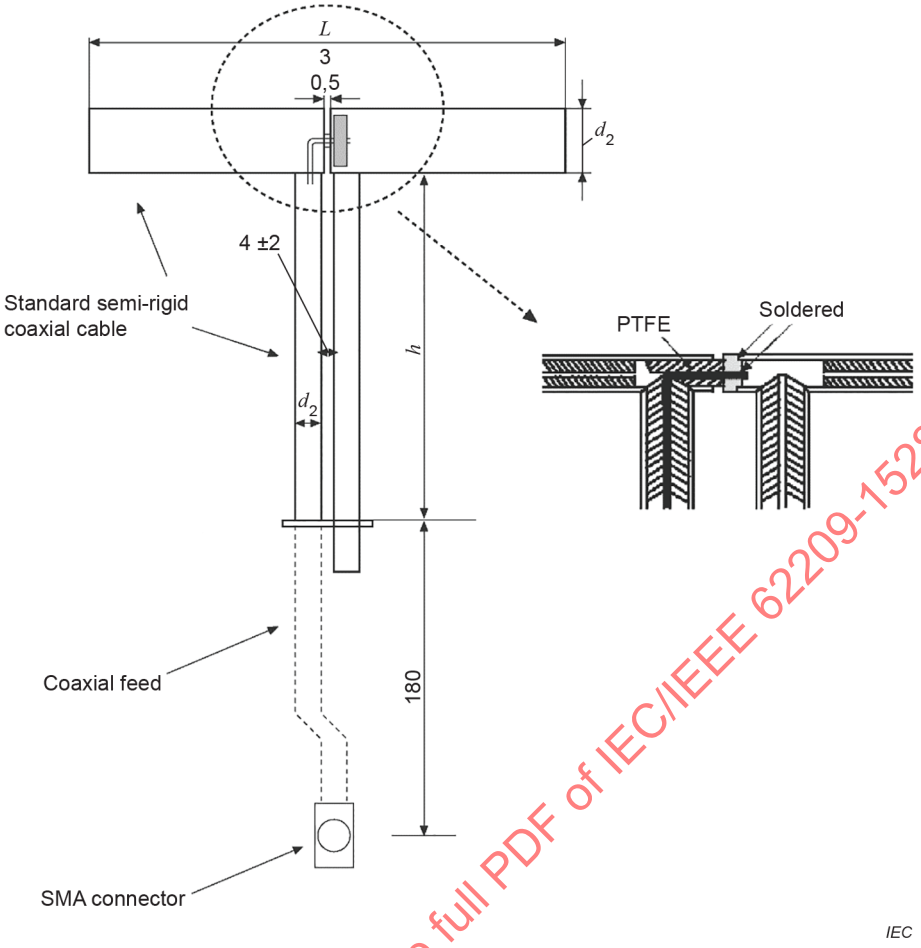
The computation of the reference values in Table D.2 for frequencies above 5 000 MHz requires specific consideration of the build structure of the small dipoles (both internal and external) and numerical values are therefore specific to the dipole antenna design. The dielectric spacer used for the dipole shall also be modelled as it can affect the numerically determined SAR value.

The reference dipole shall have a return loss better than 20 dB at the test frequency to reduce the uncertainty in the power measurement. To meet this requirement, it is acceptable to fine-tune the reference dipoles by using low-loss dielectric or metal tuning elements at the ends of the dipole (Figure A.1).

The reference dipole arms shall be parallel to the flat surface of the phantom within a tolerance of ±2° or less (Figure D.1). This can be assured by carefully positioning the empty phantom and the reference dipole to horizontal level using a spirit level.

The numerical target values above 3 GHz cannot be universally given as for below 3 GHz, due to the greater effect from the spacer, phantom bottom, and mechanical uncertainties. Thus, the numerical target values may be different from one dipole to another. It is important that for each dipole used for system validation a fully documented analysis is provided based on both numerical simulations and experimental validation.

IECNORM.COM : Click to view the full PDF of IEC/IEEE 62209-1528:2020



Key

L	length of the dipole
d_1	diameter of the dipole
d_2	diameter of the coaxial cable at the balun
h	length of the balun choke section
PTFE	polytetrafluoroethylene

Figure D.1 – Mechanical details of the standard dipoles

IECNORM.COM : Click to view the full PDF of IEC/IEEE 62209-1528:2020

Table D.1 – Mechanical dimensions of the reference dipoles

Frequency MHz	L mm	h mm	d_1 mm
300	420,0	250,0	6,35
450	290,0	166,7	6,35
750	176,0	100,0	6,35
835	161,0	89,8	3,6
900	149,0	83,3	3,6
1 450	89,1	51,7	3,6
1 500	86,2	50,0	3,6
1 640	79,0	45,7	3,6
1 750	75,2	42,9	3,6
1 800	72,0	41,7	3,6
1 900	68,0	39,5	3,6
1 950	66,3	38,5	3,6
2 000	64,5	37,5	3,6
2 100	61,0	35,7	3,6
2 300	55,5	32,6	3,6
2 450	51,5	30,4	3,6
2 600	48,5	28,8	3,6
3 000	41,5	25,0	3,6
3 500	37,0	26,4	3,6
3 700	34,7	26,4	3,6
5 000 to 6 000	20,6 [a]	40,3 [a]	3,6
6 000 to 8 000	14,5	35,1	2,2
8 000 to 10 000	12,2	25,0	2,2

NOTE The L, h, and d_1 dimensions shall be within ±2 % tolerance.

[a] These dimensions are applicable for a coaxial diameter at the balun of d_2 = 2,1 mm (Figure D.1).

IECNORM.COM : Click to view the full PDF of IEC/IEEE 62209-1528:2020

D.2.2 Numerical target SAR values

Table D.2 shows the validated numerical target SAR values for system validation (A.3.5), using the standard dipoles specified in D.2.1. The numerical target SAR values in Table D.2 were calculated using the finite-difference time-domain (FDTD) numerical-computation method using the flat phantom requirements in Clause G.3 and Table G.3, and also validated against measured results with equivalent test set-ups for 300 MHz to 10 GHz. The local SAR values in columns 5 and 6 of Table D.2 were experimentally verified for each test frequency using fourth-order polynomial extrapolation. The values above 3 GHz are dependent on the dipole spacer used and detailed construction of the dipoles; therefore, individual dipole targets may vary from the values in Table D.2 by as much as ±10 %. The reason is that the dipole length is short with respect to its diameter and the spacer dimensions, i.e. the numerical target values are not generic and need to be determined for a particular configuration. The dielectric properties used for the tissue-equivalent medium are specified in Table 2 (see 6.2.2), and the dimensions of the reference dipoles are shown in Table D.1. Different reference SAR value may apply for dipoles with mechanical dimensions that depart from those of the reference dipoles given in D.2.1.

Table D.2 – Numerical target SAR values (W/kg) for standard dipole and flat phantom

Frequency	Phantom shell thickness	1 g SAR	10 g SAR	Local SAR at surface (above feed-point)	Local SAR at surface (y =2 cm offset from feed-point)
MHz	mm	W/kg	W/kg	W/kg	W/kg
300	2,0	2,85	1,94	4,14	2,00
450	2,0	4,58	3,06	6,75	2,98
750	2,0	8,49	5,55	12,6	4,59
835	2,0	9,56	6,22	14,1	4,90
900	2,0	10,9	6,99	16,4	5,40
1 450	2,0	29,0	16,0	50,2	6,50
1 500	2,0	30,5	16,8	52,8	6,53
1 640	2,0	34,2	18,4	60,4	6,69
1 750	2,0	36,4	19,3	64,9	6,53
1 800	2,0	38,4	20,1	69,5	6,80
1 900	2,0	39,7	20,5	72,1	6,60
1 950	2,0	40,5	20,9	72,7	6,60
2 000	2,0	41,1	21,1	74,6	6,50
2 100	2,0	43,6	21,9	79,9	6,58
2 300	2,0	48,7	23,3	92,8	7,18
2 450	2,0	52,4	24,0	104	7,70
2 585	2,0	55,9	24,4	119	7,9
2 600	2,0	55,3	24,6	113	8.29
3 000	2,0	63,8	25,7	140	9,50
3 500	2,0	67,1	25,0	169	12,1
3 700	2,0	67,4	24,2	178	12,7
5 000	2,0	77,9	22,1	305	15,1
5 200	2,0	76,5	21,6	310	15,9
5 500	2,0	83,3	23,4	349	18,1
5 800	2,0	78,0	21,9	341	20,3
7 000	2,0	275,0	47,0	2 161,0	13,0
9 000	2,0	243,0	40,0	2 676,0	12,0

NOTE 1 All SAR values are normalized to 1 W forward power.

NOTE 2 The 1 g and 10 g target SAR values are only valid for the system validation specified in Clause A.1, using dipoles with the dimensions specified in D.2.1.

NOTE 3 The SAR values above 3 GHz are sensitive to the dipole and phantom geometry (dipole length, spacer length and permittivity, and phantom shell permittivity) and can vary by as much as ±10 %. See Onishi and Uebayashi [36] for details.

IECNORM.COM : Click to view the full PDF of IEC/IEEE 62209-1528:2020

D.3 Standard waveguide

D.3.1 Mechanical description

The standard waveguide of Figure D.2 with mechanical dimensions given in Table D.3 (corresponding to WR159 or UK WG-13 with an IEC-UDR58 flange according to IEC 60154-2 [42]) will produce the SAR values given in Table D.4 when the system validation test of A.3.5 is followed. The waveguide feed shall be placed at least one guide wavelength away from the matching layer, to ensure that higher order modes have attenuated. The waveguide transmission loss shall be characterized by measurement with a network analyser. If waveguides are used that have different parameters than those given in Table D.3, or if waveguides are used at frequencies other than those listed in Table D.3, the reference SAR values for those waveguides shall be documented and independently verified (e.g. by comparison of numerical simulations with measurements).

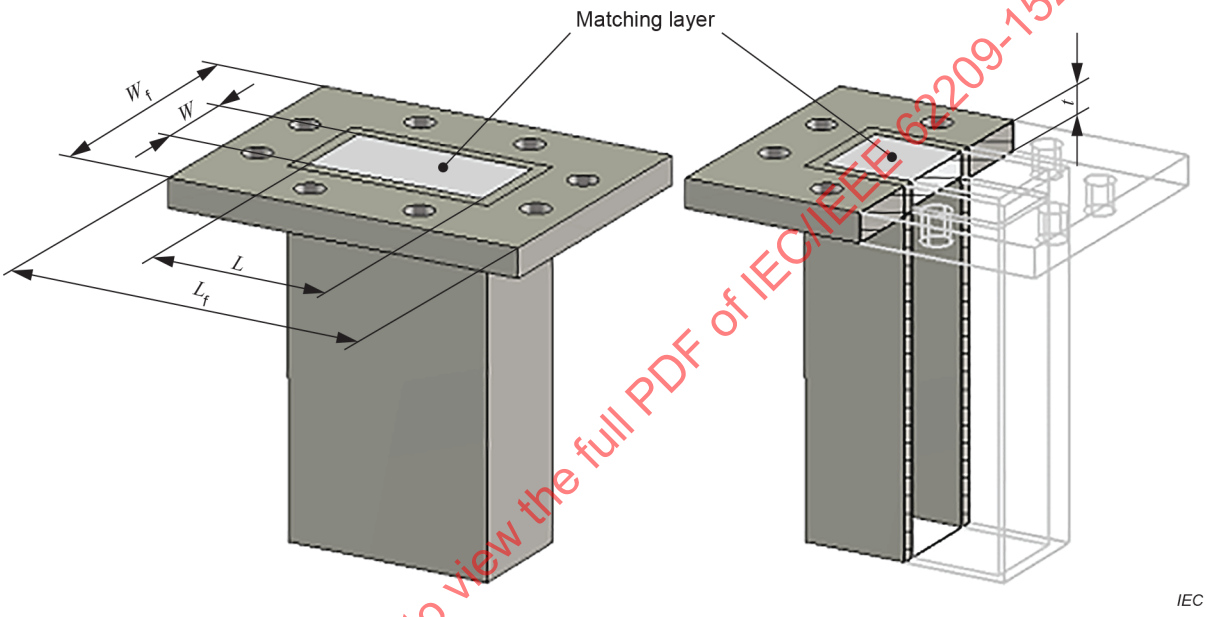


Figure D.2 – Standard waveguide (dimensions are according to Table D.3)

Table D.3 – Mechanical dimensions of the standard waveguide

Frequency	Phantom shell thickness	L	W	L_f	W_f	t	ε_r
MHz	mm	mm	mm	mm	mm	mm	
5 200	2	40,39	20,19	81,03	61,98	5,3	6
5 800	2	40,39	20,19	81,03	61,98	4,3	6

NOTE L and W are the inner length and width of the waveguide, L_f and W_f are the length and width of the waveguide flange, and t and ε_r are the thickness and relative permittivity of the matching layer. The tolerance for L and W is ±0,13 mm. The matching layer is a lossless dielectric slab that fills the cross-sectional $L \cdot W$ area of the waveguide. The waveguide and matching layer are in direct contact with the phantom shell. The minimum height of the waveguide (from the feed to the flange) is one free-space wavelength. This arrangement gives an input return loss of at least 8 dB. The uncertainty of the permittivity and thickness of the dielectric slab are included in the return loss. Therefore, these do not need to be specified independently.

IECNORM.COM : Click to view the full PDF of IEC/IEEE 62209-1528:2020

D.3.2 Numerical target SAR values

Table D.4 shows the numerically validated SAR values for system validation using the standard waveguides specified in D.3.1. The numerically validated target SAR values are dependent on the relative permittivity of the phantom shell; therefore, target values are given for phantom shell relative permittivity values of 3, 4, and 5. Linear interpolation shall be applied for phantom shell relative permittivity values between these values. The numerical target SAR values of Table D.4 are for 1 W measured net power into the waveguide, and were calculated using the finite-difference time-domain (FDTD) method with volume averaging requirements specified in IEEE Std C95.3-2002 [43] and verified by measurements [44]. The power delivered to the phantom is equal to the forward power into the waveguide minus the reflected power and waveguide transmission losses (including losses in the adapter and walls of the waveguide). The transmission loss of the adapter can be determined by measuring S_{11} at its coaxial port with three different known waveguide terminations connected to the waveguide port, for example a short plus two different offset shorts (short-circuited transmission lines at different offset lengths). The waveguide transmission loss shall be measured at least annually using a calibrated network analyser.

The waveguide used in the simulations was modelled as a perfect electric conductor with a matching dielectric window having dimensions as specified in D.3.1. The phantom used in the simulations has a length of 216 mm, a width of 152 mm, a depth of 80 mm and a shell thickness of 2 mm. The dielectric properties of the tissue-equivalent medium are as specified in Table 2 (see 6.2.2).

Table D.4 – Numerical target SAR values for waveguides

Frequency MHz	Phantom shell relative permittivity	1 g SAR W/kg	10 g SAR W/kg	Point SAR as a function of distance, d [mm] into the phantom along its centreline
5 200	3	165	53,7	$667 \exp(-2d/6{,}2)$
	4	180	56,5	$733 \exp(-2d/6{,}2)$
	5	194	59,1	$796 \exp(-2d/6{,}2)$
5 800	3	165	49,3	$804 \exp(-2d/5{,}5)$
	4	184	52,5	$907 \exp(-2d/5{,}5)$
	5	200	55,2	$982 \exp(-2d/5{,}5)$
In case the net power produces measured SAR values that are above the dynamic range of the probe, lower powers shall be used so as not to introduce additional measurement uncertainty or damage the probe. NOTE 1 The waveguide flange is placed in direct contact with the outer shell surface of the phantom. NOTE 2 All SAR values are normalized to 1 W net power (i.e. the power delivered to the phantom). NOTE 3 The 1 g and 10 g reference SAR values are only valid for the system validation specified in Clause A.1, using waveguides having dimensions and construction as specified in D.3.1.				

IECNORM.COM : Click to view the full PDF of IEC/IEEE 62209-1528:2020

D.4 System validation antennas for below 150 MHz

D.4.1 General

At frequencies of 150 MHz and below, the physical dimensions of standard dipoles and waveguides become too large to be practical. Therefore other antennas may be used that have been calibrated for 1 g and 10 g SAR.

D.4.2 Confined loop antenna

D.4.2.1 Mechanical description

An example for a confined loop antenna (CLA) is a resonant loop as shown in Figure D.3. The requirements for such antennas are:

a) resonant at the target frequency: f_{target} ± 1 MHz;

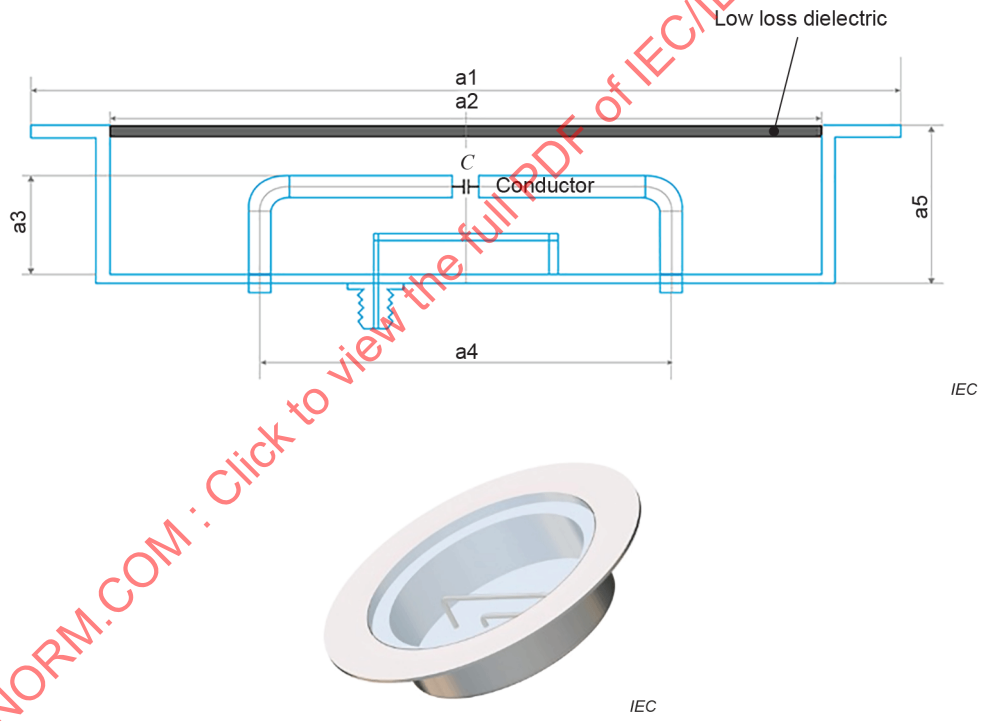
b) return loss at resonant frequency: > 10 dB;

c) stability of 1g and 10 g psSAR (at maximal specified input power): < 2 % (> 60 minutes);

d) interlaboratory reproducibility of 1 g and 10 g psSAR: < 10 %;

e) distortion (by changing the reflectivity of the floor or rotation of the structure below the phantom for typical validation configurations): < 3 %.

The return loss requirement is 10 dB compared to the 20 dB requirement for dipole antennas because the devices are considerably smaller than the wavelength. In general, antennas other than the described dipoles and waveguides have higher losses, and their efficiency can change at high input power due to thermal effects. Furthermore, high quality-factor structures are sensitive to small changes by the reflective environment. Therefore, these antennas shall be designed to minimize the influence of the environment.



Key

C capacitance

NOTE Dimensions: a1 = 220 mm, a2 = 180 mm, a3 = 25 mm, a4 = 110 mm, a5 = 45 mm.

Figure D.3 – Drawing of the CLA that corresponds to a resonant loop integrated in a metallic structure to isolate the resonant structure from the environment

IECNORM.COM : Click to view the full PDF of IEC/IEEE 62209-1528:2020

D.4.2.2 Numerical target SAR values

The target values for the CLA have been assessed by FDTD modelling of the antenna under the elliptical phantom (600 mm × 400 mm) with a 2 mm thick lossless dielectric shell (ε_r = 3,7). The antenna is fed by a stub of a coaxial cable that is terminated by a voltage source with an inner resistance of 50 Ω. The maximum mesh step is limited to 3 mm in the phantom and to 15 mm in free space. For the lower frequencies and larger meshes, the maximum mesh step is relaxed; it is always kept below λ/10. The absorbing boundary conditions terminate the computational domain at about 200 mm from the antenna. At frequencies of 64 MHz and below, this distance is increased to approximately λ/4. In all simulations, the antennas are excited with a broadband pulse. Due to their high quality factor (Q), the simulations are run for 50 periods of the operational frequencies. In particular, at the lower end of the investigated frequency range, the input impedance becomes highly reactive for small deviations from the resonance frequency, which prejudices the evaluation of the power budget of the simulations. Because the observed deviations from the nominal resonance frequency are small (< 5 %), the SAR evaluations are carried out at the actual resonance of the numerical model. To obtain reliable target values, the psSAR values are normalized to the peak of the H-fields in the plane at 5 mm distance from the medium bottom inside the phantom. Table D.5 lists the 1 g and 10 g psSAR results normalized to the H-field. The H-field normalization provides target SAR values that are independent of the internal antenna losses; the latter can be large and vary between implementations. For the same CLA type, a calibration laboratory can convert the primary H-field value to the secondary input power value that is more convenient to be used than the primary H-field values and without loss of repeatability, provided the CLA will not be opened and modified.

The assessment of the numerical uncertainty is carried out at 150 MHz, which is regarded as representative for most of the configurations. The uncertainty contribution of the power budget is evaluated for the worst case simulation at 30 MHz. For the evaluation of the grid resolution uncertainty, the mesh was further refined to a maximum step of 1,5 mm in the phantom and 7 mm in free space. In the bounding box of the antenna, the mesh step maximum was set to 1 mm. The expanded uncertainty of the numerical parameters has been assessed as 0,5 dB (k = 2).

Table D.5 – Numerical target SAR values for CLAs

	f	1 g psSAR	10 g psSAR	Local SAR at surface (above feed-point)	Local SAR at surface (20 mm offset)	Uncertainty
	MHz	W/kg/(A/m)^2	W/kg/(A/m)^2	W/kg/(A/m)^2	W/kg/(A/m)^2	dB, k = 2
CLA-6	6	0,000 84	0,000 54	0,001 33	0,000 390	0,5
CLA-13	13	0,004 04	0,002 59	0,006 36	0,001 96	0,5
CLA-30	30	0,022 3	0,014 3	0,035 5	0,010 3	0,5
CLA-64	64	0,106	0,068 1	0,168	0,047 4	0,5
CLA-128	128	0,607	0,417	0,904	0,032 6	0,5
CLA-150	150	0,842	0,586	1,24	0,489	0,5
CLA-220	220	1,20	0,818	1,82	0,686	0,5

NOTE 1 The housing of the CLA is placed in direct contact with the outer shell surface of the flat phantom.

NOTE 2 All SAR values are normalized to a peak H-field of 1 A/m measured in a plane at a distance of 5 mm from the medium bottom inside the phantom.

IECNORM.COM : Click to view the full PDF of IEC/IEEE 62209-1528:2020

D.4.3 Meander dipole antenna

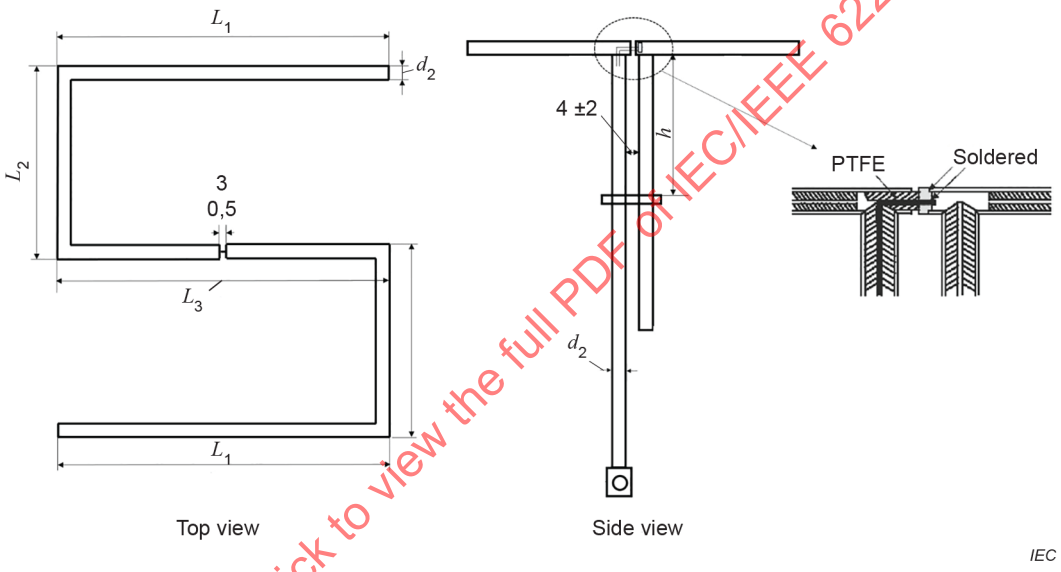
D.4.3.1 Mechanical description

Subclause D.4.3 describes a modified 150 MHz antenna, called the meander dipole, which can be installed under the standard elliptical phantom [45], [46]. Mechanical dimensions of the meander dipole are given in Figure D.4 and Table D.6. For the meander dipoles, a dielectric spacer is used to provide the distance of 15 mm ± 0,2 mm [47].

Table D.6 – Mechanical dimensions of the reference meander dipole

Frequency MHz	L_1 mm	L_2 mm	L_3 mm	h mm	d_1 mm	d_2 mm
150	197,35	129,35	197,0	165,0	6,35	6,35

Dimensions in millimetres



Key

L_1 partial length of the dipole
L_2 partial length of the dipole
L_3 partial length of the dipole
h length of the balun choke section
d_1 diameter of the dipole arms
d_2 diameter of the stub
PTFE polytetrafluoroethylene

Figure D.4 – Mechanical details of the meander dipoles for 150 MHz

D.4.3.2 Numerical target SAR values

The target values for the meander dipole antenna are shown in Table D.7 [45].

IECNORM.COM : Click to view the full PDF of IEC/IEEE 62209-1528:2020

Table D.7 – Numerical target SAR value (W/kg) for meander dipole

Frequency	1 g SAR	10 g SAR	Local SAR at surface (above feed-point)	Local SAR at surface (y = 2 cm offset from feed-point)	Uncertainty (dB, k = 2)
MHz	W/kg	W/kg	W/kg	W/kg	
150	1,71	1,23	2,16	1,22	0,2
NOTE 1 All SAR values are normalized to 1 W forward power. NOTE 2 The meander dipole is placed parallel to the surface of the flat phantom at a distance of 15 mm using a dielectric spacer.					

D.5 Orthogonal E-field source – VPIFA

D.5.1 Mechanical description

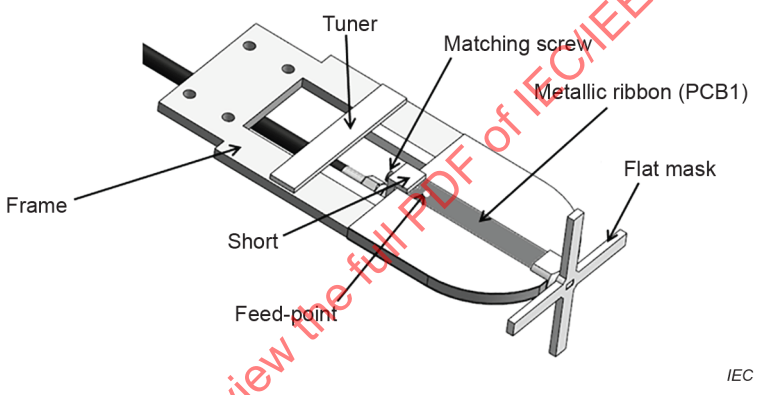
These single band antennas are designed to be placed at a wide range of locations on the curved surface of the SAM head or on a flat phantom. The design is chosen to provide a predominantly E-field coupling, as seen in a range of antenna structures where antenna metallization extends beyond the ground plane. The structure is that of a PIFA antenna. The main resonant metallic ribbon is orthogonal to the surface of the phantom. It is short-circuited on one side, and open-ended on the side that is close to the phantom, where a capacitive coupling is generated. The distance between the conductor and the phantom, and its position, are fixed by using a plastic separator, which is part of the antenna. The device should be held orthogonal to the surface. The SAR pattern is localized, with a dominant orthogonal field component. Four frequency versions for VPIFA-750, VPIFA-835, VPIFA-1950, and VPIFA-3700 are specified. At higher frequencies, the normal components dominate for $d \geq 2$ mm. Figure D.5 a) shows the basic structure of the antenna, seen from the PCB1 side. Figure D.5 b) shows the antenna as seen from the PCB2 side; the flat mask is removed in the figure to easily see the integrated spacer. The critical dimensions are shown in Figure D.5 c). Two PCB substrates are used for etching the metallic ribbon and the ground plane, respectively, and each has a thickness of 0,508 mm. Both substrates are mechanically separated by an FR4 frame. One end of this frame is used to fix the antenna to a holder. The antenna is designed to be matched to a 50 Ω coaxial connection. The dimensions for each frequency and the material properties are provided in Table D.8 and Table D.9, respectively. In order to compensate for the manufacturing errors, the antenna includes a tuning structure and a matching screw. For the tuning, a dielectric bar is adjusted to tune the resonant frequency, and for matching a brass screw integrated in the short circuit can be adjusted to change the distance between the feed-point and the short-circuit, and therefore, improve the matching. The screw implementation requires a 0,3 mm prism with a hole in order to mechanically position and fix the screw. Additionally, a lock nut is used to secure the screw position. After the antenna is fine-tuned, both elements should be fixed. The SMA connector requires a bending section to place the connection cable parallel to the antenna axis. To reduce the twisting force (torque), which can break the connector, it is recommended to first connect the bend to the cable, then connect the other side of the bend to the connector.

Figure D.6 shows the positioning mask used with the VPIFAs (see also Figure D.5 a)). The positioning tolerance using these masks is dominated by the mask uncertainty, and the corresponding SAR uncertainty is already considered in the uncertainty of the target values.

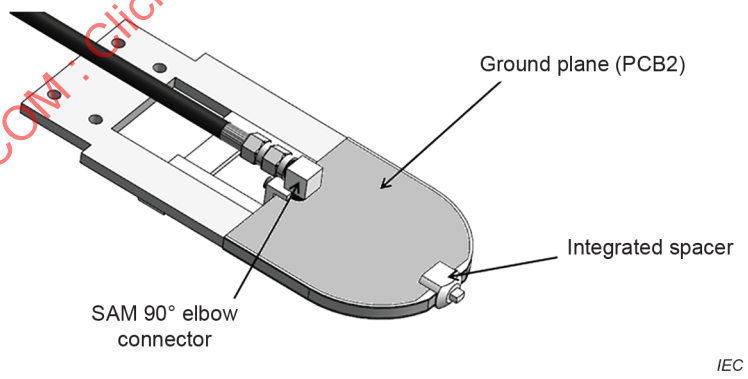
IECNORM.COM : Click to view the full PDF of IEC/IEEE 62209-1528:2020

Table D.8 – Dimensions for VPIFA antennas at different frequencies

Freq. (MHz)	Ribbon & bent width W (mm)	Length of bent width l_b (mm)	Frame thickness, l_f / radiator thickness, l_t (mm)	Frame width, W_f (mm)	Matching screw diameter / length (mm)	Tuner width W_t (mm)	$d_{b\text{-}f}$ (mm)	$d_{b\text{-}s}$ (mm)	l_{gr} (mm)	g (mm)
750	10,00 ± 0,05	1,50 ± 0,10	4,00 ± 0,05 /5,35 ± 0,05	5,00 ± 0,05	4,00 ± 0,05 / 12,00 ± 0,10	10,00 ± 0,10	58,00 ± 0,10	5,50 ± 0,10	59,90 ± 0,10	2,50 ± 0,05
835	10,00 ± 0,05	1,50 ± 0,10	4,00 ± 0,05 /5,35 ± 0,05	5,00 ± 0,05	4,00 ± 0,05 / 12,00 ± 0,10	3,50 ± 0,10	51,70 ± 0,10	5,55 ± 0,10	53,70 ± 0,10	2,50 ± 0,05
1 950	10,00 ± 0,05	1,50 ± 0,10	4,00 ± 0,05 /5,35 ± 0,05	5,00 ± 0,05	4,00 ± 0,05 / 12,00 ± 0,10	3,00 ± 0,10	77,70 ± 0,10	4,55 ± 0,10	78,45 ± 0,10	2,50 ± 0,05
3 700	3,00 ± 0,05	1,50 ± 0,10	4,00 ± 0,05 /5,35 ± 0,05	5,00 ± 0,05	4,00 ± 0,05 / 12,00 ± 0,10	2,00 ± 0,10	36,7 ± 0,10	5,77 ± 0,10	38,75 ± 0,10	2,50 ± 0,05

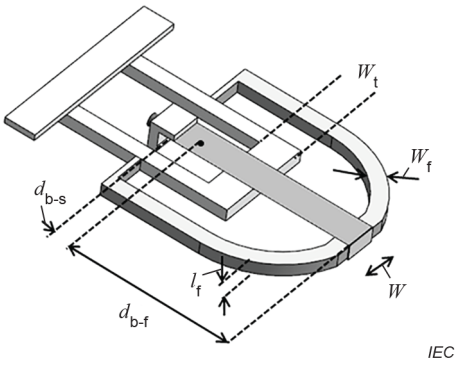


a) General schematic view from the metallic ribbon side

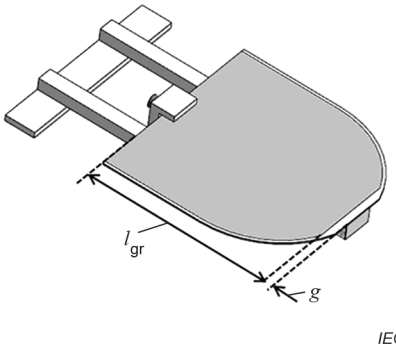


b) General schematic view from the ground plane side

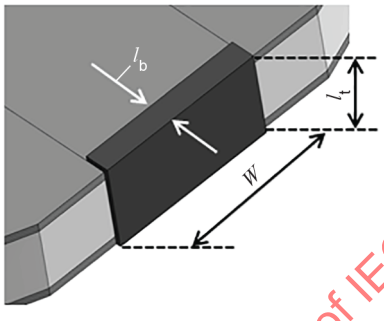
IECNORM.COM : Click to view the full PDF of IEC/IEEE 62209-1528:2020



c) Critical dimensions from front side

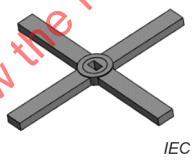


d) Critical dimensions from rear side



e) Detailed view of the bent segment

Figure D.5 – VPIFA validation antenna



The recommended tolerances for the 3D printed flat mask are ±0,10 mm.

Figure D.6 – Mask for positioning VPIFAs

Table D.9 – Electric properties for the dielectric layers for VPIFA antennas

Layer	750 MHz		835 MHz		1 950 MHz		3 700 MHz	
	ε_r	σ [S/m]	ε_r	σ [S/m]	ε_r	σ [S/m]	ε_r	σ [S/m]
Frame (FR4)	4,38	$3{,}49 \times 10^{-3}$	4,38	$3{,}84 \times 10^{-3}$	4,37	$8{,}45 \times 10^{-3}$	4,34	$15{,}7 \times 10^{-3}$
Mask (3D print)	2,22	$1{,}74 \times 10^{-3}$	2,22	$1{,}83 \times 10^{-3}$	2,22	$3{,}09 \times 10^{-3}$	2,22	$5{,}06 \times 10^{-3}$
PCB_1 (RO4350B)	3,75	463×10^{-6}	3,75	517×10^{-6}	3,75	$1{,}24 \times 10^{-3}$	3,74	$2{,}46 \times 10^{-3}$
PCB_2 (RO4350B)	3,75	463×10^{-6}	3,75	517×10^{-6}	3,75	$1{,}24 \times 10^{-3}$	3,74	$2{,}46 \times 10^{-3}$
Spacer (PET)	2,97	$7{,}52 \times 10^{-3}$	2,96	$8{,}05 \times 10^{-3}$	2,90	$14{,}5 \times 10^{-3}$	2,84	$22{,}6 \times 10^{-3}$
Tuner (FR4)	4,38	$3{,}49 \times 10^{-3}$	4,38	$3{,}84 \times 10^{-3}$	4,37	$8{,}45 \times 10^{-3}$	4,34	$15{,}7 \times 10^{-3}$

IECNORM.COM : Click to view the full PDF of IEC/IEEE 62209-1528:2020

D.5.2 Numerical target SAR values

Table D.10 provides the target values for the VPIFA antenna when the specified spacer is placed directly against the flat phantom at the centre location.

Table D.10 – Numerical target SAR values for VPIFAs on the flat phantom

Antenna	Frequency [MHz]	SAR_{1g} [W/kg]	SAR_{10g} [W/kg]	Local SAR at surface (above feed-point) [W/kg]	Local SAR at surface (y = 2 cm offset from feed-point) [W/kg]	u_c (k = 1) dB
VPIFA-750	750	12,94	3,86	66,06	0,81	0,3
VPIFA-835	835	13,22	3,82	57,02	0,729	0,3
VPIFA-1950	1 950	8,68	3,58	31,84	1,005	0,3
VPIFA-3700	3 700	9,87	4,14	27,22	0,54	0,3
NOTE All SAR values are normalized to 1 W forward power.						

IECNORM.COM : Click to view the full PDF of IEC/IEEE 62209-1528:2020

© IEC/IEEE 2020

Annex E
(normative)

Calibration and characterization of dosimetric (SAR) probes

E.1 Introductory remarks

Currently available SAR probes are based on Schottky diode detectors. The measured signal at the output of each sensor is a voltage proportional to E or E^2, depending on the magnitude of the electric field incident on the diode.

Most isotropic probes consist of three small dipole sensors with diode detectors at their centre gaps. The directivity patterns of such sensors are orthogonal, and the total E-field magnitude is proportional to the root-sum-square (RSS) of the three orthogonal field components. In the square-law region of the diode response, the sensor output voltage is proportional to the mean square of the corresponding field component. Beyond that range the output voltage is compressed, and therefore requires linearization within the dynamic range. Differences due to manufacturing tolerances will introduce somewhat different sensitivities for each sensor, which shall be accounted for during calibration and compensated during measurement.

Probe calibration for SAR testing in tissue-equivalent medium will produce either a SAR conversion factor or an E-field conversion factor. Because SAR is proportional to tissue-equivalent medium conductivity, a direct calibration in terms of SAR would be valid only for media with the exact same conductivity. The E-field sensitivity depends more on the complex permittivity and is less sensitive to the conductivity. Calibration in terms of E-field rather than SAR has a broader range of validity, and is therefore preferred for routine SAR testing in which the tissue-equivalent medium properties vary slightly over time.

Probe calibration is usually done with either one-step or two-step methods. In the two-step method, the total field is given by Formula (E.1):

$$|E|^2 = \sum_{i=1}^{3} |E_i|^2 = \sum_{i=1}^{3} \frac{f_i(V_i)}{\eta_i \psi_i} \tag{E.1}$$

Here, E_i (i = 1, 2, 3) are the components resulting from the projection of the E-field vector on the three orthogonal sensors, $f_i(V_i)$ is a linearizing function of the rectified sensor signal V_i, η_i [in μV/(V/m)^2] is the sensitivity of dipole sensor i in air, and ψ_i is the ratio of sensor response in air to the response in the dielectric media (sometimes referred to as the conversion factor). This two-step method has also been called a three-step method (Meier et al. [48]), where the third step involves the linearizing function $f_i(V_i)$.

The linearization function $f_i(V_i)$ is not only a function of the RMS value of V_i but also dependent on the signal envelope. Nadakuduti et al. [20] has shown that CW and periodic pulse-modulated signals with constant amplitude (e.g. GSM) can be more easily corrected for linearity than communication protocols employing complex modulations with stochastic signal envelopes. Acceptable linearization of complex modulations can be obtained over a wide dynamic range with a linearity uncertainty of less than 0,4 dB.

In the one-step methods specified in E.3.3, the total field is given by Formula (E.2):

$$|E|^2 = \sum_{i=1}^{3} |E_i|^2 = \sum_{i=1}^{3} \frac{f_i(V_i)}{\gamma_i} \tag{E.2}$$

IECNORM.COM : Click to view the full PDF of IEC/IEEE 62209-1528:2020

Here the η_i factors are included in the total in-tissue sensitivity γ_i. Another one-step procedure based on a standard antenna method is described in Person et al. [49].

Probe calibrations are valid only when the sensors are sufficiently far away (at least one probe-tip diameter) from any media boundaries. When the probe is close to such boundaries and compensation is not applied, the sensitivity can change. The boundary effect, as well as the isotropic response of the probe, shall be assessed using separate tests, as described in 8.4.1.5, 8.4.1.6, Clause E.4, and Clause E.6.

E.2 Linearity

Probe linearity is introduced and explained in 8.4.1.3; the associated uncertainty can be determined in accordance with the methods set forth in 8.4.1.3 for CW signals, and 8.4.2.7 for modulated signals. Clause E.2 describes a general methodology for assessing probe linearity of any signal.

The determination of the linearization function $f_i(V_i)$ shall be performed and applied prior to the assessment of the sensitivity (see Clause E.1). This is best performed using an amplitude or power scan with a well-defined incident field having the corresponding signal characteristics. Any of the following set-ups can be used, provided the dynamic range of interest is assessed in steps of 3 dB or less. A true RMS power meter, or an appropriately calibrated field probe, should be used as reference. The linearization parameters are determined for the i-th sensor by assessing and removing the linearization error between the measured response $E_{\text{inc,meas}}$ and the incident field E_{inc}, as shown in Formula (E.3):

$$error_{\text{linerarization}} = 20\lg\frac{E_{\text{inc,meas}}}{E_{\text{inc}}} \tag{E.3}$$

An approach is described by Nadakaduti et al. [20] to apply curve fitting to remove the linearization error for signals having complex signal envelopes.

E.3 Assessment of the sensitivity of the dipole sensors

E.3.1 General

The sensitivity factors can be determined by applying one-step or two-step calibration procedures. Alternatively, transfer calibration can be applied.

E.3.2 Two-step calibration procedures

E.3.2.1 General

The total field shall be evaluated according to Formula (E.2). The separation of the probe sensitivity into two factors (η_i and γ_i) allows the use of certain standardized free-space probe calibration procedures, and provides additional validation of the probe performance and calibration set-up.

E.3.2.2 Sensitivity in air (first step)

The most accurate set-ups used for the generation of well-defined fields to simulate free-space conditions for use in probe calibration are waveguides. The reasons are as follows:

- waveguide set-ups require moderate power and less space than far-field calibration set-ups;
- generation of the most accurate fields traceable to power readings is possible;

IECNORM.COM : Click to view the full PDF of IEC/IEEE 62209-1528:2020

- the uncertainty produced by the field disturbance due to the probe insertion is negligible for small near-field probes when the waveguide dimensions are considerably larger than probe dimensions;
- the set-ups allow easy access for orienting the probe axis normal or parallel to the field polarization inside the set-up;
- in addition, cross-validation of the general field strengths is possible by using a set of waveguides with overlapping frequency ranges.

As long as the resistive feed-line does not load the dipole-diode sensor and the probe is small compared to the wavelength, the sensitivity in free-space is independent of frequency. This gives an additional validation of the calibration set-ups, and checks for possible field perturbations due to the probe. Effects due to probe insertion are typically negligible if high-quality waveguide couplers and matched sources are used. An additional uncertainty source in the waveguide set-ups is due to reflections from the terminating load, which can result in a standing wave pattern within the set-up. Reflections can be kept below 1 % if high-quality waveguide loads are used. Furthermore, the uncertainty can be compensated by performing supplementary measurements with a $\lambda/4$-shifted load and averaging of the two readings.

At lower frequencies (e.g. below 750 MHz), TEM cells can be employed rather than waveguides. However, the field inside a TEM cell is less well-defined, i.e. there is rather large deviation from the predicted homogeneous field distribution [20]. The probe is generally inserted through small holes in the walls of the TEM cell and positioned at the centre (above or below the septum) where the field is mostly homogeneous over the probe dimensions. Each sensor is evaluated with respect to the field component parallel to the sensor.

E.3.2.3 Sensitivity in media (second step)

E.3.2.3.1 General

The sensitivity in tissue-equivalent medium is determined by generating locally-known field strength values inside the media. Two methods can be used:

a) transfer calibration with temperature probe;

b) calibration with analytical fields.

E.3.2.3.2 Transfer calibration with temperature probes

In lossy media, SAR is related both to the electric field (E) and the rate of temperature rise ($\mathrm{d}T/\mathrm{d}t$) in the medium having specific heat capacity c_h. Hence, based on Formula (E.4)

$$SAR = \sigma \frac{E^2}{\rho} = c_\mathrm{h} \left. \frac{\mathrm{d}T}{\mathrm{d}t} \right|_{t=0}, \tag{E.4}$$

the electric field in lossy media can be measured indirectly by measuring the rate of temperature rise in the medium. Non-perturbing temperature probes (optical probes or thermistor probes with resistive lines) with small sensors (< 2 mm) and fast response time (< 1 s) are available and can be easily calibrated with high precision [50]. The set-up and the exciting source have no influence on the calibration; only the relative positioning uncertainties of the temperature probe and the E-field probe to be calibrated shall be considered. However, several problems limit the available accuracy of probe calibrations with temperature probes.

a) The rate of temperature rise is not directly measurable, but shall be evaluated from temperature measurements that are measured over a short time duration. Special precaution is necessary to avoid measurement uncertainties caused by temperature gradients due to energy-equalizing effects or convection currents in the medium. Such effects cannot be completely avoided. With a careful set-up, these uncertainties can be kept small.

IECNORM.COM : Click to view the full PDF of IEC/IEEE 62209-1528:2020

b) The measured volume around the temperature probe is not well defined. It is difficult to calculate the energy transfer into the probe from a surrounding gradient temperature field into the probe (typically, temperature probes are calibrated in medium with homogeneous temperatures). There is no traceable standard for temperature increase measurements.

c) The calibration depends on the assessment of the mass density, the specific heat capacity, and the electrical conductivity of the medium. While mass density and specific heat capacity can be measured accurately with standardized procedures (on the order of ±2 % for c_h; much better for ρ), there is no standard for the measurement of the electrical conductivity. Depending on the method and medium, the uncertainty can be ±5 %.

d) Sufficient temperature rise is required to produce measurable temperature rises; therefore calibration is often performed at a higher power level than the E-field methods. The non-linearities in the system (e.g. power measurements, different field components, etc.) shall be compensated.

Considering these problems, the calibration accuracy of E-field probes using the temperature-rise technique in a carefully designed set-up is about ±10 % (combined standard uncertainty) [48]. A set-up using a combination of waveguide and temperature-rise techniques was presented in [51]. The estimated combined standard uncertainty of this set-up is ±5 % when the same medium is used for both the calibration and for actual measurements, and ±7 % to ±9 % when not, which is in good agreement with the estimates given in [48].

E.3.2.3.3 Uncertainty analysis for transfer calibration with temperature probes

When performing an uncertainty analysis of the transfer calibration using the temperature-rise technique, at least the parameters listed in Table E.1 shall be considered.

Table E.1 – Uncertainty analysis for transfer calibration using temperature probes

Input quantity X_i (source of uncertainty)	Probability distribution	Uncertainty ± %	Divisor	c_i	Standard uncertainty u_i ± %	v_i or v_{eff}
Positioning of E-field probe	R		√3	1		∞
Positioning of temperature probe	R		√3	1		∞
E-field probe linearity	R		√3	1		∞
Temperature probe drift and noise	R		√3	1		∞
Temperature probe linearity	R		√3	1		∞
Medium conductivity	R		√3	1		∞
Specific heat of medium	R		√3	1		∞
Medium density	R		√3	1		∞
Temperature probe accuracy	R		√3	1		∞
Combined standard uncertainty	RSS					
NOTE c_i is the sensitivity coefficient.						

The component tolerances of Table E.1 shall be determined as follows:

a) The positioning tolerances of the temperature and E-field probes are evaluated according to O.7.1 using the actual penetration depth determined from the tissue-equivalent medium dielectric properties measured at the calibration frequency. Since SAR variations at the peak location are much smaller in directions parallel to the phantom surface than in directions normal to the phantom surface, the procedures of O.7.1 are applicable when both temperature and E-field probe movements are limited to parallel directions only.

IECNORM.COM : Click to view the full PDF of IEC/IEEE 62209-1528:2020

b) Linearity uncertainty of the field probe is assessed according to Clause O.1, and for calibration shall not exceed 0,1 dB at the calibration field strength.

c) Temperature probe drifts and noise are assessed by temperature measurements at 1 s intervals for 1 h, with an integration time of less than 0,5 s in a constant temperature condition. The temperature tolerance is computed as 100 × [(T_{max} − T_{min})/ΔT_{min}], where ΔT_{min} is the minimum temperature rise for the different power levels used for the calibration.

d) The temperature probe linearity tolerance should be determined using the following procedures. The accuracy and linearity of the temperature probe readings are compared against a traceable temperature reference at 10 temperature steps in a range greater than or equal to that used during the calibration. The tolerance is computed as 100 × [(T_{max} − T_{min})/ΔT_{min}], where ΔT_{min} is the larger of the minimum temperature rise for the different power levels used for the calibration or the tolerance for the temperature reference.

e) Medium conductivity measurement tolerance during temperature calibration is determined using the same procedures as in O.9.3.

f) The specific heat tolerance of tissue-equivalent media shall be determined using calorimeter procedures ([51], [52]).

g) Medium density measurement tolerance shall be computed according to the RSS of the volume and weight tolerances obtained using standard measurement methods for volume and weight.

h) The temperature probe shall have a step response time of 1 s or less, which is specified as the time required by the measurement equipment, temperature probe, and readout electronics to reach 90 % of the expected final temperature value, after a step variation of 5 °C or more has been applied to the temperature probe.

E.3.2.3.4 Calibration with analytical fields (waveguides)

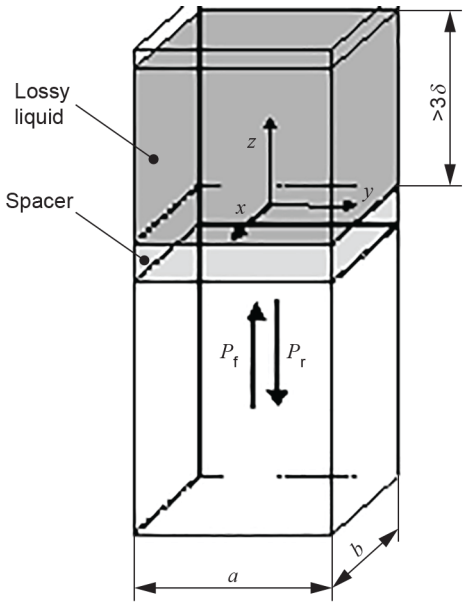
In this method, a test set-up is used in which the field can be calculated analytically from measurements of other physical magnitudes (e.g. input power). This corresponds to the standard field method for probe calibration in air; however, there is no standard specified for fields in lossy media.

When using calculated fields in lossy media for probe calibration, several points shall be considered in the estimation of the uncertainty.

- The net RF power dissipated in the waveguide shall be measured accurately. This requirement implies precise measurements of two out of the following three quantities: incident power, reflected power, reflection coefficient at the waveguide input port.
- The accuracy of the calculated field strength will depend on the assessment of the dielectric properties of the medium.
- Due to the small wavelength in media with high permittivity, higher order modes can be excited. The field distribution in the set-up shall be carefully checked for conformity with the theoretical field distribution.

Waveguides can be utilized to generate an analytically known field inside tissue-equivalent media, e.g. the set-up presented in [53]. In this set-up (Figure E.1), the upper part of a vertically-oriented open-ended waveguide is filled with liquid. A dielectric slab at a distance > λ (λ refers to the wavelength in the air section of the waveguide) from the feeding coupler provides an impedance match (> 10 dB return loss) between air and liquid. The symmetry of the construction and high losses in the liquid ensure that the field distribution inside the tissue-equivalent medium follows the TE_{10} waveguide mode pattern, although higher-order modes theoretically could exist. In [53] the absence of higher modes was carefully validated by measuring the electric field distribution in the volume of the liquid, and this was found to be within ±2 % of the theoretical TE_{10} mode pattern.

IECNORM.COM : Click to view the full PDF of IEC/IEEE 62209-1528:2020



Key

x, y, z	axes of Cartesian coordinate system
3δ	liquid depth (> 3 times the penetration depth)
a	waveguide cross-section width
b	waveguide cross-section height
P_f	incident power
P_r	reflected power

Figure E.1 – Experimental set-up for assessment of the sensitivity (conversion factor) using a vertically-oriented rectangular waveguide

Inside the liquid, the field propagates almost like a TEM wave, because of the low cut-off frequency. The liquid depth (> 3 times the penetration depth) was chosen so that the reflections at the upper surface of the liquid are negligible. Formula (E.5) shows the relationship between the SAR at the cross-sectional centre (x = y = 0) of the lossy waveguide and the longitudinal distance (z) from the dielectric slab:

$$SAR(z) = \frac{4(P_f - P_r)}{\rho ab\delta} e^{-2z/\delta} \quad \text{(E.5)}$$

where

ab is the cross-sectional area of the waveguide;

P_f is the forward power inside the air-filled section of the waveguide;

P_r is the reflected power inside the air-filled section of the waveguide;

z is the distance above the upper surface of the dielectric slab;

ρ is the liquid density;

δ is the penetration depth inside the lossy liquid.

NOTE For the purposes of this document, the density ρ is assumed to be 1 000 kg/m^3.

The penetration depth δ, which is the reciprocal of the waveguide-mode attenuation coefficient α, is determined from a scan along the z-axis and compared with the theoretical value determined from Formula (E.6) using the measured dielectric properties of the lossy liquid.

IECNORM.COM : Click to view the full PDF of IEC/IEEE 62209-1528:2020

$$\delta = \alpha^{-1} = \Re\left\{\sqrt{(\pi/a)^2 + j\omega\mu_0(\sigma + j\omega\varepsilon_0\varepsilon_r')}\right\}^{-1} \quad \text{(E.6)}$$

Table E.2 provides design guidelines for calibration waveguides with a return loss of at least 10 dB at the most important frequencies used for personal wireless communications. Values for the penetration depth for these specific fixtures and tissue-equivalent medium dielectric properties are also listed in Table E.2.

Table E.2 – Guidelines for designing calibration waveguides

Frequency MHz	Waveguide dimension	Dielectric slab[a]	
	a mm	ε_r'	Thickness mm
300	584,2	5,5	106,0
450	457,2	6,0	66,1
900	247,6	5,6	34,8
1 450	129,5	4,7	24,8
1 800 to 2 000	109,2	4,8	19,4
2 450	109,2	5,7	12,6
3 000	86,4	5,7	10,3
3 500	58,2	4,9	9,76
3 900	58,2	4,9	9,76
4 200	58,2	4,9	9,76
4 600	47,5	3,5	9,50
4 900	47,5	3,5	9,50
5 400	47,5	5,6	5,73
6 000	40,4	5,4	5,25
7 000	35,0	3,1	20,0
9 000	23,0	3,1	16,0

[a] Permittivity and thickness of the dielectric slab may vary from the values shown to accommodate commercially available materials. If the dielectric slab permittivity varies from the indicated value by more than 2 %, it is recommended to newly optimize the slab thickness for the best matching (return loss typically greater than 10 dB).

NOTE 1 The waveguides are filled with tissue-equivalent medium having dielectric properties as given in Table 2.

NOTE 2 By convention, the length of the cross-section short edge is one half that of the long edge, i.e. $b = a/2$.

NOTE 3 The waveguide dimensions are in accordance with the EIA RS-261-B: 1979 [54].

NOTE 4 These dimensions are also dependent on the frequency bandwidths of interest.

IECNORM.COM : Click to view the full PDF of IEC/IEEE 62209-1528:2020

This technique provides excellent accuracy, with a combined standard uncertainty of < ±3,6 % depending on the frequency and media. The calibration itself is reduced to power measurements traceable to a standard calibration procedure. The practical limitation given by the waveguide size to the frequency range between 750 MHz and 6 000 MHz is not severe in the context of compliance testing, because most of the operational frequencies for mobile communications systems are covered within this range. For frequencies below 750 MHz, transfer calibration with temperature probes remains the most practical way to achieve calibration with the lowest uncertainties.

E.3.2.3.5 Uncertainty analysis for calibration with analytical fields (waveguides)

When performing an uncertainty analysis of the probe calibration with analytical fields in a waveguide, at least the parameters included in Table E.3 shall be considered.

Table E.3 – Uncertainty analysis of the probe calibration in waveguide

Input quantity X_i (source of uncertainty)	Probability distribution PDF_i	Uncertainty $a(x_i)$ ± %	Divisor q_i	$u(x_i) = a(x_i)/q_i$	c_i (1 g, 10 g)	$u(y) = c_i \cdot u(x_i)$ ± %	v_i or v_{eff}
Incident or forward power	R		√3		1		∞
Reflected power	R		√3		1		∞
Liquid conductivity measurement	R		√3		1		∞
Liquid permittivity measurement	R		√3		1		∞
Liquid conductivity deviation	R		√3		1		∞
Liquid permittivity deviation	R		√3		1		∞
Frequency deviation	R		√3		1		∞
Field homogeneity	R		√3		1		∞
Field-probe positioning	R		√3		1		∞
Field-probe linearity	R		√3		1		∞
Combined standard uncertainty	RSS						

IECNORM.COM : Click to view the full PDF of IEC/IEEE 62209-1528:2020

E.3.3 One-step calibration procedure – reference antenna method

E.3.3.1 General

The procedure of E.3.2 can be combined into a one-step procedure using reference antennas. The total field shall be evaluated according to Formula (E.2). Reference antennas are small antennas designed for operating within the appropriate tissue-equivalent medium. Examples of antennas developed at 900 MHz and 1 800 MHz have been described in [49], [55]. At least two identical antennas are necessary to evaluate the gain of the main lobe for use in probe calibration.

The one-step methods in E.3.3 and also E.3.4 assess the isotropy with respect to probe rotation and polarization of the incident field. The method in E.3.4 additionally considers the angle of incidence.

Typical antennas used include simple directive patch antennas with a gain of 5 dBi or higher (see Figure E.2 for set-up). Because side lobes caused by multiple reflections at the tank wall could interfere with the calibration, it shall be verified that these are sufficiently attenuated by the tissue-equivalent medium before they reach the probe tip.

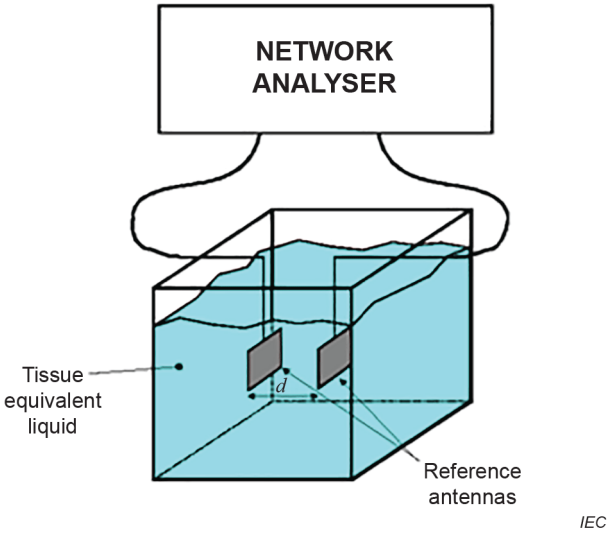


Figure E.2 – Illustration of the antenna gain evaluation set-up

E.3.3.2 Reference-antenna gain measurement

The reference antenna gain evaluation is performed according to the following protocol:

a) Position the antennas in the tissue-equivalent medium such that their main-beam axes are aligned and at a well-defined distance d, where $d \geq 2D^2/\lambda_{\text{liquid}}$, D is the largest dimension of the reference antenna, and λ_{liquid} is the wavelength in the medium. The antennas shall be at least 10 cm from any walls of the container.

b) Measure the reflection coefficients ρ_1 and ρ_2 at the input ports of each antenna.

c) Measure the transmission coefficient S_{21} between the two antennas at the same ports.

d) The gain is described in Formula (E.7):

$$G = |S_{21}(d)| \times e^{\alpha d} \left(\frac{4\pi d}{\lambda_{\text{liquid}}} \right) \times \frac{1}{\sqrt{\left(1-|\rho_1|^2\right)\left(1-|\rho_2|^2\right)}} \tag{E.7}$$

where the attenuation coefficient is described in Formula (E.8):

$$\alpha = \frac{2\pi f}{c} \times \left(\varepsilon_r'^2 + \varepsilon_r''^2\right)^{1/4} \times \sin\left[\frac{1}{2}\arctan\left(\frac{\varepsilon_r''}{\varepsilon_r'}\right)\right] \tag{E.8}$$

E.3.3.3 Uncertainty analysis for reference-antenna gain measurement

When performing an uncertainty analysis of the reference antenna measured gain, at least the parameters included in Table E.4 shall be considered. Supplemental methods for the calculation of the antenna gain can be found in E.3.3.6.

IECNORM.COM : Click to view the full PDF of IEC/IEEE 62209-1528:2020

Table E.4 – Uncertainty template for evaluation of reference antenna gain

Input quantity X_i (source of uncertainty)	Probability distribution PDF_i	Uncertainty $a(x_i)$ ± %	Divisor q_i	$u(x_i) = a(x_i)/q_i$	c_i	$u(y) = c_i \cdot u(x_i)$ ± %	v_i or v_{eff}
Incident power	R		√3		1		∞
Reflection coefficients	R		√3		1		∞
Distance	R		√3		1		∞
Medium conductivity	R		√3		1		∞
Medium permittivity	R		√3		1		∞
Combined standard uncertainty	RSS		√3				

E.3.3.4 Reference antenna method probe calibration procedure

The following protocol shall be used for evaluating the sensitivity coefficients of the probe.

a) Position one antenna in the tissue-equivalent medium. The antenna shall be at a minimum distance of 10 cm from the walls of the container.

b) Connect a power source to the input port of the reference antenna. The theoretical electric field E_{th} at a distance d_a from the antenna is given by Formula (E.9):

$$E_{th} = \left(\frac{P_{in}\left(1-|\Gamma|^2\right) G e^{-2\alpha d_a}}{4\pi d_a^2} \times \frac{120\pi}{\Re\left\{\sqrt{\varepsilon_r}\right\}} \right)^{\frac{1}{2}} \quad \text{(E.9)}$$

where

d_a is the distance from the antenna to the geometric centre of the sensors where $d \geq 2D^2/\lambda_{liquid}$;

D is the largest dimension of the reference antenna;

λ_{liquid} is the wavelength in the medium;

G is the antenna gain;

P_{in} is the input power;

Γ is the reflection coefficient of the antenna.

It is recommended to connect a bidirectional coupler to control the input power. Tune the input power so that E_{th} ~ 30 V/m.

c) Position the probe in the tissue-equivalent medium so that the centre of the detectors is at a distance d from the antenna.

d) Orient the probe in order to align the direction of the sensor with the polarization of the reference antenna.

e) Measure the voltage $V_{1,meas}$ at the transmitting antenna port.

f) The sensitivity coefficient K_1 for this antenna is $K_1 = V_{1,meas} / E_{th}^2$

g) Repeat steps d) through f) for the other two sensors to evaluate K_2 and K_3.

h) Using the sensitivity coefficients of the probe, SAR is determined by the Formula (E.10):

$$SAR = \frac{\sigma}{\rho}\left(\frac{V_{1,meas}}{K_1} + \frac{V_{2,meas}}{K_2} + \frac{V_{3,meas}}{K_3} \right) \quad \text{(E.10)}$$

where ρ is the density (1 000 kg/m^3).

IECNORM.COM : Click to view the full PDF of IEC/IEEE 62209-1528:2020

E.3.3.5 Uncertainty analysis for reference-antenna method probe calibration

When performing an uncertainty analysis of the calibration with reference antennas, at least the parameters included in Table E.5 shall be considered.

Table E.5 – Uncertainty template for calibration using reference antenna

Input quantity X_i (source of uncertainty)	Probability distribution PDF_i	Uncertainty $a(x_i)$ ± %	Divisor q_i	$u(x_i) = a(x_i)/q_i$	c_i	$u(y) = c_i \cdot u(x_i)$ ± %	v_i or v_{eff}
Incident power	R		√3		1		∞
Reflection coefficients	R		√3		1		∞
Antenna gain	N		1 or k		1		∞
Medium conductivity	R		√3		1		∞
Medium permittivity	R		√3		1		∞
Probe positioning	R		√3		1		∞
Combined standard uncertainty	RSS						

E.3.3.6 Extended formulas for the antenna gain in the near-field measurement

The antenna gain G in Formula (E.7) and the theoretical electric field strength E_{th} are based on the far-field measurement in the tissue-equivalent medium. However, it is often difficult to measure S_{21} in the far-field region due to large attenuation of the field in the tissue-equivalent medium. In such case, an extension of the Friis transmission formula in the lossy medium can be introduced to define the near-field gain of the reference antenna $G_{near}(d)$, and then E_{th} in the near-field region can be estimated [56]. The near-field gain $G_{near}(d)$ is a function of the distance from the antenna d, and can be expressed by the power series of the inverse of d. Then the procedure to determine the reference antenna gain G in E.3.3.1 a) is modified as follows.

a) Position the antennas in the medium such that their main-beam axes are aligned and at a well-defined distance d, and λ_{liquid} is the wavelength in the medium. The antennas shall be at least 10 cm from any walls of the container.

b) Measure the reflection coefficients ρ_1 and ρ_2 at the input ports of each antenna.

c) Measure the transmission coefficient $S_{21}(d)$ between the two antennas at the same ports and the same distance by changing d.

d) The near-field gain $G_{near}(d)$ can be expressed as in Formula (E.11):

$$G_{near}(d) = \frac{|S_{21}(d)|\exp(\alpha d)\cdot(2\beta d)}{\sqrt{(1-|\rho_1|^2)\cdot(1-|\rho_2|^2)}} = G \times \exp\left(\frac{a_1}{d} + \frac{a_2}{d^2} + \ldots\right) \quad \text{(E.11)}$$

where

d is the distance from the antenna;

$S_{21}(d)$ is the transmission coefficient between the two antennas;

P_{in} is the input power;

ρ_1 is the reflection coefficient of the antenna 1;

ρ_2 is the reflection coefficient of the antenna 2;

α is given by Formula (E.8);

β is $2\pi/\lambda_{liquid}$;

G is the antenna gain in dB representation given in Formula (E.12):

IECNORM.COM : Click to view the full PDF of IEC/IEEE 62209-1528:2020

$$G_{\text{neardB}}(d) = G_{\text{dB}}\left[1+\frac{1}{A\times d}+\frac{1}{B\times d^2}\right] \quad \text{(E.12)}$$

where

d is the distance from the antenna;

G_{dB} is the antenna gain.

The constants A, B or a_1, a_2,... can be determined by curve-fitting. Therefore the choice of proper curve fitting for the range of d is important. Attenuation and phase constants α and β in the liquid are obtained from the dielectric properties of the medium.

e) Then, $E_{\text{th}}(d)$ in the near-field region is given by Formula (E.13):

$$\left|E_{\text{th}}(d)\right|^2 = \frac{30P_{\text{in}}\left(1-\left|\Gamma\right|^2\right)G_{\text{near}}(d)\text{e}^{-2\alpha d}}{\Re\left\{\sqrt{\varepsilon_{\text{r}}}\right\}d^2} \quad \text{(E.13)}$$

where

α is given by Formula (E.8);

d is the distance from the antenna;

ε_{r} is the complex relative permittivity;

$G_{\text{near}}(d)$ is the near-field gain;

P_{in} is the input power;

Γ is the reflection coefficient of the antenna.

E.3.4 One-step calibration procedure – coaxial calorimeter method

E.3.4.1 General

Figure E.3 shows a coaxial calorimeter system for calibrating SAR probes by the temperature rise method at frequencies below 450 MHz, from [57]. It consists of a coaxial line with air dielectric, having an outer shield diameter 2,3 times the inner conductor diameter, which gives 50 Ω characteristic impedance. Towards the short-circuit end of the line, the inner conductor is replaced with a plastic pipe containing the tissue-equivalent medium, which is in direct contact with the metal end of the centre conductor and also the shorting plate at the top of the system. The probe is inserted through an aperture in the centre of the shorting plate. The diameter of the liquid in the pipe shall be the same as that of the metal inner conductor, and this shall be sufficiently large to prevent probe proximity errors from being significant. Power applied to the input port results in an axially polarized field in the liquid, with a fairly uniform distribution below 150 MHz.

IECNORM.COM : Click to view the full PDF of IEC/IEEE 62209-1528:2020

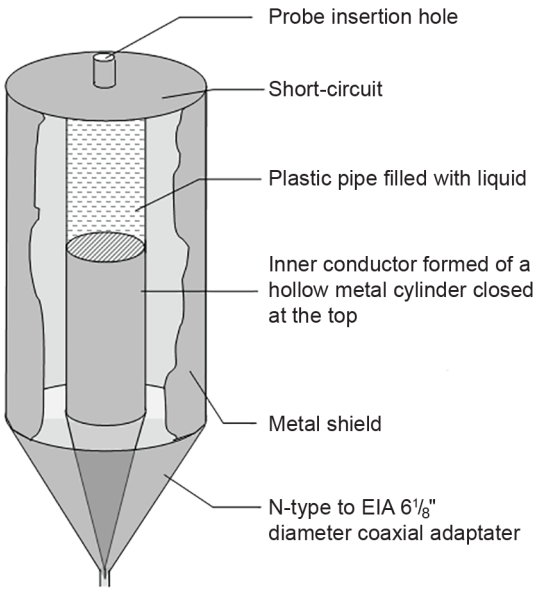


Figure E.3 – Schematic of the coaxial calorimeter system

The SAR probe is used to measure the electric field in the liquid at the reference point for approximately 1 W input power. A temperature probe is then used to measure the rate of temperature rise in the liquid at the same position, using approximately 30 W. For accuracy, it is important that the actual temperature rise is limited to 1 °C, since the conductivity of the medium changes by between 3 % and 5 % per °C. The ratio of the power for the SAR probe measurement and the temperature rise measurement shall be determined using a directional power sensor, or directional coupler and power sensor, although the absolute power is not required. Calibration is by comparing the linear output voltages from the SAR probe sensors with the electric field in the liquid that is calculated using Formula (E.14):

$$E^2_{\text{probe}} = \frac{\rho \times c_{\text{h}}}{\sigma} \frac{\mathrm{d}T}{\mathrm{d}t} \frac{P_{\text{sensor}}}{P_{\text{temperature}}} \tag{E.14}$$

where

E^2_{probe} is the electric field squared at the probe sensors;
ρ is the density of the phantom liquid;
σ is the conductivity;
c_{h} is the specific heat;
P_{sensor} is the power used in the SAR probe measurement;
$P_{\text{temperature}}$ is the power used in the temperature measurement;
$\mathrm{d}T/\mathrm{d}t$ is rate of increase in temperature in the liquid.

This system provides accurate calibrations over the frequency range 30 MHz to 450 MHz, with a standard uncertainty of around ±5 %.

E.3.4.2 Uncertainty analysis for coaxial calorimeter probe calibration

When performing the calibration using this method, at least the parameters included in Table E.6 shall be considered.

IECNORM.COM : Click to view the full PDF of IEC/IEEE 62209-1528:2020

Table E.6 – Uncertainty components for probe calibration using thermal methods

Input quantity X_i (source of uncertainty)	Probability distribution PDF_i	Uncertainty $a(x_i)$ ± %	Divisor q_i	$u(x_i) = a(x_i)/q_i$	c_i	$u(y) = c_i \cdot u(x_i)$ ± %	v_i or v_{eff}
Liquid temperature coefficient	R		√3		1		∞
Liquid heat capacity	R		√3		1		∞
Liquid density	R		√3		1		∞
Liquid conductivity	R		√3		1		∞
Power sensor linearity and drift	R		√3		1		∞
Temperature probe linearity	R		√3		1		∞
Thermal effects giving rise to non-linear temperature rise	R		√3		1		∞
Positional errors	N		1		1		∞
Combined standard uncertainty	RSS						

E.4 Isotropy

E.4.1 Axial isotropy

The probe shall be exposed to a wave with incident polarization normal to the probe axis. The axial isotropy is determined by rotating the probe along its major axis from 0° to 360° with a step size less than or equal to 15°.

E.4.2 Hemispherical isotropy

E.4.2.1 General

The probe shall be exposed to a reference wave with varying angles of incidences relative to the plane normal to the probe axis. Assessment of the hemispherical isotropy shall be done at a location where the SAR gradients are less than 3 % per mm; this can be achieved by using standing waves. The hemispherical isotropy shall be determined by either tilting the probe, or changing the polarization of the reference wave. The angles of incidence shall vary from 90° (axial) to 0° (normal), with a step size less than or equal to 30°. For each incidence angle, the probe shall be rotated through a range of 360° with a step size less than or equal to 15°.

The following four methods can be used for hemispherical isotropy, each producing similar results:

a) flat phantom with dipole at side (see E.4.2.2);

b) flat phantom with dipole beneath (see E.4.2.3);

c) spherical phantom with dipole (see E.4.2.4);

d) reference antenna method (see E.4.2.5).

E.4.2.2 Isotropy with flat phantom and dipole at side

The set-up consists of a thin-wall plastic box filled with tissue-equivalent medium exposed to a half-wave resonant dipole operating at the test frequency. The following protocol shall be used for evaluating the spherical isotropy of the probe.

IECNORM.COM : Click to view the full PDF of IEC/IEEE 62209-1528:2020

a) Mount the dipole antenna horizontally on a mounting device and position it parallel to the flat phantom (see Figure E.4). The antenna shall be positioned at a maximum distance of $e = \lambda/10$ from the adjacent wall of the medium container.

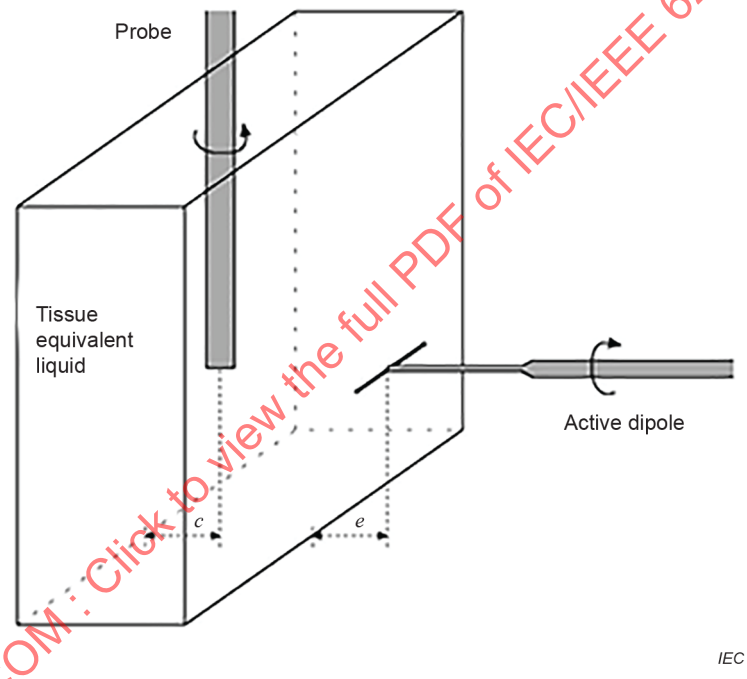
b) Insert the probe vertically in the liquid so that the centre of the three probe sensors is positioned in front of the dipole feed-point at the height of the dipole axis.

c) The horizontal position of the probe shall be, whenever possible, at the maximum of the standing wave near the back side of the box, at a distance c from the phantom/liquid interface, where the E-field is partially homogeneous and the H-field is at a minimum.

d) The dipole shall be rotated around the axis of its mounting device from at least 0° to 180° with incremental steps of less than or equal to 30°.

e) At each step the probe is rotated about its axis from 0° to 360° by the probe positioner, and measurement data is recorded in steps of less than or equal to 15°.

The deviation from spherical isotropy is then expressed as an uncertainty component with a rectangular probability distribution limited by the measured response peaks. Details can be found in [22].



Key

c Distance from probe to backwall

e Maximum distance from the front wall of the liquid container

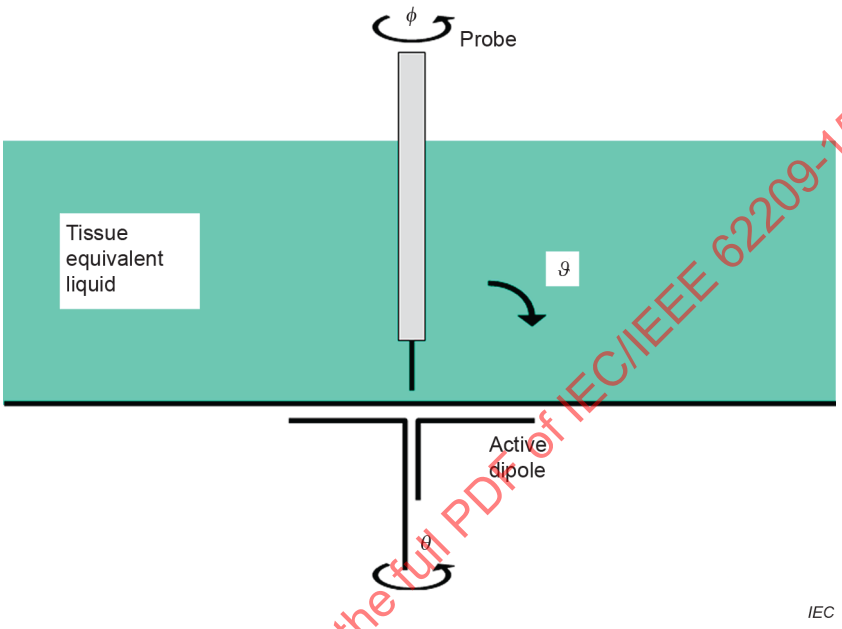
NOTE The assessment is preferably performed in the location c of minor field gradients resulting from the standing wave. The dimension e is the distance between the dipole feed-point and the interface of the front wall and the liquid.

Figure E.4 – Set-up to assess hemispherical isotropy deviation in tissue-equivalent medium

IECNORM.COM : Click to view the full PDF of IEC/IEEE 62209-1528:2020

E.4.2.3 Isotropy with flat phantom and dipole beneath

An alternative set-up for isotropy evaluation is shown in Figure E.5. A half-wave dipole mounted on a holder is positioned with arms parallel to and below a flat phantom containing tissue-equivalent medium. A probe is positioned at a point directly above the dipole feed-point. All probe rotations are performed and controlled by a high-accuracy positioner. The rotation of the probe about its axis (ϕ rotation from 0° to 360°), along with dipole rotation (θ rotation from 0° to 180°) and change of probe inclination angle ϑ (from 0° to 75°), produces a 3D evaluation of a significant portion of the hemispherical receiving pattern.



Key

ϑ probe axis tilt angle

θ rotation angle of the axis of the dipole mounting device

ϕ probe axis rotation angle of the probe

Figure E.5 – Alternative set-up to assess hemispherical isotropy deviation in tissue-equivalent medium

E.4.2.4 Isotropy with dipole and spherical phantom

The hemispherical isotropy of the probe receiving pattern can be assessed using a set-up comprised of a spherical flask filled with a tissue-equivalent medium and a dipole [58] (see Figure E.6). The probe sensors are positioned at the geometrical centre of the flask, and the probe is rotated about its axis under each excitation condition. The probe is maintained in its vertical orientation during the procedure.

The excitation conditions are provided by the dipole antenna that is external to the flask and moved at different locations to provide different incidence angles and polarizations. The dipole axis is aligned with the tangent plane of the surface of the sphere above the dipole feed-point. The impedance of the antenna is matched for this condition at the operating frequency.

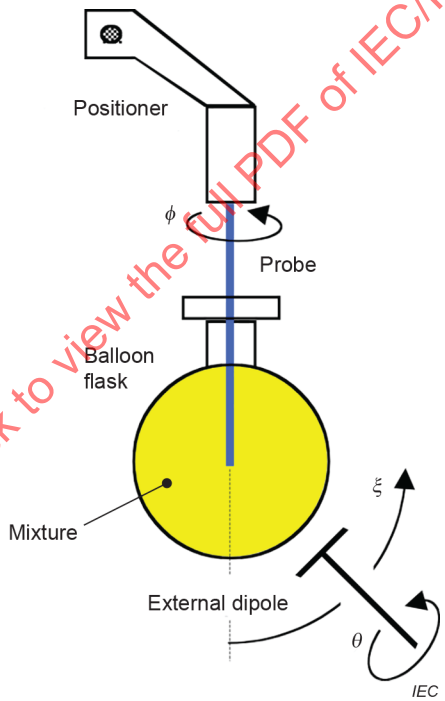
NOTE Smaller flasks can be preferred because increased medium conductivity or operating frequency implies a higher path-loss for the wave transmitted to the probe. Larger flasks feature a locally flatter surface (longer curvature radius), which produces a locally flatter wave front impinging on the probe tip and relaxes the tolerance on the position of the dipole.

IECNORM.COM : Click to view the full PDF of IEC/IEEE 62209-1528:2020

Figure E.7 [58] shows the conventions used to describe the antenna position and polarization. A 3D measurement of the probe receive pattern over a hemisphere is accomplished by rotating the probe by 360° around its axis (ϕ) while positioning the external dipole at angles $0° \leq \xi \leq 360°$. Every desired polarization of the impinging wave is achieved by rotating the dipole around its axis $0° \leq \theta \leq 180°$. Multiple θ-positions are not needed when $\xi = 0°$. While a large number of measurement points are possible with this set-up, usually steps of 30° in ξ and 15° in θ are sufficient for characterization.

The measurements consist of complete 360° rotations of the probe for each dipole position and polarization (ξ, θ). The power radiated during each rotation shall be monitored and recorded for every ϕ-position of the probe, and the SAR samples shall be normalized to a nominal value. Although it cannot be a priori excluded, there is no particular reason why any positions and polarizations of the external dipole other than what is considered here would produce significantly worse isotropic performance. However, the matrix of tests can be expanded to include any particular case of interest, e.g. polarization conditions that match the sensor orientation in some probes.

As with the flat-phantom isotropy test, a rectangular uncertainty distribution is assumed. However, the uncertainty can be substantially reduced when probe calibration is performed under a specific polarization and direction of the impinging wave and the same conditions are maintained during SAR measurements.



IECNORM.COM : Click to view the full PDF of IEC/IEEE 62209-1528:2020

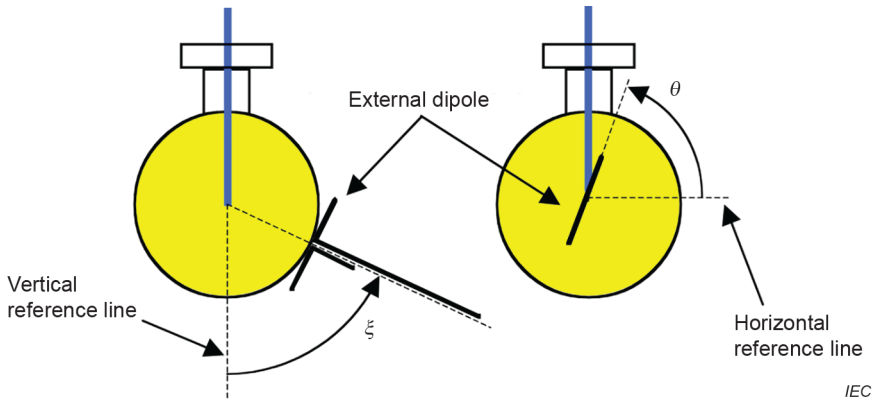
Key

ξ elevation angle to dipole axis

θ dipole rotation angle

ϕ probe axis rotation angle

Figure E.6 – Experimental set-up for the hemispherical isotropy assessment



Key

ξ elevation angle to dipole axis

θ dipole rotation angle

NOTE ξ is the angle between the probe axis and the axis of the dipole holder, and θ is the angle between the probe axis and the dipole axis.

Figure E.7 – Conventions for dipole position (ξ) and polarization (θ)

E.4.2.5 Isotropy with reference antennas

The following protocol shall be used for evaluating the isotropy of the probe using the reference antenna set-up shown in Figure E.8.

a) Position one antenna in the tissue-equivalent medium. The antenna shall be at a minimum distance of 10 cm from the walls of the liquid container, and have dimensions such that it can be placed in the position indicated in Figure E.8 .

b) Position the probe in the liquid so that the geometric centre of the sensors is at a distance d from the antenna, where $d \geq 2D^2/\lambda_{\text{liquid}}$, D is the largest dimension of the reference antenna, and λ_{liquid} is the wavelength in the liquid. It is recommended that the SAR value be set to between 0,5 W/kg and 1 W/kg at this position.

c) Orient the probe axis so that its main axis is orthogonal to the direction of propagation from the antenna (see Figure E.8).

d) Rotate the probe along its main axis from 0° to 360° with a step size less than or equal to 15°. Record the SAR values. The axial isotropy is expressed as an uncertainty component with a rectangular probability distribution based on the measured response peaks.

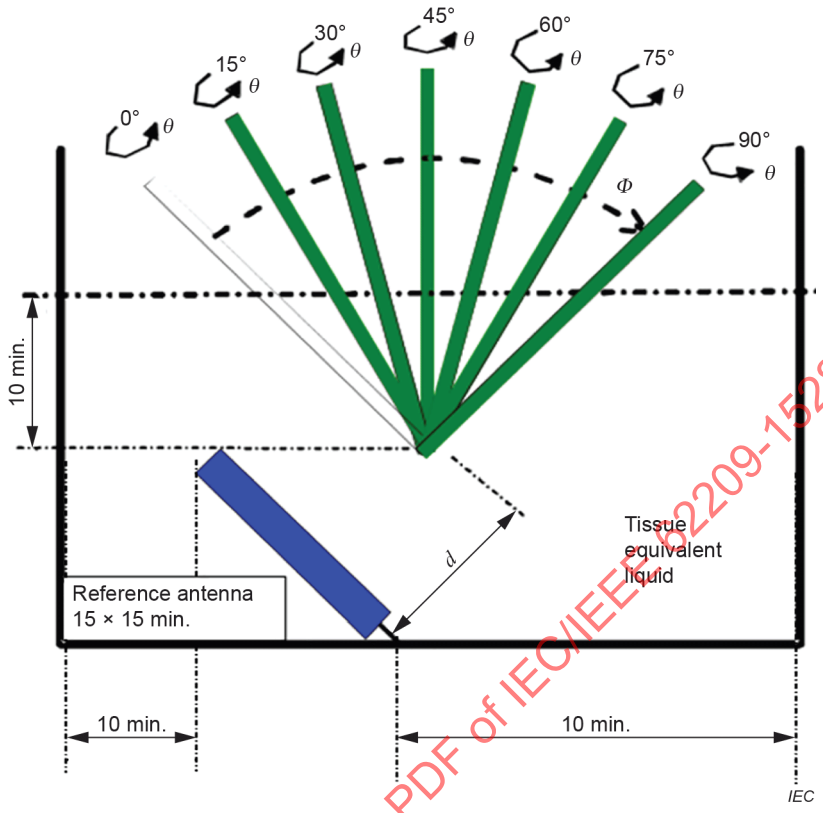
e) Vary the incidence of the reference field by tilting the reference antenna or the probe axis (see Figure E.8) from 0° to 90° with a step size of 15° or 30°.

f) For each incidence angle, rotate the probe along its main axis from 0° to 360° with a step size less than or equal to 15°. Record the SAR values.

g) The hemispherical isotropy is expressed as an uncertainty component with a rectangular probability distribution limited by the measured response peaks.

IECNORM.COM : Click to view the full PDF of IEC/IEEE 62209-1528:2020

Dimensions in centimetres



Key

θ probe axis rotation angle

Φ probe axis tilt angle

d ≥ 2 D^2/λ_{liquid}

Figure E.8 – Measurement of hemispherical isotropy with reference antenna

E.5 Lower detection limit

The lower detection limit is the minimum local SAR measurable within the overall system uncertainty. It is related to the noise level and offset of the measurement system and can be assessed by varying the output power in the same set-up as specified in Clause O.1 (i.e. by verifying that the probe is still responding linearly at the required lower detection SAR level). In actual operational conditions of the measurement system, the ambient EM environment could impair the detection limit. Therefore, verification of the lower detection limit by using the flat-phantom set-up specified in Clause G.3, or a calibration waveguide, is recommended. The lower detection limit shall be 10 mW/kg or lower.

IECNORM.COM : Click to view the full PDF of IEC/IEEE 62209-1528:2020

E.6 Boundary effect

In the closest vicinity to the inner surface of a phantom shell, probe sensitivity deviates from that which is established under typical calibration conditions. Boundary effects are evaluated with the liquid-filled open waveguide set-ups used for probe calibration. The psSAR is measured using all system components and compensation routines. The uncertainty due to boundary effects is the deviation from the analytical value at the surface, which is estimated by extrapolating the trend of measured samples to the interface of the liquid and the dielectric slab. This measurement shall be performed for each frequency band and for each averaging volume. For frequencies below 800 MHz, where calibration waveguides might not be available due to the relatively large size, an experimental set-up comprised of a half-wave dipole beneath a flat phantom may be used. In this case, extrapolation to the surface is not based on the known analytical behaviour of guided-wave modes, but on an extrapolation of measured samples. The boundary effect error is specified as the deviation between the measured SAR data and the true value in the liquid. When the probe is oriented normal to the phantom surface, the boundary effect can largely be compensated for as described in [53]. The uncertainty of the boundary effect shall be evaluated according to Clause O.3.

E.7 Response time

The response time uncertainty is the measurement error caused by movement of the probe during measurement. Field-probe signal response time uncertainty is evaluated by exposing the probe to an E-field step response producing at least 100 W/kg. The signal response time is determined as the time required by the probe and its readout electronics to reach 90 % of the expected final value produced by the step response through switching the RF power on and off. The probe shall remain stationary at each measurement location for at least three times the assessed response time to ensure a negligible probe signal response time uncertainty. Under these measurement conditions, an uncertainty value of zero may be entered in Table 9 (see 8.3). Otherwise, the SAR uncertainty due to signal response-time uncertainty shall be assessed using the signal characteristics of the test device. In this case, the signal step-response time uncertainty is equal to the percentage difference of the SAR measured with the chosen measurement time from the SAR measured with a measurement time of at least three times the assessed response time. A rectangular probability distribution shall be assumed.

IECNORM.COM : Click to view the full PDF of IEC/IEEE 62209-1528:2020

Annex F
(informative)

Example recipes for phantom tissue-equivalent media

F.1 General

The dielectric properties of the phantom shall be those listed in Table 2 of 6.2.2.

WARNING – To ensure personnel safety, users shall follow the instructions provided in the material safety data sheet (MSDS) for any material, and/or any local regulations.

F.2 Ingredients

The following ingredients are used in the example liquid recipes for producing the head tissue-equivalent media:

a) sucrose (sugar) (> 98 % pure);
b) sodium chloride (salt) (> 99 % pure);
c) de-ionized water (16 MΩ cm resistivity minimum);
d) hydroxyethyl cellulose (HEC);
e) bactericide;
f) diethylene glycol butyl ether (DGBE) (> 99 % pure);
g) diethylene glycol monohexylether;
h) polyethylene glycol mono [4-(1,1,3,3-tetramethylbutyl) phenyl ether]. This is available as Triton™ X-100.[3] The quality of the Triton X-100 shall be ultra-pure to match the composition of salt. After making the Triton X-100 based liquids, the dielectric properties are difficult to adjust in order to keep them close to the targets. Therefore, it is recommended to use alternatives when available;
i) diacetin;
j) 1,2-propanediol;
k) polyoxyethylene (20) sorbitan monolaurate (Tween 20);
l) emulsifiers;
m) mineral oil.

NOTE 1 Viscosity of HEC-based tissue-equivalent medium liquids should be low enough not to affect E-field probe movement.

NOTE 2 Add salt to water first to make a saline solution, then add the Triton X-100.

NOTE 3 Actual results and mixture percentages may vary from those shown, depending on grade and type of components used.

NOTE 4 The tolerances of ε_r and of σ in Table F.1 and Table F.2 are liquid temperature tolerances described in O.9.6 based on measurements of the applicable liquid recipes.

NOTE 5 The formulas containing Triton X-100 are under review and verification.

[3] Triton is the trademark of a product supplied by The Dow Chemical Company or an affiliated company of Dow. This information is given for the convenience of users of this document and does not constitute an endorsement by IEC of the product named. Equivalent products may be used if they can be shown to lead to the same results.

IECNORM.COM : Click to view the full PDF of IEC/IEEE 62209-1528:2020

F.3 Tissue-equivalent medium liquid formulas (permittivity/conductivity)

Table F.1 and Table F.2 provide suggested recipes.

Table F.1 – Suggested recipes for achieving target dielectric properties, 30 MHz to 900 MHz

Frequency (MHz)	**30**	**50**		**144**		**450**		**835**	**900**	
Recipe source number	3	3	2	2	3	2	4	2	2	4
Ingredients (% by weight)										
De-ionized water	48,30	48,30	53,53	55,12	48,30	48,53	56	50,36	50,31	56
Tween 20			44,70	43,31		49,51		48,39	48,34	
Oxidized mineral oil							44			44
Diethylenglycol monohexylether										
Triton X-100										
Diacetin	50,00	50,00			50,00					
DGBE										
NaCl	1,60	1,60	1,77	1,57	1,60	1,96		1,25	1,35	
Additives and salt	0,10	0,10			0,10					
Measured temperature dependence										
Temp. (°C)			21	21		21	20	21	21	20
$\varepsilon_{\text{liquid temp. unc.}}$ (%)	0,8	0,1			0,1	0,1		0,04	0,04	
$\sigma_{\text{liquid temp. unc.}}$ (%)	2,8	2,8			2,6	4,2		1,6	1,6	

IECNORM.COM : Click to view the full PDF of IEC/IEEE 62209-1528:2020

Table F.2 – Suggested recipes for achieving target dielectric properties, 1 800 MHz to 10 000 MHz

Frequency (MHz)	**1 800**		**2 450**	**4 000**	**5 000**	**5 200**	**5 800**	**6 000**	**8 000**	**10 000**
Recipe source number	2	4	4	4	4	1	1	4	5	5
Ingredients (% by weight)										
De-ionized water	54,23	56	56	56	56	65,53	65,53	56	67,8	66,0
Tween	45,27								31,1	33,0
Oxidized mineral oil		44	44	44	44			44		
Diethylenglycol monohexylether						17,24	17,24			
Triton X-100						17,24	17,24			
Diacetin										
DGBE										
NaCl	0,50									
Additives and salt										
Measured temperature dependence										
Temp. (°C)	21	20	20	20	20	22	22	20	20	20
$\varepsilon_{\text{liquid temp. unc.}}$ (%)	0,4					1,7	1,8			
$\sigma_{\text{liquid temp. unc.}}$ (%)	2,3					2,7	2,6			

NOTE 1 Multiple columns under a single frequency indicate optional recipes.

NOTE 2 Recipe source numbers: 1 verified by different labs, 2 Reference [59], 3 developed by IT'IS Foundation, 4 developed by IT'IS Foundation, 5 Reference [60].

NOTE 3 The values of $\varepsilon_{\text{liquid temp. unc.}}$ and $\sigma_{\text{liquid temp. unc.}}$ are liquid temperature uncertainties described in O.9.6, based on measurements of the applicable liquid recipes given above. These are not part of the original publications but have been subsequently developed by the project team.

NOTE 4 The recipes at 8 000 MHz and 10 000 MHz are sufficiently broadband that they cover the frequency range of 6 000 MHz to 10 000 MHz within a tolerance of ±10 % for permittivity and conductivity.

IECNORM.COM : Click to view the full PDF of IEC/IEEE 62209-1528:2020

Annex G
(normative)

Phantom specifications

G.1 Rationale for the phantom characteristics

G.1.1 General

Phantoms that represent the human anatomy are essential components of electromagnetic exposure evaluation. It is important to define and standardize the features, dimensions and material properties of the phantoms that are directly relevant to ensuring conservative exposure. It is unnecessary and impractical to specify all anatomical details. The rationales for the SAM phantom and flat phantom used in this document are provided in G.1.2 and G.1.3, respectively. Application specific phantoms are specified in Annex K and Annex L.

G.1.2 Rationale for the SAM phantom

Anthropometric studies of the human population are available to guide the specification of a conservative and realistic head phantom. Specifically, a large 1988 anthropometric study of U.S. Army personnel was particularly important in providing data to determine population coverage requirements for adults of different ages and ethnic groups [61]. Based on this study, the Specific Anthropomorphic Mannequin (SAM) is specified in this document to represent exposure of the head. The shape of the standard SAM phantom is established by a number of lines and curves as illustrated in Figure G.1 (see G.2.1).

Dosimetric studies suggest that larger heads (adult, male user) couple more energy and constitute a worst-case exposure scenario compared to smaller heads (children) [62], [63], [64], [65]. The upper 90th percentile (adult male) head dimension shall be used to ensure that well over 90 % of all users have smaller heads and would therefore sustain a lower exposure.

The back ear protrusion has a direct effect on determining the closeness of the handset and antenna to the head and is an important parameter for determining SAR. The ear protrusion was adjusted to simulate the pressure of the device on the ear. The shape of the ear is a factor in positioning the handset and was designed to enable correct and reproducible positions. A study on mobile phone exposure of the head using anatomical head phantoms of adults and children showed that the psSAR assessed with the SAM phantom yields conservative exposure for both the head and pinna tissue when regarding the pinna as an extremity that has SAR limits of at least double that of the head tissues [66].

G.1.3 Rationale for the flat phantom

The flat phantom is established to represent the torso and other regions of the body for this document. The shape and size of the flat phantom are important for accurate and representative SAR measurements. The part of the user's body exposed to the RF emissions of a wireless communication device is not always well specified and might vary with product design and usage

The flat phantom should not be excessively large compared with the size of a human torso. Large phantoms are also more difficult to construct, and SAR measurement systems might not be capable of performing measurements in phantoms that are very large or very deep.

A flat phantom represents a simple engineering structure for which the SAR can be easily and repeatably measured. It is an open-top thin dielectric shell which is filled with a tissue-equivalent medium. The physical characteristics of the standard flat phantom are intended to simulate the exposure characteristics of a human body.

IECNORM.COM : Click to view the full PDF of IEC/IEEE 62209-1528:2020

A flat-bottomed phantom provides maximal exposed surface area of flat regions of the body to the wireless (DUT). Therefore, the flat phantom generally provides conservative exposure. Flat phantoms should be large enough to allow complete coupling of the RF radiating antenna and to allow scanning of 1 g and 10 g volumes.

The use of a flat phantom as a standard phantom for SAR evaluations of devices not operating next to the ear is intended to represent maximum coupling of variations in energy absorption through irregular heterogeneous tissue boundaries. The flat phantom will produce conservative exposure in an equivalent human body, when used with prescribed test distances.

G.2 SAM phantom specifications

G.2.1 General SAM phantom specifications

The dimensions of the SAM phantom have been derived from selected 90th percentile male head data reported by Gordon et al. [61], and are listed in Table G.1 and shown in Figure G.1. Table G.2 shows other pertinent dimensions for comparison. At the ear reference point (ERP), a thickness of 6 mm including the 2 mm shell is selected to model the external ear (pinna). This thin ear spacer also simulates users with small ears, and gives conservative exposure. A system of reference points and reference lines is used to correlate the DUT positioning with the phantom (Figure G.2 and Figure G.3). The point “M” is the mouth reference point, “LE” is the left-ear ERP, and “RE” is the right-ear ERP. The ERPs are 15 mm posterior to the entrance to ear canal (EEC) along the line B-M (back-to-mouth) (Figure G.2).

The plane passing through the two ear reference points and M is specified as the reference plane. The line N-F (neck-to-front) is along the front truncated edge of the ear. Both N-F and B-M lines shall be marked on the external phantom shell to facilitate DUT positioning. These may be etched into the external surface of the phantom without affecting the specifications. Optional markings shown in Figure G.3 may also be labelled on the phantom. Posterior to the N-F line, the thickness of the phantom shell with the shape of an ear is a flat surface. The ear is 6 mm thick at the ERP. Anterior to the N-F line, the ear is truncated as illustrated in Figure G.2. The ear truncation is introduced to facilitate repeatable DUT positioning.

The phantom shall be filled with head tissue-equivalent medium. To minimize reflections within the phantom, the depth of the homogeneous medium should be at least 15 cm. Medium depth of less than 15 cm can be used if it is demonstrated (e.g. using numerical simulations) that the effect of reflections on psSAR is less than 1 %. If the effect of reflections on psSAR is more than 1 % but less than 3 %, the maximum uncertainty shall be added to the uncertainty budget.

IECNORM.COM : Click to view the full PDF of IEC/IEEE 62209-1528:2020

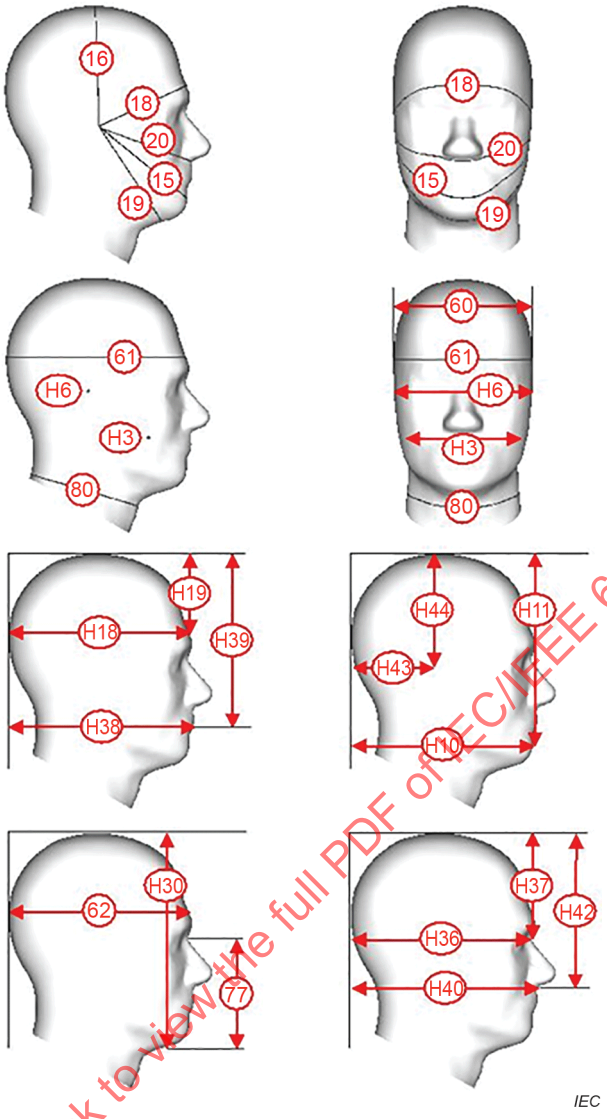


Figure G.1 – Illustration of dimensions in Table G.1 and Table G.2

IECNORM.COM : Click to view the full PDF of IEC/IEEE 62209-1528:2020

Table G.1 – Dimensions used in deriving SAM phantom from the ARMY 90th percentile male head data (Gordon et al. [61])

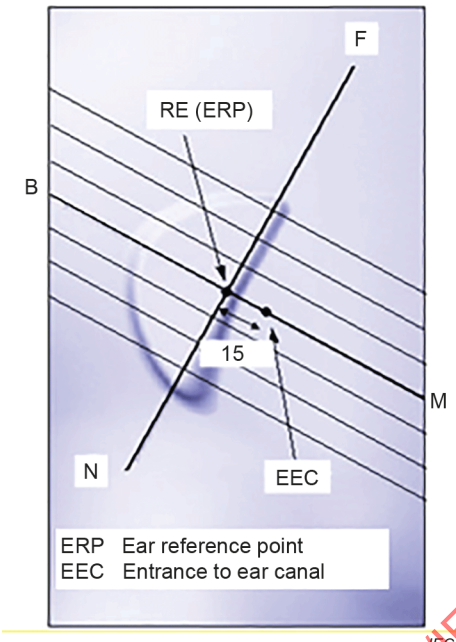
Ref.	Anatomy	Gordon report [mm]			SAM [mm]	Deviation [%]
		Mean value	Standard deviation	90th percentile		
H15	Bitragion Chin Arc	325,8	13,4	343,1	329,3	−4,0
H16	Bitragion Coronal Arc	353,3	12,9	369,7	367,3	−0,6
H18	Bitragion Frontal Arc	304,3	10,6	318,2	314,1	−1,3
H19	Bitragion Submandibular Arc	304,2	14,5	323,2	333,5	3,2
H20	Bitragion Subnasale Arc	292	11,1	306,3	305,3	−0,3
H60	Head Breadth	151,7	5,4	158,6	158,4	−0,1
H61	Head Circumference	567,7	15,4	587,3	594,8	1,3
H62	Head Length	197,1	7,1	206	206,0	0,0
H77	Menton-Sellion Length	121,9	6,5	130,4	125,0	−4,1
H80	Neck Circumference	379,6	19,7	405,3	395,4	−2,5

Table G.2 – Additional SAM dimensions compared with selected dimensions from the ARMY 90th percentile male head data (Gordon et al. [61]) – specialist head measurement section

Ref.	Anatomy	Gordon report [mm]			SAM [mm]	Deviation [%]
		Mean value	Standard deviation	90th Percentile		
H3	Bigonial Breadth	118,9	7,9	129,2	130,0	0,6
H6	Bitragion Breadth	144,8	6	152,3	152,7	0,2
H10	Chin-Back of Head	194,2	10,3	207,3	206,5	−0,4
H11	Chin-Top of Head	216,8	8,9	228,3	220,4	−3,5
H18	Glabella-Back of Head	199,7	7,2	208,5	209,2	0,3
H19	Glabella-Top of Head	96,2	7,3	105,6	104,4	−1,1
H30	Menton-Top of Head	232,0	8,8	243,3	246,7	1,4
H36	Sellion-Back of Head	197	7,1	205,9	205,3	−0,3
H37	Sellion-Top of Head	112	6,9	120,9	121,7	0,7
H38	Stomion-Back of Head	199,4	9,6	211,9	211,4	−0,2
H39	Stomion-Top of Head	186,3	7,8	196,3	196,3	0,0
H40	Subnasale-Back of Head	203,5	8,3	213,6	213,0	−0,3
H42	Subnasale-Top of Head	161,9	7,7	171,8	177,6	3,4
H43	Tragion-Back of Head	98,9	8,5	106,4	106,4	0,0
H44	Tragion-Top of Head	131	5,7	138,2	138,2	0,0

IECNORM.COM : Click to view the full PDF of IEC/IEEE 62209-1528:2020

Dimensions in millimetres



Key

B Direction of B-M line back endpoint

F Direction of N-F line front endpoint

N Direction of N-F line neck endpoint

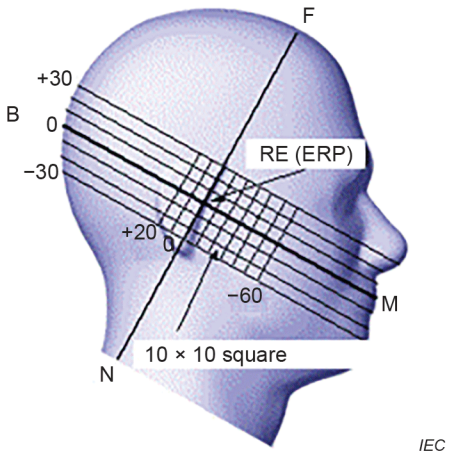
M Mouth reference point

RE Right-ear ear reference point (ERP)

Figure G.2 – Close up side view of phantom showing the ear region

IECNORM.COM : Click to view the full PDF of IEC/IEEE 62209-1528:2020

Dimensions in millimetres



Key

B Line B-M back endpoint

M Line B-M front endpoint

N Line N-F neck endpoint

F Line N-F front endpoint

RE Right-ear ear reference point (ERP)

NOTE The full-head model is shown for illustration purposes only. The procedures in this document are derived primarily for the phantom set-up shown in Figure G.4.

Figure G.3 – Side view of the phantom showing relevant markings

G.2.2 SAM phantom shell specification

The phantom shell with integral solid ear spacer, as specified in the SAM CAD model, shall be constructed from chemical-resistant, low-permittivity and low-loss material, with relative permittivity between 3 and 5; however, relative permittivity less than 3 is acceptable for frequencies up to 3 GHz. The loss tangent of the phantom shell shall be less than or equal to 0,05. It has been shown that at higher frequencies, particularly above 3 GHz, the permittivity of the phantom shell has an increasing impact on SAR measurement uncertainty [36]. According to [36], the SAR is affected by the shell even though the shell is thin and has dielectric properties much lower than the tissue-equivalent medium. Specifically, it was shown that the variation in the SAR depends not only on the frequency, but also on the relative permittivity of the shell and the distance between the antenna and the material. It was recommended that the effects of the shell be taken into account in the higher frequency range. Therefore, uncertainty evaluation shall be conducted above 3 GHz according to 8.4.2.3.

The shape of the phantom shell shall have a tolerance of less than ±0,2 mm with respect to the SAM CAD file. In any area within the projection of the DUT, the shell thickness shall be 2 mm ± 0,2 mm, except for the ear (where the thickness is specified in the CAD file with a tolerance of ±0,2 mm) and the extended perimeter walls for the SAM phantom (see Figure G.4). The phantom shell shall be made of materials resistive to the tissue-equivalent media (e.g. those listed in Annex F), to avoid damage and preserve the ±0,2 mm tolerances. This minimal thickness results in a higher SAR compared to measurements on thicker phantoms. Smaller thicknesses are not recommended due to problems with mechanical strength when holding the medium. For non-critical areas, i.e. the central strip containing the nose in the SAM phantom, as shown in Figure G.5, the thickness tolerance is allowed to be within ±1 mm.

The SAM phantom CAD file cross section for the reference plane is given in Figure G.6.

IECNORM.COM : Click to view the full PDF of IEC/IEEE 62209-1528:2020

NOTE The CAD model is for use in manufacturing the SAM phantom by groups having the necessary expertise and resources. Four *.IGES files of inner and outer surfaces for the left and right halves extracted from the CAD model of the SAM phantom are provided with this document at:

http://www.iec.ch/dyn/www/f?p=103:227:0::::FSP_ORG_ID,FSP_LANG_ID:1303,25

The four file names are:

– sam_lft_in_6_11.igs
– sam_lft_out_6_11.igs
– sam_rt_in_6_11.igs
– sam_rt_out_6_11.igs

Dimensions in millimetres

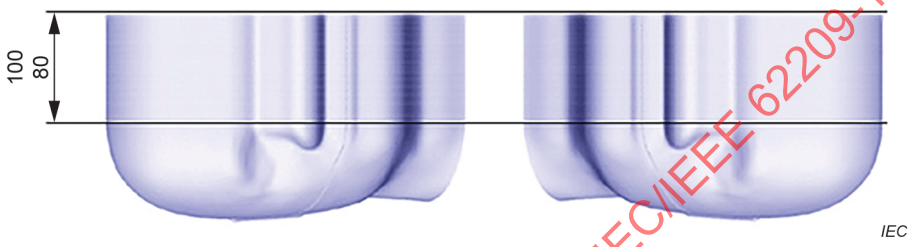
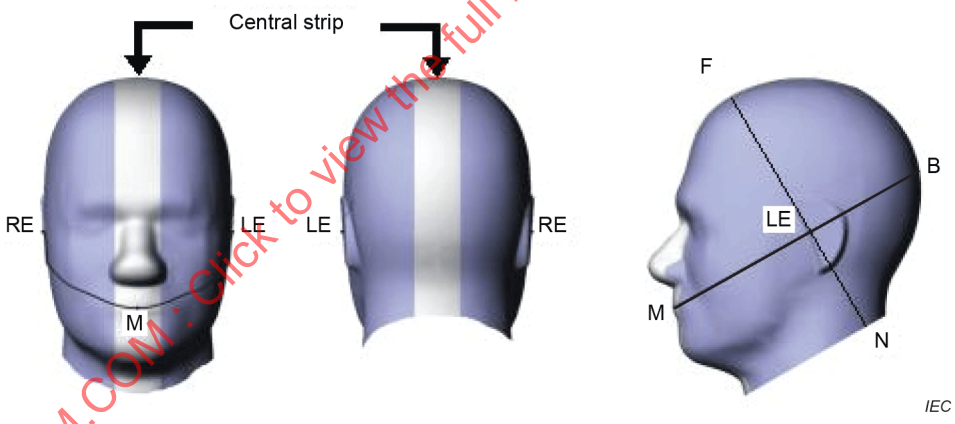


Figure G.4 – Sagittally bisected phantom with extended perimeter (shown placed on its side as used for device SAR tests)



Key

B Line B-M back endpoint
M Line B-M front endpoint
N Line N-F neck endpoint
F Line N-F front endpoint
RE Right-ear ear reference point (ERP)
LE Left-ear ear reference point (ERP)

Figure G.5 – Picture of the phantom showing the central strip

IECNORM.COM : Click to view the full PDF of IEC/IEEE 62209-1528:2020

Dimensions in millimetres

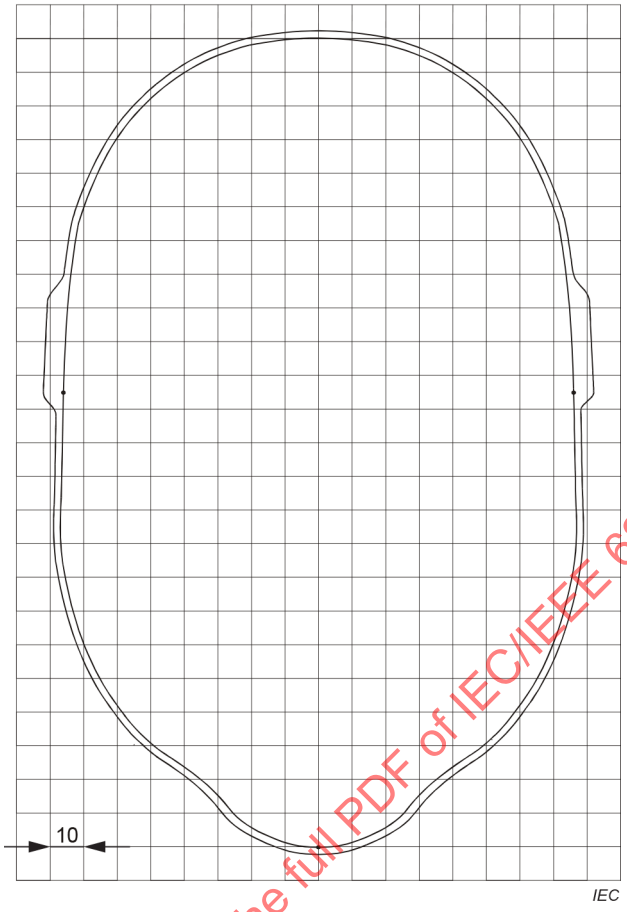


Figure G.6 – Cross-sectional view of SAM at the reference plane

G.3 Flat phantom specifications

The shell of the flat phantom shall be constructed in the form of an open-top container with a flat bottom. In this document, flat phantoms shall be used for system validation, system check, and for measurements of SAR for DUTs using positions specified in 7.2.4.1.

Any flat phantoms used shall be large enough to allow the measurement of SAR in 1 g and 10 g volumes (medium density of 1 000 kg/m^3 is used) with an influence from the phantom shape and dimensions of less than 1 %. Minimum flat phantom dimensions are specified in 6.2.4 and Clause G.4.

NOTE Use of a flat phantom as a standard phantom for SAR evaluations of body-worn and body-supported devices is intended to represent maximum coupling between the DUT and phantom compared to a significant majority of exposure situations involving people. Such coupling to the boundary while maintaining prescribed distances is likely to produce conservative exposure.

The phantom shall be filled with a tissue-equivalent medium. To minimize reflections within the phantom, the depth of the homogeneous medium should be at least 15 cm ± 0,5 cm. Medium depth of less than 15 cm can be used if it is demonstrated (e.g. using numerical simulations) that the effect of reflections on psSAR is less than 1 %. If the effect of reflections on psSAR is more than 1 % but less than 3 %, the maximum uncertainty shall be added to the uncertainty budget.

The phantom shell shall be made of low-loss and low-permittivity material, having a loss tangent ≤ 0,05 and a relative permittivity of

IECNORM.COM : Click to view the full PDF of IEC/IEEE 62209-1528:2020

$$\varepsilon_r' \leq 5 \text{ for } f \leq 3 \text{ GHz}$$

$$3 \leq \varepsilon_r' \leq 5 \text{ for } f > 3 \text{ GHz}$$

The thickness of the bottom-wall of the flat phantom shall be 2,0 mm with a tolerance of ±0,2 mm.

The phantom shell shall be made of materials resistive to the tissue-equivalent media (e.g. those listed in Annex F), to avoid damage and preserve the ±0,2 mm tolerances.

When filled with the required depth of medium, any sagging of the bottom surface of the phantom within the projection of the DUT shall be determined and considered in the uncertainty budget (see 8.4.2.4). For system check and validation testing, the sagging at the medium interface and inner surface of the phantom directly above the source (e.g. dipole or waveguide) shall be less than 1 % of the free-space wavelength in the frequency range of 800 MHz to 10 000 MHz, and less than 0,5 % of the free-space wavelength at frequencies below 800 MHz.

When the preceding requirements are met, the effect of the shape and shell thickness on the repeatability of SAR measurement results is less than 1 %. Effects on the SAR due to the influence of the deviation from the shell parameters and thickness shall be included in the uncertainty estimation.

G.4 Justification of flat phantom dimensions

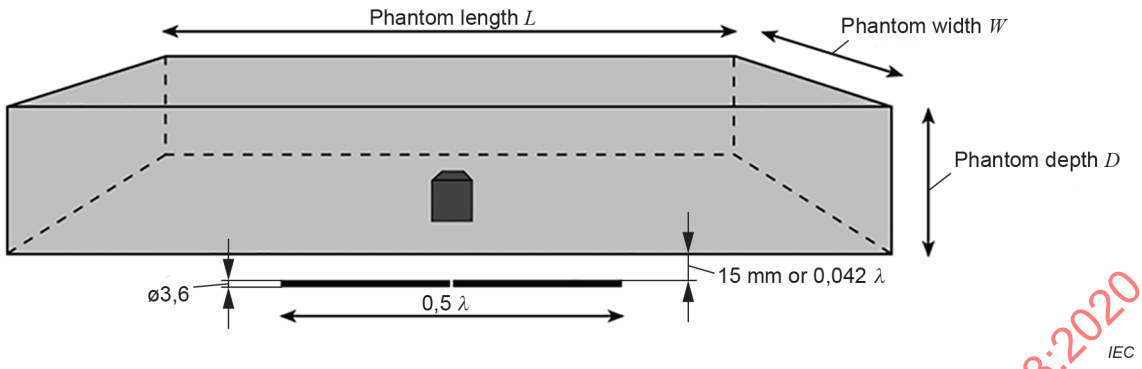
The influence of the dimensions of the flat phantom (Figure G.7) on the absorbed energy in a 10 g cube inside the medium-only phantom (without box) was assessed numerically using a commercial FDTD code. The phantom was illuminated with a matched dipole antenna at a distance of 15 mm (0,042 λ at 840 MHz). The dimensions of the phantom (W and L) were separately varied between 0,4 λ and 3 λ. The power absorbed in the cube was normalized to a feed-point current of 1 A and a feed-point power of 1 W. A length and width of at least 0,6 and 0,4 wavelength in air, respectively, was found to ensure that the effect of phantom dimensions on SAR is less than 1 % for both current and power normalization (Figure G.8). The dimensions of the phantom set-up can be scaled in terms of the free-space wavelength. The dependence on the medium properties was found to be insignificant.

Because of its larger size, a 10 g averaging cube will be more sensitive to dimension changes, i.e. the uncertainty associated with the 1 g average will be smaller than that of the 10 g average. The effects resulting in differences depend on perturbations of the dipole current magnitude and spatial distribution. Since the dipole dimensions are large compared with the SAR averaging volumes, the perturbations will increase with volume size. Although the depth used in this study was 10 cm, rather than the 15 cm required for the flat phantom in Clause G.3, it is 2,57 times the penetration depth at 840 MHz, and therefore the power reflection at the medium surface is negligible (less than 1 %).

The numerical target SAR values of Table D.2 (see D.2.2) were calculated using the FDTD method. The parameters for the lossless phantom shell used in simulations (dimensions, shell thickness, and permittivity), and the distance s between the reference dipole and tissue-equivalent medium, are given in Table G.3. The phantom dimensions in this table produce the same SAR values as a phantom that meets the requirements of Clause G.3, within the uncertainty of the SAR test system. The phantom dimensions recommended in Clause G.3 are to be used for system check and system validation. The dielectric properties used for the tissue-equivalent medium are specified in Table 2 (see 6.2.2) and the dimensions of the reference dipoles are shown in Table D.1 (see D.2.1).

IECNORM.COM : Click to view the full PDF of IEC/IEEE 62209-1528:2020

Dimensions in millimetres



Key

λ free-space wavelength

NOTE A 10 g cube is shown at the bottom centre of the flat phantom.

Figure G.7 – Dimensions of the flat phantom set-up used for deriving the minimal phantom dimensions for W and L for a given phantom depth D

IECNORM.COM : Click to view the full PDF of IEC/IEEE 62209-1528:2020

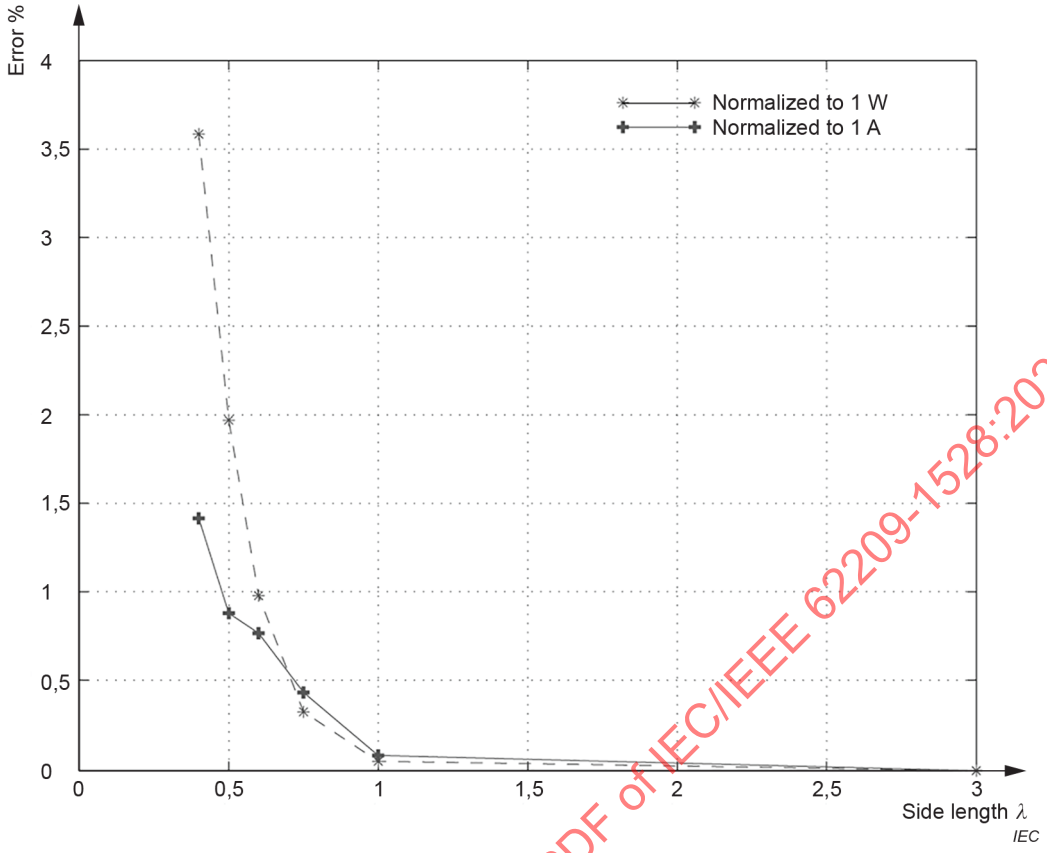


Figure G.8 – FDTD predicted error in the 10 g psSAR as a function of the dimensions of the flat phantom compared with an infinite flat phantom at 800 MHz

Table G.3 – Parameters used for calculation of reference SAR values in Table D.2

Frequency MHz	Phantom shell permittivity	Phantom dimensions used for FDTD models mm *x*; *y*; *z*	Reference dipole distance *s* from the medium mm
300	3,7	1 000; 800; 170	15
450	3,7	700; 600; 170	15
750	3,7	700; 600; 170	15
835	3,7	360; 300; 150	15
900	3,7	360; 300; 150	15
1 450	3,7	240; 200; 150	10
1 500	3,7	220; 160; 150	10
1 640	3,7	220; 160; 150	10
1 750	3,7	220; 160; 150	10
1 800	3,7	220; 160; 150	10
1 900	3,7	220; 160; 150	10
1 950	3,7	220; 160; 150	10
2 000	3,7	160; 140; 150	10
2 100	3,7	160; 140; 150	10
2 300	3,7	160; 140; 150	10
2 450	3,7	180; 120; 150	10
2 600	3,7	180; 120; 150	10

IECNORM.COM : Click to view the full PDF of IEC/IEEE 62209-1528:2020

Frequency MHz	Phantom shell permittivity	Phantom dimensions used for FDTD models mm *x*; *y*; *z*	Reference dipole distance *s* from the medium mm
3 000	3,7	220; 160; 150	10
3 500	3,7	174; 110; 150	10
3 700	3,7	174; 110; 150	10
5 000	3.7	90; 80; 35	10
5 200	3,7	90; 80; 35	10
5 500	3,7	90; 80; 35	10
5 800	3,7	90; 80; 35	10
7 000	3,7	150; 150; 75	5
9 000	3,7	150; 150; 75	5

NOTE The SAR values in Table D.2 at frequencies above 3 GHz depend on the dipole spacer and detailed construction of the dipoles and may vary by as much as ±10 %. The reasons are that the dipole dimensions are short with respect to arm diameter and spacer dimensions, i.e. the numerical reference values are not generic and need to be determined for a particular test set-up. Also, the results can be sensitive to the permittivity of the phantom shell [36].

G.5 Rationale for tissue-equivalent media

The purpose of Clause G.5 is to provide the rationale for the choice of target permittivity and conductivity for the tissue-equivalent medium used for the SAR measurements. The rationale is that the SAR induced by the inductively coupled devices is insensitive to the permittivity of the body tissue [67], [68].

The aim was to provide target properties for a homogeneous phantom that, when used in the SAM (head) and flat (body) shells, will provide 1 g and 10 g SAR values that are conservative with respect to the exposure in the human body for a significant majority of the exposed population and RF sources and device positions that fall within the scope of this document. The same tissue-equivalent medium is used for both head and body SAR assessment.

The absorption of RF energy in the body is dependent on the nature of the RF-source and its distance from the body, the region(s) of the body (and therefore the tissue types) that are exposed, and the penetration depth of the energy into these tissues. The layers of different tissues within the body can result in enhanced RF absorption at certain frequencies, and there are anatomical variations in these layers due to factors such as age, sex, BMI, etc.

The homogeneous flat phantom specified in this document is based partly on the tissue properties obtained from [69], and partly from simulation of homogeneous and layered structures to represent the body. Over the frequency range 0,15 GHz to 10 GHz, the specified real relative permittivity for the phantom is approximately 10 % greater than that of brain grey matter, and conductivity similar to that of brain white matter and muscle tissue (Figure G.9). Grey matter has lower permittivity than white matter or muscle, so this would be expected to be conservative for these materials (for a homogeneous phantom, increasing the conductivity and/or reducing the real relative permittivity will result in higher SAR values, provided that the loading effect on the transmitter is unchanged). Note that the conductivity at some frequencies has been increased to account for enhancement of absorption due to tissue layering in the body [2], and these simulations are described in more detail below.

NOTE Clause G.5 describes the rationale for selecting the tissue-equivalent medium dielectric properties used for this document. The same set of parameters is used for head and body SAR measurements.

IECNORM.COM : Click to view the full PDF of IEC/IEEE 62209-1528:2020

Below 0,15 GHz, brain and muscle tissue measurements appear to show a rapid increase in real relative permittivity as the frequency is decreased [69], and these become larger than the permittivity of water, so that a liquid phantom with these properties cannot be realized. Thus a constant target value for relative permittivity of 55 with conductivity of 0,75 S/m has been adopted for frequencies at and below 0,03 GHz.

In the case of the wireless power transfer systems operating below 30 MHz, and where it has been shown and documented that the peak normalized magnetic field strength (i.e. the ratio of the peak magnetic field strength to its reference level) exceeds the peak normalized electric field strength (i.e. the ratio of the peak electric field strength to its reference level) by 10 dB or more, a saline solution having identical conductivity (0,75 S/m) within the given tolerance (±10 %) may be used as a tissue-equivalent medium.

The effect of the tissue layers on the psSAR in the head was investigated in [2] for a region near the ear, and for 0,3 GHz to 6 GHz. The tissue layers were varied in composition and thickness to represent the anatomical variation of the exposed head region, covering the user group including adults and children (between the 10th percentile and 90th percentile). Based on the worst-case tissue layer compositions with respect to the energy absorption at each frequency, tissue-equivalent medium liquid dielectric properties for homogeneous modelling were derived to ensure that the psSAR is the same (or slightly higher) than the psSAR in the layered models. The dielectric properties of the tissues used to model the human head were computed by the 4-term Cole-Cole formula [69]. The validity of this approach for near-field exposure was demonstrated by replacing the plane-wave by half-wave dipole and quarter-wave monopole sources in the closest proximity to the layered structures, as well as by comparison with results from magnetic-resonance-imaging (MRI)-based non-homogeneous human head models of adults and children from the literature. Table 2 (see 6.2.2) shows the relative permittivity and conductivity of the resulting tissue-equivalent medium liquids as published in [2].

The study of [2] was extended for general body tissue composition [70]. It was found that standing wave effects due to reflections in the subcutaneous adipose tissue lead to a significant increase of SAR in comparison to the findings of [2]. This increase cannot be compensated by modifying the dielectric properties of the tissue-equivalent medium liquids. A comprehensive analysis of the coupling mechanism shows that the standing wave effects need only to be considered in the Fresnel zone and the far-field zone of the DUT [71]. At close distances, conservative exposure can be achieved using the parameters for tissue-equivalent medium liquids as proposed in [2]. Therefore, the established liquid parameters have been retained for the measurements of hand-held and body-worn devices up to 200 mm from the body.

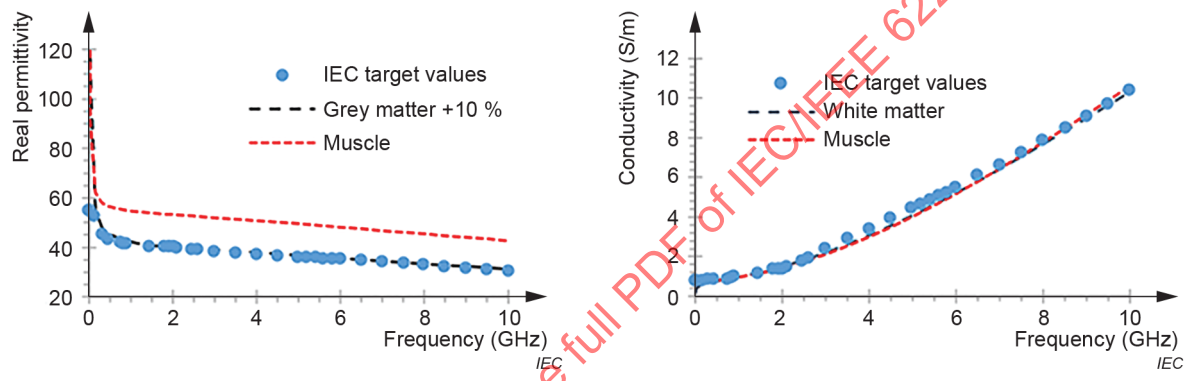
Extensive large-scale numerical studies have been performed to validate the conservativeness of the SAM and flat phantoms by comparing with SAR induced in anatomical head and body models. The first such study [14] demonstrated conservativeness of the SAM phantom at 835 MHz and 1 900 MHz for wireless devices operating at the head. This work has been extended to frequencies in the 300 MHz to 6 000 MHz range. The results obtained from the nine participating organizations show that the SAR produced in SAM for this frequency range is higher than the head SAR in the anatomical adult and child head models. The details of this study are reported in Bit-Babik [15]. A similar study has been performed for the flat phantom in the 30 MHz to 6 GHz frequency range [72] using several different anatomically correct human body models [73]. The results show the overall conservative nature of the flat phantom tissue-equivalent medium liquid parameters. Among the hundreds of exposure conditions simulated as part of this study, there were also some cases where SAR was underestimated by the flat phantom; follow-up analysis has been performed to investigate the related temperature rise in the anatomical models that could be caused by those exposure conditions. Those additional results show that the temperature increase level is not much different among all exposure conditions, including those selected cases where SAR was underestimated by the flat phantom.

IECNORM.COM : Click to view the full PDF of IEC/IEEE 62209-1528:2020

Studies also have been performed to assess whether a homogeneous phantom with the properties specified in this document is conservative with respect to absorption in the layers of tissues within the head for 6 GHz to 10 GHz. These studies showed that the phantom was conservative for the frequency range for a region above the ear, and also the cheek region [60] and [74].

Simulations showed that the tissue-equivalent medium dielectric properties proposed in Table 2 provide an overestimation of the SAR from exposure to body-worn or hand-held devices covered under this document used at 4 MHz and 150 MHz. Additional details on tissue-equivalent medium from 4 MHz to 30 MHz are provided in IEC TR 62905:2018 [18] (on exposure assessment methods for wireless power transfer systems).

For dielectric properties of head tissue-equivalent medium liquid at other frequencies within the frequency range, a linear interpolation method shall be used. Examples of recipes for liquids having parameters as specified in Table 2 are given in Annex F. The measured dielectric properties, not the values of Table 2, shall be used in the SAR calculations. This measurement can be performed using the equipment and procedures specified in Annex H.



a) Real relative permittivity **b) Conductivity**

NOTE Above 1 GHz, the permittivity decreases approximately linearly with frequency, and the conductivity increases parabolically.

Figure G.9 – Complex permittivity of human tissues compared to the phantom target properties

G.6 Definition of a phantom coordinate system and a DUT coordinate system

The offset and rotation between these optional reference coordinate systems can be used to provide a clear description of device position relative to the phantom. A definition of the phantom coordinate system for the left-ear ERP is illustrated in Figure G.10.

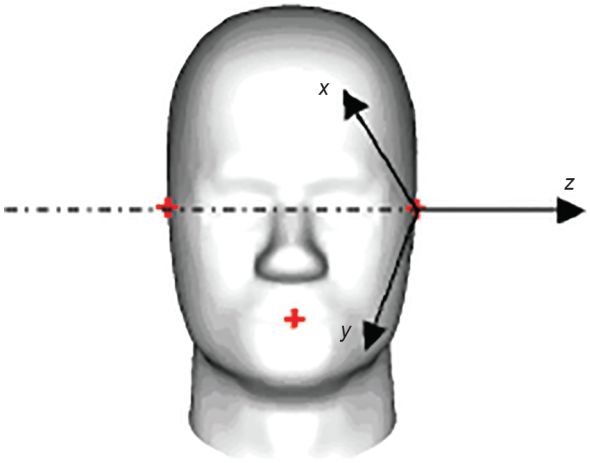
The x-, y- and z-axes form a right-handed Cartesian coordinate system. For the left-ear ERP, the axes are specified as follows.

- The z-axis is determined by a connecting line between the left-ear and the right-ear ERPs, and points from the right to the left from the point of view of the phantom. The z = 0 origin is at the left-ear ERP.
- The y-axis lies in the reference plane along the B-M line (Clause G.2).
- The x-axis is perpendicular to the reference plane along the N-F line (Clause G.2), and cuts the reference plane at the left-ear ERP.

For the right-ear ERP, the reference coordinate system can be established analogously. A definition of a DUT coordinate system is shown in Figure G.11.

IECNORM.COM : Click to view the full PDF of IEC/IEEE 62209-1528:2020

For the flat phantom, the x-axis and y-axis are parallel to the flat phantom shell, and the z-axis is perpendicular to it.



Key

x, y, z axes of the coordinate system relative to the phantom

Figure G.10 – Example reference coordinate system for the left-ear ERP of the SAM phantom

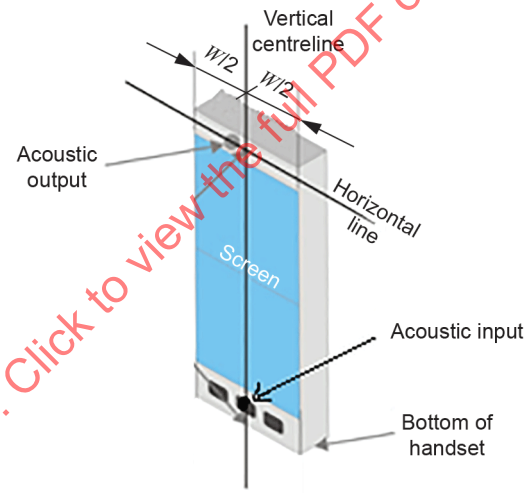


Figure G.11 – Example coordinate system on a DUT

IECNORM.COM : Click to view the full PDF of IEC/IEEE 62209-1528:2020

Annex H
(informative)

Measurement of the dielectric properties of tissue-equivalent media and uncertainty estimation

H.1 Overview

Clause H.2 describes the measurement of the dielectric properties of tissue-equivalent media required to support the SAR measurement procedures. It provides sufficient details to enable users to select a measurement method based on convenience and performance. The dielectric properties of some reference media are provided in Clause H.6 to assess the performance of the measurement procedures. General procedures to evaluate dielectric properties measurement uncertainties are provided in Clause O.9.

H.2 Measurement techniques

H.2.1 General

The dielectric properties required are the complex relative permittivity $\varepsilon_r = \varepsilon'_r - j\sigma/\omega\varepsilon_0$ of the tissue-equivalent medium at specific test frequencies and temperature. Several well-established techniques can be used for dielectric properties measurements of tissue-equivalent medium.

H.2.2 Instrumentation

The following or equivalent instrumentation is required:

- vector network analyser and S-parameter test set.
- the sample container for holding the liquid sample under test.
- application software to calculate sample dielectric properties from S-parameter measurements.

Three measurement techniques and the corresponding test methodologies are specified in Clause H.3 to Clause H.5. The achievable measurement accuracy for the different methods can vary. The dimensions of the transmission line or coaxial probe are functions of the measurement frequency ranges. The measurement accuracy is validated by measuring the dielectric properties of reference liquids in Clause H.6.

H.2.3 General principles

The following general principles should be applied for all the procedures.

a) The sample holder is thoroughly clean.

b) All cell, probes, cables, and connectors are undamaged.

c) The procedure for filling the sample holder with the sample fills the volume completely without air bubbles.

d) The temperature of the sample is recorded, and the report states that the dielectric properties are applicable at that temperature only.

e) Measurement personnel are acquainted with the nature of the measurement and what to expect at each stage of the procedure.

f) After calibration, a measurement is made on a reference liquid to validate the system prior to measuring the sample. Data for several recommended reference materials are given in Clause H.6.

IECNORM.COM : Click to view the full PDF of IEC/IEEE 62209-1528:2020

g) Data reduction methods for relating complex reflection coefficient and complex permittivity are accurate and appropriate for the sample-holder geometry being used.

H.3 Slotted coaxial transmission line

H.3.1 General

A terminated slotted coaxial line with a moveable probe can be used as a sample container [75]. A network analyser provides the RF signal at the input of the slotted line, and enables the magnitude and phase of the signal transmitted into the sample to be determined as a function of position along the line by means of the moveable probe.

The test procedure should specify the network analyser calibration and settings for the required frequency range, the starting measurement position, step size along the slot, and total number of subsequent measurement positions. The application software should interpret the measured data to yield the dielectric properties of the sample. An example procedure is given in H.3.3.

H.3.2 Equipment set-up

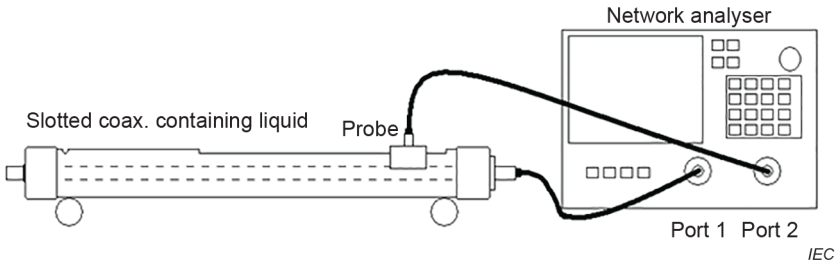
The test equipment consists of a slotted coaxial transmission line with a probe connected to a vector network analyser, as shown in Figure H.1. The sensing element of the probe is the extended centre conductor of the coaxial cable/connector. The log-magnitude and phase of S_{21} should be displayed simultaneously. Source power should be set to a level high enough to provide good signal-to-noise ratio. Since the measured quantities are magnitude and phase changes versus distance, the accuracy of the scale is very critical.

The network analyser injects a signal into one end of the slotted coaxial transmission line. The probe inserted through the slot into the tissue-equivalent medium liquid detects the RF amplitude and phase for each measurement position along the length of the line. A full two-port calibration of the network analyser should be carried out prior to filling the line with liquid, and the following precautions should be observed.

a) Fill the slotted line carefully to avoid trapping air bubbles. This operation should be performed while the slotted line is horizontal.

b) The probe should be inserted into the slot at the end nearest to the input connector of the slotted line, so that the tissue-equivalent medium liquid is flush with the inside surface of the line, and aligned with a well-defined position on the distance scale of the slotted line.

c) The probe should be inserted perpendicular to the slotted-line longitudinal axis until a stable and adequate amplitude response is achieved. Do not insert the probe too deeply into the coaxial line, because it can overly perturb the field distribution.



Although not shown, equipment for sample temperature monitoring is recommended.

Figure H.1 – Slotted line set-up

IECNORM.COM : Click to view the full PDF of IEC/IEEE 62209-1528:2020

H.3.3 Measurement procedure

a) Configure and calibrate the network analyser.

b) Measure log-magnitude and phase data at 10 to 20 positions along the slotted line, corresponding to about a 30 dB change in magnitude.

c) Plot S_{21} log-magnitude and phase against measurement distance.

d) Determine if the plotted points closely follow a straight-line approximation, based on the correlation coefficient or a similar statistical measure. The data should produce a good linear regression fit (expected correlation coefficient r^2 > 0,99 for lossy materials). If not, re-measure the liquid by increasing the number of measurement points to extend the magnitude change from 30 dB to 40 dB.

   For low-loss materials, ensure that the slotted line is long enough to avoid reflections from the load-terminated end.

e) Calculate the conductivity and relative permittivity of the tissue-equivalent medium liquid using Formulas (H.1), derived from [76].

$$\begin{aligned}
\bar{\alpha} &= \frac{m_{\mathrm{m}} \ln(10)}{20} \quad [\mathrm{Np/cm}] \\
\bar{\beta} &= \frac{m_{\mathrm{p}} \pi}{180} \quad [\mathrm{rad/cm}] \\
\varepsilon_{\mathrm{r}}' &= \frac{(\bar{\beta})^2 - (\bar{\alpha})^2}{\omega^2 \mu_0 \varepsilon_0} \\
\sigma &= \frac{2\bar{\alpha}\bar{\beta}}{\omega\varepsilon_0}\left(\frac{100\ \mathrm{cm}}{\mathrm{m}}\right) \quad [\mathrm{S/m}]
\end{aligned} \tag{H.1}$$

where

m_{m} and m_{p} are the slopes of the least-squares linear fits of the log-magnitude and phase plots, respectively;

$\bar{\alpha}$ and $\bar{\beta}$ are the average attenuation and propagation coefficients along the line.

H.4 Contact coaxial probe

H.4.1 General

Contact probes are open-ended coaxial transmission line sections, usually with an end flange serving as a ground plane for fringing fields. Coaxial probe methods can be used over the 4 MHz to 10 GHz frequency range specified in this document. Multiple probes are typically used to cover different frequency bands. A larger probe size has better sensitivity at lower frequencies. A smaller probe can measure at higher frequencies due to the suppression of non-TEM modes in the coaxial line. At frequencies below 100 MHz, special techniques may be used to mitigate electrode polarization, which is caused by charge accumulation on the probe conductors.

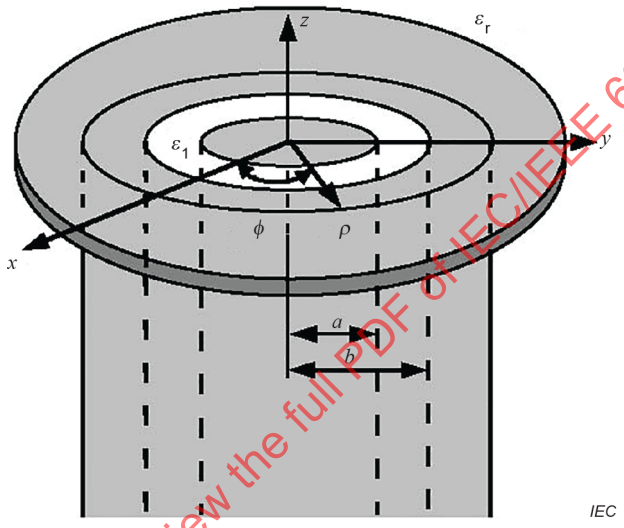
Measurements are made by placing the probe in contact with the tissue-equivalent medium sample and measuring the admittance or reflection coefficient with respect to the open-circuit end, using a network analyser or equivalent instrumentation [77], [78], and [79]. Coaxial probes can also be used to test solid dielectrics, for example bulk samples of the materials used to construct the device holder or phantom. To minimize errors with contact probes, solid surfaces should be highly polished [80].

IECNORM.COM : Click to view the full PDF of IEC/IEEE 62209-1528:2020

The network analyser should be calibrated and the test procedures should specify the equipment settings for the frequency range to be measured. The application software should use the measured data to compute the dielectric properties of the tissue-equivalent medium sample as a function of frequency. Coaxial probes are commercially available, including the application software required for use with specific network analysers. The applicable frequency range is a function of the probe size. An example procedure is given in H.4.3.

H.4.2 Equipment set-up

The equipment consists of a coaxial probe connected to one of the ports on a vector network analyser. The open-ended coaxial line construction is shown in Figure H.2. Cylindrical coordinates (ρ, ϕ, z) are used, where ρ is the radial distance from the probe axis, ϕ is the angular displacement around the axis, z is the location along the axis, a is the inner conductor radius, and b is the inner radius of the outer conductor. Coaxial probes typically include a flange to satisfy the infinite ground-plane assumption used in the admittance calculations.



Key

a	inner conductor radius
b	outer conductor inner radius
z	displacement along the axis
ε_1	permittivity of the dielectric medium filling the space between a and b
ρ	radial distance from the axis
ϕ	angular displacement around the axis
(x, y, z)	Cartesian coordinates

Figure H.2 – An open-ended coaxial probe with inner and outer radii a and b, respectively

A non-metallic container that is sufficiently large compared to the size of the probe immersed in it should be used to hold the tissue-equivalent medium sample. A probe with an outer diameter b of 2 mm to 4 mm is suitable for tissue-equivalent medium measurements in the 300 MHz to 10 GHz range. This probe size requires sample volumes of 50 cm^3 or more. Larger sample volumes are required for larger probes.

IECNORM.COM : Click to view the full PDF of IEC/IEEE 62209-1528:2020

The coaxial probe is connected to a network analyser and typically calibrated with open and short terminations, and also in a known dielectric medium such as de-ionized water. Commercially available probes are supplied with high precision shorting plugs for probe calibration. The calibration procedures are highly automated by the application software provided with commercially available probes. To ensure measurement accuracy, the probe end should be clean and free of oxidation [81]. Calibration can be checked by measuring the reference liquids of Clause H.6, and re-measuring the short circuit to ensure that a reflection coefficient of Γ = −1,0 (linear units) is obtained consistently.

Large measurement errors due to “flange resonances” can occur when the diameter of the flange is approximately equal to one half wavelength in the dielectric medium [82]. Such effects are most pronounced for high-permittivity liquids that have a loss tangent less than approximately 0,25 (at wireless device frequencies these include water, methanol, and dimethyl sulfoxide). Therefore, calibration with a liquid having a high loss tangent, e.g. ethanol, is strongly recommended for larger sensors. There could be problems calibrating 7 mm flanged coaxial sensors with water at some frequencies. Tissue-equivalent media have a loss tangent of about 0,5, which is high enough to ensure that resonance effects are practically nonexistent no matter what size of sensor is used.

H.4.3 Measurement procedure

a) Configure and calibrate the network analyser and probe system as required by the application software.

b) Place the sample in a non-metallic container and immerse the probe into the liquid. A fixture or clamp is recommended to stabilize the probe by mounting it with the probe face oriented at an angle to the liquid surface to ensure that there are no air bubbles trapped beneath the flange during insertion into the liquid.

c) Activate the application software to measure the complex admittance with respect to the probe aperture.

d) The complex relative permittivity, $\varepsilon_r = \varepsilon_r' - \mathrm{j}\sigma/\omega\varepsilon_0$, is automatically computed by the application software; for example according to Formula (H.2) [79]:

$$Y = \frac{\mathrm{j}2\omega\varepsilon_r'\varepsilon_0}{\left[\ln(b/a)\right]^2}\int_a^b\int_a^b\int_0^\pi \cos\phi' \frac{\exp\left[-\mathrm{j}\omega(\mu_0\varepsilon_r'\varepsilon_0)^{1/2} r\right]}{r}\mathrm{d}\phi'\mathrm{d}\rho'\mathrm{d}\rho \qquad \text{(H.2)}$$

where Y is the admittance of the probe in contact with the sample, the primed and unprimed coordinates refer to source and observation points, respectively, $r^2 = \rho^2 + (\rho')^2 - 2\rho\rho'\cos\phi'$, ω is the angular frequency, and j = $\sqrt{(-1)}$.

Other numerical approaches may be used, e.g. [83], [84].

H.5 TEM transmission line

H.5.1 General

This method is based on measurement of the complex transmission coefficient of a TEM-mode coaxial transmission line filled with the test liquid [85]. A transmission measurement with a vector network analyser is used to determine the magnitude and phase of the scattering coefficient S_{21}, from which the complex permittivity is calculated. The network analyser should be calibrated and the test procedures should specify the equipment settings for the frequency range to be measured. The application software should use the measured data to compute the dielectric properties of the liquid sample as a function of frequency.

IECNORM.COM : Click to view the full PDF of IEC/IEEE 62209-1528:2020

H.5.2 Equipment set-up

The measurement set-up is shown in Figure H.3. The liquid sample is contained in the open-wall stripline consisting of a centre-conductor with a circular cross-section, two planar vertical (side) ground conductors, one optically transparent plastic bottom wall, an open top, and a temperature sensor. The length d of the TEM line is chosen for a given frequency range so that the effect of multiple reflections inside the TEM line is small, and the total attenuation due to the liquid within the line does not exceed the dynamic range of the network analyser. For example, two TEM lines with different lengths can be used to cover the frequency range of 800 MHz to 2 000 MHz. The liquid sample should be carefully syringed or poured into the TEM line through the open top to avoid any air bubbles.

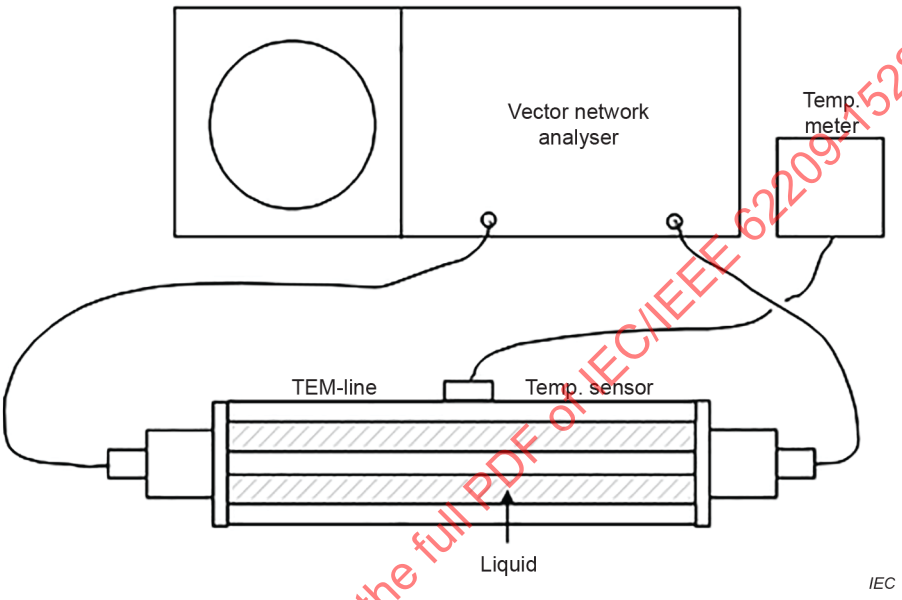


Figure H.3 – TEM line dielectric properties test set-up [85]

H.5.3 Measurement procedure

a) Configure and calibrate the network analyser.

b) Record the magnitude and phase of S_{21}^{0} of the empty cell at the desired frequencies.

c) Inject sample liquid into the cell, and repeat the measurement to obtain the transmission coefficient with the sample S_{21}^{s}.

d) Remove the liquid from the TEM line, thoroughly rinse the inside with water, and dry carefully.

e) Reconnect the coaxial line to the network analyser. Make sure that the magnitude and phase of S_{21}^{0} are unchanged (deviation less than 0,1 dB in magnitude and 0,5° in phase). This step is needed only if multiple samples are to be measured without recalibration.

f) Calculate the complex permittivity of the liquid from the magnitude and phase of S_{21}^{s}/S_{21}^{0} by a numerical solution of the Formulas (H.3).

IECNORM.COM : Click to view the full PDF of IEC/IEEE 62209-1528:2020

$$\frac{S_{21}^{s}}{S_{21}^{0}} = \frac{\left(1-\Gamma^2\right)\exp\left[-\mathrm{j}\left(k-k_0\right)d\right]}{1-\Gamma^2\exp\left(-\mathrm{j}2kd\right)}$$

$$\Gamma = \frac{1-\sqrt{\varepsilon_r}}{1+\sqrt{\varepsilon_r}} \tag{H.3}$$

$$k = \frac{2\pi f}{c_0}\sqrt{\varepsilon_r}$$

$$k_0 = \frac{2\pi f}{c_0}$$

where

Γ is the reflection coefficient at either end of the TEM line;

k is the wave number in the liquid;

k_0 is the free-space wave number;

d is the length of the sample holder (TEM line);

f is the frequency;

c_0 is the free-space speed of light;

$\varepsilon_r = \varepsilon_r' - \mathrm{j}\sigma/\omega\varepsilon_0$ is the complex relative permittivity of the sample.

H.6 Dielectric properties of reference liquids

The procedures in Clause H.2 require measurements of reference liquids that have well-established dielectric properties in order to validate the dielectric properties measurement system. It is recommended to use a reference liquid listed in Table H.1 for validating the dielectric properties measurement system. The difference between the measurement results and the calculated dielectric properties (normalized for frequency and temperature) should be within the expanded uncertainty of the dielectric properties measurement system. Two reference liquids are required, one for calibration, and one for checking the calibration. A general formula for calculating frequency-dependent dielectric properties is given by Formula (H.4):

$$\varepsilon_r = \varepsilon_\infty + \frac{\varepsilon_s - \varepsilon_\infty}{\left[1+(\mathrm{j}\omega\tau)^{1-\alpha}\right]^{\beta}} + \frac{\sigma_i}{\mathrm{j}\omega\varepsilon_0} \tag{H.4}$$

which corresponds to the Debye formula for α = 0 and β = 1, to the Cole-Cole formula for β = 1 and 0 < α < 1, and to the Cole-Davidson relationship for α = 0 and 0 < β < 1 [86], and where:

ε_s is the static or low frequency permittivity;

ε_∞ is the asymptotic high-frequency permittivity;

τ is the relaxation time;

σ_i is the ionic conductivity.

The parameters for calculating the properties of several reference liquids using this formula are given in Table H.1. These liquids are dimethyl sulfoxide, methanol, ethanediol, de-ionized water. The parameters α and σ_i are zero for all liquids listed in Table H.1. The model parameters were obtained using various test methods described in the literature [86]. In general, results obtained with two-port closed-transmission-line cells [87] are expected to be the most accurate, but results from all sources listed in the table agree relatively well. Table H.2 contains target 20 °C relative permittivity and conductivity values. If other reference liquids are used, target values and literature references should be provided in the measurement report.

IECNORM.COM : Click to view the full PDF of IEC/IEEE 62209-1528:2020

It is a good practice to choose reference liquids with dielectric properties similar to tissue-equivalent media. Any reference liquid mixture recipes should be followed exactly, and dielectric properties should be measured at the specified temperatures. In order to avoid contamination and evaporation, mixtures should not be left exposed to air. Reference liquids should be high-purity grade, e.g. analytical grade or better. After opening, reagent bottles should be stored in accordance with the manufacturer's recommendation for the duration of the recommended shelf life.

All personnel should be familiar with and apply any special handling procedures according to the Material Safety Data Sheet (MSDS) for each particular liquid.

Table H.1 – Parameters for calculating the dielectric properties of various reference liquids

Reference liquid	Temperature °C	Ref.	Model	ε_s	ε_∞	τ [ps]	β
DI water[a]	20	[88]	Debye	80,21	5,60	9,36	1
DI water[a]	25	[88]	Debye	78,36	5,20	8,27	1
DMS[b]	20	[89][c]	Debye	47,13	6,80	21,07	1
DMS[b]	25	[89][c]	Debye	46,49	6,50	19,12	1
Ethanediol	20	[89]	Cole-Davidson	41,89	4,75	165,44	0,856
Ethanediol	25	[89]	Cole-Davidson	41,75	4,70	133,70	0,859
Methanol	20	[89][c]	Debye	33,64	5,65	56,40	1
Methanol	25	[89]	Debye	32,66	5,56	50,70	1

[a] DI water is deionized water.

[b] DMS is dimethyl sulphoxide.

[c] Parameters from Gregory and Clarke [89] were derived from measurements to 5 GHz only; the accuracy of these parameters above 5 GHz has not been evaluated.

IECNORM.COM : Click to view the full PDF of IEC/IEEE 62209-1528:2020

Table H.2 – Dielectric properties of reference liquids at 20 °C

Frequency MHz	Methanol [89] [a]		DMS[b] [89] [a]		DI water[c] [88]		Ethanediol [89] [a]	
	ε'_r	σ (S/m)	ε'_r	σ (S/m)	ε'_r	σ (S/m)	ε'_r	σ (S/m)
4	33,64	0,000	47,13	0,000	80,21	0,000	41,89	0,000
10	33,64	0,000	47,13	0,000	80,21	0,000	41,89	0,000
30	33,64	0,000	47,13	0,000	80,21	0,000	41,86	0,002
150	33,56	0,012	47,11	0,007	80,20	0,005	41,19	0,041
300	33,33	0,05	47,07	0,03	80,19	0,02	39,26	0,15
450	32,94	0,11	46,99	0,06	80,16	0,05	36,51	0,31
750	31,78	0,29	46,74	0,17	80,07	0,14	30,32	0,68
835	31,37	0,35	46,64	0,20	80,03	0,17	28,66	0,78
900	31,04	0,41	46,57	0,24	80,00	0,20	27,45	0,85
1 450	27,77	0,92	45,70	0,60	79,67	0,51	19,62	1,35
1 500	27,45	0,97	45,60	0,64	79,63	0,54	19,11	1,38
1 640	26,54	1,11	45,31	0,76	79,52	0,65	17,79	1,47
1 750	25,83	1,22	45,08	0,86	79,43	0,74	16,88	1,53
1 800	25,51	1,27	44,96	0,91	79,38	0,78	16,50	1,56
1 900	24,88	1,37	44,73	1,01	79,29	0,87	15,79	1,61
2 000	24,25	1,47	44,49	1,11	79,19	0,96	15,15	1,66
2 100	23,63	1,57	44,24	1,22	79,09	1,06	14,57	1,70
2 300	22,43	1,75	43,71	1,44	78,87	1,27	13,56	1,78
2 450	21,57	1,89	43,29	1,61	78,69	1,44	12,91	1,83
2 600	20,75	2,02	42,86	1,80	78,51	1,61	12,33	1,87
3 000	18,76	2,33	41,64	2,31	77,96	2,13	11,10	1,98
3 500	16,65	2,66	40,00	3,00	77,18	2,87	10,00	2,08
4 000	14,93	2,93	38,30	3,71	76,30	3,70	9,20	2,17
4 500	13,53	3,15	36,57	4,44	75,33	4,62	8,60	2,24
5 000	12,40	3,32	34,84	5,16	74,27	5,62	8,13	2,30
5 200	12,01	3,38	34,16	5,45	73,83	6,04	7,98	2,32
5 400	11,64	3,44	33,49	5,73	73,38	6,47	7,83	2,34
5 600	11,31	3,49	32,83	6,01	72,91	6,91	7,70	2,36
5 800	11,00	3,54	32,17	6,29	72,43	7,36	7,58	2,38
6 000	10,72	3,59	31,53	6,56	71,95	7,81	7,47	2,39
7 000	9,56	3,77	28,50	7,83	69,40	10,23	7,02	2,47
8 000	8,75	3,91	25,81	8,96	66,69	12,79	6,69	2,54
9 000	8,17	3,98	23,47	9,94	63,88	15,45	6,45	2,59
10 000	7,72	4,07	21,45	10,79	61,04	18,14	6,26	2,64

[a] Parameters from Gregory and Clarke [89] were derived from measurements to 5 GHz only; the accuracy of these parameters above 5 GHz has not been evaluated.

[b] DMS is dimethyl sulphoxide.

[c] DI water is deionized water.

IECNORM.COM : Click to view the full PDF of IEC/IEEE 62209-1528:2020

Annex I
(informative)

Studies for potential hand effects on head SAR

I.1 Overview

This document is developed based on the principle of providing conservative exposure measurement protocols to assess the head SAR of handset users according to presently available science. Conservativeness of the SAM phantom is established by using the 90th percentile head dimensions of adult male population [61], [63] to ensure that the exposure corresponds to well over 90 % of the user population [62], [63], [65]. The dielectric properties of the homogeneous tissue-equivalent medium required for SAR measurement have been chosen to provide SAR overestimation when compared to results obtained from numerical simulations using anatomical models [2]. In addition, a lossless spacer with the thickness of a compressed ear is used on the SAM phantom to represent the external ear (pinna) so that the handset is positioned at a very close distance to the head; therefore, SAR is not underestimated.

For IEC 62209-1:2015, it was assumed that excluding the hand in the measurement procedures, i.e. using a lossless holder with minimal disturbance of the RF fields, provides conservative exposure. Since the publication of IEC 62209-1:2005, there have been some studies reporting an increase in head psSAR when the hand is included in the SAR assessment. The question of hand effects on head SAR was brought to the attention of IEC TC 106 in 2008 [90], and IEC TC 106 has considered two options to address the concerns of hand effects on head SAR.

a) Continue with the current test protocol and add a clause or annex to address hand effects on head SAR.

b) Revise the head SAR measurement protocol to use a modified lossy device holder or hand phantom.

A third option, to apply a correction factor to increase the measured head SAR according to influences of the hand, was also discussed within IEC TC 106. However, there was not enough data to establish an appropriate correction factor. In addition, the correction factor methodology was not pursued, because it would affect the SAR assessment of all handsets regardless of phone designs and actual hand influences on the head SAR.

The IEC National Committees were asked to vote on the preceding two options (or abstain). The voting results favoured option a) by a majority of 15 to 8. Some National Committees also requested continuing research be considered for this, to avoid delay in the completion of this document. Thus, IEC TC 106 will continue to review and analyse contributions for hand effects on head SAR. If the outcome of additional studies leads to a decision to modify the current test protocol, future revisions of this document will be amended accordingly. Following the National Committees voting results for Option a), Annex I was drafted to identify the current knowledge on hand effects on head SAR.

IECNORM.COM : Click to view the full PDF of IEC/IEEE 62209-1528:2020

I.2 Background

I.2.1 General

IEC TC 106 took action to address questions raised regarding hand effects on head SAR. Two high priority large scale studies were initiated:

- Hand Effect Measurement Interlab (HEMI) study by six participating laboratories;
- computational study by six participating laboratories on SAM conservativeness using different hand phantoms.

Final results and conclusions for these studies [91], [92], [93] were presented in multiple IEC TC 106 face-to-face meetings. The final report of the investigation on psSAR sensitivity to hand and finger positions was presented in January 2013 [94]. Besides these studies, results from several other projects were also presented at IEC TC 106 meetings [90], [95], [96], [97], [98], [99], [100], [101], [102], [103], or published elsewhere [5], [104], [105], [106], [107], [108], [109], [110], [111].

Both experimental and computational studies indicate that SAR variations are dependent on hand grips, DUT position, form factor of the DUT, antenna design and placement, as well as DUT operating frequency bands.

I.2.2 Hand phantoms

Four homogeneous hand phantoms were developed for the CTIA Certification Program Test Plan V3.0 [112] to evaluate the over-the-air (OTA) performance of DUTs using pre-defined grips. The physical dimensions of these four hand phantoms were derived from the average of 50th percentile hand data for men and women in anthropometric research publications ([113], [114], [115], and [116]). The hand grip configurations used for the phantoms were established based on studies of device size, usage, and form factor. The average wet and dry palm dielectric properties reported in [87] were used for the CTIA hand phantoms. The average anatomical characteristics were considered and were used in several experimental studies, e.g. the HEMI study as well as [96], [98], and other computational studies.

I.3 Summary of experimental studies

I.3.1 Experimental studies using fully compliant SAR measurement systems

IEC TC 106 members conducted the HEMI study to investigate hand effects on head SAR. Thirty-three DUTs with a diverse range of physical characteristics, marketed between June 2006 and June 2010, operating in the GSM 900 MHz and WCDMA 1 950 MHz bands, were tested using a single hand phantom and grip configuration, involving 42 total test configurations. Only six out of the 42 configurations show an increase in measured head SAR; the increases ranged from 5 % to 40 %, with most of the increases less than 15 %. None of the increases result in measured SAR above regulatory limits. All increases were in the WCDMA 1 950 MHz band. The remaining WCDMA and GSM configurations showed decreases of up to 78 %. The observed SAR increases were for phones exhibiting comparatively low SAR, for instance the highest increase for 10 g psSAR, including the 40 % increase, was 0,41 W/kg.

I.3.2 Experimental studies using other SAR measurement systems

The data collected in [96] using a fast SAR testing system (not fully compliant with all normative clauses of this document) have showed both increases and decreases in SAR when tested with a realistic hand phantom for 46 handsets in the 1 800 MHz frequency band; where SAR decreases outnumbered SAR increases by a ratio of approximately 2 to 1. The results in [96] and [108] also suggest that SAR increases occur more often at 1 800 MHz and above when compared to lower frequency bands. In [98] and [117], cases are reported where the head SAR increase introduced by hand effects can lead to both an unchanged local SAR distribution or a modified distribution with a shift in peak SAR location. It was also shown that the SAR is comparable for a DUT held by a CTIA hand phantom and a human hand replicating the same grip [96].

IECNORM.COM : Click to view the full PDF of IEC/IEEE 62209-1528:2020

I.4 Summary of computational studies

Several computational studies have been performed and reviewed by IEC TC 106 to investigate hand effects on head SAR [91], [94], [100], using several simplified and detailed CAD phone models at 900 MHz, 1 800 MHz, and 2 000 MHz. Several adult and child hand models were used to simulate realistic hand grip conditions for exposures in several realistic head models. The results were in general consistent with experimental data, showing a considerable prevalence of cases with psSAR decreases due to presence of the hand, and most of the SAR increases were observed at 1 800 MHz and 2 000 MHz.

The computational studies have also provided additional details on certain parameters that can introduce noticeable influences on head psSAR. One study, [118] and [119], showed higher SAR increases at frequencies around 1 800 MHz when the palm of a hand model was positioned 1 cm to 2 cm above the antenna or peak SAR location. In another study [94], involving parametric search for maximum SAR increase in varied hand grip conditions, a significant SAR increase in both the SAM phantom and anatomical head models was observed when fingers were in contact with the head. This was also observed in one of the experimental studies using a fast SAR testing system (which is not fully compliant with all normative clauses of this document) [96]. For frequencies below 2 GHz, the maximum increase in head SAR is similar for both 1 g and 10 g psSAR [96] [120].

I.5 Conclusions

a) The data show that psSAR in the head can increase due to presence of the hand for some configurations.

b) Both experimental and computational studies show:

   1) head SAR increase was observed for a small percentage of the configurations at all studied frequencies;

   2) most head SAR increases were found at frequencies between 1 800 MHz and 2 000 MHz. Data for frequencies above 2 GHz are limited;

   3) in a considerable majority of the cases where SAR increase was observed, the effect was small.

c) No particular hand configuration or grip position could be identified which yields more conservative results for all DUTs and/or for all testing conditions.

d) For a given DUT, methods do not seem to exist for predicting the transmission frequency and realistic use condition that would result in the highest possible SAR enhancement.

e) The dependency of SAR increase on phone or antenna design cannot be easily predicted.

f) There is insufficient data to scientifically justify the implementation of correction factor proposed by some National Committees.

g) IEC TC 106 will continue to review and analyse contributions related to hand effects on head SAR.

IECNORM.COM : Click to view the full PDF of IEC/IEEE 62209-1528:2020

Annex J
(informative)

Skin enhancement factor

J.1 Background

In the course of the development of this document, several studies ([70], [71], [121]) indicated that the measurements in a homogeneous phantom could result in localized SAR values lower than the maximum values in a heterogeneous and anatomically realistic body model at 1 900 MHz. Since then, several research projects and simulations were undertaken within the IEC TC 106 to verify these results. Simulations were undertaken with homogeneous phantoms and layered models simulating skin, fat, and muscle. These findings were confirmed in simulations for the metric SAR.

The exposure standard of ICES IEEE Std C95.1 and the recommendations by ICNIRP are designed to protect against established adverse health effects. The ICNIRP guidelines in [3], page 17, state:

"*Established biological and health effects in the frequency range 10 MHz to a few GHz are consistent with responses to a body temperature rise of more than 1 °C.*"

Nevertheless, simulations for temperature result in different distributions compared to SAR distributions (Figure J.1), with the temperature rise distribution being much smoother than the corresponding SAR distribution. This result indicates that local SAR enhancements do not typically produce equivalent temperature rise enhancement, due to the different nature of the underlying physics: wave phenomena for SAR, and diffusion phenomena for temperature.

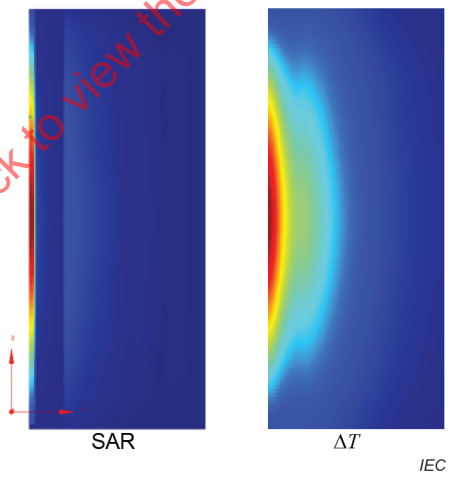


Figure J.1 – SAR and temperature increase (ΔT) distributions simulated for a three-layer (skin, fat, muscle) planar torso model

IECNORM.COM : Click to view the full PDF of IEC/IEEE 62209-1528:2020

J.2 Rationale

The reasons for the higher localized SAR values in heterogeneous tissue are standing-wave effects which can occur under far-field-like exposure conditions if a tissue layer with low water content, such as fat, bone or breast tissue, is enclosed between two tissues with high water content, e.g. muscle, skin, most inner organs, etc. The most typical structure consists of a fat layer between skin and muscle. Incident waves which pass the skin experience almost no attenuation in the subsequent fat tissue layer. If the thickness of the fat layer corresponds to approximately $\lambda/4$, the phase of the wave reflected at the muscle layer will lead to a standing wave, with its maximum in the skin layer. This will lead to a significant increase of the local SAR in the skin. Even if the SAR is averaged over a cubical volume, which in this case will contain a comparatively large amount of fat tissue, the SAR measured in the same volume of homogeneous tissue-equivalent medium will not yield conservative exposure. A detailed discussion and quantification of this effect can be found in [70], [71].

J.3 Simulations

The project team investigated the following in the existing literature with respect to age, sex, and race:

- statistical distribution of epidermis plus dermis thickness;
- statistical distribution of the fat layer thickness;
- thickness given by mean and standard deviation.

Skin anatomy and physiology undergo modifications throughout each person's entire lifespan. Diller [122] assumes that the skin thickness of children is 72 % of adult skin thickness.

Body-worn device positions according to a report of Carnegie Mellon University [123] were chosen for the study. This report from Carnegie Mellon University identified regions of the human body where radios can be carried without impeding the person's movements. Dynamic wearability is confined to body positions such as:

– arm – triceps;
– forearm;
– upper chest;
– back – subscapular;
– back – above pelvis;
– ankle;
– leg – calf;
– thigh – front;
– waist – lateral.

Body tissue thickness varies with individuals. The various thicknesses have a probability distribution. The SAR for a given skin and fat tissue (t_s, t_f) is weighted according to $P(t_s)$ $P(t_f)$ by the thickness probability.

Simulations were done for the different wearability areas with the data from the literature study on the skin and fat thicknesses of the human body [124]. Antennas with electrical lengths of 0,5 λ, 0,47 λ, 0,35 λ, 0,23 λ, 0,10 λ and 0,05 λ were analysed, at frequencies between 30 MHz and 6 GHz.

The increased SAR also varied with the distance of the antenna from the body. This distance depends on the frequency.

IECNORM.COM : Click to view the full PDF of IEC/IEEE 62209-1528:2020

J.4 Recommendation

The results of all simulations for the different thicknesses of skin, different thicknesses of fat layers, different dielectric properties, different antennas, and different distances from the body were analysed. From all the simulations, adopting a statistical coverage factor protective of 90 % of the population (Figure J.2), skin enhancement factors can be derived as shown in Table J.1 and Figure J.3.

The project team asked ICNIRP and ICES for advice whether this factor is necessary for the evaluation of the exposure. ICES came to a very clear consensus.

- It is not necessary to apply a scaling factor to limit the skin SAR.
- The measurement of SAR in a homogenous phantom without a scaling factor is adequate to protect the public.

ICNIRP responded that this issue will be considered in the general revision of their RF guidelines.

In order to quantify the possible SAR underestimation and to specify the conditions under which this underestimation will occur, Annex J is included as an informative part of this document.

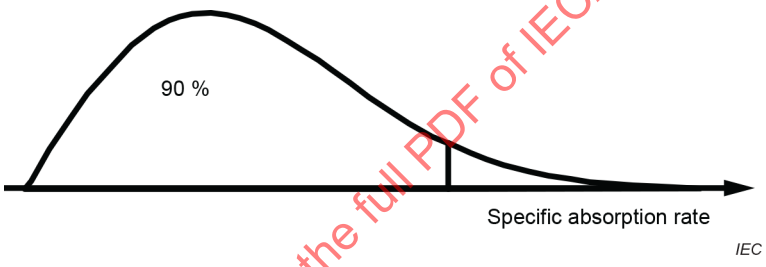


Figure J.2 – Statistical approach to protect 90 % of the population

Table J.1 –psSAR correction factors

Frequency band	Device to phantom distance	Skin enhancement factor [a,b]
300 MHz to 800 MHz	0 mm to 200 mm	1,0
800 MHz to 1 000 MHz	0 mm to 40 mm	1,0
	40 mm to 45 mm	linearly interpolate between 1,0 and 1,1
	45 mm to 200 mm	1,1
1 700 MHz to 3 000 MHz	0 mm to 20 mm	1,0
	20 mm to 35 mm	linearly interpolate between 1,0 and 1,5
	35 mm to 200 mm	1,5
5 000 MHz to 6 000 MHz	0 mm to 200 mm	1,0

[a] This represents the enhancement of the psSAR (1 g and 10 g). It is referred to as the skin enhancement factor because the SAR enhancement is in the skin layer.

[b] For all other frequencies and distances, use linear interpolation.

IECNORM.COM : Click to view the full PDF of IEC/IEEE 62209-1528:2020

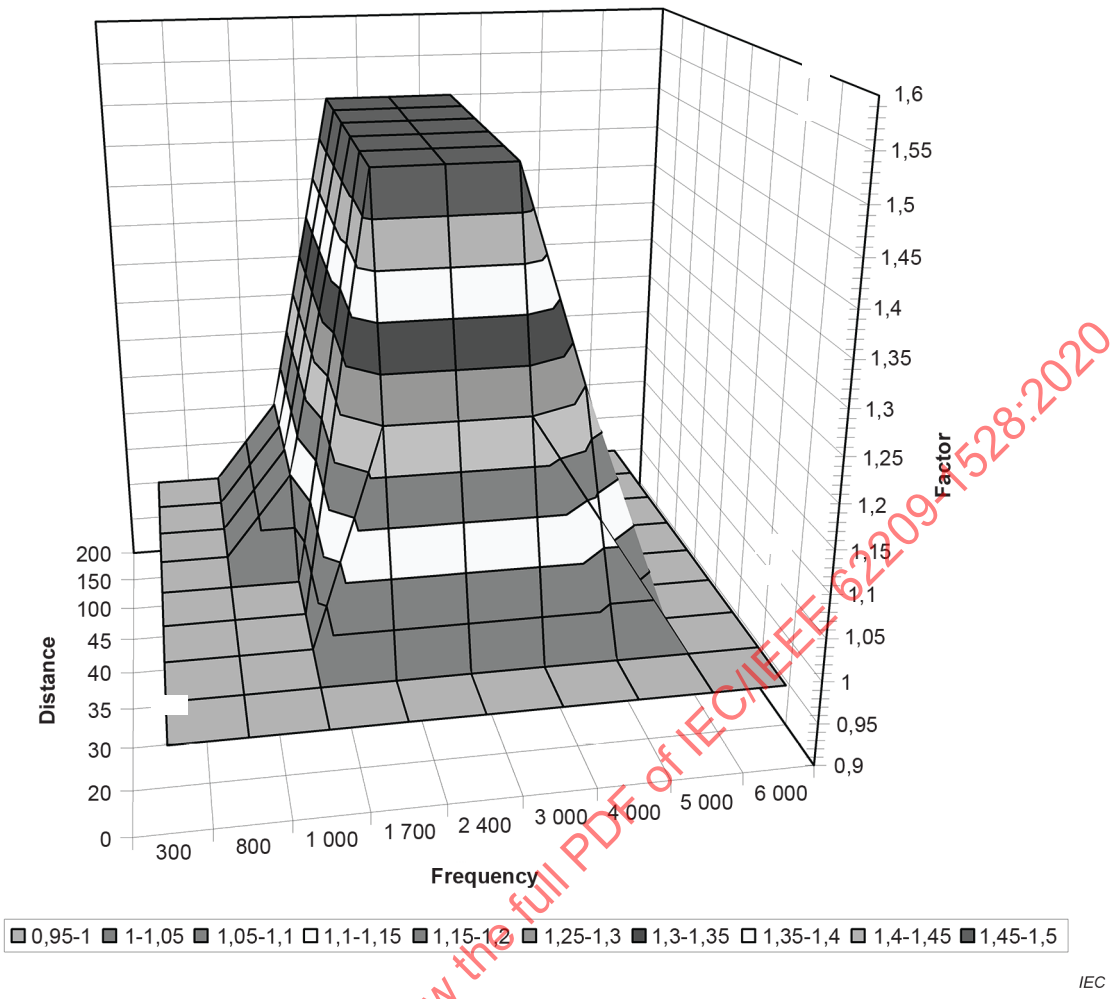


Figure J.3 – psSAR skin enhancement factors

IECNORM.COM : Click to view the full PDF of IEC/IEEE 62209-1528:2020

Annex K
(normative)

Application-specific phantoms

K.1 General

Some wireless communication devices (e.g. smart glasses, hearing aids, smart watches) have form factors and/or usage scenarios such that assessments performed with the standard phantoms of Clause 6 (sagittally-bisected SAM, and the elliptical or rectangular flat phantoms) are either not applicable or are inappropriate. For example, some wireless communication devices expose the top of the head, the front of the face, or specific body parts, e.g. wrist, hands, or ankles. Specific phantoms are proposed that allow the exposed regions of the body to be evaluated in accordance with the intended use of the device, and reduced measurement uncertainty. Annex K describes the requirements for appropriate phantoms, scanning measurements, and reporting.

K.2 Phantom basic requirements

The phantom and procedure shall enable conservative exposure. The shape and tissue-equivalent medium shall be selected such that the assessed psSAR is higher than the 90th percentile of the highest exposure in the user population. This is usually derived by numerical parameter variations using anatomical models that represent the user population [73].

The phantom shell shall ensure stable shape within 2 % relative to the provided CAD file of the phantom, even when filled with tissue-equivalent medium and with a mounted device under test (DUT).

Justification for the appropriateness of phantom and tissue-equivalent medium for the exposure conditions, and evidence that the test system (phantom and tissue-equivalent medium) is conservative, shall be provided. These items are typically demonstrated, using validation studies and other results, by the equipment manufacturer, including the SAR measurement set-up; for example, test device and phantom positioning, field probe positioning and scanning, or post-processing requirements, etc.

K.3 Examples of specific alternative phantoms

K.3.1 Face-down SAM phantom

The SAM face-down phantom shown in Figure K.1 is recommended for devices where the exposure is at the front side of the head. It is the same as the SAM phantom specified in Annex G, but oriented with the front of the face facing downward. This phantom is truncated along a plane behind the ear reference point. Above this plane, an upper extension is added to ensure that the tissue-equivalent medium liquid is deep enough to measure in the relevant regions of the SAM phantom. The upper extension is flanged, to allow measurement probe access. The shell thickness shall be 2 mm ± 0,2 mm (not including the upper extension). The phantom is filled with head tissue-equivalent medium having dielectric properties as specified in 6.2. The same phantom could be used for some transmitters mounted on eyeglasses or eyewear. If the psSAR location is in the eye region, the user shall either show that the tissue-equivalent medium provides conservative exposure or propose an alternative medium. The conservativeness of the assessment shall be determined by numerical evaluation, or with an equivalent method (e.g. with the Virtual Family phantoms).

IECNORM.COM : Click to view the full PDF of IEC/IEEE 62209-1528:2020

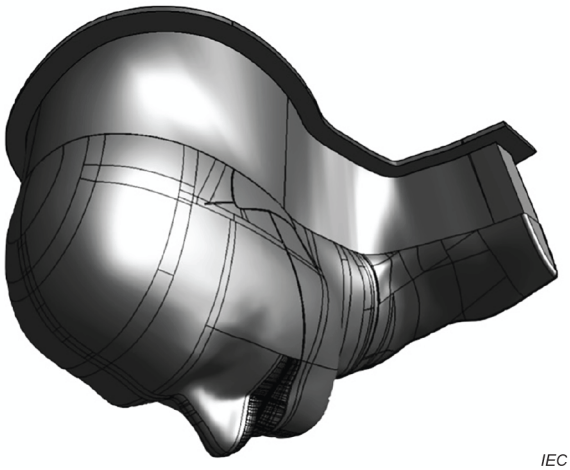


Figure K.1 – SAM face-down phantom

K.3.2 Head-stand SAM phantom

The head-stand phantom (Figure K.2) is recommended for devices where the exposure is at the top side of the head (e.g. head-mounted devices). It is the same as the SAM phantom specified in Annex G, but oriented with the top of the head facing downward. It is truncated along a plane above the bottom of the ear reference point. Above this plane, an upper extension is added to ensure that the tissue-equivalent medium liquid is deep enough to measure in the relevant regions of the SAM phantom. The upper extension is flanged, to allow better measurement probe access for the top of the head (bottom of the head-stand phantom). The shell thickness shall be 2 mm ± 0,2 mm (not including the upper extension). The phantom is filled with tissue-equivalent medium having dielectric properties as specified in 6.2.

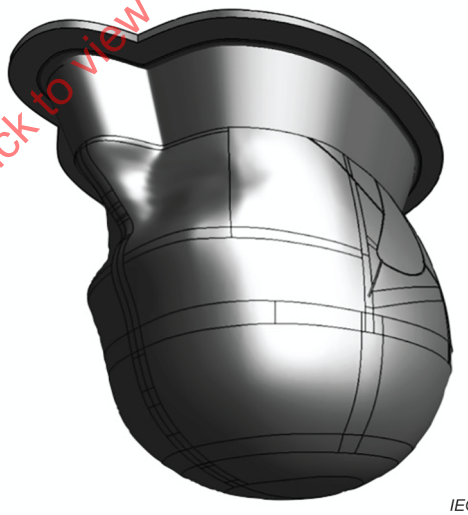


Figure K.2 – SAM head-stand phantom

K.3.3 Wrist phantom

The wrist phantom (Figure K.3), to test wrist-worn wearables (watches, bracelets, etc.) that are equipped with transmitters, is based on CTIA forearm phantom with a shell thickness of 2 mm. The conservativeness of the tissue-equivalent medium shall be demonstrated. The wrist phantom is recommended when the flat phantom is inappropriate (e.g. when wrist-worn wearables do not conform to the flat phantom, when test distances or gaps between the device and the phantom are inconsistent with intended use conditions, or when wrist band straps operate correctly only when closed).

IECNORM.COM : Click to view the full PDF of IEC/IEEE 62209-1528:2020

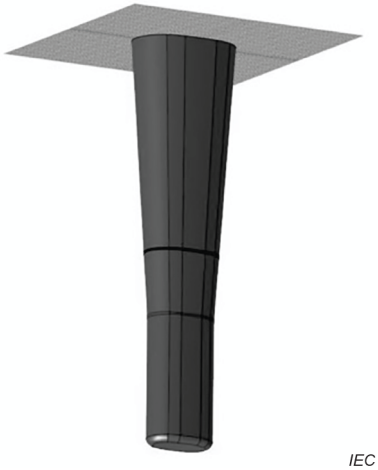


Figure K.3 – Wrist phantom

K.4 Scanning and evaluation requirements

For application-specific phantoms, the measurement requirements of Clause 7 shall be applied where possible. If the geometry of the specific phantom does not allow the requirements to be applied (e.g. due to probe orientation, scan volume), the details of the assessment method shall be documented, and associated additional uncertainty analysis shall be reported.

If the probe orientation can be maintained within ±30° of the normal to the phantom surface (see 7.4), the positioning accuracy of the probe geometrical centre (centre of the probe detector) relative to the phantom shell shall be better than ±0,2 mm, as specified in 6.4. However, if it is not possible to maintain the probe orientation within the ±30° tolerance, a larger positioning tolerance of up to ±0,5 mm is acceptable, if the additional uncertainty analysis is provided. In this case, the boundary effect compensation is expected to have a higher uncertainty, and the full hemispherical isotropy shall be evaluated (Clause E.4); the method for extrapolation to the surface shall be assessed for all angles of incidence relative to the probe orientation, and uncertainty assessed and documented (Clause K.5 and Clause K.6). The scan area shall be larger than the projection of the device on the phantom. If the SAR averaging volume includes portions outside the tissue-equivalent medium, the psSAR evaluation shall be performed in compliance with methods from the numerical standard IEC/IEEE 62704-1 [41], and the same uncertainty as in IEC/IEEE 62704-1 shall be applied.

K.5 Uncertainty assessment

All uncertainty parameters specified in Clause 8 shall be determined for assessment using application-specific phantoms. Additional uncertainties related to the specific phantom and associated measurement procedures shall also be addressed. When an alternative phantom is used, it is the user's responsibility to ensure proper validation and justification is available, including clear documentation and acceptable uncertainty assessment.

K.6 Reporting

In addition to the reporting requirements of Clause 9, the report shall include the justification of the choice of phantom used, and the uncertainty assessment of the evaluation, especially variations from Clause 8.

IECNORM.COM : Click to view the full PDF of IEC/IEEE 62209-1528:2020

Annex L
(normative)

Fast compliance evaluations using a flat-bottom phantom with a curved corner (Uniphantom)

L.1 General

In Annex L, the main focus is methods to reduce the number of tests for evaluating the compliance of a DUT by using a flat-bottom phantom with a curved edge, known as a "Uniphantom," and specified in Clause L.2. The techniques utilize a conventional SAR measurement system, which complies with the basic requirements of this document, apart from the shape of the phantom. Two handset form factors, straight and clamshell, may be tested, as specified in Clause L.3 and Clause L.4.

L.2 Uniphantom

The Uniphantom is a flat-bottom container based on the rectangular flat phantom used for body-worn devices (Clause G.3), and has a curvature that is representative of the SAM phantom (Clause G.2) at a bottom edge, as shown in Figure L.1. The curvature cross-section along the edge is a quarter elliptic arc with horizontal axis dimension of 90 mm and vertical axis dimension of 75 mm. The ear reference point (ERP) is set at 135 mm from the adjacent inner sidewall of the phantom. The curvature of this phantom approximately follows the line along the ERP and the cheek-chin curve of the cross section of the SAM phantom (see Figure G.6). The Uniphantom shall satisfy the specifications on dielectric properties of the material and the mechanical requirements are the same as for the standard phantoms. The thickness and width requirements of the flat bottom, curved edge, and sidewalls of the Uniphantom are the same as the flat phantom for body-worn devices.

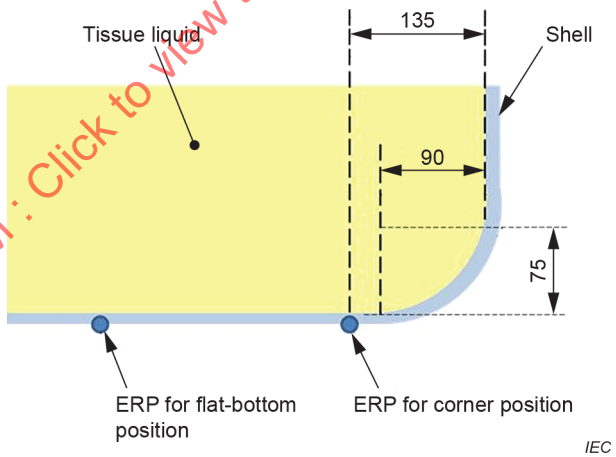


Figure L.1 – Cross section of the unified phantom (Uniphantom) with its dimensions

IECNORM.COM : Click to view the full PDF of IEC/IEEE 62209-1528:2020

L.3 Device positions for compliance testing and definitions of handset shapes

L.3.1 General

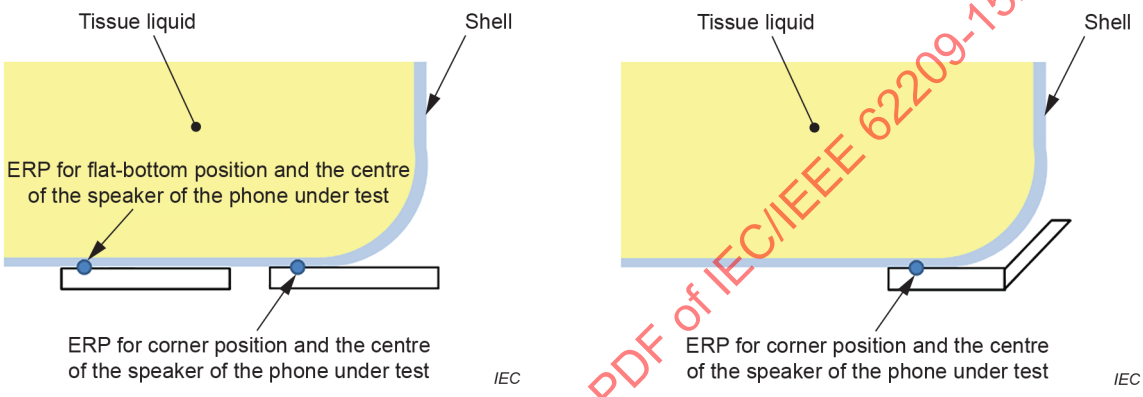
Different device positions apply depending on the form factor of the handset. Subclauses L.3.2 and L.3.3 describe devices with straight and clamshell form factors.

L.3.2 Handsets with a straight form factor

Typical handsets categorized under this type include slider phones, bar phones, and smart phones. With slider phones the keyboard can slide out. A phone of this category is placed at the flat-bottom position or at the curved-edge position as shown in Figure L.2 a). The centre of the speaker is at the ERP, same as in case of the full-compliance SAR measurement set-up using the SAM phantom.

L.3.3 Handsets with a clamshell form factor

These handsets consist of two or more sections, and can be folded via one or more hinges. A phone of this category is set at the curved-edge position as shown in Figure L.2 b). The centre of the speaker is at ERP, same as in the case of the full-compliance SAR measurement set-up using the SAM phantom.



a) Straight form factor **b) Clamshell form factor**

Figure L.2 – Measurement positions of handsets with straight and clamshell form factors

L.4 Testing procedure

L.4.1 General

When comparing the measured SAR with the SAR limit, a margin shall be considered, to prevent underestimation of the SAR measured with the Uniphantom. This margin shall be appropriately determined based on statistical data. Examples of the statistical determination of the margin are specified in Annex U.

L.4.2 Handsets with straight form factors

Figure L.3 shows a flowchart of the testing procedure for handsets with straight form factors. In detail, the steps are as follows:

a) Step 1: Go to step 5 if measurement at the flat bottom of the Uniphantom will be omitted.

b) Step 2: Set the DUT at the flat bottom of the Uniphantom, with the front side in direct contact with the phantom shell, as shown in Figure L.2 a).

c) Step 3: Measure psSAR (SAR_{flat}).

d) Step 4: If SAR_{flat} is lower than the compensated SAR limit ($SAR_{\text{limit}} - SAR_{\text{margin_straight_flat}}$), the phone is deemed to be compliant and the evaluation may stop; otherwise go to step 5.

e) Step 5: Set the phone at the curved-edge (cross-section corner) of the Uniphantom, with the front side in direct contact with the phantom shell, as shown in Figure L.2 a).

f) Step 6: Measure psSAR (SAR_{corner}).

IECNORM.COM : Click to view the full PDF of IEC/IEEE 62209-1528:2020

g) Step 7: If SAR_{corner} is smaller than the compensated SAR limit (SAR_{limit} – $SAR_{margin_straight_corner}$), the phone is deemed to be compliant and the evaluation may stop; otherwise go to step 8.

h) Step 8: Perform full-compliance psSAR evaluation using the SAM phantom.

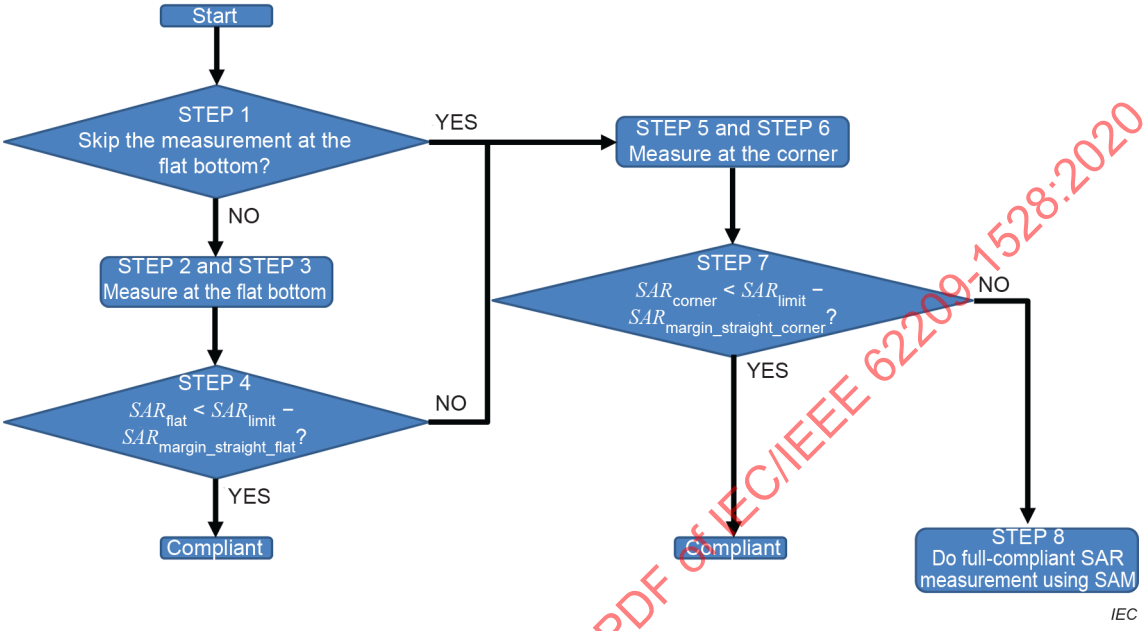


Figure L.3 – Flow chart of testing procedure for handsets with straight form factors

L.4.3 Handsets with clamshell form factors

Figure L.4 shows a flowchart of the testing procedure for handsets with clamshell form factors. In detail, the steps are as follows:

a) Step 1: Set the phone at the curved-edge (cross-section corner) of the Uniphantom, with the front side in direct contact with the phantom shell, as shown in Figure L.2 b).

b) Step 2: Measure psSAR (SAR_{corner}).

c) Step 3: If SAR_{corner} is lower than the compensated SAR limit (SAR_{limit} + $SAR_{margin_clamshell_corner}$), the phone is deemed to be compliant and the evaluation may stop; otherwise go to step 4.

d) Step 4: Perform full-compliance psSAR evaluation using the SAM phantom.

IECNORM.COM : Click to view the full PDF of IEC/IEEE 62209-1528:2020

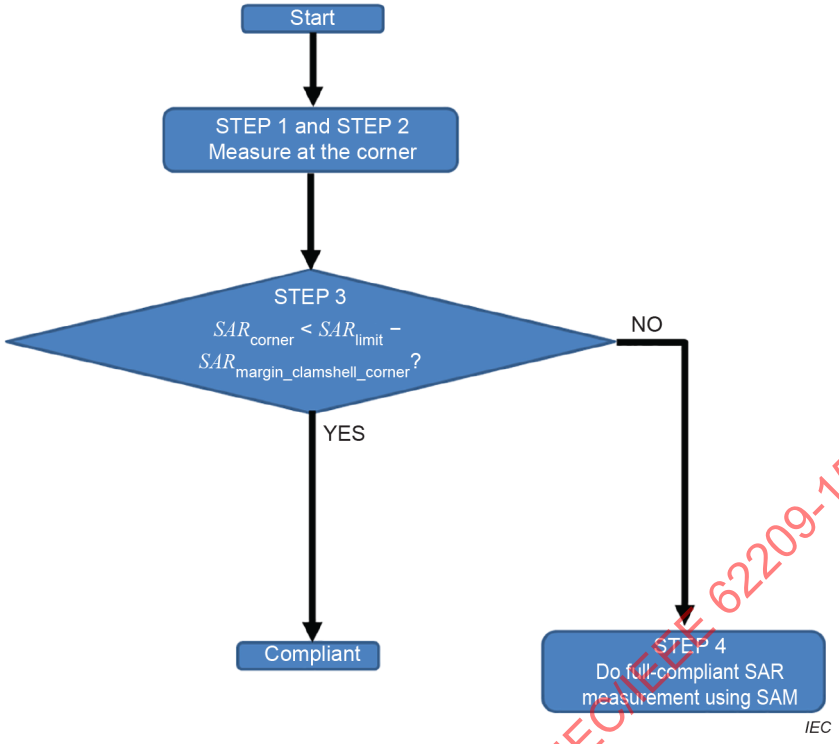


Figure L.4 – Flow chart of testing procedure for handsets with clamshell form factors

L.5 Uncertainty of SAR measurement results using Uniphantom

The uncertainty evaluation of SAR measurement results using the Uniphantom can be performed by the methodology specified in Clause 8. When the measurement is carried out only at the flat bottom of the Uniphantom, and the same device holder as that in the full-compliance SAR evaluation is used, the same uncertainty table as in Clause 8 can be applied.

Notwithstanding the uncertainty evaluation scheme for specified in Clause 8, for compliance evaluation using the Uniphantom, several Type A uncertainty items may be evaluated separately.

The uncertainties related to the items listed below are identical to those of the full-compliance SAR measurement specified in Clause 8:

- mechanical restrictions of the probe positioner;
- phantom shape and thickness;
- postprocessing;
- test sample positioning;
- device holder.

IECNORM.COM : Click to view the full PDF of IEC/IEEE 62209-1528:2020

Annex M
(informative)

Wired hands-free headset testing

M.1 Concept

Annex M describes a procedure that is suitable for assessing the SAR in the head from a wired personal hands-free headset. Note that other procedures following the same principles can also be suitable.

- An experimental test set-up designed in accordance with the principles set out in this document shall be used.
- For correct comparison, the configurations shown in Figure M.1 and Figure M.2 shall be used.

Annex M only describes how to make an informed assessment of hands-free kits.



IEC

Figure M.1 – Configuration of a personal wired hands-free headset

IECNORM.COM : Click to view the full PDF of IEC/IEEE 62209-1528:2020



IEC

Figure M.2 – Configuration without a personal wired hands-free headset

The tissue-equivalent medium at the appropriate operating frequency should be used, as specified in this document.

The two conditions to be tested are:

– the head region of the head-and-torso phantom is filled with the tissue-equivalent medium;
– the entire head-and-torso phantom is filled with tissue-equivalent medium.

In both set-ups, the DUT should be placed next to the ear, and then at the waist with the headset connected to the phone via lead-wires and taped at the ear. Scanning shall be focused on finding SAR changes close to the ear. The psSAR in the head shall also be measured.

Human phantoms used for measurements involving a hands-free accessory shall include the torso; i.e. measurements shall not be performed on the head phantom alone. Use of only a head phantom alone can have significant (and anomalous) impact on the results, because the RF energy coupled into the leads of hands-free accessories is strongly attenuated by the body.

M.2 Example results

The example results are given for the phantom partially filled with tissue-equivalent medium, and the DUT speaker centred at the phantom ear. The maximum 1 g psSAR of 1,2 W/kg is located below the ear. The maximum 1 g psSAR at the ear position is about 0,4 W/kg. There is no significant change in the results of this measurement if the torso is also filled with tissue-equivalent medium, because the DUT interacts mainly with the head.

When the headset accessory is used and the phone is worn at the chest, the following results have been obtained. The headset earpiece is centred at the phantom ear canal and the DUT at the belt (Figure M.1). In this case (with the unfilled torso), the maximum 1 g psSAR measured at the ear (32 mm × 32 mm) is 0,05 W/kg, showing an 87 % (9 dB) reduction compared to the with the DUT at the ear position. If the phantom chest is completely filled with tissue-equivalent medium, a maximum 1 g psSAR of 0,02 W/kg near the ear is obtained, which corresponds to a 95 % (13 dB) reduction from the case with the DUT at the ear.

IECNORM.COM : Click to view the full PDF of IEC/IEEE 62209-1528:2020

M.3 Discussion

From these example measurements it is clear that: 1) the SAR near the ear where the headset earpiece is located is low compared to the peak SAR produced by the DUT; 2) the whole-phantom maximum psSAR is not located near the ear with the headset accessory; 3) the presence of the torso attenuates the field from the headset accessory, resulting in a lower SAR compared to that measured without the torso. It should be noted that in the preceding situations, the coupling between the DUT and headset accessory was very strong, as shown by the additional measurement of the whole-phantom maximum SAR in the head from the headset without the presence of the torso. These measurements yield a peak 1 g psSAR of 0,9 W/kg. Again, it should be noted that the location of this peak is not near the headset earpiece, but it is shifted down to the cheek where the corresponding current on the headset cable is stronger. This is close to the results of computations with best coupling between the wire and RF source, which indicates that the presence of the torso leads to a strong decrease of the whole-phantom maximum SAR in the head, even when the wire is strongly coupled to the RF source (DUT).

The measurements also show that the SAR from the headset accessories near the ear is always lower than when the phone is near the head. It should be noted that if the primary RF source is removed from the ear, the secondary radiator (headset) produces a much lower exposure at this location.

Though the attenuation effect of the body can vary depending on the position of the wire relative to the body, if a large part of the hands-free accessory wire is close to the user's body then the psSAR measured in the ear region can be more than 10 dB lower than psSAR measured from the DUT alone when placed near the head.

IECNORM.COM : Click to view the full PDF of IEC/IEEE 62209-1528:2020

Annex N
(informative)

Applying the head SAR test procedures

Annex N illustrates an example of how to apply the SAR test protocol of 7.3. A DUT supporting GSM mode in 850 MHz, 900 MHz, 1 800 MHz, and 1 900 MHz bands is used for illustration. The device has a sliding keypad that can be used for voice calls with the slide in open and closed positions. The test procedures in 7.4.2 are applied according to the following steps.

Step 1: SAR measurements are performed at the channel having the highest output power for each transmit frequency band according to procedures in 7.4. The corresponding channel numbers are 190 at 836,6 MHz for GSM 850, 38 at 897,6 MHz for GSM 900, 699 at 1 747,6 MHz for GSM 1800, and 661 at 1 880 MHz for GSM 1900. All device test configurations specified in 7.2.4.2.2 and 7.2.4.2.3 for cheek and tilt positions on the left and right sides of the SAM phantom are tested, with the sliding keypad open and closed. The device supports only GSM voice mode for head use; therefore other GSM modes are not applicable for this example.

Step 2: SAR measurements are performed for additional frequency channels in each frequency band and mode as required by 7.2.8 for the highest psSAR test configuration of step 1. In addition, SAR is also measured at other frequency channels as required by 7.2.8 for all configurations tested per step 1 where the psSAR is greater than or equal to half of the applicable SAR limit.

Step 3: The SAR measurement results are shown in Table N.1, Table N.2, Table N.3, and Table N.4. The highest 10 g psSAR among all GSM frequency bands is 1,205 W/kg, on channel 251 at 848,8 MHz for GSM 850.

Table N.1 – SAR results tables for example test results in GSM 850 band

Mode and Band	Device configuration (slide position)	SAM phantom test position		10 g psSAR [W/kg][a]		
				Ch 128[b] 824,2 MHz	Ch 190[b] 836,6 MHz	Ch 251[b] 848,8 MHz
GSM 850	closed	Left	Cheek	0,776	0,653[c]	0,552
			Tilt	-	0,492	-
		Right	Cheek	-	0,626	-
			Tilt	-	0,448	-
	open	Left	Cheek	1,011	1,192[d,e]	1,195
			Tilt	-	0,430	-
		Right	Cheek	0,892	1,120[e]	1,205[f]
			Tilt	-	0,418	-

[a] The applicable regulatory SAR limit is 2,0 W/kg averaged over a 10 g tissue volume.

[b] According to 7.2.8, the number of channels to be tested is N_c = 3 for all of the modes (see step 2).

[c] This is the highest psSAR measured for the mid-band channel with slide closed. Hence, the other two channels in this frequency band also require SAR measurement (see step 2).

[d] This is the highest psSAR measured for the mid-band channel with slide open. Hence, the other two channels in this frequency band also require SAR measurement (see step 2).

[e] The measured psSAR is within 3 dB of the applicable SAR limit. Hence the other two channels in this frequency band also require SAR measurement (see step 2).

[f] This is the highest psSAR measured among all GSM frequency bands and test configurations (see step 3).

IECNORM.COM : Click to view the full PDF of IEC/IEEE 62209-1528:2020

Table N.2 – SAR results tables for example test results in GSM 900 band

Mode & Band	Device configuration	Device position		SAR, averaged over 10 g [W/kg][a]		
				Ch 975[b] 880,2 MHz	Ch 38[b] 897,6 MHz	Ch 124[b] 914,8 MHz
GSM 900	closed	Left	Cheek	0,766	0,730[c]	0,652
			Tilt	-	0,522	-
		Right	Cheek	-	0,631	-
			Tilt	-	0,482	-
	open	Left	Cheek	0,618	0,723[d]	0,833
			Tilt	-	0,443	-
		Right	Cheek	-	0,620	-
			Tilt	-	0,406	-

[a] The applicable regulatory SAR limit is 2,0 W/kg averaged over a 10 g tissue volume.

[b] According to 7.2.8, the number of channels to be tested is N_c = 3 for all of the modes (see step 2).

[c] This is the highest psSAR measured for the mid-band channel with slide closed. Hence, the other two channels in this frequency band also require SAR measurement (see step 2).

[d] This is the highest psSAR measured for the mid-band channel with slide open. Hence, the other two channels in this frequency band also require SAR measurement (see step 2).

Table N.3 – SAR results tables for example test results in GSM 1800 band

Mode & Band	Device configuration	Device position		SAR, averaged over 10 g [W/kg][a]		
				Ch 512[b] 1 710,2 MHz	Ch 699[b] 1 747,6 MHz	Ch 885[b] 1 784,8 MHz
GSM 1800	closed	Left	Cheek	-	0,254	-
			Tilt	-	0,230	-
		Right	Cheek	0,336	0,343[c]	0,466
			Tilt	-	0,215	-
	open	Left	Cheek	-	0,154	-
			Tilt	-	0,162	-
		Right	Cheek	-	0,174	-
			Tilt	0,188	0,192[d]	0,211

[a] The applicable regulatory SAR limit is 2,0 W/kg averaged over a 10 g tissue volume.

[b] According to 7.2.8, the number of channels to be tested is N_c = 3 for all of the modes (see step 2).

[c] This is the highest psSAR measured for the mid-band channel with slide closed. Hence, the other two channels in this frequency band also require SAR measurement (see step 2).

[d] This is the highest psSAR measured for the mid-band channel with slide open. Hence, the other two channels in this frequency band also require SAR measurement (see step 2).

IECNORM.COM : Click to view the full PDF of IEC/IEEE 62209-1528:2020

Table N.4 – SAR results tables for example test results in GSM 1900 band

Mode & Band	Device configuration	Device position		SAR, averaged over 10 g [W/kg][a]		
				Ch 512[b] 1 850,2 MHz	Ch 661[b] 1 880,0 MHz	Ch 810[b] 1 909,8 MHz
GSM 1900	closed	Left	Cheek	-	0,240	-
			Tilt	-	0,233	-
		Right	Cheek	0,246	0,353[c]	0,387
			Tilt	-	0,221	-
	open	Left	Cheek	-	0,158	-
			Tilt	-	0,178	-
		Right	Cheek	-	0,169	-
			Tilt	0,188	0,195[d]	0,301

[a] The applicable regulatory SAR limit is 2,0 W/kg averaged over a 10 g tissue volume.

[b] According to 7.2.8, the number of channels to be tested is N_c = 3 for all of the modes (see step 2).

[c] This is the highest psSAR measured for the mid-band channel with slide closed. Hence, the other two channels in this frequency band also require SAR measurement (see step 2).

[d] This is the highest psSAR measured for the mid-band channel with slide open. Hence, the other two channels in this frequency band also require SAR measurement (see step 2).

IECNORM.COM : Click to view the full PDF of IEC/IEEE 62209-1528:2020

Annex O
(normative)

Uncertainty analysis for measurement system manufacturers and calibration laboratories

O.1 Probe linearity and detection limits

Because the non-linear response of the probe does not depend on the surrounding media but only on the sensor diodes, evaluation of the linearizing functions $f_i(V_i)$ for a CW signal may be done either in free space or in the tissue-equivalent medium (for modulated signals, use the procedure specified in Clause R.3). This is performed by a power sweep covering the specified psSAR detection range, or a range at least from 0,12 W/kg to 100 W/kg in steps of 3 dB or less. Small TEM cells or waveguides as field generators are preferable, because high field strengths can be produced with medium power amplifiers. The linearity uncertainty is specified as the maximum deviation in the SAR versus power characteristics from the best-fit straight reference line going through zero ($SAR = a \cdot P$, where a is the best-fit slope of the line, using the method of least-squares) specified over the interval 0,12 W/kg to 100 W/kg. The linearity uncertainty for CW signal is determined in Formula (O.1):

$$SAR_{\text{CW linearity uncertainty}}\,[\%] = \max_{j\in\{x,y,z\}}\left[\max_{SAR(P_i)_{\text{CW},j}=0{,}12\text{W/kg}}^{SAR(P_i)_{\text{CW},j}=100\text{W/kg}}\left(100\times\left|\frac{SAR(P_i)_{\text{CW},j}}{P_i\cdot a}-1\right|\right)\right] \tag{O.1}$$

Here, $SAR(P_i)_{\text{CW},j}$ is the SAR measured for a CW signal at the i-th power level, P_i. The index j refers to the field sensor for each of which the procedure shall be repeated. A rectangular probability distribution is assumed for the probe linearity uncertainty.

At SAR levels as high as 100 W/kg, the tissue-equivalent medium temperature can rise significantly, causing deviations in the dielectric properties. To avoid this problem, care should be taken to ensure that the tissue-equivalent medium is exposed to high SAR levels only for short periods of time.

The probe detection limit uncertainty is determined as in Formula (O.2) by comparing the measured psSAR (SAR_{meas}) at a reference power level P_{ref} to the calculated SAR, $SAR_{\text{ref}} = a \cdot P_{\text{ref}}$, using the best-fit slope as in the preceding paragraph.

$$U_{\text{detection limit}}\,[\%] = 100\times\left|\frac{SAR_{\text{meas}}}{SAR_{\text{ref}}}\right| = 100\times\left|\frac{SAR_{\text{meas}}}{a\cdot P_{\text{ref}}}\right| \tag{O.2}$$

The reference power level P_{ref} shall be chosen such that the signal to noise ratio (determined at the measurement time) is 6 dB. This shall be verified using the data from the power sweep. A rectangular probability distribution shall be assumed for detection limit uncertainty in Table 9.

The uncertainty posed by the non-linear response can be rather high and depends on the various probe components, i.e. it shall be determined for each probe individually. A rectangular probability distribution has been assumed for probe linearity uncertainty in Table 9.

IECNORM.COM : Click to view the full PDF of IEC/IEEE 62209-1528:2020

O.2 Broadband signal uncertainty

Electric field-strength probes used for SAR measurements are electrically small dipoles that do not have a constant frequency response (Annex E). In addition, the probes are immersed in a tissue-equivalent medium with frequency dependent dielectric properties. This frequency dependence can be neglected when measuring narrowband signals. If the signal bandwidth exceeds 100 MHz, an additional uncertainty term shall be included in the uncertainty budget.

As a first approximation, the frequency dependence of the probe sensitivity S_f can be assumed to be linear with frequency f. The uncertainty can be estimated using Formula (O.3):

$$SAR_{\text{uncertainty}}[\%] = k_{\text{w}} \times \frac{S_{f+1} - S_{f-1}}{S_f} \times \frac{BW}{f_{+1} - f_{-1}} \quad \text{(O.3)}$$

where

BW is the bandwidth of the signal being measured (in hertz);

f_{+1} is the closest calibrated frequency that is above the centre frequency of the signal being measured (in hertz);

f_{-1} is the closest calibrated frequency that is below the centre frequency of the signal being measured (in hertz);

$f_{+1} - f_{-1} > BW$;

S_{f+1} is the sensitivity of the sensor at frequency f_{+1};

S_{f-1} is the sensitivity of the sensor at frequency f_{-1};

S_f is the sensitivity of the sensor at the centre frequency of the signal being measured;

k_{w} is a weighting factor of the spectral non-symmetry of the signal time average envelope with respect to the centre frequency. A conservative value shall be applied that is determined by measurements.

This uncertainty is assumed to have a rectangular distribution.

O.3 Boundary effect

The probe boundary effect introduces measurement uncertainty. For the purposes of this document, this uncertainty is negligible if the closest distance between the probe tip and the phantom inner surface is always larger than the probe-tip diameter.

In some cases, measurements at distances closer than the probe tip diameter can be required in order to reduce interpolation and extrapolation uncertainties. Then the boundary effect uncertainty of Clause E.6 shall be assessed preferably by using the waveguide system specified in E.3.2.3.4. Alternatively, the temperature method specified in E.3.2.3.2 may be used below 800 MHz. The following method is applicable assuming that the angle between the probe axis and the surface normal line is within the requirements of Table 3 and Table 4. Because the boundary effect is a characteristic of a specific probe, it shall be determined during probe calibration (i.e. influence of the probe tip diameter). If algorithms are applied to compensate for the boundary effect, then the SAR uncertainty shall be determined with the same evaluation hardware and software that is used for SAR measurements. The boundary effect uncertainty can be estimated according to Formula (O.4) and Formula (O.5), as based on linear and exponential extrapolations between the surface and $d_{\text{be}} + d_{\text{step}}$ along lines that are approximately normal to the surface.

$$SAR_{\text{uncertainty}}[\%] = \Delta SAR_{\text{be}}[\%] \frac{\left(d_{\text{be}} + d_{\text{step}}\right)^2}{2d_{\text{step}}} \frac{\left(\mathrm{e}^{-d_{\text{be}}/(\delta/2)}\right)}{\delta/2}; \quad \left(d_{\text{be}} + d_{\text{step}}\right) < 10\,\text{mm}, \quad f \le 3\,\text{GHz} \quad \text{(O.4)}$$

IECNORM.COM : Click to view the full PDF of IEC/IEEE 62209-1528:2020

$$SAR_{\text{uncertainty}}[\%] = \Delta SAR_{\text{be}}[\%]\frac{\delta}{\delta - d_{\text{be}}};\quad d_{\text{be}} < \delta,\quad f > 3\,\text{GHz} \tag{O.5}$$

where

$SAR_{\text{uncertainty}}$ is the uncertainty, as a percentage, of the probe boundary effect;

d_{be} is the distance between the surface and the closest measurement point;

d_{step} is the separation distance between the first and second measurement points that are closest to the phantom surface, assuming that the boundary effect at the second location is negligible;

δ is the penetration depth of the tissue-equivalent medium;

ΔSAR_{be} is the deviation of the measured SAR value, as a percentage, at the distance d_{be} from the boundary, from the analytical reference SAR value for waveguide systems SAR_{ref}; SAR_{ref} is calculated using Formula (E.5) (see E.3.2.3.4).

If waveguide systems are not available for certain frequency ranges, temperature probes shall be used to assess the reference values SAR_{ref} at the locations d_{be} and (d_{be} + d_{step}), and the SAR uncertainty of the temperature probe shall be accounted for. If temperature methods are used, then SAR_{ref} is the value at this location determined using the temperature probe. Note that the actual calibration shall be performed at distances between the probe tip and boundary that are larger than the probe tip diameter, where the boundary effect is negligibly small. Enter the uncertainty of the probe boundary effect in the appropriate row and column in Table 9 using rectangular distribution.

O.4 Field-probe readout electronics uncertainty

All uncertainties related to the probe readout electronics, including the gain and linearity of the instrumentation amplifier, its loading effect on the probe, and accuracy of the signal conversion algorithm, shall be evaluated to estimate the maximum SAR uncertainty. One method to determine these uncertainty components is by replacing the probe with an equivalent source having the same source impedance as the probe under consideration, according to the manufacturer's specifications for the probe. This evaluation is generally performed by the system manufacturer. Each uncertainty shall be converted to a standard uncertainty using normal probability distribution. The RSS value of these uncertainties shall then be used to determine the overall readout electronics uncertainty.

O.5 Signal step-response time uncertainty

Field-probe signal step-response time uncertainty is evaluated by exposing the probe to an E-field step response producing at least 100 W/kg near the phantom surface. The signal response time is evaluated as the time required by the probe and its readout electronics to reach 90 % of the expected final value produced by the step response by switching the RF power on and off. During the SAR measurement, the probe shall remain stationary at each measurement location for at least twice the assessed response time, so that the probe signal response time uncertainty is negligible. Under these measurement conditions, a tolerance value of zero may be entered in Table 9 Otherwise, the SAR uncertainty due to signal response-time uncertainty shall be assessed, using the signal characteristics of the test device. In this case, the signal step-response time uncertainty is equal to the percentage difference between the SAR measured at the chosen measurement time and the SAR measured at twice the chosen measurement time. A rectangular probability distribution shall be assumed.

IECNORM.COM : Click to view the full PDF of IEC/IEEE 62209-1528:2020

O.6 Probe integration-time uncertainty

O.6.1 General

Probe integration-time uncertainties can arise when test devices do not emit a continuous signal. When the integration time and discrete sampling intervals used in the probe electronics are not synchronized with the pulsed characteristics of the measured signal, the RF energy at each measurement location might not be fully or correctly captured. This uncertainty shall be evaluated according to the signal characteristics of the test device prior to the SAR measurement.

O.6.2 Probe integration-time uncertainty for periodic pulsed signals

For signals with periodic pulse modulation and a pulse period greater than 1 % of the probe integration time, additional SAR uncertainty shall be considered when the probe integration time is not an exact multiple of the longest periodicity. The uncertainty shall be assessed according to the maximum uncertainty expected for unsynchronized probe integration time, with an assumed rectangular probability distribution. For a signal with an envelope $s(t)$, the average signal read by the probe during the integration time t_{int} starting at time t_0 is given by $s_{\text{int}}(t_0,t_{\text{int}})$ in Formula (O.6):

$$s_{\text{int}}(t_0,t_{\text{int}}) = \frac{1}{t_{\text{int}}} \int_{t_0}^{t_0+t_{\text{int}}} s(t)\,\mathrm{d}t, \qquad 0 \le t_0 \le T \tag{O.6}$$

Formula (O.6) assumes that the filtering by the probe does not significantly alter the signal envelope $s(t)$. If t_0 is not synchronized with the longest period T of $s(t)$, the probe integration-time uncertainty can be specified as shown in Formula (O.7):

$$SAR_{\text{uncertainty}}[\%] = 100 \times \frac{\max\left(s_{\text{int}}(t)\right) - \left\langle s_{\text{int}}(t)\right\rangle}{\left\langle s_{\text{int}}(t)\right\rangle} \tag{O.7}$$

Here $\langle\cdot\rangle$ denotes the average value. Formula (O.6) and Formula (O.7) can be used to derive the probe integration-time uncertainty of any pulsed signal.

A simple alternative formula for the uncertainty of a TDMA system is shown in Formula (O.8):

$$SAR_{\text{uncertainty}}[\%] = 100 \times \sum_{\text{all sub-frames}} \frac{t_{\text{frame}}}{t_{\text{int}}} \frac{slot_{\text{idle}}}{slot_{\text{total}}} \tag{O.8}$$

Formula (O.8) is an approximation that typically overestimates the uncertainty. Here $slot_{\text{idle}}$ is the number of idle slots in a frame, with $slot_{\text{total}}$ being the total number of slots. The frame duration is t_{frame}, with $t_{\text{frame}} < t_{\text{int}}$. The total probe integration-time uncertainty is the sum of the errors for all subframes in the frame structure that have idle slots. For example, the basic frame for GSM systems has a frame duration t_{frame} = 4,6 ms, with 7 idle slots in an 8-slot frame, and the multiframe duration is $t_{\text{multiframe}}$ = 120 ms, i.e. 1 idle slot in a 26-slot frame. For a probe integration time of 0,2 s, the uncertainty is estimated to be 0,020 1 + 0,023 1 = 0,043 2, or 4,32 % for GSM using Formula (O.8), compared with 3,84 % using Formula (O.6) and Formula (O.7). GPRS is the same as GSM, except that the number of idle slots can be 6, 5, …, 1, where 7 idle slots is the worst case.

A rectangular probability distribution shall be assumed for probe integration-time uncertainty. For continuous or CW-equivalent signals, an uncertainty value of zero shall be entered.

IECNORM.COM : Click to view the full PDF of IEC/IEEE 62209-1528:2020

O.6.3 Probe integration-time uncertainty for non-periodic signals

For other than periodic pulsed signals, the probe integration time should be determined from SAR measurements using a stable source with the same signal characteristics and the same probe type that is used for DUT measurements. Measurements at a single point (where the SAR is at least 1 W/kg) shall be made consecutively using the chosen integration time and successively larger integration times. The integration time shall be doubled for each consecutive measurement, until the last and next to last measurement results are within 0,5 % of each other. Each measurement at a given integration time shall be repeated several times to verify that the measurement result is stable, and the average SAR of the repeated measurements shall be used for that integration time. For the probe integration time, a rectangular probability distribution shall be assumed. The uncertainty is the percentage difference between the average SAR at the selected integration time and the average SAR at the longest integration time.

O.7 Contribution of mechanical constraints

O.7.1 Mechanical tolerances of the probe positioner (directions parallel to phantom surface)

The mechanical tolerances of the field probe positioner can introduce deviations in the accuracy and repeatability of probe positioning, which add to the uncertainty of the measured SAR. The uncertainty may be estimated from the specifications of the probe positioner relative to the position required by the actual measurement location determined by the geometrical centre of the field probe sensors, and is expressed as maximum deviation d_{ss}. By assuming a rectangular probability distribution, the psSAR uncertainty contributions due to mechanical tolerances of the probe positioner may be calculated using d_{ss}, according to a first-order error approximation as described in Formula (O.9):

$$SAR_{\text{uncertainty}}\left[\%\right] = \frac{d_{ss}}{\delta/2} \times 100 \qquad \text{(O.9)}$$

where

$SAR_{\text{uncertainty}}$ is the uncertainty as a percentage;

d_{ss} is the maximum position uncertainty between the calculated position at the centre of the probe sensors and the actual position with respect to a reference point specified by the system manufacturer;

δ is the penetration depth of the tissue-equivalent medium specified in this document.

If the system manufacturer does not specify the mechanical tolerances of the probe positioner, this shall be evaluated to determine the contribution to SAR measurement uncertainty. This can be done by evaluating the relative accuracy of probe movements within the area-scan region. The largest distance difference between the target and actual positions shall be used to assess the SAR uncertainty. The SAR uncertainty shall be entered in Table 9 assuming rectangular distribution.

O.7.2 Probe positioning with respect to phantom shell surface

The uncertainty of the probe positioner relative to the phantom shell shall be estimated as the maximum deviation of the distance between the probe tip and the phantom surface d_{ph}. By assuming a rectangular probability distribution, the psSAR uncertainty contribution is calculated using Formula (O.10):

$$SAR_{\text{uncertainty}}\left[\%\right] = \frac{d_{ph}}{\delta/2} \times 100 \qquad \text{(O.10)}$$

IECNORM.COM : Click to view the full PDF of IEC/IEEE 62209-1528:2020

where

$SAR_{\text{uncertainty}}$ is the uncertainty as a percentage;

d_{ph} is the maximum deviation of the distance between probe tip and phantom shell, i.e. the uncertainty of determining the probe tip location;

δ is the penetration depth of the head tissue-equivalent medium specified in this document.

O.7.3 First-order approximation of exponential decay

Formula (O.9) and Formula (O.10) are first-order error approximations of the SAR error corresponding to a positioning error Δz at location z. They are derived according to Formula (O.11):

$$\frac{\Delta SAR}{SAR} = \frac{SAR_0 \mathrm{e}^{-2\alpha(z+\Delta z)} - SAR_0 \mathrm{e}^{-2\alpha z}}{SAR_0 \mathrm{e}^{-2\alpha z}} = \left(\mathrm{e}^{-2\alpha z} - 1\right)$$
$$= 1 - 2\alpha\,\Delta z + \frac{1}{2}(2\alpha\,\Delta z)^2 + \ldots + (-1) \approx -2\alpha\,\Delta z \qquad \text{(O.11)}$$

Here α is the reciprocal of the field penetration depth δ, and SAR_0 is the SAR value at the surface of the phantom (z = 0). $\Delta SAR/SAR$ is an estimate of the SAR sensitivity for the exponential decay.

O.8 Contribution of post-processing

O.8.1 General

The estimation of the uncertainty resulting from the post-processing of the discrete measured data to determine the 1 g and 10 g psSAR is described, i.e. the combined uncertainty of interpolation, extrapolation, averaging, and maximum-finding algorithms. These algorithms can add uncertainty due to assumptions on the general field behaviour and therefore might not perfectly predict the SAR distribution in the tissue-equivalent medium for a specific DUT. The algorithm uncertainty is a function of the resolution chosen for the measurement, and the post-processing methods used in the area scans and zoom scan.

The actual SAR distribution at the peak location is strongly dependent on the operating frequency and design of the DUT, test position, and proximity to the tissue-equivalent medium. SAR distributions can have a rather flat gradient when a low frequency source is a large distance away, or can have a very steep gradient when a small high frequency source (such as a helix antenna) is placed next to the tissue. In some cases, the maximum SAR is offset into the medium rather than at the surface of the phantom, due to cancellation of magnetic fields at the surface [64].

The analytical SAR distribution functions presented in O.8.2 are intended to simulate the preceding conditions, and were developed for the purpose of this uncertainty estimation. These empirically derived reference functions are used to create artificial or “dummy” SAR data sets, for testing the system software post-processing subroutines. Computed reference function values at coarse and fine grid spacing, the same as those used in measurements, are input to the SAR system software. SAR values at grid points corresponding to the area-scan and zoom-scan measurement grids are computed according to the three SAR distribution functions given in O.8.2, then processed by the system interpolation, extrapolation, and integration algorithms as if they were actually measured. The resulting 1 g and 10 g psSAR values are compared with reference SAR values listed in O.8.2. Procedures for evaluating the SAR uncertainty of the area-scan and zoom-scan post-processing algorithms are specified in O.8.3. The test functions assume a planar tissue-equivalent medium and phantom interface. The applicability of these functions for curved interfaces is discussed in O.8.3.3. This uncertainty concept assumes that there are no errors in location of the grid points calculated

IECNORM.COM : Click to view the full PDF of IEC/IEEE 62209-1528:2020

with the analytical distribution functions, and probe positioning and measurement uncertainties are not included.

O.8.2 Evaluation test functions

Three analytical functions, f_1, f_2, and f_3, are used to represent the possible range of SAR distributions expected for DUTs tested according to the procedures of this document. The distribution f_1 in Formula (O.12) is based on the evaluation of SAR footprints of actual wireless communication devices, and is applicable for frequencies up to 2 GHz. Because f_1 takes into account devices placed in close proximity to SAM phantom at frequencies above 900 MHz, f_1 is also used to model very steep SAR gradients. Two parameter sets are given for f_1, such that SAR distributions with single and double maxima can be evaluated.

The function f_2 in Formula (O.13) is used at frequencies up to 3 GHz to account for exposure conditions with H-field cancellation at the phantom-tissue surface.

The third reference function f_3 in Formula (O.14) is specified for testing in the frequency range 3 GHz to 10 GHz. It is also valid for capacitively-coupled sources. Because noise can affect the extrapolation at these frequencies, a noise term is included. The distribution functions are specified for the phantom surface at z = 0, and the half-space tissue-equivalent medium for all z > 0 in Formula (O.12):

$$f_1(x,y,z) = A_1 \exp\left[-\frac{(x'+x_d/2)^2}{2\sigma_{x,\text{peak}}^2}\right]\exp\left(-\frac{(y')^2}{2\sigma_{y,\text{peak}}^2}\right)\mathrm{e}^{-\frac{z}{a}} + A_2 \exp\left[-\frac{(x'-x_d/2)^2}{2\sigma_{x,\text{sec}}^2}\right]\exp\left(-\frac{(y')^2}{2\sigma_{y,\text{sec}}^2}\right)\mathrm{e}^{-\frac{z}{a}} \quad \text{(O.12)}$$

$$f_2(x,y,z) = A\mathrm{e}^{-\frac{z}{a}}\frac{a^2}{a^2+(x')^2}\left(3-\mathrm{e}^{-\frac{2z}{a}}\right)\cos^2\left(\frac{\pi}{2}\frac{y'}{3a}\right) \quad \text{(O.13)}$$

$$f_3(x,y,z) = A\exp\left[-\frac{\left((x')^2+(y')^2/2\right)}{(a/4)^2}\right]\mathrm{e}^{-\frac{8z}{a}} + N_{\text{rms}}\,\text{rnd}(\zeta) \quad \text{(O.14)}$$

Note that due to the noise term in the function f_3, it should be evaluated at least 4 000 times, to verify that the standard deviation converges to the correct value. x, y, and z are the spatial Cartesian coordinates of the SAR distribution. The SAR averaging cube shall be assumed to be directly against the surface of a planar phantom. The z-axis is normal to the phantom surface, and the axes of the averaging cube are aligned with the axes of the coordinate system.

In Formula (O.12), the parameters $\sigma_{x,\text{peak}}$, $\sigma_{y,\text{peak}}$, $\sigma_{x,\text{sec}}$, and $\sigma_{y,\text{sec}}$ are set as described in Formula (O.15) through Formula (O.18):

$$\sigma_{x,\text{peak}} = \begin{cases} \sigma_{x,\text{pp}}, & x' \geq -x_d/2 \\ \sigma_{x,\text{pn}}, & x' < -x_d/2 \end{cases} \quad \text{(O.15)}$$

$$\sigma_{y,\text{peak}} = \begin{cases} \sigma_{y,\text{pp}}, & y' \geq 0 \\ \sigma_{y,\text{pn}}, & y' < 0 \end{cases} \quad \text{(O.16)}$$

IECNORM.COM : Click to view the full PDF of IEC/IEEE 62209-1528:2020

$$\sigma_{x,\text{sec}} = \begin{cases} \sigma_{x,\text{sp}}, & x' \geq x_d / 2 \\ \sigma_{x,\text{sn}}, & x' < x_d / 2 \end{cases} \quad \text{(O.17)}$$

$$\sigma_{y,\text{sec}} = \begin{cases} \sigma_{y,\text{sp}}, & y' \geq 0 \\ \sigma_{y,\text{sn}}, & y' < 0 \end{cases} \quad \text{(O.18)}$$

These parameters have been selected based on the evaluations of different DUTs at 1 950 MHz, and are given in Table O.1. The decay parameter a was derived by fitting experimental zoom scan data at 1 950 MHz with an exponential decay curve, and by averaging the results of different DUTs.

Table O.1 – Parameters for the reference function f_1 in Formula (O.12)

No. of peaks	A_1 [W/kg]	A_2 [W/kg]	a [mm]	x_d [mm]	$\sigma_{x,\text{pp}}$ [mm]	$\sigma_{y,\text{pp}}$ [mm]	$\sigma_{x,\text{sp}}$ [mm]	$\sigma_{y,\text{sp}}$ [mm]	$\sigma_{x,\text{pn}}$ [mm]	$\sigma_{y,\text{pn}}$ [mm]	$\sigma_{x,\text{sn}}$ [mm]	$\sigma_{y,\text{sn}}$ [mm]
1	1,2	0,0	11,9	n.a.	19,6	15,5	n.a.	n.a.	21,9	17,2	n.a.	n.a.
2	1,2	1,0	11,9	60,47	22,6	19,7	19,4	19,6	22,0	15,5	17,9	24,2
n.a. = not applicable												

In Formula (O.12), Formula (O.13), and Formula (O.14), the parameters are set as follows:

$$x' = x + d, \quad y' = y + d$$

Where d is the offset parameter, a is 20 mm, and A is1 W/kg.

The preceding parameters a and A are used for the generation of the appropriate SAR distributions. A value of d = 2,5 mm, for example, provides a lateral shift of the SAR distribution, so that the peak location is not aligned with a measurement grid having a 5 mm increment. This offset is used to test the software peak search subroutines and uncertainty.

N_{rms} represents the variance of the system noise in SAR (in W/kg) in the tissue-equivalent medium for A = 5. This parameter is system dependent, and corresponds to random SAR values measured in the absence of an RF signal [rnd(ζ)]. Suitable functions are available in typical math applications. The variable ζ is an arbitrary seed.

The reference SAR values from the distribution functions f_1, f_2, and f_3 for 1 g and 10 g averaging cubes aligned with the (x, y, z) coordinate axes are given in Table O.2. These SAR values were calculated with an accuracy of 0,01 %.

When function f_1 is considered, the maximum deviation from reference values obtained considering the single-peak and two-peaks cases shall be used for post-processing uncertainty computations.

These reference values are applied in O.8.3 for testing the post-processing algorithms used by the area scans and zoom scans.

IECNORM.COM : Click to view the full PDF of IEC/IEEE 62209-1528:2020

Table O.2 – Reference SAR values from the distribution functions f_1, f_2, and f_3

Function (condition)	SAR 1 g, W/kg	SAR 10 g, W/kg
f_1 (single peak)	0,791	0,494
f_1 (two peak, cube centred on primary peak)	0,796	0,503
f_1 (two peak, cube centred on secondary peak)	0,686	0,438
f_2	1,796	1,375
f_3	0,015 7	0,026 8

O.8.3 Data-processing algorithm uncertainty evaluations

O.8.3.1 Evaluation of the coarse area scan

The area-scan interpolation algorithms shall be capable of locating psSAR coordinates with an accuracy of $\pm L_z/2$ mm or better, where L_z is the side length of the zoom-scan volume. If this precondition is satisfied, which is tested with the procedures of O.8.3.1, the evaluation of the area scan does not contribute to the uncertainty budget.

The reference function values calculated at the usual area-scan grid points are input to the system software. The interpolation algorithm treats these data points as if they were measured to complete the area scan and determine the psSAR location (x_{eval}, y_{eval}). This is compared with the actual peak location determined by the analytical functions at (x_{ref}, y_{ref}), with an offset parameter d, as specified in O.8.2 for x' and y' for Formula (O.12), Formula (O.13), and Formula (O.14). The subscripts "eval" and "ref" refer to evaluated and reference, respectively. In other words, Formula (O.19) shall be satisfied:

$$|x_{ref} - x_{eval}| \le L_z / 2, \quad |y_{ref} - y_{eval}| \le L_z / 2 \tag{O.19}$$

The following procedure shall be used to assess the uncertainty of the interpolation algorithms used in the area scan for determining the peak SAR location.

a) Choose the measurement resolution $(\Delta x, \Delta y)$, and number of evaluation (corresponding to measurement) points (N_x, N_y). The centre of the area scan shall be set to $(x_0, y_0) = (0, 0)$.

b) SAR values are computed using the functions f_1, f_2, and f_3 at the evaluation grid points of the area scan within the ranges of Formula (O.20) and Formula (O.21):

$$x_0 - \Delta x \times \left[(N_x - 1)/2 \right] \le x \le x_0 + \Delta x \times \left[(N_x - 1)/2 \right], \tag{O.20}$$

$$y_0 - \Delta y \times \left[(N_y - 1)/2 \right] \le y \le y_0 + \Delta y \times \left[(N_y - 1)/2 \right], \tag{O.21}$$

where N_x and N_y are odd integers. A value of $z = 0$ is assumed, because the peak location is independent of z for these three functions.

The SAR values computed by the three distribution functions are interpolated by the SAR measurement system with a spatial resolution of $(\Delta x_i, \Delta y_i)$, according to the interpolation functions $g_i(x)$ and $g_i(y)$ used by the system to determine the psSAR location (x_{eval}, y_{eval}). If the measurement system does not allow SAR values to be imported to perform the assessment, the same algorithm shall be implemented independently by other means, to determine the interpolation and peak-search uncertainties.

IECNORM.COM : Click to view the full PDF of IEC/IEEE 62209-1528:2020

The psSAR location determined by the interpolation algorithms shall satisfy the requirements of the inequalities in Formula (O.19). Otherwise, the data-processing and measurement systems shall use a finer grid resolution and/or a larger number of interpolation points to repeat the assessment starting at step b).

The centre of the area scan (x_0, y_0) shall be shifted in 1 mm steps within the range $0 < x_0 \leq \Delta x/2$ and $0 < y_0 \leq \Delta y/2$ to repeat the assessment starting at step b) for each of the shifted (x_0, y_0) in these ranges.

O.8.3.2 Evaluation of the zoom scan

The zoom scan is evaluated by comparing the highest 1 g or 10 g SAR values with the reference SAR values in O.8.2. From the area scan procedure in O.8.3.1, the true peak location (x_{ref}, y_{ref}) will be displaced from the estimated peak location (x_{eval}, y_{eval}) by an amount given by inequalities in Formula (O.19). This displacement is accounted for in the reference functions f_1, f_2, and f_3 in O.8.2 by incorporating the distance d. Because this displacement will vary in practice, the value of d shall be varied over the range of Formula (O.22):

$$|d| \leq (L_z - L_c)/2 \tag{O.22}$$

where L_c is the averaging cube side length (10 mm for 1 g, 21,5 mm for 10 g). For each distance d, the largest uncertainty produced by any of the three functions is recorded. The RMS of the largest uncertainty values for several distances d is entered as the uncertainty due to extrapolation, interpolation, and integration.

Although the requirement for the area scan is that the local psSAR be located within $|d| \leq L_z/2$, a smaller range of $|d| \leq (L_z - L_c)/2$ is used here to ensure that the 1 g or 10 g cube can be computed on the first attempt. For values of $(L_z - L_c)/2$ and $|d| \leq L_z/2$, the measurement software shall alert that the 1 g or 10 g cube is not captured and the measurement shall be re-attempted. This will not affect the uncertainty, so it is not necessary to consider this case here.

a) Choose a displacement d for the evaluation of the functions f_1, f_2, and f_3. d shall vary from $-(L_z - L_c)/2$ to $+(L_z - L_c)/2$ in small increments (e.g. 1 mm steps). The displacement shall also vary separately in the x- and y-directions.

b) SAR values are computed according to the functions f_1, f_2, and f_3 at the evaluation grid points that correspond to measured zoom-scan volume points. The zoom-scan volume shall be centred at the point in Formula (O.23):

$$(x, y, z) = (0, 0, (L_h/2 + d_{be})) \tag{O.23}$$

where

L_h is the height of the zoom-scan volume, and

d_{be} is the distance of the closest measurement point from the inner surface of the phantom.

c) The computed SAR values are extrapolated to the phantom surface at $z = 0$ by the system software, to obtain the additional points in the zoom-scan volume that cannot be measured due to probe constraints. Both the computed and extrapolated data points are then interpolated to a finer resolution by the system software, which subsequently applies the integration algorithms as well as the search algorithm for finding the psSAR within the zoom-scan volume, to determine the highest 1 g or 10 g psSAR. Alternatively, other procedures are possible. If the system does not allow SAR values to be imported to perform the assessment, the same algorithm shall be implemented independently by other means to test the extrapolation, interpolation, and integration algorithms.

IECNORM.COM : Click to view the full PDF of IEC/IEEE 62209-1528:2020

d) The 1 g and 10 g psSAR values determined by the system or data processing software (SAR_{eval}) are compared to the reference SAR values given in O.8.2. The standard deviation caused by the random noise (SAR_{stdev} (N_{rms})) is determined by evaluating f_3 at least 4 000 times, and with each of the 4 000 or more evaluations using different random noise parameters. The SAR uncertainty for distribution functions f_1 and f_2 is calculated using Formula (O.24):

$$SAR_{uncertainty}[\%] = 100 \times \left| \frac{SAR_{eval} - SAR_{ref}}{SAR_{ref}} \right| \quad \text{(O.24)}$$

The SAR uncertainty for distribution function f_3 is calculated using Formula (O.25):

$$SAR_{uncertainty}[\%] = 100 \times \left| \frac{SAR_{eval} - SAR_{ref}}{SAR_{ref}} \right| + 100\sqrt{3} \times \left| \frac{SAR_{stdev}(N_{rms})}{SAR_{ref}} \right| \quad \text{(O.25)}$$

e) The highest SAR uncertainty estimated by the three distribution functions is recorded.

f) Repeat steps b) to e) for other displacement values d.

g) Compute the RMS value of the uncertainties calculated in step d) for each displacement d above. This value shall be entered as the uncertainty due to extrapolation, interpolation, and integration in the corresponding row and column of Table 9, and a rectangular probability distribution shall be used.

h) Record the following parameters used to estimate the zoom-scan uncertainty:

1) the dimension of the grid used to sample the reference functions, both in terms of number of points and sample steps in the three dimensions;

2) the number of interpolation points included between two test points, or the interpolation resolution in the three directions, for the reference functions;

3) the dimension of the extrapolation region, i.e. the distance between the probe sensor location at the first measurement point and the phantom surface (also considering that measurement point is behind the probe tip);

4) the interpolation, extrapolation, and averaging algorithms used.

The computational conditions (such as the number of grid points, the grid increments, and the number of interpolation points in the three directions) shall be the same for all the functions.

O.8.3.3 SAR evaluation with curved surfaces

The procedures in O.8.3.1 and O.8.3.2 assume that the tissue-equivalent medium and phantom boundary is planar. However, the uncertainty estimated with these functions for flat tissue-equivalent medium and phantom boundaries is also valid for smoothly-varying curved surfaces, provided that the four side faces are parallel to the line normal to the phantom at the centre of the cube face next to the phantom surface. The fact that the function is based on a flat surface does not impose any restrictions with respect to applicability for the test, provided the procedure is based on equivalent distances of the grid from surfaces. This produces averaging volumes such as illustrated in Figure O.1. Figure O.1 illustrates an acceptable method for shaping the cube during SAR post-processing. The front face of the volume facing the phantom/medium interface conforms to the curved boundary, to ensure that all SAR peaks are captured. The back face shall be equally distorted to maintain the correct averaging mass.

IECNORM.COM : Click to view the full PDF of IEC/IEEE 62209-1528:2020

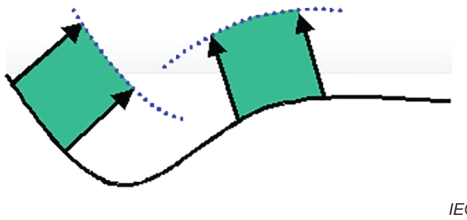


Figure O.1 – Orientation and surface of averaging volume relative to phantom surface

O.9 Tissue-equivalent medium properties uncertainty

O.9.1 General

Details of dielectric properties test methods are given in Annex H, and uncertainty estimation methods are given in O.9.5.

In accordance with usual metrological practices, the measurement uncertainty for each of the dielectric properties is required to be less than or equal to the allowable variations (see 7.2.1) from the target values of the measured dielectric properties.

O.9.2 Medium density

A tissue-equivalent medium density of 1 000 kg/m^3 shall be applied for the SAR calculation and averaging, regardless of the actual density of the medium used. This ensures that the SAR and the volumes of the 1 g and 10 g averaging masses are independent of the chosen recipe, where only the permittivity and conductivity are relevant. Therefore, no uncertainty is associated with the density.

O.9.3 Medium conductivity uncertainty

The uncertainty due to the medium conductivity arises from two different sources. The first source of uncertainty is the allowable tolerance from the target value of Table 2 (see 6.2.2), and the second source of uncertainty arises from the measurement procedures used to assess conductivity. The uncertainty shall be estimated using a normal probability. See 7.2.1 for applicable tolerances, and 7.8 for corrections of the measured SAR for the deviations in conductivity.

O.9.4 Medium permittivity uncertainty

The uncertainty due to the medium relative permittivity arises from two different sources. The first source of uncertainty is the deviation from the target value of Table 2 (see 6.2.2), and the second source of uncertainty arises from the measurement procedures used to assess relative permittivity. The uncertainty shall be estimated using a normal probability. See 7.2.1 for applicable tolerances, and 7.8 for corrections of the measured SAR for the deviations in permittivity.

O.9.5 Assessment of dielectric properties measurement uncertainties

The measurement procedures specified in Annex H use vector network analysers for dielectric properties measurements. Network analysers require calibration in order to account for and remove inherent losses and reflections. The uncertainty budget for dielectric properties measurements derives from inaccuracies in the calibration data, analyser drift, and random errors. Other sources of errors are the uncertainties of the sample holder hardware, deviations from the optimal dimensions for the specified frequencies, and sample properties. This applies regardless of the type of sample holder and the nature of the scattering parameters being measured. Uncertainties due to the straight-line fit in the slotted-line method can be evaluated using a least-squares analysis [125].

IECNORM.COM : Click to view the full PDF of IEC/IEEE 62209-1528:2020

An example uncertainty template is shown in Table O.3. All uncertainty parameters might or might not apply to a specific test set-up or procedure, and other components not listed might be relevant in some test set-ups. Measurement of well-characterized reference liquids can be used to estimate the uncertainty of the measurement of the dielectric properties [126], [127], [128], [129], using the following procedure.

a) Configure and calibrate the network analyser in a frequency span large enough around the centre frequency of interest, of the tissue-equivalent medium used in the SAR measurement.

b) Measure a reference material.

c) Repeat steps a) and b) at least n times (where n is at least three and is sufficient such that the measurements have stabilized. n should be large enough to keep the repeatability in step d) within the applicable tolerances as specified in 7.2.1 at all frequencies of interest. Make the measurements at the same medium temperature at which the target dielectric properties of the reference liquids are known. At each frequency, perform steps d) to g).

d) Calculate the repeatability as the sample standard deviation divided by the mean value. For the permittivity, this is given by Formula (O.26):

$$repeatability[\%] = 100 \times \frac{1}{\overline{\varepsilon'_{\mathrm{r}}}} \sqrt{\frac{1}{n-1} \sum_{i=1}^{n} \left(\varepsilon'_{\mathrm{r},i} - \overline{\varepsilon'_{\mathrm{r}}} \right)^2} \tag{O.26}$$

where the mean value is specified in Formula (O.27):

$$\overline{\varepsilon'_{\mathrm{r}}} = \frac{1}{n} \sum_{i=1}^{n} \varepsilon'_{\mathrm{r},i} \tag{O.27}$$

Do the same for the conductivity.

e) Enter the repeatability in Table O.3, and the number of degrees of freedom $v_i = n - 1$. Determine the deviation of the dielectric properties from the target values $\varepsilon_{\mathrm{r,ref}}$ and σ_{ref}. For the permittivity, this is given by Formula (O.28):

$$deviation[\%] = 100 \times \left| \frac{\overline{\varepsilon'_{\mathrm{r}}} - \varepsilon'_{\mathrm{r,ref}}}{\varepsilon'_{\mathrm{r,ref}}} \right| \tag{O.28}$$

f) Enter the deviation in Table O.3, and the number of degrees of freedom $v_i = n - 1$. Do the same for the conductivity.

g) Estimate the Type B uncertainties for the other components of Table O.3 (and other relevant components if needed) in the frequency range under consideration.

h) Determine the combined standard uncertainty as the RSS of the uncertainty components from steps d), e), and f). Enter this value in Table O.3.

i) For the relative permittivity, choose the frequency that gives the largest value for the combined standard uncertainty in step g). Enter this uncertainty and the corresponding degrees of freedom v_i into the appropriate row of Table 9. Do the same for the conductivity.

In Table 9, the sensitivity coefficients c_i for the measurement uncertainties of the conductivity and permittivity of tissue-equivalent media are needed. These sensitivity coefficients are c_σ for conductivity and c_ε for permittivity. They are calculated using Formula (9) through Formula (12) (see 7.8.2).

For inductively-coupled sources, the highest sensitivity coefficients over the 30 MHz to 6 000 MHz frequency range were found to be c_σ = 0,79 (at 180 MHz) and c_ε = 0,23 (at 2 000 MHz) for 1 g averaging, and c_σ = 0,77 (at 30 MHz) and c_ε = 0,26 (at 5 500 MHz) for 10 g averaging. For capacitively-coupled sources, the sensitivity coefficients can be different from this, and should be evaluated using an approach similar to that of [28].

IECNORM.COM : Click to view the full PDF of IEC/IEEE 62209-1528:2020

These maximum values are entered into Table 9. Alternatively, maximum values for specific tested frequency ranges may be entered.

Table O.3 – Example uncertainty template and example numerical values for permittivity (ε_r') and conductivity (σ) measurement

Input quantity X_i (source of uncertainty)	Probability distribution PDF_i	Uncertainty $a(x_i)$ ± %	Divisor q_i	$u(x_i) = a(x_i)/q_i$	c_i (1 g, 10 g)	$u(y) = c_i \cdot u(x_i)$ ± %	v_i
Repeatability of ε_r' or σ (N repeats)	N	5,2	1		1	5,2	4
Deviation from reference liquid target ε_r' or σ	R	3,0	√3		1	1,73	4
Network analyser-drift, linearity, etc.	R	0,5	√3		1	0,29	∞
Test-port cable variations	U	0,5	√2		1	0,35	∞
Combined standard uncertainty						5,50	5

O.9.6 Medium temperature uncertainty

The measurements of both SAR and tissue-equivalent medium dielectric properties shall be performed at an ambient temperature between 18 °C and 25 °C, inclusively. These two measured temperatures shall not differ by more than 2 °C. The following evaluation shall be performed for each recipe to determine the uncertainty caused by the temperature tolerance. This evaluation is typically done only once per recipe at the frequencies of interest. This evaluation shall be performed for every new recipe, or whenever modifications are made to a recipe.

Measurements of the dielectric properties at medium temperatures T_{low} = 18 °C and T_{high} = 25 °C shall be used to compute temperature uncertainty, according to Formula (O.29). The conditions that apply here only concern the evaluation of the medium temperature uncertainty, but do not affect the temperature requirements during testing.

$$\varepsilon_{\text{liquid temperature uncertainty}}\,[\%] = 100 \times \left| \frac{2 \times \left[\varepsilon_r(T_{high}) - \varepsilon_r(T_{low}) \right]}{\varepsilon_r(T_{high}) + \varepsilon_r(T_{low})} \times \frac{2\,°C}{T_{high} - T_{low}} \right|$$

$$\sigma_{\text{liquid temperature uncertainty}}\,[\%] = 100 \times \left| \frac{2 \times \left[\sigma(T_{high}) - \sigma(T_{low}) \right]}{\sigma(T_{high}) + \sigma(T_{low})} \times \frac{2\,°C}{T_{high} - T_{low}} \right| \quad \text{(O.29)}$$

where

$\varepsilon_{\text{liquid temperature uncertainty}}$ is the temperature uncertainty for the medium permittivity as a percentage;

$\sigma_{\text{liquid temperature uncertainty}}$ is the temperature uncertainty for the medium conductivity as a percentage;

$\varepsilon_r(T_{high})$ is the relative permittivity at temperature T_{high};

$\varepsilon_r(T_{low})$ is the relative permittivity at temperature T_{low};

$\sigma(T_{high})$ is the conductivity at temperature T_{high};

$\sigma(T_{low})$ is the conductivity at temperature T_{low};

T_{high} is the highest temperature in °C at which the dielectric properties were measured;

IECNORM.COM : Click to view the full PDF of IEC/IEEE 62209-1528:2020

T_{low} is the lowest temperature in °C at which the dielectric properties were measured.

These formulas can be used to derive the temperature uncertainty for the particular tissue-equivalent medium. The uncertainty of the measurements for T_{low} and T_{high} shall be less than 0,1 °C. Note that this tolerance is applicable only for this uncertainty evaluation; this does not affect nor apply for the temperature requirements during DUT testing.

The values of $\varepsilon_{\text{liquid temperature uncertainty}}$ and $\sigma_{\text{liquid temperature uncertainty}}$ are entered into the appropriate rows and column in Table 9. Calculated values for some recipes are provided in Annex F. A rectangular probability distribution is assumed for the temperature uncertainty in Table 9.

IECNORM.COM : Click to view the full PDF of IEC/IEEE 62209-1528:2020

Annex P
(normative)

Post-processing techniques

P.1 Extrapolation and interpolation schemes

P.1.1 General

The local SAR inside the phantom shall be measured using small dipole sensing elements enclosed in a probe cover/case. Probe calibration (involving E-field measurement) may be carried out with respect to the geometric centre of the internal dipoles set, in which case the spatial offset of the dipoles of a few millimetres from the physical tip of the probe shall be taken into account when defining the measurement positions. In order to minimize probe boundary effect uncertainties, the probe tip shall not be in contact with the phantom surface although this usually is where the highest local SAR values usually occur. The assessment of these highest local SAR values is essential to determine the psSAR, and shall therefore be obtained by extrapolation from measurements carried out at a range of distances from the phantom surface. The accurate assessment of the psSAR requires a fine spatial resolution according to Table 4 within a three-dimensional scanned volume. The measured data shall be extrapolated and interpolated to provide a data array with sufficient resolution to accurately calculate the overall psSAR. The measurement uncertainty resulting from these interpolation, extrapolation, and other numerical procedures (integration, averaging, etc.) shall be determined. The location uncertainty of measurement points is determined as a separate uncertainty component.

P.1.2 Extrapolation schemes

Since the actual measurement location of the field probe corresponds to the geometrical centre of the dipole sensors, which is displaced from the tip of the probe, the SAR values between the surface of the phantom and the closest measurable points required for computing the 1 g or 10 g psSAR shall be determined by extrapolation.

Extrapolation can be performed using splines, biharmonic splines, wavelets, polynomials, or rational functions. Various computational mathematics books describe how to implement some of these methods.

P.1.3 Interpolation schemes

The measured and extrapolated SAR values within the zoom-scan volume are interpolated to a 1 mm grid in order to determine the 1 g or 10 g psSAR, for example by using three staggered one-dimensional cubic splines [130].

Interpolation can be performed using various mathematical techniques, such as statistics [131], basis function curve-fits [132], Fourier analysis [133], and wavelet [134], polynomial, or spline curve fits [135]. Various numerical analysis textbooks, e.g. [130], describe how to implement some of these methods.

P.2 Averaging scheme and maximum finding

P.2.1 Volume average schemes

After extrapolation and interpolation, the cubical volumes evaluated to average the local SAR shall extend to the phantom surface, in order to include the highest values of local SAR. The contour of the bottom surface of the averaging volume shall follow the contour of the phantom surface (Figure O.1). The top surface of the averaging volume shall be the same shape as the bottom surface. The other four side surfaces of the averaging volume shall each be parallel to

IECNORM.COM : Click to view the full PDF of IEC/IEEE 62209-1528:2020

the normal of the centre of the bottom surface. This ensures that the extruded volume is close to a cubical shape and conformal to the phantom surface.

P.2.2 Finding the psSAR and estimating the uncertainty

The psSAR is found by moving the averaging volume specified in P.2.1 over the zoom scan volume. At each point (with a resolution of 1 mm or better) the SAR is averaged over the averaging volume. Averaging may use the trapezoidal algorithm or other methods. The psSAR is the highest of these averaged SAR values over all locations.

If the highest 1 g or 10 g cube touches the boundary of a zoom-scan volume, the entire zoom scan shall be repeated with the new centre located at the maximum psSAR location indicated by the preceding zoom scan measurement.

The uncertainty contribution of the averaging scheme and maximum finding is included in the evaluation methods of Clause O.8; the methods of Clause O.8 serve not only as benchmarks for the interpolation and extrapolation schemes, but also for the averaging and maximum-finding schemes.

IECNORM.COM : Click to view the full PDF of IEC/IEEE 62209-1528:2020

© IEC/IEEE 2020

Annex Q
(informative)

Rationale for time-period averaged SAR test procedure

The SAR measurement procedures specified in 7.4 refer to handsets, laptops, tablets, and other devices within the scope of this document that do not have autonomous and real-time capability to calculate and control their transmission power and/or duty factor. Recent devices have evolved significantly in this respect, and the measurement procedures shall take these capabilities into account.

RF exposure guidelines specify basic restrictions in terms of the psSAR integrated over a certain period of time. A six-minute averaging time is specified by the ICNIRP Guidelines [3] and by IEEE Std C95.1-2019 [4]. Until now the SAR measurement and testing standards have not taken these integration times into account, because historically the DUTs were not able to calculate or limit their transmit power or duty factor.

Traditionally there are two basic components needed to ensure that the exposure of the user does not exceed SAR exposure limits.

- The detection component detects when the exposure of a user could exceed the limits.
- The mitigation component provides a method to reduce the exposure when high exposure has been detected.

Typically devices have utilized a proximity sensor for body detection, and look-up tables for static power reduction as a means of SAR mitigation. Typically such an implementation detects the physical proximity of the user to the antenna. When the proximity sensor is triggered, the device reduces its transmit power if needed to ensure that the psSAR levels are within the specified limits.

More recent devices apply algorithms which accurately track, calculate, and control the transmit power level and/or duty factor over the averaging period with high precision and accuracy. Such devices typically limit the transmission duty factor, output power, or both when necessary to reduce the time-period averaged SAR.

These algorithms and techniques can be tested for compliance according to the procedure specified in 7.6.

IECNORM.COM : Click to view the full PDF of IEC/IEEE 62209-1528:2020

Annex R
(normative)

Measurement uncertainty analysis for testing laboratories

R.1 RF ambient conditions

The ambient RF level shall be evaluated by performing SAR measurements using the same equipment set-up as used for testing a DUT, but with the RF power switched off. For both 1 g and 10 g averaging mass, the SAR due to RF ambient shall be less than or equal to 0,012 W/kg (i.e. 3 % of 0,4 W/kg).

It is not necessary to check RF ambient noise prior to each SAR test, provided the laboratory can demonstrate that there are no new RF sources.

The test configurations specified in Clause A.2 are used to assess the effects of reflections from nearby objects at the test site. The total amount of reflections shall comply with requirements of 6.1. In addition, the RF ambient noise shall be determined by performing SAR measurements with all local RF sources switched off. The allowable variation shall be within ±3 % of 0,4 W/kg, and the uncertainty shall be estimated assuming a rectangular probability distribution.

When SAR is measured in a controlled environment, such as an anechoic chamber, RF ambient effects shall be assessed at least once per year. Otherwise, RF ambient effects should be assessed before performing any SAR measurement on a DUT, and ambient conditions shall be monitored during the measurement so that any nearby high output sources, such as walkie-talkies, do not affect the SAR measurements.

The rationale for the non-controlled environment RF check evaluation is that there is no reason to assess this uncertainty contribution before every SAR measurement if it can be demonstrated that RF sources are sufficiently far from the SAR measurement system, even if the measurement system is placed in a non-controlled environment, due to the near field nature of the SAR measurement. The rationale on calibration intervals is specified in ISO 10012:2003 [136]. It is recommended to periodically evaluate the RF ambient effects on SAR measurements.

R.2 Device positioning and holder uncertainties

R.2.1 General

A device holder is used to keep the test position of the DUT at the phantom during a SAR measurement. Because the device holder can influence the characteristics of a DUT, the SAR uncertainty due to the device holder perturbation shall be estimated using the procedures in R.2.2. Procedures to assess the SAR uncertainties due to positioning variations due to mechanical uncertainties of the device holder are discussed in R.2.2.2 and R.2.2.3. Both subclauses include procedures for device-specific and predetermined uncertainties. If predetermined uncertainties are used, in most cases multiple repetitions of device-specific tests are required to further reduce the predetermined standard deviations.

IECNORM.COM : Click to view the full PDF of IEC/IEEE 62209-1528:2020

R.2.2 Device holder perturbation uncertainty

R.2.2.1 General

The device holder shall be made of low-loss dielectric material, with a loss tangent ≤ 0,05 and relative permittivity ≤ 5. (These material parameters can be determined, for example, using the coaxial contact probe method.) Nevertheless, some holders might still affect the DUT, so the uncertainty due to the holder (i.e. the deviation relative to a set-up without the holder) shall be estimated. The uncertainty of the device holder for testing a specific DUT shall be estimated according to the Type B method specified in R.2.2.2. Alternatively, the Type A method specified in R.2.2.3 can be used to assess the uncertainty for a group of DUTs with similar SAR characteristics, if they are tested with the same device holder.

R.2.2.2 Device holder perturbation uncertainty for a specific DUT: Type B

The uncertainty for a specific DUT operating in a specific device holder shall be estimated by performing the following two tests using a flat phantom:

a) assessment of the 1 g or 10 g psSAR ($SAR_{\text{w/ holder}}$) by placing the device in the holder in the way the DUT would be held when tested next to the head, then by positioning the DUT in direct contact with a flat phantom (horizontal and vertical centreline of the DUT parallel to the bottom of the flat phantom);

b) assessment of the 1 g or 10 g psSAR ($SAR_{\text{w/o holder}}$) by placing the device in the same position as in a), but held in place using foamed polystyrene or an equivalent low-loss and non-reflective material (permittivity not greater than 1,2, and loss tangent not greater than 10^{-5}).

The SAR uncertainty to be used in Table 9 is in Formula (R.1):

$$SAR_{\text{uncertainty}}\ [\%] = \left(\frac{SAR_{\text{w/ holder}} - SAR_{\text{w/o holder}}}{SAR_{\text{w/o holder}}} \right) \times 100 \qquad \text{(R.1)}$$

where

$SAR_{\text{uncertainty}}$ is the uncertainty as a percentage;

$SAR_{\text{w/ holder}}$ is the SAR with device holder in W/kg;

$SAR_{\text{w/o holder}}$ is the SAR without device holder in W/kg.

This uncertainty has an assumed rectangular probability distribution, and v_i = ∞ degrees of freedom.

R.2.2.3 Device holder perturbation uncertainty for a specific test device: Type A

The specific-device holder-disturbance uncertainty data evaluated according to the Type B method described in R.2.2.2, for a group of DUTs with the same shape and with substantially equivalent SAR distribution characteristics, shall be statistically compiled and applied to selected groups of devices tested in the same device holder and the same configurations. The statistical procedures shall include at least six devices, each evaluated according to the Type B method described in R.2.2.2. As more DUTs with similar SAR characteristics are evaluated with the same device holder, the perturbation error may be included in a Type A uncertainty analysis, and applied to future SAR evaluations of similar device and holder configurations. Increasing the number of test devices will increase the degrees of freedom (v_i) and lower the coverage factor (k_p). The coverage factor (k_p) for such conditions shall be determined as $k_p = t_p(v_{\text{eff}})$ where $t_p(v_{\text{eff}})$ is the coverage factor of the t-distribution, and v_{eff} is the effective number of degrees of freedom estimated using the Welch-Satterthwaite formula (see ISO/IEC Guide 98-3). The effect of the device holder for N different models of DUTs in the different configurations shall be estimated by performing the tests of R.2.2.2 according to the Type B method described in this paragraph for each model (N shall be at least 6).

IECNORM.COM : Click to view the full PDF of IEC/IEEE 62209-1528:2020

The corresponding uncertainty for Table 9 shall be estimated by using the RMS of the individual uncertainties, with $v_i = N - 1$ degrees of freedom. It is recommended that the database be updated yearly, in order to account for new DUT designs.

R.2.3 DUT positioning uncertainty with a specific test device holder: Type A

R.2.3.1 General

The deviation of the actual DUT position from the positions specified in 7.2.4 depends on the precision of the DUT positioner, as well as on the interpretation and handling by the person performing the test. In addition, the magnitude of this deviation on the psSAR values depends on the DUT design. Since these parameters cannot be separated, the Type A tests specified in R.2.3.2 and R.2.3.3 shall be performed.

R.2.3.2 Positioning uncertainty of a specific DUT in a specific device holder

The positioning uncertainty of a specific DUT tested in a specific device holder is assessed by repeating measurements of the 1 g or 10 g psSAR. This positioning uncertainty shall be evaluated using the antenna position, frequency channel, and device position for the operating mode that produced the highest SAR among all frequency bands. In addition to the original SAR measurement, the DUT shall be repositioned and the tests repeated at least four more times. This minimum of five tests is sufficient to establish a reasonable value for the degrees of freedom. If the positioning uncertainty of an individual device is suspected to be large, more tests might need to be performed, to reduce the impact on the total measurement uncertainty. Increasing the number of tests will increase the effective degrees of freedom (v_{eff}) and decrease the coverage factor. The average SAR for the total number of measurements (N) is used to determine the SAR uncertainty, according to the standard deviation and degrees of freedom ($v_i = N - 1$) of the number of tests performed.

R.2.3.3 Positioning uncertainty of specific types of DUTs in a specific device holder

A Type A uncertainty analysis can be applied for a group of DUTs with predominantly the same shape and substantially equivalent physical dimensions and SAR distributions. The tests shall include at least six separate devices, each evaluated according to the procedures for a specific DUT in a specific device holder described in R.2.3.2. The number of tests n shall be at least 5, and each of the n tests shall be performed for all M devices. For the sagitally-bisected SAM phantom, the n tests shall include the cheek position and the tilt position. For other phantoms, relevant device positions should be used. The corresponding uncertainty shall be estimated by applying the RMS of the M individual standard deviations. The value to be filled in the uncertainty table shall be the standard uncertainty with $k = 1$. The degrees of freedom are determined according to the total number of tests $N = n \times M$. For the M devices included in the specific group of DUTs, $v_i = N - 1$. If this procedure is applied to determine uncertainty, it might be unnecessary to apply the procedures for a specific DUT in a specific device holder described in R.2.3.2 to individual DUTs. It is recommended that the database be updated yearly, in order to account for new DUT designs.

R.3 Probe modulation response

Probe sensor responses to modulated signals that are based on diode detectors can be complex because the diodes are non-linear elements. The diode response theory for complex signals is described in Nadakuduti et al. [20]. The linearization parameters for a particular operating mode shall be determined by relative experimental calibration, i.e. by evaluating a power sweep for a particular operating mode, as specified in Clause E.2. The linearization parameters shall be determined for each sensor separately.

IECNORM.COM : Click to view the full PDF of IEC/IEEE 62209-1528:2020

The following uncertainty can be determined by using any source (e.g. waveguide or dipole) with a set-up equivalent to that specified in Figure A.1. The signal generation set-up shall simulate the operating mode for which the uncertainty is determined, according to the specification of the operating mode standard. The power shall be increased from a probe sensor voltage equivalent to lower than P_0 – the power transmitted to produce a SAR of 0,1 W/kg – to the equivalent of higher than P_1 – the power transmitted to produce a SAR of 10 W/kg – for the investigated sensor, in 5 dB steps. At each power level, the SAR shall be measured with the modulated signal, and with a CW signal at the same RMS power. (It shall be verified that the power meter uses a true RMS detector, and that the amplifier is sufficiently linear over the entire dynamic range of the signals.) This procedure shall be repeated for each field sensor.

Formula (R.2) is used to derive the modulation uncertainty of a particular modulation operating mode mod_{X}.

$$SAR_{\text{modulation uncertainty},mod\mathrm{X}}[\%] = \max_{j\in\{x,y,z\}}\left(\max_{P_i=P_0}^{P_0+20\ \mathrm{dB}}\left(100\times\left|\frac{SAR(P_i)_{mod\mathrm{X},j}}{SAR(P_i)_{\text{cal X},j}}-1\right|\right)\right) \quad \text{(R.2)}$$

where

$SAR_{\text{modulation uncertainty},mod\mathrm{X}}$ is the uncertainty for the particular operating mode mod_{X} as a percentage;

$SAR(P_i)_{mod\mathrm{X},j}$ is the SAR measured with the modulated signal at power level P_i for sensor index j;

$SAR(P_i)_{\text{cal X},j}$ is the SAR measured with the calibrated signal at the same RMS power for sensor index j.

The SAR uncertainty is determined as the maximum of all $SAR(P_i)_{mod\mathrm{X}}$ at each step for all three sensors. The index j refers to the field sensor, for each of which the procedure shall be repeated. A rectangular probability distribution has been assumed for probe modulation response uncertainty in Table 9.

R.4 Time-period averaged SAR

R.4.1 General

The uncertainty of time-period averaged SAR (TPAS) is the combined uncertainty of the TX factor uncertainty assessment (TXF) and the uncertainty of SAR measurement of a DUT (ΔSAR).

R.4.2 TX factor uncertainty

a) When the TX factor is assessed using SAR measurement, its uncertainty (TXF) is evaluated by measuring a CW signal with a pulse modulated amplitude. The amplitude variation shall be appropriate for the signal being measured. As an example, a signal amplitude may be used that has a square pulse shape (with 1 ms rise time) that varies in sequence such that is produces SAR results between three levels: 0,3 W/kg, 0,5 W/kg, and 1 W/kg, with amplitude durations of 1 s, 5 s, and 10 s. The measured TX factor is compared to its theoretical value (0,6 W/kg in this case). The worst-case deviation is taken as the sampling rate uncertainty assuming rectangular distribution.

b) When the TX factor is assessed using conducted power measurements (e.g. with a power meter) the uncertainty for pulse signals (applicable to the DUT testing) is considered to be the TX factor uncertainty assessment (TXF).

NOTE The requirement on the signal amplitude variation might change as more DUTs applying time averaging are developed (see Annex Q).

IECNORM.COM : Click to view the full PDF of IEC/IEEE 62209-1528:2020

R.5 Measured SAR drift

R.5.1 General

The SAR measurement drift of the DUT is accounted for by the first and last step of the measurement process specified in 7.4.2, by using the following two methods.

a) As the preferred method, local SAR measurements are made by the SAR measurement system prior to the area scan. A secondary measurement is made by the system at the same point after completion of the psSAR measurement. The measurement is performed within the tissue-equivalent medium at a reference point where the SAR values for both primary and secondary measurements exceed the lower detection limit of the measurement system. The distance from the reference point to the inner phantom surface in the normal direction shall be less than or equal to 10 mm.

b) Alternatively, and if the preferred method in a) is not sensitive enough, conducted power measurements can be made on the device at the antenna port, using equipment capable of measuring RF power prior to device placement for SAR testing. A secondary RF power measurement shall be made after the SAR testing is completed.

c) In either case, the drift is recorded as the percentage difference of the secondary reference measurement, $Ref_{\text{secondary}}$ (SAR or conducted power), from the primary reference measurement, Ref_{primary} as described in Formula (R.3):

$$drift = 100\ \% \times \frac{\left(Ref_{\text{secondary}} - Ref_{\text{primary}}\right)}{Ref_{\text{primary}}} \tag{R.3}$$

Commercial DUTs shall have SAR drifts within ±5 %. Some devices could have significant fluctuations in output power that are not classifiable as undesirable power drift, but rather are a characteristic of the normal operating behaviour of the device. In this case, other methods, such as SAR scaling, shall be considered to ensure that an accurate and conservative SAR is obtained.

d) If the SAR drift cannot meet the 5 % threshold while performing the SAR testing in accordance with 7.4.2, then a drift measurement for the longest intended measurement evaluation time shall be performed without recharging the battery. This is done by performing a measurement according to method a) or b) of this subclause continuously over the evaluation time (at least once every 5 s). This time sweep measurement shall be performed at each frequency band for the operating mode with the highest time-averaged output power.

   – If the difference between the maximum and minimum in the time sweep is less than 5 % of the average value, or if the difference is less than 10 % and the SAR primarily decreases during the time sweep (i.e. if it does not increase by more than 2 % at any time during the time sweep), it is sufficient to perform reference measurements at the beginning of the area scan and at end of the last zoom scan, as specified in 7.4.2 a) and f).

   – Otherwise, additional reference measurements shall be taken during the zoom scan, and the zoom scan measurements shall be corrected prior to performing extrapolation, integration, and averaging. Linear interpolation between the reference measurements is performed prior to the correction. The SAR values measured during the zoom scan shall be corrected by the difference between the interpolated values and the first reference value measured before the area scan. The time between reference measurements during the zoom scan shall be sufficiently small, such that correction of the time sweep curve specified in this paragraph shall be conservative for all points.

R.5.2 Accounting for drift

a) If the SAR drift is within 5 %, then it can be treated either as an uncertainty (i.e. random error), or a systematic offset. If the drift is larger than 5 %, the measurement drift shall be considered a systematic offset rather than an uncertainty.

IECNORM.COM : Click to view the full PDF of IEC/IEEE 62209-1528:2020

b) If treated as an uncertainty, the absolute value of the drift shall be entered into the uncertainty table. The drift shall not be added to the assessed SAR value. The uncertainty value reported in the uncertainty budget shall either be the value corresponding to the highest SAR measurement drift reported, or the maximum allowed 5 %.

c) If treated as a systematic offset, compensation to the measured SAR shall be applied by adding the absolute difference to the determined SAR value if the drift is either negative or positive, as described in Formula (R.4):

$$SAR_{\text{compensated}} = SAR_{\text{measured}} \times \left(1 + \left|drift\right| / 100\ \%\right) \tag{R.4}$$

In this case it is not necessary to record the drift in the uncertainty budget (i.e. u_i = 0 %).

d) To maintain a conservative value for the resulting SAR, drifts shall not be subtracted from the assessed SAR. If different assessed operating modes of the device exhibit different drift ratios, all the corresponding measured SAR values may be compensated by the same ratio, provided that the applied drift ratio is the largest one detected during the SAR testing over all operating modes of the device. The uncertainty shall be estimated assuming a rectangular probability distribution.

R.6 SAR scaling uncertainty

Uncertainties of the SAR scaling (7.2.3.2) are associated with non-linearities of the signal and RF amplifier stages, the modulation signal bandwidth, and antenna impedance.

For SAR scaling uncertainty, a rectangular probability distribution shall be assumed. The uncertainty is evaluated by determination of the SAR of mod_{Y} at the psSAR location (x_{p}, y_{p}, z_{p}) using the following procedure.

a) Perform an area scan with mod_{X} according to 7.4.2.

b) Move the probe to the peak location of the area scan.

c) Take the SAR reading at the peak location with mod_{X}.

d) Switch the device to mod_{Y} (without moving the device).

e) Take the SAR reading with mod_{Y}.

f) Calculate the ratio of the measured and scaled $SAR_{mod\text{Y}}$ using Formula (R.5):

$$SAR_{\text{scaling uncertainty}} = \left(\frac{SAR\left(x_{\text{p}}, y_{\text{p}}, z_{\text{p}}\right)_{mod\text{Y}}}{SAR\left(x_{\text{p}}, y_{\text{p}}, z_{\text{p}}\right)_{mod\text{X}} \cdot R_{\text{p}}} - 1 \right) \times 100\ \% \tag{R.5}$$

with R_{p} as the time-averaged RF output power ratio of mod_{X} and mod_{Y}, according to 7.2.3.2.

If $SAR_{\text{scaling uncertainty}}$ > 5 %, do not use the scaling; instead perform full SAR testing for mod_{Y}.

IECNORM.COM : Click to view the full PDF of IEC/IEEE 62209-1528:2020

Annex S
(normative)

Validation antenna SAR measurement uncertainty

S.1 Deviation of experimental antennas

The system validation antennas in Annex D are well specified, and were simulated to obtain numerical reference values using validated numerical codes. However, the mechanical and electrical uncertainties of each specific antenna affect the resulting psSAR values, due to, for example, different feed-point impedance and current distribution as function of distance, phantom shell, tissue-equivalent medium, etc. In other words, the numerical target values are valid for the specific antennas and set-up configuration requirements. The deviation from the target values shall be determined either by Type A or Type B evaluations. Type A evaluations should use statistical evaluation of several measurements using different tissue-equivalent media, probes, and phantoms. For Type B evaluations, all parameters need to be assessed experimentally. Numerical target values are established by numerical simulations and validated laboratory calibration.

For the standard waveguide, Table S.1 provides the contributions to the deviations of the waveguide from theory.

For the standard dipole, confined loop antenna, meander dipole, and VPIFA, contributions to the deviation of experimental antennas from theory include variations in the physical parameters specified in Annex D.

The combined uncertainty from the deviations in experimental antennas from theory is entered into Table 9, with an assumed normal probability distribution.

Table S.1 – Uncertainties relating to the deviations of the parameters of the standard waveguide from theory

Symbol	Input quantity X_i (source of uncertainty)	Prob. Dist. PDF_i	Uncert'nty $a(x_i)$ ± %	Div. q_i	$u(x_i) = a(x_i)/q_i$	c_i (1 g, 10 g)	$u(y) = c_i \cdot u(x_i)$ ± %	v_i
ΔTE_{01}	Variation from theoretical waveguide mode in medium	R	5,0	√3	2,9	1	2,9	∞
L, W	Waveguide dimensions	N	1,0	1	1,0	1	1,0	∞
$u_c(y)$	Combined uncertainty	RSS					3,1	∞

S.2 Other uncertainty contributions when using system validation antennas

In addition to the uncertainty terms for the system validation antenna discussed elsewhere, there are additional terms to be added in the uncertainty budget. These terms depend on the type of system validation antenna used. For a dipole antenna, meander dipole, or VPIFA, such a term can be the distance of the feed-point to the tissue-equivalent medium, and for a waveguide or confined loop antenna, such a term can be the mismatch error. Table S.2 and Table S.3 show the uncertainty terms for the dipole antenna and the waveguide, respectively. The expanded measurement uncertainty shall be within ±10 % for k = 2. These additional uncertainty terms are entered into the row VAL of Table 9. The numerical values in this table are examples only, and should not be assumed to represent the values for specific antennas.

NOTE The waveguide is placed directly against the phantom, as specified in Annex D. Therefore, no uncertainty term is needed to account for the distance to the phantom, like with the dipole antenna.

IECNORM.COM : Click to view the full PDF of IEC/IEEE 62209-1528:2020

Table S.2 – Other uncertainty contributions relating to the dipole antennas specified in Annex D.

Input quantity X_i (source of uncertainty)	Probability distribution PDF_i	Uncertainty $a(x_i)$ ± %	Divisor q_i	$u(x_i) = a(x_i)/q_i$	c_i	$u(y) = c_i \cdot u(x_i)$ ± %	v_i
Dipole axis to medium distance	R	2,0	√3		1	1,2	∞

Table S.3 – Other uncertainty contributions relating to the standard waveguides specified in Annex D

Input quantity X_i (source of uncertainty)	Probability distribution PDF_i	Uncertainty $a(x_i)$ ± %	Divisor q_i	$u(x_i) = a(x_i)/q_i$	c_i	$u(y) = c_i \cdot u(x_i)$ ± %	v_i
Mismatch error for system [a]	U-shaped	5,0	√2		1	3,5	∞
Uncertainty in measurement of power transmission loss of adapter and waveguide.	N	1,0	2		1	0,5	∞
Combined uncertainty	RSS				±	3,5	∞

[a] This is calculated for 8 dB return loss to the waveguide, 30 dB return loss for the power sensor, and 25 dB return loss for the output port of the coupler.

IECNORM.COM : Click to view the full PDF of IEC/IEEE 62209-1528:2020

Annex T
(normative)

Interlaboratory comparisons

T.1 Purpose

The purpose of the interlaboratory comparison is to validate various SAR measurement systems by comparing results from several different laboratories. The general concept is to use reference DUTs and the required phantoms specified in this document. The SAR assessment methodologies specified in Clause 7 are used.

The measured data from various laboratories shall be compared. Also, a comparison of measurement uncertainty analyses among the test laboratories shall be performed. If the differences and discrepancies between the measured data can be attributed to differences in the measurement uncertainties, the interlaboratory comparison is deemed to be successful. If not, all sources of uncertainties shall be investigated in accordance with the recommendations of Clause 8. Also, other possible sources of uncertainties different from those specified in Clause 8 shall be considered.

NOTE General guidelines for accomplishing interlaboratory comparison tests are given for example in [137] and [138].

T.2 Phantom set-up

The required phantoms are specified in this document. The phantom shall have a mounting structure made of a rugged material, with low permittivity (less than 5) and low loss tangent (less than 0,05). Metallic parts closer than 50 cm from the structure shall be avoided. The phantom shall be irradiated using a reference DUT, mounted according to the test positions specified in 7.2.4.

T.3 Reference devices

Reference devices are commercial wireless DUTs. The set of reference devices may also be extended to include non-commercial sources. Each reference device shall have evaluated target SAR values with associated measurement uncertainty. The designation of the supplier is based on the agreement between the participating parties.

T.4 Power set-up

The power set-up is dependent on the precision of the output power measurement of the reference device used for the interlaboratory comparison. Each device is individually checked by the participating laboratory, so that the maximum conducted output power of each reference device is in the range of ±0,3 dB from the reference value. The measured output power shall be reported to the monitor laboratory. The device output power shall be adjusted via test software to a predetermined value. The device battery shall be fully charged.

Careful effort shall be expended to ensure an accurate output power measurement. Some devices may allow easy and accurate output power measurements at the antenna port. The ease of output-power measurement shall be considered when designating reference devices for use in the comparison tests. If deemed necessary, the reference devices shall be returned to a monitor laboratory periodically during the comparison campaign, for verification of SAR, output power, and frequency. Also, the battery condition shall be checked by the monitor laboratory, to ensure uniform power output at all laboratories.

IECNORM.COM : Click to view the full PDF of IEC/IEEE 62209-1528:2020

T.5 Interlaboratory comparison – procedure

Measurement procedures for SAR assessment used in the interlaboratory comparison are the same as those used for compliance testing, in accordance with Clause 7. When a full SAR testing system or a fast SAR testing system is used, the interlaboratory comparison shall be performed with a calibrated and validated system. Each laboratory shall provide a full measurement report in accordance with the requirements of Clause 8 and Clause 9, including system validation, dielectric properties measurements, system-contributed uncertainty data, and measured output power data. If a fast SAR testing system that does not meet all of the specifications of this document is used to perform SAR measurements, the uncertainty should follow general guidance provided in Clause C.1, if applicable.

Results of the interlaboratory comparison shall be compared to their respective target values. Each result shall fall within the expanded measurement uncertainty of the measured value and target value. The reports from different laboratories are to be evaluated and compared by the designated monitor laboratory.

IECNORM.COM : Click to view the full PDF of IEC/IEEE 62209-1528:2020

Annex U
(informative)

Determination of the margin for compliance evaluation using the Uniphantom

U.1 General

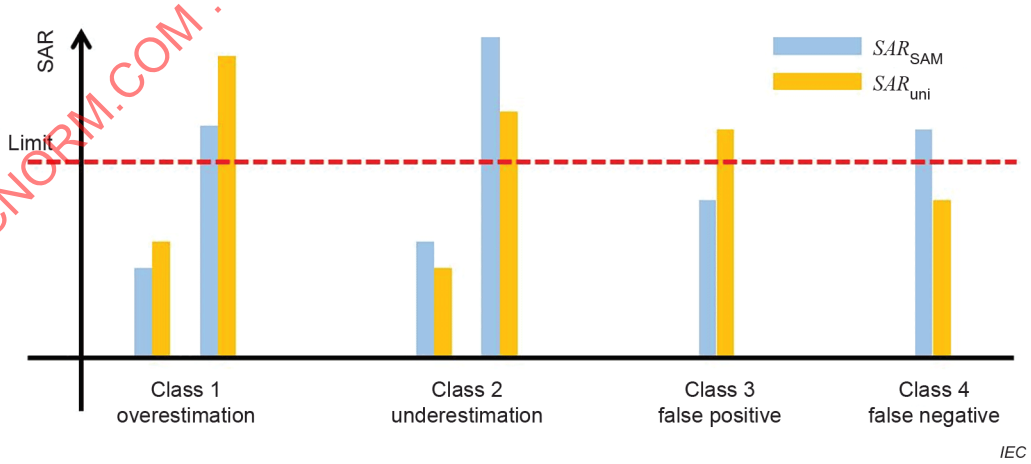
When comparing the psSAR measured with the Uniphantom with the psSAR limit, it is necessary to consider a margin in order to compensate the possibility of the underestimation of measured psSAR. This margin shall be appropriately determined based on statistical data. Some examples of the determination of the margin are specified in Annex U.

U.2 Deviation of the psSAR measured using the Uniphantom from the psSAR measured using the SAM phantom

The Uniphantom is designed to obtain a more conservative SAR value in comparison to the SAM phantom. In some cases, however, the SAR value measured using the Uniphantom can be lower than the psSAR measured with the SAM phantom. The compared results of the measured psSAR between the Uniphantom and the SAM phantom are can be categorized into four “Classes,” as shown in Figure U.1.

It is important to avoid a false negative as shown by the Class 4 results of Figure U.1, whereas a false positive can be checked by a full-compliance SAR measurement following after the evaluation using the Uniphantom. A margin is therefore necessary to compensate the measured SAR using the Uniphantom. However, an overly-large margin is inappropriate, because then most cases would be categorized as false positives, which would need full SAR testing using the SAM phantom.

The 95 % confidence interval of the deviation of the measured SAR between the Uniphantom and the SAM phantom is used to determine the margin in Annex U. This margin means that 5 % of the cases are misclassified if the measured SAR of the Uniphantom is higher than the compensated SAR limit, which generally is very rare if the 95 % confidence interval is relatively small.



NOTE The psSAR limit is also shown as a dashed red line.

Figure U.1 – Categories (classes) for comparison of the measured psSAR between the Uniphantom (SAR_{uni}) and the SAM phantom (SAR_{SAM})

IECNORM.COM : Click to view the full PDF of IEC/IEEE 62209-1528:2020

U.3 Determination of margin based on 95 % confidence interval

a) Measure maximum psSAR values using the Uniphantom (SAR_{flat} and SAR_{corner}) and the SAM phantom (SAR_{SAM}) for handsets of the same shape. SAR_{flat} is the measured SAR for the handset positioned at the flat bottom of the Uniphantom, and SAR_{corner} is the measured SAR for the handset positioned at the curved edge (cross-section corner) of the Uniphantom. SAR_{SAM} is the highest value of the maximum condition among the left and right sides and the cheek and tilt positions, and so on. The number of handsets is N.

b) Calculate the deviations of the measured SAR between the Uniphantom and the SAM phantom (Dev) for each handset as in Formula (U.1):

$$Dev = SAR_{\text{uni}} - SAR_{\text{SAM}} \tag{U.1}$$

where SAR_{uni} is SAR_{flat} or SAR_{corner}.

c) Calculate the average (Dev_{ave}) and the standard deviation (Dev_{std}) of Dev for N handsets.

d) Calculate the 95 % confidence interval, based on the t-distribution with $N - 1$ degrees of freedom ($Int_{95\ \%}$).

e) Calculate the margin ($SAR_{\text{limit margin}}$) as in Formula (U.2):

$$SAR_{\text{limit margin}} = Dev_{\text{std}} \times Int_{95\ \%} - Dev_{\text{ave}} \tag{U.2}$$

f) If $SAR_{\text{limit margin}}$ is negative, do not apply the margin (i.e. $SAR_{\text{limit margin}} = 0$). If $SAR_{\text{limit margin}}$ is larger than the psSAR limit value (SAR_{limit}), do not apply the evaluation using the Uniphantom.

g) Test for compliance by comparing the SAR_{uni} and the compensated psSAR limit as follows:

1) compliant if $SAR_{\text{uni}} \leq SAR_{\text{limit}} - SAR_{\text{limit margin}}$;

2) not compliant if $SAR_{\text{uni}} > SAR_{\text{limit}} - SAR_{\text{limit margin}}$.

NOTE Some national regulatory authorities might have other or different requirements for compliance demonstration.

The uncertainty shall also be considered into SAR_{uni} if the uncertainty is larger than 30 %, same as for the full-compliance SAR measurement using the SAM phantom.

U.4 Examples of the determination of the margin factor

U.4.1 Margin for handsets with straight form factors at flat-bottom position

In Clause U.4, 45 handsets with straight form factors are considered to determine the margin for the 10 g psSAR limit (2 W/kg), and 40 handsets are considered for the 1 g psSAR limit (1,6 W/kg). The information used for the determination of the margin is summarized in Table U.1. The statistical distributions are also shown in Figure U.2 and Figure U.3.

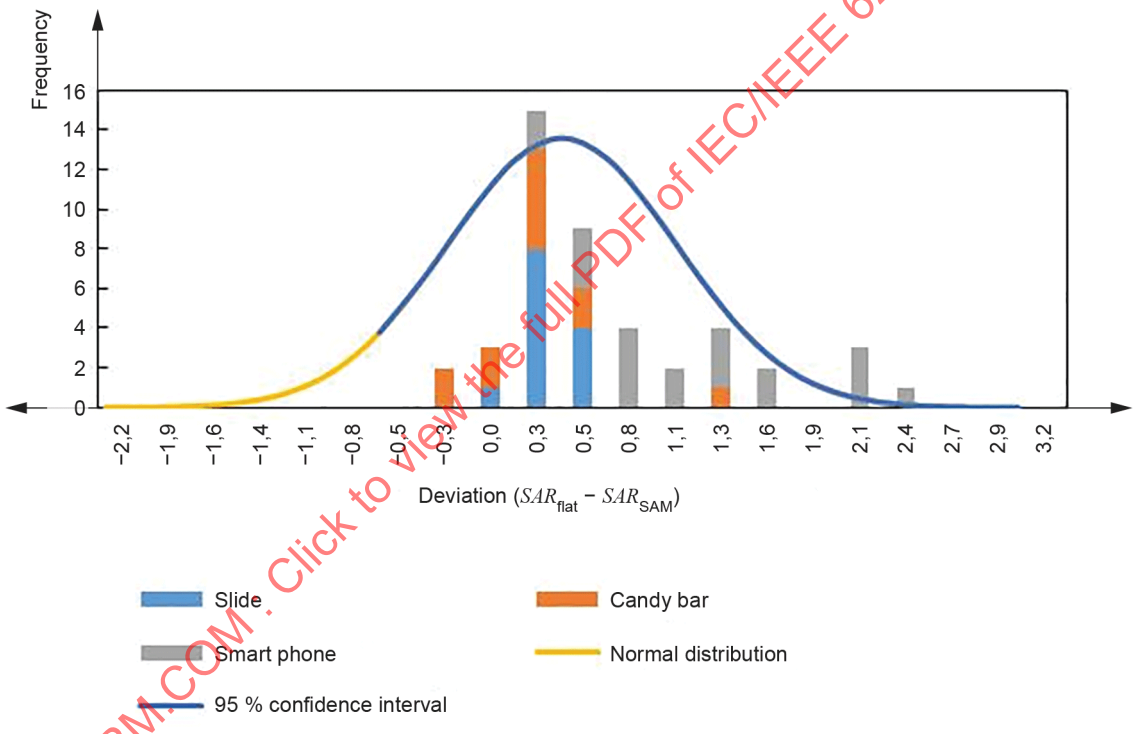
Figure U.2 and Figure U.3 show that the margin based on the 95 % confidence interval is conservative. Note that this high ratio of the number of false-positive handsets is caused by the inclusion of the SAR results of the smart phones. This result suggests that the smart phones and the other handsets could be separately considered to apply the SAR margin, or the measurement of the flat bottom of the Uniphantom could be skipped. The margins for the smart phone and the other handsets are determined in U.4.2 to U.4.5.

IECNORM.COM : Click to view the full PDF of IEC/IEEE 62209-1528:2020

Table U.1 – Summary of information to determine the margin for handsets with straight form factors positioned at the flat bottom of the Uniphantom

Contribution	10 g psSAR	1 g psSAR
Number of handsets (N)	45	40
Average of the deviation (Dev_{ave}) (W/kg)	0,53	1,30
Standard deviation of the deviation (Dev_{std}) (W/kg)	0,67	1,58
t value of 95 % with N − 1 degree of freedom	1,68	1,68
Margin ($SAR_{limit\ margin}$) (W/kg)	0,60	1,36
Compensated psSAR limit (SAR_{limit} − $SAR_{limit\ margin}$) (W/kg)	1,40	0,24
Ratio of false-positive handsets to all of the measured handsets (Class 3 in Figure U.1)[a]	29 %	98 %

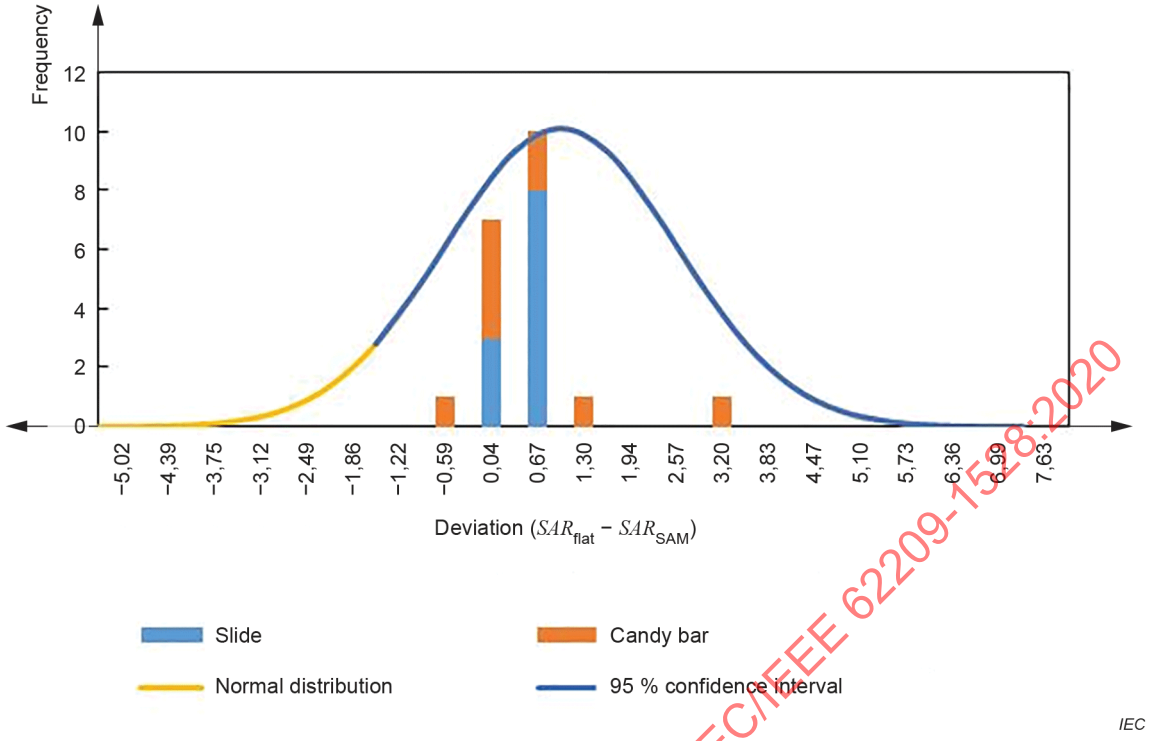
[a] The handsets should be measured at the curved edge (corner) of the Uniphantom or using the SAM phantom in the same way as in the full-compliance SAR measurement.



NOTE The normal distribution and its 95 % confidence interval with the same average and standard deviation are also shown.

Figure U.2 – Histogram of the deviation of the 10 g psSAR of 45 handsets with straight form factors positioned at the flat bottom of the Uniphantom

IECNORM.COM : Click to view the full PDF of IEC/IEEE 62209-1528:2020



NOTE The normal distribution and its 95 % confidence interval with the same average and standard deviation are also shown.

Figure U.3 – Histogram of the deviation of the 1 g psSAR of 40 handsets with straight form factors positioned at the flat bottom of the Uniphantom

U.4.2 Margin for handsets with straight form factors (except smart phones at flat-bottom position)

In U.4.2, 25 handsets with straight form factors, including slide-type handsets and bar phones, but not smart phones, are considered to determine the margin for the 10 g psSAR limit (2 W/kg), and 20 handsets are considered for the 1 g psSAR limit (1,6 W/kg). The information used for the determination of the margin is summarized in Table U.2. The statistical distributions are also shown.

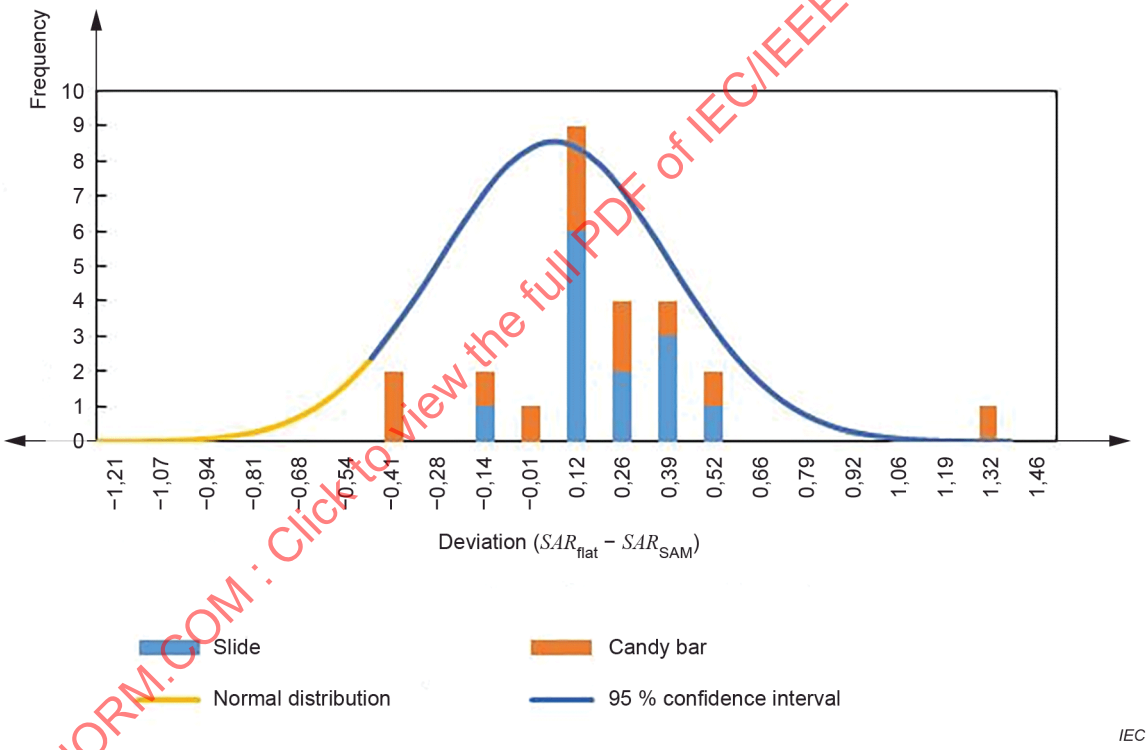
Figure U.4 and Figure U.5 show that the margin based on the 95 % confidence interval is conservative, which results in a lower ratio of false-positive handsets than in the cases wherein all handsets with straight form factors including smart phones are considered (U.4.1).

IECNORM.COM : Click to view the full PDF of IEC/IEEE 62209-1528:2020

Table U.2 – Summary of information to determine the margin for handsets with straight form factors, including slide-type and bar handsets (except smart phones), positioned at the flat bottom of the Uniphantom

Contribution	10 g psSAR	1 g psSAR
Number of handsets (N)	25	20
Average of the deviation (Dev_{ave}) (W/kg)	0,12	0,26
Standard deviation of the deviation (Dev_{std}) (W/kg)	0,33	0,68
t value of 95 % with N − 1 degree of freedom	1,71	1,73
Margin ($SAR_{limit\ margin}$) (W/kg)	0,45	0,92
Compensated psSAR limit (SAR_{limit} − $SAR_{limit\ margin}$) (W/kg)	1,55	0,68
Ratio of false-positive handsets to all of the measured handsets (Class 3 in Figure U.1) [a]	12 %	40 %

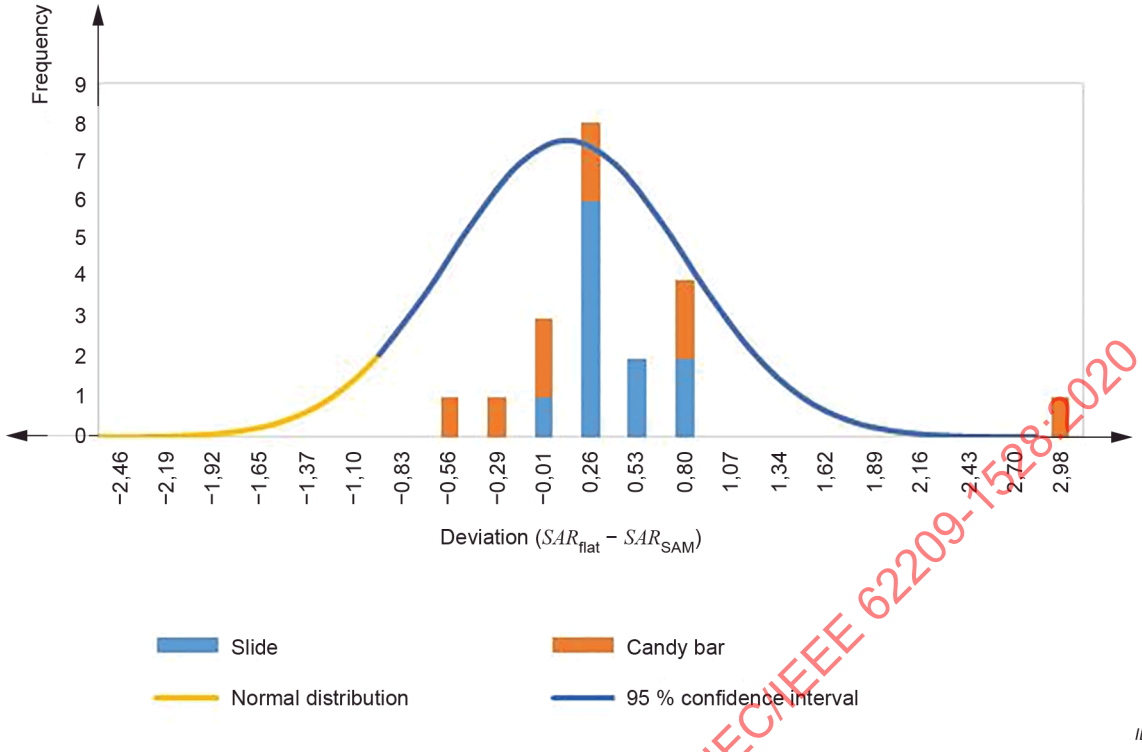
[a] The handsets should be measured at the curved edge (corner) of the Uniphantom or using the SAM phantom in the same way as in the full-compliance SAR measurement.



NOTE The normal distribution and its 95 % confidence interval with the same average and standard deviation are also shown.

Figure U.4 – Histogram of the deviation of the 10 g psSAR of 25 handsets with straight form factors positioned at the flat bottom of the Uniphantom

IECNORM.COM : Click to view the full PDF of IEC/IEEE 62209-1528:2020



NOTE The normal distribution and its 95 % confidence interval with the same average and standard deviation are also shown.

Figure U.5 – Histogram of the deviation of the 1 g psSAR from 20 handsets with straight form factors positioned at the flat bottom of the Uniphantom

U.4.3 Margin for smart phones at flat-bottom position

In U.4.3, 20 handsets with straight form factors or smart phones are considered to determine the margin for the 10 g psSAR limit (2 W/kg), and 20 handsets are considered for the 1 g psSAR limit (1,6 W/kg). The information used for the determination of the margin is summarized in Table U.3. The statistical distributions are also shown.

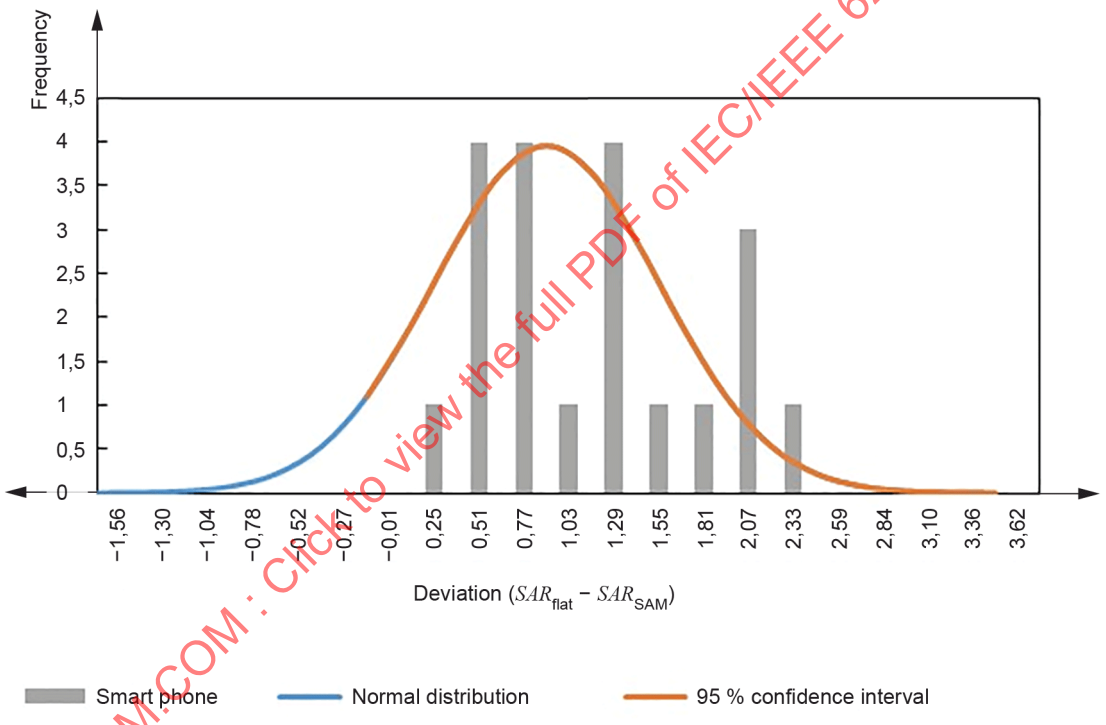
Figure U.6 and Figure U.7 show that the margin based on the 95 % confidence interval is conservative. Note that the ratio of the false-positive handsets for 10 g psSAR is more reasonable than that in the cases where all handsets with straight form factors, and with including smart phones, are considered (U.4.1). However, the ratio for 1 g psSAR is still considerably high, which means that the SAR measurement at the flat bottom of the Uniphantom should be omitted.

IECNORM.COM : Click to view the full PDF of IEC/IEEE 62209-1528:2020

Table U.3 – Summary of information to determine the margin for the smart phones positioned at the flat bottom of the Uniphantom

Contribution	10 g psSAR	1 g psSAR
Number of handsets (N)	20	20
Average of the deviation (Dev_{ave}) (W/kg)	1,03	2,35
Standard deviation of the deviation (Dev_{std}) (W/kg)	0,65	1,53
t value of 95 % with N − 1 degree of freedom	1,73	1,73
Margin ($SAR_{limit\ margin}$) (W/kg)	0,09	0,30
Compensated psSAR limit (SAR_{limit} − $SAR_{limit\ margin}$) (W/kg)	1,91	1,30
Ratio of false-positive handsets to all of the measured handsets (Class 3 in Figure U.1) [a]	30 %	85 %

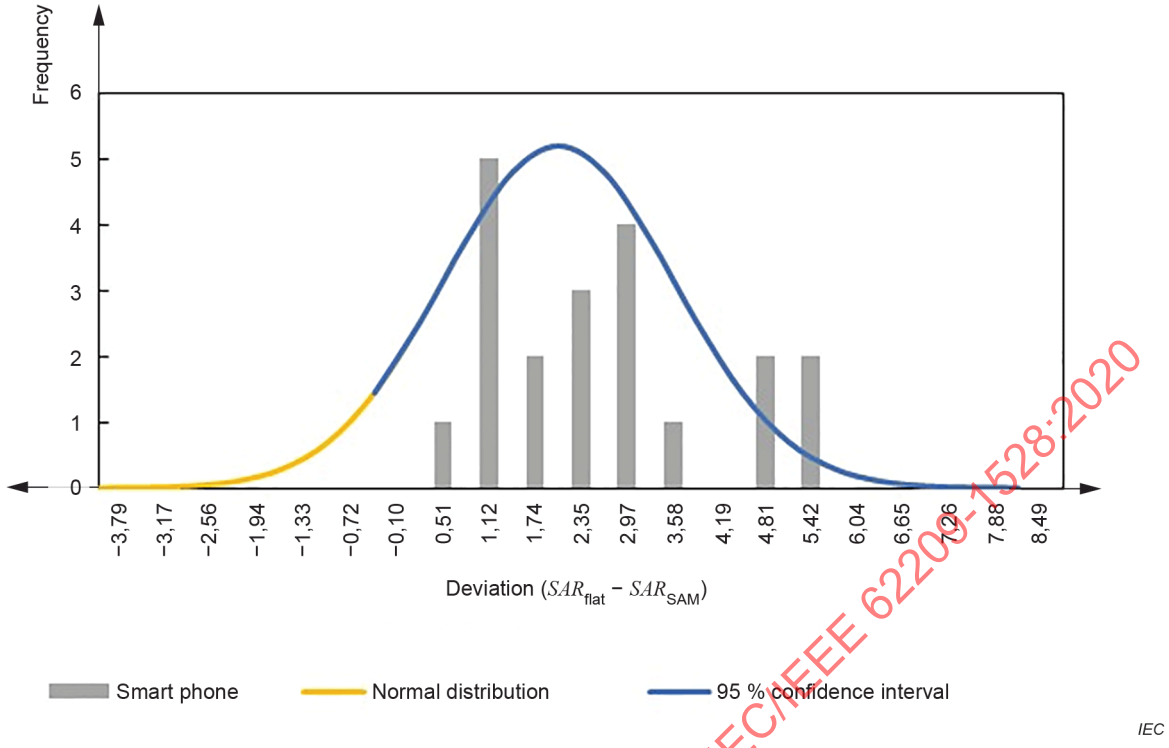
[a] The handsets should be measured at the curved edge (corner) of the Uniphantom or using the SAM phantom in the same way as in the full-compliance SAR measurement.



NOTE The normal distribution and its 95 % confidence interval with the same average and standard deviation are also shown.

Figure U.6 – Histogram of the deviation of the 10 g psSAR of 20 handsets with straight form factors or smart phones positioned at the flat bottom of the Uniphantom

IECNORM.COM : Click to view the full PDF of IEC/IEEE 62209-1528:2020



NOTE The normal distribution and its 95 % confidence interval with the same average and standard deviation are also shown.

Figure U.7 – Histogram of the deviation of the 1 g psSAR of 20 handsets with straight form factors or smart phones positioned at the flat bottom of the Uniphantom

U.4.4 Margin for smart phones at corner position

In U.4.4, 20 smart phones are considered to determine the margin for the 10 g psSAR limit (2 W/kg), and 19 smart phones are considered for the 1 g psSAR limit (1,6 W/kg). The information used for the determination of the margin is summarized in Table U.4. The statistical distributions are also shown.

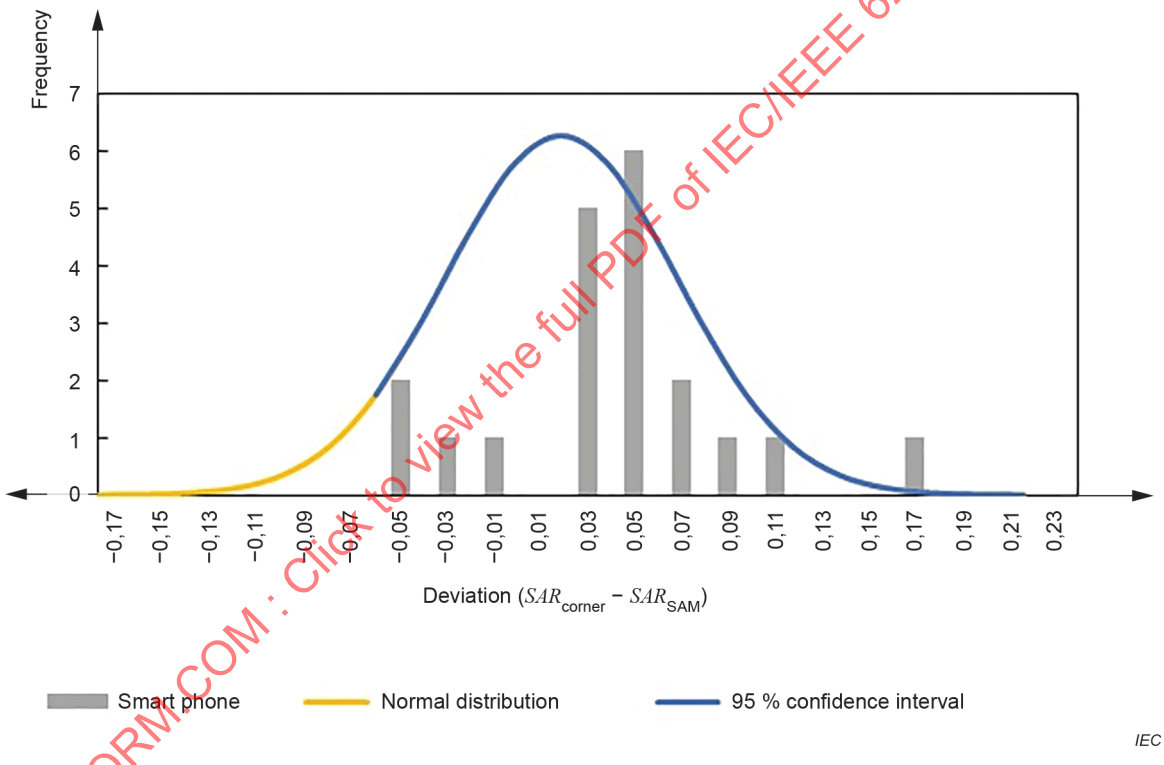
Figure U.8 clearly shows that the margin based on the 95 % confidence interval is conservative for the 10 g psSAR limit. On the other hand, there is one case where the deviation is outside the 95 % confidence interval, as shown in Figure U.9. However, this is not a false-negative case, i.e. Class 2 but not Class 4 per Figure U.1. Note that the ratio of the false-positive handsets, which require further measurements, is extremely good; i.e. 0 %, which is a significant improvement with respect to the cases of the measurement at the flat bottom of the Uniphantom (Table U.5), because the deviation is significantly small, which implies that the Uniphantom is an appropriate substitute for the SAM phantom.

IECNORM.COM : Click to view the full PDF of IEC/IEEE 62209-1528:2020

Table U.4 – Summary of information to determine the margin for smart phones positioned at the corner of the Uniphantom

Contribution	10 g psSAR	1 g psSAR
Number of handsets (N)	20	19
Average of the deviation (Dev_{ave}) (W/kg)	0,03	−0,03
Standard deviation of the deviation (Dev_{std}) (W/kg)	0,05	0,08
t value of 95 % with N − 1 degree of freedom	1,73	1,73
Margin ($SAR_{limit\ margin}$) (W/kg)	0,06	0,17
Compensated psSAR limit (SAR_{limit} − $SAR_{limit\ margin}$) (W/kg)	1,94	1,43
Ratio of false-positive handsets to all of the measured handsets (Class 3 in Figure U.1)[a]	0 %	0 %

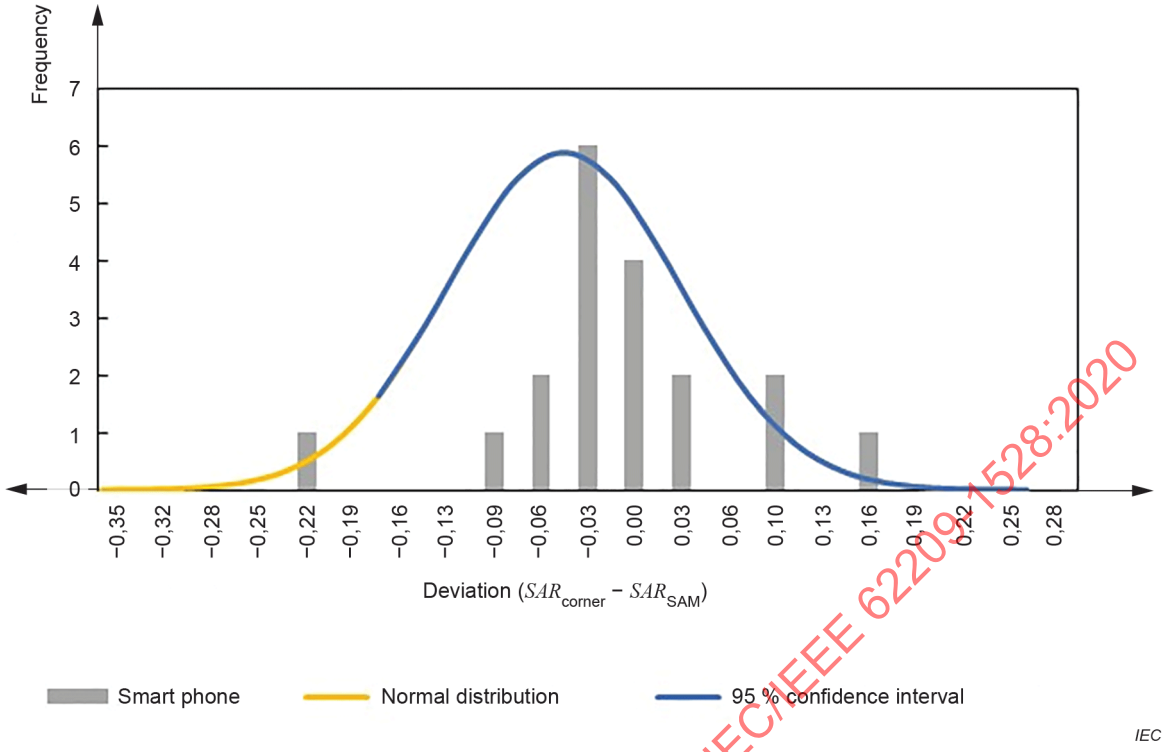
[a] The handsets should be measured at the curved edge (corner) of the Uniphantom or using the SAM phantom in the same way as in the full-compliance SAR measurement.



NOTE The normal distribution and its 95 % confidence interval with the same average and standard deviation are also shown.

Figure U.8 – Histogram of the deviation of the 10 g psSAR of 20 handsets with straight form factors or smart phones positioned at the corner of the Uniphantom

IECNORM.COM : Click to view the full PDF of IEC/IEEE 62209-1528:2020



NOTE The normal distribution and its 95 % confidence interval with the same average and standard deviation are also shown.

Figure U.9 – Histogram of the deviation of the 1 g psSAR of 19 handsets with straight form factors or smart phones positioned at the corner of the Uniphantom

Table U.5 – Statistical analysis results of P(Tilt/Cheek > x) for various device types

x	P(Tilt/Cheek > x)			
	Bar	Clamshell	Slide (Open)	Slide (Closed)
1,0	$6{,}853 \times 10^{-3}$	$2{,}992 \times 10^{-8}$	$5{,}441 \times 10^{-4}$	$1{,}771 \times 10^{-3}$
1,1	$1{,}334 \times 10^{-3}$	$3{,}769 \times 10^{-10}$	$2{,}138 \times 10^{-5}$	$1{,}739 \times 10^{-4}$
1,2	$1{,}982 \times 10^{-4}$	$2{,}801 \times 10^{-12}$	$4{,}385 \times 10^{-7}$	$1{,}131 \times 10^{-5}$
1,3	$2{,}240 \times 10^{-5}$	$1{,}221 \times 10^{-14}$	$4{,}658 \times 10^{-9}$	$4{,}844 \times 10^{-7}$
2,0	$1{,}998 \times 10^{-15}$	$0{,}000 \times 10^{0}$	$0{,}000 \times 10^{0}$	$0{,}000 \times 10^{0}$

IECNORM.COM : Click to view the full PDF of IEC/IEEE 62209-1528:2020

U.4.5 Margin for handsets with clamshell form factors at corner position

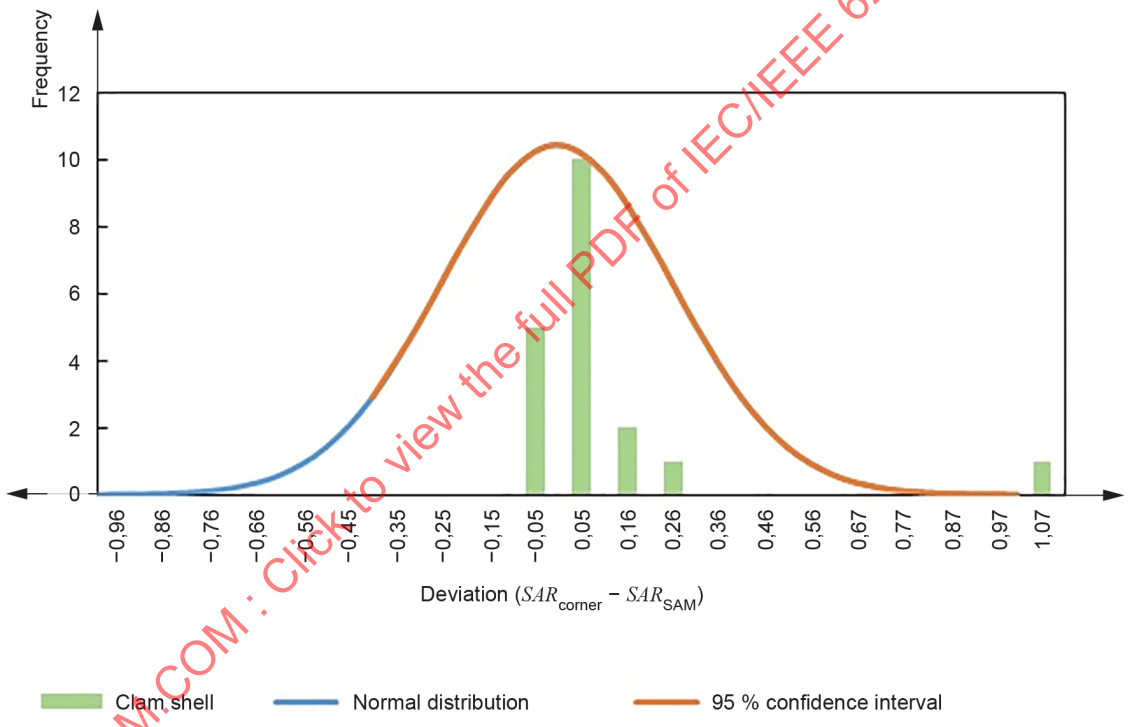
In U.4.5, 19 handsets with clamshell form factors are considered to determine the margin for the 10 g psSAR limit (2 W/kg), and 19 handsets are considered for the 1 g psSAR limit (1,6 W/kg). The information used for the determination of the margin is summarized in Table U.6. The statistical distributions are also shown.

Figure U.10 and Figure U.11 clearly show that the margin based on the 95 % confidence interval is conservative, which results in a good or low ratio of the false-positive handsets, i.e. 0 % for 10 g psSAR, and 11 % for 1 g psSAR. This also means that the curved-edge (cross-section corner) of the Uniphantom is an appropriate substitute for the SAM phantom for handsets with clamshell form factors.

Table U.6 – Summary of information to determine the margin for handsets with clamshell form factors positioned at the corner of the Uniphantom

Contribution	10 g psSAR	1 g psSAR
Number of handsets (N)	19	19
Average of the deviation (Dev_{ave}) (W/kg)	0,05	0,03
Standard deviation of the deviation (Dev_{std}) (W/kg)	0,25	0,20
t value of 95 % with N − 1 degree of freedom	1,73	1,73
Margin ($SAR_{limit\ margin}$) (W/kg)	0,39	0,31
Compensated psSAR limit (SAR_{limit} − $SAR_{limit\ margin}$) (W/kg)	1,61	1,29
Ratio of false-positive handsets to all of the measured handsets (Class 3 in Figure U.1)[a]	0 %	11 %

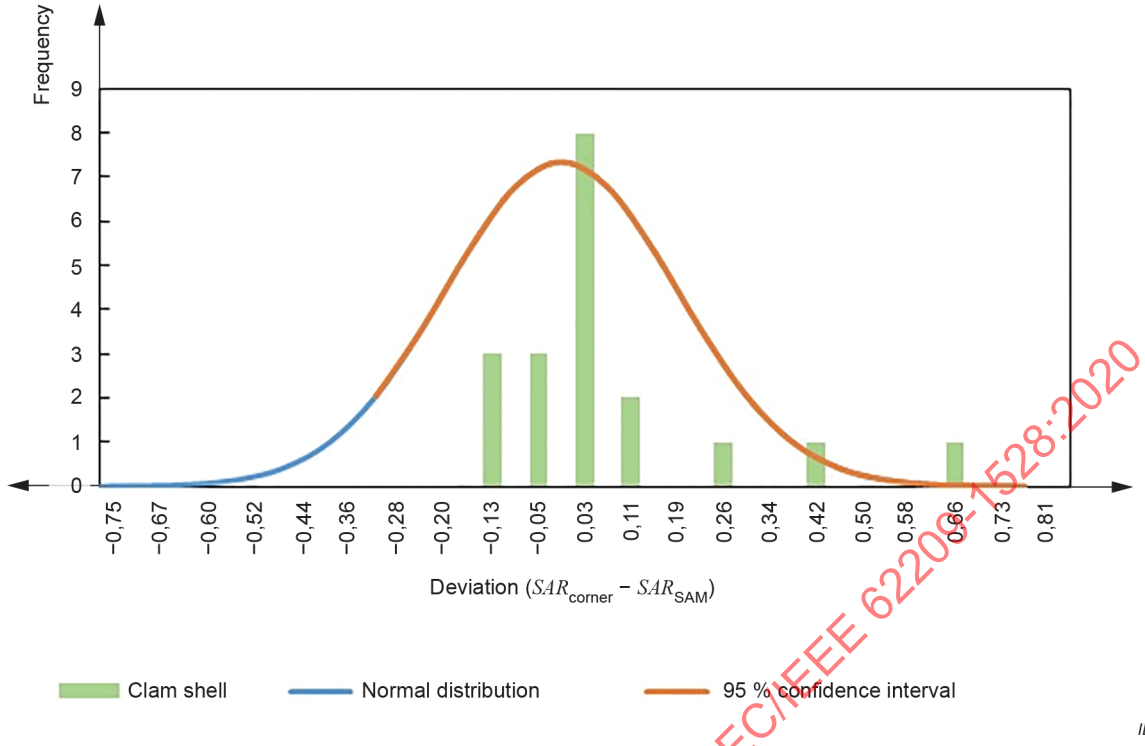
[a] The handsets should be measured at the curved edge (corner) of the Uniphantom or using the SAM phantom in the same way as in the full-compliance SAR measurement.



NOTE The normal distribution and its 95 % confidence interval with the same average and standard deviation are also shown.

Figure U.10 – Histogram of the deviation of the 10 g psSAR of 20 handsets with clamshell form factors at the corner of the Uniphantom

IECNORM.COM : Click to view the full PDF of IEC/IEEE 62209-1528:2020



NOTE The normal distribution and its 95 % confidence interval with the same average and standard deviation are also shown.

Figure U.11 – Histogram of the deviation of the 1 g psSAR of 19 handsets with clamshell form factors at the corner of the Uniphantom

IECNORM.COM : Click to view the full PDF of IEC/IEEE 62209-1528:2020

Annex V
(informative)

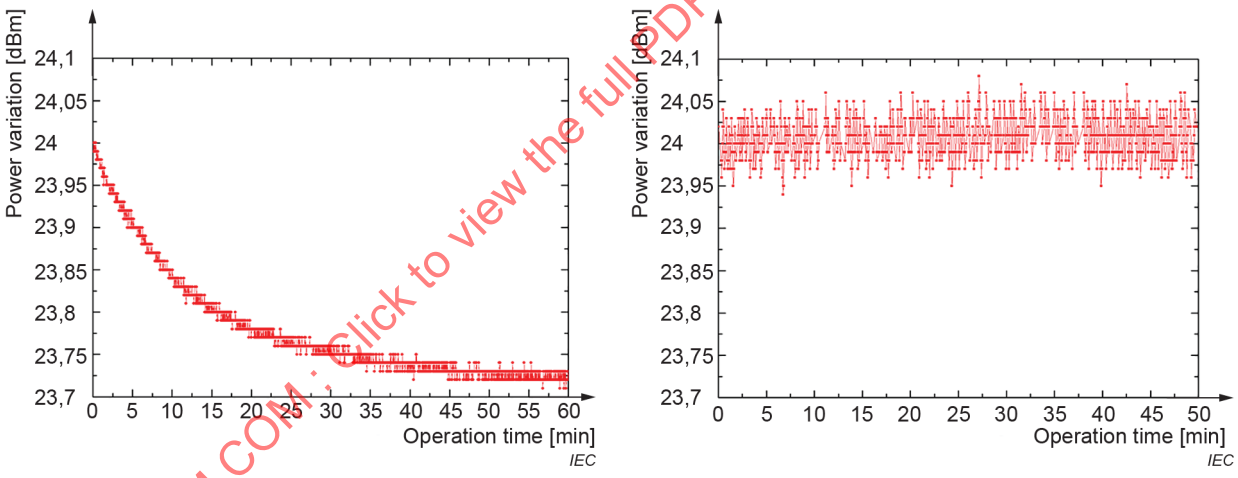
Automatic input power level control for system validation

V.1 General

The input power level (i.e. forward power to the antenna) in system validation and calibration should be stable enough for reliable measurements. Typically, the input power for system validation or probe calibration is controlled manually during the process, and the equipment needs time (e.g. half an hour) to warm up such that the power from the signal generator and amplifier stabilizes. For the reduction of the power uncertainty contribution, it is recommended to apply automatic input power level control (AIPLC) methodology. The AIPLC is applied to the system validation and probe calibration process, and helps to keep the input power constant during the tests by controlling the signal generator and/or the amplifier.

The expanded uncertainty for the SAR measurement system is limited to 30 %; therefore, for example a 5 % power drift contributes a significant amount to the total measurement uncertainty.

Figure V.1 shows the power drift before applying AIPLC (left) and after applying AIPLC (right), which can be compared with the power drift to operation time after its application.



a) Without AIPLC b) With AIPLC

Figure V.1 – Generated RF input power variations to operation time without and with application of AIPLC

IECNORM.COM : Click to view the full PDF of IEC/IEEE 62209-1528:2020

V.2 Operational mechanism of AIPLC

A schematic diagram of AIPLC scheme is shown in Figure V.2. A computer reads the power meter, and controls the signal generator or the amplifier automatically through GPIB or a RS-232C cable.

Two adjusting methods are available to control the RF power output level: one is to adjust the amplifier, and the other is to adjust the signal generator. Figure V.3 shows the power variation patterns when AIPLC is applied by adjusting the amplifier or the signal generator. The power variation by adjusting the amplifier is about ±0,125 dB (shown in Figure V.3 a)), whereas it is less than ±0,05 dB by adjusting the signal generator (shown in Figure V.3 b)).

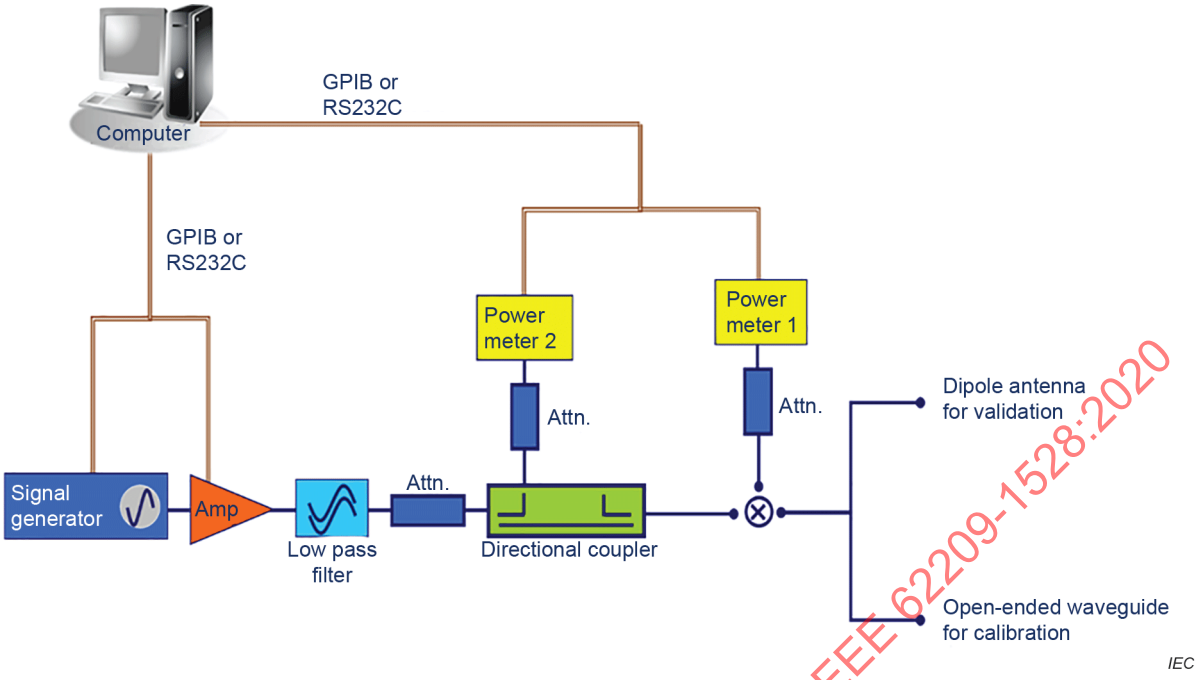
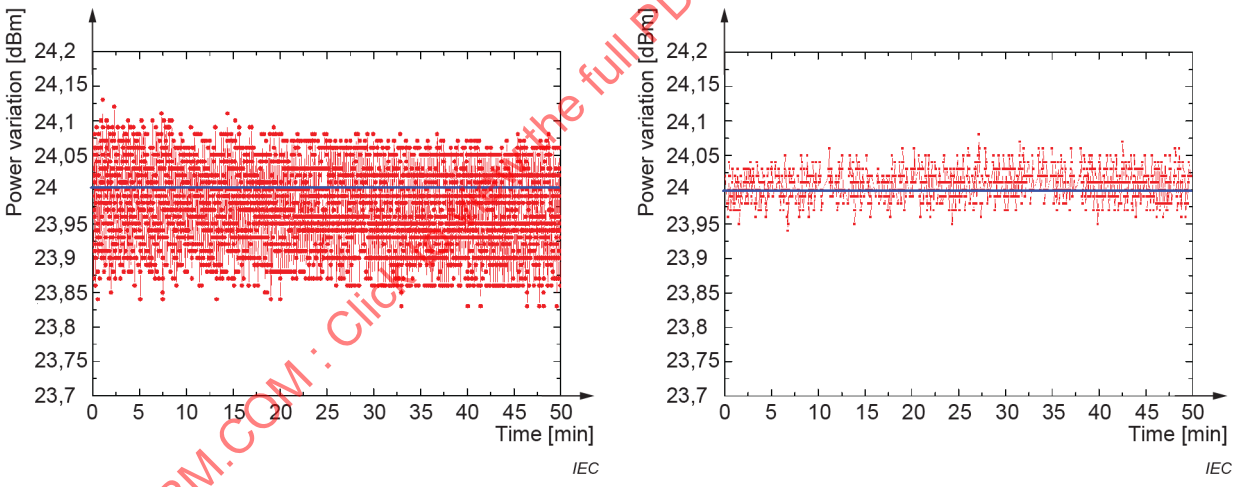


Figure V.2 – The system block diagram of the AIPLC



a) By adjusting the amplifier output **b) By adjusting the signal generator output**

NOTE Control step-size of signal generator is higher resolution than the amplifier.

Figure V.3 – Power variation characteristics by adjusting the amplifier or signal generator outputs

IECNORM.COM : Click to view the full PDF of IEC/IEEE 62209-1528:2020

Annex W
(informative)

LTE test configurations supporting information

W.1 General

The relationship between RF conducted power and psSAR is investigated using the following formula, where m indicates a specific LTE mode in a frequency band:

$$SAR(m) = \alpha(m) P(m) \quad \text{(W.1)}$$

The psSAR is proportional to conducted RF power P. However due to antenna mismatch, phantom coupling, and other conditions, the ratio between SAR and conducted power, designated as α, is expected to vary among the LTE modes (m). In order to evaluate the deviation of α among LTE modes, two independent studies were conducted, as described in Clause W.2 and Clause W.3.

W.2 Study 1

This study is fully described in [139], [140] and [141]. This study was performed according to the protocol in IEC 62209-1, and therefore refers to low, middle, and high channels. The protocol of 7.9.3.6 to commence SAR testing with the LTE mode having the highest conducted RF power was recommended after the results of Study 1 and Study 2 were combined. The following is a summary of the test configurations.

- Device type and characteristics: smart phones.
- Frequency and channels tested: band 1 (1 920 MHz to 1 980 MHz); low, middle, and high channels.
- Phantoms and test positions: SAM and flat.
- Conducted power measurement configurations: Figure W.1.

  NOTE Green colour bars in Figure W.1 mean measurements were not performed for these conditions, because these are the same as those with 20 MHz bandwidth (i.e. largest channel bandwidth used in device).

- Number of DUTs: four different devices from three different manufacturers.
- Number of measurements: 42, for both conducted power and SAR.

The results shown in Figure W.2 are summarized in the following list.

– Deviations: α has a relative standard deviation of less than 11,5 % (Table W.1).
– RF conducted power is the highest without maximum power reduction (MPR) for the devices with the highest psSAR.
– The deviation of α for the SAM phantom is slightly larger than for the flat phantom. This might be due to DUT placement uncertainty.

IECNORM.COM : Click to view the full PDF of IEC/IEEE 62209-1528:2020

Table W.1 – Relative standard deviation of α found in Study 1 (without MPR)

Phantom (test position)	Coefficient of variation [a]	
	SAR	
	1 g	10 g
Flat	7,90 %	7,90 %
SAM (Cheek)	9,90 %	9,40 %
SAM (Tilt)	11,40 %	10,90 %
[a] Coefficient of variation (CV) is the standard deviation divided by the average value.		

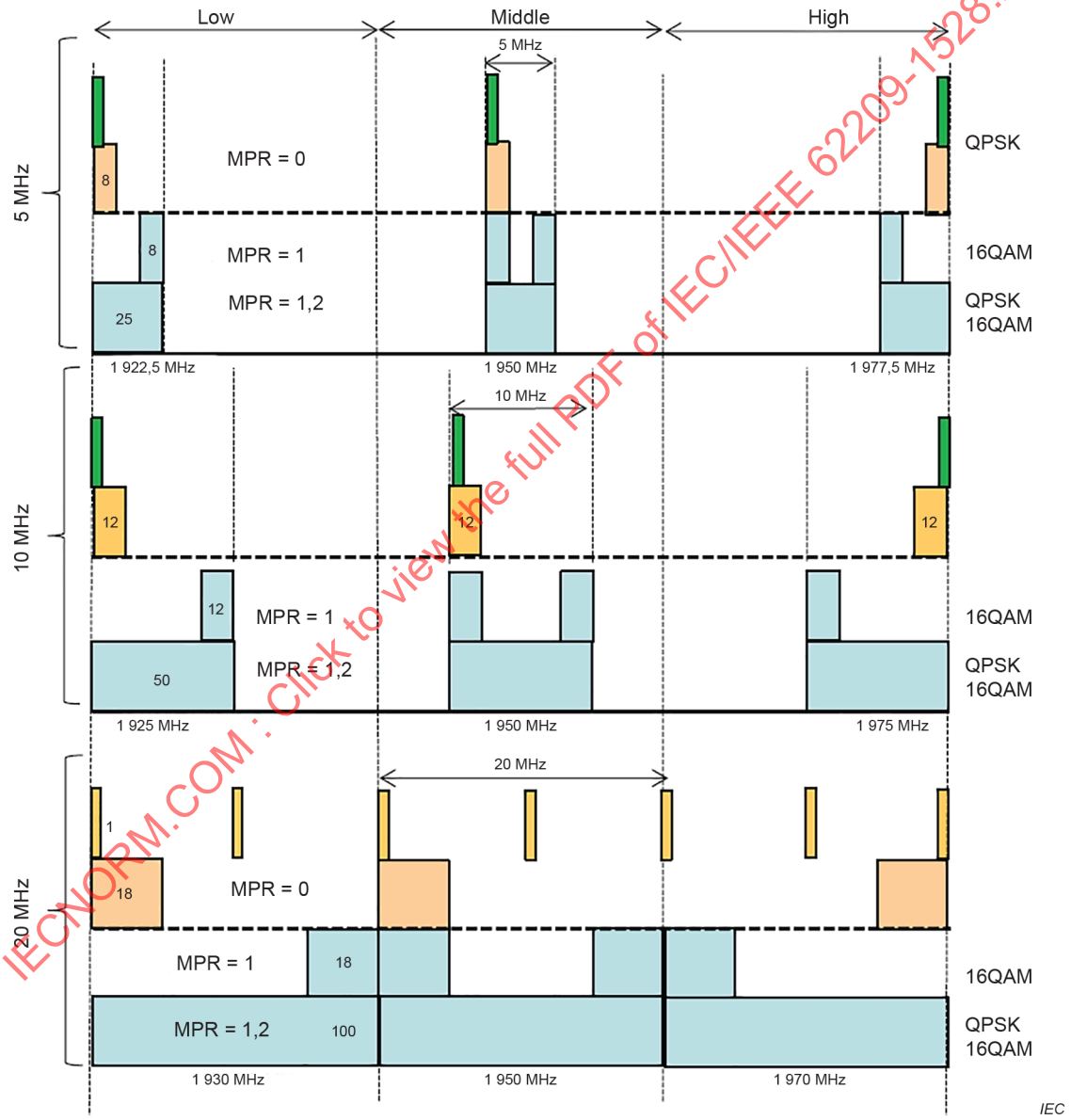
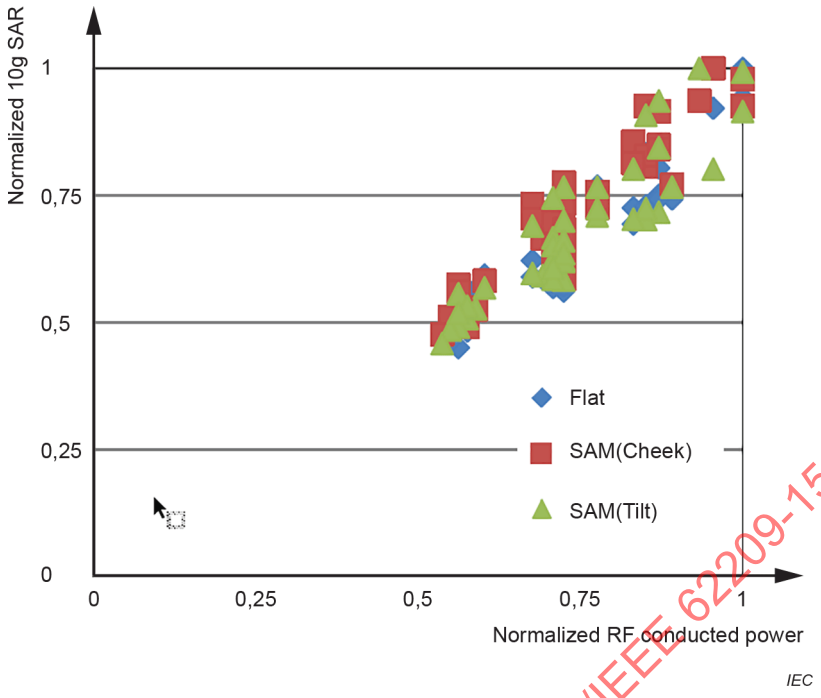


Figure W.1 – Low, middle, and high channels at 2 GHz band (Band 1)

IECNORM.COM : Click to view the full PDF of IEC/IEEE 62209-1528:2020



NOTE The three clusters of results along the horizontal axis are due to differences in maximum output power or MPR associated with the LTE modes tested for the LTE conditions.

Figure W.2 – RF conducted power versus 10 g psSAR

W.3 Study 2

This study is fully described in [33]. The test configurations are as follows.

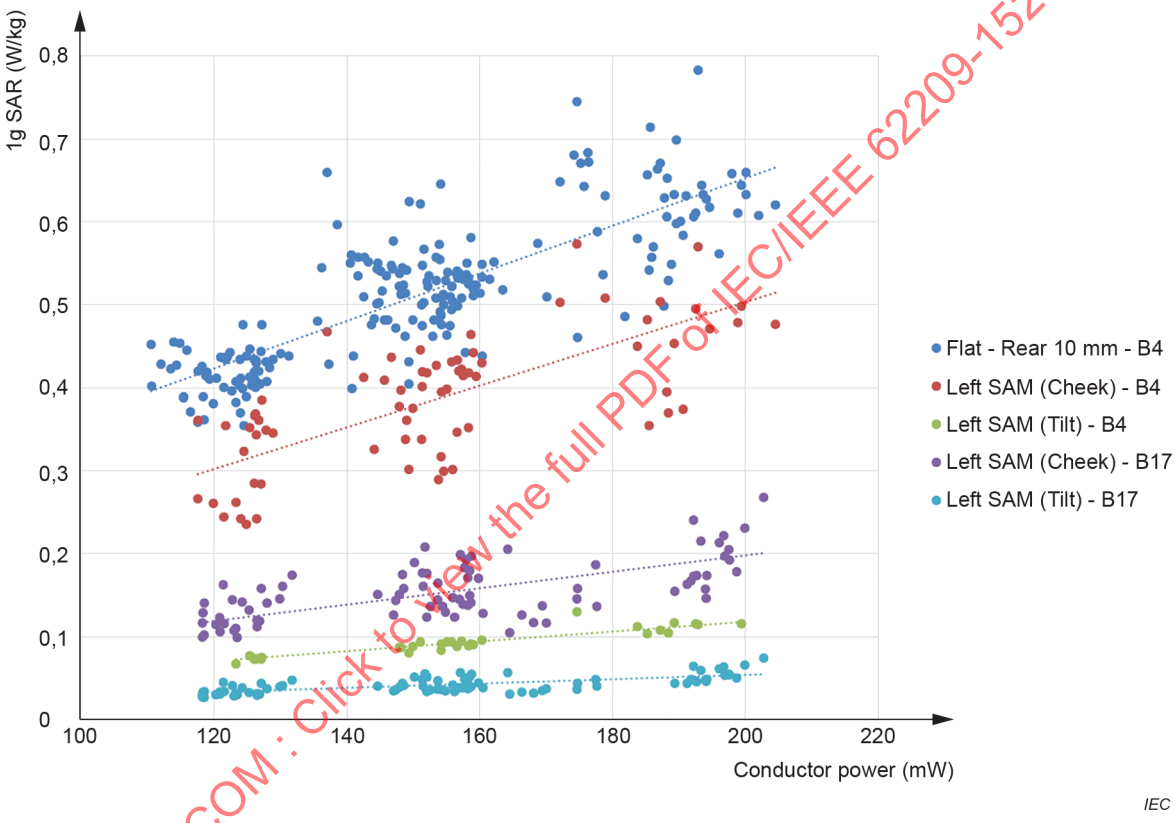
- Two DUTs.
- Positions: body rear 10 mm, SAM left-side cheek/tilt, SAM right-side cheek/tilt.
- Bands: LTE FDD band 4, LTE FDD band 17.
- Channels:
  - Band 4: 19975 (1 712,5 MHz), 20000 (1 715 MHz), 20025 (1 717,5 MHz), 20050 (1 720 MHz), 20175 (1 732,5 MHz), 20300 (1 745 MHz), 20325 (1 747,5 MHz), 20350 (1 750 MHz), 20375 (1 752,5 MHz);
  - Band 17: 23755 (706,5 MHz), 23780 (709 MHz), 23790 (710 MHz), 23800 (711 MHz), 23825 (713,5 MHz), 23825 (713,5 MHz).
- Bandwidths:
  - Band 4: 5 MHz, 10 MHz, 15 MHz, 20 MHz;
  - Band 17: 5 MHz, 10 MHz.
- RB sizes:
  - Band 4: 1, 12, 25, 36, 50, 75, 100;
  - Band 17: 1, 12, 25, 50.
- RB offsets:
  - Band 4: 0, 6, 12, 13, 18, 24, 25, 36, 39, 49, 50, 74, 99;
  - Band 17: 0, 6, 12, 24, 25, 49.
- Modulations: QPSK, 16-QAM.
- Number of measurements: 2 510.

IECNORM.COM : Click to view the full PDF of IEC/IEEE 62209-1528:2020

A summary of the measurements including LTE modes, conducted power measurements, device positions, and test conditions can be found in [33]. Figure W.3 and Table W.2 show the results.

Table W.2 – Maximum relative standard deviation of α found in Study 2 (with MPR)

Phantom (test position)	Coefficient of variation
	1 g SAR
Flat	12,90 %
SAM (Cheek)	17,10 %
SAM (Tilt)	16,80 %



NOTE The three clusters of results along the horizontal axis are due to differences in maximum output power or MPR associated with the LTE Modes tested for the LTE Conditions. Dashed lines indicate linear regressions.

Figure W.3 – 1 g SAR as a function of RF conducted power in various test conditions

IECNORM.COM : Click to view the full PDF of IEC/IEEE 62209-1528:2020

W.4 Justifications of relative standard deviations

The probability density function of the ratio of two normal random variables was derived by Hinkley in [142]. Assuming the peak spatial-average SAR for a given LTE mode m is a random normal variable with a maximum of 15 % relative standard deviation (30 % k = 2 uncertainty), and the conducted power $P(m)$ is a random normal variable with a maximum 5 % relative standard deviation, then $\alpha(m)$ follows a distribution as described by Hinkley such that:

a) if $SAR(m)$ and $P(m)$ are uncorrelated, then the 95 % confidence interval of $\alpha(m)$ is about 31 % maximum, or ±15,5 % on average;

b) if $SAR(m)$ and $P(m)$ correlate with a coefficient of more than 0,9, then the 95 % confidence interval of $\alpha(m)$ is about 22 % maximum, or ±11 % on average.

In other words, for the preceding assumption, the k = 2 uncertainty of $\alpha(m)$ determination for a given LTE mode m can be as high as 15,5 %. In addition, $\alpha(m)$ varies with the mode m, so that relative standard deviation of α across modes is likely to be higher than 8 %.

To investigate the highest relative standard deviation that can be expected, 100 samples of $\alpha(m)$ were artificially generated as the output of a ratio of two uncorrelated normal random variables, $SAR(m)$ and $P(m)$, with respective relative standard deviations of 15 % and 5 %. For a mode $m1$, $SAR(m1)$ was chosen with a mean value of 0,66 W/kg and a mean conducted power $P(m1)$ of 137 mW. For a mode $m2$, the average of $SAR(m2)$ and $P(m2)$ were chosen respectively equal to 0,66 W/kg and 124,5 mW. In fact, $\alpha(m1)$ and $\alpha(m2)$ were logically found to exhibit an average relative difference over the 100 realizations of about 10 %. However, the maximum relative difference on a specific set of realizations of $\alpha(m1)$ and $\alpha(m2)$ was observed to be as high as 54 %. This approach is conservative, because the entire uncertainty budget of the measurement system is not exploited when comparing SAR values across LTE modes in a given position. In addition, averaging the uncertainty contributions across a variety of modes decreases the overall observed dispersion of α. Based on this analysis, a 95th percentile value of 1,35 for α has been determined to be conservative, as applied in 7.9.3.6.3.

IECNORM.COM : Click to view the full PDF of IEC/IEEE 62209-1528:2020

Bibliography

[1] IEC TR 62630:2010, *Guidance for evaluating exposure from multiple electromagnetic sources*

[2] Drossos, A., Santomaa, V., and Kuster, N., "The dependence of electromagnetic energy absorption upon human head tissue composition in the frequency range of 300-3000 MHz," IEEE Trans. Microwave Theory Tech., Nov. 2000, vol. 48, no. 11, pp. 1988–1995

[3] ICNIRP, "International Commission on Non-Ionizing Radiation Protection guidelines for limiting exposure to time-varying electric, magnetic and electromagnetic fields (Up to 300 GHz)," Health Physics, Vol. 74, No. 4, pp. 494–522, 1998

[4] IEEE Std C95.1-2019, *IEEE Standard for Safety Levels with Respect to Human Exposure to Radio Frequency Electromagnetic Fields, 3 kHz to 300 GHz*

[5] Francavilla, M., Schiavoni, A., Bertotto, P., and Richiardi, G., "Effect of the hand on cellular phone radiation," IEE Proceedings Microwaves, Antennas and Propagation, Vol. 148, No. 4, pp. 247–253, Aug. 2001

[6] Gandhi, O. P., Lazzi, G., and Furse, C. M., "Electromagnetic absorption in the human head and neck for mobile telephones at 835 and 1900 MHz," IEEE Transactions on Microwave Theory and Techniques, Vol. 44, No. 10, pp. 1884–1897, Oct. 1996

[7] Jensen, M. A., and Rahmat-Samii, Y., "Performance analysis of antennas for hand-held transceivers using FDTD," IEEE Transactions on Antennas and Propagation, Vol. 42, No. 8, pp. 1106–1113, Aug. 1994

[8] Jensen, M. A. and Rahmat-Samii, Y., "EM interaction of handset antenna and a human in personal communications," Proceedings of the IEEE, vol. 83, no.1, pp. 7–17, Jan. 1995

[9] Kuster, N., Kästle, R., and Schmid, T., "Dosimetric evaluation of mobile communications equipment with known precision," IEICE Trans. Commun., May 1997, vol. E80-B, no. 5, pp. 645–652

[10] Watanabe, S., Taki, M., Nojima, T., and Fujiwara, O., "Characteristics of the SAR distribution in a head exposed to electromagnetic fields radiated by a hand-held portable radio," IEEE Transactions on Microwave Theory and Techniques, Vol. 44, No. 10, pp. 1874–1883, Oct. 1996

[11] IEEE Std 1528, *Recommended Practice for Determining the Peak Spatial-Average Specific Absorption Rate (SAR) in the Human Head from Wireless Communications Devices: Measurement Techniques*, New York: Institute Electrical and Electronics Engineers, Sep. 2013

[12] Balzano, Q., Garay, O., and Manning, T., "Electromagnetic energy exposure of the users of portable cellular telephones," IEEE Transactions on Vehicular Technology, Vol. 44, No. 3, pp. 390–403, Aug. 1995

[13] Meyer, F. J. C., Palmer, K. D., and Jakobus, U., "Investigation into the accuracy, efficiency and applicability of the method of moments as numerical dosimetry tool for the head and hand of a mobile phone user," Applied Computational Electromagnetics Society Journal, Vol. 16, No. 2, pp. 114–125, July 2001

IECNORM.COM : Click to view the full PDF of IEC/IEEE 62209-1528:2020

[14] Beard, B. B., et al., “Comparisons of Computed Mobile Phone Induced SAR in the SAM Phantom to that in Anatomically Correct Models of the Human Head,” IEEE Transactions on Electromagnetic Compatibility, Vol. 48, No. 2, May 2006

[15] Bit-Babik, G., “Computational comparison of SAR in SAM phantom and anatomically correct head models at 300 MHz–5.8 GHz: Summary comparison of the results,” report to ICES TC34 SC1, October 2008

[16] Kainz, W., et al., “Dosimetric comparison of the specific anthropomorphic mannequin (SAM) to 14 anatomical head models using a novel definition for the mobile phone positioning,” Phys. Med. Biol., Vol. 50, pp. 3423–3445, July 2005

[17] ISO/IEC 17025:2017, *General requirements for the competence of testing and calibration laboratories*

[18] IEC TR 62905:2018, *Exposure assessment methods for wireless power transfer systems*

[19] Di Nallo, C., and Faraone, A., “Effect of amplitude modulation of the CDMA IS-95 signal on SAR measurements,” IEEE Transactions on Electromagnetic Compatibility, vol. 48, no. 3, pp. 552–562, August 2006

[20] Nadakuduti, J., Kühn, S., Fehr, M., Douglas, M., Poković, K., and Kuster, N., "Effect of Diode Response of Electromagnetic Field Probes for the Measurements of Complex Signals," IEEE Transactions on Electromagnetic Compatibility, vol. 54, no. 6, pp. 1195–1204, December, 2012

[21] IEC 106/465/INF, *Supporting Information for Amendment 1 to IEC 62209-2 Ed.1 (Document 106/460/CDV)*, 2018-07-27

[22] Poković, K., “Advanced Electromagnetic Probes for Near Field Evaluation,” Doc. Tech. Sci. Diss. ETH Nr. 13334. Switzerland, Zurich: Swiss Federal Institute of Technology, 1999

[23] Bolomey, J. C., “Efficient near-field techniques for human exposure evaluation: Applications to mobile and fixed antennas,” presented at the Electromagnetic Environment and Human Exposure Evaluation Workshop of EMC, Sorrento, Italy, 2002

[24] Kanda, M. Y., Douglas, M.G., Mendivil, E. D., Ballen, M., Gessner, A. V. Chou, C-K., “Faster Determination of Mass-Averaged SAR From 2-D Area Scans,” IEEE Transactions on Microwave Theory and Techniques, vol. 52, no. 8, pp. 2013–2020, August, 2004

[25] Manning, M., Massey, P., “Rapid SAR testing of mobile phone prototype using a spherical test geometry,” in IEE Tech. on Antenna Measurements and SAR Seminar, Loughborough, U.K., May 28–29, 2002

[26] Merckel, O., Fleury, G., Bolomey, J.-C., “Rapid SAR measurement via parametric modeling,” Proc. 5th International Congress of the European BioElectromagnetics Association (EBEA), p. 75–77, Helsinki, Finland, Sep. 2001

[27] Merckel, O., Bolomey, J.-Ch., Joisel, A., “Near-field approach to Rapid SAR Measurement of Mobile Phones,” Symp. of the Association for Measurement and Testing of Antennas (AMTA 2003), Irvine, Denver, USA, Oct. 2003

IECNORM.COM : Click to view the full PDF of IEC/IEEE 62209-1528:2020

[28] Douglas, M.G., Kanda, M.Y., Luengas, W.G., Ballen, M., Babij, T.M. and Chou, C-K., "An Algorithm for Predicting the Change in SAR in a Human Phantom due to Deviations in its Complex Permittivity," IEEE Transactions on Electromagnetic Compatibility, 2007, vol. 51, no 2, May 2009

[29] Douglas, M.G., and Chou, C-K., "Enabling the Use of Broadband Tissue Equivalent Liquids for Specific Absorption Rate Measurements," IEEE Electromagnetic Compatibility Symposium, July 2007

[30] Kuster, N. and Balzano, Q., "Energy absorption mechanism by biological bodies in the near field of dipole antennas above 300 MHz," IEEE Transactions on Vehicular Technology, Vol. 41, No. 1, pp. 17–23, Feb. 1992

[31] Bit-Babik, G., Faraone, A., Ballen, M. and Chou, C-K., "Sensitivity of the Spatial-Average Peak SAR to the Dielectric properties of Media Used for Compliance Testing in the Frequency Range 0.3 – 3 GHz," Antennas and Propagation Society International Symposium Digest, Vol. 3, pp. 722–725, June 2002

[32] IEC 62479:2010, *Assessment of the compliance of low-power electronic and electrical equipment with the basic restrictions related to human exposure to electromagnetic fields (10 MHz to 300 GHz)*

[33] Derat, B., "Experimental Study on the Relationship between Specific Absorption Rate and RF Conducted Power for LTE Wireless Devices," Proc. European Microwave Conf., Paris, France, Sep. 2015

[34] IEC 62311:2019, *Assessment of electronic and electrical equipment related to human exposure restrictions for electromagnetic fields (0 Hz to 300 GHz)*

[35] ISO/IEC Guide 98-1:2009, *Uncertainty of measurement – Part 1: Introduction to the expression of uncertainty in measurement*

[36] Onishi, T. and Uebayashi S., "Influence of phantom shell on SAR measurement in 3-6 GHz frequency range," IEICE Trans. Commun., vol., E88-B, no. 8, pp. 3257–3262, 2005

[37] Niskala, K., "Multimode SAR test reduction," Final report, IEC MT1 meeting, Tokyo-Japan, May 2014

[38] Schiavoni, A., Francavilla, M., Forigo, D., Deplano, M., "A Procedure to Reduce the Qualification Time in SAR Compliance Tests," BEMS 2005, June 2005

[39] Francavilla, M., "Time reduction in SAR compliance of GSM/UMTS mobile phones," BEMS 2011, Halifax, Canada, June 2011

[40] Montgomery, D.C., Design and Analysis of Experiments (4th edition), New York: John Wiley and Sons. (1997)

[41] IEC/IEEE 62704-1:2017, *Determining the peak spatial-average specific absorption rate (SAR) in the human body from wireless communications devices, 30 MHz to 6 GHz – Part 1: General requirements for using the finite-difference time-domain (FDTD) method for SAR calculations*

[42] IEC 60154-2, *Flanges for waveguides – Part 2: Relevant specifications for flanges for ordinary rectangular waveguides*

IECNORM.COM : Click to view the full PDF of IEC/IEEE 62209-1528:2020

[43] IEEE Std C95.3-2002, *IEEE Recommended Practice for Measurements and Computations of Radio Frequency Electromagnetic Fields With Respect to Human Exposure to Such Fields, 100 kHz–300 GHz*

[44] Loader, B., "Computer Simulation of WR159 Waveguide against a Flat Dielectric Phantom at 5.2 GHz and 5.8 GHz," NPL Report DEM EM 008, 2007

[45] Choi, D.-G., Kim, K.-H., Choi, J.-H., "New Numerical Target SAR Values and an Optimized Flat Phantom for SAR Validation Test in the 150 MHz Band," IEICE TRANS. COMMUN., Vol. E98-B, No. 7, July 2015

[46] Kim, K.-H., Jang, J.-D., Chung, S.-Y., and Gimm, Y.-M., "A Study on the Meander-Type Dipole Antenna for SAR Validation Test at 150 MHz Band," Proceedings of 2016 URSI AP-RASC (Asia-Pacific Radio Science Conference), pp. 911–913, August 21–25, 2016, Grand Hilton Seoul Hotel, Seoul, Korea

[47] Kim, K.-H., Choi. D.-G., Gimm, Y.-M., "Automatic RF Input Power Level Control Methodology for SAR Measurement Validation," Journal of Electromagnetic Engineering and Science, Vol. 15, No. 3, pp. 181–184, Jul. 2015

[48] Meier, K., Burkhardt, M., Schmid, T., and Kuster, N., "Broadband calibration of E-field probes in lossy media," IEEE Trans. Microwave Theory Tech., Oct. 1996, vol. 44, no. 10, pp. 1954-1962

[49] Person, C., Tanné, G., Ahlonsou, L.N, Ngounou, C., and Grangeat, C., "New reference antennas for SAR probe calibration in tissue equivalent liquid," Millennium Conference on Antennas and Propagation, AP2000, Davos, Switzerland: April 9–14, 2000

[50] Kuster, N., and Balzano, Q., "Experimental and numerical dosimetry," in Kuster, N., Q. Balzano, and J. C. Lin, eds., Mobile Communications Safety, New York: Chapman & Hall, pp. 13–64, 1997

[51] Jokela, K., Hyysalo, P., and Puranen, L., "Calibration of specific absorption rate (SAR) probes in waveguide at 900 MHz," IEEE Trans. Instrumen. Meas., Apr. 1998, vol. 47, no. 2, pp. 432-438

[52] Magee, J. W., "Molar heat capacity (Cv) for saturated and compressed liquid and vapor nitrogen from 65 to 300 K at pressures to 35 MPa," Journal of Research of the National Institute of Standards and Technology, Vol. 96, No. 6, pp. 725–740, Nov./Dec. 1991

[53] Poković, K., Schmid, T., and Kuster, N., "Robust setup for precise calibration of E-field probes in tissue simulating liquids at mobile communication frequencies," in Proceedings ICECOM '97. Dubrovnik, Croatia, Oct. 12–17, 1997, pp. 120–124

[54] EIA RS-261-B: 1979, Rectangular Waveguides (WR3 to WR2300)

[55] Person, C., Ahlonsou, L.N, and Grangeat, C., "New test bench for the characterization of SAR measurement probes used in tissue equivalent liquids," Bioelectromagnetics Society 22nd Annual Meeting, Munich Germany, June 11–16, 2000

[56] Ishii, N., Sato, K., Hamada, L., Watanabe, S., "Gain calibration in near-field region of antenna in tissue-equivalent liquid for SAR assessment," 2008 Asia-Pacific Symposium on Electromagnetic Compatibility, Singapore, pp.112–115, May, 2008

[57] Loader, B. G, Gregory, A.P., and Bownds, D., "Coaxial artefact standard for specific absorption rate 100 kHz to 400 MHz," Progress in Electromagnetic Research Symposium (PIERS), 23–27 March, 2009, Beijing, China

IECNORM.COM : Click to view the full PDF of IEC/IEEE 62209-1528:2020

[58] Faraone, A., McCoy, D.O., Chou, C.K., and Balzano, Q., “Characterization of miniaturized E-field probes for SAR measurements,” IEEE Intl. Symp. Electromag. Compat., Washington, DC, 2000, pp. 749–754

[59] Fukunaga, K., Watanabe, S., Wake, K. and Yamanaka, Y., "Time dependence of tissue-equivalent dielectric liquid materials and its effect on SAR," EMC Europe Symp., Sorrento, Italy, Sep. 2002

[60] Loader, B. G., Gregory A.P., Mouthaan, R., “Formulation and properties of liquid phantoms 1 MHz to 10 GHz,” NPL Report TQE 9, June 2017

[61] Gordon, C.C., Churchill, T., Clauser, C.E., Bradtmiller, B., McConville, J.T., Tebbetts, I., and Walker, R.A., “1988 Anthropometric Survey of U.S. Army Personnel: Methods and Summary Statistics,” Technical Report NATICK/TR-89/044, U.S. Army Natick Research, Development and Engineering Center, Massachusetts: Natick, Sep. 1989

[62] Lee, A.K., and Pack, J.K., “Effect of head size for cellular telephone exposure on EM absorption,” IEICE Trans. Commun., Mar. 2002, vol. E85-B, no. 3, pp. 698–701

[63] Lee, A.K., Choi, H.D., Lee, H.S., and Pack, J.K., “Human head size and SAR characteristics for handset exposure,” ETRI J., Apr. 2002, vol. 24, no. 2, pp. 176–179

[64] Leisten, O., Vardaxaglou, Y., Schmid, T., Rosenberger, B., Agboraw, E., Kuster, N. and Nicolaidis, G., “Miniature dielectric-loaded personal telephone antennas with low user exposure,” Electron. Lett., Aug. 20, 1998, vol. 34, no. 17, pp. 1628–1629

[65] Schönborn, F., Burkhardt, M., and Kuster, N., “The difference of EM energy absorption between adults and children,” Health Phys., Feb. 1998, vol. 74, no. 2, pp. 160–168

[66] Keshvari, J., Kivento, M., Christ, A., and Bit-Babik, G., “Large scale study on the variation of RF energy absorption in the head & brain regions of adults and children and evaluation of the SAM phantom conservativeness,” Physics in Medicine & Biology, 61(8), 2991, 2016

[67] Hirata, A., Ito, F., and Laakso, I., "Confirmation of quasi-static approximation in SAR evaluation for a wireless power transfer system," Physics in Medicine and Biology, vol. 58, p. N241, 2013.

[68] Laakso, I., Shimamoto, T., Hirata, A., and Feliziani, M., "Quasistatic Approximation for Exposure Assessment of Wireless Power Transfer," IEICE Transactions on Communications, vol. E98.B, pp. 1156–1163, 2015

[69] Gabriel, S., Lau, R.W., and Gabriel, C., “The dielectric properties of biological tissues: 3. Parametric models for the dielectric spectrum of tissues,” Phys. Med. Bio., 1996, vol. 41, no. 11, pp. 2271–2293

[70] Christ, A., Klingenböck, A., Samaras, T., Goiceanu, C., and Kuster, N., “The dependence of electromagnetic far-field absorption on body tissue composition in the frequency range from 300 MHz to 6 GHz,” IEEE Transactions on Microwave Theory and Techniques, vol. 54, no. 5, pp. 2188–2195, May 2006

[71] Christ, A., Samaras, T., Klingenböck, A., and Kuster, N., “Characterization of the electromagnetic near-field absorption in layered biological tissue in the frequency range from 30 MHz to 6000 MHz,” Physics in Medicine and Biology, vol. 51, no. 19, October 2006

IECNORM.COM : Click to view the full PDF of IEC/IEEE 62209-1528:2020

[72] Kangas, I., and Hyttinen, J., “Thermal Simulations for Anatomical Human Models, Part III of Dielectric properties for Tissue Simulating Liquids Study: Extension and Validation Covering a Frequency Range from 30 MHz to 6 GHz,” Technical Report, Tampere University of Technology, April 22, 2016

[73] Christ, A., et al. “The Virtual Family—development of surface-based anatomical models of two adults and two children for dosimetric simulations,” Physics in Medicine & Biology, vol. 55, no. 2, p. N23, 2009

[74] Poković, K., Christ, A., Samaras, T., Douglas, M., Kuster, N., “Methods and Instrumentation for Reliable Experimental SAR Assessment at 6 – 10 GHz,” The joint annual meeting of the Bioelectromagnetics Society and the European BioElectromagnetics Association, Hangzhou, China, June 5–9, 2017

[75] Chou, C.-K., Chen, G.W., Guy, A.W. and Luk, K.H., “Formulas for preparing phantom muscle tissue at various radiofrequencies,” Bioelectromag., 1984, vol.5, pp. 435–441

[76] Von Hippel, A., Dielectric Materials and Applications. Cambridge: MA: MIT Press, 1954

[77] Blackham, D.V., and Pollard, R.D., “An improved technique for permittivity measurements using a coaxial probe,” IEEE Trans. Instrumen. Meas., Oct. 1997, vol. 46, no. 5, pp. 1093–1099

[78] Gabriel, C., Chan, T.Y.A, and Grant, E.H., “Admittance models for open ended coaxial probes and their place in dielectric spectroscopy,” Phys. Med. Biol., 1994. vol. 39, no.12, pp. 2183–2200

[79] Pournaropoulos, C.L., and Misra, D.K., “The co-axial aperture electromagnetic sensor and its application in material characterization,” Meas. Sci. Tech., 1997, vol. 8, pp. 1191–1202

[80] Arai, M.J., Binner, G.P., and Cross, T.E., “Estimating errors due to sample surface roughness in microwave complex permittivity measurements obtained using a coaxial probe,” Electron. Lett., Jan. 19, 1995, vol. 32, no. 2, pp. 115–117

[81] Bao, J.Z, Swicord, M.L., and Davis, C.C., “Microwave dielectric characterization of binary mixtures of water, methanol, and ethanol,” J. Chem. Phys., Mar. 12, 1996, vol. 104, no. 12, pp. 4441–4450

[82] Clarke, R.N., Gregory, A.P., Hodgetts, T.E., and Symm, G.T., “Improvements in coaxial sensor dielectric measurement: relevance to aqueous dielectrics and biological tissue,” in Microwave Aquametry: Electromagnetic Wave Interaction With Water-containing Materials, A. Kraszewski, ed., New York: IEEE Press, 1996, pp. 279–297

[83] Mosig, J.R., Besson, J.C.E, Gex-Fabry, M., and Gardiol, F.E., “Reflection of an open-ended coaxial line and application to non-destructive measurement of materials,” IEEE Trans. Instrumen. Meas., 1981, IM-30, pp 46–51

[84] Nevels, R.D., Butler, C.M., and Yablon, W., “The annular slot antenna in a lossy biological medium,” IEEE Trans. Microwave Theory Tech., 1985, MTT-30, pp 314–319

[85] Toropainen, A., Vainikainen, P., and Drossos, A., “Method for accurate measurement of complex permittivity of tissue equivalent liquids,” Electron. Lett., 2000, vol. 36, no. 1, pp. 32–34

[86] Hill, N.E., Vaughan, W.E., Price, A.H., and Davies, M., *Dielectric Properties and Molecular Behaviour*, London: Van Nostrand Reinhold, 1969

IECNORM.COM : Click to view the full PDF of IEC/IEEE 62209-1528:2020

[87] Gabriel, S., Lau, R. W., and Gabriel, C., “The dielectric properties of biological tissues: II. Measurement in the frequency range 10 Hz to 20 GHz,” Physics in Medicine and Biology, Vol. 41, No. 11, pp. 2251–2269, 1996

[88] Kaatze, U., “Complex permittivity of water as function of frequency and temperature,” J. Chem. Engin. Data, 1989, vol. 34, no. 4, pp. 371–374

[89] Gregory, A.P. and Clarke, R.N., “Tables of the Complex Permittivity of Dielectric Reference Liquids at Frequencies up to 5 GHz,” NPL Report MAT 23, Materials Division, Teddington, England: National Physical Laboratory, Revised Jan 2012, ISSN 1754-2979

[90] Rocher, F., Julien, T., Derat, B., "Impact of a Hand Phantom on the Measured Average SAR," presentation to ICES TC-34 committee, December 11, 2008

[91] Bit-Babik, G., Summary and Review of the SAM Study Phase III, April 2012

[92] Derat, B., Gabriel, S., Faraone, A., “Hand effect measurement interlab: final report,” presentation to IEC MT 62209, August 2011

[93] Derat, B., Gabriel, S., Faraone, A., “Hand effect measurement interlab: Conclusions of the study,” presentation to IEC MT 62209, Dec 2011

[94] Christ, A., “Analysis of the exposure of the hand and its impact on the absorption in the heads of cell phone users,” presentation to IEC MT 62209, January 2013

[95] Kuster, N., Douglas, M., "Proposal for inclusion of the hand for IEC 62209," IEC MT 62209 meeting, Thessaloniki Greece, June 2013

[96] Douglas, M., Bucher, C., Ofli, E., Derat, B., Gabriel, S., Kuster, N., "Investigation of the influence of the Hand on Head SAR," IEC MT 62209 meeting, Newbury UK, March 2010

[97] Douglas, M., Kuster, N., "Summary of two studies of hand effect on SAR in head," IEC MT 62209 meeting, Brisbane Australia, June 17, 2012

[98] Li, C-H., Douglas, M., Ofli, E. Derat, B. and Kuster, N., "Investigation of the influence of the Hand on Head SAR," report to IEC PT 62209 MT-1, April, 2010

[99] Nesterova, M., Review of Head-Hand Studies between 1997-1999, April 2012

[100] Kivento, M., Keshvari, J., “Hand effect during the use of real mobile phones,” Jan 2013

[101] Park, G. B., Joyner, K., Jang, J. D. ”Modified DUT Holder for SAR Measurement,” IEC 62209 MT1 Meeting Turin, 11–13 Sept. 2012

[102] Joyner, K., Jang, J.D., Park, G.B., Park, Y. H., “2nd Modified DUT Holder for SAR measurement,” IEC 62209 MT1 Meeting, Ft Lauderdale, 22–24 Jan. 2013

[103] Joyner K., “The Case to Exclude the Hand,” IEC 62209 MT1 Meeting, Newbury, 7–9 May 2013

[104] Monebhurrun, V., Wong, M. F., Gati, A., Wiart, J., “Study of the influence of the hand on the specific absorption rate evaluation of mobile phones,” in Proc. URSI, Istanbul, Aug. 2011

IECNORM.COM : Click to view the full PDF of IEC/IEEE 62209-1528:2020

[105] Monebhurrun, V., Wong, M. F., Gati, A., Wiart, J., “Numerical and experimental investigations of the influence of the hand on the specific absorption rate evaluations of mobile phones,” in Proc. 33rd Annual Meeting of the Bioelectromagnetics Society, Halifax, June 2011

[106] Monebhurrun, V., “Influence of the hand on the specific absorption rate assessments of mobile phones,” Microwave Optical Technology Letters, 54, 3, 2012, pp. 654–656

[107] Monebhurrun, V., “Study of the influence of a CTIA hand phantom on the specific absorption rate measurements of mobile phones,” in Proc. BioEM 2013, Thessaloniki, June 2013

[108] Francavilla, M. and Schiavoni, A., "Effect of the Hand in SAR Compliance Tests of Body Worn Devices," Applied Computational Electromagnetic Society Conference, Verona, Italy, March 21, 2007

[109] Li, C.H., Douglas. M., Ofli, E., Chavannes, N., Balzano, Q., Kuster, N., "Mechanisms of RF Electromagnetic Field Absorption in Human Hands and Fingers," IEEE Transactions on Microwave Theory and Techniques, vol. 60, no. 7, pp. 2267–2276, July 2012

[110] Li, C.H., Douglas, M., Ofli, E., Derat, B., Gabriel, S., Chavannes, N., Kuster, N., "Influence of the Hand on the Specific Absorption Rate in the Head from a Mobile Phone," IEEE Transactions on Antennas and Propagation, vol. 60, no. 2, pp. 1066–1074, February 2012

[111] Li, C.-H., Ofli, E., Chavannes, N., and Kuster, N., “Effects of hand phantom on mobile phone antenna performance,” IEEE Transactions on Antennas and Propagation, vol. 57, no. 9, pp. 2763–2770, Sep. 2009

[112] CTIA, “CTIA test plan for wireless device over-the-air performance, revision 3.7.1,” CTIA Wireless Association, Feb. 2018

[113] Greiner, T.M., “Hand Anthropometry of US Army Personal,” Army Natick Research Development and Engineering Center, Technical Report Natick/TR-92/011, Dec. 1991

[114] Tilley, A.R., and Henry Dreyfuss Associates, “The Measure of Man and Woman: Human Factors in Design,” Wiley, Dec. 31, 2001

[115] Buchholz, B., Armstrong, T.J. and Goldstein, S.A., “Anthropometric data for describing the kinematics of the human hand,” Ergonomics vol. 35, no. 3, pp. 261–273, 1992

[116] Bugbee, W.D., and Botte, M.J, “Surface Anatomy of the Hand: The Relationships Between Palmar Skin Creases and Osseous Anatomy,” Clinical Orthopaedics and Related Research, 296, 122–126, 1993

[117] Derat, B., "Impact of the hand on the averaged SAR in the head: simulation of a CAD phone model," presentation to IEC PT62209 MT-1, April 22, 2009

[118] Pelosi, M., Franek, O., Knudsen, M. B., Christensen, M., and Pedersen, G. F., “A grip study for talk and data modes in mobile phones,” IEEE Transactions on Antennas and Propagation, vol. 57, no. 4, pp. 856–865, Apr. 2009

[119] Pelosi, M., Franek, O., Pedersen, G.F., Knudsen, M., "User's Impact on PIFA Antennas in Mobile Phones," IEEE 69th Vehicular Technology Conference, Barcelona, Spain, 26–29 April 2009

IECNORM.COM : Click to view the full PDF of IEC/IEEE 62209-1528:2020

[120] Wu, T., Lin, X., Yang, J., Zhao, C., Zhang, C. and Shao, Q., "TD-SCDMA Mobile Phone's SAR Measurement about OTA Hand Phantom," Progress in Electromagnetics Research Symposium, Xi'an, China, March 22–26, 2010

[121] Pradier, A., Colas, O., Celin, P., Sarrebourse, T., Laudru, D., Wong, M.-F., Fouad Hanna, V., Wiart, J. "Evaluation of the Specific Absorption Rate Induced by the Handset Close to the Body," in BEMS 28th Annual Meeting, 2006

[122] Diller, K.R., Adapting adult scald safety standards to children (2006) J Burn Care Res 27: 314–22

[123] Gemperle, F., Kasabach, C., Stivoric, J., Bauer, M., and Martin, R., *Design for Wearability*, Techn. Rep. [online]. Carnegie Mellon University, PA (USA) [viewed 2019-07-16], Available at https://www.cs.cmu.edu/~15-821/READINGS/PAPERS/gemperle1998.pdf

[124] Douglas, M., Bit-Babik, G., Nadakuduti, J., Faraone, A., and Chou, C-K., "Modeling of SAR in the User for Body-Worn Wireless communication devices," Proc. 29th Annual Meeting of the Bioelectromagnetics Society (BEMS 2007), Kanazawa, Japan, June 11–15, 2007

[125] Taylor, J.R., An Introduction to Error Analysis: The Study of Uncertainties In Physical Measurements. 2nd ed. Sausalito, CA: University Science Books, 1997

[126] Evans, S., and Michelson, S.C., "Intercomparison of dielectric reference materials available for the calibration of an open-ended probe at different temperatures," Meas. Sci. Tech., Dec. 1995, vol. 6, no. 12, pp. 1721–1732

[127] Jenkins, S., Hodgetts, T.E., Clarke, R.N., and Preece, A.W., "Dielectric measurements on reference liquids using automatic network analysers and calculable geometries," Meas. Sci. Tech., July 1990, vol. 1, no. 7, pp. 691–702

[128] Migliore, M.D., "Partial self-calibration method for permittivity measurement using truncated coaxial cable," Electron. Lett., July 20, 2000, vol. 36, no. 15, pp. 1275–1277

[129] Nyshadam, A., Sibbald, C.L, and Stuchly, S.S., "Permittivity measurements using open-ended sensors and reference liquid calibration – an uncertainty analysis," IEEE Trans. Microwave Theory Tech., Feb. 1992, vol. 40, no. 2, pp. 305–314

[130] Press, W.H., Flannery, B.P., Teukolsky, S.A., and Vetterling, W.T., *Numerical Recipes in FORTRAN 77: The Art of Scientific Computing*, New York: Cambridge University Press, 1992

[131] Fieguth, P.W., Karl, W.C., Willsky, A.S., and Wunsch, C., "Multi-resolution optimal interpolation and statistical analysis of TOPEX/POSEIDON satellite altimetry," IEEE Trans. Geosci. Remote Sens., Mar. 1995, vol. 33, pp. 280–292

[132] Lancaster, P., and Salkauska, K., *Curve and Surface Fitting: An Introduction*. New York: Academic Press, 1986

[133] Ferreira, P.J.S.G., "Non-iterative and fast iterative methods for interpolation and extrapolation," IEEE Trans. Sig. Proc., Nov 1994, vol. 41, pp. 3278–3282

[134] Ford, C., and Etter, D.M., "Wavelet basis reconstruction of nonuniformly sampled data," IEEE Trans. Circuits Sys. II: Analog Dig. Sig. Proc., Aug. 1998, vol. 45, no. 8, pp. 1165–1168

IECNORM.COM : Click to view the full PDF of IEC/IEEE 62209-1528:2020

[135] Ustuner, K.F., and Ferrai, L.A., “Discrete splines and spline filters,” IEEE Trans. Circuits Sys., July 1991, vol. 39, no. 7, pp 417–422

[136] ISO 10012:2003, *Measurement management systems – Requirements for measurement processes and measuring equipment*

[137] EA-2/07 (rev.01), *EAL Strategy to Achieve Comparability of Results in Calibration and Testing*, Mar. 1997

[138] ISO/IEC 17043:2010, *Conformity assessment – General requirements for proficiency testing*

[139] Onishi, T., et. al, “LTE SAR measurement consideration,” IEC TC106 MT1 meeting in Turin, Sept. 2012

[140] Onishi, T., “Considerations on SAR measurement for recent trend of the usages and new technologies,” 7th European Conference on Antennas and Propagation (EuCAP) 2013, March 2013

[141] Onishi, T., “Investigation on SAR measurement procedure using SAM and Flat phantoms for LTE handsets,” IEC TC106 MT1 meeting in Ottawa, Sept. 2013

[142] Hinkley, D.V., “On the ratio of two correlated normal random variables,” Biometrika, Vol. 56, No. 3, pp. 635–639, Dec. 1969

IECNORM.COM : Click to view the full PDF of IEC/IEEE 62209-1528:2020

IECNORM.COM : Click to view the full PDF of IEC/IEEE 62209-1528:2020

SOMMAIRE

AVANT-PROPOS 295
INTRODUCTION 298
1 Domaine d'application 299
2 Références normatives 299
3 Termes et définitions 300
4 Symboles et abréviations 308
4.1 Grandeurs physiques 308
4.2 Constantes 308
4.3 Abréviations 308
5 Guide de démarrage rapide et liste de contrôle du plan d'évaluation 310
6 Spécifications du système de mesure 313
6.1 Exigences générales pour les essais de DAS complet 313
6.2 Spécifications du fantôme 314
6.2.1 Généralités 314
6.2.2 Paramètres du fantôme de base 315
6.2.3 Fantôme de tête 316
6.2.4 Fantôme plan 317
6.2.5 Fantômes spécifiques au dispositif 318
6.3 Influence de la main sur le DAS dans la tête 318
6.4 Exigences du système de balayage 319
6.5 Spécifications du support de dispositif 319
6.6 Caractéristiques de la lecture électronique 320
7 Protocole pour l'évaluation du DAS 320
7.1 Généralités 320
7.2 Préparation des mesurages 321
7.2.1 Préparation du milieu équivalent au tissu et contrôle du système 321
7.2.2 Préparation du DUT de communication sans fil 321
7.2.3 Exigences relatives aux modes de fonctionnement du DUT 322
7.2.4 Positionnement du DUT par rapport au fantôme 324
7.2.5 Configurations de l'antenne 344
7.2.6 Options et accessoires 344
7.2.7 DUT à facteur de forme différent 344
7.2.8 Fréquences d'essai pour le DUT 345
7.3 Essais à effectuer pour les DUT 346
7.3.1 Généralités 346
7.3.2 Approche fondamentale des essais du DUT 346
7.4 Procédure de mesure 349
7.4.1 Généralités 349
7.4.2 Procédures d'essai complet du DAS 349
7.4.3 Dérive 355
7.4.4 Mesurages de DAS de DUT avec des antennes multiples ou des émetteurs multiples 356
7.5 Post-traitement de données de mesure de DAS 364
7.5.1 Interpolation 364
7.5.2 Extrapolation 364
7.5.3 Définition du volume d'intégration 364

IECNORM.COM : Click to view the full PDF of IEC/IEEE 62209-1528:2020

7.5.4 Recherche des maxima 364
7.6 Considérations relatives au DAS moyenné sur une période 364
7.6.1 Généralités 364
7.6.2 Puissance conduite RF 365
7.6.3 Paramètres de mesure du DAS moyenné sur une période pour les méthodes de mesure du DAS 365
7.6.4 Considérations en matière de conditions d'exposition et de position d'essai 365
7.6.5 DAS moyenné sur une période pour les émissions simultanées 366
7.6.6 Évaluation du facteur TX 366
7.6.7 Mesurages de DAS 367
7.6.8 Incertitude dans les évaluations de TPAS 367
7.7 Considérations relatives aux capteurs de proximité 367
7.7.1 Généralités 367
7.7.2 Procédures de détermination des distances de déclenchement du capteur de proximité 369
7.7.3 Procédure de détermination de la zone de couverture du capteur de proximité 372
7.7.4 Procédures de mesure de DAS impliquant des capteurs de proximité 373
7.8 Correction de DAS pour les écarts de permittivité complexe par rapport aux cibles 374
7.8.1 Généralités 374
7.8.2 Formule de correction du DAS 374
7.8.3 Incertitude de la formule de correction 375
7.9 Réduction le plus possible de la durée d'essai 376
7.9.1 Généralités 376
7.9.2 Essai rapide de DAS 376
7.9.3 Réduction d'essai de DASs 383
8 Estimation de l'incertitude de mesure 396
8.1 Généralités 396
8.2 Exigences relatives à l'évaluation de l'incertitude 397
8.3 Description des modèles d'incertitude 397
8.3.1 Généralités 397
8.3.2 Mesurage de DAS d'un DUT 397
8.3.3 Mesurage de validation du système et de contrôle du système 398
8.3.4 Répétabilité et reproductibilité du contrôle du système 398
8.3.5 Essai rapide de DAS (mesure relative) 398
8.4 Paramètres contribuant à l'incertitude 400
8.4.1 Erreurs du système de mesure 400
8.4.2 Erreurs de fantôme et de dispositif (DUT ou antenne de validation) 401
8.4.3 Corrections du résultat de DAS (si appliqué) 404
9 Rapport de mesure 404
9.1 Généralités 404
9.2 Éléments à consigner dans le rapport de mesure 404
Annexe A (normative) Vérification du système de mesure de DAS 409
A.1 Vue d'ensemble 409
A.2 Contrôle du système 409
A.2.1 Objet 409
A.2.2 Montage du fantôme 410
A.2.3 Antenne de contrôle du système 410

IECNORM.COM : Click to view the full PDF of IEC/IEEE 62209-1528:2020

A.2.4 Mesurage de la puissance d'entrée de la source de contrôle du système 411
A.2.5 Procédure de contrôle du système 413
A.2.6 Critères d'acceptation du contrôle du système 413
A.3 Validation du système 414
A.3.1 Objet 414
A.3.2 Montage du fantôme 414
A.3.3 Antennes de validation du système 414
A.3.4 Mesurage de la puissance d'entrée 414
A.3.5 Procédure de validation du système 414
A.4 Validation du système et contrôle du système d'essai rapide de DAS 416
A.4.1 Généralités 416
A.4.2 Validation du système d'essai rapide de DAS 417
A.4.3 Contrôle du système d'essai rapide de DAS 418
Annexe B (informative) Informations de support de réduction d'essai DAS 420
B.1 Généralités 420
B.2 Réduction d'essai fondée sur les caractéristiques de conception du DUT 420
B.2.1 Généralités 420
B.2.2 Vue d'ensemble de l'analyse statistique 420
B.2.3 Résultats d'analyse 421
B.2.4 Conclusions 424
B.2.5 Extension à la transmission à plusieurs antennes 425
B.3 Réduction d'essai fondée sur l'analyse des résultats de DAS sur d'autres modulations de signal 425
B.3.1 Généralités 425
B.3.2 Résultats d'analyse 426
B.4 Réduction d'essai fondée sur l'analyse de niveau de DAS 428
B.4.1 Généralités 428
B.4.2 Analyse statistique 428
B.4.3 Exemple d'applicabilité de réduction d'essai 432
B.5 Autres approches statistiques pour rechercher les configurations d'essai de DAS élevé 434
B.5.1 Généralités 434
B.5.2 Réductions d'essai fondées sur un plan d'expérience 435
B.5.3 Recherche "un facteur à la fois" (OFAT) 435
B.5.4 Analyse de données non structurées 435
Annexe C (informative) Incertitude de mesure des résultats obtenus à partir des méthodes d'essai rapide de DAS spécifiques 436
C.1 Généralités 436
C.2 Évaluation d'incertitude de mesure – paramètres de contribution 436
C.2.1 Généralités 436
C.2.2 Étalonnage de sonde et dérive d'étalonnage du système 437
C.2.3 Isotropie 438
C.2.4 Positionnement de la sonde 438
C.2.5 Couplage mutuel de capteur 439
C.2.6 Diffraction à l'intérieur du réseau de sondes 440
C.2.7 Erreur d'échantillonnage 440
C.2.8 Limites du réseau 440
C.2.9 Couplage de sonde ou de réseau de sonde avec le DUT 441
C.2.10 Immunité / réception secondaire du système de mesure 441

IECNORM.COM : Click to view the full PDF of IEC/IEEE 62209-1528:2020

C.2.11 Écarts de forme de fantôme 441
C.2.12 Variation spatiale des propriétés diélectriques 441
C.2.13 Reconstruction 441
C.3 Bilan d'incertitude 442
Annexe D (normative) Antennes de validation du système DAS 445
D.1 Exigences générales relatives aux antennes 445
D.2 Antenne doublet normalisée 445
D.2.1 Description mécanique 445
D.2.2 Valeurs de DAS numériques cibles 448
D.3 Guide d'ondes normalisé 450
D.3.1 Description mécanique 450
D.3.2 Valeurs de DAS numériques cibles 451
D.4 Antennes de validation du système au-dessous de 150 MHz 452
D.4.1 Généralités 452
D.4.2 Antenne cadre confinée 452
D.4.3 Antenne doublet en serpentin 455
D.5 Source de champ E orthogonal – VPIFA 456
D.5.1 Description mécanique 456
D.5.2 Valeurs de DAS numériques cibles 459
Annexe E (normative) Étalonnage et caractérisation de sondes dosimétriques (DAS) 460
E.1 Remarques introductives 460
E.2 Linéarité 461
E.3 Évaluation de la sensibilité des capteurs-dipôles 461
E.3.1 Généralités 461
E.3.2 Procédures d'étalonnage en deux étapes 461
E.3.3 Procédures d'étalonnage en une étape – méthode de l'antenne de référence 468
E.3.4 Procédures d'étalonnage en une étape – méthode du calorimètre coaxial 473
E.4 Isotropie 475
E.4.1 Isotropie axiale 475
E.4.2 Isotropie hémisphérique 475
E.5 Limite inférieure de détection 482
E.6 Effet de proximité de bord 483
E.7 Temps de réponse 483
Annexe F (informative) Exemples de formules pour les milieux équivalents aux tissus du fantôme 484
F.1 Généralités 484
F.2 Constituants 484
F.3 Formules de liquides de milieu équivalent au tissu (permittivité/conductivité) 485
Annexe G (normative) Spécifications du fantôme 487
G.1 Justification relative aux caractéristiques du fantôme 487
G.1.1 Généralités 487
G.1.2 Justification relative au fantôme SAM 487
G.1.3 Justification relative au fantôme plan 487
G.2 Spécifications relatives au fantôme SAM 488
G.2.1 Spécifications relatives au fantôme SAM – Généralités 488
G.2.2 Spécifications relatives à l'enveloppe du fantôme SAM 492
G.3 Spécifications relatives au fantôme plan 495

IECNORM.COM : Click to view the full PDF of IEC/IEEE 62209-1528:2020

G.4 Justification relative aux dimensions du fantôme plan 496
G.5 Justification relative aux milieux équivalents aux tissus 499
G.6 Définition du système de coordonnées d'un fantôme et du système de coordonnées d'un DUT 502
Annexe H (informative) Mesurages des propriétés diélectriques des milieux équivalents aux tissus et estimation de l'incertitude 504
H.1 Vue d'ensemble 504
H.2 Techniques de mesure 504
H.2.1 Généralités 504
H.2.2 Instrumentation 504
H.2.3 Principes généraux 504
H.3 Ligne de transmission coaxiale de banc de mesure 505
H.3.1 Généralités 505
H.3.2 Montage de l'équipement 505
H.3.3 Procédure de mesure 506
H.4 Sonde coaxiale de contact 507
H.4.1 Généralités 507
H.4.2 Montage de l'équipement 507
H.4.3 Procédure de mesure 509
H.5 Ligne de transmission TEM 509
H.5.1 Généralités 509
H.5.2 Montage de l'équipement 509
H.5.3 Procédure de mesure 510
H.6 Propriétés diélectriques des liquides de référence 511
Annexe I (informative) Études des effets potentiels de la main sur le DAS de la tête 514
I.1 Vue d'ensemble 514
I.2 Contexte 515
I.2.1 Généralités 515
I.2.2 Fantômes de main 515
I.3 Récapitulatif des études expérimentales 515
I.3.1 Études expérimentales utilisant des systèmes de mesure de DAS entièrement conformes 515
I.3.2 Études expérimentales utilisant d'autres systèmes de mesure de DAS 516
I.4 Récapitulatif des études informatiques 516
I.5 Conclusions 516
Annexe J (informative) Facteur d'amplification de la peau 518
J.1 Contexte 518
J.2 Justification 519
J.3 Simulations 519
J.4 Recommandation 520
Annexe K (normative) Fantômes spécifiques à l'application 522
K.1 Généralités 522
K.2 Exigences de base relatives au fantôme 522
K.3 Exemples d'autres fantômes spécifiques 522
K.3.1 Fantôme SAM visage vers le bas 522
K.3.2 Fantôme SAM avec appui renversé sur la tête 523
K.3.3 Fantôme de poignet 524
K.4 Balayage et exigences d'évaluation 524
K.5 Évaluation d'incertitude 525

IECNORM.COM : Click to view the full PDF of IEC/IEEE 62209-1528:2020

K.6 Consignation 525
Annexe L (normative) Évaluations rapides de la conformité à l'aide d'un fantôme à base plane avec un coin arrondi (unifantôme) 526
L.1 Généralités 526
L.2 Unifantôme 526
L.3 Positions du dispositif pour les essais de conformité et définitions des formes de combiné 527
L.3.1 Généralités 527
L.3.2 Combinés avec facteur de forme droit 527
L.3.3 Combinés avec facteur de forme en coquille 527
L.4 Procédure d'essai 528
L.4.1 Généralités 528
L.4.2 Combinés avec facteurs de forme droits 528
L.4.3 Combinés avec facteurs de forme en coquille 529
L.5 Incertitude des résultats de mesure de DAS avec l'unifantôme 530
Annexe M (informative) Essai du kit mains libres à oreillettes avec fil 532
M.1 Concept 532
M.2 Exemples de résultats 533
M.3 Commentaires 534
Annexe N (informative) Application des procédures d'essai pour le DAS de la tête 535
Annexe O (normative) Analyse d'incertitude pour les fabricants de systèmes de mesure et les laboratoires d'étalonnage 538
O.1 Linéarité et limites de détection de sonde 538
O.2 Incertitude du signal à large bande 539
O.3 Effet de proximité de bord 539
O.4 Incertitude des lectures électroniques de la sonde de champ 541
O.5 Incertitude sur le temps de réponse à un échelon du signal 541
O.6 Incertitude de temps d'intégration de sonde 541
O.6.1 Généralités 541
O.6.2 Incertitude de temps d'intégration de sonde pour des signaux pulsés périodiques 541
O.6.3 Incertitude de temps d'intégration de sonde pour des signaux non périodiques 542
O.7 Contribution des contraintes mécaniques 543
O.7.1 Tolérances mécaniques du positionneur de la sonde (directions parallèles à la surface du fantôme) 543
O.7.2 Positionnement de sonde par rapport à la surface de l'enveloppe du fantôme 543
O.7.3 Approximation de premier ordre de la décroissance exponentielle 544
O.8 Contribution du post-traitement 544
O.8.1 Généralités 544
O.8.2 Fonctions d'essai d'évaluation 545
O.8.3 Évaluations des incertitudes des algorithmes de traitement de données 547
O.9 Incertitudes des propriétés du milieu équivalent au tissu 550
O.9.1 Généralités 550
O.9.2 Masse volumique du milieu 550
O.9.3 Incertitude de conductivité du milieu 550
O.9.4 Incertitude de permittivité du milieu 551
O.9.5 Évaluation des incertitudes de mesure de propriétés diélectriques 551
O.9.6 Incertitude de température du milieu 553

IECNORM.COM : Click to view the full PDF of IEC/IEEE 62209-1528:2020

Annexe P (normative) Techniques de post-traitement 554
P.1 Schémas d'extrapolation et d'interpolation 554
P.1.1 Généralités 554
P.1.2 Schémas d'extrapolation 554
P.1.3 Schémas d'interpolation 554
P.2 Schéma d'intégration et recherche du maximum 555
P.2.1 Schémas d'intégration par le volume 555
P.2.2 Recherche du psDAS et évaluation de l'incertitude 555
Annexe Q (informative) Justification pour la procédure d'essai de DAS moyenné sur une période 556
Annexe R (normative) Analyse de l'incertitude de mesure pour les laboratoires d'essai 557
R.1 Conditions RF ambiantes 557
R.2 Incertitudes de positionnement du dispositif et du support 557
R.2.1 Généralités 557
R.2.2 Incertitude due aux perturbations du support de dispositif 558
R.2.3 Incertitude de positionnement du DUT avec un support de dispositif d'essai spécifique: Type A 559
R.3 Réponse en modulation de la sonde 560
R.4 DAS moyenné sur une période 561
R.4.1 Généralités 561
R.4.2 Incertitude du facteur TX 561
R.5 Dérive de DAS mesuré 561
R.5.1 Généralités 561
R.5.2 Prise en compte de la dérive 562
R.6 Incertitude de mise à l'échelle du DAS 563
Annexe S (normative) Incertitude de mesure de DAS de l'antenne de validation 564
S.1 Écart des antennes expérimentales 564
S.2 Autres contributions à l'incertitude lors de l'utilisation des antennes de validation du système 565
Annexe T (normative) Comparaisons interlaboratoires 566
T.1 Objet 566
T.2 Montage du fantôme 566
T.3 Dispositifs de référence 566
T.4 Réglage de la puissance 566
T.5 Comparaison interlaboratoire – procédure 567
Annexe U (informative) Détermination de la marge pour l'évaluation de conformité à l'aide de l'unifantôme 568
U.1 Généralités 568
U.2 Écart du psDAS mesuré avec l'unifantôme par rapport au psDAS mesuré avec le fantôme SAM 568
U.3 Détermination de la marge selon l'intervalle de confiance de 95 % 569
U.4 Exemples de détermination du facteur de marge 570
U.4.1 Marge pour les combinés avec facteurs de forme droits en position sur base plane 570
U.4.2 Marge pour les combinés avec facteurs de forme droits en position sur fond plat (à l'exception des mobiles multifonctions en position sur base plane) 572
U.4.3 Marge pour les mobiles multifonctions en position sur base plane 574
U.4.4 Marge pour les mobiles multifonctions en position en coin 576

IECNORM.COM : Click to view the full PDF of IEC/IEEE 62209-1528:2020

U.4.5 Marge pour les combinés avec facteur de formes en coquille en position en coin 579
Annexe V (informative) Commande du niveau de puissance d'entrée automatique pour la validation du système 582
V.1 Généralités 582
V.2 Mécanisme opérationnel de l'AIPLC 583
Annexe W (informative) Informations de support des configurations d'essai LTE 585
W.1 Généralités 585
W.2 Étude 1 585
W.3 Étude 2 587
W.4 Justifications des écarts types relatifs 589
Bibliographie 591

Figure 1 – Guide de démarrage rapide 312
Figure 2 – Dimensions du fantôme elliptique 318
Figure 3 – Montage du DUT dans le support de dispositif à l'aide d'une mousse à faible permittivité et à faibles pertes pour éviter les variations de performances du DUT selon le matériau du support 320
Figure 4 – Désignation des points de référence du DUT 325
Figure 5 – Mesurages réalisés en déplaçant un dispositif volumineux sur la zone de mesure efficace du système incluant les zones de chevauchement – dans ce cas: six essais réalisés 326
Figure 6 – Positions d'essai des dispositifs portés près du corps 327
Figure 7 – Dispositif équipé d'une antenne à rotule 328
Figure 8 – Positions d'essai pour les appareils posés sur le corps 331
Figure 9 – Positions d'essai pour les appareils de bureau 332
Figure 10 – Positions d'essai pour les appareils placés devant le visage 334
Figure 11 – Position d'essai des appareils tenus à la main, mais non à proximité de la tête ou du torse 334
Figure 12 – Positions d'essai des appareils fixés à un membre 335
Figure 13 – Position d'essai pour les dispositifs de communication sans fil intégrés aux vêtements 336
Figure 14 – Positions d'essai possibles d'un appareil générique 337
Figure 15 – Lignes de référence verticale et horizontale et points de référence A et B sur deux exemples types de dispositifs: un mobile multifonction avec écran tactile complet (en haut) et un DUT à clavier (en bas) 339
Figure 16 – Position "joue" du DUT sur le côté gauche du SAM dans laquelle le dispositif doit être maintenu pour la configuration d'essai du fantôme 343
Figure 17 – Position "incliné" du DUT sur le côté gauche du SAM 344
Figure 18 – DUT à facteur de forme différent avec points de référence et lignes de référence 345
Figure 19 – Schéma de principe des essais à effectuer 349
Figure 20 – Orientation de la sonde par rapport à la droite perpendiculaire à la surface du fantôme, pour les fantômes de la tête et les fantômes plans, à deux emplacements différents 354
Figure 21 – Procédure de mesure des différents types de signaux corrélés 363
Figure 22 – Positionnement des surfaces et des bords du DUT pour déterminer la distance de déclenchement du capteur de proximité 371

IECNORM.COM: Click to view the full PDF of IEC/IEEE 62209-1528:2020

Figure 23 – Positionnement des bords du DUT pour déterminer les variations de distance de déclenchement du capteur de proximité avec le bord positionné selon différents angles par rapport à la position perpendiculaire 372
Figure 24 – Procédure A de DAS rapide 380
Figure 25 – Procédure B de DAS rapide 383
Figure 26 – Organigramme modifié de la Figure 19 388
Figure 27 – Utilisation de la puissance conduite pour le choix du mode LTE, pour la Bande 1 (1 920 MHz à 1 980 MHz) (les valeurs MPR sont en dB) 392
Figure 28 – Utilisation de la puissance conduite pour le choix du mode LTE, pour la Bande 17 (704 MHz à 716 MHz) (les valeurs MPR sont en dB) 393
Figure A.1 – Montage d'essai pour le contrôle du système 411
Figure B.1 – Distribution de "Incliné/Joue" 422
Figure B.2 – DAS par rapport au DAS en position avec le DAS maximal en mode GSM 427
Figure B.3 – Deux points identifiant la distance minimale entre la position du DAS maximal interpolé et les points à 0,6 × DAS_{max} 429
Figure B.4 – Histogramme pour D_{min} dans le cas de GSM 900 et d'un isoniveau à 0,6 × DAS_{max} 430
Figure B.5 – Histogramme pour la variable aléatoire $Facteur_{1g,1800}$ 432
Figure D.1 – Informations détaillées mécaniques relatives au doublet normalisé 447
Figure D.2 – Guide d'ondes normalisé (dimensions conformes au Tableau D.3) 450
Figure D.3 – Dessin de la CLA correspondant à un cadre résonant intégré dans une structure métallique pour isoler la structure résonante de l'environnement 453
Figure D.4 – Informations détaillées mécaniques relatives aux doublets en serpentin pour 150 MHz 455
Figure D.5 – Antenne de validation VPIFA 458
Figure D.6 – Masque de positionnement des VPIFA 458
Figure E.1 – Montage expérimental pour l'évaluation de la sensibilité (facteur de conversion) utilisant un guide d'ondes rectangulaire vertical 466
Figure E.2 – Représentation graphique du montage d'évaluation du gain de l'antenne 469
Figure E.3 – Schéma du système de calorimètre coaxial 473
Figure E.4 – Montage utilisé pour évaluer l'écart de l'isotropie hémisphérique dans le milieu équivalent au tissu 477
Figure E.5 – Autre montage utilisé pour évaluer l'écart de l'isotropie hémisphérique dans le milieu équivalent au tissu 478
Figure E.6 – Montage expérimental pour l'évaluation de l'isotropie hémisphérique 480
Figure E.7 – Conventions pour la position (ξ) du doublet et la polarisation (θ) 481
Figure E.8 – Mesurage de l'isotropie hémisphérique avec l'antenne de référence 482
Figure G.1 – Représentation graphique des dimensions du Tableau G.1 et du Tableau G.2 489
Figure G.2 – Vue de côté rapprochée du fantôme montrant la région de l'oreille 491
Figure G.3 – Vue de côté du fantôme montrant les marquages pertinents 492
Figure G.4 – Bissection sagittale du fantôme avec périmètre étendu (montrée sur le côté comme lors des essais de DAS du dispositif) 493
Figure G.5 – Représentation du fantôme représentant la bande central 494
Figure G.6 – Section du SAM au niveau du plan de référence 495

IECNORM.COM : Click to view the full PDF of IEC/IEEE 62209-1528:2020

Figure G.7 – Dimensions du montage de fantôme plan utilisé pour déduire les dimensions minimales du fantôme pour W et L pour une profondeur de fantôme donnée D 497
Figure G.8 – Erreur prévue de FDTD dans le psDAS à 10 g en fonction des dimensions du fantôme plan comparées à un fantôme plan infini à 800 MHz 498
Figure G.9 – Permittivité complexe des tissus humains comparée aux propriétés cibles du fantôme 502
Figure G.10 – Exemple de système de coordonnées de référence pour l'ERP de l'oreille gauche du fantôme SAM 503
Figure G.11 – Exemple de système de coordonnées sur un DUT 503
Figure H.1 – Montage du banc de mesure 506
Figure H.2 – Sonde coaxiale sans terminaison avec des rayons intérieur et extérieur a et b, respectivement 508
Figure H.3 – Montage d'essai diélectrique des propriétés diélectriques de ligne TEM [85] 510
Figure J.1 – Distributions du DAS et de l'échauffement (ΔT) simulées pour un modèle de torse planaire à trois couches (peau, graisse, muscle) 518
Figure J.2 – Approche statistique pour protéger 90 % de la population 520
Figure J.3 – Facteur d'amplification de la peau du psDAS 521
Figure K.1 – Fantôme SAM visage vers le bas 523
Figure K.2 – Fantôme SAM avec appui renversé sur la tête 523
Figure K.3 – Fantôme de poignet 524
Figure L.1 – Section du fantôme unifié (unifantôme) avec ses dimensions 526
Figure L.2 – Positions de mesure des combinés avec des facteurs de forme droit et en coquille 527
Figure L.3 – Organigramme de la procédure d'essai des combinés avec facteurs de formes droits 529
Figure L.4 – Organigramme de la procédure d'essai des combinés avec facteurs de formes en coquille 530
Figure M.1 – Configuration d'un kit mains libres à oreillettes avec fil 532
Figure M.2 – Configuration sans kit mains libres à oreillettes avec fil 533
Figure O.1 – Orientation et surface du volume d'intégration par rapport à la surface du fantôme 550
Figure U.1 – Catégories (classes) pour la comparaison du psDAS mesuré entre l'unifantôme (DAS_{uni}) et le fantôme SAM (DAS_{SAM}) 569
Figure U.2 – Histogramme de l'écart du psDAS à 10 g de 45 combinés avec facteurs de forme droits positionnés sur la base plane de l'unifantôme 571
Figure U.3 – Histogramme de l'écart du psDAS à 1 g de 40 combinés avec facteurs de forme droits positionnés sur la base plane de l'unifantôme 572
Figure U.4 – Histogramme de l'écart du psDAS à 10 g de 25 combinés avec facteurs de forme droits positionnés sur la base plane de l'unifantôme 573
Figure U.5 – Histogramme de l'écart du psDAS à 1 g de 20 combinés avec facteurs de forme droits positionnés sur la base plane de l'unifantôme 574
Figure U.6 – Histogramme de l'écart du psDAS à 10 g de 20 combinés avec facteurs de forme droits ou de mobiles multifonctions positionnés sur la base plane de l'unifantôme 575
Figure U.7 – Histogramme de l'écart du psDAS à 1 g de 20 combinés avec facteurs de forme droits ou de mobiles multifonctions positionnés sur la base plane de l'unifantôme 576

IECNORM.COM : Click to view the full PDF of IEC/IEEE 62209-1528:2020

Figure U.8 – Histogramme de l'écart du psDAS à 10 g de 20 combinés avec facteurs de forme droits ou de mobiles multifonctions positionnés au niveau du coin de l'unifantôme 577

Figure U.9 – Histogramme de l'écart du psDAS à 1 g de 19 combinés avec facteurs de forme droits ou de mobiles multifonctions positionnés au niveau du coin de l'unifantôme 578

Figure U.10 – Histogramme de l'écart du psDAS à 10 g de 20 combinés avec facteurs de forme en coquille au niveau du coin de l'unifantôme 580

Figure U.11 – Histogramme de l'écart du psDAS à 1 g de 19 combinés avec facteurs de forme en coquille au niveau du coin de l'unifantôme 581

Figure V.1 – Variations de puissance d'entrée RF générées sur le temps de fonctionnement sans et avec application de l'AIPLC 582

Figure V.2 – Schéma de principe du système de l'AIPLC 583

Figure V.3 – Caractéristiques de variation de puissance en réglant les sorties de l'amplificateur ou du générateur de signal 584

Figure W.1 – Canaux inférieur, central et supérieur au niveau de la bande de 2 GHz (Bande 1) 587

Figure W.2 – Puissance conduite RF en fonction du psDAS à 10 g 587

Figure W.3 – DAS à 1 g en fonction de la puissance conduite RF dans différentes conditions d'essai 589

Tableau 1 – Liste de contrôle du plan d'évaluation 310

Tableau 2 – Propriétés diélectriques du milieu équivalent au tissu 315

Tableau 3 – Paramètres de balayage de surface 352

Tableau 4 – Paramètres de balayage-zoom 352

Tableau 5 – Exemple de méthode pour déterminer la valeur de DAS combiné utilisant la Variante 1 360

Tableau 6 – Formule de correction du DAS d'erreur quadratique en fonction de la variation maximale de permittivité et de conductivité [28] 375

Tableau 7 – Valeurs de seuil $TH(f)$ utilisées dans le protocole de réduction d'essai proposé 387

Tableau 8 – Diviseurs pour les fonctions de densité de probabilité (PDF) 397

Tableau 9 – Modèle de bilan d'incertitude pour l'évaluation de l'incertitude dans la valeur mesurée du psDAS à 1 g ou 10 g à partir d'un DUT ou d'une antenne de validation (N = normal, R = rectangulaire) 399

Tableau 10 – Incertitude de la Formule (8) (voir 7.8.2) en fonction de la variation maximale de permittivité et de conductivité 404

Tableau B.1 – Nombre de DUT utilisés pour l'étude statistique 421

Tableau B.2 – Résultats d'analyse statistique de P(Incliné/Joue > x) pour différentes valeurs de x 422

Tableau B.3 – Résultats d'analyse statistique de P(Incliné/Joue > x) pour un psDAS à 1 g et 10 g 423

Tableau B.4 – Résultats d'analyse statistique de P(Incliné/Joue > x) pour différentes positions d'antenne 423

Tableau B.5 – Résultats d'analyse statistique de P(Incliné/Joue > x) pour différentes bandes de fréquences 424

Tableau B.6 – Résultats d'analyse statistique de P(Incliné/Joue > x) pour différents types de dispositifs 424

Tableau B.7 – Distance D^*_{min} pour différentes valeurs de "l'isoniveau" 430

IECNORM.COM : Click to view the full PDF of IEC/IEEE 62209-1528:2020

Tableau B.8 – Seuils expérimentaux pour avoir une probabilité de 95 % que la valeur de DAS maximal mesurée à partir du balayage de surface ait également un psDAS 432
Tableau B.9 – Valeur de DAS à partir du balayage de surface (bande GSM 900): Exemple 1 433
Tableau B.10 – Valeur de DAS à partir du balayage de surface (bande GSM 900): Exemple 2 434
Tableau C.1 – Bilan d'incertitude de mesure pour des mesurages de DAS relatifs à l'aide d'un essai rapide de DAS de Classe 2, pour les essais effectués dans une bande de fréquences et modulation 443
Tableau C.2 – Bilan d'incertitude de mesure pour le contrôle du système à l'aide d'un essai rapide de DAS de Classe 2 444
Tableau D.1 – Dimensions mécaniques des doublets de référence 448
Tableau D.2 – Valeurs de DAS numériques cibles (W/kg) pour un doublet normalisé et un fantôme plan 449
Tableau D.3 – Dimensions mécaniques du guide d'ondes normalisé 451
Tableau D.4 – Valeurs numériques cibles de DAS pour les guides d'ondes 452
Tableau D.5 – Valeurs numériques cibles de DAS pour les CLA 454
Tableau D.6 – Dimensions mécaniques du doublet en serpentin de référence 455
Tableau D.7 – Valeurs numériques cibles de DAS (W/kg) pour les antennes en serpentin 456
Tableau D.8 – Dimensions des antennes VPIFA à différentes fréquences 457
Tableau D.9 – Propriétés diélectriques des couches diélectriques des antennes VPIFA 459
Tableau D.10 – Valeurs de DAS numériques cibles pour les VPIFA sur le fantôme plan 459
Tableau E.1 – Analyse de l'incertitude de l'étalonnage du transfert avec des sondes de température 464
Tableau E.2 – Lignes directrices de conception de guides d'ondes d'étalonnage 467
Tableau E.3 – Analyse d'incertitude de l'étalonnage de sonde dans le guide d'ondes 468
Tableau E.4 – Modèle d'incertitude pour l'évaluation du gain de l'antenne de référence 470
Tableau E.5 – Modèle d'incertitude pour l'étalonnage à l'aide de l'antenne de référence 471
Tableau E.6 – Composantes d'incertitude pour l'étalonnage de sonde en utilisant des méthodes thermiques 475
Tableau F.1 – Formules suggérées pour obtenir les propriétés diélectriques cibles: 30 MHz à 900 MHz 485
Tableau F.2 – Formules suggérées pour obtenir les paramètres diélectriques cibles: 1 800 MHz à 10 000 MHz 486
Tableau G.1 – Dimensions utilisées pour déduire le fantôme SAM à partir des données de l'ARMÉE sur le 90^{e} percentile de la tête masculine (Gordon et al. [61]) 490
Tableau G.2 – Dimensions SAM supplémentaires comparées aux dimensions sélectionnées à partir des données de l'ARMÉE sur le 90^{e} percentile de la tête masculine (Gordon et al. [61])– section spécifique de mesure de la tête 490
Tableau G.3 – Paramètres utilisés pour calculer les valeurs de DAS de référence du Tableau D.2 499
Tableau H .1 – Paramètres pour le calcul des propriétés diélectriques de différents liquides de référence 512
Tableau H.2 – Propriétés diélectriques de liquides de référence à 20 °C 513
Tableau J.1 – Facteurs de correction du psDAS 521
Tableau N.1 – Tableau de résultats de DAS pour des exemples de résultats d'essai dans la bande GSM 850 536

IECNORM.COM : Click to view the full PDF of IEC/IEEE 62209-1528:2020

Tableau N.2 – Tableau de résultats de DAS pour des exemples de résultats d'essai dans la bande GSM 900 536

Tableau N.3 – Tableau de résultats de DAS pour des exemples de résultats d'essai dans la bande GSM 1800 537

Tableau N.4 – Tableau de résultats de DAS pour des exemples de résultats d'essai dans la bande GSM 1900 537

Tableau O.1 – Paramètres de la fonction de référence f_1 de la Formule (O.12) 546

Tableau O.2 – Valeurs de DAS de référence issues des fonctions de distribution f_1, f_2 et f_3 547

Tableau O.3 – Exemple de modèle d'incertitude et de valeurs numériques pour la mesure de la permittivité (ε_r') et de la conductivité (σ) 552

Tableau S.1 – Incertitudes associées aux écarts des paramètres de la source de guide d'ondes normalisé par rapport à la théorie 564

Tableau S.2 – Autres contributions à l'incertitude associées aux antennes doublets décrites à l'Annexe D. 565

Tableau S.3 – Autres contributions à l'incertitude associées aux guides d'ondes normalisés spécifiés à l'Annexe D 565

Tableau U.1 – Récapitulatif des informations permettant de déterminer la marge pour les combinés à facteurs de forme droits positionnés sur la base plane de l'unifantôme 570

Tableau U.2 – Récapitulatif des informations permettant de déterminer la marge pour les combinés à facteurs de forme droits, y compris les combinés à glissière et les combinés à barre (à l'exception des mobiles multifonctions) positionnés sur la base plane de l'unifantôme 573

Tableau U.3 – Récapitulatif des informations permettant de déterminer la marge pour les mobiles multifonctions positionnés sur la base plane de l'unifantôme 575

Tableau U.4 – Récapitulatif des informations permettant de déterminer la marge pour les mobiles multifonctions positionnés au niveau du coin de l'unifantôme 577

Tableau U.5 – Résultats d'analyse statistique de P(Incliné/Joue > x) pour différents types de dispositifs 578

Tableau U.6 – Récapitulatif des informations permettant de déterminer la marge pour les combinés à facteurs de forme en coquille positionnés au niveau du coin de l'unifantôme 579

Tableau W.1 – Écart type relatif de α déterminé dans l'Étude 1 (sans MPR) 586

Tableau W.2 – Écart type relatif maximal de α déterminé dans l'Étude 2 (avec MPR) 588

IECNORM.COM : Click to view the full PDF of IEC/IEEE 62209-1528:2020

© IEC/IEEE 2020

COMMISSION ÉLECTROTECHNIQUE INTERNATIONALE

_____

PROCÉDURE DE MESURE POUR L'ÉVALUATION DU DÉBIT D'ABSORPTION SPÉCIFIQUE DE L'EXPOSITION HUMAINE AUX CHAMPS RADIOFRÉQUENCE PRODUITS PAR LES DISPOSITIFS DE COMMUNICATIONS SANS FIL TENUS À LA MAIN OU PORTÉS PRÈS DU CORPS –

Partie 1528: Modèles humains, instrumentation et procédures (plage de fréquences comprise entre 4 MHz et 10 GHz)

AVANT-PROPOS

1) La Commission Électrotechnique Internationale (IEC) est une organisation mondiale de normalisation composée de l'ensemble des comités électrotechniques nationaux (Comités nationaux de l'IEC). L'IEC a pour objet de favoriser la coopération internationale pour toutes les questions de normalisation dans les domaines de l'électricité et de l'électronique. À cet effet, l'IEC – entre autres activités – publie des Normes internationales, des Spécifications techniques, des Rapports techniques, des Spécifications accessibles au public (PAS) et des Guides (ci-après dénommés "Publication(s) de l'IEC"). Leur élaboration est confiée à des comités d'études, aux travaux desquels tout Comité national intéressé par le sujet traité peut participer. Les organisations internationales, gouvernementales et non gouvernementales, en liaison avec l'IEC, participent également aux travaux.

   Les normes de l'IEEE sont élaborées par les Sociétés de l'IEEE, ainsi que par les Comités de coordination des normes du Conseil de normalisation de l'IEEE Standards Association (IEEE-SA). Ces normes sont l'aboutissement d'un consensus qui rassemble des bénévoles représentant divers points de vue et intérêts. Les participants bénévoles ne sont pas nécessairement membres de l'IEEE et leur intervention n'est pas rétribuée. Si l'IEEE administre le déroulement de cette procédure et définit les règles destinées à favoriser l'équité du consensus, l'IEEE lui-même n'évalue pas, ne teste pas et ne vérifie pas l'exactitude de toute information contenue dans ses normes. L'utilisation de normes de l'IEEE est entièrement volontaire. *Les documents de l'IEEE sont disponibles à des fins d'utilisation, à condition d'être assortis d'avis importants et de clauses de non-responsabilité (voir* http://standards.ieee.org/IPR/disclaimers.html *pour de plus amples informations).*

   L'IEC collabore étroitement avec l'IEEE selon des conditions fixées par accord entre les deux organisations. Cette norme internationale double logo a été développée conjointement par l'IEC et l'IEEE selon les termes de cet accord.

2) Les décisions officielles de l'IEC concernant les questions techniques représentent, dans la mesure du possible, un accord international sur les sujets étudiés, étant donné que les Comités nationaux de l'IEC intéressés sont représentés dans chaque comité d'études. Une fois le consensus établi entre les Sociétés de l'IEEE et les Comités de coordination des normes, les décisions officielles de l'IEEE relatives aux questions techniques sont déterminées en fonction du vote exprimé par un groupe à la composition équilibrée, composé de parties intéressées qui manifestent leur intérêt pour la révision des normes proposées. L'approbation finale de la norme de l'IEEE est soumise au Conseil de normalisation de l'IEEE Standards Association (IEEE-SA).

3) Les Publications IEC/IEEE se présentent sous la forme de recommandations internationales et sont agréées comme telles par les Comités nationaux de l'IEC/Sociétés de l'IEEE. Tous les efforts raisonnables sont entrepris afin de s'assurer de l'exactitude du contenu technique des Publications IEC/IEEE; l'IEC ou l'IEEE ne peuvent pas être tenus responsables de l'éventuelle mauvaise utilisation ou interprétation qui en est faite par un quelconque utilisateur final.

4) Dans le but d'encourager l'uniformité internationale, les Comités nationaux de l'IEC s'engagent, dans toute la mesure possible, à appliquer de façon transparente les Publications de l'IEC (y compris les Publications IEC/IEEE) dans leurs publications nationales et régionales. Toutes divergences entre toutes Publications IEC/IEEE et toutes publications nationales ou régionales correspondantes doivent être indiquées en termes clairs dans ces dernières.

5) L'IEC et l'IEEE eux-mêmes ne fournissent aucune attestation de conformité. Des organismes de certification indépendants fournissent des services d'évaluation de conformité et, dans certains secteurs, accèdent aux marques de conformité de l'IEC. L'IEC et l'IEEE ne sont responsables d'aucun des services effectués par les organismes de certification indépendants.

6) Tous les utilisateurs doivent s'assurer qu'ils sont en possession de la dernière édition de cette publication.

7) Aucune responsabilité ne doit être imputée à l'IEC ou à l'IEEE, à ses administrateurs, employés, auxiliaires ou mandataires, y compris ses experts particuliers et les membres de ses comités d'études et des Comités nationaux de l'IEC, ou les bénévoles des Sociétés de l'IEEE et des Comités de coordination des normes du Conseil de normalisation de l'IEEE Standards Association (IEEE-SA), pour tout préjudice causé en cas de dommages corporels et matériels, ou de tout autre dommage de quelque nature que ce soit, directe ou indirecte, ou pour supporter les coûts (y compris les frais de justice) et les dépenses découlant de la publication ou de l'utilisation de cette Publication IEC/IEEE ou toute autre publication de l'IEC ou de l'IEEE, ou au crédit qui lui est accordé.

IECNORM.COM : Click to view the full PDF of IEC/IEEE 62209-1528:2020

8) L'attention est attirée sur les références normatives citées dans cette publication. L'utilisation de publications référencées est obligatoire pour une application correcte de la présente publication.

9) L'attention est attirée sur fait que la mise en application de cette Publication IEC/IEEE peut requérir l'utilisation de matériels protégés par des droits de brevet. En publiant cette norme, aucun parti n'est pris concernant l'existence ou la validité de droits de brevet y afférents. Ni l'IEC ni l'IEEE ne peuvent être tenus d'identifier les revendications de brevet essentielles pour lesquelles une autorisation peut s'avérer nécessaire, d'effectuer des recherches sur la validité juridique ou l'étendue des revendications des brevets, ou de déterminer le caractère raisonnable ou non discriminatoire des termes ou conditions d'autorisation énoncés dans le cadre d'un Certificat d'assurance, lorsque la demande d'un tel certificat a été formulée, ou contenus dans tout accord d'autorisation. Les utilisateurs de cette norme sont expressément informés du fait que la détermination de la validité de tous droits de propriété industrielle, ainsi que les risques qu'implique la violation de ces droits, relève entièrement de leur seule responsabilité.

La Norme internationale IEC/IEEE 62209-1528 a été établie par le comité d'études 106 de l'IEC: Méthodes d'évaluation des champs électriques, magnétiques et électromagnétiques en relation avec l'exposition humaine, en coopération avec l'International Committee on Electromagnetic Safety de l'IEEE Standards Association, selon l'accord double logo IEC/IEEE.

Cette première édition de l'IEC/IEEE 62209-1528 annule et remplace l'IEC 62209-1:2016, IEC 62209-2:2010, IEC 62209-2:2010/AMD1:2019 et l'IEEE Std 1528-2013. Cette édition constitue une révision technique.

Cette édition inclut les modifications techniques majeures suivantes par rapport à l'édition précédente:

a) extension de la plage de fréquences de 4 MHz jusqu'à 10 GHz;
b) essai des dispositifs équipés de capteurs de proximité;
c) fantômes spécifiques à l'application;
d) spécification du support de dispositif;
e) procédures d'essai de DAS rapide;
f) procédures de réduction de l'essai;
g) procédure d'évaluation de l'ELT;
h) révision de l'article de validation, y compris les antennes de validation;
i) révision de la procédure d'évaluation du DAS;
j) procédure de mesure du DAS moyenné dans le temps;
k) analyse de l'incertitude;

Ce document est publié en tant que norme double logo IEC/IEEE.

Cette publication contient des fichiers joints sous la forme d'un assistant DAS rapide décrit en 7.9.2.2 et de fichiers CAO pour le fantôme SAM. Ces fichiers sont disponibles à l'adresse suivante:

http://www.iec.ch/dyn/www/f?p=103:227:0::::FSP_ORG_ID,FSP_LANG_ID:1303,25.

Ces fichiers sont destinés à être utilisés comme complément et ne font pas partie intégrante de la publication.

La présente version bilingue (2021-04) correspond à la version anglaise monolingue publiée en 2020-10.

La version française de cette norme n'a pas été soumise au vote.

Les Normes internationales sont rédigées conformément aux règles données dans les Directives ISO/IEC, Partie 2.

IECNORM.COM : Click to view the full PDF of IEC/IEEE 62209-1528:2020

Le comité d'études de l'IEC et le comité d'études de l'IEEE ont décidé que le contenu de cette publication ne sera pas modifié avant la date de stabilité indiquée sur le site web de l'IEC sous "http://webstore.iec.ch" dans les données relatives à la publication recherchée. À cette date, la publication sera

- reconduite,
- supprimée,
- remplacée par une édition révisée, ou
- amendée.

IMPORTANT – Le logo "colour inside" qui se trouve sur la page de couverture de cette publication indique qu'elle contient des couleurs qui sont considérées comme utiles à une bonne compréhension de son contenu. Les utilisateurs devraient, par conséquent, imprimer cette publication en utilisant une imprimante couleur.

IECNORM.COM : Click to view the full PDF of IEC/IEEE 62209-1528:2020

INTRODUCTION

Le présent document a pour objet de fournir les procédures de mesure de l'exposition humaine des dispositifs destinés à être utilisés proches de la tête ou du corps. Il a été développé pour établir les procédures d'évaluation de l'exposition aux champs électromagnétiques (CEM) produits par des appareils d'émission de radiofréquences (RF) utilisés proches de l'oreille, devant le visage ou sur le corps en combinaison avec d'autres dispositifs ou accessoires de transmission RF ou pas (une attache de ceinture, par exemple) ou intégrés aux vêtements. Les types de dispositifs incluent, entre autres, les téléphones mobiles, les téléphones sans fil, les micros sans fil et les émetteurs radio dans les ordinateurs personnels. La plage de fréquences applicables est comprise entre 4 MHz et 10 GHz. Le document définit:

– les exigences relatives au système de mesure (Article 6),
– les protocoles pour le mesurage du DAS (Article 7),
– l'évaluation de l'incertitude de mesure du DAS (Article 8), et
– les exigences relatives à la consignation (Article 9).

Au moment du développement du présent document, deux projets informatiques et de mesure communs IEC/IEEE traitant de l'évaluation de la densité de puissance à ondes millimétriques étaient en cours de développement et couvraient la plage de fréquences comprise entre 6 GHz et 300 GHz. De ce fait, il existe un chevauchement de fréquence entre le présent document, qui traite du DAS, et les projets communs IEC/IEEE traitant de la densité de puissance entre 6 GHz et 10 GHz. Conscient de ce fait, le groupe de travail commun IEC/IEEE a estimé que cela permettrait d'apporter une certaine souplesse quant à l'utilisation des métriques adaptées au cas considéré d'évaluation de la conformité.

IECNORM.COM : Click to view the full PDF of IEC/IEEE 62209-1528:2020

© IEC/IEEE 2020

PROCÉDURE DE MESURE POUR L'ÉVALUATION DU DÉBIT D'ABSORPTION SPÉCIFIQUE DE L'EXPOSITION HUMAINE AUX CHAMPS RADIOFRÉQUENCE PRODUITS PAR LES DISPOSITIFS DE COMMUNICATIONS SANS FIL TENUS À LA MAIN OU PORTÉS PRÈS DU CORPS –

Partie 1528: Modèles humains, instrumentation et procédures (plage de fréquences comprise entre 4 MHz et 10 GHz)

IECNORM.COM : Click to view the full PDF of IEC/IEEE 62209-1528:2020

1 Domaine d'application

Le présent document spécifie les protocoles et procédures d'essai pour le mesurage reproductible et répétable du DAS maximal moyenné dans l'espace (psDAS) d'exposition prudente induit à l'intérieur d'un modèle simplifié de tête et de corps humain par des dispositifs d'émission de radiofréquence (RF), avec une incertitude de mesure définie. Ces protocoles et procédures s'appliquent à une grande partie de la population, y compris les enfants, lors de l'utilisation de dispositifs de communication sans fil portatifs et portés près du corps. Ces dispositifs incluent un ou plusieurs émetteurs ou antennes, et fonctionnent en maintenant leur(s) structure(s) de rayonnement à des distances de la tête et du corps atteignant 200 mm. Il a été développé pour établir les procédures d'évaluation de l'exposition aux champs électromagnétiques (CEM) produits par des appareils d'émission de radiofréquences (RF) utilisés proches de l'oreille, devant le visage ou sur le corps en combinaison avec d'autres dispositifs ou accessoires de transmission RF ou pas (une attache de ceinture, par exemple) ou intégrés aux vêtements. La plage de fréquences applicables est comprise entre 4 MHz et 10 GHz. Les dispositifs fonctionnant dans la plage de fréquences applicable peuvent être soumis à l'essai à l'aide de fantômes et d'autres exigences définies dans le présent document.

Les catégories de dispositifs couvertes incluent, entre autres, les téléphones mobiles, les micros sans fil et les émetteurs radio dans les ordinateurs personnels, les ordinateurs de bureau et les ordinateurs portables, pour les opérations à plusieurs bandes à l'aide d'une ou de plusieurs antennes, y compris les dispositifs à boutons-poussoirs. Le présent document peut également être appliqué pour les dispositifs de transfert de puissance sans fil fonctionnant à plus de 4 MHz.

Le présent document ne concerne pas les dispositifs médicaux implantés.

2 Références normatives

Les documents suivants sont cités dans le texte de sorte qu'ils constituent, pour tout ou partie de leur contenu, des exigences du présent document. Pour les références datées, seule l'édition citée s'applique. Pour les références non datées, la dernière édition du document de référence s'applique (y compris les éventuels amendements).

IEC 62209-3:2019, *Procédure de mesure pour l'évaluation du débit d'absorption spécifique de l'exposition humaine aux champs radiofréquence produits par les dispositifs de communications sans fil tenus à la main ou portés près du corps – Partie 3: Systèmes basés sur la mesure vectorielle (plage de fréquences comprise entre 600 MHz et 6 GHz).*

ISO/IEC Guide 98-3:2008, *Incertitude de mesure – Partie 3: Guide pour l'expression de l'incertitude de mesure (GUM:1995)*

3 Termes et définitions

Pour les besoins du présent document, les termes et définitions suivants s'appliquent.

L'ISO, l'IEC et l'IEEE tiennent à jour des bases de données terminologiques destinées à être utilisées en normalisation, consultables aux adresses suivantes:

- IEC Electropedia: disponible à l'adresse http://www.electropedia.org/
- ISO Online browsing platform: disponible à l'adresse http://www.iso.org/obp/ui/fr/
- IEEE Dictionary Online: disponible à l'adresse http://dictionary.ieee.org

3.1
accessoire
fixation ou composant facultatif qui peut être utilisé conjointement avec le dispositif en essai (DUT)

EXEMPLE 1 Des accessoires de maintien, de fixation, de transport, de port ou de fixation du dispositif ou ayant un usage particulier sur le corps de l'utilisateur (une attache de ceinture, une dragonne ou toute autre dragonne, ou un cordon permettant de porter le dispositif en collie).

EXEMPLE 2 Des accessoires électroniques permettant d'exécuter des tâches spécialisées ou qui assurent une fonction supplémentaire (modules GPS, imprimantes extérieures, lecteurs MP3, caméras ou dispositifs d'affichage, par exemple).

EXEMPLE 3 Des accessoires électroniques fournissant une entrée ou une sortie audio ou vidéo (casques, micros, caméras, par exemple).

EXEMPLE 4 Des accessoires offrant une capacité RF améliorée au dispositif (antennes d'origine, de remplacement ou auxiliaires, par exemple).

EXEMPLE 5 Batteries et composants d'alimentation en courant continu connexes.

EXEMPLE 6 Des combinaisons d'accessoires, dans lesquelles au moins deux des éléments ci-dessus sont combinés pour former un seul composant.

Note 1 à l'article: L'abréviation "DUT" est dérivée du terme anglais développé correspondant "*device under test*".

3.2
isotropie axiale
écart maximal du DAS mesuré lorsque la sonde tourne autour de son axe principal pendant qu'elle est exposée à une onde diffractant depuis une direction coïncidant avec son axe principal

3.3
restriction de base
limites de conformité de l'exposition de l'homme aux champs électriques, magnétiques et électromagnétiques variables dans le temps, mesurées à l'intérieur du corps et fondées sur des effets néfastes établis sur la santé

Note 1 à l'article: Dans les limites du domaine d'application du présent document, la grandeur physique utilisée comme restriction de base est le débit d'absorption spécifique (DAS).

3.4
dispositif porté près du corps
dispositif contenant au moins un émetteur ou émetteur-récepteur sans fil, qui est placé proche du torse ou des membres d'une personne (à l'exclusion de la tête) au moyen d'un accessoire de transport, et permettant de prendre en charge les opérations prévues dans le cadre de l'utilisation

Note 1 à l'article: Le présent document utilise le terme "porté près du corps" comme synonyme du terme "porté sur le corps", qui était utilisé dans les versions précédentes.

IECNORM.COM : Click to view the full PDF of IEC/IEEE 62209-1528:2020

3.5
dispositif posé sur le corps
dispositif contenant au moins un émetteur ou émetteur-récepteur sans fil, dont une quelconque partie est maintenue directement sur le corps de l'utilisateur

3.6
effet de proximité de bord
modification de la sensibilité d'une sonde de champ électrique quand la sonde est située à proximité (moins d'un diamètre d'extrémité de sonde) des limites du milieu

Note 1 à l'article: Cet effet est provoqué par la distorsion du champ diffracté à l'extrémité de la sonde en raison de la surface du fantôme diélectrique à proximité. Cet effet peut être compensé pour une orientation connue de la sonde par rapport à la surface du fantôme.

3.7
câble
fil nécessaire au fonctionnement du dispositif dans la configuration opérationnelle prévue

3.8
canal
canal RF
subdivision spécifique de la plage de fréquences disponible, selon les paramètres de fonctionnement d'une technologie sans fil

Note 1 à l'article: Le nombre de canaux RF et la largeur de bande du canal correspondante peuvent varier en fonction de chaque technologie sans fil. Pour les besoins du présent document, les mesurages de DAS sont effectués sur des canaux spécifiques; par exemple, les canaux supérieur, central ou inférieur de la bande d'émission.

3.9
puissance conduite
puissance délivrée par l'amplificateur de puissance au dispositif jusqu'à une charge correspondante

3.10
exposition prudente
estimation du psDAS, prenant en compte les incertitudes définies dans la présente norme, qui est représentative et légèrement supérieure à celles attendues dans la tête et le corps d'une majorité significative de personnes lors de l'utilisation prévue du dispositif d'émission sans fil

3.11
mode à enveloppe constante
mode d'émission dans lequel l'amplitude du signal ne varie pas dans le temps

3.12
signaux corrélés
champs électromagnétiques associés à des formes d'ondes de signaux distinctes, donnant une intégrale de corrélation dans le domaine temporel non nulle à un instant donné

Note 1 à l'article: Des informations détaillées sont spécifiées dans l'IEC TR 62630 [1].

3.13
appareil de bureau
appareil posé ou monté sur un bureau, une table ou une structure d'appui similaire, et dont l'antenne est prévue pour fonctionner à moins de 200 mm du corps humain

3.14
support de dispositif
fixation fabriquée en un matériau à faible perte diélectrique, utilisée pour maintenir le dispositif en essai dans la position d'essai exigée pendant le mesurage de DAS

IECNORM.COM : Click to view the full PDF of IEC/IEEE 62209-1528:2020

3.15
dispositif en essai
DUT
appareil portable contenant au moins un émetteur-récepteur sans fil et soumis à l'essai selon les méthodes du présent document

Note 1 à l'article: Un dispositif en essai peut être classé parmi les dispositifs portés près du corps, posés sur le corps, les dispositifs de bureau, devant le visage, portatifs, portés sur les membres, intégrés aux vêtements ou génériques.

Note 2 à l'article: L'abréviation "DUT" est dérivée du terme anglais développé correspondant "*device under test*".

3.16
facteur d'utilisation
rapport de la durée d'émission d'un émetteur sur une période spécifique

3.17
essais rapides de DAS
utilisation de techniques, méthode ou algorithmes particuliers pour diminuer le temps de mesure du DAS comparé à l'essai complet de DAS

Note 1 à l'article: L'essai rapide de DAS de Classe 1 utilise un matériel satisfaisant aux exigences du présent document pour l'essai complet du DAS. Toutefois, il utilise des procédures d'essai plus rapides que celles satisfaisant aux procédures d'essai complet du DAS.

Note 2 à l'article: L'essai rapide de DAS de Classe 2 utilise un matériel et des procédures d'essai ne satisfaisant pas aux exigences du présent document pour l'essai complet du DAS.

3.18
bande de fréquences
plage de fréquences d'émission associée à un mode de fonctionnement sans fil particulier

Note 1 à l'article: En règle générale, il est fait référence à la bande de fréquences avec des chiffres arrondis. Toutefois, l'allocation de fréquence réelle peut être légèrement différente (la bande GSM 850 MHz utilise actuellement une plage comprise entre 824 MHz et 849 MHz et entre 869 MHz et 894 MHz, et la bande GSM 900 MHz utilise une plage comprise entre 880 MHz et 915 MHz et entre 925 MHz et 960 MHz, par exemple). Dans d'autres cas, la nomenclature 3GPP officielle peut être utilisée. Par exemple, la bande LTE 12 (liaison montante 699 MHz à 716 MHz; liaison descendante 729 MHz à 746 MHz).

3.19
appareil placé devant le visage
appareil tenu à la main et contenant au moins un émetteur ou émetteur-récepteur sans fil mis en marche très près du visage

Note 1 à l'article: Les types de dispositifs placés devant le visage comprennent les dispositifs à boutons-poussoirs, les radios bidirectionnelles et les appareils équipés d'une caméra optique.

3.20
essais complets du DAS
utilisation de méthodes, de procédures et de matériel spécifique qui satisfont totalement à toutes les exigences normatives du présent document, à l'exception de celles spécifiées en 7.9.2

3.21
appareil générique
dispositif qui ne peut pas être classé comme étant l'un quelconque des types de dispositifs spécifiques

3.22
appareil tenu à la main
appareil portable dont l'utilisation prévue implique que l'utilisateur le tienne à la main à plus de 200 mm de la tête ou du torse pendant son utilisation prévue

IECNORM.COM : Click to view the full PDF of IEC/IEEE 62209-1528:2020

3.23
combiné
appareil de communication sans fil destiné à être tenu à la main et utilisé proche de l'oreille, composé d'une sortie acoustique (écouteur) et d'une entrée acoustique (micro) et contenant un émetteur ou émetteur-récepteur radio

Note 1 à l'article: Pour les synonymes tels que "téléphone mobile", les termes "mobile" et "portable" ont des significations spécifiques, mais génériques, dans l'IEC 60050 – mobile: capable de fonctionner en déplacement (IEC 60050-151:2001, 151-16-46); portable: capable d'être porté par une personne seule (IEC 60050 151:2001, 151-16-47). Le terme "portable" fait souvent référence à l'aptitude à fonctionner d'un appareil porté sur l'utilisateur. Ces définitions sont utilisées indifféremment dans différentes réglementations et spécifications de l'industrie sans fil, faisant dans certains cas référence à des types d'appareils de communication et dans d'autres cas à leur utilisation prévue.

3.24
dispositif installé sur la tête
dispositif contenant au moins un émetteur ou émetteur-récepteur sans fil, qui est placé très proche de la tête ou du cou d'une personne au moyen d'un accessoire de transport, si nécessaire, et permettant de prendre en charge les opérations prévues dans le cadre de l'utilisation

Note 1 à l'article: Cette définition exclut les appareils tenus à la main.

3.25
isotropie hémisphérique
écart maximal du DAS quand la sonde est en rotation sur son axe principal tandis qu'elle est exposée à une onde de référence ayant différents angles d'incidence par rapport à l'axe de la sonde et une incidence dans le demi-espace face à la sonde

3.26
hôte
équipement qui nécessite d'être utilisé avec un appareil ou module sans fil pendant l'essai offrant des fonctionnalités d'émission en fonction de son utilisation prévue

3.27
utilisation prévue
conditions d'utilisation auxquelles un produit est destiné en fonction de l'éventail complet des fonctions disponibles, selon les spécifications, les instructions et les informations fournies par le fabricant dans la documentation d'utilisation

3.28
appareil fixé à un membre
appareil contenant au moins un émetteur ou émetteur-récepteur sans fil et dont l'utilisation prévue suppose d'être attaché au bras ou à la jambe de l'utilisateur pendant l'émission

Note 1 à l'article: Les types d'appareils fixés à un membre sont notamment les appareils fixés au poignet, les appareils fixés à la cheville et les appareils fixés à l'avant-bras. Certaines juridictions de réglementation spécifient différentes exigences relatives aux dispositifs portés sur d'autres membres que les poignets ou les chevilles.

3.29
erreur de linéarité
écart maximal d'une grandeur mesurée sur la plage de mesure par rapport à la dépendance linéaire prévue

3.30
dérive de mesure
variation continue ou incrémentielle au fil du temps de la grandeur mesurée, en raison de variations des propriétés métrologiques d'un instrument de mesure

IECNORM.COM : Click to view the full PDF of IEC/IEEE 62209-1528:2020

3.31
incertitude de mesure

3.31.1
évaluation de l'incertitude
<Type A> évaluation de l'incertitude par l'analyse statistique d'une série d'observations (mesurages)

3.31.2
évaluation de l'incertitude
<Type B> évaluation de l'incertitude par des moyens autres que l'analyse statistique d'une série d'observations (mesurages)

3.31.3
incertitude-type
écart type estimé du résultat d'un mesurage, égal à la racine carrée positive de la variance estimée

3.31.4
incertitude composée
écart type estimé du résultat d'un mesurage obtenu en combinant les incertitudes-types individuelles des évaluations de type A et de type B en utilisant la méthode usuelle de "somme quadratique" de combinaison d'écarts types qui sont obtenus en utilisant la racine carrée positive des variances estimées

3.31.5
incertitude élargie
grandeur définissant un intervalle autour du résultat d'un mesurage et qui est considérée comme englobant une distribution des valeurs dans un intervalle de confiance défini qui peuvent être raisonnablement attribuées à la grandeur mesurée

3.32
multibande
<dispositif de communication sans fil> capable de fonctionner dans plus d'une bande de fréquence

3.33
mode de fonctionnement
protocole sans fil ou norme utilisé(e) par un dispositif pour communiquer avec un autre terminal ou réseau

Note 1 à l'article: Le mode de fonctionnement inclut tous les paramètres permettant d'établir la communication sur le réseau sans fil. Les paramètres de mode de fonctionnement spécifiques incluent, la liste n'étant pas exhaustive, la norme de communication, la bande de fréquences, le canal, la modulation de signal, le protocole de communication, le débit de données, la bande passante, le nombre d'intervalles de temps et leur position, et le nombre de blocs de ressource et leur position. Certains modes de fonctionnement ne comportent pas certains de ces paramètres.

Note 2 à l'article: Les terminaux modernes peuvent avoir plusieurs modes de fonctionnement pour une émission individuelle ou simultanée. Les modes de fonctionnement incluent, entre autres, des protocoles sans fil tels que GSM, EDGE, EVDO, GPRS, CDMA, WCDMA, LTE, 5 G NR, Bluetooth®[1] et Wi-Fi®[2]. Plusieurs modes de fonctionnement peuvent émettre sur une ou plusieurs bandes de fréquences. Par exemple, un DUT peut prendre en charge plusieurs technologies sans fil dans une bande de fréquences, et permettre plusieurs modes d'émission sans fil au sein d'une technologie sans fil (GSM, GPRS, EDGE ou WCDMA et HSPA ou 5 G NR, par exemple).

---

1 Bluetooth® est une marque de Bluetooth Special Interest Group (SIG). Cette information est donnée à l'intention des utilisateurs du présent document et ne signifie nullement que l'IEC approuve ou recommande l'emploi exclusif du produit cité.

2 Wi-Fi® est une marque de Wi-Fi Alliance. Cette information est donnée à l'intention des utilisateurs du présent document et ne signifie nullement que l'IEC approuve ou recommande l'emploi exclusif du produit cité.

IECNORM.COM : Click to view the full PDF of IEC/IEEE 62209-1528:2020

3.34
puissance de sortie
puissance à la sortie de l'émetteur RF lorsqu'il est connecté à l'antenne ou à une charge de la même impédance que l'antenne

3.35
valeur primaire du DAS crête
valeur de DAS local interpolée la plus élevée déterminée dans le cadre d'un mesurage de balayage de surface

3.36
valeur secondaire du DAS crête
dans un mesurage de balayage de surface, DAS local interpolé maximal inférieur à la valeur primaire du DAS crête

3.37
DAS maximal moyenné dans l'espace
psDAS
DAS maximal moyenné dans une région locale en fonction d'une masse moyennée spécifique (1 g ou 10 g de tissus en forme d'un cube, par exemple)

Note 1 à l'article: Dans le présent document, les termes psDAS (sur 1 g ou 10 g) et les termes DAS sur 1 g et DAS sur 10 g sont utilisés indifféremment.

Note 2 à l'article: L'abréviation "ps" est dérivée du terme anglais développé correspondant "*peak spatial-average*".

3.38
profondeur de pénétration
profondeur à laquelle le DAS d'une onde plane incidente associée, pénétrant un milieu homogène avec pertes, est ramenée à $1/e^2$ de sa valeur juste au-dessous de la surface du milieu

Note 1 à l'article: Pour une onde plane incidente perpendiculaire sur un demi-espace planaire, la profondeur de pénétration δ du champ E est donnée par:

$$\delta = \frac{1}{\omega}\left[\frac{\mu_0 \varepsilon'_r \varepsilon_0}{2}\left(\sqrt{1+\left(\frac{\sigma}{\omega \varepsilon'_r \varepsilon_0}\right)^2}-1\right)\right]^{-\frac{1}{2}}$$

où

ω est la fréquence angulaire;

μ_0 est la perméabilité magnétique du vide, en henry par mètre;

μ_0 est la permittivité diélectrique du vide, en farad par mètre;

ε'_r est la permittivité diélectrique relative du milieu avec pertes, sans unité;

σ est la conductivité électrique du milieu avec pertes, en siemens par mètre.

3.39
fantôme
modèle physique similaire en apparence à l'anatomie humaine et composé d'un milieu équivalent au tissu ayant les propriétés électriques spécifiées dans le présent document

3.40
pavillon de l'oreille
partie cartilagineuse extérieure de l'oreille, consistant en l'hélix, le lobe et l'anthélix

IECNORM.COM : Click to view the full PDF of IEC/IEEE 62209-1528:2020

3.41
algorithme de régulation de puissance
protocole du DUT pour définir et régler la puissance de sortie maximale de l'émetteur sur une période de moyennage spécifiée

3.42
variation de production
plage de la puissance de sortie parmi les échantillons de production du DUT réglée pour émettre au niveau maximal

3.43
dispositif à bouton-poussoir
émetteur-récepteur radio tenu à la main sur lequel l'utilisateur active un commutateur mécanique pour basculer entre l'émission et la réception radio (mode de fonctionnement simplex)

EXEMPLE Une radio bidirectionnelle.

3.44
isotropie de la sonde
propriété relative à la mesure dans laquelle la réponse d'une sonde de champ électrique ou de champ magnétique est indépendante de la polarisation et de la direction de propagation de l'onde incidente

Note 1 à l'article: Voir également "isotropie axiale" (3.2) et "isotropie hémisphérique" (3.25).

3.45
capteur de proximité
capteur capacitif ou combinaison de capteurs dans le DUT utilisé(e) pour détecter la proximité d'un utilisateur afin de limiter la puissance de l'émetteur et assurer la conformité aux limites d'exposition RF

3.46
lecture électronique
composant du système de mesure relié à la sonde de champ E et qui fournit au postprocesseur du système de mesure une conversion analogique-numérique des valeurs mesurées

3.47
temps de réponse
temps nécessaire à l'équipement de mesure pour atteindre 90 % de sa valeur finale après une variation du signal d'entrée

3.48
système de balayage
système de positionnement automatique capable de placer la sonde de mesure à des positions spécifiées selon les exigences du présent document

3.49
sensibilité
rapport de l'amplitude de la réponse du système (par exemple, tension) sur l'amplitude de la grandeur mesurée (exemple: carré d'un champ électrique)

3.50
distance de séparation
distance entre le dispositif en essai et la surface extérieure du fantôme

Note 1 à l'article: La distance de séparation représente la distance pendant l'utilisation prévue.

IECNORM.COM : Click to view the full PDF of IEC/IEEE 62209-1528:2020

3.51
débit d'absorption spécifique
DAS
mesure du débit d'absorption de l'énergie par le corps humain lorsqu'il est exposé à un champ électromagnétique RF

Note 1 à l'article: Le DAS dans le milieu équivalent au tissu peut être déterminé par la vitesse d'élévation de la température ou par les mesurages de champ E, selon les formules suivantes:

$$DAS = \frac{\sigma E^2}{\rho}$$

$$DAS = c_h \left.\frac{\partial T}{\partial t}\right|_{t=0}$$

où:

DAS est le débit d'absorption spécifique en watts par kilogramme;

E est la valeur efficace du champ électrique dans le milieu équivalent au tissu en volts par mètre;

σ est la conductivité électrique du milieu équivalent au tissu en siemens par mètre;

ρ est la masse volumique du milieu équivalent au tissu en kilogrammes par mètre cube;

c_h est la capacité thermique massique du milieu équivalent au tissu en kilogramme par kelvin;

$\left.\frac{\partial T}{\partial t}\right|_{t=0}$ est la dérivée initiale en fonction du temps de la température dans le milieu équivalent au tissu en kelvin par seconde.

3.52
configuration d'essai
ensemble de paramètres du DUT applicables au mesurage du DAS, composé de la position du DUT sur le fantôme applicable, de la configuration d'utilisation du DUT (la position de l'antenne, par exemple) et du mode de fonctionnement

3.53
DAS moyenné sur une période
TPAS
DAS moyenné sur une période spécifiée lorsque l'algorithme de régulation de puissance est appliqué

Note 1 à l'article: L'abréviation "TPAS" est dérivée du terme anglais développé correspondant "*time-period averaged SAR*".

3.54
DAS moyenné dans le temps
DAS mesuré sur une durée d'intégration suffisamment longue pour obtenir un résultat stable sur le facteur d'utilisation et d'autres caractéristiques du signal modulé

3.55
spécification finement établie
tolérance de puissance de sortie lors du réglage d'un échantillon du DUT pour émettre au niveau maximal de puissance sortie

3.56
facteur TX
rapport de la puissance de sortie moyenne sur la puissance de sortie maximale du DUT sur une période de moyennage dans le temps spécifiée

IECNORM.COM : Click to view the full PDF of IEC/IEEE 62209-1528:2020

4 Symboles et abréviations

4.1 Grandeurs physiques

Le Système international d'unités (SI) est utilisé tout le long du présent document.

Symbole	Grandeur	Unité	Dimensions
α	Coefficient d'atténuation	inverse du mètre	1/m
P	Puissance absorbée moyenne (temporelle)	watt	W
J	Densité de courant	ampère par mètre carré	A/m^2
σ	Conductivité électrique	siemens par mètre	S/m
E	Champ électrique	volt par mètre	V/m
f	Fréquence	hertz	Hz
ρ	Masse volumique	kilogramme par mètre cube	kg/m^3
δ	Profondeur de pénétration	mètre	m
μ	Perméabilité	henry par mètre	H/m
c_h	Capacité thermique massique	joule par kilogramme par kelvin	J/(kg K)
ε	Permittivité	farad par mètre	F/m
DAS	Débit d'absorption spécifique	watt par kilogramme	W/kg
T	Température	kelvin	K
λ	Longueur d'onde	mètre	m

NOTE Dans le présent document, la température est exprimée en degrés Celsius et définie par: T(°C) = T(K) – 273,15 K.

4.2 Constantes

Symbole	Constante physique	Amplitude
c_0	Vitesse de la lumière dans le vide	$2{,}998 \times 10^8$ m/s
ε_0	Permittivité de l'espace libre	$8{,}854 \times 10^{-12}$ F/m
μ_0	Perméabilité de l'espace libre	$4\pi \times 10^{-7}$ H/m

4.3 Abréviations

5G NR	Nouvelle radio cinquième génération
AIPLC	Automatic Input Power Level Control (contrôle automatique du niveau de puissance d'entrée)
APS	Absolute psSAR (psDAS absolu)
CAO	Conception assistée par ordinateur
AMRC	Accès multiple par répartition en code
CLA	Confined-Loop Antenna (antenne cadre confinée)
CW	Continuous Wave (onde entretenue)
DCS	Digital Cellular Service (service de téléphonie cellulaire numérique)
DOE	Design Of Experiments (plan d'expériences)
DUT	Device Under Test (dispositif en essai)

IECNORM.COM : Click to view the full PDF of IEC/IEEE 62209-1528:2020

EDGE	Enhanced Data rates for GSM Evolution (GSM à débit amélioré)
champ E	Champ électrique
ERP	Ear Reference Point (point de référence de l'oreille)
FDTD	Finite-Difference Time-Domain (différences finies dans le domaine temporel)
GPRS	General Packet Radio Service (service général de radiocommunication par paquets)
GSM	Global System for Mobile Communications (système global de communications mobiles)
champ H	Champ magnétique
ICES	International Committee on Electromagnetic Safety (comité international de sécurité électromagnétique)
ICNIRP	International Commission on Non-Ionizing Radiation Protection (commission internationale de protection contre les rayonnements non ionisants)
OG	Oreille gauche
ELT	Évolution à long terme
MIMO	Multiple Input Multiple Output (entrées multiples, sorties multiples)
MPR	Maximum Power Reduction (réduction de puissance maximale)
OFAT	One-Factor-At-a-Time (un facteur à la fois)
OFDM	Orthogonal Frequency-Division Multiplexing (multiplexage par répartition orthogonale de la fréquence)
OFDMA	Orthogonal Frequency-Division Multiple Access (accès multiple par répartition orthogonale de la fréquence)
PCS	Personal Communications Service (service de communication personnelle)
PDF	Probability Density Function (fonction de densité de probabilité)
psDAS	DAS maximal moyenné
PTT	Push-To-Talk (bouton-poussoir)
OD	Oreille droite
RF	Radiofréquence
RMS	Root Mean Square (valeur efficace)
RSS	Root Sum Square (somme quadratique)
SAM	Specific Anthropomorphic Mannequin (mannequin anthropomorphe spécifique)
DAS	Débit d'absorption spécifique
STBC	Space-Time Block Coding (code de bloc espace-temps)
AMRT	Accès multiple par répartition temporelle
TX	Transmission
UMTS	Universal Mobile Telecommunications System (système universel de télécommunications mobiles)
VPIFA	Vertical Planar Inverted F-Antenna (antenne F inversée planaire verticale)
WCDMA	Wideband Code Division Multiple Access (AMRC à bande élargie)
WiMax	Worldwide Interoperability for Microwave Access (interopérabilité mondiale des accès d'hyperfréquences)
WLAN	Wireless Local Area Network (réseau local sans fil)

IECNORM.COM : Click to view the full PDF of IEC/IEEE 62209-1528:2020

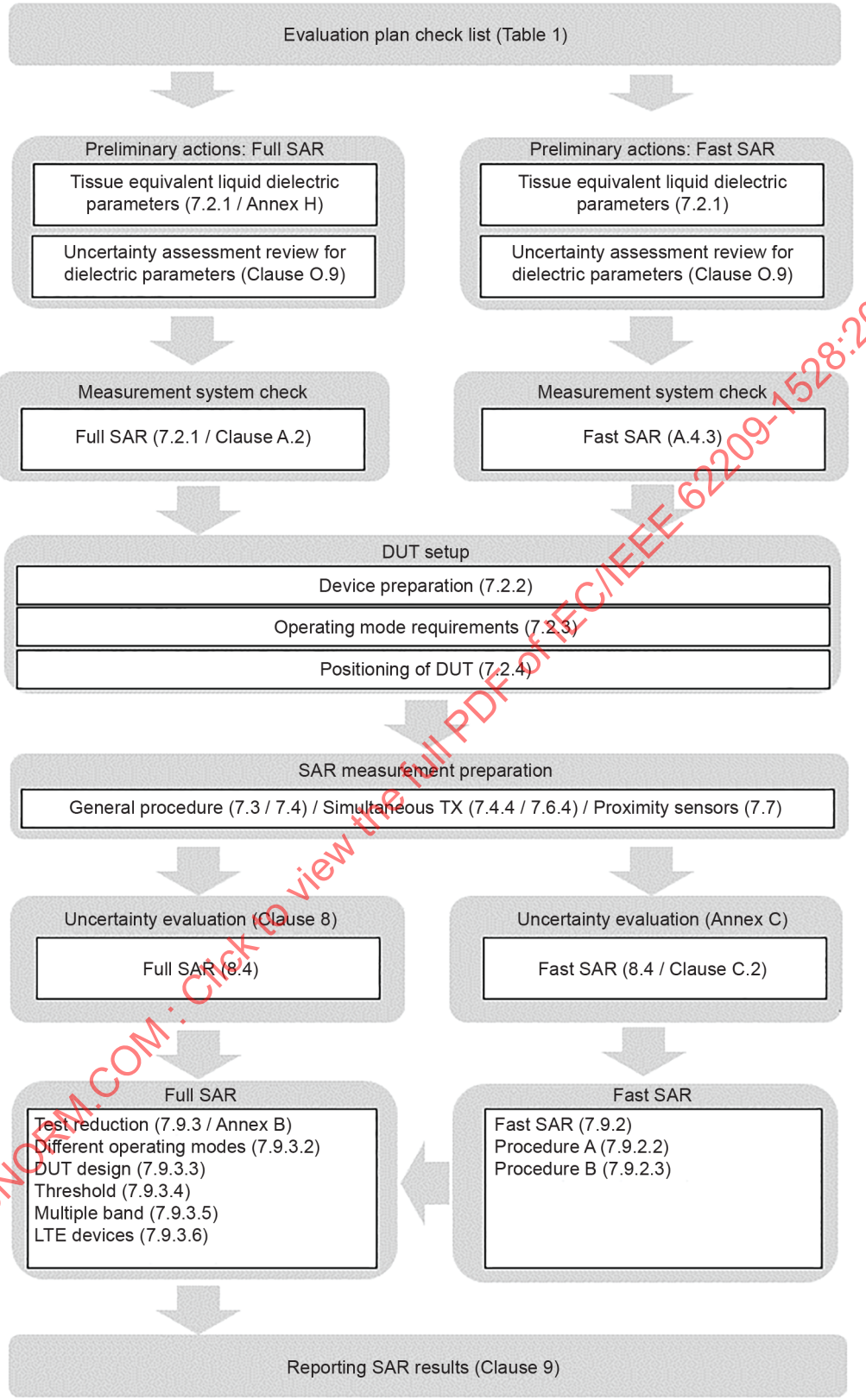
5 Guide de démarrage rapide et liste de contrôle du plan d'évaluation

Le guide de démarrage rapide représenté à la Figure 1 et la liste de contrôle du plan d'évaluation présentée dans le Tableau 1 donnent une très bonne vue d'ensemble des procédures de mesure du DAS du présent document. Chaque étape est détaillée à l'article correspondant spécifié à la Figure 1 et dans le Tableau 1.

Tableau 1 – Liste de contrôle du plan d'évaluation

Phase	Étapes d'évaluation	Action
Liste de contrôle du plan d'évaluation Planification des configurations de mesure	– Quel type de dispositif est en cours d'évaluation? – Examen des antennes et des technologies sans fil prises en charge, seules ou en combinaison. – Quelles sont les positions d'essai applicables? – Travailler dans des conditions de laboratoire et suivre les bonnes pratiques et documentations de laboratoire pour se préparer à effectuer les évaluations nécessaires.	Remplir la liste de contrôle par rapport au plan d'évaluation.
Actions préliminaires et vérification du système de mesure	– Les propriétés diélectriques d'un liquide doivent être mesurées les données consignées **Pour les systèmes matriciels, elles sont en général fournies par le fabricant* – Il est nécessaire de contrôler le système afin de vérifier le bon fonctionnement des composants du système.	Il convient de les effectuer avant de commencer un projet et de les répéter.
Configuration du DUT	Le protocole d'évaluation de DAS définit toutes les permutations de conditions de fonctionnement qu'il convient de soumettre à l'essai. Les étapes essentielles incluent: – Préparation du DUT par l'établissement d'une connexion à un simulateur de station de base. – Configuration du DUT pour qu'il fonctionne sur les fréquences d'essai appropriées. – Positionnement du DUT par rapport au fantôme.	Vérifier que le DUT est configuré de la bonne manière et qu'il rayonne correctement lorsqu'il est placé conte le fantôme.
Évaluation de l'incertitude	– Des lignes directrices et des formules d'approximation sont fournies afin de permettre l'estimation de chaque composante individuelle de l'incertitude. – Le bilan d'incertitude doit couvrir la plage de fréquences appropriée en ce qui concerne le matériel utilisé dans le système DAS.	Déterminer l'incertitude et compléter le tableau d'incertitudes.
Procédures de mesure de DAS	– Cette phase est la procédure réelle de mesure de DAS. – La procédure est itérative pour assurer que la valeur la plus élevée du DAS maximal moyenné d'un DUT est capturée. – Cela est réalisé par un processus systématique prenant en compte, de façon adéquate, l'ensemble des positions, configurations et modes de fonctionnement du dispositif dans toutes les bandes de fréquences. – Les systèmes de mesure peuvent intégrer une seule sonde ou des sondes matricielles. Des essais rapides de DAS ou des techniques de réduction d'essai peuvent être utilisées. Des techniques reconnues peuvent être utilisées pour réduire ou accélérer le processus de mesure.	Détermination du DAS le plus élevé. Assurer que la justification de la réduction d'essai ou de l'essai de DAS rapide est enregistrée et consignée dans un rapport s'ils ont été utilisés.
Consignation des résultats de DAS	– Le rapport final décrit les résultats des évaluations, fournit suffisamment d'informations détaillées techniques pour permettre la répétabilité des évaluations réalisées et consigne les résultats en comparaison avec la limite applicable. – Le rapport de mesure doit contenir suffisamment de détails et d'informations pour démontrer la satisfaction aux exigences du présent document.	Préparer le rapport de mesure final et la formulation des exigences.

IECNORM.COM : Click to view the full PDF of IEC/IEEE 62209-1528:2020



IECNORM.COM : Click to view the full PDF of IEC/IEEE 62209-1528:2020

Anglais	Français
Evaluation plan check list (Table 1)	Liste de contrôle du plan d'évaluation (Tableau 1)
Preliminary actions: Full SAR	Action préliminaire: DAS complet
Tissue equivalent liquid dielectric parameters (7.2.1/Annex H)	Paramètres diélectriques du liquide équivalent au tissu (7.2.1/Annexe H)
Uncertainty assessment review for dielectric parameters (Clause O.9)	Examen d'évaluation de l'incertitude des paramètres diélectriques (Article O.9)
Preliminary actions: Fast SAR	Action préliminaire: DAS rapide
Tissue equivalent liquid dielectric parameters (7.2.1)	Paramètres diélectriques du liquide équivalent au tissu (7.2.1)
Uncertainty assessement review for dielectric parameters (Clause O.9)	Examen d'évaluation de l'incertitude des paramètres diélectriques (Article O.9)
Measurement system check	Contrôle du système de mesure
Full SAR (7.2.1/Clause A.2)	DAS complet (7.2.1/Article A.2)
DUT setup	Configuration du DUT
Device preparation (7.2.2)	Préparation du dispositif (7.2.2)
Operating mode requirements (7.2.3)	Exigences relatives aux modes de fonctionnement (7.2.3)
Positioning of DUT (7.2.4)	Positionnement du DUT (7.2.4)
SAR measurement preparation	Préparation du mesurage de DAS
General procedure (7.3/7.4) / Simultaneous TX (7.4.4/7.6.4) / Proximity sensors (7.7)	Procédure générale (7.3/7.4) / Émission simultanée (7.4.4/7.6.4) / Capteurs de proximité (7.7)
Uncertainty evaluation (Clause 8)	Évaluation de l'incertitude (Article 8)
Full SAR (8.4)	DAS complet (8.4)
Uncertainty evaluation (Annex C)	Évaluation de l'incertitude (Annexe C)
Fast SAR (8.4/Clause C.2)	DAS rapide (8.4/Article C.2)
Full SAR	DAS complet
Test reduction (7.9.3/Annex B)	Réduction d'essai (7.9.3/Annexe B)
Different operating modes (7.9.3.2)	Différents modes de fonctionnement (7.9.3.2)
DUT design (7.9.3.3)	Conception du DUT (7.9.3.3)
Threshold (7.9.3.4)	Seuil (7.9.3.4)
Multiple band (7.9.3.5)	Multibande (7.9.3.5)
LTE devices (7.9.3.6)	Dispositifs ELT (7.9.3.6)
Fast SAR	DAS rapide
Fast SAR (7.9.2)	DAS rapide (7.9.2)
Procedure A (7.9.2.2)	Procédure A (7.9.2.2)
Procedure B (7.9.2.3)	Procédure B (7.9.2.3)
Reporting SAR results (Clause 9)	Rapport des résultats de DAS (Article 9)

IECNORM.COM : Click to view the full PDF of IEC/IEEE 62209-1528:2020

Figure 1 – Guide de démarrage rapide

6 Spécifications du système de mesure

6.1 Exigences générales pour les essais de DAS complet

Un système de mesure du DAS est composé du fantôme (un fantôme SAM représentant la tête et/ou un fantôme plan représentant le corps humain) rempli d'un milieu équivalent au tissu, d'instruments électroniques de mesure, d'un système de balayage et d'un support de DUT. Les procédures d'essai de DAS complet sont décrites en 7.4. Les essais de DAS réalisés selon le présent document doivent satisfaire aux exigences suivantes.

a) Le DAS doit être mesuré en utilisant une sonde qui est positionnée automatiquement pour mesurer la distribution interne du champ E dans le fantôme. Les valeurs de champ E mesurées, la distribution de DAS et la valeur psDAS doivent être calculées.

b) Le fantôme doit être rempli avec le milieu équivalent au tissu exigé, représentant les propriétés diélectriques des tissus de la tête ou du corps humain.

c) Le milieu équivalent au tissu doit être un liquide de faible viscosité pour permettre le libre mouvement de la sonde dans le liquide.

d) Pour les milieux équivalents aux tissus, une densité ρ de 1 000 kg/m^3 doit être utilisée.

e) Au moins trois points de référence doivent être définis sur le fantôme par le fabricant du fantôme afin d'aligner le système de balayage sur le fantôme. Ces points doivent être visibles par l'utilisateur, incluant au moins 80 % de la face supérieure du fantôme et doivent être espacés d'au moins 20 cm.

f) La température ambiante et la température du milieu équivalent au tissu doivent être comprises entre 18 °C et 25 °C inclus. Voir O.9.6 pour déterminer l'incertitude de température.

g) Avant de mesurer les propriétés diélectriques du milieu équivalent au tissu et le DAS, le DUT, l'équipement d'essai, le milieu et le fantôme doivent avoir été conservés au laboratoire assez longtemps pour que leurs températures se soient stabilisées (c'est-à-dire qu'ils ne doivent pas avoir été déplacés récemment depuis une autre zone à une température ambiante différente, par exemple un réfrigérateur ou un espace de stockage).

NOTE En fonction de la forme, de la taille, du volume et de la température initiale du milieu et du conteneur, une période d'au moins 24 h peut être exigée pour stabiliser la température.

h) La température du milieu équivalent au tissu pendant les mesurages de DAS ne doit pas varier de plus de 2 °C (ou doit représenter une différence de température correspondant à une variation de 5 % de la permittivité ou de la conductivité, selon la valeur la plus faible) par rapport à celle à laquelle les propriétés diélectriques ont été mesurées. Si la variation de température dépasse cette tolérance, les propriétés diélectriques doivent faire l'objet d'un nouveau mesurage.

i) L'effet des réflexions des câbles, de l'équipement d'essai ou d'autres réflecteurs doit être déterminé par la procédure de contrôle du système DAS décrite à l'Article A.2, en comparant le DAS mesuré en présence ou en l'absence des réflecteurs ou, le cas échéant, avec le positionnement judicieux de matériaux absorbants et/ou l'utilisation de perles de ferrite sur les câbles.

j) Les mesurages de DAS des DUT ne doivent être effectués que lorsque les effets des réflexions, des émetteurs RF secondaires, etc., donnent lieu à un psDAS (pour une masse de 1 g ou de 10 g, suivant la valeur applicable à l'essai) inférieur à 0,012 W/kg en mesurant le psDAS à (environ) 0,4 W/kg (utilisé pour établir la limite de détection minimale de 3 %, voir 8.4.1.7). Lorsque l'effet des câbles et des réflecteurs est supérieur à 0,012 W/kg, des perles de ferrite, des absorbeurs RF et d'autres techniques d'atténuation doivent être appliqués pour réduire l'erreur de DAS.

Si la limite précédente ne peut pas être atteinte, une valeur supérieure à 3 % (0,012 W/kg) peut être prise en considération dans le bilan d'incertitude dans la colonne "conditions ambiantes RF – réflexions" des tableaux applicables de l'Annexe C, à condition qu'il puisse être démontré que la contribution de DAS en raison des réflexions déterminées par la procédure de contrôle du système est inférieure à 10 % du DAS mesuré pour le DUT.

IECNORM.COM : Click to view the full PDF of IEC/IEEE 62209-1528:2020

k) Les exigences liées aux réflexions doivent être vérifiées au moins chaque année ou chaque fois que le contrôle du système indique des résultats inattendus.

l) Au cours de l'essai, le DUT ne doit pas être connecté à un quelconque réseau sans fil, sauf à un simulateur de station de base dans le laboratoire.

m) La validation d'un système selon le protocole défini à l'Article A.3 doit être effectuée au moins une fois par an, et lors de la mise en exploitation d'un nouveau système de mesure et à chaque modification du système (une nouvelle version de logiciel, l'introduction d'un type ou une version différente de lecture électronique ou de sondes différente, par exemple). Les sources d'émission utilisées pour la validation du système doivent être conçues et validées pour satisfaire aux exigences spécifiées à l'Annexe D. Des sources d'émission supplémentaires de types dipôles et guides d'ondes à des fréquences spécifiques ne figurant actuellement pas dans le Tableau D.1, dans le Tableau D.2, dans le Tableau D.3, dans le Tableau D.4, dans le Tableau D.5, dans le Tableau D.6, dans le Tableau D.7, dans le Tableau D.8, dans le Tableau D.9 et dans le Tableau D.10 peuvent être utilisées en tant que sources à condition qu'elles satisfassent aux exigences spécifiées à l'Annexe D. Dans le présent document, les fantômes plans doivent être utilisés pour contrôler et valider le système.

n) Le système de mesure doit être validé comme un système complet.

o) La sonde doit être étalonnée dans un milieu équivalent au tissu dans la plage de fréquences et de températures d'étalonnage exigée, selon la méthodologie spécifiée à l'Annexe E. L'étalonnage de la sonde séparément du système de mesure est permis, à condition que les mêmes caractéristiques électriques d'interface entre la sonde et la lecture électronique soient utilisées lors des mesurages. La ou les sondes doivent être étalonnées avec un amplificateur, un dispositif de mesure et un système d'acquisition de données identiques.

p) La limite de détection inférieure doit être inférieure ou égale à 0,01 W/kg, et la limite de détection maximale doit être supérieure à 100 W/kg.

q) L'isotropie de la sonde doit être inférieure à l'incertitude élargie pour la composante d'isotropie axiale en utilisant les procédures du Tableau 9 et de 8.4.1.5 ou ±0,2 dB (±5 %), selon la valeur qui est la plus faible, telle que déterminée dans le milieu équivalent au tissu.

r) Le diamètre extérieur de l'extrémité de la sonde ne doit pas dépasser 8 mm dans la zone des éléments de mesure pour des fréquences inférieures ou égales à 2 GHz.

s) Pour les fréquences supérieures à 2 GHz, le diamètre de l'extrémité de la sonde ne doit pas dépasser $\lambda/3$, où λ est la longueur d'onde dans le milieu. Le diamètre de l'extrémité de la sonde peut être plus important s'il peut être démontré que le champ E de toute distribution de champ potentielle peut être mesuré avec une incertitude inférieure à ±15 % (k = 2) aux distances de la surface du fantôme, comme cela est indiqué dans le Tableau 3 et dans le Tableau 4 ou aux distances recommandées par le fabricant du système de mesure de DAS (suivant la valeur la plus faible).

t) La linéarité du système doit être dans les limites de ±0,5 dB sur la plage de DAS comprise entre 0,12 W/kg et 100 W/kg.

u) Lorsque le présent document spécifie de manière explicite les caractéristiques de performances de toute ou partie du système de mesure, le fabricant du système ou du sous-système, ou l'intégrateur de système, doit documenter la conformité aux dispositions du présent document.

IECNORM.COM : Click to view the full PDF of IEC/IEEE 62209-1528:2020

6.2 Spécifications du fantôme

6.2.1 Généralités

Le 6.2 spécifie les fantômes à utiliser pour mesurer le psDAS du DUT. Le 6.2.3 définit le fantôme de tête à utiliser pour évaluer l'exposition dans la tête, proche de l'oreille. Le 6.2.4 définit le fantôme plan à utiliser pour évaluer l'exposition dans le torse ou d'autres parties du corps. Si les fantômes de tête ou les fantômes plans ne sont pas applicables, en raison des contraintes physiques liées au système de balayage ou aux conditions d'utilisation prévue du DUT, les fantômes spécifiques décrits en 6.2.5 peuvent être utilisés.

6.2.2 Paramètres du fantôme de base

Le matériau de l'enveloppe du fantôme doit résister aux dégradations ou réactions chimiques dans le milieu équivalent au tissu. L'enveloppe du fantôme doit être constituée d'un matériau à faible perte et à faible permittivité, ayant une tangente de perte $\tan\delta \leq 0{,}05$ et une permittivité relative de:

- $\varepsilon_r' \leq 5$, pour $f \leq 3$ GHz
- $3 \leq \varepsilon_r' \leq 5$, pour $f > 3$ GHz

Les propriétés diélectriques cibles du milieu équivalent au tissu dans le fantôme sont spécifiées dans le Tableau 2 pour des fréquences discrètes comprises entre 4 MHz et 10 GHz. Pour d'autres fréquences dans les limites de cette plage, les propriétés diélectriques nominales doivent être obtenues par interpolation linéaire entre les chiffres supérieurs et inférieurs du tableau. Des exemples de formules de préparation des milieux équivalents aux tissus conçus pour générer des propriétés diélectriques à certaines fréquences dans la plage comprise entre 4 MHz et 10 GHz sont donnés à l'Annexe F. Les propriétés diélectriques du milieu sont justifiées à l'Article G.5. Les spécifications de température du liquide sont données en 6.1.

NOTE 1 Les valeurs nominales sont les propriétés diélectriques cibles avec une exigence de tolérance spécifique.

Pour réduire le plus possible les réflexions de la surface supérieure du milieu équivalent au tissu, il convient que la profondeur du milieu soit d'au moins 15 cm. Une profondeur de moins de 15 cm ne peut être utilisée que s'il est démontré (en utilisant des simulations numériques, par exemple) que l'effet sur le psDAS est inférieur à 1 % lors de la validation du système (voir l'Annexe A). Si elle est supérieure à 1 %, mais inférieure à 3 %, l'incertitude de la valeur la plus élevée issue de la validation du système doit être ajoutée au bilan d'incertitude.

Les propriétés diélectriques doivent être mesurées et comparées aux valeurs données dans le Tableau 2 à l'aide d'une interpolation linéaire. Ce mesurage peut être effectué en utilisant l'équipement et les procédures décrits à l'Annexe H. Les propriétés diélectriques mesurées, et non les valeurs du Tableau 2, doivent être utilisées pour les calculs du DAS.

NOTE 2 Les propriétés diélectriques (permittivité et conductivité) du milieu ont été spécifiées pour donner une exposition prudente (voir l'Article G.5 pour les justificatifs utilisés pour déduire les propriétés diélectriques du milieu).

NOTE 3 Voir 7.2.1 pour les variations admissibles entre les propriétés diélectriques mesurées et les propriétés diélectriques cibles indiquées dans le Tableau 2.

Tableau 2 – Propriétés diélectriques du milieu équivalent au tissu

Fréquence MHz	Partie réelle de la permittivité relative complexe, ε_r'	Conductivité, σ S/m	Profondeur de pénétration (champ E), δ mm
4	*55,0*	*0,75*	293,0
13	*55,0*	*0,75*	165,5
30	55,0	0,75	112,8
150	52,3	0,76	62,0
300	45,3	0,87	46,1
450	43,5	0,87	43,0
750	*41,9*	*0,89*	39,8
835	41,5	0,90	39,0
900	41,5	0,97	36,2
1 450	40,5	1,20	28,6
1 800	40,0	1,40	24,3

IECNORM.COM : Click to view the full PDF of IEC/IEEE 62209-1528:2020

Fréquence MHz	Partie réelle de la permittivité relative complexe, ε_r'	Conductivité, σ S/m	Profondeur de pénétration (champ E), δ mm
1 900	40,0	1,40	24,3
1 950	40,0	1,40	24,3
2 000	40,0	1,40	24,3
2 100	*39,8*	*1,49*	22,8
2 450	39,2	1,80	18,7
2 600	*39,0*	*1,96*	17,2
3 000	38,5	2,40	14,0
3 500	*37,9*	*2,91*	11,4
4 000	*37,4*	*3,43*	10,0
4 500	*36,8*	*3,94*	9,7
5 000	*36,2*	*4,45*	1,5
5 200	*36,0*	*4,66*	8,4
5 400	*35,8*	*4,86*	8,1
5 600	*35,5*	*5,07*	7,5
5 800	35,3	5,27	7,3
6 000	*35,1*	*5,48*	7,0
6 500	*34,5*	*6,07*	6,7
7 000	*33,9*	*6,65*	6,4
7 500	*33,3*	*7,24*	6,1
8 000	*32,7*	*7,84*	5,9
8 500	*32,1*	*8,46*	5,3
9 000	*31,6*	*9,08*	4,8
9 500	*31,0*	*9,71*	4,4
10 000	*30,4*	*10,40*	4,0

NOTE À des fins de commodité, les valeurs de permittivité et de conductivité font l'objet d'une interpolation linéaire à des fréquences qui ne font pas partie des données originales fournies par Drossos et al. [2]. Elles sont présentées en italique dans le Tableau 2. Les valeurs en italique font l'objet d'une interpolation linéaire (sous 5 800 MHz) ou d'une extrapolation (au-dessus de 5 800 MHz) à partir des valeurs qui ne sont pas en italique immédiatement au-dessus et au-dessous de ces valeurs.

IECNORM.COM : Click to view the full PDF of IEC/IEEE 62209-1528:2020

6.2.3 Fantôme de tête

Le fantôme du mannequin anthropomorphe spécifique (SAM) doit être utilisé pour évaluer l'exposition dans la tête. La justification du choix du modèle de fantôme de tête spécifique (c'est-à-dire le SAM) de ce document repose sur les critères suivants.

a) Le psDAS doit assurer une exposition prudente.

b) Les résultats d'essai ne doivent pas inutilement surestimer le DAS maximal prévu chez les utilisateurs réels.

c) Le fantôme doit permettre un positionnement stable et répétable du dispositif pour les mesurages de psDAS et être efficace pour vérifier la répétabilité de mesure selon les procédures de contrôle du système, et la reproductibilité de mesure par des comparaisons interlaboratoires.

d) Le fantôme doit être pratique pour l'évaluation de DAS en routine.

e) Le fantôme doit prendre en charge ces critères pour les conceptions actuelles et futures d'appareils sans fil et être neutre vis-à-vis de toute conception ou forme particulière.

f) Sur la base des données scientifiques, des ouvrages de référence et de l'expérience actuellement disponibles, la conception d'un fantôme SAM qui satisfait aux critères ci-dessus dépend des paramètres suivants au moins:

1) taille et forme de l'enveloppe du fantôme de tête;

2) propriétés diélectriques et homogénéité du matériau des milieux équivalents aux tissus et de l'enveloppe du fantôme;

3) taille, forme, emplacement et propriétés du matériau de pavillon de l'oreille;

4) exclusion de la main pour mesurer le DAS dans la tête (Annexe I, 6.3).

6.2.4 Fantôme plan

a) Pour évaluer l'exposition dans le corps, les exigences suivantes s'appliquent.

1) Le fantôme plan doit être utilisé.

2) Son enveloppe doit avoir la forme d'un conteneur à dessus ouvert avec une base plane.

3) Tout fantôme plan utilisé doit être assez grand pour permettre de mesurer le DAS dans des volumes de 1 g et 10 g, l'influence de la forme du conteneur étant inférieure 1 % (Article G.4).

b) La forme et les dimensions du fantôme plan doivent être les suivantes (Figure 2).

1) Sauf dans le cas spécifié en b) 2), la paroi de la base plane du fantôme doit avoir une forme d'ellipse d'une longueur de 600 mm et d'une largeur de 400 mm.

2) Pour des fréquences supérieures à 150 MHz, et pour les distances de séparation inférieures ou égales à 25 mm de la surface extérieure de la base de l'enveloppe du fantôme, les fantômes de formes différentes et de dimensions inférieures sont admis comme suit:

i) entre 150 MHz et 800 MHz, la paroi de la base plane du fantôme peut avoir une forme quelconque englobant une ellipse d'une longueur de 0,6 λ_0 et d'une largeur de 0,4 λ_0, où λ_0 est la longueur d'onde dans l'air;

ii) entre 800 MHz et 10 GHz, le fantôme peut avoir une forme quelconque de paroi de base plane englobant une ellipse de 225 mm de longueur et 150 mm de largeur.

c) L'épaisseur de la paroi de la base du fantôme plan doit être égale à 2,0 mm, avec une tolérance de ±0,2 mm. S'il est rempli de liquide jusqu'à la profondeur exigée, toute flèche éventuelle de la surface de la base du fantôme à l'intérieur de la projection du DUT doit être déterminée et prise en considération dans le bilan d'incertitude (voir 8.4.2.4). Si les précédentes exigences de dimensions sont satisfaites, l'effet de la forme et de l'épaisseur sur la répétabilité des résultats de mesure du DAS est inférieur à 1 % (voir l'Article G.4). Les effets sur le DAS dus à l'influence de l'écart par rapport aux paramètres et à l'épaisseur exigés de l'enveloppe doivent être inclus dans l'estimation d'incertitude (voir 8.4.2.3).

NOTE L'utilisation d'un fantôme plan en tant que fantôme normalisé pour évaluer le DAS des appareils portés près du corps et posés sur le corps a pour but de représenter le couplage maximal entre le DUT et le fantôme de l'homme. Ce couplage effectué sur le fantôme, tout en conservant les distances recommandées, est susceptible de donner une exposition prudente. L'Annexe J fournit des informations détaillées supplémentaires sur ce sujet.

IECNORM.COM : Click to view the full PDF of IEC/IEEE 62209-1528:2020

Dimensions en millimètres

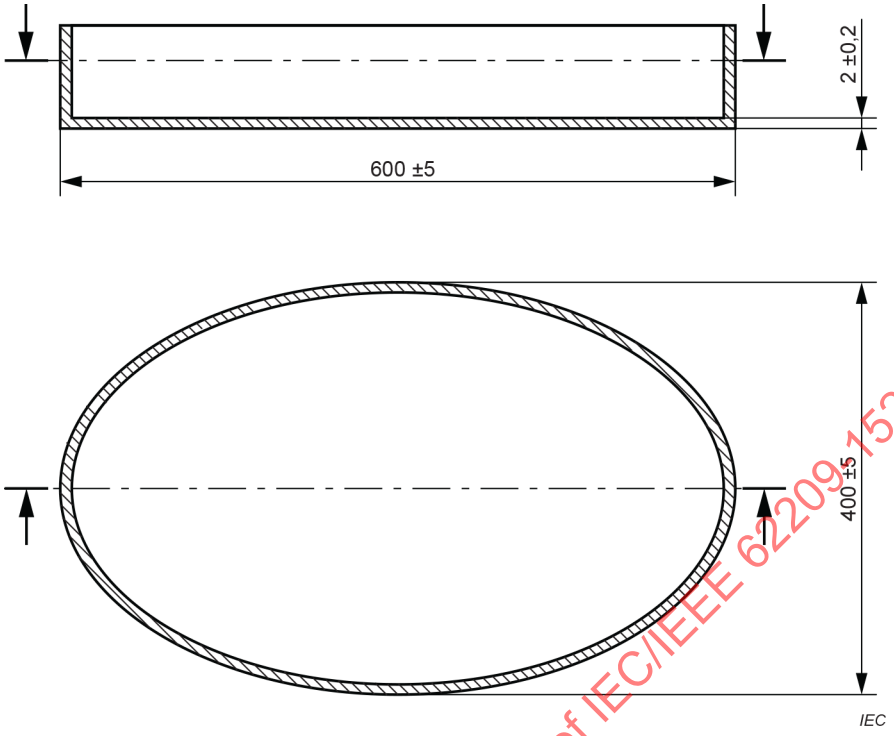


Figure 2 – Dimensions du fantôme elliptique

6.2.5 Fantômes spécifiques au dispositif

Des fantômes spécifiques au dispositif, autres que ceux spécifiés en 6.2.3 ou en 6.2.4, peuvent être utilisés si le fantôme plan ou le SAM ne prend pas en charge les conditions d'exposition ou si l'un des éléments suivants s'applique:

a) le dispositif est destiné à fonctionner sur différentes parties du corps autres que la tête ou le torse (le poignet, par exemple);

b) les contraintes physiques imposées par le fantôme au système de balayage ne permettent pas de déterminer le psDAS du DUT selon l'exactitude exigée.

Des exemples d'autres fantômes spécifiques au dispositif sont donnés à l'Annexe K et à l'Annexe L. Les justifications et spécifications scientifiques ou techniques de ces fantômes sont présentées dans les annexes mentionnées ci-dessus. D'autres procédures de positionnement du dispositif peuvent également être exigées. Celles-ci, ainsi que les justifications de l'utilisation d'autres fantômes spécifiques, doivent être consignées.

6.3 Influence de la main sur le DAS dans la tête

Pendant le fonctionnement normal, la tête et la main sont dans le champ proche du DUT lorsqu'il est utilisé à côté de l'oreille et donc, absorbent toutes deux de l'énergie. Pour les extrémités telles que la main, une limite de DAS plus élevée est admise (par exemple, 4 W/kg moyennée sur 10 g de tissu dans les lignes directrices ICNIRP pour l'exposition RF [3] et la Norme IEEE C95.1-2019 [4]). Des études numériques et expérimentales ont démontré qu'il n'est pas prévu que le DAS dans la main aux niveaux de puissance utilisés par des DUT classiques dépasse ces limites (Francavilla et al. [5], Gandhi et al. [6], Jensen and Rahmat-Samii [7], [8], Kuster et al. [9], Watanabe et al. [10]). De plus, aucun fantôme pratique pour le mesurage de DAS dans la main n'est actuellement disponible. Par conséquent, le mesurage de DAS dans la main n'est pas traité dans le présent document.

IECNORM.COM : Click to view the full PDF of IEC/IEEE 62209-1528:2020

L'influence d'une main tenant un DUT sur la tête pendant les mesurages de DAS a été prise en considération dans l'IEEE 1528-2013 [11]. Les travaux antérieurs de Balzano et al. [12] et de Kuster et al. [9] ont indiqué que la présence de la main a diminué ou n'a pas eu d'effet significatif sur le DAS de la tête. Toutefois, les résultats numériques de Meyer et al. [13] ont mis en évidence un cas avec une augmentation de 7 % du DAS de la tête due à la main. Il a été conclu que ces écarts de DAS de la tête sont compatibles avec le niveau de prudence correspondant au fantôme SAM. Sur la base de ces études, l'exclusion de la main des procédures d'essai conduit à une surestimation du DAS de la tête dans la majorité des cas, comme le confirment des résultats récents de recherches [14], [15], [16] sur les niveaux de DAS du DUT. Pour ces raisons, les modèles de main ne sont pas pris en considération dans le présent document.

L'état des recherches dosimétriques sur l'effet de la main sur le DAS de la tête produit par des DUT est présenté à l'Annexe I. Ces recherches démontrent qu'il existe des cas dans lesquels le DAS produit par des DUT dans le fantôme SAM peut augmenter et également diminuer significativement lorsque la main tient le DUT, du fait de conceptions de DUT, de bandes de fonctionnement et de prises de main spécifiques. Ces observations initiales ont démontré que le fantôme SAM à lui seul peut toujours surestimer le DAS de la tête dans un certain nombre de cas statistiquement significatifs par rapport au moment auquel la main est présente pour le mesurage. Cependant, elles méritent des investigations complémentaires, ce qui peut entraîner des modifications futures du présent document.

6.4 Exigences du système de balayage

Le système de balayage de la sonde de DAS doit pouvoir balayer les régions de mesure exigées du fantôme qui se situent dans les projections d'un DUT afin d'évaluer le balayage de surface et le balayage-zoom. La tolérance du positionnement de l'extrémité de la sonde à un point de mesure du fantôme doit être ≤ 0,2 mm. L'exactitude du système de positionnement de la sonde par rapport au fantôme doit être vérifiée en fonction des points de référence du fantôme définis par le fabricant du fantôme. La structure mécanique du système de balayage ne doit pas gêner les mesurages de DAS. La plage de balayage doit couvrir au moins 90 % des dimensions du fantôme dans toutes les directions.

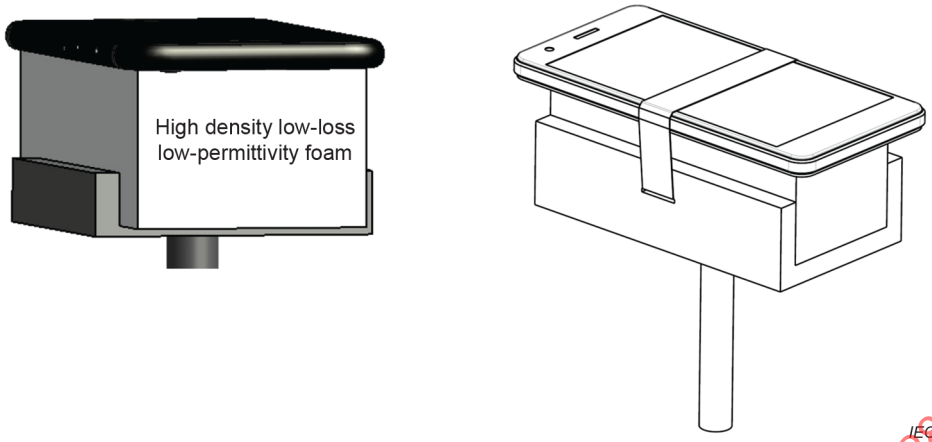
6.5 Spécifications du support de dispositif

Le support de dispositif doit permettre de positionner le DUT conformément aux définitions données en 7.2.4. Il doit être constitué de matériaux à faible perte et à faible permittivité: tangente de perte ≤ 0,05 et permittivité relative ≤ 5.

Le DUT est de préférence monté sur un élément de faible permittivité relative (< 1,2) et en mousse à faible perte avant d'être monté dans le support de dispositif. Il s'agit d'éviter tout contact direct entre le support de dispositif et le DUT (Figure 3). Si cela s'avère impossible, le support de dispositif doit être le moins possible en contact avec le DUT afin d'assurer une prise sûre et de maintenir la position exigée pendant le mesurage. Si un positionnement relatif par défaut ne peut pas être réalisé, du fait par exemple de l'interaction du support de dispositif avec des boutons et des capteurs sur le DUT, il convient d'appliquer les décalages de position minimale dans une direction prédéfinie pour obtenir la position d'essai exigée du DUT. Les informations détaillées doivent être fournies dans le rapport de mesure.

Le support de dispositif doit garantir un positionnement précis et répétable du DUT pour le mesurage de DAS. Les incertitudes de positionnement doivent être estimées selon les procédures spécifiées en 8.4.2.5 et 8.4.2.6. Si le psDAS le plus élevé est déterminé selon l'étape 3 du protocole d'essai de 7.3.2, l'effet d'incertitude du support de dispositif sur la valeur de DAS consignée est considéré comme étant négligeable.

IECNORM.COM : Click to view the full PDF of IEC/IEEE 62209-1528:2020



Anglais	Français
High density low-loss low-permittivity foam	Mousse haute densité à faibles pertes et faible permittivité

NOTE Le DUT peut être fixé en haut de la mousse (à gauche) ou maintenu en bas à l'aide d'une fine longe (à droite).

Figure 3 – Montage du DUT dans le support de dispositif à l'aide d'une mousse à faible permittivité et à faibles pertes pour éviter les variations de performances du DUT selon le matériau du support

6.6 Caractéristiques de la lecture électronique

La sortie de la sonde est traitée par la lecture électronique et les instruments associés qui combinent les tensions provenant des capteurs de la sonde pour fournir une sortie qui est proportionnelle à l'amplitude quadratique du champ E incident sur les capteurs. Des diodes de détecteur au niveau du point d'alimentation du dipôle sont utilisées pour corriger les tensions des capteurs. Les signaux corrigés sont transmis par l'intermédiaire de lignes résistives (RF transparentes) au système de lecture électronique. Pour un signal à onde entretenue à faibles niveaux d'intensité de champ, la sortie de la sonde est proportionnelle au carré de l'amplitude du champ E incident. À des niveaux de signal plus élevés (au-dessus du point de compression de la diode), la sortie n'est pas linéairement proportionnelle à $|E|^2$, mais devient proportionnelle à $|E|$. Cette compression du signal donne lieu à une sous-estimation du DAS réel dans des conditions de haute intensité de champ si elle n'est pas compensée correctement par l'étalonnage de la sonde. De même, les amplificateurs contenus dans la lecture électronique peuvent s'écarter d'une réponse linéaire idéale et créer une incertitude supplémentaire. Pour les incertitudes associées à la lecture électronique de la sonde, voir 8.4.1.6.

7 Protocole pour l'évaluation du DAS

7.1 Généralités

Il convient d'effectuer tous les mesurages sur la base des bonnes pratiques de laboratoire, par exemple conformément à l'ISO/IEC 17025 [17] ou à toute autre exigence nationale relative à la certification des dispositifs. Le présent document ne contient aucune méthode de vérification des paramètres du mode de fonctionnement du DUT (modulation, débit de données, intervalles de temps, blocs de ressources, par exemple. Voir 3.33).

IECNORM.COM : Click to view the full PDF of IEC/IEEE 62209-1528:2020

7.2 Préparation des mesurages

7.2.1 Préparation du milieu équivalent au tissu et contrôle du système

a) Les propriétés diélectriques mesurées du milieu équivalent au tissu doivent être appliquées dans l'évaluation du DAS. Les propriétés diélectriques doivent être mesurées dans les 24 h précédant les mesurages de DAS et toutes les 48 h d'utilisation continue. Si le laboratoire prouve la conformité au Tableau 2 et aux exigences de 6.2.2 en utilisant des intervalles de mesure allant jusqu'à une semaine au maximum, des mesurages de propriétés diélectriques moins fréquents sont acceptables. Si la série d'essais dure plus de 48 h, les propriétés du milieu doivent également être mesurées à la fin de la série d'essais.

b) Les milieux équivalents aux tissus doivent produire des valeurs mesurées de permittivité relative et de conductivité à ±5 % des valeurs cibles aux fréquences auxquelles le DAS est mesuré. Si la méthode de 7.8 est utilisée pour corriger le DAS mesuré pour les écarts de permittivité et de conductivité, la tolérance peut être établie à ±10 % au maximum des cibles. Si des mesurages hors tolérance des propriétés diélectriques sont réalisés sur un intervalle de mesure de plus de 48 h, toutes les données de DAS mesurées depuis le dernier mesurage des propriétés diélectriques doivent être ignorées.

c) Pour les systèmes d'essai de DAS rapide hermétiquement scellés, le fabricant doit fournir une procédure de mesure exacte des propriétés diélectriques, ou une documentation sur les propriétés diélectriques du milieu (avec la température du milieu et la température ambiante correspondantes), qui ont été mesurées pour le fantôme spécifique lors de sa fabrication ou pendant le nouvel étalonnage du système.

d) La température du milieu équivalent au tissu doit être mesurée et consignée au moment du mesurage des propriétés diélectriques et avant le contrôle du système et les mesurages du DAS.

e) Le système doit être contrôlé à chaque bande de fréquences à soumettre à l'essai, afin de détecter les éventuelles dérives sur de courtes périodes et d'autres erreurs de mesure dans le système. Un contrôle du système selon les procédures de l'Article A.2 doit être effectué dans les 24 h qui précèdent la réalisation des mesurages de DAS pour un DUT.

f) La procédure de contrôle du système doit être effectuée sur le même système de mesure de DAS, avec la même ou les mêmes sondes de DAS et le même milieu équivalent au tissu que pour l'évaluation de DAS du dispositif pour chaque bande de fréquences soumise à l'essai. Pour limiter la fluctuation de puissance lors du contrôle du système, un contrôle automatique du niveau de puissance d'entrée peut être mis en œuvre, comme cela est spécifié à l'Annexe V.

7.2.2 Préparation du DUT de communication sans fil

a) Tous les éléments rayonnants, batteries et accessoires doivent être ceux spécifiés par le fabricant et documentés dans le rapport de mesure. La charge de la batterie doit être complète avant chaque mesurage et le DUT être positionné sans connexion ou câble externe non exigé pour le fonctionnement normal.

b) La puissance de sortie RF et la fréquence (canal) doivent être commandées par une liaison sans fil à une station de base ou un simulateur de réseau pour les modes de fonctionnement pris en charge. Si aucune liaison sans fil ne peut être établie avec un simulateur de station de base, un logiciel d'essai et des codes d'essai interne peuvent être utilisés.

NOTE 1 Certains organismes de réglementation nationaux peuvent exiger que le fabricant du dispositif procède à une vérification des essais réalisés sur des prototypes, afin d'assurer que la version disponible dans le commerce présente les mêmes caractéristiques mécaniques et électriques que le prototype soumis à l'essai.

c) Le DUT doit être réglé pour transmettre au plus haut niveau de puissance de sortie maximale moyenné, dans les limites de la plage des spécifications finement établies et des variations de production du produit.

Pour les essais des dispositifs de transfert de puissance sans fil, il convient d'appliquer d'autres procédures de préparation, comme cela est spécifié dans l'IEC TR 62905 [18].

NOTE 2 Pour les dispositifs qui peuvent surveiller et contrôler leur puissance d'émission afin de maintenir le DAS moyenné dans le temps sous la limite de DAS applicable, voir 7.6.

IECNORM.COM : Click to view the full PDF of IEC/IEEE 62209-1528:2020

7.2.3 Exigences relatives aux modes de fonctionnement du DUT

7.2.3.1 Exigences relatives aux paramètres de puissance et de signal de sortie du DUT

Les objectifs de 7.2.3.1 sont les suivants.

- Déterminer que le DAS du DUT est évalué à son niveau de puissance maximale, en prenant en considération la tolérance de puissance de sortie maximale et les variations de production.
- Appliquer correctement la compensation de linéarité de la sonde pour des signaux variables dans le temps et vérifier que le signal est correctement échantillonné.

Les exigences de puissance sont les suivantes.

a) Les niveaux de puissance maximale moyennés dans le temps du DUT doivent être vérifiés par le fabricant du dispositif (par des essais de puissance réalisés avec une batterie complètement chargée, par exemple) pour prendre en charge la mise à l'échelle du DAS.

b) Tous les modes de fonctionnement applicables doivent être pris en considération pour les essais, même si les essais de certains d'entre eux peuvent ne pas être exigés (7.9.3).

c) Un DUT fonctionnant dans les modes à enveloppe constante doit être soumis à l'essai à la puissance de sortie maximale de son signal (porteuse) équivalent à CW.

d) Un DUT fonctionnant dans les modes d'enveloppe pulsée doit être soumis à l'essai avec les mêmes caractéristiques d'impulsion (facteur d'utilisation, période d'impulsion). Si le DUT peut émettre plusieurs modes en modifiant les caractéristiques d'impulsion (transmission dans plusieurs intervalles, par exemple) dans une technologie sans fil, le signal avec la puissance de sortie maximale moyennée dans le temps la plus élevée par bande de fréquences doit être soumis à l'essai, après avoir pris en considération la puissance de sortie maximale du DUT pour chaque mode.

e) Si le mode à enveloppe pulsée présente une longue période d'impulsion, de sorte que la composante de fréquence la plus basse de l'enveloppe du signal est inférieure à la fréquence de coupure du filtre passe-bas du sous-système d'acquisition de mesure de DAS, le temps d'intégration et/ou la période d'acquisition d'échantillon doivent être choisis pour mesurer exactement la valeur efficace du signal, par exemple à l'aide d'un nombre entier de périodes d'impulsion pour éviter le repliement spectral.

f) Un DUT dans des modes de fonctionnement dans lesquels l'enveloppe du signal varie de manière aléatoire dans le temps (AMRC, OFDM, par exemple) doit être soumis à l'essai dans le mode entraînant la puissance de sortie maximale moyennée dans le temps émise par le dispositif pour chaque technologie sans fil. La sonde doit être étalonnée sur sa plage dynamique et la sortie doit inclure la compensation de linéarité de la sonde. La compensation de linéarité dépend souvent du mode de fonctionnement, comme l'indiquent Di Nallo et Faraone [19] et Nadakuduti et.al [20].

g) Si le DUT ne peut pas fonctionner pendant la durée de mesure du DAS à son plus haut niveau de puissance de sortie maximale moyenné dans le temps, dans les limites de la plage de spécifications finement établies du produit et des variations de production, ce qui suit doit s'appliquer.

   1) Le DUT peut fonctionner à une puissance de sortie inférieure ou à un facteur d'utilisation inférieur, et le DAS doit être mis à l'échelle au plus haut niveau de puissance de sortie maximale moyenné dans le temps exigé. Toutefois, la puissance de sortie moyennée dans le temps doit être dans les limites de la plage de tolérances spécifiée pour le dispositif.

   2) Il doit être démontré que le DAS du dispositif augmente de manière linéaire avec la puissance conduite.

   3) Les dispositifs qui fonctionnent avec des amplificateurs à double sortie, si les deux amplificateurs ne sont pas exigés dans le cadre d'un fonctionnement à de faibles niveaux de puissance, ou ceux conçus pour fonctionner de manière intermittente à de très faibles facteurs d'utilisation, peuvent exiger des considérations supplémentaires pour être sûr que le DAS peut être mis à l'échelle de manière linéaire.

IECNORM.COM : Click to view the full PDF of IEC/IEEE 62209-1528:2020

NOTE Certaines autorités de réglementation peuvent imposer des exigences supplémentaires en matière de réduction de puissance de sortie maximale moyennée dans le temps admise pour les essais de DAS du dispositif.

La procédure de mise à l'échelle de la puissance est donnée en 7.2.3.2.

7.2.3.2 Procédure de mise à l'échelle du DAS pour les variations de puissance ou de signal

La mise à l'échelle du DAS est l'extrapolation du DAS d'un DUT déterminée avec un mode de fonctionnement soumis à l'essai (mod_X) par rapport à un DAS du même dispositif, dans la même position d'essai d'exposition et le même canal de fréquences, avec un mode de fonctionnement différent (mod_Y). La différence peut être dans le niveau de puissance et/ou le mode de fonctionnement. Le rapport de puissance de sortie RF moyennée de mod_X et mod_Y doit être déterminé soit en mesurant la puissance moyenne pour les deux ou par l'intégration numérique de l'enveloppe de puissance si les signaux sont suffisamment connus. La mise à l'échelle du DAS est possible si:

a) le même étage d'amplificateur RF est utilisé pour mod_X et mod_Y;

b) la même antenne est utilisée pour mod_X et mod_Y, et aucune technique MIMO ou autre technique de diversité d'antenne n'est appliquée;

c) l'incertitude de réponse de la modulation de la sonde a été évaluée pour le signal modulé mod_X (8.4.2.7) et le DAS a été déterminé pour mod_X;

d) le rapport de puissance de sortie RF moyennée dans le temps (R_p) de mod_X et mod_Y après l'étage d'amplificateur RF est connu d'après la Formule (1):

$$R_p = \frac{P_{\max,\,mod\,Y}}{P_{mod\,X}} \tag{1}$$

où $P_{\max,mod Y}$ correspond à la valeur de réglage de la puissance de sortie moyennée dans le temps la plus élevée. Si les deux signaux diffèrent dans le mode de fonctionnement, le signal d'essai est alors réglé à la puissance de sortie maximale moyennée dans le temps: $P_{mod X} = P_{\max,mod X}$.

Le facteur R_p doit être déterminé par des moyens expérimentaux (par exemple, un mesurage en utilisant un wattmètre moyen).

e) la fréquence porteuse RF de mod_X est la même que pour mod_Y;

f) le rapport de bande passante de signal RF R_m de mod_X et mod_Y satisfait à la Formule (2):

$$R_m = \left| \frac{BW_{mod\,Y}}{BW_{mod\,X}} - 1 \right| \times 100 \le 30\,\% \tag{2}$$

g) les largeurs de bandes de canal de mod_X et mod_Y sont chacune à 5 % de la fréquence porteuse.

Si les exigences mentionnées ci-dessus sont satisfaites, une mise à l'échelle du DAS de mod_X et mod_Y doit être effectuée conformément à la Formule (3) et l'incertitude de la mise à l'échelle doit être déterminée comme cela est spécifié en 8.4.3.2:

$$DAS_{mod\,Y} = R_m \cdot DAS_{mod\,X} \tag{3}$$

Si l'approche de 7.2.3.2 est utilisée, il doit être indiqué dans le rapport de mesure que les points de a) à g) sont respectés.

IECNORM.COM : Click to view the full PDF of IEC/IEEE 62209-1528:2020

Pour les dispositifs prenant en charge les modes PTT ou d'autres opérations TDD spécifiques à la technologie, le facteur d'utilisation maximal doit être évalué.

7.2.4 Positionnement du DUT par rapport au fantôme

7.2.4.1 Distance d'essai et positionnement par rapport au fantôme plan

7.2.4.1.1 Généralités

Le 7.2.4.1 décrit comment le DUT, avec ou sans accessoire, doit être positionné, orienté et configuré par rapport au fantôme pour le mesurage de DAS. Les positions d'essai spécifiées sont applicables pour les séparations de surface entre le dispositif et le fantôme jusqu'à 200 mm inclus.

Le 7.2.4.1 décrit les procédures de positionnement pour les types de dispositifs suivants:

– dispositifs qui sont grands par rapport à la surface du fantôme (7.2.4.1.4);
– dispositifs utilisés avec des accessoires portés près du corps (7.2.4.1.5);
– dispositifs équipés d'une antenne à charnière ou à rotule (7.2.4.1.6);
– dispositifs utilisés proches ou contre le corps sans accessoire (7.2.4.1.7);
– appareil de bureau (7.2.4.1.8);
– appareil placé devant le visage (7.2.4.1.9);
– appareil utilisé tenu en main, mais non à proximité de la tête ou du torse (7.2.4.1.10);
– appareil fixé à un membre (7.2.4.1.11);
– appareil intégré aux vêtements (7.2.4.1.12);
– appareil générique (7.2.4.1.13);

NOTE Les chiffres de 7.2.4.1 sont donnés à titre d'exemple uniquement, ils ne sont ni à l'échelle ni représentatifs des zones nécessitant un mesurage de DAS.

7.2.4.1.2 Distance de séparation entre le DUT et le fantôme

Lors des mesurages par rapport au fantôme plan, la distance de séparation entre le DUT et le fantôme peut être définie selon la hiérarchie suivante.

a) Exigence réglementaire: Si une exigence réglementaire nationale spécifie la distance de séparation du DUT par rapport au fantôme, le DUT doit être positionné selon cette exigence.
b) "Distance d'utilisation prévue" spécifiée par le fabricant: En l'absence d'exigence réglementaire, la condition ou distance d'utilisation prévue spécifiée par le fabricant doit être utilisée. Ces informations doivent se trouver dans la documentation d'utilisation qui accompagne le DUT.
c) Distance de séparation par défaut: En l'absence d'exigence réglementaire et de distance d'utilisation prévue spécifiée par le fabricant, le DUT doit être mesuré avec chaque face accessible en contact direct avec la surface du fantôme (voir également l'appareil générique de 7.2.4.1.13).

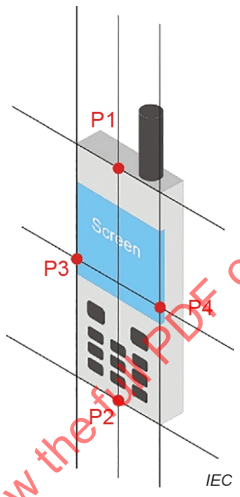
La distance de séparation indiquée peut être déterminée avec l'accessoire de transport fixé au DUT, si cet état est soumis à l'essai (voir 7.2.4.1.5).

Il convient de veiller à vérifier le positionnement précis aux distances de séparation applicables, par exemple en utilisant des cales étalons ou des moyens similaires pour assurer la répétabilité.

IECNORM.COM : Click to view the full PDF of IEC/IEEE 62209-1528:2020

7.2.4.1.3 Points de référence du DUT

Des recommandations générales pour identifier l'orientation d'un DUT, ou s'il est placé dans un accessoire de transport pour le positionner par rapport au fantôme, sont présentées ci-dessous. P1, P2, P3 et P4 sont définis comme étant les points médians sur chaque bord de la surface faisant face au fantôme, comme cela est représenté à la Figure 4. La ligne P1-P2 et la ligne P3-P4 doivent être parallèles à la surface du fantôme, de sorte que la distance entre P1 et la surface du fantôme soit égale à la distance entre P2 et la surface du fantôme. De la même manière, la distance entre P3 et la surface du fantôme doit être égale à la distance entre P4 et la surface du fantôme. La distance de séparation est spécifiée comme étant la distance entre l'enveloppe du fantôme et le point le plus proche sur le DUT positionné comme cela est indiqué précédemment. Il peut s'avérer nécessaire d'adapter cette recommandation générale aux conceptions particulières (les dispositifs ou accessoires de transport aux surfaces arrondies, par exemple) qui exigent de positionner le dispositif différemment pour les essais. Les informations détaillées précises relatives aux positions d'essai réelles utilisées doivent être documentées de manière exhaustive dans le rapport de mesure.



Anglais	Français
Screen	Écran

Figure 4 – Désignation des points de référence du DUT

7.2.4.1.4 Positionnement pour les dispositifs qui sont grands par rapport à la surface du fantôme

Si le DUT est plus grand que la région mesurable du fantôme plan spécifié en 6.2.4, ce qui suit s'applique.

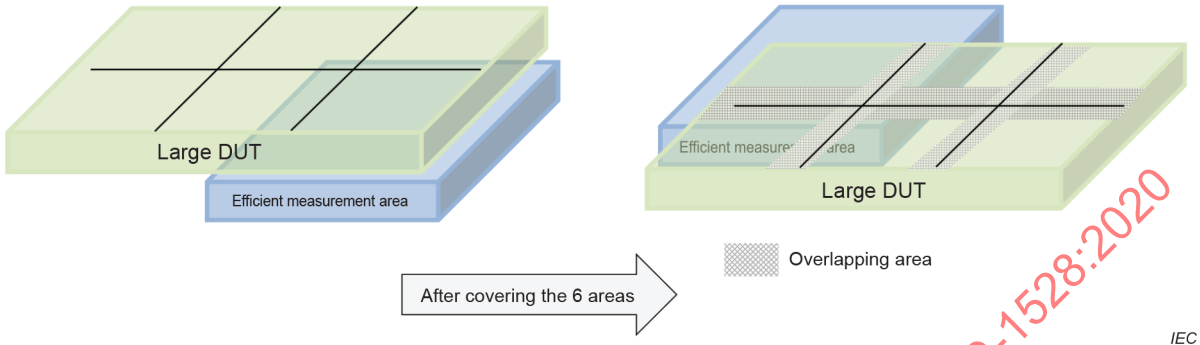
a) Le DUT doit être déplacé de sorte que plusieurs balayages de surface puissent couvrir la distribution de DAS du DUT. Lorsque le DUT est déplacé, le couplage RF entre le DUT et le fantôme peut changer, entraînant une distribution de DAS différente de celle utilisant un fantôme plus grand. Toutefois, un fantôme plus grand peut ne pas être représentatif de la grande majorité des situations d'exposition impliquant des personnes (voir la NOTE en 6.2.4).

b) Afin de limiter les écarts de DAS mesuré dus aux variations du couplage, deux balayages successifs doivent avoir une zone de chevauchement au moins égale à un tiers de la taille de la zone combinée, comme cela est représenté à la Figure 5.

c) Dans la zone de chevauchement, la distribution de DAS doit être similaire, de sorte que l'écart de DAS en tout point par rapport à la géométrie du DUT soit inférieur à l'incertitude élargie de répétabilité. Sinon, le DUT doit être légèrement déplacé, de sorte que l'écart de DAS soit dans les limites de l'incertitude.

IECNORM.COM : Click to view the full PDF of IEC/IEEE 62209-1528:2020

Le déplacement n'est pas nécessaire si les structures de rayonnement sont petites comparées au DUT et au fantôme et/ou que le premier balayage de surface indique que la distribution de DAS est entièrement capturée dans la zone de balayage. Si le déplacement a été omis, la justification doit être clairement documentée dans le rapport de mesure.



Anglais	Français
Large DUT	Grand DUT
Efficient measurement area	zone de mesure efficace
Overlapping area	Zone de chevauchement
After covering the 6 areas	Après avoir couvert les 6 zones

Figure 5 – Mesurages réalisés en déplaçant un dispositif volumineux sur la zone de mesure efficace du système incluant les zones de chevauchement – dans ce cas: six essais réalisés

7.2.4.1.5 Dispositifs utilisés avec des accessoires portés près du corps

Un dispositif relevant du domaine d'application du présent document et destiné à être utilisé avec un accessoire porté près du corps approuvé ou spécifié par le fabricant du dispositif, doit être évalué selon les exigences suivantes.

a) Si les instructions d'utilisation fournies par le fabricant spécifient l'utilisation prévue avec un accessoire de transport (attache de ceinture, étui, mallette de transport ou analogue), le dispositif doit être placé dans cet accessoire de transport et positionné dans les conditions d'utilisation prévue par rapport au fantôme plan.

b) En ce qui concerne les accessoires de transport construits avec des matériaux non conducteurs et qui peuvent maintenir le DUT à des distances variables par rapport au fantôme, il est prévu que l'accessoire de transport offrant la distance de séparation la plus proche produise le DAS le plus élevé. Il n'est donc pas utile de soumettre à l'essai un accessoire de transport offrant des distances de séparation plus importantes, sauf s'il contient des matériaux conducteurs.

c) En présence de plusieurs accessoires de transport maintenant le DUT à la même distance, il convient de soumettre au moins l'un d'eux à l'essai. Il est à noter que tous les accessoires de transport contenant des matériaux conducteurs doivent être soumis à l'essai.

d) En ce qui concerne les accessoires de transport qui ne contiennent pas de matériaux conducteurs (des parties non métalliques, par exemple), il est acceptable de remplacer l'accessoire de transport par un entrefer qui maintient le DUT à une distance de la surface du fantôme inférieure ou égale à la distance offerte par l'accessoire de transport.

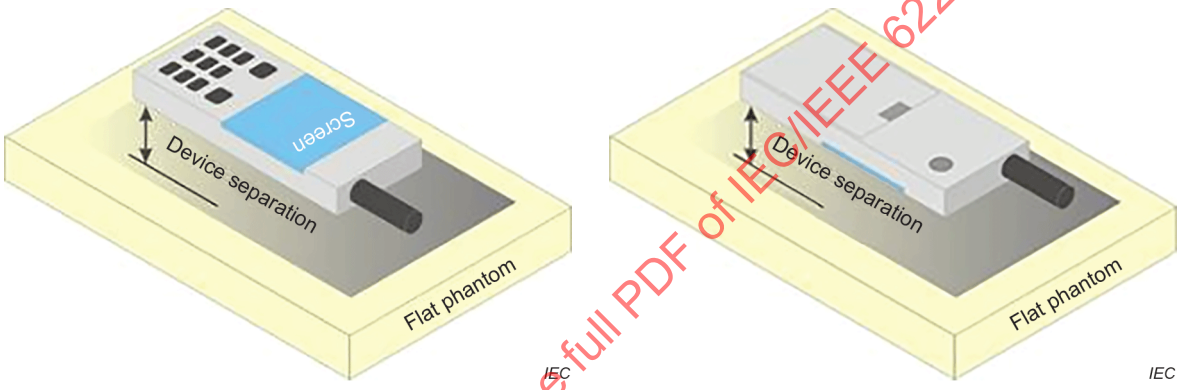
e) Le dispositif doit être positionné dans la configuration d'utilisation prévue avec l'accessoire porté près du corps dont la distance par rapport à la surface extérieure du fantôme est établie par l'accessoire spécifique (Figure 6).

IECNORM.COM : Click to view the full PDF of IEC/IEEE 62209-1528:2020

f) Si aucun dispositif d'évaluation n'est fourni avec les accessoires portés près du corps, mais si l'utilisateur peut obtenir des accessoires portés près du corps par ses propres moyens, le DAS de l'accessoire porté près du corps doit être mesuré avec une distance de séparation selon les conditions de 7.2.4.1.2.

g) Il convient de positionner la surface du dispositif orienté vers le fantôme plan à la surface du fantôme, conformément à 7.2.4.1.3. Toutefois, tous les dispositifs n'ont pas de surface plane. Par conséquent, les informations détaillées relatives à la position du dispositif (la définition de la distance et la relation physique entre le dispositif et le fantôme en fonction des accessoires portés près du corps, par exemple) doivent être documentées dans le rapport de mesure.

h) Si le fonctionnement de plusieurs surfaces d'un accessoire porté près du corps face à l'utilisateur peut ne pas paraître évident, le DUT doit être soumis à l'essai avec toutes les surfaces applicables placées à la distance de séparation la plus prudente par rapport au fantôme plan. Les informations détaillées relatives à la position du dispositif fixé à l'accessoire doivent être documentées dans le rapport de mesure. Si les essais de certaines surfaces (pas toutes) ne sont pas exigés, cela doit être documenté avec une justification associée dans le rapport de mesure.



Anglais	Français
Screen	Écran
Device separation	Distance de séparation de l'appareil
Flat phantom	Fantôme plan

Figure 6 – Positions d'essai des dispositifs portés près du corps

7.2.4.1.6 Dispositifs équipés d'une ou de plusieurs antennes à charnière ou à rotule

Pour les appareils utilisant une ou plusieurs antennes externes avec des positions variables (une antenne déployée, rétractée, tournée, par exemple), ce qui suit s'applique.

a) Le DUT doit être positionné selon 7.2.4.1.2 et 7.2.4.1.3.

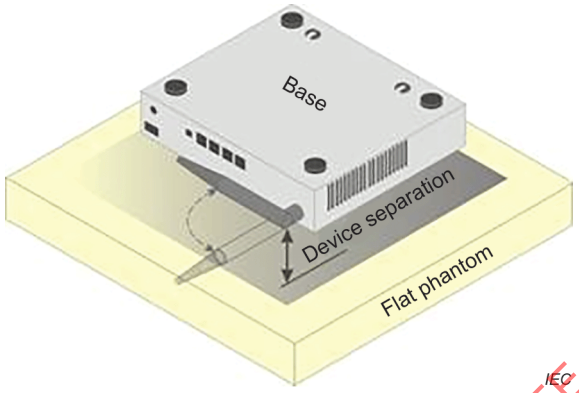
b) Si certaines positions d'antenne ne paraissent pas claires, les essais doivent être réalisés pour les positions d'antenne et les polarisations prévues par l'utilisateur (Figure 7), par exemple avec l'antenne déployée et rétractée de manière à obtenir la condition d'exposition la plus élevée.

c) Pour les antennes pouvant pivoter sur un ou deux plans, il convient de procéder à une investigation préliminaire et de la documenter dans le rapport de mesure, afin de déterminer le scénario d'exposition la plus élevée de manière à ce que seules la ou les positions correspondant à ce scénario nécessitent d'être soumises à l'essai.

IECNORM.COM : Click to view the full PDF of IEC/IEEE 62209-1528:2020

d) Pour les appareils équipés de plusieurs antennes amovibles, il convient de prendre en considération chaque antenne de manière séparée afin de déterminer les exigences d'essai de DAS. Par exemple, si les antennes sont pratiquement similaires (équivalentes), certaines considérations en matière de réduction d'essai peuvent être appliquées (7.9.3.3).

Le 7.2.4.1.6 peut être appliqué conjointement avec les configurations d'essai spécifiées dans d'autres paragraphes, selon ce qui est approprié pour le dispositif.



Anglais	Français
Base	Base
Device separation	Distance de séparation de l'appareil
Flat phantom	Fantôme plan

Figure 7 – Dispositif équipé d'une antenne à rotule

7.2.4.1.7 Dispositifs utilisés proches ou contre le corps sans accessoire

Un exemple classique de dispositif près du corps est un ordinateur portable ou une tablette sans fil contenant un émetteur radio enfichable qui peut être placé sur le corps de l'utilisateur. D'autres appareils entrant dans cette catégorie sont les tablettes de tailles équivalentes ou plus volumineuses qu'un ordinateur léger (écran de plus de 20 cm de diagonale), les cartes de crédit, les terminaux de point de vente et/ou d'inventaire. L'exemple de la Figure 8 a) représente un ordinateur portable en forme de tablette pour lequel il convient d'évaluer séparément le DAS avec chaque surface et bord contenant une antenne en position contre le fantôme plan selon les conditions de 7.2.4.1.2. Certaines tablettes peuvent limiter les orientations de l'écran de sorte que les bords avec les antennes ne soient pas utilisés proches de l'utilisateur. Ces bords peuvent donc ne pas nécessiter d'être soumis à l'essai.

Pour évaluer ces types de conditions d'utilisation, ce qui suit s'applique.

a) Le DUT doit être positionné avec sa base (surface de la base) et les bords applicables contre le fantôme plan. Les orientations et autres positions d'utilisation peuvent être spécifiques au dispositif hôte. Par conséquent, il convient de les déterminer en fonction des emplacements de l'émetteur et de l'antenne sur le dispositif hôte.

NOTE 1 Les émetteurs RF qui peuvent fonctionner sur des hôtes différents peuvent faire l'objet de considérations supplémentaires.

b) Pour les antennes intégrées dans l'écran d'un ordinateur portable, d'un bloc-notes ou d'ordinateurs légers, les essais doivent être réalisés avec l'écran ouvert à 90°, comme cela est représenté à la Figure 8 b) (côté gauche), ou selon un angle moins prononcé permettant aux antennes d'être plus proches du fantôme pour évaluer les conditions d'exposition de l'utilisateur.

IECNORM.COM : Click to view the full PDF of IEC/IEEE 62209-1528:2020

c) En règle générale, il n'est pas nécessaire de soumettre à l'essai les dispositifs relevant du domaine d'application de 7.2.4.1.7 et équipés d'un écran qu'il convient d'ouvrir pendant le fonctionnement normal, à condition que les antennes placées sur l'écran soient suffisamment éloignées du corps de l'utilisateur selon la puissance de sortie maximale de l'antenne.

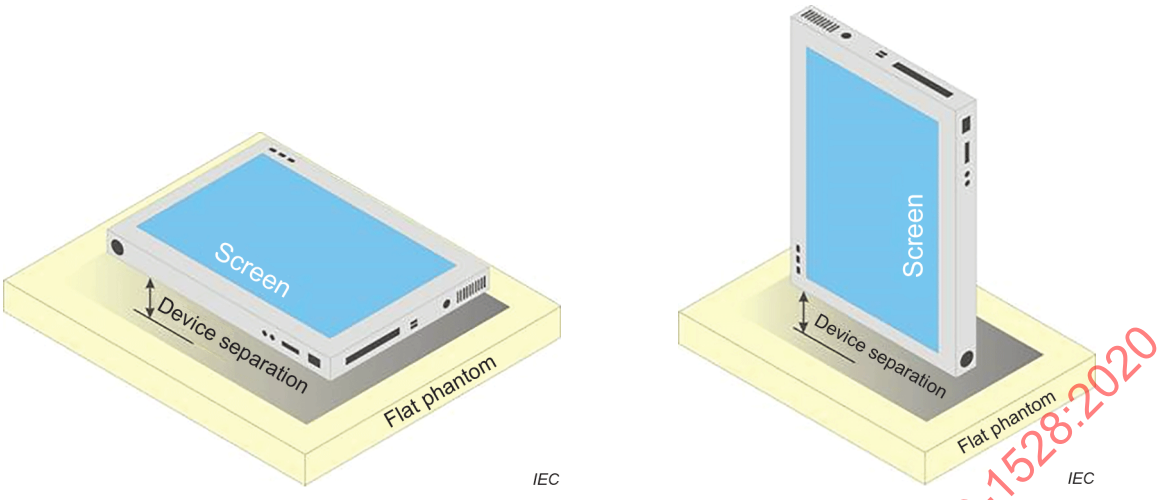
d) En présence d'une antenne montée sur l'écran, le mesurage du DAS pour une exposition des personnes doit être réalisé en positionnant l'écran parallèle au fantôme plan, comme le représente la Figure 8 b) (côté droit).

NOTE 2 Une distance de séparation de 2,5 cm est considérée comme prudente pour la couverture d'un large éventail de conditions prévues d'exposition des personnes.

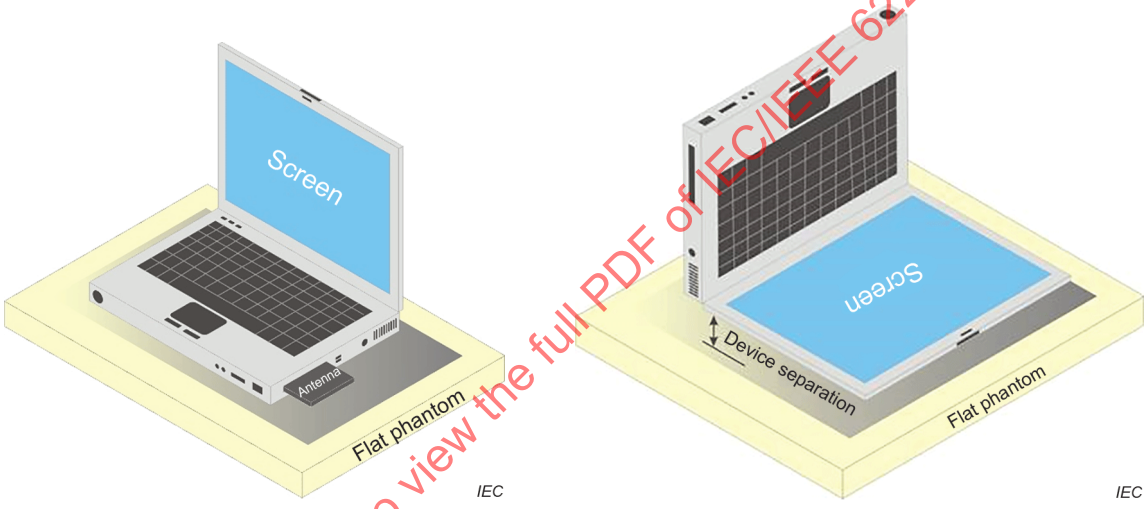
e) Les dispositifs posés sur le corps avec une alimentation externe (adaptateur en courant alternatif, par exemple) en complément de la batterie doivent être soumis à l'essai avec et sans cette alimentation externe.

f) Pour les appareils utilisant une antenne externe avec des positions variables, il convient d'utiliser les procédures relatives aux antennes à rotule et aux antennes détachables (7.2.4.1.6 et Figure 7).

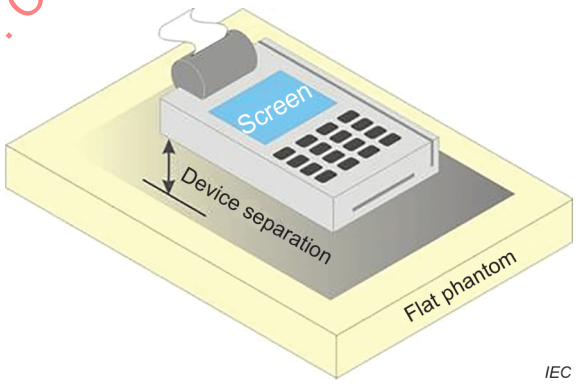
IECNORM.COM : Click to view the full PDF of IEC/IEEE 62209-1528:2020



a) Ordinateur portable sous forme de tablette



b) Ordinateur portable avec antenne externe sous forme de carte enfichable (à gauche) ou avec antenne interne située dans l'écran (à droite)



c) Terminal d'autorisation de transaction des cartes de crédit sans fils

IECNORM.COM : Click to view the full PDF of IEC/IEEE 62209-1528:2020

Anglais	Français
Screen	Écran
Device separation	Distance de séparation de l'appareil
Flat phantom	Fantôme plan
Antenna	Antenne

Figure 8 – Positions d'essai pour les appareils posés sur le corps

7.2.4.1.8 Appareil de bureau

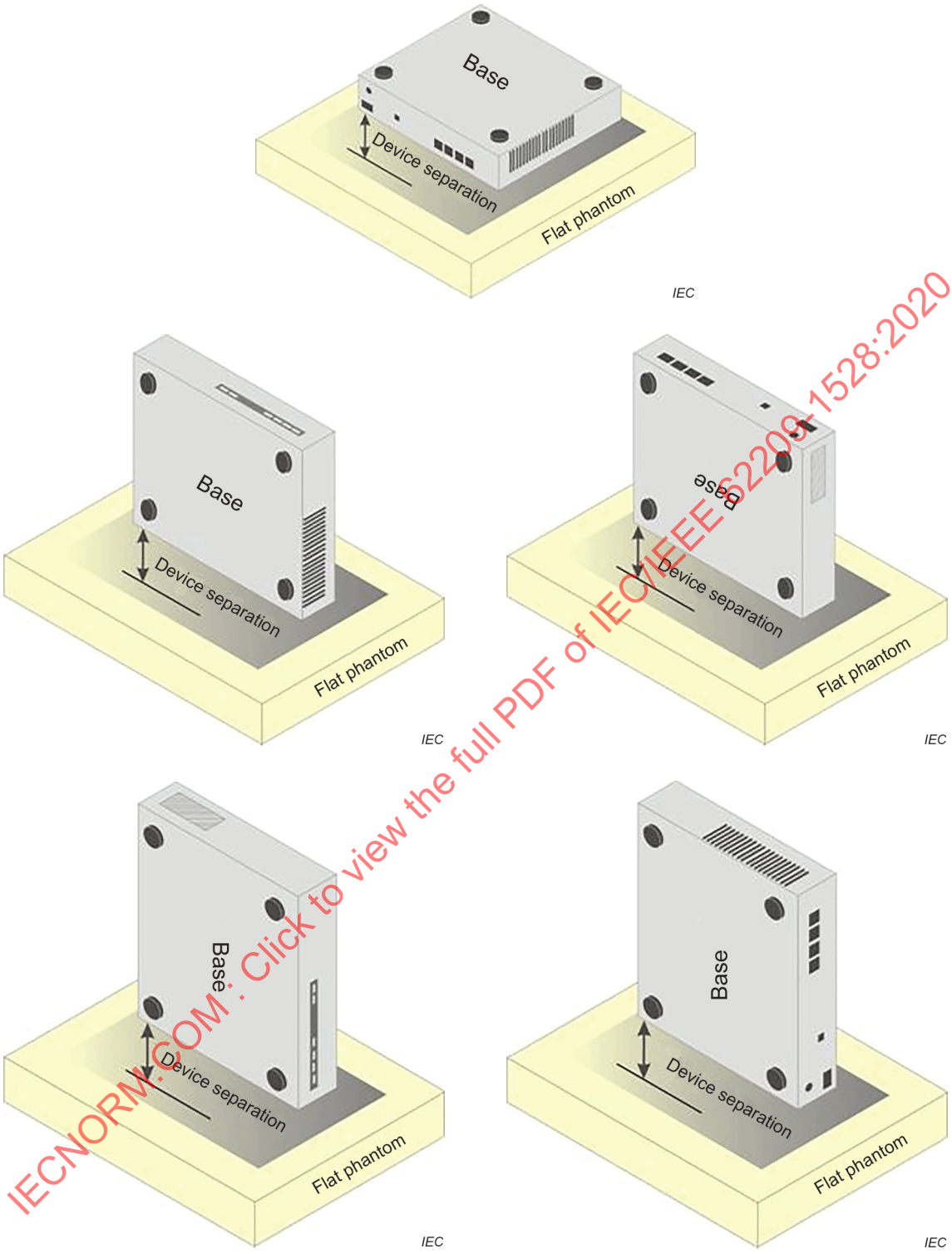
Un exemple classique d'appareil de bureau est un ordinateur de bureau sans fils posé sur une table ou un bureau à 200 mm des utilisateurs lorsqu'il est utilisé.

Pour évaluer ce type de dispositif, ce qui suit s'applique.

- Le DUT doit être placé contre le fantôme plan selon les conditions de 7.2.4.1.2.
- Pour les dispositifs utilisant une antenne externe avec des positions variables, les essais doivent être effectués pour toutes les positions d'antenne spécifiées. La Figure 7 et la Figure 9 représentent les positions d'essai de DAS d'un appareil de bureau.

En raison de la conception physique, certaines surfaces de dispositif peuvent ne pas exiger d'essai (la base d'un appareil posé sur le bureau, par exemple).

IECNORM.COM : Click to view the full PDF of IEC/IEEE 62209-1528:2020



IECNORM.COM : Click to view the full PDF of IEC/IEEE 62209-1528:2020

Anglais	Français
Flat phantom	Fantôme plan
Device separation	Distance de séparation de l'appareil

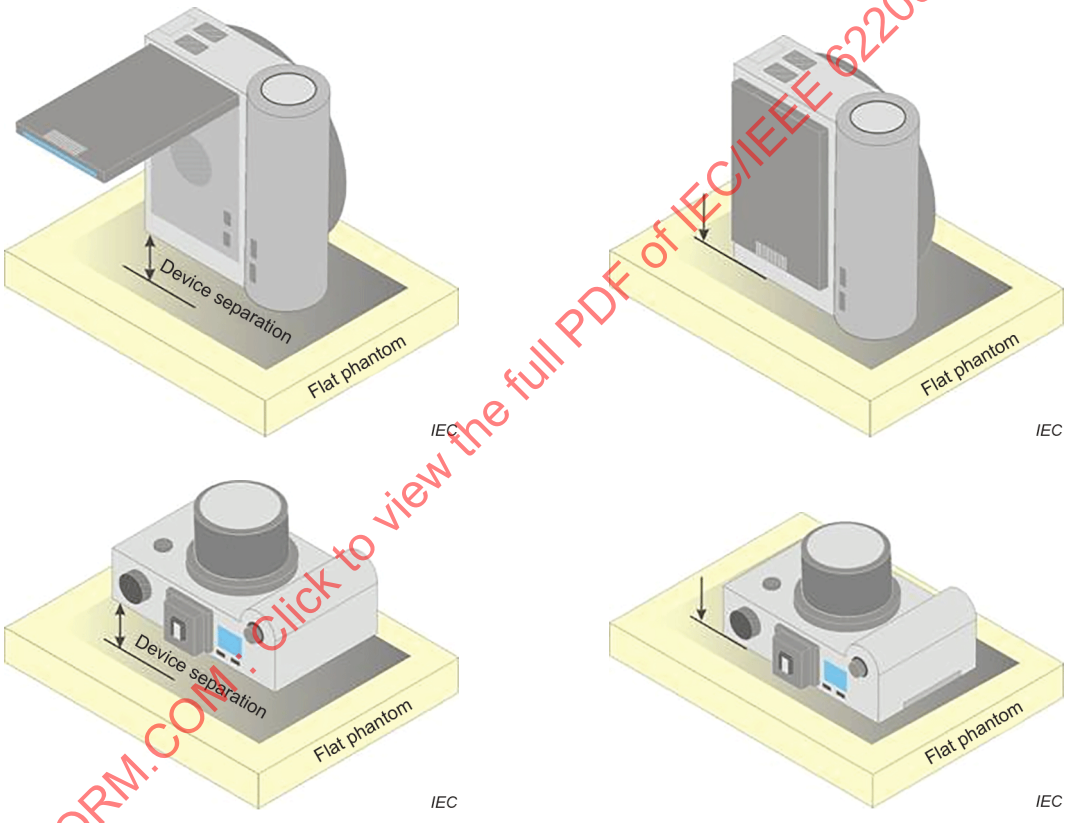
Figure 9 – Positions d'essai pour les appareils de bureau

7.2.4.1.9 Appareil placé devant le visage

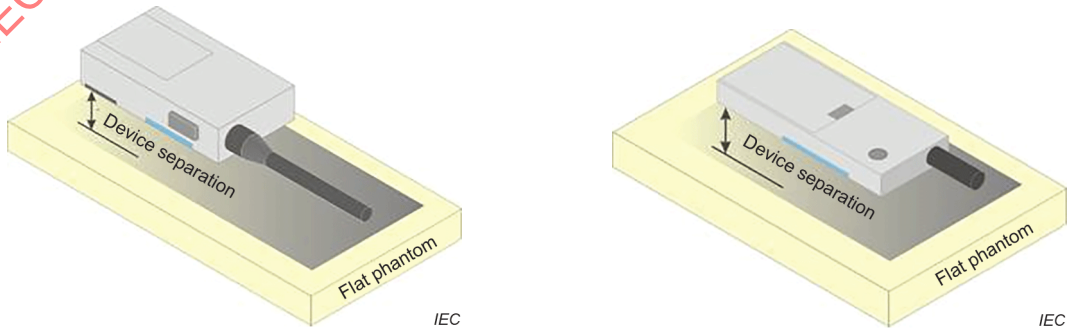
Un exemple classique d'appareil placé devant le visage est une radio bidirectionnelle tenue à une distance proche du visage de l'utilisateur pendant l'émission. D'autres dispositifs entrant dans cette catégorie sont, par exemple, les appareils photographiques et les caméras vidéo sans fils pouvant envoyer des données vers un réseau ou un autre dispositif (Figure 10 a)).

Pour évaluer ce type de dispositif, ce qui suit s'applique:

- Le DUT doit être placé à une distance de séparation d'essai par rapport au fantôme plan selon les conditions de 7.2.4.1.2.
- Pour un dispositif dont l'utilisation prévue exige que le visage de l'utilisateur soit en contact avec l'appareil (un appareil équipé d'un viseur optique, par exemple), ce dernier doit être placé directement contre le fantôme (Figure 10 a), côté droit).



a) Appareils photographiques et caméras vidéo



b) Radios bidirectionnelles

IECNORM.COM : Click to view the full PDF of IEC/IEEE 62209-1528:2020

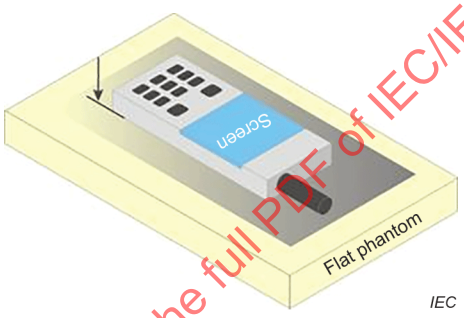
Anglais	Français
Device separation	Distance de séparation de l'appareil
Flat phantom	Fantôme plan

Figure 10 – Positions d'essai pour les appareils placés devant le visage

7.2.4.1.10 Appareil utilisé tenu en main, mais non à proximité de la tête ou du torse

S'il s'avère nécessaire de mesurer le DAS pour les appareils tenus à la main qui n'émettent pas lorsqu'ils sont sur la tête ou le torse, un fantôme plan peut être utilisé. Pour évaluer ce type de dispositif, ce dernier doit être placé directement contre le fantôme plan, comme cela est représenté à la Figure 11 pour les côtés du dispositif qui sont en contact avec la main dans le cadre de l'utilisation prévue.

NOTE Concernant un fantôme de mesure représentant la main, il est difficile, sur le plan pratique, de spécifier une position unique de main tenant un appareil applicable à tous les dispositifs. Des études complémentaires restent nécessaires pour élaborer une méthode représentative d'évaluation du DAS de la main pour les appareils tenus à la main (qu'il s'agisse ou pas d'appareils à commande manuelle). Il est prévu que les futures versions du présent document contiennent une méthode d'essai reposant sur des données et des justifications scientifiques.



Anglais	Français
Screen	Écran
Flat phantom	Fantôme plan

Figure 11 – Position d'essai des appareils tenus à la main, mais non à proximité de la tête ou du torse

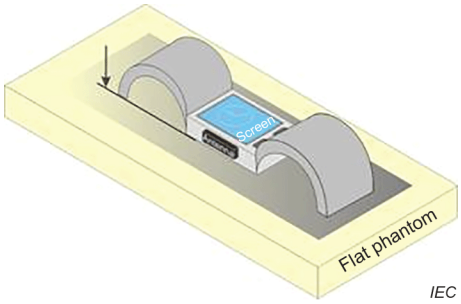
7.2.4.1.11 Appareil fixé à un membre

Les appareils fixés à un membre sont attachés au bras ou à la jambe de l'utilisateur pendant l'émission. Il est similaire à un appareil porté près du corps.

Pour évaluer ce type de dispositif, ce qui suit s'applique.

- Les positions d'essai de 7.2.4.1.5 doivent s'appliquer.
- Le dispositif doit être placé contre le fantôme de sorte que le DAS mesuré soit une exposition prudente (en ouvrant ou retirant la dragonne comme cela est indiqué à la Figure 12, le cas échéant).
- Si le fantôme plan ou une section courbe du fantôme SAM n'est pas applicable, des fantômes spécifiques peuvent être pris en considération (voir l'Annexe K et l'Annexe L, par exemple).

IECNORM.COM : Click to view the full PDF of IEC/IEEE 62209-1528:2020



Anglais	Français
Screen	Écran
Flat phantom	Fantôme plan

Figure 12 – Positions d'essai des appareils fixés à un membre

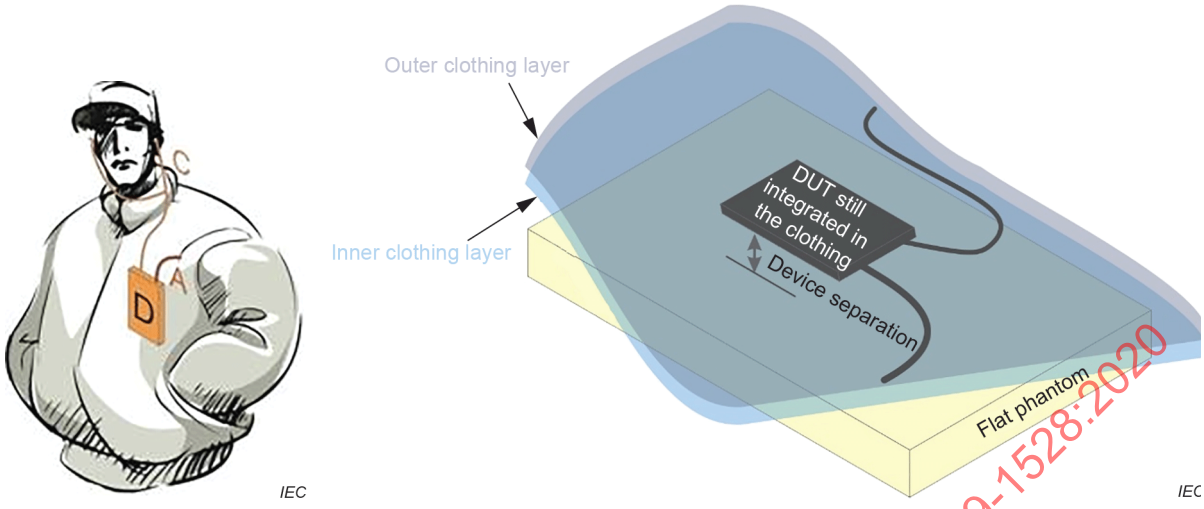
7.2.4.1.12 Appareil intégré aux vêtements

Un exemple classique d'appareil intégré aux vêtements est un dispositif de communication sans fil intégré dans une veste afin de fournir une communication vocale par l'intermédiaire d'un haut-parleur et d'un micro intégrés. Cette catégorie inclut également les dispositifs installés sur la tête avec dispositifs de communication sans fil intégrés.

Pour évaluer ce type de dispositif, ce qui suit s'applique.

- Tous les composants sans fil ou à émission RF doivent être placés contre le fantôme plan (ou des fantômes spécifiques, voir l'Annexe K et l'Annexe L) correspondant aux conditions d'utilisation prévues lorsqu'ils sont intégrés au vêtement (Figure 13).
- Les appareils intégrés dans des dispositifs installés sur la tête peuvent être soumis à l'essai à l'aide du fantôme plan (si cela est approprié) ou de fantômes spécifiques (6.2.3 ou 6.2.5).

IECNORM.COM : Click to view the full PDF of IEC/IEEE 62209-1528:2020



Anglais	Français
Outer clothing layer	Couche de vêtement extérieure
Inner clothing layer	Couche de vêtement intérieure
DUT still integrated in the clothing	DUT toujours intégré dans le vêtement
Device separation	Distance de séparation de l'appareil
Flat phantom	Fantôme plan

Figure 13 – Position d'essai pour les dispositifs de communication sans fil intégrés aux vêtements

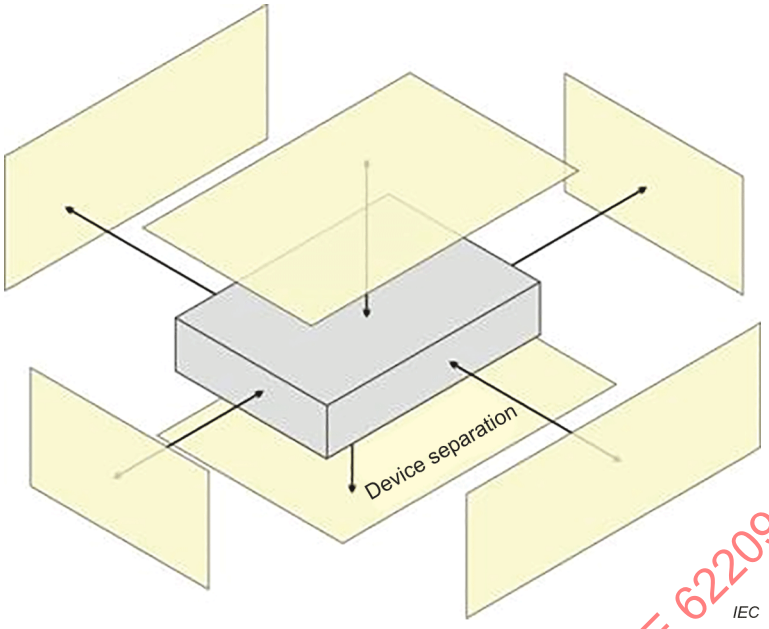
7.2.4.1.13 Appareil générique

Un dispositif ne pouvant pas être classé dans l'un quelconque des autres types spécifiques de dispositifs de 7.2.4.1.5 à 7.2.4.1.12 est considéré comme générique, c'est-à-dire représenté par une boîte fermée comprenant au moins un émetteur RF interne et une antenne. Le principe d'appareil générique peut être appliqué à n'importe quel dispositif. Lorsqu'un émetteur est ajouté au à l'appareil hôte afin que l'hôte et l'émetteur fonctionnent comme un dispositif unique, la catégorie générique peut être considérée uniquement si les dispositions de 7.2.4.1.5 à 7.2.4.1.12 ne sont pas applicables. Lorsque l'antenne ou l'émetteur RF ajouté est externe à l'hôte et que le positionnement de l'antenne ou de l'émetteur RF ajouté est indépendant du positionnement de l'hôte (l'émetteur est relié par un câble et 7.2.4.1.6 ne s'applique pas, par exemple), il doit être évalué en appliquant les procédures de l'appareil générique.

La hiérarchie de distance du DUT spécifiée en 7.2.4.1.2 doit être utilisée pour évaluer les appareils génériques.

L'essai des six faces du DUT (voir la Figure 14) peut ne pas être exigé. L'omission des essais de certaines faces doit être justifiée. La surface de l'appareil générique dirigée vers le fantôme plan doit être conforme à 7.2.4.1.3.

IECNORM.COM : Click to view the full PDF of IEC/IEEE 62209-1528:2020



Anglais	Français
Device separation	Distance de séparation de l'appareil

Figure 14 – Positions d'essai possibles d'un appareil générique

7.2.4.2 Positionnement par rapport au fantôme de tête

7.2.4.2.1 Généralités

Le présent document spécifie deux positions d'essai du DUT par rapport au fantôme de tête (la position "joue" et la position "incliné"). Ces deux positions d'essai sont spécifiées en 7.2.4.2.2 et en 7.2.4.2.3. Le DUT doit être soumis à l'essai dans ces deux positions, sur les côtés gauche et droit du fantôme SAM.

Dans certains cas (des DUT asymétriques ou d'autres facteurs de forme, par exemple), les procédures de positionnement du DUT de 7.2.4.2.2 et 7.2.4.2.3 ne peuvent pas être utilisées. Dans de tels cas, des procédures d'alignement adaptées peuvent être appliquées. Les positions d'essai obtenues doivent refléter les conditions d'utilisation prévues aussi fidèlement que possible.

Les informations détaillées précises relatives aux positions d'essai réelles utilisées, y compris les procédures d'alignement adaptées (si cela est nécessaire) doivent être documentées de manière exhaustive dans le rapport de mesure.

7.2.4.2.2 Définition de la position "joue"

La position "joue" est établie comme cela est décrit dans les points a) à j) ci-dessous.

a) Si nécessaire, configurer le DUT en mode de fonctionnement vocal. Par exemple, pour un DUT avec un capot pliable, pivotant ou coulissant, ouvrir le capot si celui-ci est compatible avec le mode vocal. Si le DUT peut également être utilisé avec le capot fermé, les deux configurations doivent être soumises à l'essai.

b) Définir deux lignes imaginaires sur le DUT, la ligne centrale verticale et la ligne horizontale, le DUT étant en orientation verticale, comme cela est représenté à la Figure 15.

IECNORM.COM : Click to view the full PDF of IEC/IEEE 62209-1528:2020

c) La ligne centrale verticale passe par deux points sur la face avant du DUT: le point central de la largeur w_t du DUT au niveau de la sortie acoustique (Point A sur la Figure 15) et le point central de la largeur w_b de la base du DUT (Point B). La ligne horizontale est perpendiculaire à la ligne centrale verticale et passe par le centre de la sortie acoustique (Figure 15). L'intersection des deux lignes est au Point A. Il est à noter que pour beaucoup de DUT, le Point A coïncide avec le centre de la sortie acoustique. Cependant la sortie acoustique peut être située n'importe où sur la ligne horizontale. Noter également que la ligne centrale verticale n'est pas nécessairement parallèle à la face avant du DUT, en particulier pour les DUT en forme de coquille, les DUT pliables et autres DUT de forme irrégulière.

d) Placer le DUT à proximité de la surface du fantôme de telle sorte que le Point A soit en prolongement (virtuel) de la droite passant par les Points OD (point de référence de l'oreille droite) et OG (point de référence de l'oreille gauche) sur le fantôme (voir la Figure 16a) et la Figure 16 b)). Le plan défini par la ligne centrale verticale et la ligne horizontale du DUT doit être parallèle au plan sagittal du fantôme.

e) Déplacer le DUT vers le fantôme le long de la droite passant par OD et OG jusqu'à ce que le DUT touche l'oreille (voir la Figure 16c)).

f) Faire tourner le DUT autour de la ligne (virtuelle) OD-OG jusqu'à ce que la ligne centrale verticale du DUT soit dans le plan de référence (voir la Figure 16 d)).

g) Faire tourner le DUT autour de sa ligne centrale verticale jusqu'à ce que le plan défini par la ligne centrale verticale du DUT et la ligne horizontale soit parallèle à la ligne N-F (voir l'Annexe G), puis déplacer le DUT vers le fantôme le long de la ligne OD-OG jusqu'à ce que le Point A du DUT touche l'oreille à l'ERP (point de référence de l'oreille) (voir la Figure 16e)).

h) Tout en maintenant le Point A sur la ligne passant par OD et OG et en maintenant le DUT en contact avec le pavillon de l'oreille, faire tourner le DUT autour de la ligne N-F jusqu'à ce qu'un point quelconque du DUT soit en contact avec le point du fantôme sous le pavillon de l'oreille (joue) (voir la Figure 16f)). Les angles de rotation doivent être notés.

i) Tout en maintenant le Point A du DUT en contact avec l'ERP, faire tourner le DUT autour d'une ligne perpendiculaire au plan défini par la ligne centrale verticale du DUT et la ligne horizontale, et passant par le Point A du DUT, jusqu'à ce que la ligne centrale verticale du DUT soit dans le plan de référence (voir la Figure 16g)).

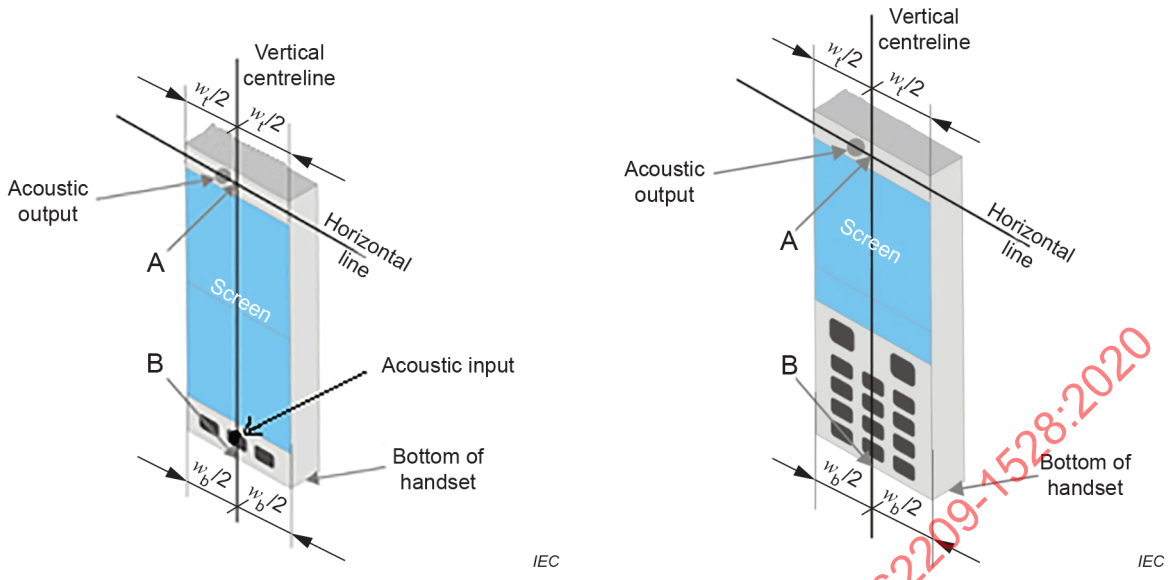
j) Vérifier que la position "joue" est correcte, comme suit:

   1) la ligne N-F est dans le plan défini par la ligne centrale verticale du DUT et la ligne horizontale;

   2) le Point A du DUT touche le pavillon de l'oreille à l'ERP;

   3) la ligne centrale verticale du DUT est dans le plan de référence.

IECNORM.COM : Click to view the full PDF of IEC/IEEE 62209-1528:2020



Anglais	Français
Acoustic output	Sortie acoustique
Horizontal line	Ligne horizontale
Vertical centerline	Ligne centrale verticale
Acoustic input	Entrée acoustique
Bottom of handset	Base du combiné

Légende

w_t Largeur du DUT au niveau de la sortie acoustique

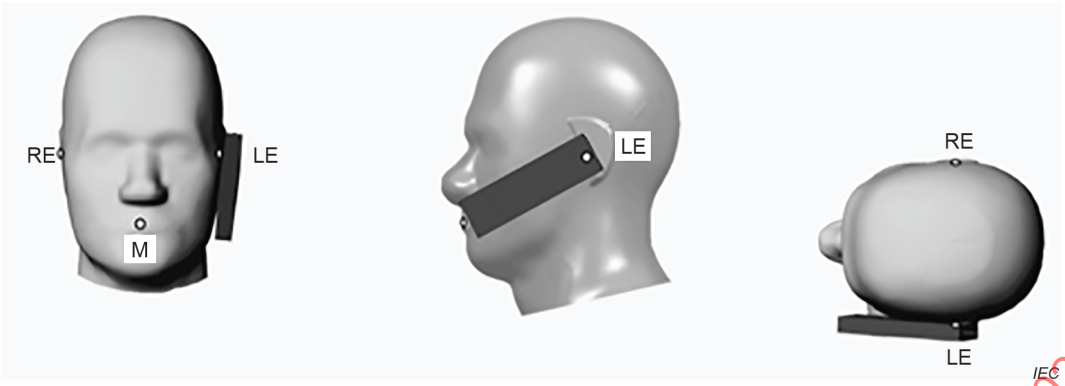
w_b Largeur à la base du DUT

A Point central de la largeur w_t du DUT au niveau de la sortie acoustique

B Point central de la largeur w_b à la base du DUT

Figure 15 – Lignes de référence verticale et horizontale et points de référence A et B sur deux exemples types de dispositifs: un mobile multifonction avec écran tactile complet (en haut) et un DUT à clavier (en bas)

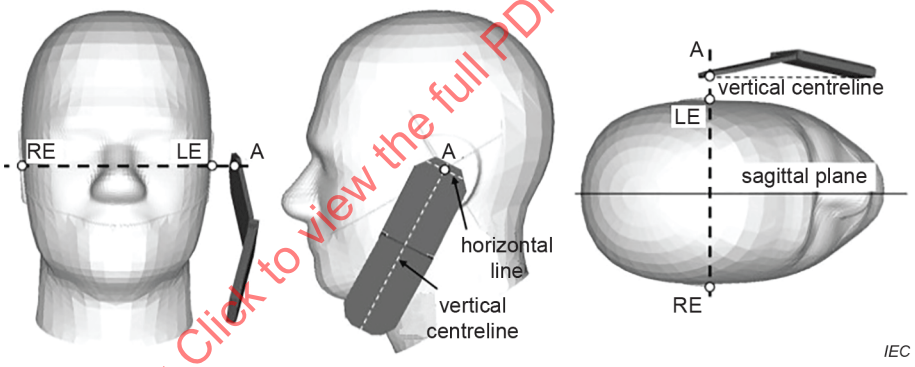
IECNORM.COM : Click to view the full PDF of IEC/IEEE 62209-1528:2020



Anglais	Français
RE	OD
LE	OG
M	B

NOTE Les points de référence pour l'oreille droite (OD), l'oreille gauche (OG) et la bouche (B), qui définissent le plan de référence pour le positionnement du DUT, sont indiqués. Cette position de dispositif doit être maintenue pour la configuration d'essai sagittale de fantôme représentée à la Figure G.4.

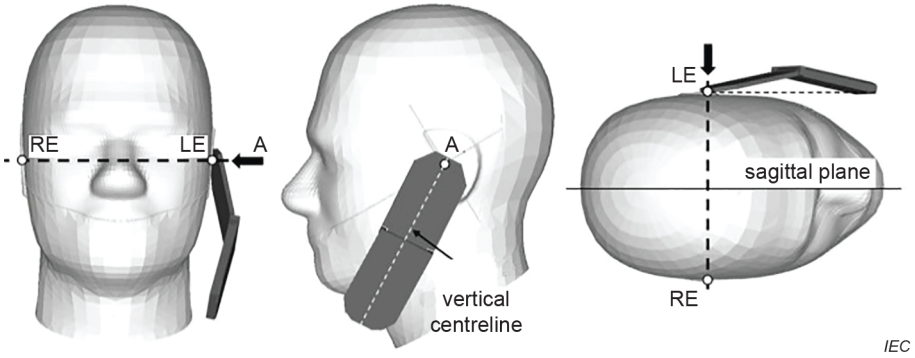
a) Position de téléphone 1 – position joue



Anglais	Français
RE	OD
LE	OG
Horizontal line	Ligne horizontale
Vertical centerline	Ligne centrale verticale
Sagittal plane	Plan sagittal

b) Position de DUT possible contre la tête après application de 7.2.4.2.2 c)

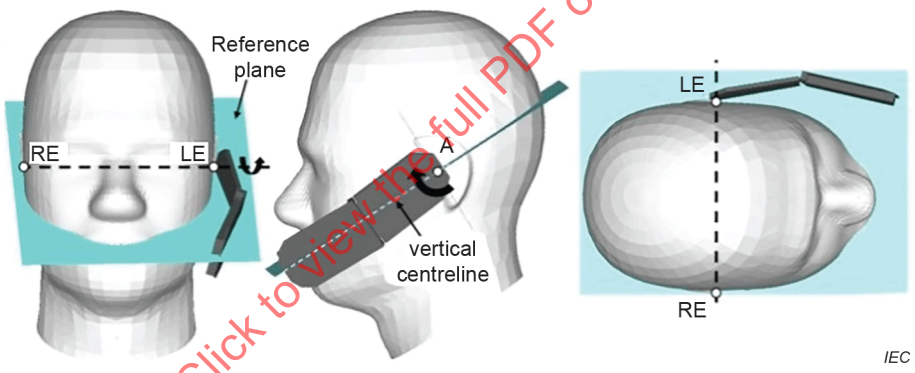
IECNORM.COM : Click to view the full PDF of IEC/IEEE 62209-1528:2020



Anglais	Français
RE	OD
LE	OG
Vertical centerline	Ligne centrale verticale
Sagittal plane	Plan sagittal

NOTE Les flèches noires indiquent la direction de déplacement du DUT pour 7.2.4.2.2 d).

c) Position du DUT après application de 7.2.4.2.2 d)

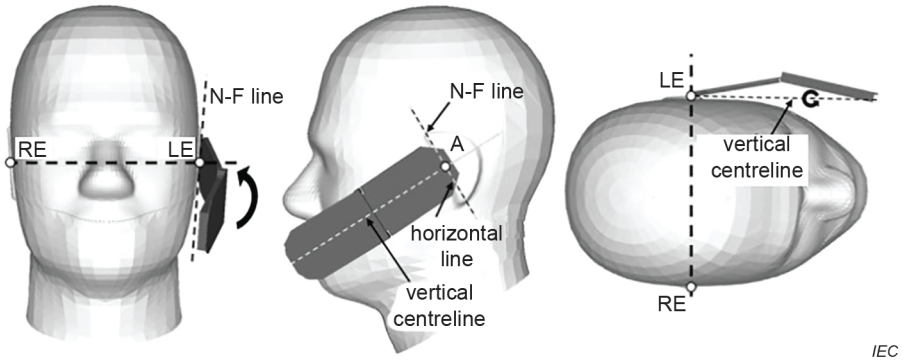


Anglais	Français
RE	OD
LE	OG
Vertical centerline	Ligne centrale verticale
Reference plane	Plan de référence

NOTE Les flèches noires indiquent la direction de rotation du DUT pour 7.2.4.2.2 e).

d) Position du DUT après application de 7.2.4.2.2 e)

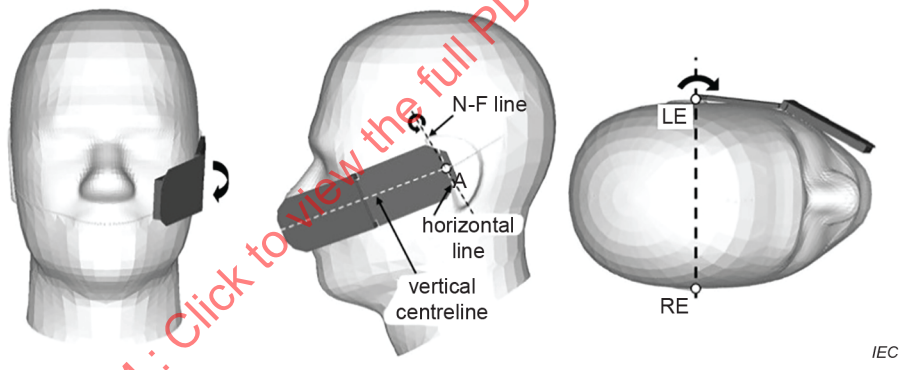
IECNORM.COM : Click to view the full PDF of IEC/IEEE 62209-1528:2020



Anglais	Français
LE	OG
RE	OD
N-F line	Ligne N-F
horizontal line	ligne horizontale
vertical centerline	ligne centrale verticale

NOTE Les flèches noires courbées indiquent la direction de rotation du DUT pour 7.2.4.2.2 f).

e) Position du DUT après application de 7.2.4.2.2 f)

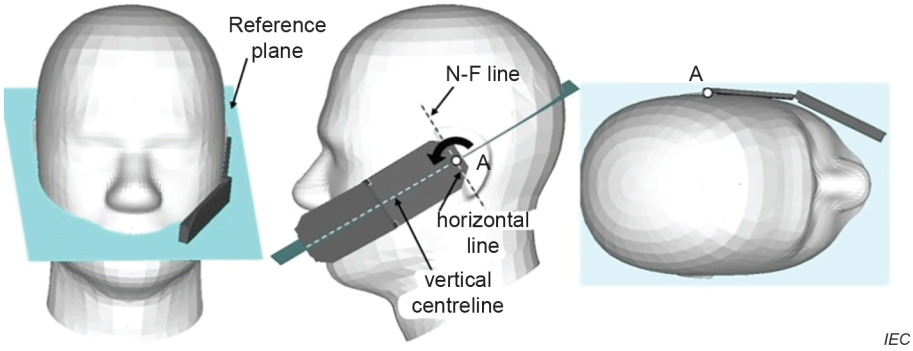


Anglais	Français
LE	OG
RE	OD
N-F line	Ligne N-F
horizontal line	ligne horizontale
vertical centerline	ligne centrale verticale

NOTE Les flèches noires courbées indiquent la direction de rotation du DUT pour 7.2.4.2.2 g)

f) Position du DUT après application de 7.2.4.2.2 g)

IECNORM.COM : Click to view the full PDF of IEC/IEEE 62209-1528:2020



Anglais	Français
Reference plane	Plan de référence
N-F line	Ligne N-F
horizontal line	ligne horizontale
vertical centerline	ligne centrale verticale

NOTE Les flèches noires courbées indiquent la direction de rotation du DUT pour 7.2.4.2.2 h).

g) Position du DUT après application de 7.2.4.2.2 h)

Figure 16 – Position "joue" du DUT sur le côté gauche du SAM dans laquelle le dispositif doit être maintenu pour la configuration d'essai du fantôme

7.2.4.2.3 Définition de la position "incliné"

La position "incliné" est établie comme cela est décrit dans les points a) à d) ci-dessous.

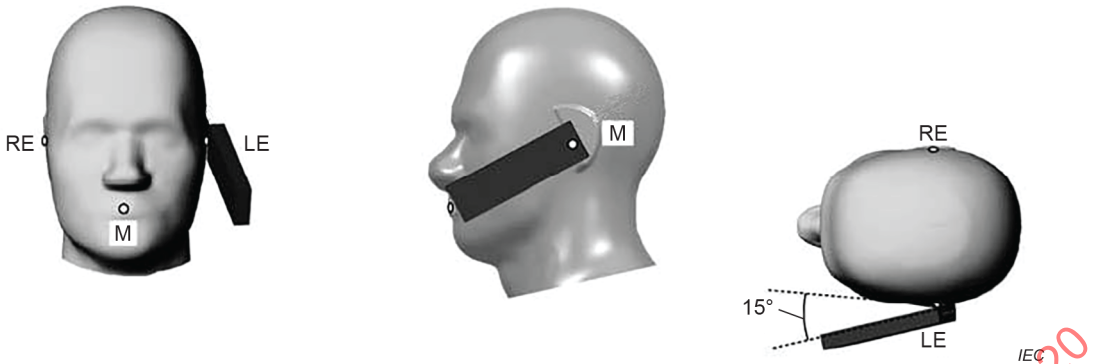
a) Répéter les Étapes a) à j) de 7.2.4.2.2 pour placer le DUT dans la position "joue" (voir la Figure 16).

b) Tout en maintenant l'orientation du DUT, éloigner le DUT du pavillon de l'oreille le long de la ligne passant par OD et OG suffisamment loin pour permettre une rotation du DUT loin de la joue de 15°.

c) Faire tourner le DUT de 15° autour de la ligne horizontale (voir la Figure 17).

d) Tout en maintenant l'orientation du DUT, déplacer celui-ci vers le fantôme sur une ligne passant par OD et OG jusqu'à ce qu'une partie quelconque du DUT touche l'oreille. La position "incliné" est atteinte lorsque le contact avec le pavillon de l'oreille est réalisé. Si le contact a lieu ailleurs qu'avec le pavillon de l'oreille (une antenne déployée en contact avec l'arrière du fantôme de tête, par exemple), l'angle du DUT doit être réduit. Dans ce cas, la position "incliné" est obtenue si une partie quelconque du DUT est en contact avec le pavillon de l'oreille et si un second point du DUT est en contact avec le fantôme (l'antenne avec l'arrière de la tête, par exemple).

IECNORM.COM : Click to view the full PDF of IEC/IEEE 62209-1528:2020



Anglais	Français
RE	OD
LE	OG
M	B

Légende

B Point de référence de la bouche

OG Point de référence de l'oreille gauche

OD Point de référence de l'oreille droite

Cette position du dispositif doit être maintenue pendant les réglages d'essai du fantôme.

Figure 17 – Position "incliné" du DUT sur le côté gauche du SAM

7.2.5 Configurations de l'antenne

Pour les dispositifs qui utilisent une ou plusieurs antennes externes avec des positions variables (antenne déployée, rétractée, tournée, par exemple), ceux-ci doivent être positionnés conformément aux instructions d'utilisation fournies par le fabricant. Si aucune position d'antenne prévue n'est spécifiée, les essais doivent être réalisés avec l'antenne ou les antennes orientées de manière à obtenir les conditions d'exposition maximale tout en maintenant le dispositif dans les positions de 7.2.4. Pour les antennes qui peuvent être déployées, l'essai doit être effectué avec l'antenne totalement déployée et totalement rétractée. Les configurations d'antenne doivent être documentées dans le rapport de mesure. Les antennes à diversité d'émission doivent être soumises à l'essai séparément pour le DAS.

7.2.6 Options et accessoires

D'autres accessoires qui affectent la puissance de sortie RF ou la distribution de courant RF du DUT lorsqu'il est utilisé à côté d'une personne doivent être soumis à l'essai conformément aux conditions d'utilisation prévue spécifiées par le fabricant. Voir 7.2.4.1.5 pour le positionnement proche du corps, et 7.2.4.2 pour le positionnement proche de la tête. Par exemple, a) antennes facultatives, b) blocs de batteries facultatifs qui modifient les performances ou le DAS du dispositif de communication sans fil, etc., et c) fils connectés pendant l'utilisation prévue. En règle générale, les accessoires de communication en champ proche basse puissance ou de transfert de puissance sans fil récepteurs uniquement n'exigent aucun mesurage de DAS, mais leur influence sur le DAS d'autres émetteurs doit être prise en considération.

7.2.7 DUT à facteur de forme différent

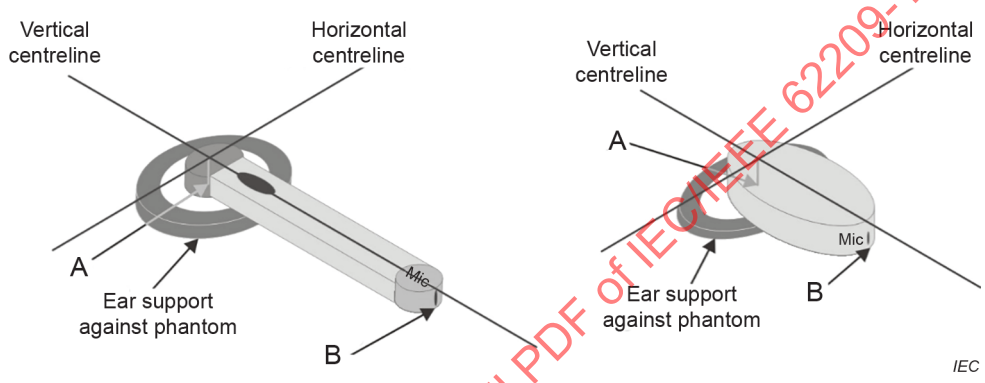
Les principes de base définis et spécifiés en 7.2.4 peuvent être appliqués à des dispositifs aux facteurs de forme similaires. Les casques sans fil (reliés par Bluetooth, par exemple) sont des exemples de dispositifs installés sur la tête qui peuvent être évalués en appliquant ces principes.

IECNORM.COM : Click to view the full PDF of IEC/IEEE 62209-1528:2020

La géométrie et le système de mise en correspondance des coordonnées représentés à la Figure 18 sont applicables. Le point A, qui est la sortie acoustique, se trouve au point central de la largeur, et le point B, qui est le micro primaire, se trouve à la base du dispositif (l'extrémité la plus proche de la bouche). Il est à noter que pour les besoins de l'application des procédures de positionnement, le DUT est considéré comme un facteur de forme (rectangulaire, cubique) de type "barre classique".

Avant d'appliquer 7.2.7, il faut prendre en considération les modes de fonctionnement disponibles et les niveaux de puissance de fonctionnement maximaux, car certains dispositifs peuvent ne pas exiger d'essai.

Toutes les informations détaillées relatives aux DUT à facteur de forme différent doivent être entièrement documentées dans le rapport de mesure, y compris des diagrammes ou des photographies. Des principes techniques appropriés doivent être appliqués pour mettre en œuvre la mise en correspondance d'un dispositif à facteur de forme différent.



Anglais	Français
Vertical centerline	Ligne centrale verticale
Horizontal centerline	Ligne centrale horizontale
Ear support against phantom	Support d'oreille contre le fantôme

Figure 18 – DUT à facteur de forme différent avec points de référence et lignes de référence

7.2.8 Fréquences d'essai pour le DUT

Un DUT doit être conforme aux normes d'exposition applicables à toutes les fréquences d'émission. Cependant, la conduite des essais pour tous les canaux n'est ni réalisable ni nécessaire. L'Article 7.2.8 a pour objet de définir un sous-ensemble utilisable de canaux pour lesquels les mesurages de DAS doivent être effectués. Ce sous-ensemble de canaux est choisi de façon à caractériser un DUT pour le comparer avec toute norme d'exposition applicable.

Avant de procéder aux essais à l'aide des canaux spécifiques exigés par le présent document, la puissance de sortie maximale des canaux doit être vérifiée pour déterminer si les canaux choisis produisent la sortie assignée la plus élevée du dispositif. Le processus utilisé pour établir les canaux pour les besoins de l'essai doit être documenté dans le rapport de mesure.

Pour chaque mode de fonctionnement d'une technologie sans fil utilisée par le DUT:

a) les essais doivent être réalisés avec le canal produisant la puissance de sortie assignée la plus élevée;

b) si la largeur de la bande de fréquences transmise ($\Delta f = f_{haut} - f_{bas}$) dépasse 1 % de sa fréquence centrale f_c, les canaux aux fréquences la plus basse et la plus élevée de la bande d'émission doivent également être soumis à l'essai;

IECNORM.COM : Click to view the full PDF of IEC/IEEE 62209-1528:2020

c) si la largeur de la bande d'émission dépasse 10 % de sa fréquence centrale, la Formule (4) doit être appliquée pour déterminer le nombre de canaux N_c à soumettre à l'essai:

$$N_c = 2 \times \text{roundup}\left[10 \times \left(f_{haut} - f_{bas}\right)/f_c\right] + 1 \quad (4)$$

où

f_c est le canal de la fréquence centrale de la bande d'émission en Hz;

f_{haut} est le canal de la plus haute fréquence de la bande d'émission en Hz;

f_{bas} est le canal de la plus basse fréquence de la bande d'émission en Hz;

N_c est le nombre de canaux.

NOTE 1 La fonction roundup(x) arrondit son argument x à l'entier supérieur. Par conséquent, le nombre de canaux, N_c, est toujours un nombre impair.

NOTE 2 Les organismes de réglementation nationaux peuvent avoir différentes exigences sur le nombre de canaux à soumettre à l'essai par bande d'émission, en fonction des allocations de fréquence et d'autres exigences des technologies sans fil. Un exemple est donné dans la Formule (5):

$$N_c = \text{arrondi}\left[\sqrt{\frac{100\left(f_{haut} - f_{bas}\right)}{f_c}}\left(\frac{f_c}{100}\right)^{0,2}\right]_{\perp} \quad (5)$$

Il convient que le nombre de canaux, N_c, soit espacé de manière égale. Ce nombre doit satisfaire aux exigences précédentes.

Les étalonnages de sonde doivent être valides pour toutes les fréquences d'essai et les paramètres diélectriques du milieu à ces fréquences. Plusieurs points d'étalonnage de sonde et différents milieux équivalents aux tissus couvrant l'ensemble de la bande de fréquences peuvent être exigés pour les dispositifs présentant des bandes d'émission sensiblement plus larges.

7.3 Essais à effectuer pour les DUT

7.3.1 Généralités

La procédure d'essai du DUT englobe les deux principaux processus suivants:

– le choix des configurations d'essai à mesurer à l'aide des techniques de réduction d'essai présentées en 7.9.3 (facultatives), et

– l'évaluation de DAS de ces configurations d'essai à l'aide de la procédure d'essai complet de DAS présentée en 7.4.2. Éventuellement, l'essai rapide de DAS selon les exigences définies en 7.9.2 peut être utilisé.

Dans tous les cas où des réductions d'essai (7.9.3) ont été appliquées, le dispositif contenant des combinaisons d'accessoires ayant été exclus du mesurage de DAS, et la justification de ces réductions d'essai, doivent être clairement documentés dans le rapport de mesure.

7.3.2 Approche fondamentale des essais du DUT

Pour déterminer le psDAS d'un DUT, toutes les positions, configurations et modes de fonctionnement d'essai exigés du dispositif doivent être soumis à l'essai pour chaque bande de fréquences conformément aux étapes 1 à 3. Pour les dispositifs capables d'émission simultanée, appliquer la procédure appropriée décrite en 7.4.4. Le processus d'essai est représenté à la Figure 19. Des exemples d'application sont donnés à l'Annexe N.

Pour les modes ELT, la procédure de 7.9.3.6.3 doit être utilisée à la place de celle de 7.3.2.

IECNORM.COM : Click to view the full PDF of IEC/IEEE 62209-1528:2020

Étape 1: La procédure de mesure décrite en 7.4 doit être réalisée au niveau du canal produisant la puissance de sortie assignée la plus élevée pour chaque antenne d'émission utilisée:

a) pour toutes les positions d'essai du dispositif (comme cela est spécifié en 7.2.4),

b) pour toutes les configurations d'utilisation pour chaque position du dispositif en a), par exemple, avec la glissière ou le couvercle du dispositif ouvert et fermé ou l'antenne déployée et rétractée, et

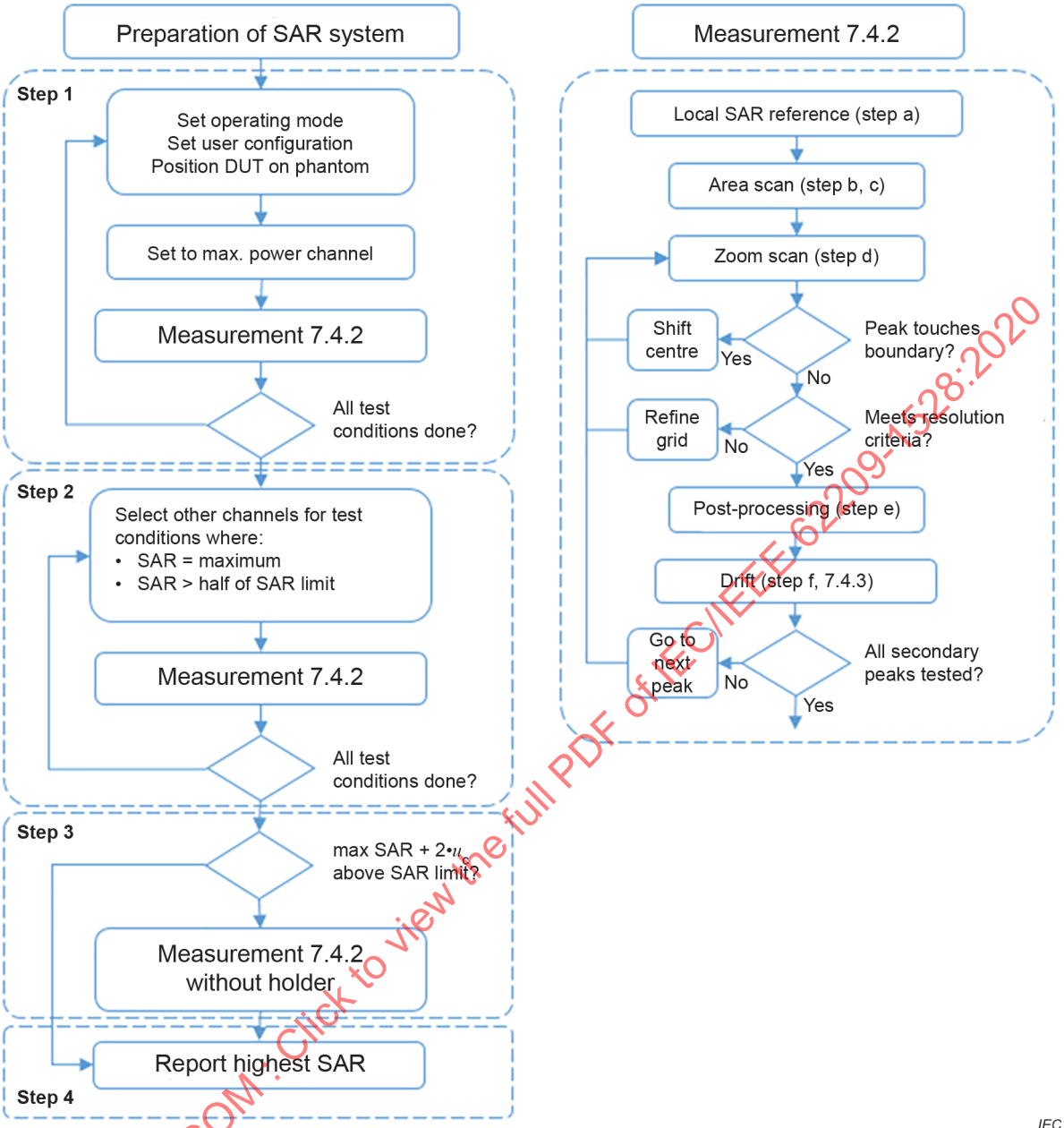
c) pour tous les modes de fonctionnement (voir 3.33), pour chaque position du dispositif en a) et chaque configuration en b) pour chaque bande de fréquences.

Étape 2: Pour la configuration d'essai donnant le psDAS le plus élevé déterminé à l'Étape 1 et pour chaque essai en a), b) et c), effectuer tous les essais décrits en 7.4 au niveau de tous les autres canaux de fréquences d'essai applicables, par exemple, les canaux le plus bas et le plus haut (7.2.8). De plus, pour chaque position, configuration et mode de fonctionnement du dispositif dans lesquels la valeur du psDAS déterminée aux étapes 1 a), b) et c) est supérieure ou égale à la moitié de la limite applicable du DAS, il est exigé de soumettre à l'essai tous les canaux de 7.2.8. Dans le cas contraire, une telle exigence n'est pas applicable

Étape 3: Si le psDAS le plus élevé de l'étape 1 et de l'étape 2 est supérieur à la limite applicable du DAS diminuée de l'incertitude de mesure élargie et si, pour cette configuration d'essai, le DUT était en contact direct avec des parties du support de dispositif dont la permittivité relative est supérieure à 1,2, cette configuration d'essai doit être de nouveau soumise à l'essai après le montage du dispositif sur un élément en mousse, comme cela est spécifié en 6.5 et à la Figure 3. Les deux valeurs doivent être consignées.

Étape 4: Examiner toutes les données et consigner le psDAS mesuré à l'étape 1, l'étape 2 et l'étape 3 selon les exigences réglementaires.

IECNORM.COM : Click to view the full PDF of IEC/IEEE 62209-1528:2020



IECNORM.COM : Click to view the full PDF of IEC/IEEE 62209-1528:2020

Anglais	Français
Preparation of SAR system	Préparation du système DAS
Step 1	Étape 1
Set operating mode	Définir le mode de fonctionnement
Set user configuration	Définir la configuration de l'utilisateur
Position DUT on phantom	Positionner le DUT sur le fantôme
Set to max. power channel	Régler au canal de puissance max.
Measurement 7.4.2	Mesurage 7.4.2
All test conditions done?	Toutes les conditions d'essai sont-elles réalisées?
Step 2	Étape 2
Select other channel for test conditions where:	Sélectionner un autre canal pour les conditions d'essai lorsque:
SAR = maximum	DAS = maximum
SAR > half of SAR limit	DAS > moitié de la limite de DAS

Anglais	Français
Measurement 7.4.2	Mesurage 7.4.2
All test conditions done?	Toutes les conditions d'essai sont-elles réalisées?
Step 3	Étape 3
max SAR + 2 above SAR limit?	max DAS + 2 au-dessus de la limite de DAS?
Measurement 7.4.2 without holder	Mesurage 7.4.2 sans support
Report highest SAR	Consigner le DAS le plus élevé
Step 4	Étape 4
Measurement 7.4.2	Mesurage 7.4.2
Local SAR reference (step a)	Référence de DAS local (étape a)
Area scan (step b, c)	Balayage de surface (étape b, c)
Zoom scan (step d)	Balayage-zoom (étape d)
Shift centre	Déplacer le centre
Yes	Oui
No	Non
Peak touches boundary?	La valeur crête touche-t-elle la limite?
Refine grid	Affiner la grille
Yes	Oui
No	Non
Meet resolution criteria?	Satisfait aux critères de résolution?
Post-processing (step e)	Post-traitement (étape e)
Drift (step f, 7.4.3)	Dérive (étape f, 7.4.3)
Go to next peak?	Aller à la valeur crête suivante?
All secondary peaks tested?	Toutes les valeurs crêtes secondaires ont-elles été soumises à l'essai?

Figure 19 – Schéma de principe des essais à effectuer

7.4 Procédure de mesure

7.4.1 Généralités

Le 7.4 décrit la procédure d'évaluation du psDAS du DUT, y compris le nombre minimal de mesurages de dérive à effectuer. Si la dérive est élevée pour un mode de fonctionnement et un canal de fréquences particuliers, davantage de mesurages de dérive peuvent être nécessaires, comme cela est décrit en 7.4.3.

7.4.2 Procédures d'essai complet du DAS

La procédure suivante doit être effectuée pour chaque condition d'essai (Figure 19) décrite en 7.3. Le Tableau 3 présente les paramètres de mesure utilisés dans le balayage de surface et le Tableau 4 ceux utilisés pour le balayage-zoom.

a) Mesurer le DAS local à un point d'essai situé dans les limites de 5 mm de la surface interne du fantôme où le DAS local mesuré dépasse la limite de détection inférieure du système de mesure. De préférence, le point d'essai est au-dessus de l'emplacement de DAS maximal prévu dans ladite limite de distance de la surface du fantôme. Comme cela est décrit à l'étape f), un mesurage comparatif doit être effectué par le système au même point à l'issue du mesurage de DAS.

IECNORM.COM : Click to view the full PDF of IEC/IEEE 62209-1528:2020

b) Mesurer la distribution du DAS à deux dimensions dans le fantôme (c'est-à-dire le balayage de surface). Le Tableau 3 présente les paramètres de mesure exigés pour la zone de balayage.

1) La zone sur laquelle le mesurage de DAS est effectué doit couvrir au moins une zone plus grande que la projection du DUT et de son antenne. Pour certains DUT, la zone projetée sur le fantôme peut être si grande que la sonde peut ne pas atteindre tous les points. Dans ce cas, les fantômes peuvent être tournés et la zone peut être évaluée au moyen de balayages multiples avec des zones de chevauchement. La résolution de mesure et la résolution spatiale pour l'interpolation doivent être choisies pour permettre l'identification des emplacements du maximum local à la moitié de la dimension linéaire du côté correspondant du volume de balayage-zoom.

2) Pour le fantôme plan, la limite de la zone de mesure ne doit pas être inférieure à 20 mm des parois latérales du fantôme.

c) À partir de la distribution de DAS de balayage de surface, identifier la position de la valeur maximale de DAS. De plus, identifier également les positions de tous les maxima locaux éventuels avec des valeurs de DAS à 2 dB au plus de la valeur maximale et qui ne sont pas dans le balayage-zoom d'autres pics. Les balayages-zooms supplémentaires doivent être mesurés uniquement si ce type de pics est dans les limites de 2 dB de la limite de conformité de DAS (par exemple, 1 W/kg pour 1,6 W/kg, limite 1 g; ou 1,26 W/kg pour 2 W/kg, limite 10 g).

d) Mesurer la distribution tridimensionnelle de DAS aux emplacements des maxima locaux identifiés à l'étape c) (c'est-à-dire le balayage-zoom).

1) Pour des fréquences inférieures ou égales à 3 GHz, la procédure suivante doit être appliquée (voir le Tableau 4).

i) La taille minimale du volume de balayage-zoom doit être de (30 x 30 x 30) mm.

ii) Le pas de grille horizontal doit être de 8 mm au maximum.

iii) Le pas de grille dans la direction verticale doit être de 5 mm ou moins si un espacement uniforme est utilisé.

iv) Si un espacement variable est utilisé dans la direction verticale, l'espacement maximal entre les deux points mesurés les plus proches de l'enveloppe du fantôme (M1 et M2, voir la Figure 20) doit être de 4 mm au maximum, et l'espacement entre les points les plus éloignés doit augmenter selon un facteur de 1,5 au maximum.

v) Pour les autres paramètres, voir le Tableau 4 et la Figure 20.

2) Pour des fréquences supérieures à 3 GHz, la procédure suivante doit être appliquée.

i) La taille minimale du volume de balayage-zoom peut être réduite à (22 x 22 x 22) mm.

ii) Le pas de grille horizontal doit être de $(24/f[\text{GHz}])$ mm au maximum.

iii) Si un espacement uniforme dans la direction verticale est utilisé, le pas de grille dans la direction verticale doit être de $(10/(f[\text{GHz}]-1))$ mm au maximum.

iv) Si un espacement variable est utilisé dans la direction verticale, l'espacement maximal entre les deux points mesurés les plus proches de l'enveloppe du fantôme doit être de $(12/f[\text{GHz}])$ mm au maximum, et l'espacement entre les points les plus éloignés doit augmenter selon un facteur de 1,5 au maximum.

v) Pour les autres paramètres, voir le Tableau 4 et la Figure 20.

3) Si le cube au DAS 1 g ou 10 g le plus élevé touche le bord du volume de balayage-zoom, le balayage-zoom doit être entièrement répété avec un nouveau centre situé à la position de psDAS maximal indiquée par le mesurage précédent de balayage-zoom. Il est également acceptable de développer le balayage-zoom pendant le mesurage tant que le cube 1 g ou 10 g touche le bord du volume de balayage-zoom.

4) Si le balayage-zoom mesuré comme cela est indiqué dans les précédents alinéas satisfait à i) et ii) ou si le psDAS est inférieur à 0,1 W/kg, aucun mesurage supplémentaire n'est nécessaire.

IECNORM.COM : Click to view the full PDF of IEC/IEEE 62209-1528:2020

i) La plus courte distance horizontale entre les pics de DAS local et tous les points 3 dB sous le pic de DAS doit être supérieure aux pas de grille horizontaux dans les directions x et y- (Δx, Δy). Cela doit être vérifié pour le plan de balayage-zoom mesuré conforme au fantôme à une distance z_{M1}. La distance minimale doit être consignée dans le rapport d'essai de DAS.

ii) Le rapport du DAS au second point de mesure (M2) sur le DAS au point mesuré le plus proche (M1) à l'emplacement x-y de la valeur de DAS maximale mesurée doit être d'au moins 30 % (Figure 20). Le rapport (en %) doit être consigné dans le rapport d'essai de DAS.

NOTE 1 L'évaluation du balayage-zoom est en général effectuée par le postprocesseur, par interpolation et extrapolation, et dans reconstruction du champ. Des distributions de DAS induit plus concentrées (pour des sources plus localisées comme des sources à couplage capacitif, par exemple) exigent une grille plus dense, de manière à pouvoir utiliser les mêmes algorithmes d'intégration et d'extrapolation pour la même incertitude d'évaluation.

NOTE 2 Le rapport minimal de 30 % est déduit de la profondeur de pénétration d'onde plane à 6 GHz.

5) Si une ou les deux étapes d) 4) i) et ii) ne sont pas respectées, le mesurage du balayage-zoom doit être répété avec une résolution plus fine tout en conservant les autres paramètres de balayage-zoom compatibles avec le Tableau 4. De nouvelles étapes de grille horizontale et verticale doivent être définies à partir de la distribution de DAS mesuré de manière à satisfaire à d) 4) i) et ii). La conformité à d) 4) i) et ii) doit être démontrée pour le nouveau balayage-zoom mesuré. La taille du balayage-zoom de résolution plus élevée et les autres paramètres du Tableau 4 doivent s'appliquer. Le point le plus proche de l'enveloppe du fantôme doit être à 2 mm au maximum des grilles nivelées et le facteur de nivelage doit être de 1,5 au maximum.

6) Il convient également de réduire le plus possible les incertitudes dues à la distorsion de champ entre la limite de milieu et l'enceinte diélectrique de la sonde, ce qui est obtenu si la distance entre la surface du fantôme et l'extrémité physique de la sonde est supérieure au diamètre de l'extrémité de la sonde. D'autres méthodes peuvent utiliser des procédures de correction pour compenser les effets de proximité de bord, qui peuvent permettre de procéder à des mesurages d'une plus grande précision à une distance inférieure à la moitié du diamètre de sonde [22]. Pour tous les points de mesure, l'angle de la sonde par rapport à la surface du fantôme doit être inférieur à 5° pour les fantômes plans et à 30° pour les fantômes de tête. Si ces angles ne peuvent pas être atteints, une évaluation d'incertitude supplémentaire est exigée (voir l'Article O.3).

e) Utiliser les procédures de post-traitement (c'est-à-dire l'interpolation et l'extrapolation) définies en 7.5 pour déterminer les valeurs de psDAS.

f) Mesurer le DAS local exactement au même emplacement de point d'essai que celui de l'étape a). L'écart de DAS du DUT peut être évalué par la différence entre les deux valeurs de DAS local mesurées en a) et f). Voir 7.4.3 pour plus d'informations relatives au traitement de la dérive de mesure du DAS.

IECNORM.COM : Click to view the full PDF of IEC/IEEE 62209-1528:2020

Tableau 3 – Paramètres de balayage de surface

Paramètre	Fréquence d'émission du DUT soumis à l'essai	
	$f \leq 3$ GHz	3 GHz < $f \leq 10$ GHz
Distance maximale entre les points mesurés (centre géométrique des capteurs) et la surface interne du fantôme (z_{M1} de la Figure 20 en mm)	5 ± 1	$\delta \ln(2)/2 \pm 0{,}5$ [a]
Espacement maximal entre des points de mesure adjacents, en mm (voir O.8.3.1)[b]	20 ou la moitié de la longueur de balayage-zoom correspondante, suivant la valeur la plus faible	$60/f$ ou la moitié de la longueur de balayage-zoom correspondante, suivant la valeur la plus faible
Angle maximal entre l'axe de sonde et la normale de la surface du fantôme (α de la Figure 20)[c]	5° (fantôme plan uniquement) 30° (autres fantômes)	5° (fantôme plan uniquement) 20° (autres fantômes)
Tolérance d'angle de sonde	1°	1°

[a] δ est la profondeur de pénétration pour une onde plane incidente perpendiculairement sur un demi-espace planaire.

[b] Voir l'Article O.8 sur la façon dont Δx et Δy peuvent être choisies pour les exigences individuelles de balayage de surface.

[c] L'angle de sonde par rapport à la normale de la surface du fantôme est limité en raison de la dégradation de l'exactitude de mesure dans des champs avec des gradients spatiaux prononcés. L'exactitude de mesure diminue lorsque l'angle de sonde et la fréquence augmentent. C'est pourquoi la restriction d'angle de sonde est plus stricte à des fréquences au-dessus de 3 GHz.

Tableau 4 – Paramètres de balayage-zoom

Paramètre	Fréquence d'émission du DUT soumis à l'essai	
	$f \leq 3$ GHz	3 GHz < $f \leq 10$ GHz
Distance maximale entre les points mesurés les plus proches et la surface du fantôme (z_{M1} de la Figure 20 et du Tableau 3, en mm)	5	$\delta \ln(2)/2$ [a]
Angle maximal entre l'axe de sonde et la normale de la surface du fantôme (α de la Figure 20)	5° (fantôme plan uniquement) 30° (autres fantômes)	5° (fantôme plan uniquement) 20° (autres fantômes)
Espacement maximal entre des points mesurés dans les directions x et y (Δx et Δy, en mm)	8	$24/f$ [b]
Pour les grilles uniformes: Espacement maximal entre des points mesurés dans la direction perpendiculaire à l'enveloppe du fantôme (Δz_1 de la Figure 20, en mm)	5	$10/(f - 1)$
Pour les grilles nivelées: Espacement maximal entre les deux points mesurés les plus proches dans la direction perpendiculaire à l'enveloppe du fantôme (Δz_1 de la Figure 20, en mm)	4	$12/f$
Pour les grilles nivelées: Augmentation incrémentielle maximale de l'espacement entre les points mesurés dans la direction perpendiculaire à l'enveloppe du fantôme ($R_z = \Delta z_2/\Delta z_1$ de la Figure 20)	1,5	1,5
Longueur d'arête minimale du volume de balayage-zoom dans les directions x et y (L_z de O.8.3.2, en mm)	30	22

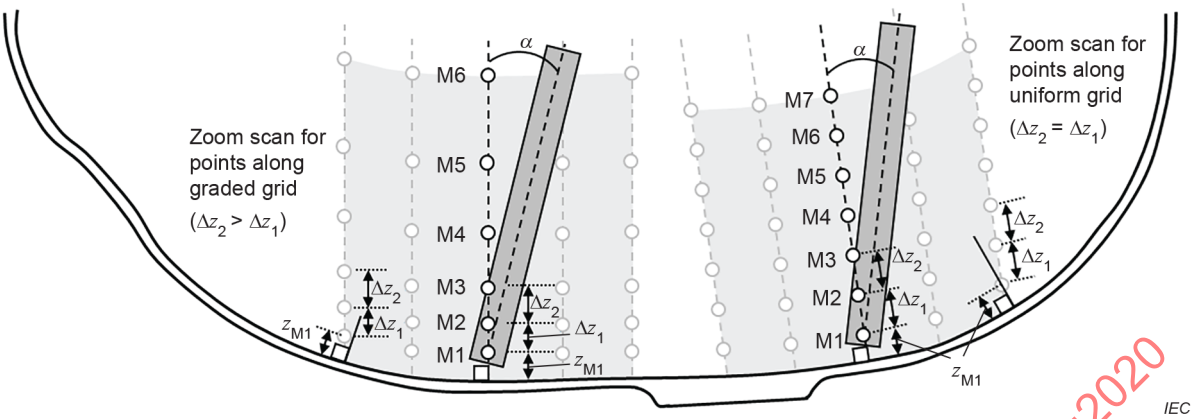
IECNORM.COM : Click to view the full PDF of IEC/IEEE 62209-1528:2020

Paramètre	Fréquence d'émission du DUT soumis à l'essai	
	$f \leq 3$ GHz	3 GHz < $f \leq 10$ GHz
Longueur d'arête minimale du volume de balayage-zoom dans la direction perpendiculaire à l'enveloppe du fantôme (L_h de O.8.3.2, en mm)	30	22
Tolérance d'angle de sonde	1°	1°

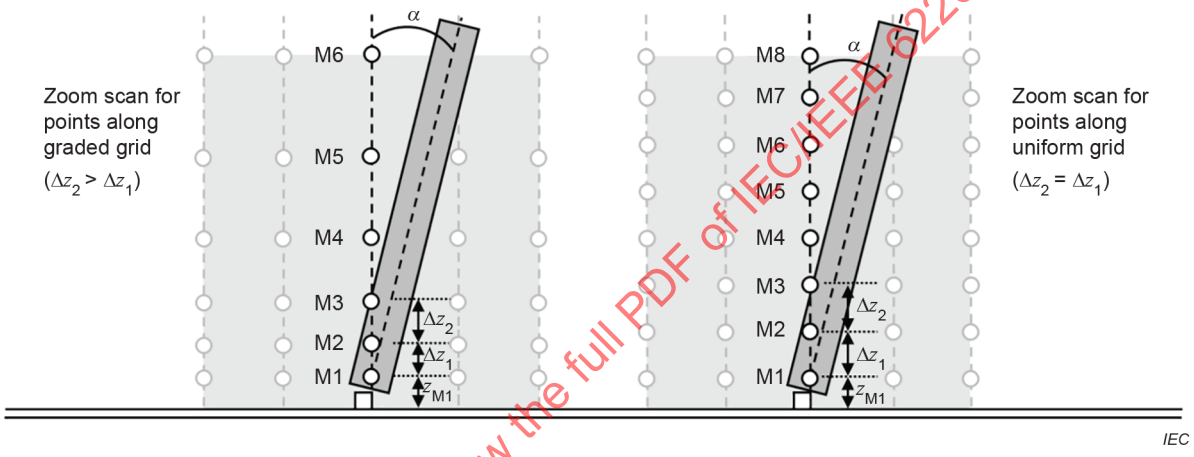
[a] δ est la profondeur de pénétration pour une onde plane incidente perpendiculairement sur un demi-espace planaire.

[b] Il s'agit de l'espacement maximal admis, qui peut ne pas être adapté dans toutes les situations.

IECNORM.COM : Click to view the full PDF of IEC/IEEE 62209-1528:2020



a) Fantôme de tête



Anglais	Français
Zoom scan for points along graded grid	Balayage-zoom des points le long de la grille nivelée
Zoom scan for points along uniform grid	Balayage-zoom des points le long de la grille uniforme

b) Fantôme plan

NOTE M1 à M8 sont des exemples de points de mesure utilisés pour l'extrapolation à la surface. Le maximum de l'angle α entre l'axe d'évaluation et la droite perpendiculaire à la surface est présenté dans le Tableau 3 et dans le Tableau 4. La distance z_{M1} est la distance entre l'enveloppe du fantôme et le premier point de mesure M1, et sa valeur maximale est indiquée dans le Tableau 3 et dans le Tableau 4. Les distances Δz_i (i = 1, 2, 3, …) sont les distances entre les points de mesure M_i et M_{i+1}. Pour des grilles uniformes, tous les Δz_i sont égaux. Pour les grilles nivelées $\Delta z_{i+1} > \Delta z_i$. Le terme $R_z = \Delta z_{i+1}/\Delta z_i$ est un rapport avec une valeur maximale indiquée dans le Tableau 4. La direction z correspond à la direction verticale, la direction x à l'horizontale et la direction y à l'horizontale dans la page.

Figure 20 – Orientation de la sonde par rapport à la droite perpendiculaire à la surface du fantôme, pour les fantômes de la tête et les fantômes plans, à deux emplacements différents

IECNORM.COM : Click to view the full PDF of IEC/IEEE 62209-1528:2020

7.4.3 Dérive

a) La dérive de mesure de DAS du DUT est prise en compte par la première étape et la dernière étape de la procédure de mesure définie en 7.4.2 en utilisant les deux méthodes suivantes.

   1) Dans la méthode préférentielle, des mesurages de DAS local sont effectués par le système de mesure de DAS avant de réaliser le balayage de surface. Un mesurage secondaire est effectué par le système au même point à l'issue du mesurage de DAS. Le mesurage est réalisé dans le milieu équivalent au tissu à un point de référence auquel les valeurs de DAS pour les premier et second mesurages doivent dépasser la limite de détection inférieure du système de mesure. La distance entre le point de référence et la surface interne du fantôme, dans la direction perpendiculaire à la surface interne du fantôme, doit être inférieure ou égale à 5 mm.

   2) Par ailleurs, et si la méthode préférentielle de a) n'est pas assez sensible, les mesurages de la puissance conduite peuvent être effectués sur le dispositif à l'accès d'antenne en utilisant un équipement capable de mesurer la puissance RF avant le placement du dispositif pour l'essai de DAS. Un second mesurage de puissance RF doit être effectué à l'issue de l'essai de DAS.

b) Pour le cas a) 1) ou a) 2), la dérive est enregistrée comme étant la différence en pourcentage entre le second mesurage de référence, $Ref_{\text{secondaire}}$ (DAS ou puissance conduite) et le premier mesurage de référence Ref_{primaire}, comme cela est décrit dans la Formule (6):

$$dérive = 100\ \% \times \frac{Ref_{\text{secondaire}} - Ref_{\text{primaire}}}{Ref_{\text{primaire}}} \tag{6}$$

   La dérive de DAS pendant le mesurage du dispositif sans fil doit être dans les limites de ±5 %. Certains dispositifs peuvent avoir des fluctuations significatives de puissance de sortie qui ne sont pas classifiables comme une dérive de puissance indésirable, mais plutôt comme une caractéristique du comportement fonctionnel normal du dispositif. Dans ce cas, d'autres méthodes telles que la mise à l'échelle de DAS doivent être envisagées pour assurer l'obtention d'un DAS exact et prudent.

c) Si la dérive de DAS ne peut pas respecter le seuil de 5 % pendant la réalisation de l'essai de DAS selon 7.4.2, un mesurage de dérive pendant le temps d'évaluation de mesure le plus long prévu doit alors être effectué sans recharger la batterie. Pour ce faire, procéder à un mesurage selon la méthode a) 1) ou a) 2), en continu pendant le temps d'évaluation (au moins une fois toutes les 5 s). Ce mesurage de balayage temporel doit être effectué pour chaque bande de fréquences pour le mode de fonctionnement ayant la puissance de sortie moyennée la plus élevée. Si la différence entre le maximum et le minimum dans le balayage temporel est inférieure à 5 % de la valeur moyenne, ou si la différence est inférieure à 10 % et si le DAS diminue principalement pendant le balayage temporel (il n'augmente pas de plus de 2 % à un moment quelconque pendant le balayage temporel), il est suffisant d'effectuer des mesurages de référence au début du balayage de surface et à la fin du dernier balayage-zoom, comme cela est décrit en 7.4.2 a) et f). Sinon, des mesurages de référence supplémentaires doivent être effectués pendant le balayage-zoom, et les mesurages de balayage-zoom doivent être corrigés avant d'effectuer l'extrapolation, l'intégration et le calcul de moyenne.

d) L'interpolation linéaire entre les mesurages de référence est réalisée avant la correction. Les valeurs de DAS mesurées pendant le balayage-zoom doivent être corrigées par la différence entre les valeurs interpolées et la première valeur de référence mesurée avant le balayage de surface. Le temps entre les mesurages de référence pendant le balayage-zoom doit être suffisamment court pour que la correction de la courbe de balayage temporel dans le précédent alinéa conduise à une mesure prudente pour tous les points.

IECNORM.COM : Click to view the full PDF of IEC/IEEE 62209-1528:2020

e) Si la dérive de DAS est inférieure ou égale à 5 %, elle peut être traitée comme une incertitude (c'est-à-dire, une erreur aléatoire) ou un décalage systématique. Si la dérive est supérieure à 5 %, la dérive de mesure doit être considérée comme un décalage systématique plutôt qu'une incertitude. Si elle est traitée comme une incertitude, la valeur absolue de la dérive est enregistrée dans le tableau d'incertitudes. De même, la dérive n'est pas ajoutée à la valeur de DAS évaluée. La valeur d'incertitude consignée dans le bilan d'incertitude doit être la valeur correspondant à la dérive de mesure la plus élevée de DAS consignée ou le maximum admis (c'est-à-dire 5 %). Si elle est traitée comme un décalage systématique, appliquer une compensation au DAS mesuré, c'est-à-dire en ajoutant la différence absolue à la valeur de DAS déterminée si la dérive est négative ou positive, comme cela est décrit dans la Formule (7):

$$DAS_{\text{compensé}} = DAS_{\text{mesuré}} \times \left(1 + \left|dérive\right| / 100\ \%\right) \quad (7)$$

Dans ce cas, il n'est pas nécessaire d'enregistrer la dérive dans le bilan d'incertitude (c'est-à-dire u_i = 0 %). Afin de maintenir une exposition prudente, les dérives ne sont pas soustraites du DAS évalué. Si différents modes de fonctionnement évalués du dispositif présentent des rapports de dérive différents, toutes les valeurs de DAS mesurées correspondantes peuvent être compensées par le même rapport, à condition que le rapport de dérive appliqué soit le plus grand détecté pendant l'essai de DAS dans tous les modes de fonctionnement du dispositif. L'incertitude doit être estimée en prenant pour hypothèse une loi de probabilité rectangulaire.

7.4.4 Mesurages de DAS de DUT avec des antennes multiples ou des émetteurs multiples

7.4.4.1 Généralités

Les DUT avec des antennes multiples ou des émetteurs multiples (avec des antennes uniques ou multiples) émettant simultanément exigent des considérations d'essai spéciales. Les méthodes pour combiner les champs afin de déterminer la distribution de DAS combinée diffèrent suivant que les émetteurs RF correspondants émettent ou non des formes d'onde qui sont corrélées ou non corrélées dans le temps. La méthode de sommation de champ et les exigences des instruments de mesure associées pour les formes d'onde de signaux corrélés sont différentes de celles applicables aux signaux non corrélés (voir l'IEC TR 62630 [1]).

Une procédure adaptée à l'évaluation du DAS dans la tête à partir d'un kit mains libres à oreillettes avec fil est décrite à l'Annexe M.

7.4.4.2 Mesurages de DAS pour des signaux non corrélés

7.4.4.2.1 Généralités

Les procédures suivantes sont applicables à des dispositifs incorporant plusieurs modes de fonctionnement destinés à fonctionner simultanément.

a) Pour les fréquences multiples (f_1, f_2, etc.) qui sont séparées par plus que la plage de fréquences valide de l'étalonnage de sonde ou du milieu équivalent au tissu, suivant celui qui est le plus faible, le DAS ne peut normalement pas être évalué simultanément en utilisant les mêmes sonde et milieu. La plage de fréquences valide de l'étalonnage de sonde est généralement étroite (par exemple ±50 MHz à ±100 MHz) pour les sondes de champ électrique dans la plupart des systèmes actuellement utilisés. De plus, les sondes de champ électrique utilisées dans les systèmes actuels ayant généralement une tension continue en sortie, elles ne peuvent pas distinguer les signaux aux différentes fréquences. La plage de fréquences valide du milieu équivalent au tissu désigne la plage de fréquences dans laquelle les propriétés diélectriques sont dans les limites de tolérance des valeurs cibles (voir le Tableau 2 et [2]). En raison de ces limitations, les valeurs de DAS doivent dans un premier temps être évaluées séparément, puis combinées de façon arithmétique.

IECNORM.COM : Click to view the full PDF of IEC/IEEE 62209-1528:2020

b) Dans le cas d'antennes multiples émettant différents modes de fonctionnement à la même fréquence, les mesurages peuvent être effectués avec des signaux émis simultanément. Cependant, cela n'est pas nécessaire si le psDAS est mesuré séparément pour chaque mode de fonctionnement, puis additionné comme cela est décrit dans la Variante 1 ci-dessous (voir 7.4.4.2.2) étant donné que cette méthode donne une exposition prudente du DAS combiné. Pour le cas d'antennes multiples émettant des signaux corrélés (par exemple, certaines configurations MIMO), voir 7.4.4.3.

c) En 7.4.4.2, une combinaison d'essai est définie comme une combinaison particulière de positions de dispositif (joue gauche, inclinaison droite, etc.), de configuration (par exemple, position d'antenne) et d'accessoire (batterie). Les paragraphes 7.4.4.2.2 à 7.4.4.2.5 spécifient d'autres procédures d'évaluation pour l'émission simultanée dans différentes bandes de fréquences. Les procédures s'appliquent également à l'émission simultanée dans la même bande de fréquences, si cela est exigé par les conditions de configuration d'essai du dispositif ou par les configurations de logiciel en mode d'essai. Les conditions préalables suivantes s'appliquent pour les méthodes alternatives.

   1) Le balayage de surface, le balayage-zoom et le psDAS sont évalués séparément à chaque fréquence (conformément à 7.4.2) avec l'émission à cette fréquence activée et l'émission aux autres fréquences désactivée.

   2) Les données de DAS de différentes fréquences ou antennes sont combinées uniquement lorsque la combinaison d'essai est la même pour les bandes de fréquences ou antennes, et si la combinaison d'essai est destinée à un fonctionnement simultané.

d) Différentes autres méthodes peuvent être utilisées pour différentes combinaisons d'essais. Les variantes sont résumées ci-dessous:

   1) Variante 1: Sommation de valeurs de psDAS – méthode la plus simple, mais la plus prudente pour déterminer la limite supérieure; toujours applicable (7.4.4.2.2).

   2) Variante 2: Sélection de la valeur de psDAS – méthode simple, applicable lorsque certaines distributions de DAS présentent peu, voire pas du tout, de chevauchement (7.4.4.2.3).

   3) Variante 3: Calcul de DAS volumétrique combiné à partir de balayages de surface et/ou balayages-zoom existants – méthode exacte et rapide; toujours applicable (7.4.4.2.4).

   4) Variante 4: Balayage volumétrique – méthode la plus exacte, toujours applicable (7.4.4.2.5).

e) Le mesurage du DUT est considéré comme satisfaisant totalement aux exigences du présent document s'il satisfait aux exigences de l'une de ces procédures d'évaluation alternatives.

f) L'incertitude selon l'Article 8 doit être évaluée et documentée dans le rapport de mesure.

L'Alternative 1 est la plus prudente et la plus simple en matière de calculs et n'exige pas de mesurage de DAS supplémentaire. La Variante 2 et la Variante 3 réduisent successivement le degré de surestimation, mais exigent plus de calcul et une plus grande analyse d'essai. La Variante 4 fournit la surestimation minimale et exige le plus d'effort.

7.4.4.2.2 Variante 1: Évaluation par sommation de valeurs de psDAS

Cette procédure est appliquée pour déterminer de manière prudente la limite supérieure du DAS combiné lorsque la même puissance de sortie maximale de chaque émetteur ou antenne est utilisée pour les émissions autonomes et simultanées. Il est à noter que les différentes valeurs sommées de psDAS peuvent être à différents emplacements spatiaux. Cette procédure est toujours applicable, et il est à noter qu'elle surestime le DAS combiné. Les procédures suivantes doivent être appliquées en utilisant des essais complets du DAS qui satisfont à toutes les exigences normatives du présent document. Les essais rapides de DAS peuvent être utilisés pour identifier les configurations d'essai de DAS les plus élevées pour chaque bande de fréquences, comme cela est spécifié en 7.9.2.

a) Pour une combinaison d'essai dans laquelle un fonctionnement simultané est prévu, ajouter les valeurs de psDAS pour chaque antenne et bande de fréquences lorsqu'un fonctionnement simultané est prévu (voir NOTE 1, NOTE 2 et NOTE 3).

IECNORM.COM : Click to view the full PDF of IEC/IEEE 62209-1528:2020

b) Vérifier si la valeur sommée de DAS maximal est dans les limites de 3 dB de la limite applicable de DAS. Si c'est le cas, veiller à ce que tous les canaux de fréquences d'essai exigés en 7.2.8 aient été mesurés dans toutes les bandes de fréquences et pour toutes les antennes pour lesquelles un fonctionnement simultané est prévu. Répéter les étapes a) et b) pour déterminer les valeurs de psDAS d'émission simultanée.

c) La valeur sommée de DAS maximal aux étapes a) et b) est le DAS combiné.

NOTE 1 La valeur de DAS pour chaque bande de fréquences correspond au canal de fréquence soumis à l'essai dans cette bande dans laquelle le psDAS mesuré est le plus élevé. En 7.2.8, le sous-ensemble approprié de fréquences à mesurer pour chaque bande de fréquences est spécifié, et les procédures de mesure à des fréquences plus faibles que ce sous-ensemble sont décrites en 7.3. Par exemple, si le DAS a été mesuré aux canaux inférieur, central et supérieur dans une bande, et si le DAS le plus élevé se trouve au canal de fréquence inférieur, le psDAS au canal de fréquence inférieur est utilisé comme valeur de DAS pour cette bande de fréquences. Si seul le DAS au canal de fréquence central a été mesuré conformément aux procédures de 7.3, le psDAS au canal de fréquence central est utilisé comme valeur de DAS pour cette bande de fréquences.

NOTE 2 Une variation acceptable de 7.4.4.2.2 a) consiste à ajouter les valeurs de psDAS les plus élevées applicables à toutes les combinaisons d'émissions simultanées, quelles que soient les conditions d'essai. Pour ce faire, le psDAS le plus élevé pour une bande de fréquences (parmi toutes les conditions d'essai dans cette bande de fréquences) est ajouté à la valeur de psDAS la plus élevée dans l'autre bande de fréquences (parmi l'ensemble des conditions d'essai), et ainsi de suite pour les autres bandes de fréquences lorsqu'un fonctionnement simultané est prévu. Chacune des combinaisons d'essai prises en considération en utilisant cette méthode est ensuite évaluée en 7.4.4.2.2 b) et c). Cette méthode est plus prudente que la méthode de 7.4.4.2.2 a).

NOTE 3 Dès lors que la configuration d'essai de DAS maximal est identifiée, il est acceptable de réaliser un balayage volumétrique sur cette configuration d'essai, selon 7.4.4.2.5, pour obtenir une estimation plus réaliste du DAS combiné maximal. Le balayage volumétrique peut être utilisé si la position d'essai et la configuration du dispositif sont identiques pour les différentes bandes de fréquences ou antennes.

7.4.4.2.3 Variante 2: Évaluation par sélection de valeurs de psDAS maximal évalué les plus élevées

Cette procédure donne une estimation du DAS combiné lorsque les distributions de balayage-zoom de DAS mesurées séparément ont peu ou pas de chevauchement. Les maxima sont ensuite séparés à un degré tel que la valeur de psDAS maximal de chaque distribution n'augmente pas de plus de 5 % lorsque les distributions de DAS de tous les autres modes de fonctionnement simultané sont ajoutées. Cette variante est applicable uniquement si le psDAS le plus élevé est inférieur à 70 % de la limite de conformité, calculée à partir des balayages-zooms à chaque fréquence. La procédure doit être appliquée en utilisant des essais complets du DAS qui satisfont à toutes les exigences normatives du présent document.

a) Mesurer le psDAS à chaque fréquence, séparément, conformément à 7.4.2. Les balayages de surface doivent être effectués dans le même plan à chaque fréquence. La distance z_{M1} pour tous les balayages de surface doit être inférieure ou égale à la valeur la plus faible de z_{M1} indiquée dans le Tableau 4 pour les fréquences d'intérêt. Le diamètre de l'extrémité de la sonde doit satisfaire aux exigences de 6.1 r) à toutes les fréquences d'intérêt, et l'étalonnage de sonde doit satisfaire aux exigences du présent document.

b) Les balayages de surface séparés doivent être interpolés de sorte que la zone de chevauchement ait la même grille. La résolution de la grille interpolée doit être d'au moins 1 mm. Déterminer la valeur de crête dans chacun des balayages de surface.

c) La zone de chevauchement doit contenir toutes les valeurs de crête de DAS.

d) Pour tous les balayages de surface mesurés, créer une distribution de DAS en ajoutant les balayages de surface interpolés spatialement (c'est-à-dire, point par point) à l'intérieur de la zone de chevauchement.

e) Si la valeur de crête dans la nouvelle distribution de DAS créée à l'étape c) ne dépasse pas les valeurs de DAS maximal les plus élevées séparées obtenues à l'étape b) de plus de 5 %, le DAS combiné est choisi comme étant la plus élevée des valeurs de psDAS séparées, calculées à partir du balayage-zoom, telles que calculées à l'Étape a).

IECNORM.COM : Click to view the full PDF of IEC/IEEE 62209-1528:2020

7.4.4.2.4 Variante 3: Évaluation par les données de DAS volumétrique calculées

Cette procédure utilise des balayages de surface et des balayages-zooms existants, en combinaison avec l'interpolation et l'extrapolation, pour la génération de données de DAS volumétrique, et est un moyen rapide d'obtention du DAS combiné. Différents algorithmes utilisés à cet effet ont été présentés en [23], [24], [25], [26] et [27]. L'incertitude de la méthode utilisée doit être bien documentée conformément aux procédures de l'Article 8 et doit être consignée. Cette méthode est toujours applicable. Cette procédure doit être appliquée en utilisant des essais complets du DAS qui satisfont à toutes les exigences normatives du présent document.

a) Pour une combinaison d'essai dans laquelle un fonctionnement simultané est prévu, calculer la distribution de DAS volumétrique sur une région correspondant au balayage de surface pour chaque bande de fréquences lorsqu'un fonctionnement simultané est prévu.

b) Ajouter les distributions de DAS volumétrique de toutes les bandes de fréquences spatialement, en utilisant l'interpolation conformément à 7.5.1. Pour chaque bande de fréquences, lorsqu'un fonctionnement simultané est prévu, cette étape doit être effectuée pour chaque canal de fréquence mesuré conformément aux exigences de 7.2.8 et aux procédures de 7.3 (voir NOTE 1 de 7.4.4.2.2).

c) Utiliser les procédures de post-traitement définies en 7.5 et à l'Annexe P pour déterminer les valeurs de psDAS à partir des distributions de DAS de l'étape b).

d) Vérifier si la valeur de psDAS maximal est dans les limites de 3 dB de la limite de conformité. Si c'est le cas, veiller à ce que tous les canaux de fréquences d'essai exigés en 7.2.8 aient été mesurés dans toutes les bandes de fréquences dans lesquelles un fonctionnement simultané est prévu, puis répéter les étapes a) à c).

7.4.4.2.5 Variante 4: Évaluation par balayage volumétrique

Cette procédure est la façon la plus exacte d'évaluer le DAS combiné et est toujours applicable. Les données de DAS sont combinées pour chaque configuration d'essai (voir 3.52) dans lesquelles une émission simultanée est prévue. Cette procédure doit être appliquée en utilisant des essais complets du DAS qui satisfont à toutes les exigences normatives du présent document.

a) Pour une combinaison d'essai dans laquelle un fonctionnement simultané est prévu, veiller à ce que le balayage-zoom ait été mesuré conformément à 7.4.2 à tous les canaux de fréquences d'essai spécifiés en 7.2.8 pour chaque bande de fréquences à laquelle un fonctionnement simultané est prévu.

b) Déterminer une grille volumétrique qui couvre les balayages-zooms aux fréquences d'essai déterminées à l'étape a) sur toutes les bandes de fréquences auxquelles un fonctionnement simultané est prévu. Si les balayages-zoom aux fréquences f_1, f_2, etc., sont éloignés à tel point que la grille volumétrique est très grande, entraînant des temps de mesure très longs, une variation acceptable consiste à identifier tous les emplacements des balayages-zooms pour chaque canal de fréquences de l'étape a), puis à appliquer la variante de procédure de l'étape c).

c) À chaque canal de fréquences déterminé à l'étape a), mesurer la grille volumétrique observée à l'étape b). Ce mesurage de grille volumétrique satisfait à toutes les exigences de 7.4.2, étapes c) et d) si ce n'est que la grille volumétrique est plus grande que le balayage-zoom. S'il a été décidé à l'étape b) d'utiliser les emplacements des balayages-zooms au lieu d'une grille volumétrique, alors à chaque canal de fréquences déterminé à l'étape a), mesurer le balayage-zoom pour les autres fréquences exactement aux mêmes emplacements que ceux des balayages-zooms précédemment mesurés à l'étape a). Le mesurage est réalisé avec le mode de fonctionnement à cette fréquence activé et les modes de fonctionnement aux autres fréquences désactivés.

IECNORM.COM : Click to view the full PDF of IEC/IEEE 62209-1528:2020

d) Ajouter les distributions de DAS obtenues à l'étape c) spatialement pour obtenir une distribution de DAS sommée. Calculer le DAS combiné maximal à partir de la distribution sommée en utilisant les procédures de post-traitement (interpolation, extrapolation et calcul de moyenne) définies en 7.5 pour déterminer le psDAS. Lorsque des balayages volumétriques sont réalisés pour chaque fréquence, ils doivent être sommés et la valeur de crête maximale est déterminée en fonction de la distribution totale. Dans le cas où seuls des balayages-zooms sont effectués à l'étape c), les balayages-zooms à chaque emplacement du maximum dans chaque bande de fréquences sont combinés et le plus élevé est identifié pour calculer le psDAS.

Il convient de fixer le DUT sur le fantôme lorsque les milieux sont modifiés de sorte que la sommation des distributions de DAS soit aussi exacte que possible. Si la batterie du dispositif nécessite d'être rechargée, le câble du chargeur doit être raccordé au DUT lorsqu'il reste positionné sur le fantôme. Le câble doit être raccordé uniquement pendant la charge de la batterie entre des mesurages de DAS et doit être détaché pendant l'essai.

7.4.4.2.6 Exemple de calcul de DAS combiné utilisant la Variante 1

Le 7.4.4.2.6 donne un exemple de l'application de la méthode de sommation des valeurs de psDAS (Variante 1). Il n'est donné qu'à titre d'illustration. Le Tableau 5 donne un exemple de DUT ayant deux antennes et quatre modes de fonctionnement, pour lequel les valeurs de psDAS pour 10 g provenant de mesurages de bande unique sont données dans la troisième colonne et la troisième ligne pour les quatre modes de fonctionnement et les antennes. Les valeurs de DAS sont indiquées dans la troisième ligne pour l'Antenne 1 et la troisième colonne pour l'Antenne 2. Les cellules en bas et à droite de ces valeurs présentent les valeurs de DAS combiné. Dans cet exemple, les cellules sans signe "–" sont les seules à être évaluées. Les quatre modes de fonctionnement sont constitués de deux modes vocaux et deux modes de données, chacun dans deux bandes de fréquences. Les valeurs de psDAS pour 10 g ont toutes été mesurées au canal central des bandes de fréquences respectives pour un fonctionnement à bande unique (un mode de fonctionnement et une antenne émettent, tandis que les autres bandes et antennes sont désactivées). Les valeurs de DAS combiné sont calculées à l'aide de l'Alternative 1 (c'est-à-dire simple sommation des valeurs de psDAS pour 10 g dans la ligne 3 et la colonne 3). Pour cet exemple, le DUT prend en charge un seul mode vocal à la fois, et un mode de données à la fois et il prend en charge l'émission simultanée de parole et de données. Par conséquent, un mode vocal n'est pas combiné avec un autre mode vocal, par exemple. De même, des mesurages de DAS sur le côté gauche de la tête ne sont pas combinés avec des mesurages de DAS sur le côté droit. Cependant, il est prévu dans cet exemple que les deux antennes puissent émettre simultanément.

Tableau 5 – Exemple de méthode pour déterminer la valeur de DAS combiné utilisant la Variante 1

Antenne 2			Antenne 1							
			Bande vocale 1		Bande vocale 2		Bande de données 1		Bande de données 2	
			Gauche	Droite	Gauche	Droite	Gauche	Droite	Gauche	Droite
			0,285	0,250	0,333	0,315	0,512	0,489	0,593	0,574
Bande vocale 1	Gauche	0,141	–	–	–	–	0,653	–	0,734	–
	Droite	0,120	–	–	–	–	–	0,609	–	0,694
Bande vocale 2	Gauche	0,131	–	–	–	–	0,643		0,724	–
	Droite	0,130	–	–	–	–	–	0,619	–	0,704
Bande de données 1	Gauche	0,220	0,505	–	0,553	–	–	–	–	–
	Droite	0,213	–	0,463	–	0,528	–	–	–	–
Bande de données 2	Gauche	0,225	0,510	–	0,558	–	–	–	–	–
	Droite	0,216	–	0,466	–	0,531	–	–	–	–

IECNORM.COM : Click to view the full PDF of IEC/IEEE 62209-1528:2020

7.4.4.3 Mesurages de DAS pour des signaux corrélés

Des DUT avec des antennes multiples émettant simultanément des signaux corrélés représentent un cas particulier de dispositifs, tels que des émetteurs MIMO avec des capacités de formation de faisceau numérique, et exigent des considérations d'essai spéciales. Les signaux de ces DUT peuvent être classés en fonction du changement de phases relatives dans une communication normale. En général, deux types de signaux peuvent être observés dans la plupart des émetteurs à plusieurs antennes de dernière génération.

Le premier type représente les signaux avec des phases relatives inchangées pendant une durée relativement longue par rapport à la durée d'un symbole. Il s'agit du Type 1 pour les besoins du présent document. Les signaux de Type 1 sont utilisés dans les systèmes d'antennes en réseau à commande de phase, dans lesquels les phases relatives des signaux envoyés aux antennes sont commandées pour former la caractéristique de rayonnement de l'antenne en réseau dans une certaine direction. Dans des environnements de fonctionnement différents, les phases relatives peuvent varier pour obtenir différentes caractéristiques de rayonnement souhaitées. Dès que la direction d'émission est déterminée et que la caractéristique est formée, les phases relatives sont fixées pendant une certaine durée, et ne varient que lorsque la caractéristique de rayonnement est configurée pour une autre forme. En fait, la durée pendant laquelle les phases relatives sont maintenues inchangées est relativement longue par rapport à la durée d'un symbole dans une communication normale.

D'autre part, le second type de signaux représente les signaux avec des phases relatives qui varient rapidement pendant une durée relativement courte. Il s'agit du Type 2 pour les besoins du présent document. Les signaux de Type 2 peuvent être observés dans les systèmes utilisant des techniques MIMO. Les phases relatives des signaux varient de symbole à symbole en raison de la fonction de code de bloc espace-temps (STBC) dans les systèmes MIMO. Les phases relatives des signaux varient de symbole à symbole selon le codage STBC, mais la formation de faisceau n'est pas utilisée au cours d'une communication normale.

Comme cela est décrit dans l'IEC TR 62630 [1], les signaux corrélés peuvent uniquement être émis à la même fréquence porteuse et le DAS dépend de la ou des phases relatives entre les signaux. Par conséquent, le psDAS ne peut pas être évalué avec exactitude en utilisant des sondes de champ E scalaires à partir d'un mesurage avec plusieurs émetteurs réglés sur des conditions de phase relative fixes si ces phases sont soumises à une variation pendant le fonctionnement normal du dispositif. En revanche, pour une évaluation exacte de DAS, des mesurages répétés correspondant à toutes les combinaisons de phases entre les émetteurs sont nécessaires. Il s'agit d'une évaluation plutôt longue et fastidieuse, qui peut ne pas être réalisable sauf si certains systèmes DAS sont utilisés, permettant des essais rapides de DAS combinés avec la commande logicielle de DUT pour le cyclage par toutes les combinaisons de phases possibles des signaux émis simultanément à leurs puissances de sortie maximales moyennées dans le temps. En général, il est également possible d'évaluer avec exactitude le psDAS de chaque émetteur individuel émettant séparément à la puissance de sortie maximale moyennée dans le temps en utilisant des mesurages de DAS individuels. Cependant, cela exige des mesurages vectoriels complexes de champ E (c'est-à-dire, des mesurages d'amplitude et de phase des trois composantes de champ E) et est par conséquent moins pratique.

L'autre méthode qui utilise des systèmes DAS conventionnels s'appuie sur des mesurages de DAS pour chaque émetteur émettant séparément à la puissance maximale de sortie moyennée dans le temps, et combine les résultats de DAS individuels comme cela est décrit dans l'IEC TR 62630 [1]. Cette approche conduit à des mesurages de DAS beaucoup plus rapides, mais ne produit qu'une limite supérieure de DAS, susceptible de surestimer les résultats. L'IEC TR 62630 [1] décrit deux méthodes de combinaison du DAS à partir de mesurages individuels en utilisant les sondes de champ E scalaires conventionnelles.

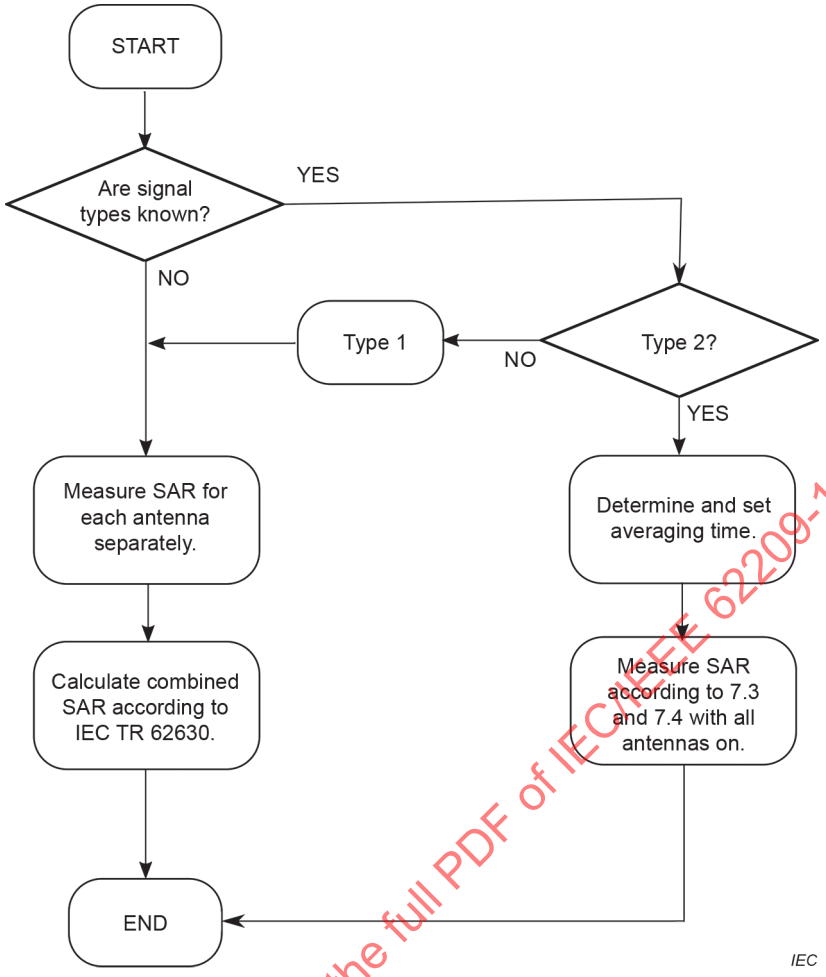
IECNORM.COM : Click to view the full PDF of IEC/IEEE 62209-1528:2020

Les deux méthodes décrites dans l'IEC TR 62630 [1] peuvent être mises en œuvre à l'aide de systèmes de mesure de DAS conventionnels et n'exigent qu'un nombre limité de balayages de DAS égal au nombre d'émetteurs. La première méthode repose sur une combinaison des amplitudes des valeurs de champ E individuelles, et la seconde sur les amplitudes des composantes de champ E individuelles. En particulier pour les signaux de Type 1 ou les signaux non spécifiés, il convient d'utiliser la seconde approche reposant sur la combinaison de composantes de champ E individuelles, car elle conduit à un degré moindre de surestimation potentielle de DAS et de nombreux systèmes DAS produisent aisément les données d'entrée exigées pour le post-traitement décrit en [1]. La procédure de mesure pour les différents types de signaux corrélés est décrite à la Figure 21. Pour les signaux de Type 2, il convient d'utiliser l'approche des mesurages de DAS moyenné dans le temps (voir NOTE), qui exige uniquement d'utiliser la procédure de mesure définie en 7.4, avec l'utilisation de sondes scalaires conventionnelles.

NOTE Une autre méthode consiste à mesurer le DAS moyenné dans le temps dans une certaine période d'intégration en utilisant les systèmes de mesure de DAS scalaires conventionnels. Cette méthode peut s'appliquer uniquement aux dispositifs générant des signaux corrélés de Type 2. Une propriété de signal part du principe que la combinaison de phases relatives qui génère le DAS maximal ne se produit pas souvent, et même lorsque c'est le cas, elle se produit pendant très peu de temps avant d'être dominée par d'autres combinaisons qui produisent un DAS inférieur. Étant donné que le DAS est déterminé par l'énergie électromagnétique (EM) absorbée par le milieu équivalent au tissu exposé, l'utilisation de la procédure de calcul de moyenne convient à l'évaluation de DAS dans ces champs électromagnétiques à fluctuations rapides. Pour évaluer le DAS moyenné dans le temps de ces dispositifs, toutes les antennes d'émission sont activées en même temps dans le cadre d'une communication normale, et les valeurs de DAS instantané sont mesurées à chaque point de mesure avec un intervalle de temps d'échantillonnage et sont moyennées sur une durée appropriée pour capturer les caractéristiques des signaux.

Cette méthode présente l'avantage d'utiliser des sondes DAS scalaires conventionnelles et, en outre, fournit un DAS mesuré qui est proche du DAS réel. Cette méthode n'exige également qu'un seul mesurage de moyenne temporelle à chaque point de mesure conformément à la procédure de 7.4, quel que soit le nombre d'antennes d'émission. Cependant, le temps d'intégration pour le système à plusieurs antennes est plus long que celui du système classique d'antenne d'émission unique. De même, lorsque le nombre d'antennes augmente, le temps d'intégration est légèrement plus long pour obtenir un DAS convergent, du fait de la fluctuation dans le temps du DAS instantané avec l'augmentation du nombre d'antennes. Le temps d'intégration dépend également de la fréquence d'échantillonnage des sondes des systèmes de mesure de DAS. Il se réduit au fur et à mesure que la fréquence d'échantillonnage augmente, et inversement. Par exemple, pour un système de mesure de DAS avec une cadence de mesure de 1 250 échantillons par seconde, le temps d'intégration de 1 s conduit à ce que l'écart type des valeurs de DAS instantané en raison d'antennes d'émission multiples soit maintenu au-dessous de 2 %. Dans un tel cas, l'incertitude de mesure totale est évaluée à l'aide de valeurs classiques et du bilan d'incertitude présenté à l'Article 8, le niveau d'incertitude pour plusieurs antennes d'émission est similaire à celui des systèmes d'antenne unique (généralement à 8,7 %).

IECNORM.COM : Click to view the full PDF of IEC/IEEE 62209-1528:2020



Anglais	Français
START	DÉBUT
Are signal types known?	Les types de signaux sont-ils connus?
YES	OUI
NO	NON
Type 1	Type 1
NO	NON
Type 2?	Type 2 ?
YES	OUI
Measure SAR for each antenna separately.	Mesurer le DAS de chaque antenne séparément.
Determine et set the average time	Déterminer et définir le temps moyen
Calculate combined SAR according to IEC TR 62630	Calculer le DAS composé selon l'IEC TR 62630
Measure SAR according to 7.3 and 7.4 with all antennas on.	Mesurer le DAS selon 7.3 et 7.4 avec toutes les antennes activées.
END	FIN

IECNORM.COM : Click to view the full PDF of IEC/IEEE 62209-1528:2020

Figure 21 – Procédure de mesure des différents types de signaux corrélés

7.5 Post-traitement de données de mesure de DAS

7.5.1 Interpolation

La résolution de la grille de mesure n'est pas aussi fine que celle exigée par les exigences d'interpolation pour le balayage de surface et le balayage-zoom pour calculer le psDAS. L'interpolation doit être appliquée aux points de mesure. Des exemples de processus d'interpolation sont donnés à l'Annexe P.

7.5.2 Extrapolation

Les sondes de champ électrique utilisées pour mesurer le DAS sont habituellement constituées de trois dipôles orthogonaux très proches les uns des autres et placés dans un protecteur/boîtier de protection. Le point de mesure (étalonnage) est situé à quelques millimètres de l'extrémité de la sonde et ce décalage doit être pris en compte pour identifier la position du DAS mesuré. En raison des erreurs de l'effet de proximité de bord de sonde et du décalage du capteur de sonde, le DAS n'est pas mesuré à la surface du fantôme. Les points mesurés les plus proches de la surface sont extrapolés pour estimer le DAS le plus élevé à la surface du fantôme. Des exemples de processus d'extrapolation sont donnés à l'Annexe P.

7.5.3 Définition du volume d'intégration

Le volume d'intégration doit être de forme cubique avec un côté qui établit une masse de 1 g ou 10 g. La longueur du côté du cube de 1 g doit être de 10 mm, et la longueur du côté du cube de 10 g doit être de 21,5 mm. L'orientation du volume cubique est donnée à l'Annexe P.

7.5.4 Recherche des maxima

Le volume d'intégration cubique doit être déplacé dans tout le volume interpolé et extrapolé de balayage-zoom à la surface interne du fantôme à proximité du DAS local maximal, en tenant compte des considérations données à l'Annexe P. Le cube ayant le psDAS le plus élevé ne doit pas être au bord/à la périphérie du volume de balayage-zoom. Si c'est le cas, le volume de balayage-zoom doit être déplacé et les mesurages doivent être effectués à nouveau.

7.6 Considérations relatives au DAS moyenné sur une période

7.6.1 Généralités

Le 7.6 spécifie les procédures d'essai permettant d'évaluer le DAS moyenné sur une période (TPAS) lorsque le DUT utilise une commande de puissance limitée dans le temps. La période de moyennage dans le temps applicable est spécifiée dans les lignes directrices internationales (l'ICNIRP, par exemple) ou les règlements nationaux. Cette procédure d'essai est différente des procédures d'essai de DAS spécifiées en 7.4 et qui sont applicables aux DUT sans algorithme de régulation de puissance. L'évaluation du TPAS est justifiée à l'Annexe Q.

NOTE Certains règlements de DAS nationaux peuvent contenir des définitions différentes des exigences de moyennage dans le temps pour leur limite de DAS.

Une procédure et ses exigences d'évaluation du TPAS sont fournies de 7.6.3 à 7.6.7. La procédure peut être appliquée si les exigences suivantes sont satisfaites.

a) Les algorithmes de régulation de puissance du DUT ne doivent pas être modifiables ni accessibles par l'utilisateur.

b) Le fabricant du DUT doit fournir une documentation suffisante relative aux algorithmes de régulation de puissance et à leur mise en œuvre, de sorte que les mesurages permettent d'obtenir une exposition prudente.

Si les précédentes exigences ne sont pas satisfaites, le DAS doit être évalué au niveau de puissance de sortie maximale décrit en 7.4.

D'autres procédures de 7.6.2 à 7.6.7 peuvent être appliquées si cela est justifié et documenté.

IECNORM.COM : Click to view the full PDF of IEC/IEEE 62209-1528:2020

7.6.2 Puissance conduite RF

Les mesures de puissance conduite RF peuvent être utilisées pour déterminer les facteurs TX.

Les paramètres de détection de puissance, de temps d'intégration et de moyennage d'échantillon du wattmètre permettent d'être sûr que la composante d'incertitude du TPAS est dans les limites de la valeur évaluée en 7.6.8. Les mesures de puissance conduite doivent également être exactes pour le mode de fonctionnement respectif. Les relevés linéaires (milliwatt, par exemple) doivent être utilisés.

7.6.3 Paramètres de mesure du DAS moyenné sur une période pour les méthodes de mesure du DAS

7.6.3.1 Généralités

Le 7.6.3 donne les exigences de mesure du TPAS et de calcul du facteur TX pour des périodes jusqu'à six minutes.

7.6.3.2 Systèmes de DAS d'un réseau

Pour les essais rapides de DAS de Classe 2 (voir 7.9.2), le $DAS_{\text{moyenné dans le temps}}$ doit être mesuré sur une période de moyennage, et le $DAS_{\text{pleine puissance}}$ doit être mesuré sur une période suffisamment longue pour que le mesurage soit stable. Ni le DUT ni les capteurs ne doivent être déplacés pendant la période de moyennage. Le taux d'échantillonnage du mesurage doit être suffisant pour être sûr que la composante d'incertitude du TPAS est dans les limites de la valeur évaluée en 7.6.8.

7.6.3.3 Systèmes de DAS de balayage

Pour les systèmes de DAS à sonde de balayage, y compris les systèmes de DAS à sonde unique et les systèmes d'essais rapides de DAS de Classe 1 (voir 7.9.2), ce qui suit s'applique.

a) Le $DAS_{\text{pleine-puissance}}$ et le $DAS_{\text{moyenné dans le temps}}$ sont des mesurages du DAS local.

b) La sonde doit être positionnée à l'emplacement du DAS maximal à partir d'un balayage de surface réalisé selon les exigences de 7.4.2.

c) Le niveau de DAS à cet emplacement doit être supérieur au niveau de bruit.

d) La sonde ou le réseau de sondes doit être dans la même position pour les mesurages du $DAS_{\text{pleine-puissance}}$ et du $DAS_{\text{moyenné dans le temps}}$.

e) Le $DAS_{\text{moyenné dans le temps}}$ doit être mesuré sur la période définie.

f) Le $DAS_{\text{pleine-puissance}}$ doit être mesuré sur une période suffisamment longue pour obtenir un mesurage stable.

g) Le taux d'échantillonnage du mesurage doit être suffisant pour être sûr que la composante d'incertitude du TPAS est dans les limites de la valeur évaluée en 7.6.8.

7.6.4 Considérations en matière de conditions d'exposition et de position d'essai

Le TPAS doit être évalué séparément pour chaque bande de fréquences et mode de fonctionnement, sauf s'il peut être démontré que le même facteur TX peut être appliqué à plusieurs bandes de fréquences et/ou modes de fonctionnement sans fil. Deux approches sont prises en considération, selon que le dispositif est capable de détecter et de distinguer de manière fiable sa position d'usage (détecter les positions de la tête et portées près du corps en fonction de l'acheminement audio vers le récepteur téléphonique d'un dispositif pendant un appel vocal, par exemple).

IECNORM.COM : Click to view the full PDF of IEC/IEEE 62209-1528:2020

a) Si les différentes positions d'usage ne sont pas détectées et distinguées par le dispositif, le TPAS maximal parmi toutes les positions et conditions d'essai/d'utilisation applicables, y compris toutes les positions de la tête, portées près du corps et autres, est utilisé pour déterminer la conformité. Il s'agit de l'approche la plus simple et la plus prudente qui s'applique à toutes les conditions d'utilisation.

b) Sinon, les positions d'essai de DAS peuvent être regroupées comme suit.

   1) Position d'essai de la tête: Le TPAS maximal parmi toutes les positions d'essai de la tête (joue gauche, inclinaison gauche, joue droite et inclinaison droite) correspondant à des appels vocaux vers le récepteur téléphonique, est utilisé pour déterminer la conformité du DAS d'exposition de la tête.

   2) Positions portées près du corps et autres positions d'essai: Le TPAS maximal parmi toutes les positions portées près du corps et autres positions d'essai applicables, reposant sur les distances de séparation applicables pour les positions d'utilisation correspondantes, en l'absence d'appel vocal adressé au récepteur téléphonique, est utilisé pour déterminer la conformité du DAS non relatif à la tête.

7.6.5 DAS moyenné sur une période pour les émissions simultanées

La combinaison des émissions simultanées avec le TPAS se révélant complexe, les exigences suivantes s'appliquent pour déterminer le psDAS le plus élevé:

a) l'évaluation du facteur TX (7.6.6) doit être appliquée à une émission simultanée au maximum;

b) toutes les émissions simultanées, outre celles de a), doivent être évaluées à la puissance de sortie maximale;

c) le DAS combiné de tous les émetteurs simultanés doit être évalué selon 7.4.4.

7.6.6 Évaluation du facteur TX

Le facteur TX permet de mettre à l'échelle le DAS mesuré à la puissance de sortie maximale (voir 7.6.7) jusqu'au DAS moyenné sur une période. Il est appliqué séparément pour chaque mode de fonctionnement (GSM, WCDMA, LTE, 5G NR, par exemple) et pour chaque bande de fréquences applicable, sauf s'il peut être démontré que le même facteur TX peut être appliqué à plusieurs bandes de fréquences et/ou modes de fonctionnement sans fil.

La procédure suivante doit être réalisée pour déterminer les facteurs TX.

a) L'algorithme de régulation de puissance doit être en premier lieu désactivé.

b) Le DUT doit être sous le contrôle d'un ensemble d'essais de communication radio (boîte téléphonique).

c) L'ensemble d'essais de communication radio doit être réglé à une puissance TX maximale et un facteur d'utilisation à partir du DUT selon les exigences de la technologie sans fil.

d) Si un système de mesure du DAS est utilisé pour évaluer le facteur TX, le DUT doit être positionné selon 7.6.4.

e) Mesurer la puissance conduite (voir 7.6.2) ou le DAS local. La puissance conduite ou les données de DAS doivent être consignées et documentées dans le rapport de mesure. Cette valeur doit être notée $P_{\text{pleine-puissance}}$ ou $DAS_{\text{pleine puissance}}$, respectivement pour le mesurage de la puissance ou du DAS.

f) Activer l'algorithme de régulation de puissance. Vérifier que la position du DUT par rapport au fantôme est maintenue pendant cette étape.

g) Mesurer la puissance conduite ou le DAS local sur au moins la période de moyennage dans le temps. Consigner la puissance conduite moyenne ou le DAS sur la période de moyennage dans le temps. Cette valeur doit être notée $P_{\text{moyenne-temps}}$ ou $DAS_{\text{moyenne-temps}}$.

h) Le facteur TX est $P_{\text{moyenne-temps}}$ / $P_{\text{pleine-puissance}}$ ou $DAS_{\text{moyenne-temps}}$ / $DAS_{\text{pleine-puissance}}$.

IECNORM.COM : Click to view the full PDF of IEC/IEEE 62209-1528:2020

7.6.7 Mesurages de DAS

Le DAS doit être mesuré pour toutes les positions et conditions d'essai exigées spécifiées en 7.2.4. Les algorithmes de régulation de puissance dans le DUT doivent être désactivés pendant ces mesurages de DAS.

Il existe deux options de mesurage de DAS.

– Option 1: Pendant les mesurages de DAS, la puissance d'émission doit être à la valeur maximale spécifiée pour le DUT (7.2.3.1). Les facteurs TX obtenus à l'étape h) de 7.6.6 doivent être appliqués aux résultats de DAS pleine puissance maximale obtenus, c'est-à-dire être multipliés par le facteur TX. Les résultats TPAS calculés sont comparés directement à la limite de DAS applicable afin de déterminer la conformité.

– Option 2: La puissance d'émission doit être limitée au niveau de puissance moyenné sur une période $P_{\text{moyenne-temps}}$, déterminé à l'étape h) de 7.6.6, afin que le DAS mesuré corresponde au facteur TX. Si les facteurs TX sont déterminés par le mesurage de DAS local de l'étape h) de 7.6.6, et s'il est démontré que le DAS et la puissance sont évolutifs de manière linéaire pour la configuration sans fil utilisée dans le DUT (7.2.3.2), le niveau de puissance moyenné sur une période $P_{\text{moyenne-temps}}$ est déterminé en mettant à l'échelle la puissance maximale (7.2.3.1) utilisée pour établir le facteur TX. Les résultats TPAS sont comparés directement à la limite de DAS applicable afin de déterminer la conformité.

7.6.8 Incertitude dans les évaluations de TPAS

L'incertitude liée au calcul du TPAS doit être évaluée conformément aux recommandations générales de l'Article 8, et documentée dans le rapport de mesure.

L'incertitude supplémentaire liée à l'évaluation du TPAS est due au taux d'échantillonnage du mesurage. L'incertitude du TPAS peut être ignorée en fonction de la méthode choisie pour déterminer le facteur TX (c'est-à-dire l'utilisation des mesurages de DAS (7.6.3) ou des mesurages de la puissance conduite (7.6.2)).

L'incertitude du TPAS est différente de l'incertitude de modulation de signal (MOD) et des erreurs d'acquisition de données (DAE) spécifiées en 8.4.

Si l'incertitude composée de la méthode de mesure de DAS et du calcul moyenné dans le temps (fondée sur le DAS ou sur la puissance conduite) dépasse la limite d'incertitude supérieure spécifiée dans le présent document, un facteur de mise à l'échelle ($U_{\text{TPAS}} - U_{\text{DAS}}$) doit être appliqué au résultat de mesure, où U_{TPAS} est l'incertitude de l'évaluation de TPAS et U_{DAS} l'incertitude des mesurages de DAS à pleine puissance et au cycle de service maximal. Les informations détaillées relatives au calcul de l'incertitude doivent être obtenues auprès du fabricant du système de mesure.

7.7 Considérations relatives aux capteurs de proximité

7.7.1 Généralités

Les capteurs de proximité sont utilisés pour réduire la puissance de sortie du DUT en fonction de la distance par rapport aux utilisateurs et aux objets proches. Si le dispositif fonctionne à une distance plus proche que la distance de déclenchement du capteur de proximité, la puissance de sortie maximale d'un DUT est réduite pour assurer la conformité du DAS. À des distances plus éloignées que la distance de déclenchement du capteur, le capteur de proximité est désactivé et la puissance de sortie maximale est rétablie. Selon la dimension de l'antenne et son emplacement, un DUT peut intégrer un ou plusieurs capteurs de proximité pour assurer la couverture du capteur.

IECNORM.COM : Click to view the full PDF of IEC/IEEE 62209-1528:2020

La procédure spécifiée en 7.7 s'applique uniquement aux capteurs de proximité conçus pour couvrir une seule antenne d'émission. Les procédures s'appliquent à un seul capteur ou à plusieurs capteurs si les réponses du capteur sont combinées de manière à assurer un déclenchement unique et sans condition. La procédure ne concerne pas plusieurs capteurs qui déclenchent plusieurs antennes. Toutefois, elle peut être appliquée séparément pour plusieurs antennes, à condition que chaque antenne se déclenche séparément.

NOTE 1 La procédure n'est pas destinée au déclenchement sous condition pour différentes conditions d'utilisation. La procédure ne couvre pas non plus une émission simultanée.

NOTE 2 La procédure spécifiée en 7.7 s'applique uniquement à la réduction de puissance en une seule étape avec une distance de déclenchement du capteur de proximité. Si une réduction de puissance en plusieurs étapes est appliquée à l'aide de plusieurs distances de séparation, les autorités de réglementation peuvent être consultées pour déterminer les procédures et exigences d'essai.

NOTE 3 La procédure spécifiée en 7.7 a été établie pour les dispositifs utilisés près du corps, si le fantôme plan est applicable pour les essais de DAS. La procédure ne tient pas compte des cas d'essai sur la tête ou les fantômes spécifiques à l'application décrits à l'Annexe K, dans lesquels des modifications des contours du corps exigent des considérations d'essai plus complexes pour valider les caractéristiques de fonctionnement du capteur de proximité.

NOTE 4 En règle générale, les DUT permettent d'assurer que, si le capteur de proximité n'est pas fonctionnel, il passe par défaut à la puissance de sortie réduite.

Le 7.7 doit être utilisé pour déterminer la distance de déclenchement et la zone de couverture des capteurs de proximité pour assurer que:

a) la réduction de puissance est déclenchée de manière cohérence et fiable à la distance spécifiée entre le DUT et l'utilisateur (7.7.2);

b) le capteur de proximité couvre une zone ou région suffisante autour de l'emplacement du DAS maximal pour assurer un déclenchement cohérent à partir de toutes les orientations de DUT applicables par rapport à l'utilisateur (7.7.3);

c) la distance de séparation d'essai pour l'essai de DAS à pleine puissance est déterminée. Il s'agit de la distance de déclenchement la plus petite pour l'orientation perpendiculaire du DUT (7.7.2.2) et de la distance de déclenchement pour l'orientation inclinée du DUT (7.7.2.3) moins 1 mm. L'espacement moins 1 mm est en général exigé pour assurer que toutes les unités de production sont conformes. Si une plus grande variation de production est prévue dans la distance de déclenchement, elle doit être prise en compte en conséquence.

d) tout effet d'hystérèse dans la distance de déclenchement est pris en considération.

Les procédures doivent être réalisées pour toutes les antennes mettant en œuvre une réduction de puissance par capteur de proximité. Chaque paramètre de sensibilité du capteur de proximité mis en œuvre doit être soumis à l'essai une seule fois dans l'une des combinaisons correspondantes de mode de fonctionnement et de bande de fréquences. Si les paramètres de sensibilité du capteur de proximité mis en œuvre ne sont pas connus, les procédures doivent être réalisées pour toutes les combinaisons de mode de fonctionnement et de bande de fréquences.

Les capteurs capacitifs sont en général utilisés pour la détection de proximité. La présence d'objets proches au voisinage du capteur peut être détectée par des variations de capacité du capteur. En fonction de la dimension de l'antenne et de l'étendue de la distribution de DAS, au moins un capteur peut être exigé pour assurer une couverture adéquate pour la distribution de DAS correspondante. Les procédures de détermination de la couverture du capteur sont spécifiées en 7.7.3.

NOTE 5 Les capteurs de proximité peuvent utiliser des techniques autres que la détection capacitive. Les procédures de 7.7 ont été rédigées pour des capteurs capacitifs uniquement, qui doivent être adaptées ou peuvent se révéler inadaptées aux essais autres que les technologies de détection. Selon le cas, les autorités de réglementation peuvent être consultées afin de déterminer les exigences d'essai et de validation pour d'autres techniques de détection.

IECNORM.COM : Click to view the full PDF of IEC/IEEE 62209-1528:2020

7.7.2 Procédures de détermination des distances de déclenchement du capteur de proximité

7.7.2.1 Généralités

Les capteurs de proximité sont en général intégrés sur des surfaces planes ou sur les bords d'un dispositif où se trouve l'antenne, de sorte que le déclenchement de la réduction de puissance de sortie puisse opportunément limiter le DAS. Les procédures de 7.7.2 permettent de satisfaire aux exigences suivantes.

a) La distance de déclenchement minimale doit être déterminée et utilisée pour établir une distance de séparation d'essai pour les mesurages de conformité du DAS à pleine puissance, lorsque la réduction de puissance est inactive.

b) La distance de déclenchement minimale doit tenir compte des variations dues à l'hystérèse et aux variations dans les unités de production dues aux tolérances de mise en œuvre.

c) Pour les capteurs se trouvant sur les bords d'un dispositif, la distance de déclenchement minimale doit couvrir les différents angles et orientations du bord par rapport à l'utilisateur afin de déterminer la distance de séparation d'essai pour le mesurage de DAS.

d) Tous les capteurs de proximité dans le DUT doivent être soumis à l'essai dans les conditions d'utilisation réelle, comme si le dispositif était utilisé par l'utilisateur, y compris plusieurs capteurs de proximité utilisés pour couvrir une distribution de DAS élargie d'une antenne. Toutes les interactions entre les capteurs de proximité doivent être prises en compte pendant l'essai.

e) Si des capteurs de proximité sont exigés pour couvrir différentes conditions d'utilisation (des capteurs qui s'enroulent sur le bord d'un dispositif pour prendre en charge la détection des bords et des surfaces, par exemple), toutes les conditions d'utilisation applicables doivent être soumises à l'essai.

f) Chaque antenne déclenchée pour diminuer sa puissance de sortie doit être soumise à l'essai séparément. Les procédures doivent être réalisées pour toutes les combinaisons de mode de fonctionnement et de bande de fréquences qui s'appliquent à l'antenne.

g) Les fantômes et milieux équivalents aux tissus spécifiés dans le présent document doivent être utilisés pour déterminer la distance de déclenchement minimale du capteur. Les propriétés diélectriques du milieu équivalent au tissu doivent être dans les limites des tolérances spécifiées dans le Tableau 2 dans la bande de fréquences à l'étude pour chaque essai de capteur de proximité.

h) La puissance de sortie maximale pleine et réduite correspondant aux conditions de déclenchement activées et désactivées doit être vérifiée. Cela peut être réalisé à l'aide d'un logiciel d'essai intégré, en mesurant la puissance conduite ou en mesurant la puissance rayonnée. Si un logiciel d'essai est utilisé pour identifier le déclenchement, la puissance conduite ou rayonnée doit être mesurée séparément pour vérifier les niveaux de puissance réels. Il est préférable de mesurer la puissance conduite plutôt que la puissance rayonnée.

i) Si la puissance conduite est mesurée, les pertes des câbles RF doivent être prises en compte pour vérifier la puissance maximale exigée pour le mesurage de DAS dans les états de déclenchement correspondants.

j) Si la puissance rayonnée est mesurée, les niveaux de puissance de sortie maximale pour les conditions de déclenchement doivent être identifiés sans équivoque en tenant compte des effets de la propagation RF et des perturbations environnementales. Le DAS local à l'emplacement du DAS maximal peut être enregistré pour identifier la variation de condition de déclenchement liée au changement de stade dans la puissance de sortie du dispositif. Le DAS local mesuré peut être corrélé au même emplacement que le mesurage de conformité du DAS à 1 g ou 10 g.

k) Tous les câbles et connecteurs utilisés pour mesurer la puissance conduite doivent être configurés et positionnés de manière à ne perturber ni les caractéristiques de détection de proximité ni les niveaux et distributions de DAS (pour le DAS local) comparés à des situations sans câbles et connecteurs.

l) Le rapport d'essai de DAS doit contenir des données tabulaires de la puissance de sortie mesurée et des états du capteur en fonction de la distance entre les DUT et le fantôme.

IECNORM.COM : Click to view the full PDF of IEC/IEEE 62209-1528:2020

7.7.2.2 Distance de déclenchement pour l'orientation perpendiculaire du DUT

La procédure de détermination de la distance de déclenchement des capteurs de proximité (un seul capteur de proximité ou une combinaison de capteurs tel que cela est spécifié en 7.7.2.1) intégrés sur une surface plane ou sur le bord d'un dispositif et approchant le fantôme (utilisateur) de manière perpendiculaire est présentée en 7.7.2.2. La variation de distance de déclenchement due à des orientations inclinées du DUT est couverte en 7.7.2.3.

Pour une approche normale du DUT au fantôme, la procédure est la suivante.

a) Chaque antenne du DUT qui exige une détection de proximité doit être soumise à l'essai dans les bandes de fréquences applicables à l'aide d'un fantôme plan spécifié en 6.2.4.

b) La surface ou le bord du DUT qui contient le capteur doit être positionné perpendiculairement au fantôme plan, à une distance initiale inférieure à 10 mm au-delà de la distance de déclenchement du capteur de proximité.

NOTE Cette procédure de distance de déclenchement s'applique uniquement aux mesurages de DAS dans un fantôme plan. En règle générale, elle ne s'applique pas au fantôme SAM ou à d'autres conditions d'utilisation du dispositif tenu en main.

c) La surface ou le bord du DUT doit être déplacé vers le fantôme par incréments de 5 mm tant que la puissance de sortie maximale n'est pas réduite.

d) La surface ou le bord du DUT doit être éloigné du fantôme par incréments d'au moins 5 mm tant que la puissance de sortie maximale n'est pas revenue à son niveau maximal.

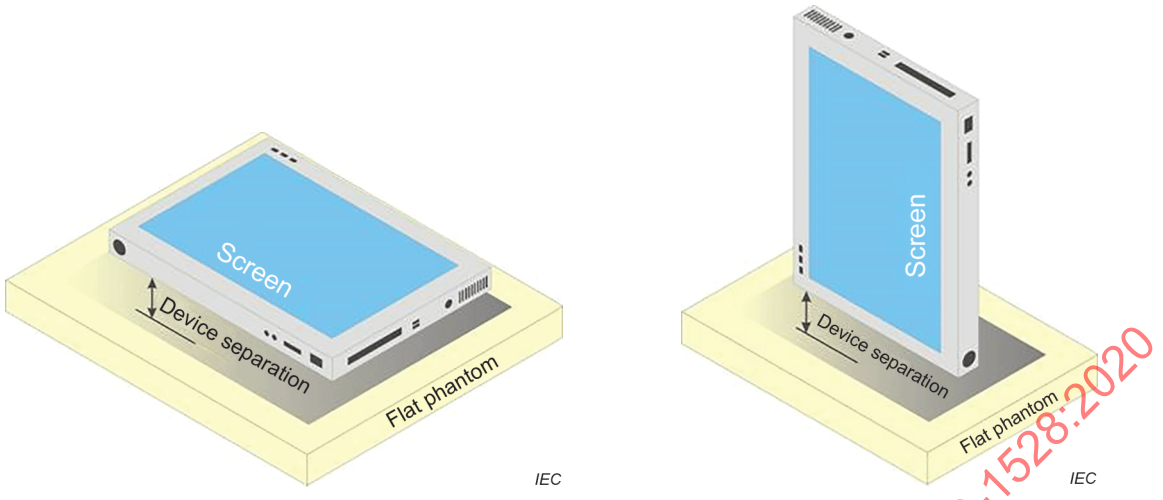
e) La surface ou le bord du DUT doit de nouveau être déplacé vers le fantôme, mais par incréments de 1 mm tant qu'il n'a pas dépassé le point de déclenchement d'au moins 5 mm ou qu'il n'est pas entré en contact avec le fantôme.

f) Si le DUT ne touche pas le fantôme, il doit être déplacé par incréments de 3 mm tant qu'il ne touche pas le fantôme, afin de confirmer que le capteur reste actif et que la puissance maximale reste réduite.

g) Le DUT doit être éloigné du fantôme selon les mêmes incréments que ceux indiqués de c) à f) afin de déterminer la distance à laquelle le déclenchement se termine. Il convient que le mouvement se poursuive jusqu'à au moins 50 mm au-delà du point qui déclenche le retour de la puissance maximale normale.

h) La plus petite distance de séparation déterminée par la procédure de déclenchement du capteur avec des mouvements d'approche et d'éloignement par rapport au fantôme doit être la distance de déclenchement minimale pour un mouvement perpendiculaire de la surface ou du bord correspondant vers l'utilisateur.

IECNORM.COM : Click to view the full PDF of IEC/IEEE 62209-1528:2020



Anglais	Français
Device separation	Séparation de dispositif
Screen	Écran
Flat phantom	Fantôme plan

Figure 22 – Positionnement des surfaces et des bords du DUT pour déterminer la distance de déclenchement du capteur de proximité

7.7.2.3 Distance de déclenchement pour une orientation inclinée du DUT

Pour les capteurs placés sur le bord d'un dispositif, outre le déclenchement perpendiculaire, l'influence du bord du DUT sur la distance de déclenchement doit également être évaluée en positionnant le bord du dispositif selon différents angles par rapport à la perpendiculaire du fantôme (Figure 22). La procédure de détermination des variations de déclenchement dues au bord d'un dispositif orienté selon différents angles par rapport au fantôme est la suivante.

a) Positionner le bord du DUT à la distance de déclenchement minimale déterminée en 7.7.2.2.

b) Vérifier que le capteur de proximité se déclenche lorsque le DUT est dans l'orientation perpendiculaire spécifiée en 7.7.2.2.

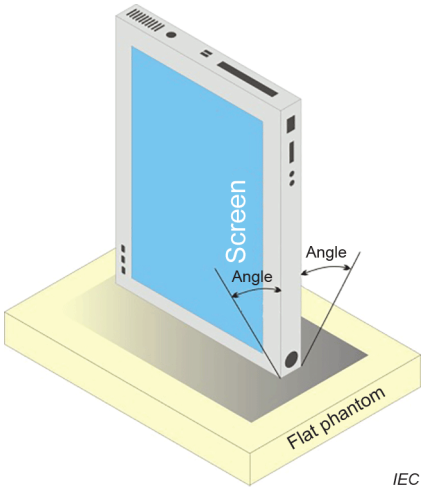
c) Faire pivoter le DUT comme cela est indiqué à la Figure 23. L'angle doit varier de ±40° par rapport à l'orientation perpendiculaire et par incréments de 10°. À chacun de ces angles, vérifier que le capteur de proximité est toujours déclenché.

d) Réduire de 1 mm la distance de bord par rapport au fantôme et revenir à l'étape b) si le déclenchement du capteur est terminé ou si la puissance de sortie maximale normale est rétablie à celle de l'étape c).

e) La plus petite distance de séparation déterminée à l'étape a) et à l'étape b) est la distance de déclenchement du capteur pour des conditions de déclenchement de bord non perpendiculaire.

f) La plus petite distance de déclenchement déterminée pour le bord dans les conditions perpendiculaires et de pivotement doit être la distance de déclenchement minimale pour ce bord.

IECNORM.COM : Click to view the full PDF of IEC/IEEE 62209-1528:2020



Anglais	Français
Screen	Écran
Flat phantom	Fantôme plan

Figure 23 – Positionnement des bords du DUT pour déterminer les variations de distance de déclenchement du capteur de proximité avec le bord positionné selon différents angles par rapport à la position perpendiculaire

7.7.3 Procédure de détermination de la zone de couverture du capteur de proximité

Cette procédure permet de vérifier que la zone de couverture des capteurs de proximité contient le cube psDAS applicable. Cela permet d'assurer que le capteur se déclenche de manière adaptée en fonction du DAS enregistré au niveau de puissance réduite.

Les capteurs de proximité couvrent une zone ou une région autour de l'emplacement du DAS maximal associé à la distribution de DAS d'une antenne. En fonction de la mise en œuvre, le capteur peut partager l'espace avec l'antenne ou en être décalé spatialement.

Les surfaces ou les bords sur lesquels l'essai de zone de couverture du capteur est réalisé sont déterminés comme suit.

– Toutes les surfaces et tous les bords qui exigent une détection de proximité pour déclencher la réduction de puissance doivent être soumis à l'essai, sauf si l'antenne et le capteur partagent l'espace avec le cube psDAS.
– Deux bords du DUT doivent être soumis à l'essai si le capteur ou l'antenne concernée se trouve à moins de 50 mm du coin des deux bords adjacents et si l'essai des deux bords est exigé (7.2.4.1).

NOTE Cette distance de 50 mm est considérée comme étant suffisamment éloignée du coin pour que le bord adjacent n'ait aucun impact sur l'antenne/le capteur. Elle correspond également à la taille classique des parties significatives de la distribution de DAS pour des antennes dans des dispositifs pour lesquels la procédure présentée en 7.7.3 a été développée.

Si la procédure de détermination de la zone de couverture du capteur est modifiée (c'est-à-dire que la procédure est inadéquate en raison de problèmes liés au placement de l'antenne, à l'étendue de la distribution de DAS ou au décalage du capteur), toutes les modifications doivent être documentées.

Selon la distribution de DAS de l'antenne et le décalage du capteur, si la réduction de la distance de déclenchement élargit la zone de couverture pour inclure l'emplacement du DAS maximal, la plus petite distance de déclenchement peut être prise en considération pour éviter des problèmes de couverture du capteur.

IECNORM.COM : Click to view the full PDF of IEC/IEEE 62209-1528:2020

L'essai de la zone de couverture du capteur de proximité est le suivant.

a) Orienter le DUT pour que la surface ou le bord applicable (déterminé ci-dessus) entre en contact avec le fantôme plan. Aligner le grand axe de la surface ou du bord du DUT sur le grand axe du fantôme.

b) Éloigner le DUT du fantôme d'au moins la distance de déclenchement déterminée en 7.7.2.2. La surface ou le bord doit être maintenu parallèle à l'enveloppe du fantôme plan.

c) Établir la position initiale du DUT en déplaçant le DUT de manière latérale par rapport au fantôme tant que l'antenne et le capteur de proximité ne sont pas hors du périmètre du fantôme. La surface ou le bord doit être maintenu parallèle à l'enveloppe du fantôme plan. Si l'emplacement précis de l'antenne ou du capteur de proximité n'est pas connu, vérifier que de toute la surface ou tout le bord est hors du périmètre du fantôme.

d) Vérifier que le capteur de proximité ne se déclenche pas dans la position initiale du DUT. Si c'est le cas, contrôler le montage pour vérifier que d'autres objets aux alentours ne déclenchent pas le capteur de proximité.

e) Déplacer le DUT de manière latérale par rapport au fantôme tant que le capteur de proximité ne se déclenche pas. La surface ou le bord doit être maintenu parallèle à l'enveloppe du fantôme plan. Enregistrer cet emplacement du DUT par rapport au bord du fantôme.

f) Faire pivoter le DUT de 90°. L'axe de rotation est perpendiculaire à la surface du fantôme plan.

g) Remettre le DUT dans la position initiale de l'étape c).

h) Répéter l'étape d) et l'étape e). Enregistrer l'emplacement du DUT lorsque le capteur de proximité se déclenche.

i) Répéter l'étape f), l'étape g) et l'étape h) pour que le déclenchement soit soumis à l'essai à des orientations de 0°, 90°, 180° et 270° de la surface ou du bord applicable. Quatre emplacements de DUT (un pour chaque orientation) sont enregistrés.

j) Déterminer la zone de couverture comme étant la région se trouvant entre les quatre emplacements de DUT enregistrés ci-dessus.

k) Déterminer l'emplacement du psDAS par rapport à la surface ou au bord du DUT.

   Vérifier que le cube psDAS se trouve intégralement dans les limites de la zone de couverture. Si ce n'est pas le cas, l'essai de DAS à puissance réduite de 7.7.4 ne doit pas être réalisé sans justification supplémentaire.

7.7.4 Procédures de mesure de DAS impliquant des capteurs de proximité

Deux niveaux de puissance de sortie maximale différents sont appliqués en fonction des conditions de déclenchement du capteur de proximité. Le DAS doit être mesuré pour les deux combinaisons différentes de l'état de puissance de sortie et de distance d'essai.

a) Pleine puissance: Les essais de DAS doivent être réalisés à la distance de séparation d'essai correspondant à la distance de déclenchement minimale du capteur parmi tous les essais de déclenchement et de couverture de 7.7, moins 1 mm, comme cela est spécifié en 7.7.2 et en 7.7.3.

b) Puissance réduite: Les essais de DAS doivent être réalisés à la distance d'utilisation prévue la plus proche ou à la distance la plus proche exigée par l'autorité de réglementation.

Les mesurages de DAS à ces deux combinaisons de puissance et de distance suffisent à assurer la conformité aux conditions d'utilisation exigeant une détection de proximité et une réduction puissance au dispositif applicable en fonction de la distance de l'utilisateur.

Les photos du montage d'essai, le mesurage de puissance exigé et les résultats de la distance de déclenchement, pour la prise en charge du déclenchement du capteur et de la couverture du capteur, doivent être documentés dans le rapport de mesure.

IECNORM.COM : Click to view the full PDF of IEC/IEEE 62209-1528:2020

7.8 Correction de DAS pour les écarts de permittivité complexe par rapport aux cibles

7.8.1 Généralités

Dans le présent document, les propriétés diélectriques du milieu équivalent au tissu utilisées pour le mesurage du DAS sont choisies afin de donner une exposition prudente. Les écarts des propriétés diélectriques par rapport aux valeurs cibles peuvent conduire à une incertitude de mesure. Une manière de réduire l'incertitude de mesure consiste à conserver les propriétés diélectriques des milieux équivalent au tissu dans une tolérance serrée des cibles (par exemple, de l'ordre de ±5 %). Cependant, il peut s'avérer difficile de trouver des formulations de liquides adaptées et stables dont les propriétés diélectriques sont proches des cibles, en particulier à des fréquences supérieures à 2 GHz. Voici trois solutions permettant de remédier à ce problème:

a) en modifiant les paramètres propriétés cibles pour qu'ils correspondent à celles des formulations disponibles;

b) en élargissant la tolérance (sans corriger le DAS compte tenu de l'écart des propriétés diélectriques)

c) en élargissant la tolérance et en corrigeant la valeur de DAS compte tenu de l'écart des propriétés diélectriques mesurées par rapport aux valeurs cibles.

La troisième solution est la meilleure parce que la modification des cibles restreint l'applicabilité du document à des formulations particulières, et parce que le simple élargissement de la tolérance augmente l'incertitude de mesure.

La méthodologie utilisée pour déterminer la correction du DAS est décrite en 7.8.2. La méthodologie a été appliquée sur une plage de fréquences comprise entre 4 MHz et 10 GHz. Elle a également été étudiée pour des plages de permittivité et de conductivité de ±20 % par rapport aux valeurs cibles indiquées dans le Tableau 2, mais des plages de ±10 % ont été choisies pour le présent document, comme cela est spécifié ci-dessous. Étant donné que la modification des propriétés diélectriques influence le facteur de conversion de la sonde, cette influence est faible si une plage de ±10 % est utilisée.

7.8.2 Formule de correction du DAS

À partir des publications de Douglas et al. ([28], [29]), une relation linéaire a été identifiée entre la variation de pourcentage du DAS (désigné ΔDAS) et la variation de pourcentage de la permittivité et de la conductivité par rapport aux valeurs cibles indiquées dans le Tableau 2 ($\Delta\varepsilon_r$ et $\Delta\sigma$, respectivement). Cette relation linéaire concorde avec les résultats de Kuster et Balzano [30] et ceux de Bit-Babik et al. [31]. La relation est donnée par:

$$\Delta DAS = c_\varepsilon \Delta\varepsilon_r + c_\sigma \Delta\sigma \tag{8}$$

où

c_ε = $\partial(\Delta DAS)/\partial(\Delta\varepsilon)$ est le coefficient représentant la sensibilité du DAS à la permittivité lorsque le DAS est normalisé à la puissance de sortie;

c_σ = $\partial(\Delta DAS)/\partial(\Delta\sigma)$ est le coefficient représentant la sensibilité du DAS à la conductivité lorsque le DAS est normalisé à la puissance de sortie.

Les valeurs de c_ε et c_σ ont une relation simple avec la fréquence, qui peut être décrite par des équations polynomiales. Pour les antennes doublets à des fréquences comprises entre 4 MHz et 6 GHz, les valeurs de DAS moyen sur 1 g c_ε et c_σ sont données par

$$c_\varepsilon = -7{,}854\times10^{-4} f^3 + 9{,}402\times10^{-3} f^2 - 2{,}742\times10^{-2} f - 0{,}202\,6 \tag{9}$$

IECNORM.COM : Click to view the full PDF of IEC/IEEE 62209-1528:2020

$$c_\sigma = 9{,}804\times10^{-3} f^3 - 8{,}661\times10^{-2} f^2 + 2{,}981\times10^{-2} f + 0{,}782\ 9 \quad (10)$$

où f est la fréquence en GHz. Au-dessus de 6 GHz, la sensibilité est invariable avec la fréquence en raison d'une faible profondeur de pénétration. Les valeurs de c_ε = −0,198 et c_σ = 0 doivent être utilisées.

Pour des fréquences comprises entre 4 MHz et 6 GHz, le DAS moyen sur 10 g c_ε et c_σ est donné par:

$$c_\varepsilon = 3{,}456\times10^{-3} f^3 - 3{,}531\times10^{-2} f^2 + 7{,}675\times10^{-2} f - 0{,}186\ 0 \quad (11)$$

$$c_\sigma = 4{,}479\times10^{-3} f^3 - 1{,}586\times10^{-2} f^2 - 0{,}197\ 2 f + 0{,}771\ 7 \quad (12)$$

où f est la fréquence en GHz. Au-dessus de 6 GHz, la sensibilité est invariable avec la fréquence en raison d'une faible profondeur de pénétration. Les valeurs de c_ε = −0,250 et c_σ = 0 doivent être utilisées. Pour des antennes et fréquences spécifiques, la procédure de O.9.5 peut être appliquée afin de déterminer les coefficients de sensibilité, selon le cas.

7.8.3 Incertitude de la formule de correction

L'incertitude de puissance moyenne des formules données en 7.8.2, définie dans Douglas et al. [28] comme l'erreur quadratique entre l'écart de DAS prédit par les formules et l'écart simulé sur 440 cas analysés, est indiquée dans le Tableau 6 pour le psDAS sur 1 g et le psDAS sur 10 g. Le Tableau 6 indique l'accroissement de l'erreur de puissance moyenne à mesure qu'augmente la valeur maximale admissible de $\Delta\varepsilon_r$ et $\Delta\sigma$. [28] indique également que ces corrections sont valables pour des modèles de DUT combinés réalistes.

Avec cette approche, l'incertitude de mesure est moins grande, étant donné que cette correction élimine le besoin en éléments d'incertitude qui expliquent l'écart des propriétés diélectriques par rapport aux cibles. Au lieu de cela, il existe un élément d'incertitude qui représente l'erreur de la formule de correction. La valeur de cet élément d'incertitude est indiquée dans le Tableau 6. Pour un écart de permittivité et de conductivité de ±10 %, entrer respectivement 1,9 % et 1,6 % dans le bilan d'incertitude pour le psDAS moyen sur 1 g et 10 g. Il convient que ces valeurs d'incertitude soient enregistrées dans la ligne appropriée du Tableau 9, en partant de l'hypothèse d'une distribution de probabilité normale.

Tableau 6 – Formule de correction du DAS d'erreur quadratique en fonction de la variation maximale de permittivité et de conductivité [28]

Variation max. de ε_r ou σ	Incertitude quadratique du DAS_{1g} %	Incertitude quadratique du DAS_{10g} %
±5 %	1,2	0,97
±10 %	1,9	1,6

IECNORM.COM : Click to view the full PDF of IEC/IEEE 62209-1528:2020

7.9 Réduction le plus possible de la durée d'essai

7.9.1 Généralités

Le 7.9 donne des méthodes de réduction le plus possible de la durée d'essai afin d'identifier un sous-ensemble des conditions de DAS le plus élevé pour un DUT. L'essai complet du DAS, c'est-à-dire l'essai satisfaisant totalement aux exigences de 7.4 du présent document, doit être réalisé pour le sous-ensemble des configurations de dispositif identifiées comme ayant les valeurs de DAS définies par ces essais. L'une des deux méthodes de réduction de la durée globale de l'essai d'un DUT peut être utilisée:

a) les méthodes de réduction d'essai dans lesquelles un ensemble de règles est appliqué afin de réduire le nombre total de configurations de dispositif qui exigent de procéder aux essais spécifiés en 7.9.3;

b) l'essai rapide de DAS qui réduit la durée de mesure pour chaque configuration de dispositif, comme cela est spécifié en 7.9.2.

Les méthodes de réduction d'essai ne doivent pas être utilisées conjointement avec l'essai rapide de DAS.

NOTE Des études sont en cours pour une future révision du présent document afin de vérifier si les méthodes de réduction d'essai et l'essai rapide de DAS peuvent être utilisés conjointement, tout en garantissant le caractère prudent du DAS consigné.

7.9.2 Essai rapide de DAS

7.9.2.1 Généralités

L'essai complet du DAS utilise des systèmes et procédures de mesure satisfaisant parfaitement aux exigences du présent document et appelés systèmes de "DAS complet" (voir également 3.20). Les procédures décrites en 7.9.2 s'appliquent aux essais rapides de DAS. L'essai rapide de DAS diffère de l'essai complet de DAS en ce sens qu'il utilise des techniques, méthodes ou algorithmes spéciaux ou différents équipements de mesure qui ne satisfont pas à toutes les exigences normatives du présent document, mais qui diminuent la durée de mesure (voir également 3.17).

L'essai rapide de DAS peut être utilisé conjointement avec l'essai complet du DAS pour réduire la durée de mesure nécessaire à l'évaluation d'un dispositif de communication sans fil. L'essai rapide de DAS peut être utilisé pour identifier les configurations d'essai de DAS le plus élevé, et donc pour évaluer les niveaux de DAS relatifs. L'essai complet du DAS doit être utilisé pour évaluer les niveaux de DAS absolu. L'essai complet du DAS doit être réalisé sur au moins la configuration d'essai de DAS le plus élevé et celles dans les niveaux de confiance donnés dans les procédures spécifiées en 7.9.2.2 et 7.9.2.3.

NOTE 1 Ces autres essais ne sont pas obligatoires. L'utilisateur du présent document reste libre d'appliquer la procédure d'essai complet du DAS spécifiée de 7.1 à 7.5 pour tous les essais.

L'essai rapide de DAS n'entre pas dans la catégorie des méthodes de réduction d'essai (voir 7.9.3). En règle générale, l'essai rapide de DAS a pour objectif de diminuer le temps passé au mesurage, alors que les méthodes de réduction d'essai visent à réduire le nombre total de mesurages à réaliser.

Compte tenu du temps moindre nécessaire pour procéder à l'essai rapide de DAS, il peut être prévu d'utiliser plusieurs méthodes d'essai rapide de DAS à l'aide d'une seule charge de batterie lors de l'essai d'un dispositif. Les exigences de 7.4.3 doivent être satisfaites en ce qui concerne la fluctuation de puissance restant dans les limites de ±5 % de la valeur moyenne tout au long de l'intervalle de mesure.

Les procédures suivantes ne concernent pas toutes les formes d'évaluations de DAS d'un émetteur multiple. Un essai complet du DAS supplémentaire peut s'avérer nécessaire pour satisfaire aux exigences de 7.4.4.

IECNORM.COM : Click to view the full PDF of IEC/IEEE 62209-1528:2020

Deux classes d'essai rapide de DAS sont désignées pour les besoins du présent document.

a) Classe 1: Il s'agit de méthodes d'essai rapide de DAS reposant sur des mesurages réalisés avec un équipement conforme à tous les articles normatifs du présent document, mais où des techniques spéciales sont appliquées afin d'améliorer la vitesse de mesure, par exemple en mesurant des nombres réduits de points, puis en utilisant un post-traitement supplémentaire. L'essai rapide de DAS de Classe 1 s'appuie sur les exigences de balayage et de post-traitement de la méthode individuelle d'essai rapide de DAS utilisée pour réduire la durée de mesure, mais avec une exactitude moindre ou une incertitude de mesure plus importante que pour l'essai complet de DAS. L'incertitude de mesure doit être déterminée selon l'Article 8 et l'Annexe C, et doit être documentée. Chaque méthode individuelle d'essai rapide de DAS doit être intégralement validée afin de déterminer son applicabilité pour soumettre à l'essai différents dispositifs de communication sans fil, comme cela est spécifié en A.4.2. La plage de fréquences valide, les distributions de DAS et les niveaux de DAS applicables pour la méthode d'essai rapide de DAS doivent être documentés, comme cela est décrit en A.4.2. Les utilisateurs d'une méthode d'essai rapide de DAS doivent effectuer un contrôle du système pour démontrer la fiabilité et la cohérence de la méthode, comme cela est décrit en A.4.3.

b) Classe 2: Il s'agit de méthodes d'essai rapide de DAS reposant sur des mesurages réalisés avec des équipements qui ne sont pas conformes à tous les articles normatifs du présent document. Les systèmes de balayage ou les systèmes matriciels qui utilisent des algorithmes de reconstruction de champ entrent dans cette classe. Les systèmes d'essai rapide de DAS de Classe 2 doivent satisfaire à toutes les exigences de vérification et de validation du système de mesure du DAS de l'IEC 62209-3, si ce n'est que l'incertitude de mesure n'est pas limitée à un seuil de 30 %, et que la validation et la vérification du système peuvent également être réduites aux plages des modes de fonctionnement et des fréquences soumises à l'essai. Utilisé conjointement avec la Procédure A de mesure rapide de DAS (voir 7.9.2.3), l'essai rapide de DAS de Classe 2 peut avantageusement identifier les configurations d'essai de DAS le plus élevé qui doivent ensuite être mesurées avec un essai complet du DAS pour évaluer le DAS maximal qui se produit dans la tête ou le corps (pour les besoins de la démonstration de conformité, par exemple). Comme avec l'essai rapide de DAS de Classe 1, les systèmes d'essai rapide de DAS de Classe 2 doivent être étalonnés et intégralement validés afin de déterminer leur applicabilité pour soumettre à l'essai différents dispositifs de communication sans fil pour des technologies de communication, conditions d'exposition et configurations de dispositif spécifiques évalués pour le DAS. L'incertitude de mesure doit être déterminée et documentée (voir l'Annexe C).

Les exigences relatives aux systèmes de mesure vectorielle sont données dans l'IEC 62209-3. Il est recommandé d'appliquer ces exigences au présent document.

NOTE 2 Les techniques de reconstruction de champ sont spécifiées dans l'IEC 62209-3.

7.9.2.2 Procédure A d'essai rapide de DAS

La procédure A peut être appliquée pour déterminer le DAS maximal d'un DUT pour toutes les configurations d'essai exigées ou un sous-ensemble de ces configurations. L'essai rapide de DAS de Classe 1 et l'essai rapide de DAS de Classe 2 peuvent utiliser la Procédure A. Cette procédure doit être appliquée séparément pour les types de fantômes de tête et de corps. Pour le type de fantôme de tête, les données de la tête gauche et de la tête droite peuvent être considérées comme un seul ensemble de données. Pour le type de fantôme de corps, toutes les configurations (si plusieurs tailles de fantôme ont été utilisées, par exemple) peuvent être considérées comme un seul ensemble de données.

NOTE 1 Une étude interlaboratoire de grande ampleur a été réalisée pour évaluer la robustesse de la Procédure A d'essai rapide de DAS. Dans cette étude, prise en charge par le comité d'études 106 de l'IEC et organisée par l'ISED (Innovation, Science and Economic Development) au Canada, 10 laboratoires ont procédé à plus de 7 500 mesurages avec des essais complets de DAS et des essais rapides de DAS de Classe 1 et de Classe 2. Un résultat de l'étude a amené à la révision de la Procédure A pour améliorer son taux de réussite. Les résultats obtenus dans le cadre de cette étude ont démontré que les méthodes de Classe 1 et de Classe 2 peuvent être utilisées conjointement avec la Procédure A d'essai rapide de DAS avec un niveau de confiance très élevé, tout en réduisant considérablement la durée et les efforts nécessaires pour procéder à l'évaluation conforme d'un DUT.

La Figure 24 est un flux de travail simplifié décrivant en détail les étapes de la Procédure A.

IECNORM.COM : Click to view the full PDF of IEC/IEEE 62209-1528:2020

Afin d'augmenter sensiblement la convivialité de cette procédure et d'assurer que les étapes de la Procédure A sont bien respectées, un outil appelé Fast SAR Wizard a été développé. Le Fast SAR Wizard peut être téléchargé à l'adresse suivante:

http://www.iec.ch/dyn/www/f?p=103:227:0::::FSP_ORG_ID,FSP_LANG_ID:1303,25

Les étapes de la Procédure A sont les suivantes:

a) Utiliser l'essai rapide de DAS pour procéder aux mesurages sur un ensemble choisi de configurations d'essai (voir 3.52). Les configurations d'essai doivent être regroupées séparément dans N combinaisons de bande de fréquences et de mode de fonctionnement, chacune ayant M_i configurations d'essai. Ces valeurs d'essai rapide de DAS sont désignées $DAS_{\text{rapide},(i,j)}$ (i = 1 à N et j = 1 à M_i). Si un système d'essai rapide de DAS de Classe 1 est utilisé, il est suffisant d'inclure le canal central pour chaque configuration d'essai. Si un essai rapide de DAS de Classe 2 est utilisé, tous les canaux exigés en 7.2.8 doivent être soumis à l'essai pour chaque configuration d'essai.

b) Utiliser l'essai complet de DAS pour mesurer la configuration d'essai du DAS le plus élevé provenant de chacun des N groupes. Ces N valeurs d'essai rapide de DAS sont désignées $DAS_{\text{max,rapide},i}$ (i = 1 à N). Choisir la valeur d'essai rapide de DAS maximale $DAS_{\text{max,rapide}} = \max(DAS_{\text{max,rapide},i})$.

   Avec l'essai rapide de DAS de Classe 1, il n'est pas nécessaire de répéter le balayage de surface entier pendant l'essai complet de DAS lorsque le nombre de valeurs de crête DAS est déjà connu à partir de l'essai rapide de DAS. La méthode d'essai complet du DAS de cette étape peut utiliser une surface réduite, lorsque toutes les exigences de 7.4.2 b) et du Tableau 3 s'appliquent, si ce n'est que la surface peut être plus petite que la projection du DUT et de l'antenne. Le balayage de surface réduit doit inclure au moins le point de grille à chaque valeur de crête de DAS trouvée à l'étape a), et les huit points adjacents qui entourent chaque valeur de crête de DAS. Le balayage de surface obtenu est valable s'il identifie également les mêmes crêtes de DAS et les emplacements du maximum trouvés à l'étape a), dans les limites de tolérance de positionnement.

c) Utiliser l'essai complet de DAS pour mesurer toutes les autres configurations d'essai (i,j), au niveau du canal donnant le résultat d'essai rapide de DAS le plus élevé, lorsque la condition de la Formule (13) est satisfaite. Le deuxième alinéa de l'étape b) s'applique.

$$DAS_{\text{rapide},(i,j)} \geq DAS_{\text{max,rapide}} \times \left(B_{\text{rapide},i} - \sqrt{B_{\text{rapide},i}^2 - 1} \right) \quad (13)$$

   $B_{\text{rapide},i}$ est calculé selon la Formule (14).

$$B_{\text{rapide},i} = \frac{1}{1 - \left(1{,}64\, U_{\text{rapide},i}\right)^2} \quad (14)$$

   $U_{\text{rapide},i}$ de la Formule (14) est l'incertitude de mesure type (k = 1) des résultats d'essai rapide de DAS à la i-e combinaison de bande de fréquences et de mode de fonctionnement.

   Lorsque le système de Classe 2 est utilisé pour l'essai rapide de DAS, $U_{\text{rapide},i}$ doit être défini sur l'incertitude-type ou sur 35 %/2 = 17,5 %, selon la valeur la plus élevée. Le chiffre de 35 % repose sur l'analyse d'une étude comparative interlaboratoire de l'essai rapide de DAS réalisée en 2017.

NOTE La Formule (13) et la Formule (14) sont déduites pour un intervalle de confiance à 95 % où

$$DAS_{\text{rapide},(i,j)} \leq DAS_{\text{max,rapide},i}$$

IECNORM.COM : Click to view the full PDF of IEC/IEEE 62209-1528:2020

Cet intervalle de confiance est donné par:

$$\left(DAS_{\text{max,rapide}} - DAS_{\text{rapide},(i,j)}\right) - 1{,}64U_{\text{rapide},i}\sqrt{S^2_{\text{max,rapide}} + S^2_{\text{rapide},(i,j)}} \le 0 .$$

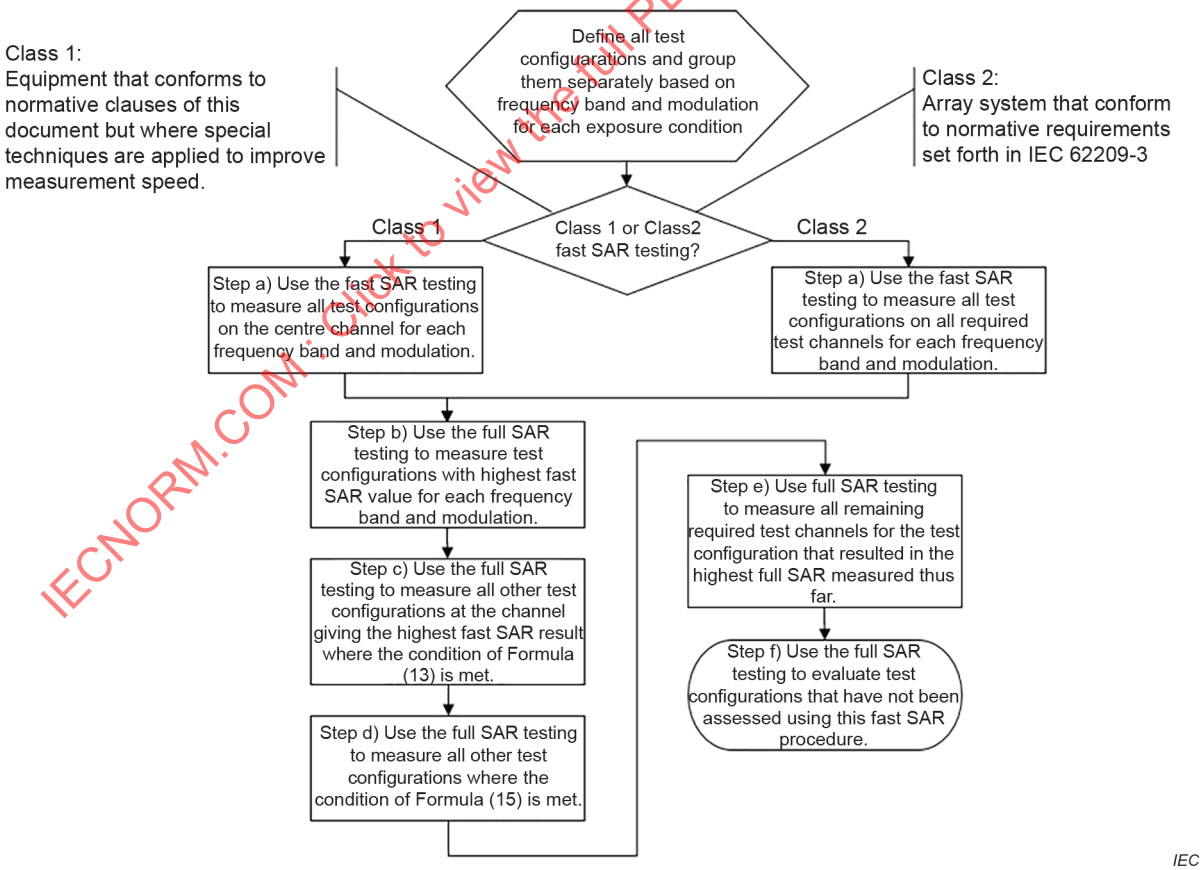
La résolution de $DAS_{\text{rapide},(i,j)}$ conduit à la Formule (13) et à la Formule (14), où $U_{\text{rapide},i}$ est l'incertitude-type et a une loi gaussienne. La valeur de 1,64 est le facteur pour un intervalle de confiance unilatéral à 95 % d'une variable aléatoire à loi gaussienne.

d) Utiliser l'essai complet de DAS pour mesurer toutes les autres configurations d'essai lorsque la condition de la Formule (15) est satisfaite. Le deuxième alinéa de l'étape b) et le dernier alinéa de l'étape c) s'appliquent.

$$DAS_{\text{rapide},(i,j)} \ge DAS_{\text{limité}} \times \left(B_{\text{rapide},i} - \sqrt{B^2_{\text{rapide},i} - 1}\right) \quad (15)$$

e) Utiliser l'essai complet de DAS pour mesurer tous les canaux exigés spécifiés en 7.2.8 sur la bande de fréquences correspondant à la configuration d'essai qui a donné le psDAS le plus élevé, $DAS_{\text{plus élevé,complet}}$ = max($DAS_{\text{complet},(i,j)}$), si cela n'a pas déjà été fait. Les exigences de balayage de surface réduit présentées à l'étape b) pour les méthodes de Classe 1 s'appliquent.

f) Utiliser l'essai complet de DAS conformément à 7.3 pour mesurer toutes les autres configurations d'essai qui n'ont pas été soumises à l'essai rapide de DAS de l'étape a) et qui ne sont pas exclues des essais par le présent document ou par les règlements applicables.



IECNORM.COM : Click to view the full PDF of IEC/IEEE 62209-1528:2020

Anglais	Français
Class 1: Equipment that conforms to normative clauses of this document but where special techniques are applied to improve measurement speed.	Classe 1: Équipements conformes à tous les articles normatifs du présent document, mais où des techniques spéciales sont appliquées afin d'améliorer la vitesse de mesure.
Define all test configurations and group them separately based on frequency band and modulation for each exposure condition	Définir toutes les configurations d'essai et les regrouper séparément en fonction de la bande de fréquences et de la modulation pour chaque condition d'exposition
Class 2: Array system that conform to normative requirements set forth in IEC 62209-3	Classe 2: Système matriciel conforme aux exigences normatives de l'IEC 62209-3
Class 1	Classe 1
Class 1 or Class 2 fast SAR testing?	Essai rapide de DAS de Classe 1 ou de Classe 2?
Class 2	Classe 2
Step a) Use the fast SAR testing to measure all test configurations on the centre channel for each frequency band and modulation.	Étape a) Utiliser les essais rapides de DAS pour mesurer toutes les configurations d'essai sur le canal central pour chaque bande de fréquences et modulation.
Step a) Use the fast SAR testing to measure all test configurations on all required test channels for each frequency band and modulation.	Étape a) Utiliser les essais rapides de DAS pour mesurer toutes les configurations d'essai sur tous les canaux d'essai exigés pour chaque bande de fréquences et modulation.
Step b) Use the full SAR testing to measure test configurations with highest fast SAR value for each frequency band and modulation.	Étape b) Utiliser les essais complets de DAS pour mesurer les configurations d'essai avec la valeur de DAS rapide le plus élevé pour chaque bande de fréquences et modulation.
Step c) Use the full SAR testing to measure all other test configurations at the channel giving the highest fast SAR result where the condition of Formula (13) is met.	Étape c) Utiliser les essais complets de DAS pour mesurer toutes les autres configurations d'essai au niveau du canal donnant le résultat rapide de DAS le plus élevé lorsque la condition de la Formule (13) est satisfaite.
Step d) Use the full SAR testing to measure all other test configurations where the condition of Formula (15) is met.	Étape d) Utiliser les essais complets de DAS pour mesurer toutes les autres configurations d'essai lorsque la condition de la Formule (15) est satisfaite.
Step e) Use the full SAR testing to measure all remaining required test channels for the test configuration that resulted in the highest full SAR measured thus far.	Étape e) Utiliser les essais complets de DAS pour mesurer tous les canaux d'essai exigés restants pour la configuration d'essai qui a donné le DAS complet le plus élevé mesuré jusqu'ici.
Step f) Use the full SAR testing to evaluate test configurations that have not been assessed using this fast SAR procedure.	Étape f) Utiliser les essais complets de DAS pour évaluer les configurations d'essai qui ne l'ont pas été en utilisant cette procédure rapide de DAS.

IECNORM.COM : Click to view the full PDF of IEC/IEEE 62209-1528:2020

Figure 24 – Procédure A de DAS rapide

7.9.2.3 Procédure B d'essai rapide de DAS

La procédure B peut être appliquée pour déterminer le DAS maximal d'un DUT pour toutes les configurations d'essai exigées ou un sous-ensemble de ces configurations. Seul l'essai rapide de DAS de Classe 1 peut utiliser la Procédure B. Cette procédure doit être appliquée séparément pour les types de fantômes de tête et de corps. Pour le type de fantôme de tête, les données de la tête gauche et de la tête droite peuvent être regroupées. Pour le type de fantôme de corps, tous les fantômes de corps (si plusieurs tailles de fantôme ont été utilisées, par exemple) peuvent être regroupés.

La Figure 25 représente un flux de travail simplifié décrivant en détail les étapes de la Procédure B.

Les étapes de la Procédure B sont les suivantes:

a) Utiliser l'essai rapide de DAS pour procéder aux mesurages sur un ensemble choisi de configurations d'essai (voir 3.52). Les configurations d'essai doivent être regroupées séparément dans N combinaisons de bande de fréquences et de mode de fonctionnement, chacune ayant M_i configurations d'essai. Ces valeurs d'essai rapide de DAS sont désignées $DAS_{\text{rapide},(i,j)}$ (i = 1 à N et j = 1 à M_i). Il est suffisant d'inclure le canal central pour chaque configuration d'essai, mais le mesurage des autres canaux d'essai exigés doit également être réalisé pour la configuration donnant le DAS le plus élevé pour chaque N groupes.

b) Utiliser l'essai complet de DAS pour mesurer la configuration d'essai du DAS le plus élevé provenant de chacun des N groupes.

c) Utiliser l'essai complet de DAS pour mesurer toutes les autres configurations d'essai (i,j), au niveau du canal donnant le résultat d'essai rapide de DAS le plus élevé, lorsque la condition de la Formule (15) est satisfaite. Ces valeurs de l'étape b) et de l'étape c) sont désignées $DAS_{\text{complet},(i,j)}$.

   L'essai complet de DAS peut être limité au canal donnant le résultat d'essai rapide de DAS le plus élevé uniquement lorsque les distributions relatives de DAS entre les canaux sont identiques. Sinon l'essai complet de DAS pour tous les canaux est exigé. Dans certains cas spécifiques (par exemple, des signaux à bande étroite), une comparaison visuelle des tracés de mesure de DAS pour différents canaux peut être appliquée pour assurer que les distributions de DAS sont identiques.

d) Pour toutes les valeurs d'essai complet de DAS de l'étape b) et de l'étape c), calculer et consigner $R_{i,j}$ selon la Formule (16):

$$R_{i,j} = \frac{DAS_{\text{rapide},(i,j)} - DAS_{\text{complet},(i,j)}}{DAS_{\text{complet},(i,j)}} \tag{16}$$

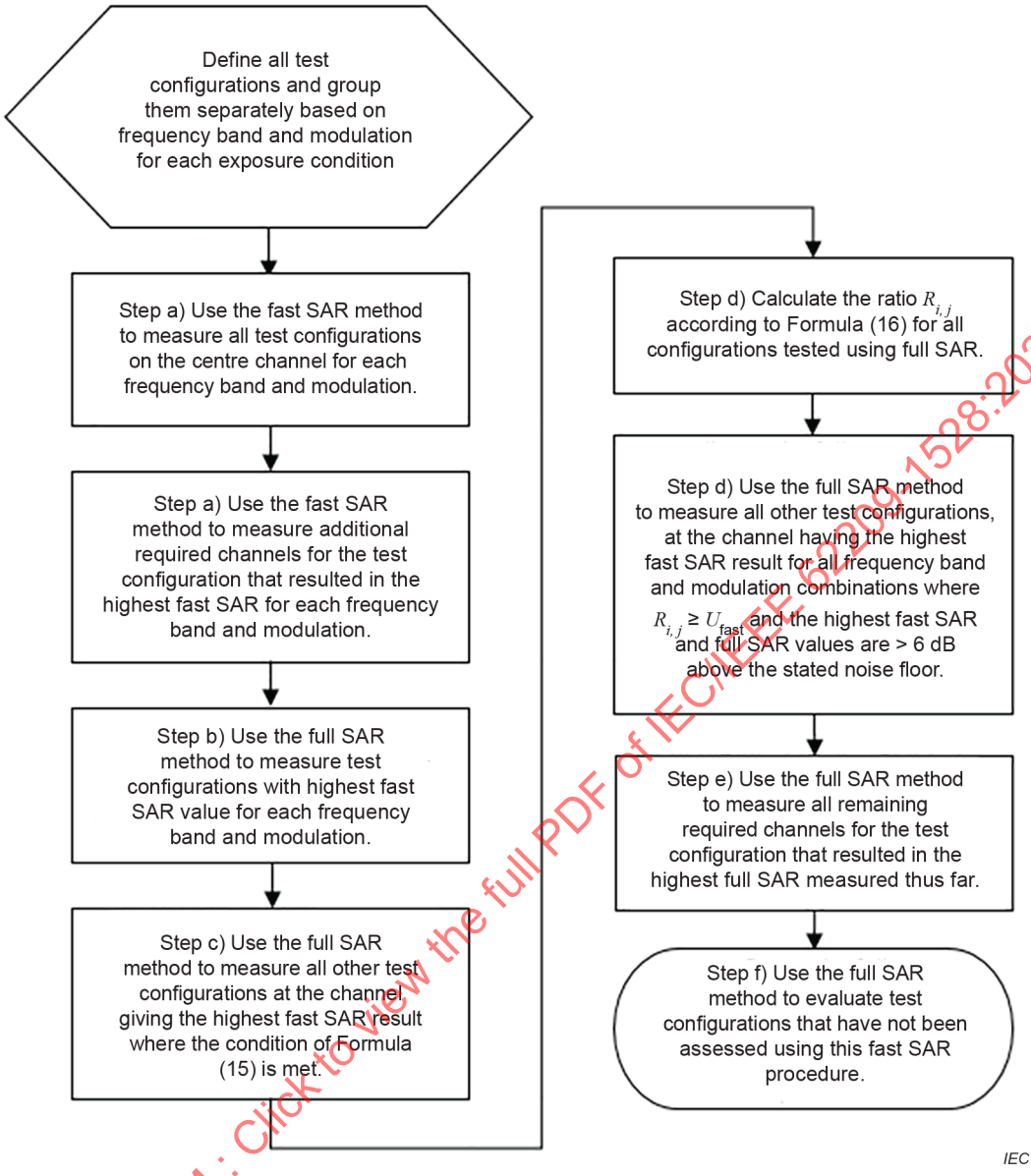
   Utiliser l'essai complet de DAS pour mesurer toutes les autres configurations d'essai, pour tous les groupes N où $R_{i,j} \geq U_{\text{rapide},i}$ et où $DAS_{\text{rapide},(i,j)}$ et $DAS_{\text{complet},(i,j)}$ les plus élevés sont d'au moins 6 dB au-dessus de leurs seuils de bruit établis. Cet essai est réalisé au niveau du canal ayant le résultat d'essai rapide de DAS le plus élevé.

   Certaines configurations d'essai peuvent avoir un seul résultat d'essai rapide de DAS disponible, qui doit être interprété comme étant le résultat le plus élevé.

e) Utiliser l'essai complet de DAS pour mesurer tous les canaux exigés spécifiés en 7.2.8 sur la bande de fréquences correspondant à la configuration d'essai qui a donné le psDAS le plus élevé, $DAS_{\text{le plus élevé,complet}} = \max[DAS_{\text{complet},(i,j)}]$, si cela n'a pas déjà été fait.

f) Utiliser l'essai complet de DAS conformément à 7.3 pour mesurer toutes les autres configurations d'essai qui n'ont pas été soumises à l'essai selon la méthode d'essai rapide de DAS de l'étape a) et de l'étape e) et qui ne sont pas exclues des essais par le présent document ou par les règlements applicables.

IECNORM.COM : Click to view the full PDF of IEC/IEEE 62209-1528:2020



Anglais	Français
Define all test configurations and group them separately based on frequency band and modulation for each exposure condition	Définir toutes les configurations d'essai et les regrouper séparément en fonction de la bande de fréquences et de la modulation pour chaque condition d'exposition
Step a) Use the fast SAR method to measure all test configurations on the centre channel for each frequency band and modulation.	Étape a) Utiliser la méthode rapide de DAS pour mesurer toutes les configurations d'essai sur le canal central pour chaque bande de fréquences et modulation.
Step a) Use the fast SAR method to measure additional required channels for the test configuration that resulted in the highest fast SAR for each frequency band and modulation.	Étape a) Utiliser la méthode rapide de DAS pour mesurer les canaux exigés supplémentaires pour la configuration d'essai qui a donné le DAS rapide le plus élevé pour chaque bande de fréquences et modulation.
Step b) Use the full SAR method to measure test configurations with highest fast SAR value for each frequency band and modulation.	Étape b) Utiliser la méthode complète de DAS pour mesurer les configurations d'essai avec la valeur de DAS rapide le plus élevé pour chaque bande de fréquences et modulation.
Step c) Use the full SAR method to measure all other test configurations at the channel giving the highest fast SAR result where the condition of Formula (15) is met.	Étape c) Utiliser la méthode complète de DAS pour mesurer toutes les autres configurations d'essai au niveau du canal donnant le résultat rapide de DAS le plus élevé lorsque la condition de la Formule (15) est satisfaite.

IECNORM.COM : Click to view the full PDF of IEC/IEEE 62209-1528:2020

Anglais	Français
Step d) Calculate the ratio $R_{i,j}$ according to Formula (16) for all configurations tested using full SAR.	Étape d) Calculer le rapport $R_{i,j}$ selon la Formule (16) pour toutes les configurations soumises à l'essai à l'aide du DAS complet.
Step d) Use the full SAR method to measure all other test configurations, at the channel having the highest fast SAR result for all frequency band and modulation combinations where $R_{i,j} \geq U_{fast}$ and the highest fast SAR and full SAR values are > 6 dB above the stated noise floor.	Étape d) Utiliser la méthode complète de DAS pour mesurer toutes les autres configurations d'essai, au niveau du canal ayant le résultat de DAS rapide le plus élevé pour toutes les combinaisons de bande de fréquences et de modulation dans lesquelles $R_{i,j} \geq U_{rapide}$ et les valeurs de DAS rapide et de DAS complet le plus élevé sont > 6 dB au-dessus du bruit de fond indiqué .
Step e) Use the full SAR method to measure all remaining required channels for the test configuration that resulted in the highest full SAR measured thus far.	Étape e) Utiliser la méthode complète de DAS pour mesurer tous les canaux exigés restants pour la configuration d'essai qui a donné le DAS complet le plus élevé mesuré jusqu'ici.
Step f) Use the full SAR method to evaluate test configurations that have not been assessed using this fast SAR procedure	Étape f) Utiliser la méthode complète de DAS pour évaluer les configurations d'essai qui ne l'ont pas été en utilisant cette procédure rapide de DAS

Figure 25 – Procédure B de DAS rapide

7.9.3 Réduction d'essai de DASs

7.9.3.1 Généralités

Le nombre d'essais de DAS exigé pour identifier la configuration donnant le psDAS maximal peut être plus important pour un DUT pouvant émettre dans plusieurs bandes de fréquences et avec différentes configurations d'utilisation. C'est également le cas si le DUT peut être utilisé avec différents accessoires. La durée de mesure totale exigée pour soumettre à l'essai un dispositif de communication personnel sans fil peut être réduite en utilisant des techniques de mesure rapides qui réduisent la durée de mesure de chaque série d'essais (selon 7.9.2) ou en réduisant directement le nombre d'essais à réaliser (selon 7.9.3). La combinaison des techniques de réduction d'essai avec les essais rapides de DAS exige d'autres investigations qui vont être prises en considération dans les versions futures du présent document. Les méthodes de réduction d'essai de DAS appliquées pendant les essais doivent être consignés comme cela est décrit en 9.2 f).

D'autres approches pour réduire le nombre d'essais sont présentées en 7.9.3. Ces approches sont:

a) réduction d'essai pour différents modes de fonctionnement à la même bande de fréquences d'essai en utilisant la même technologie sans fil;

b) réduction d'essai fondée sur les caractéristiques de conception du DUT;

c) réduction d'essai fondée sur l'analyse de niveau de DAS maximal;

d) réduction d'essai fondée sur des considérations d'émission multibande simultanée.

NOTE 1 Par exemple GSM, GPRS et EDGE (tous utilisant la modulation GMSK) sont définis comme appartenant à la même technologie sans fil, contrairement à GSM et UMTS.

NOTE 2 Les procédures de réduction d'essai de DAS décrites en 7.9.3 permettent aux utilisateurs du présent document de réduire la durée exigée pour les essais. Ces autres essais ne sont pas obligatoires.

Des informations complémentaires relatives à la réduction d'essai de DAS peuvent consultées à l'Annexe B.

IECNORM.COM : Click to view the full PDF of IEC/IEEE 62209-1528:2020

7.9.3.2 Réduction d'essai pour différents modes de fonctionnement à faible puissance dans la même bande de fréquences en utilisant la même technologie sans fil

Si différents modes de fonctionnement (mod_X, mod_Y, etc.) fonctionnent dans la même bande de fréquences, des procédures peuvent être utilisées dans certains cas pour réduire le nombre de mesurages pour les modes de fonctionnement à faible puissance (mod_Y, etc.) sans compromettre la fiabilité des essais pour évaluer le psDAS d'exposition prudente. Les procédures peuvent être appliquées si les conditions suivantes sont satisfaites.

a) Le même étage d'amplificateur RF est utilisé pour mod_X et mod_Y.

b) La même antenne est utilisée pour mod_X et mod_Y.

c) Aucune technique MIMO (entrées multiples et sorties multiples) n'est appliquée pour mod_X et mod_Y.

d) La même technologie sans fil est utilisée pour mod_X et mod_Y.

e) Soit la même modulation de signal est utilisée et cette modulation a une amplitude constante, soit la puissance de sortie moyennée de mod_Y est au moins 2 dB au-dessous de la puissance de sortie de mod_X.

f) L'étalonnage de sonde DAS est valide à la fois pour mod_X et mod_Y (c'est-à-dire que le certificat d'étalonnage de sonde définit la validité et l'incertitude de l'étalonnage applicable à la fois à mod_X et à mod_Y).

g) Le même système de mesure de DAS (sonde, fantôme, milieu équivalent au tissu et éléments électroniques) est utilisé pour soumettre à l'essai tous les modes de fonctionnement.

h) La fréquence porteuse RF de mod_X est la même que pour mod_Y.

i) Le rapport de largeur de bande de canal (R_m) de mod_X et mod_Y satisfait à la Formule (17):

$$R_m = \left| \frac{BW_{modY}}{BW_{modX}} - 1 \right| \leq 0{,}3 \tag{17}$$

Afin de réduire le nombre d'essais exigés, la procédure suivante peut être appliquée si toutes les conditions ci-dessus sont remplies:

Étape 1 Essai de tous les modes de fonctionnement (mod_X, mod_Y etc.) dans l'une quelconque des configurations d'essai normalisé (par exemple, oreille gauche, position de toucher).

Étape 2 Essai complet dans toutes les configurations d'essai normalisé du mode de fonctionnement qui a la valeur la plus élevée de DAS à l'Étape 1.

Étape 3 Essai complet dans toutes les configurations d'essai normalisé de tous les autres modes de fonctionnement évalués à l'Étape 1, pour lesquels les deux conditions suivantes s'appliquent:

- si la valeur de DAS mesurée à l'Étape 1 pour le mode de fonctionnement à l'étude est inférieure ou égale à 15 % de la valeur de DAS mesurée à l'Étape 1 du mode de fonctionnement de DAS le plus élevé (c'est-à-dire, le mode de fonctionnement choisi pour utilisation à l'Étape 2), et
- si la valeur de DAS le plus élevé à l'Étape 2 est inférieure ou égale à 15 % de la limite applicable de DAS.

La marge de 15 % correspond approximativement à la moitié de l'incertitude de mesure élargie maximale de 30 %.

IECNORM.COM : Click to view the full PDF of IEC/IEEE 62209-1528:2020

NOTE GSM et GPRS utilisent GMSK, qui est une modulation d'amplitude constante. Par conséquent, la puissance de sortie maximale moyennée par rapport au nombre maximal d'intervalles de temps utilisés dans chaque mode de fonctionnement peut être utilisée pour déterminer le mode de fonctionnement le plus prudent pour l'essai de DAS. De manière similaire, EGPRS (qui utilise GMSK et 8PSK) peut être inclus avec GSM et GPRS dans cette détermination du mode de fonctionnement le plus prudent pour l'essai de DAS, en raison de ses similarités intrinsèques avec GSM et GPRS. D'autre part, WiMAX utilise OAMRF avec un rapport puissance de crête à puissance moyenne élevé s'il est attendu que l'erreur de mesure de DAS varie avec la puissance.

7.9.3.3 Réduction d'essai fondée sur les caractéristiques de conception du DUT

Il existe une large plage de conceptions différentes de combinés sur le marché. L'analyse de données DAS de l'Article B.2 a démontré que les principes suivants de réduction et d'exclusion d'essai peuvent être appliqués à des combinés utilisés proche de la tête avec des antennes à montage interne et des fréquences de fonctionnement comprises entre 800 MHz et 2 GHz. Ces critères dépendent des emplacements d'antenne dans un DUT et des différents modèles de DUT. Une extension au-dessus de 2 GHz peut être envisagée si des données supplémentaires venant à l'appui deviennent disponibles.

Les exigences suivantes relatives à plusieurs modes de communication au sein de la même technologie sans fil et des mêmes bandes de fréquences doivent être satisfaites pour appliquer la procédure de réduction d'essai de 7.9.3.3.

a) Le même circuit RF doit être utilisé (émetteur, point d'alimentation de l'antenne, éléments d'adaptation, etc.).

b) Les mêmes antenne et mise à la terre de l'antenne doivent être utilisées.

c) Aucune technique MIMO (entrées multiples et sorties multiples) ne doit être appliquée.

d) Le même système de mesure de DAS (sonde, fantôme, milieu équivalent au tissu et éléments électroniques) doit être utilisé.

Pour un DUT avec une antenne interne montée en bas (c'est-à-dire, une antenne interne montée dans la moitié inférieure du DUT) qui est totalement incorporée à 2,5 cm au plus du bas du dispositif, lorsque le psDAS le plus élevé de la position "joue" pour une bande de fréquences et un mode de fonctionnement est au moins à 3 dB de la limite de DAS, l'essai dans la position "incliné" n'est pas exigé. Pour les autres emplacements d'antenne, lorsque le DAS mesuré en position "incliné" en utilisant le canal de DAS le plus élevé soumis à l'essai pour la position "joue" est d'au moins 3 dB inférieur à la limite de DAS, l'essai des autres canaux exigés pour la position "incliné" n'est pas exigé.

Pour appliquer une réduction d'essai supplémentaire pour le DUT en utilisant la même antenne interne montée en bas pour plusieurs modes de communication au sein de la même technologie sans fil et des mêmes bandes de fréquences, sélectionner le système de communication avec la puissance de sortie maximale moyennée la plus élevée et effectuer la procédure d'essai complet de DAS, y compris toutes les configurations et positions d'essai spécifiées en 7.3. L'essai dans des positions "incliné"s pour d'autres modes de fonctionnement au sein de cette même bande de fréquences n'est pas exigé, quel que soit le niveau de DAS en position "joue", si les deux conditions suivantes sont remplies.

- La position "joue" a la valeur de psDAS la plus élevée pour une bande de fréquences.
- Les valeurs de psDAS pour les configurations dans la position "incliné" sont au moins à 30 % au-dessous de la limite de DAS.

Le rapport de mesure de DAS doit comprendre des dessins ou des photos représentant la configuration et les emplacements d'antennes dans le DUT, et décrivant les modes de fonctionnement sans fil applicables à chaque antenne afin d'étayer la réduction et l'exclusion d'essai envisagée. Si la réduction d'essai relative à des dispositifs avec la même antenne interne montée en bas pour plusieurs modes de fonctionnement dans une même bande de fréquences doit être appliquée, l'antenne et les circuits d'adaptation RF et d'antenne doivent être décrits pour chaque mode de fonctionnement dans le rapport de mesure de DAS.

L'Article B.2 présente la justification et les informations venant à l'appui pour l'analyse effectuée pour étayer ces principes de réduction et d'exclusion d'essai.

IECNORM.COM : Click to view the full PDF of IEC/IEEE 62209-1528:2020

7.9.3.4 Réduction d'essai fondée sur l'analyse de niveau de DAS

Cette approche de réduction d'essai a pour objet d'éliminer la session de "balayage-zoom" pour chaque mesurage individuel (7.4.2 d)) lorsque le DAS maximal mesuré à partir du "balayage de surface" est au-dessous d'un seuil, en veillant à ce que la valeur de psDAS maximal soit:

- correctement évaluée et pas sous-estimée, en particulier si elle peut générer un psDAS proche de la limite de conformité applicable;
- correctement identifiée, même si la session de "balayage-zoom" n'est pas exécutée.

NOTE Cette procédure de réduction d'essai est différente de la procédure d'essai rapide de DAS décrite en 7.9.2. Dans ce protocole de réduction d'essai, la décision d'appliquer la procédure d'essai complet du DAS est prise après avoir examiné les valeurs mesurées à partir du balayage de surface (pas le psDAS final). De plus, une valeur de seuil est nécessaire étant donné que l'objectif est d'éviter le balayage-zoom pour des configurations de mesure particulières et de ne pas dépendre d'un algorithme d'essai rapide de DAS particulier pour estimer le psDAS.

La justification et les études soutenant cette approche de réduction d'essai sont indiquées à l'Article B.4.

Lors de l'application du protocole décrit ci-dessous, il est nécessaire:

– d'ajuster les paramètres de "balayage de surface" spécifiés dans le Tableau 3 afin d'utiliser un espacement de grille ne dépassant pas 10 mm;

– d'effectuer les balayages de surface à une distance maximale fixe de 4 mm entre les points mesurés (centre géométrique des capteurs) et la surface interne du fantôme.

Le protocole de réduction d'essai monobande (valable pour chaque mode de fonctionnement pris en charge par le DUT) est décrit ci-dessous.

a) Mesurer le DAS local comme cela est décrit en 7.4.2 a).

b) Effectuer la procédure de balayage de surface pour l'une des positions définies en 7.4.2, au niveau du canal de la bande à l'étude ayant la puissance de sortie assignée la plus élevée, comme cela est indiqué dans le schéma de mesure complet décrit en 7.4.2.

c) Déterminer le DAS local maximal du balayage de surface. Celui-ci est défini comme étant le psDAS absolu (APS).

d) Effectuer le balayage-zoom, comme cela est indiqué dans le schéma de mesure complet décrit en 7.4.2.

e) Procéder au post-traitement pour déterminer le psDAS, comme cela est indiqué en 7.4.2 e).

f) Mesurer le DAS local et évaluer la dérive de mesure comme cela est indiqué en 7.4.2 f).

g) Pour toutes les autres positions et tous les autres canaux de fréquences à soumettre à l'essai, répéter les étapes 1) à 5) suivantes.

   1) Mesurer le DAS local comme cela est décrit en 7.4.2 a).

   2) Procéder au balayage de surface comme cela est indiqué dans le schéma de mesure complet décrit en 7.4.2 b).

   3) Évaluer le DAS local maximal du balayage de surface. Si cette valeur est supérieure à l'APS, l'APS doit alors être attribué au DAS maximal du balayage de surface, après exécution de l'Étape 4).

   4) Effectuer le balayage-zoom exigé par 7.4.2 si le DAS maximal de balayage de surface n'est pas inférieur à 1,3 W/kg (80 % de 1,6 W/kg) ou si le DAS maximal est supérieur ou égal à $TH(f) \times APS$, où la valeur de seuil $TH(f)$ qui dépend de la fréquence est définie dans le Tableau 7 et APS est le psDAS absolu. S'il est exigé de mesurer des valeurs de crête multiples (comme cela est décrit en 7.4.2 c)), appliquer cette étape à toutes les valeurs de crête.

   5) Procéder au post-traitement pour déterminer le psDAS, comme cela est indiqué en 7.4.2 e).

   6) Évaluer la dérive de mesure comme cela est indiqué en 7.4.2 f). Si la dérive est supérieure à 5 %, elle doit être traitée comme cela est indiqué en 7.4.2 f).

IECNORM.COM : Click to view the full PDF of IEC/IEEE 62209-1528:2020

h) L'Étape g) doit être effectuée de façon séquentielle pour toutes les bandes applicables. Les valeurs de seuil qui dépendent de la fréquence utilisée à l'Étape g) 4) sont résumées dans le Tableau 7.

i) Si la procédure de réduction'essai de 7.9.3.4 est suivie:

   1) Le schéma de principe à gauche de la Figure 19 doit être appliqué.

   2) Le schéma de principe à droite de la Figure 19 ne doit être appliqué que pour le premier mesurage de DAS. Des mesurages de DAS ultérieurs doivent être effectués selon la Figure 26, qui est une modification de la procédure décrite à la Figure 19.

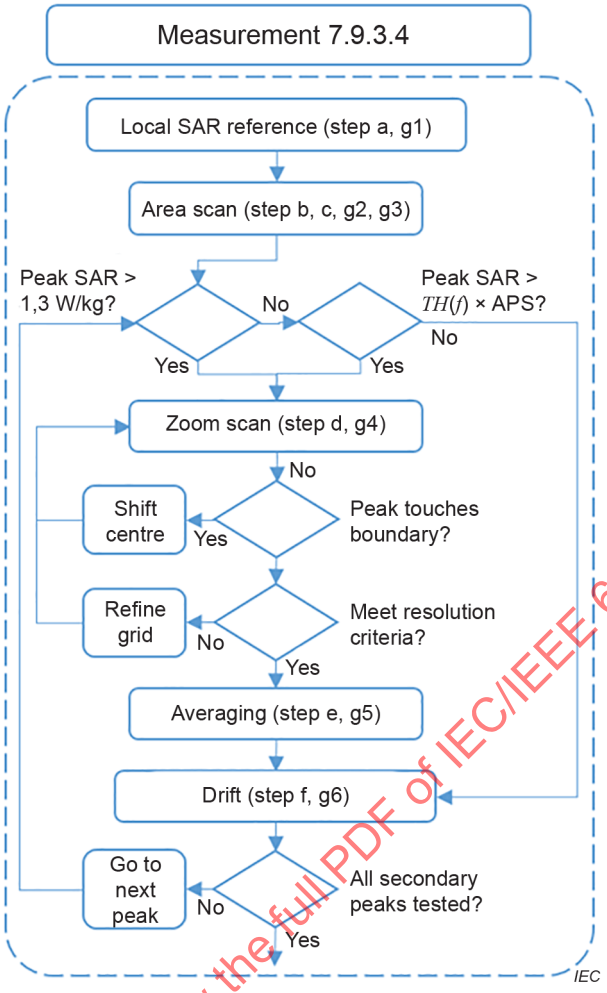
L'Article B.4 présente la justification des niveaux de seuil utilisés dans le présent protocole de réduction d'essai, fondé sur l'analyse spatiale du gradient de DAS.

Tableau 7 – Valeurs de seuil $TH(f)$ utilisées dans le protocole de réduction d'essai proposé

Mode de fonctionnement	$TH(f)$
GSM900	0,75
UMTS VI [a]	0,75
DCS1800	0,60
UMTS IX [a]	0,60
UMTS I	0,60

[a] Les Bandes VI et IX de 3GPP UMTS-FDD ont des fréquences de liaison montante très proches de GSM900 et DCS1800, respectivement. Même si seuls les dispositifs fonctionnant dans les bandes GSM900, DCS1800 et UMTS I ont été pris en considération à l'Article B.2, les seuils du présent tableau doivent être appliqués pour la Bande VI de UMTS-FDD et la Bande IX de UMTS-FDD.

IECNORM.COM : Click to view the full PDF of IEC/IEEE 62209-1528:2020



IECNORM.COM : Click to view the full PDF of IEC/IEEE 62209-1528:2020

Anglais	Français
Measurement 7.9.3.4	Mesurage 7.9.3.4
Local SAR reference (step a, g1)	Référence de DAS local (étape a, g1)
Area scan (step b, c, g2, g3)	Balayage de surface (étape b, c, g1, g2)
Peak SAR > 1,3 W/kg?	DAS maximal > 1,3 W/kg?
No	Non
Yes	Oui
Peak SAR > *TH(f)* × APS?	DAS maximal > *TH(f)* × APS?
Zoom scan (step d, g4)	Balayage-zoom (étape d, g4)
Shift centre	Déplacer le centre
Peak touches boundary?	La valeur crête touche-t-elle la limite?
Refine grid	Affiner la grille
Meet resolution criteria?	Satisfait aux critères de résolution?
Averaging (step e, g5)	Moyennage (étape e, g5)
Drift (step f, g6)	Dérive (étape f, g6)
Go to next peak?	Aller à la valeur crête suivante?
All secondary peaks tested?	Toutes les valeurs crêtes secondaires ont-elles été soumises à l'essai?

Figure 26 – Organigramme modifié de la Figure 19

7.9.3.5 Réduction d'essai fondée sur des considérations d'émission multibande simultanée

Dans une émission multibande simultanée, le dispositif peut émettre dans des bandes de fréquences multiples en même temps, par exemple, une émission AMRC à bande élargie (WCDMA) à 2 GHz et une émission de réseau local sans fil (WLAN) à 2,45 GHz. La puissance de sortie moyennée dans le temps d'un émetteur secondaire (c'est-à-dire, l'émetteur de plus faible puissance, par exemple Bluetooth, WLAN) peut être beaucoup plus faible que celle de l'émetteur primaire (c'est-à-dire, l'émetteur de puissance plus élevée, par exemple, AMRC à bande élargie). Dans certains cas, l'émetteur secondaire peut être exclu de l'essai de DAS lorsqu'il est utilisé seul. Cependant, lorsque les émetteurs primaire et secondaire sont utilisés conjointement (émission simultanée), la limite de DAS peut encore être dépassée. Un moyen de détermination de la puissance de seuil pour l'émetteur secondaire qui lui permet d'être exclu de l'essai de DAS est exigé.

Une façon de déterminer le niveau de puissance de seuil pour l'émetteur secondaire ($P_{\text{disponible}}$) consiste à le calculer à partir du psDAS mesuré de l'émetteur primaire (DAS_1) selon la Formule (18):

$$P_{\text{disponible}} = P_{\text{max},m} \times (DAS_{\text{lim}} - DAS_1) / DAS_{\text{lim}} \quad (18)$$

où $P_{\text{max},m}$ est le niveau de puissance d'exclusion de seuil maximal, qui est calculé par $DAS_{\text{lim}} \times m$, et où m est une masse d'intégration.

Par exemple, une limite d'exposition de DAS_{lim} = 2,0 W/kg et une masse d'intégration de m = 10 g donnent une puissance d'émission totale de $P_{\text{max},m}$ = 20 mW.

Par exemple, une limite d'exposition de DAS_{lim} = 1,6 W/kg et une masse d'intégration de m = 1 g donnent une puissance d'émission totale de $P_{\text{max},m}$ = 1,6 mW.

La Formule (18) peut aisément être généralisée au cas dans lequel plus de deux émetteurs émettent simultanément. En présence de N émetteurs simultanés et si le psDAS des $N - 1$ premiers émetteurs est connu (DAS_i), alors le niveau de puissance de seuil pour le N-e émetteur peut être déduit de la Formule (19):

$$P_{\text{disponible}} = P_{\text{max},m} \times (DAS_{\text{lim}} - \sum_{i=1}^{N-1} DAS_i) / DAS_{\text{lim}} \quad (19)$$

NOTE L'applicabilité de seuils de puissance tels que définis à l'Annexe B de l'IEC 62479:2010 [32] exige une investigation pour remplacer $P_{\text{max},m}$ si: i) le DUT est mesuré à l'oreille du SAM et ii) les parties rayonnantes du DUT sont à moins de 5 mm de la surface du fantôme. La définition de nouveaux seuils de puissance pour une telle configuration est nécessaire.

IECNORM.COM : Click to view the full PDF of IEC/IEEE 62209-1528:2020

7.9.3.6 Mesurages de DAS et réductions d'essai pour les dispositifs ELT

7.9.3.6.1 Considérations générales relatives aux essais de DAS ELT

La technologie ELT présente une complexité supplémentaire sur les précédents schémas radio. Pour configurer et soumettre à l'essai les dispositifs ELT, de nombreux paramètres de signaux sont pris en compte: la bande de fréquences, la largeur de bande de canal (entre 1,4 MHz et 20 MHz, par exemple), la modulation (QPSK, 16-QAM et QAM d'ordre supérieur, par exemple), le nombre de blocs de ressources (BR) attribués, le décalage des blocs de ressources à l'intérieur de la largeur de bande de canal, ainsi que la réduction de puissance maximale (MPR). Les combinaisons de paramètres dans une bande de fréquences donnée peuvent donner lieu à des centaines de modes ELT et configurations d'essai de DAS. Pour en tenir compte, un protocole particulier est nécessaire pour l'évaluation du DAS des dispositifs ELT. Ce protocole a pour principal objet de démontrer la conformité du DUT aux limites applicables selon un nombre raisonnable d'évaluations de DAS.

NOTE 1 Les organismes de réglementation nationaux peuvent avoir différentes exigences sur les configurations d'essai des dispositifs ELT.

Pour un mode ELT et une position de dispositif donnés, le psDAS est associé à la puissance de sortie RF maximale. Par conséquent, les mesures de puissance conduite RF peuvent être utilisées pour identifier rapidement les modes ELT de DAS élevé. Le DAS et la puissance conduite RF ne sont toutefois pas directement proportionnels, car:

a) la puissance conduite RF est mesurée avec une impédance de charge de 50 Ω;

b) l'impédance d'antenne d'un DUT n'est en général pas de 50 Ω et varie en fonction de la fréquence;

c) la position du dispositif et les conditions d'accouplement du fantôme peuvent avoir un impact sur l'impédance d'antenne.

Par conséquent, un mesurage de DAS individuel utilisant le mode ELT avec la puissance de sortie conduite maximale mesurée dans une bande de fréquences peut ne pas être suffisant pour démontrer la conformité, sauf si la valeur de DAS est nettement inférieure à la limite de conformité applicable. Les conditions d'essai exigées sont établies en appliquant le protocole de 7.9.3.6.3.

NOTE 2 Les procédures de mesure de puissance s'appliquent aux modes ELT dans une certaine bande de fréquences. Le DAS est mesuré pour la condition de puissance mesurée la plus élevée dans une bande de fréquences pour toutes les positions d'essai de dispositif selon les conditions ELT.

Les conditions d'essai ELT sont mesurées selon les protocoles de mesure de DAS du présent document. Le présent document spécifie uniquement les procédures d'identification des configurations d'essai ELT qui sont les plus susceptibles de donner les niveaux de DAS les plus proches des valeurs maximales, et une exposition prudente peut être obtenue selon les procédures de 7.9.3.6.2.

Ce sont les raisons pour lesquelles des études sur les relations entre la puissance conduite RF et le DAS ont été menées par le comité d'études 106 de l'IEC à l'aide de DUT fonctionnant dans les bandes ELT 3GPP 1, 4 et 17. Les résultats de l'Annexe W donnent ce qui suit.

– La modulation QPSK avec 1 allocation RB produit en général le psDAS le plus élevé. La réduction de puissance maximale (MPR) ne s'applique pas dans ce cas.

– Le psDAS présente une bonne corrélation avec la puissance de sortie conduite RF mesurée. La relation s'écarte de la proportionnalité de moins de 25 % (k = 2).

– Pour les modes LTE avec une puissance conduite maximale inférieure à 85 % de P_{max}, où P_{max} est la puissance de sortie RF maximale mesurée la plus élevée de tous les modes LTE de la bande de fréquences, il est très peu probable que les résultats de DAS les plus élevés soient prévus.

IECNORM.COM : Click to view the full PDF of IEC/IEEE 62209-1528:2020

7.9.3.6.2 Description du choix du mode LTE

La puissance conduite doit être mesurée pour la plus grande largeur de bande de canal prise en charge par les modes LTE dans chaque bande de fréquences, à l'aide d'une modulation QPSK avec allocation 1 RB. Les canaux d'essai exigés doivent être déterminés selon 7.2.8.

– Si un seul canal est exigé, 1 RB doit être alloué au décalage = centre.
– Si trois canaux sont exigés, 1 RB doit être alloué: i) décalage = 0, ii) centre, et iii) maximum à l'intérieur de la largeur de bande de canal.
– Si cinq canaux sont exigés, 1 RB doit être alloué: i) décalage = 0, ii) sous le centre, iii) centre, iv) au-dessus du centre et v) maximum à l'intérieur de la largeur de bande de canal, respectivement, pour les canaux du plus bas au plus élevé.

Outre "Modulations QPSK avec allocation 1 RB", les autres modes LTE doivent être mesurés pour les différentes configurations de largeur de bande de canal utilisant les modulations et les allocations RB spécifiées par 3GPP pour les essais de conformité. Les paramètres de réduction de puissance maximale (MPR) se trouvent dans la documentation 3GPP correspondante.

La puissance de sortie maximale conduite doit être mesurée en utilisant le canal d'essai et les configurations de décalage RB.

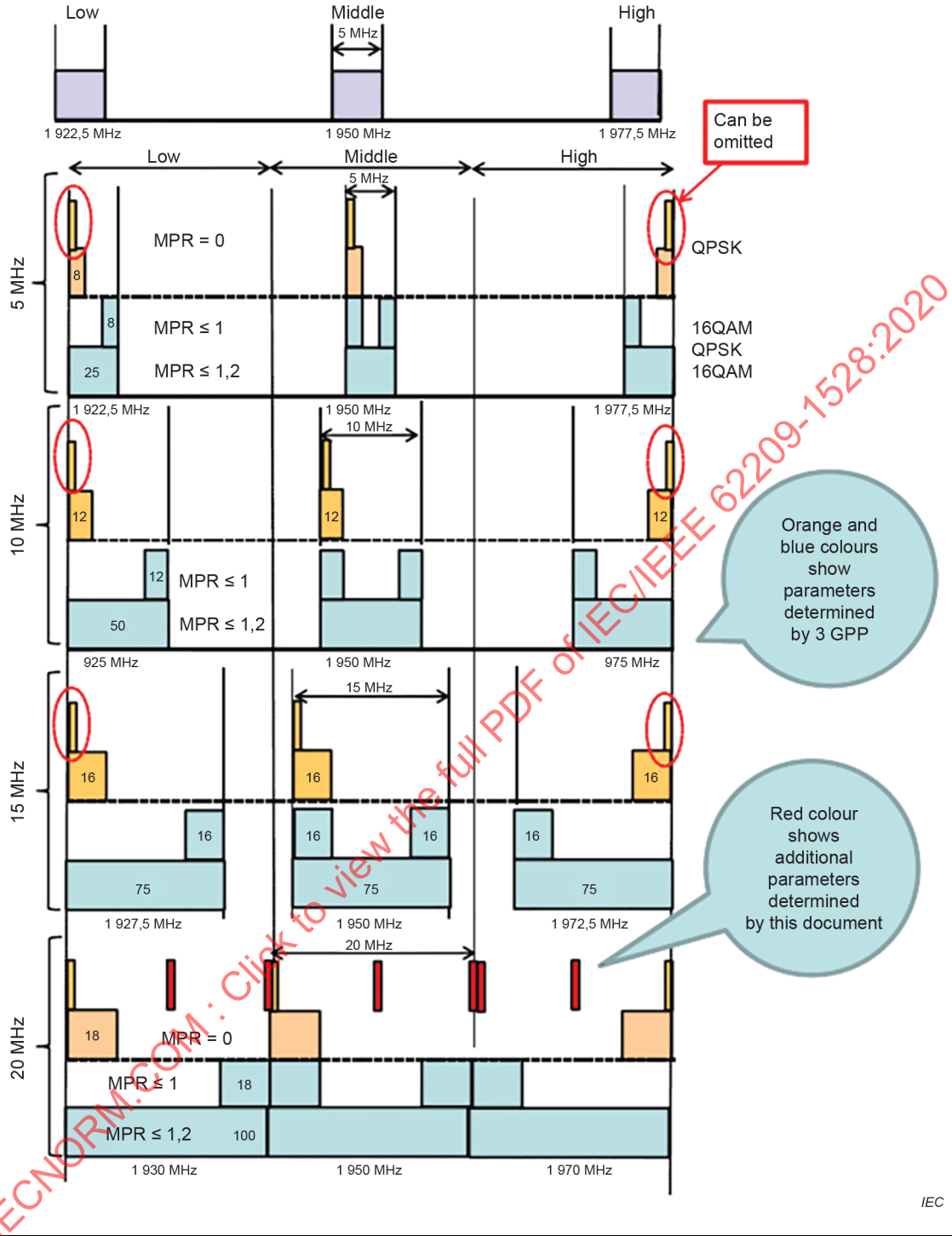
a) Si la réduction de puissance maximale ne s'applique pas, les configurations de l'Article W.2 sont mesurées pour les canaux inférieur et médian avec "décalage RB = 0" et "décalage RB = maximum" pour le canal supérieur.
b) Si la réduction de puissance maximale s'applique, les configurations de l'Article W.3 sont mesurées
    1) pour le canal inférieur avec "décalage RB = maximum",
    2) pour le canal médian avec "décalage RB = 0 et maximum",
    3) pour le canal supérieur avec "décalage RB = 0",

Pour "Modulation QPSK avec allocation 1 RB" dans les plus petites configurations de largeur de bande de canal, si le même décalage RB a déjà été mesuré dans la largeur de bande la plus élevée, ledit décalage RB peut être ignoré. Cela correspond à des RB alloués proches de bords du canal. Par exemple, décalage = 0 pour le canal inférieur et "maximum" pour le canal supérieur, pour des largeurs de bande de canal de 5 MHz, 10 MHz, 15 MHz dans la Bande 1 peuvent être ignorés.

Les conditions de mesure de la puissance de sortie conduite sont représentées à la Figure 27 pour les largeurs de bande de canal de 5 MHz, 10 MHz, 15 MHz et 20 MHz dans la Bande 1 (1 920 MHz à 1 980 MHz), et à la Figure 28 pour les largeurs de bande de canal de 5 MHz et 10 MHz dans la Bande 17 (704 MHz à 716 MHz). Les RB orange et bleu correspondent aux conditions d'essai spécifiées par 3GPP pour les essais de conformité. Les RB rouges représentent les configurations supplémentaires exigées pour QPSK et l'allocation 1 RB dans la configuration de largeur de bande de canal la plus grande, non spécifiée pour les essais de conformité 3GPP. Les canaux exigés sont déterminés selon 7.2.8.

Les essais de puissance conduite pour les modes LTE supplémentaires sont admis si les résultats constituent un surensemble des exigences ci-dessus (essai de puissance conduite selon les exigences FCC, par exemple). Si ce type de surensemble de puissance conduite est consigné, tous les résultats doivent être pris en compte dans les procédures d'essai de DAS suivants.

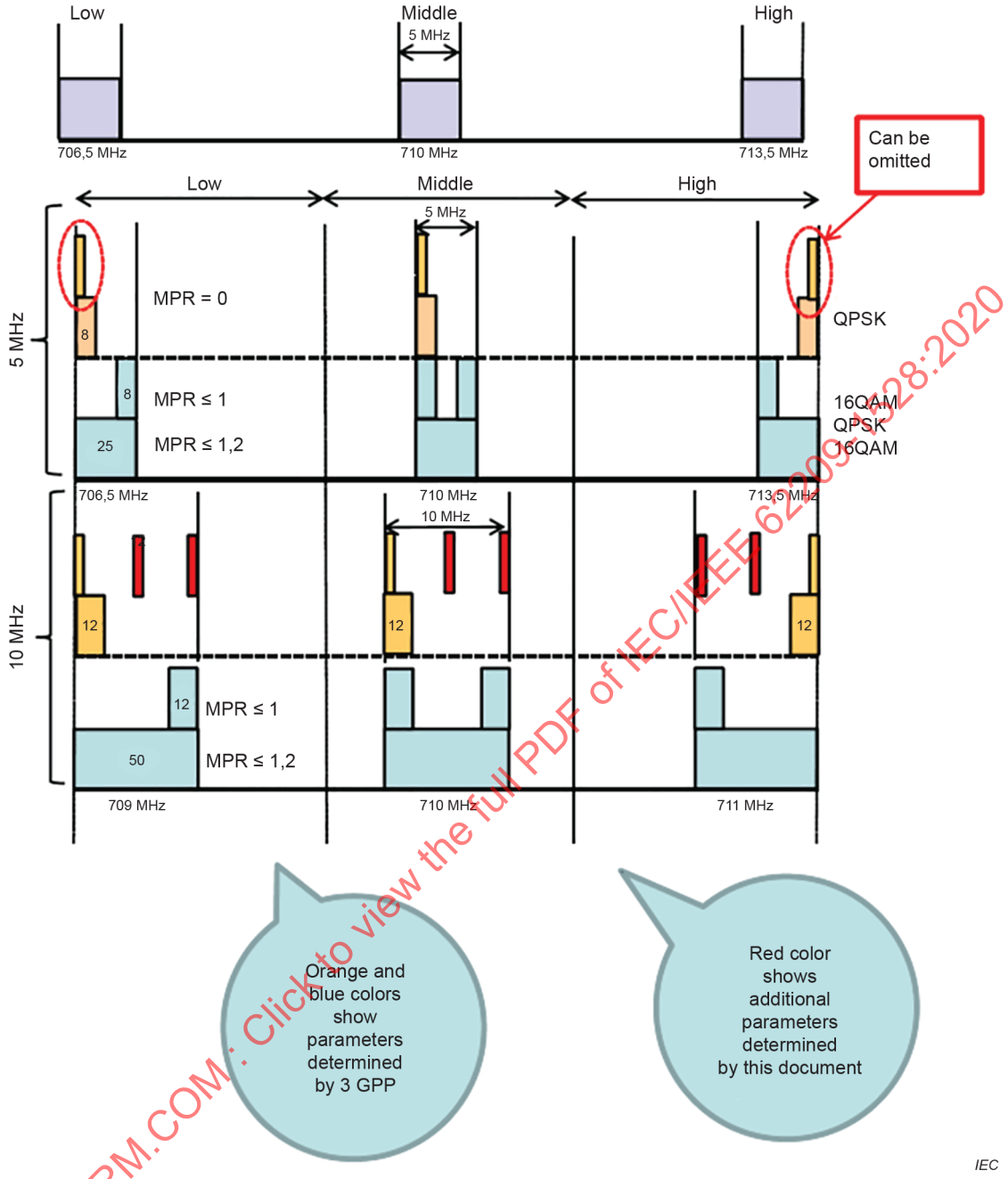
IECNORM.COM : Click to view the full PDF of IEC/IEEE 62209-1528:2020



IECNORM.COM : Click to view the full PDF of IEC/IEEE 62209-1528:2020

Anglais	Français
Low	Inférieur
Middle	Médian
High	Supérieur
Can be omitted	Peut être ignoré
Orange and blue colors show parameters determined by 3 GPP	Les couleurs orange et bleue indiquent les paramètres déterminés par 3 GPP
Red color shows additional parameters determiner by this document	La couleur rouge présente les paramètres supplémentaires déterminés par le présent document

Figure 27 – Utilisation de la puissance conduite pour le choix du mode LTE, pour la Bande 1 (1 920 MHz à 1 980 MHz) (les valeurs MPR sont en dB)



IECNORM.COM : Click to view the full PDF of IEC/IEEE 62209-1528:2020

Anglais	Français
Low	Inférieur
Middle	Médian
High	Supérieur
Can be omitted	Peut être ignoré
Orange and blue colors show parameters determined by 3 GPP	Les couleurs orange et bleue indiquent les paramètres déterminés par 3 GPP
Red color shows additional parameters determiner by this document	La couleur rouge présente les paramètres supplémentaires déterminés par le présent document

Figure 28 – Utilisation de la puissance conduite pour le choix du mode LTE, pour la Bande 17 (704 MHz à 716 MHz) (les valeurs MPR sont en dB)

7.9.3.6.3 Protocole de mesure de la puissance et du DAS

Le DAS est soumis à l'essai au mode LTE de puissance de sortie conduite la plus élevée pour toutes les positions de dispositif dans chaque bande de fréquences, tel que déterminé par les procédures de mesure de la puissance de 7.9.3.6.1. Le nombre d'essais de DAS qui suivent est réduit le plus possible selon les trois autres approches décrites à l'étape 3.

Le protocole de mesure suivant est en principe identique au protocole de 7.3, si ce n'est qu'il commence par le mode LTE dont la puissance conduite est la plus élevée, plutôt que par le centre de la bande de fréquences d'émission. Le protocole s'applique si les paramètres de puissance de sortie maximale du DUT sont les mêmes quelle que soit la condition d'utilisation (porté près du corps/mode vocal, par exemple).

a) Étape 1 – Mesurage de la puissance conduite RF.

   1) La puissance conduite RF doit être mesurée pour tous les modes LTE spécifiés en 7.9.3.6.2, où $P(m)$ est la puissance mesurée pour les m modes LTE. Le protocole de mesure de la puissance de sortie conduite RF est spécifié en 7.9.3.6.4.

   2) Le mode LTE avec la puissance de sortie conduite maximale mesurée la plus élevée dans chaque bande de fréquences est identifié par P_{max}.

   3) Le sous-ensemble des modes LTE dans une bande de fréquences avec une puissance mesurée supérieure ou égale à 85 % de P_{max} est identifié par S.

b) Étape 2 – Mesurage de DAS pour le mode LTE générant la puissance conduite RF maximale (P_{max}) et la position de dispositif provoquant le DAS maximal.

   Le DAS doit être mesuré pour toutes les positions de dispositif du mode LTE avec la puissance conduite RF maximale (P_{max}) afin de déterminer la position de dispositif avec le psDAS le plus élevé, identifié par $DAS_{étape2}$.

c) Étape 3 – Les trois approches suivantes peuvent être appliquées pour déterminer le psDAS le plus élevé.

   1) Approche 1 (AP1) – Sélectionner le mesurage de DAS à la position de dispositif générant le DAS maximal de l'étape 2.

      – Pour la position d'essai correspondant à $DAS_{étape2}$, multiplier par α_{95} pour obtenir le psDAS le plus élevé mis à l'échelle, identifié par AP1 $DAS_{étape3}$. Le facteur α_{95} est le 95e percentile (moyenne plus deux écarts types) du rapport $\alpha(m)$ entre le DAS et la puissance conduite (Formule (W.1)). Une valeur de α_{95} = 1,35 a été déduite des deux études, comme cela est indiqué à l'Annexe W. D'autres facteurs de α_{95} peuvent être utilisés si une justification est donnée dans le rapport d'essai.

      – L'Approche 1 est une méthode rapide donnant une exposition prudente. Si les résultats de DAS maximal obtenus avec cette approche dépassent la limite de DAS, l'Approche 2 peut être utilisée pour obtenir des résultats de DAS maximal plus précis.

   2) Approche 2 (AP2) – Mesurage de DAS à la position de dispositif générant le DAS maximal pour les modes LTE inclus dans un sous-ensemble S.

      – Pour la position d'essai correspondant à $DAS_{étape}$, mesurer le DAS dans cette position d'essai pour les autres modes LTE inclus dans le sous-ensemble S. Le psDAS le plus élevé est identifié par AP2 $DAS_{étape}$.

      – L'Approche 2 est la méthode la plus précise, mais elle exige de soumettre à l'essai les modes LTE dans chaque sous-ensemble S.

   3) Approche 3 (AP3) – Mesurage de DAS limité à la position de dispositif générant le DAS maximal pour les modes LTE inclus dans un sous-ensemble S.

      – Pour la position d'essai correspondant à $DAS_{étape2}$, mesurer le DAS dans cette position d'essai pour un autre mode LTE ayant la puissance conduite la plus élevée parmi tous les modes LTE non soumis à l'essai inclus dans le sous-ensemble S.

IECNORM.COM : Click to view the full PDF of IEC/IEEE 62209-1528:2020

– Multiplier le psDAS mesuré par α_{95} pour obtenir le nouveau psDAS mis à l'échelle, identifié par AP3 $DAS_{\text{mis à l'échelle}}$.

– Si AP3 $DAS_{\text{mis à l'échelle}}$ n'est pas inférieur à la limite de DAS, répéter le mesurage de DAS pour le mode LTE suivant tel que cela est spécifié ci-dessus dans cette étape. Sinon, choisir la valeur la plus élevée parmi tous les résultats de psDAS mesuré et la dernière valeur mise à l'échelle AP3 $DAS_{\text{mis à l'échelle}}$, et l'identifier par AP3 $DAS_{\text{étape3}}$.

4) $DAS_{\text{étape3}}$ d'AP1, AP2 ou AP3 doit être consigné en tant que DAS maximal pour la bande de fréquences LTE.

NOTE Lors de l'évaluation du DAS multiémission simultané (LTE + WLAN, par exemple), la valeur de DAS LTE maximale pour chaque position d'essai obtenue dans le cadre des précédentes approches AP1 et/ou AP2 et/ou AP3, est appliquée conformément aux procédures de DAS d'émission simultanée du présent document pour cette évaluation.

7.9.3.6.4 Mesurage de la puissance de sortie conduite RF pour les modes LTE

Comme cela est indiqué en 7.9.3.6.1, les mesurages de la puissance de sortie conduite RF sont utilisés pour identifier les configurations d'essai peu susceptibles de produire les valeurs de DAS le plus élevé pour les modes LTE dans la bande de fréquences. Il est primordial de définir les lignes directrices permettant d'assurer des mesurages répétables et précis de la puissance conduite RF pour les dispositifs LTE. Les études menées par le comité d'études 106 de l'IEC [32] ont démontré que ces mesurages peuvent être affectés par la présence ou l'absence du chargeur de dispositif et par le nombre de trames de données (10 ms pour LTE) utilisées pour le moyennage de puissance efficace.

De ce fait, les exigences suivantes s'appliquent au mesurage de la puissance de sortie conduite.

a) L'accès de sortie RF du dispositif doit être relié à l'instrument de mesure (le wattmètre, par exemple) et le câble ne doit pas bouger pendant l'évaluation de la puissance conduite pour une bande de fréquences donnée.

b) Le dispositif doit être alimenté par une batterie et aucun chargeur ne doit être relié au dispositif. La batterie doit être chargée pour tous les mesurages de puissance.

c) La même allocation de sous-trame doit être utilisée pour les mesurages de puissance de tous les modes LTE dans un canal de fréquences donné. Par exemple, les mesurages pour tous les modes LTE de la Bande 17 peuvent être réalisés avec le schéma suivant: seule la sous-trame #0 émet activement dans chaque trame de données, les neuf sous-trames restantes étant inactives.

d) La puissance de sortie conduite RF doit être moyennée sur au moins 20 trames.

Les résultats du mesurage de puissance conduite doivent être documentés, et l'incertitude de mesure doit être prise en compte. Pour un canal de fréquence et un mode LTE m donnés, $U[P(m)]$ désigne l'écart type relatif des résultats de mesure de puissance conduite du mode m obtenu sur au moins cinq mesurages répétés. L'écart type relatif est l'écart type divisé par la moyenne $\overline{P}(m)$ sur cinq mesurages.

La puissance de sortie conduite $P(m)$ pour un mode LTE m donné à un canal de fréquence spécifié est défini par $\overline{P}(m)$. La puissance conduite de sortie maximale sur les m modes LTE est désignée par $\max_{m=1:M}\left\{\overline{P}(m)_{\max}\right\}$. $U(P, k = 2)$ désigne l'incertitude $k = 2$ de l'évaluation de la puissance conduite, désignée par $\max_{m=1:M}\left\{U\left[P(m)\right]\right\}$. Les notations $P(m)$ et $P_{\max}$ sont utilisées à des fins de simplicité.

IECNORM.COM : Click to view the full PDF of IEC/IEEE 62209-1528:2020

8 Estimation de l'incertitude de mesure

8.1 Généralités

Le bilan d'incertitude s'applique aux résultats de mesure de DAS de la tête et du corps. L'estimation de la répétabilité du mesurage, vérifiée dans le cadre de la procédure de contrôle du système, est obtenue en ignorant les contributions de Type B du bilan d'incertitude. Le Tableau 9 (voir 8.3) est un exemple de bilan d'incertitude pour le mesurage de DAS à 1 g ou 10 g d'un DUT ou d'une antenne de validation.

Chaque grandeur d'entrée est décrite avec un exemple de la manière d'évaluer l'incertitude-type associée. Des exemples généraux peuvent ne pas être applicables à tous les systèmes de mesure, et des grandeurs supplémentaires non traitées dans le présent document peuvent être exigées dans des cas particuliers.

Des informations supplémentaires sur l'évaluation des contributions à l'incertitude destinées aux fabricants de systèmes et aux laboratoires d'étalonnage sont données de 8.4.1.1 à 8.4.1.6, en 8.4.1.8, en 8.4.1.9 et en 8.4.2.1.

L'incertitude de mesure élargie est calculée par la Formule (20):

$$U = k \cdot u_c(y) \tag{20}$$

Un facteur d'élargissement de k = 2 est utilisé dans le présent document, correspondant à un intervalle de confiance de 95 %. L'incertitude-type composée $u_c(y)$ est calculée par la Formule (21):

$$u_c(y) = \sqrt{\sum_{i=1}^{N} c_i^2 \cdot \left[a(x_i)/q_i\right]^2} = \sqrt{\sum_{i=1}^{N} c_i^2 \cdot u^2(x_i)} = \sqrt{\sum_{i=1}^{N} u_i^2(y)} \tag{21}$$

où

x_i est la valeur estimée de la i-e grandeur d'entrée X_i qui influence l'incertitude;

y est la valeur de la grandeur de sortie Y qui correspond à l'incertitude composée;

$a(x_i)$ est la valeur d'incertitude de x_i ayant une fonction de densité de probabilité PDF_i;

q_i est le diviseur correspondant à la fonction de densité de probabilité PDF_i de x_i;

$u(x_i)$ = $a(x_i)/q_i$ est l'incertitude-type de x_i, correspondant à une distribution normale;

c_i est le coefficient de sensibilité associé à x_i. Il décrit la mesure dans laquelle y varie avec de petites modifications de x_i. Il est calculé comme étant la dérivée partielle de la fonction de modèle f par rapport à x_i, voir la Formule (22):

$$c_i = \partial f / \partial x_i \tag{22}$$

$u_i(y) = c_i \cdot u(x_i)$ est l'incertitude-type de y, correspondant à une distribution normale.

Les diviseurs q_i doivent être appliqués conformément à la fonction de densité de probabilité PDF_i spécifiée dans l'ISO/IEC Guide 98-3. Le Tableau 8 donne les diviseurs pour les fonctions de densité de probabilité habituelles.

IECNORM.COM : Click to view the full PDF of IEC/IEEE 62209-1528:2020

Tableau 8 – Diviseurs pour les fonctions de densité de probabilité (PDF)

PDF	Normal	Rectangulaire	Triangulaire	En forme de U
Diviseur q	k	√3	√6	√2

8.2 Exigences relatives à l'évaluation de l'incertitude

L'incertitude de mesure élargie, U, est le résultat de l'évaluation de l'incertitude, dont les informations détaillées spécifiques sont consignées dans un bilan d'incertitude. Les bilans d'incertitude élargie doivent être évalués pour les mesurages de DAS conformément à ce qui suit.

a) L'incertitude élargie dans la valeur mesurée de psDAS (1 g ou 10 g) doit être évaluée conformément aux recommandations et aux explications données dans l'ISO/IEC Guide 98-3.

b) La plage de fréquences et les conditions de mesure pour lesquelles l'analyse d'incertitude est valable doivent être spécifiées.

c) L'incertitude consignée doit représenter l'incertitude élargie maximale dans les limites de cette plage.

d) L'incertitude élargie dans les mesurages de contrôle et de validation du système doit également être évaluée. L'incertitude doit être indiquée au niveau de confiance de 95 %, et l'incertitude élargie ne doit pas dépasser 30 % de la valeur de psDAS dans la plage comprise entre 0,4 W/kg et 10 W/kg. Pour les valeurs de psDAS inférieures à 0,4 W/kg, l'incertitude élargie ne doit pas dépasser 0,12 W/kg (30 % de 0,4 W/kg).

e) Lorsque cela est acceptable dans le cadre des exigences nationales, si l'incertitude élargie est supérieure à 30 %, il est nécessaire que les données consignées tiennent compte de la différence de pourcentage entre l'incertitude réelle et la valeur cible de 30 % (voir la méthode de [34], par exemple).

8.3 Description des modèles d'incertitude

8.3.1 Généralités

Les modèles d'incertitude de 8.3 sont décrits dans le format de la Formule (23):

$$Y = X_1 + X_1 + \cdots + X_N \tag{23}$$

$Y = \Delta DAS$ est la grandeur de sortie correspondant à l'incertitude d'évaluation de DAS composée. Les grandeurs de sortie X_i sont décrites par les symboles de 8.4. La Formule (21) (voir 8.1) doit être utilisée pour calculer l'incertitude-type composée $u_c(y)$.

En référence aux lignes directrices en matière d'évaluation de l'incertitude de l'ISO/IEC Guide 98-1 [35] et de l'ISO/IEC Guide 98-3, les modèles d'incertitude des processus suivants sont spécifiés à l'aide des symboles décrits en 8.4.

8.3.2 Mesurage de DAS d'un DUT

La formule du modèle d'incertitude de mesure (équation du modèle) correspondant aux résultats des mesurages de DAS du DUT est donnée par la Formule (24).

$$\begin{aligned}\Delta DAS = {} & CF + CF_{\text{dérive}} + LIN + BBS + ISO + DAE + AMB + \frac{2}{\delta}\Delta_{xyz} + DAT + LIQ(\sigma) \\ & + LIQ(T_c) + 0{,}25EPS + 2DIS + D_{xyz} + H + MOD + TAS + RF_{\text{dérive}} + C(\varepsilon', \sigma) + C(R)\end{aligned} \tag{24}$$

IECNORM.COM : Click to view the full PDF of IEC/IEEE 62209-1528:2020

Le Tableau 9 présente le modèle de bilan d'incertitude des résultats de mesure du psDAS d'un DUT, ainsi que les descriptions des symboles utilisés dans la Formule (24).

8.3.3 Mesurage de validation du système et de contrôle du système

La formule du modèle d'incertitude de mesure correspondant aux résultats des mesurages de DAS de validation du système et de contrôle du système est donnée par la Formule (25).

$$\Delta DAS = CF + CF_{\text{dérive}} + LIN + ISO + DAE + AMB + \frac{2}{\delta}\Delta_{xyz} + DAT + LIQ(\sigma) + LIQ(T_{\text{c}}) + 0{,}25EPS + 2DIS + RF_{\text{dérive}} + P_{\text{in}} + VAL + C(\varepsilon', \sigma) \quad (25)$$

Le Tableau 9 présente le modèle de bilan d'incertitude des résultats de mesure du psDAS de validation du système, ainsi que les descriptions des symboles utilisés dans la Formule (25).

8.3.4 Répétabilité et reproductibilité du contrôle du système

La formule du modèle d'incertitude de mesure correspondant aux résultats des mesurages de DAS de répétabilité et de reproductibilité du contrôle du système est donnée par la Formule (26). Les symboles sont décrits dans le Tableau 9.

$$\Delta DAS = CF_{\text{dérive}} + \frac{2}{\delta}\Delta_{xyz} + LIQ(\sigma) + LIQ(T_{\text{c}}) + 0{,}25EPS + 2DIS + RF_{\text{dérive}} + P_{\text{in}} + C(\varepsilon', \sigma) \quad (26)$$

8.3.5 Essai rapide de DAS (mesure relative)

La formule du modèle d'incertitude de mesure correspondant aux résultats des mesurages (relatifs) rapides de DAS est donnée par la Formule (27). Les symboles sont décrits dans le Tableau 9.

$$\Delta DAS = LIN + ISO + DAE + AMB + \frac{2}{\delta}\Delta_{xyz} + DAT + 2DIS + H + D_{xyz} + MOD + RF_{\text{dérive}} \quad (27)$$

IECNORM.COM : Click to view the full PDF of IEC/IEEE 62209-1528:2020

Tableau 9 – Modèle de bilan d'incertitude pour l'évaluation de l'incertitude dans la valeur mesurée du psDAS à 1 g ou 10 g à partir d'un DUT ou d'une antenne de validation (N = normal, R = rectangulaire)

Symbole	Grandeur d'entrée X_i (source d'incertitude)	Réf.	Prob. Dist.[a] PDF_i	Unc. $a(x_i)$	Div.[a] q_i	$u(x_i) = a(x_i)/q_i$	c_i	$u(y) = c_i \cdot u(x_i)$	v_i
Erreurs du système de mesure									
CF	Étalonnage de sonde	8.4.1.1	N (k = 2)		2		1		∞
$CF_{\text{dérive}}$	Dérive de l'étalonnage de sonde	8.4.1.2	R		√3		1		∞
LIN	Linéarité et limites de détection de sonde	8.4.1.3	R		√3		1		∞
BBS	Signal à large bande	8.4.1.4	R		√3		1		∞
ISO	Isotropie de la sonde	8.4.1.5	R		√3		1		∞
DAE	Autres erreurs de sonde et d'acquisition de données	8.4.1.6	N		1		1		∞
AMB	Bruit ambiant et bruit RF	8.4.1.7	N		1		1		∞
Δ_{xyz}	Erreurs de positionnement de la sonde	8.4.1.8	N		1		$2/\delta$		
DAT	Erreur de traitement de données	8.4.1.9	N		1		1		∞
Erreurs de fantôme et de dispositif (DUT ou antenne de validation)									
$LIQ(\sigma)$	Mesurage de la conductivité (σ) du fantôme	8.4.2.1	N		1		c_ε, c_σ		∞
$LIQ(T_c)$	Effets de la température (milieu)	8.4.2.2	R		√3		c_ε, c_σ		∞
EPS	Permittivité de l'enveloppe	8.4.2.3	R		√3		voir 8.4.2.3		∞
DIS	Distance entre l'élément rayonnant du DUT et le milieu du fantôme	8.4.2.4	N		1		2		∞
D_{xyz}	Répétabilité du positionnement du DUT ou de la source contre le fantôme	8.4.2.5	N		1		1		5
H	Effets du support de dispositif	8.4.2.6	N		1		1		
MOD	Effet du mode de fonctionnement sur la sensibilité de la sonde	8.4.2.7	R		√3		1		∞
TAS	DAS moyenné dans le temps	8.4.2.8	R		√3		1		∞
$RF_{\text{dérive}}$	Variation du DAS due à la dérive dans la sortie du DUT	8.4.2.9	N		1		1		
VAL	Incertitude de l'antenne de validation (mesure de validation uniquement)	8.4.2.10	N		1		1		
P_{in}	Incertitude dans la puissance acceptée (mesure de validation uniquement)	8.4.2.11	N		1		1		
Corrections du résultat de DAS (si appliqué)									
$C(\varepsilon',\sigma)$	Écart du fantôme par rapport à la cible (ε',σ)	8.4.3.1	N		1		1		
$C(R)$	Mise à l'échelle du DAS	8.4.3.2	R		√3		1		
$u(\Delta DAS)$	Incertitude composée								
U	Incertitude élargie et degrés efficaces de liberté						U =		v_{eff} =

[a] D'autres distributions de probabilité et diviseurs peuvent être utilisés s'ils représentent mieux la connaissance disponible des grandeurs concernées.

IECNORM.COM : Click to view the full PDF of IEC/IEEE 62209-1528:2020

8.4 Paramètres contribuant à l'incertitude

8.4.1 Erreurs du système de mesure

8.4.1.1 Étalonnage de sonde

CF – Incertitude d'étalonnage pour la sensibilité de la sonde DAS dans le fantôme, obtenue à partir du certificat d'étalonnage. Un protocole d'évaluation des coefficients d'étalonnage de sonde DAS et de l'estimation d'incertitude est donné à l'Annexe E.

8.4.1.2 Dérive de l'étalonnage de sonde

$CF_{\text{dérive}}$ – Dérive de *CF* pendant l'intervalle d'étalonnage, estimée à partir de l'historique d'étalonnage de sonde, de la connaissance de sondes similaires ou des spécifications du fabricant.

8.4.1.3 Linéarité et limites de détection de sonde

LIN – Variation de la sensibilité de la sonde en fonction du DAS appliqué pour des signaux à ondes entretenues entre le DAS mesuré et le niveau auquel la sonde a été étalonnée. Les erreurs de linéarité et limites de détection de sonde, mesurées conformément à l'Article O.1 sur la plage comprise entre au moins 0,12 W/kg et 100 W/kg, sont données dans le certificat d'étalonnage ou dans les spécifications du fabricant.

8.4.1.4 Signal à large bande

BBS – Incertitude due à la réponse variable de la sonde en fonction de la fréquence. Ce terme est négligeable pour le mesurage des signaux à bande étroite. Sinon, il doit être calculé comme cela est spécifié à l'Article O.2.

8.4.1.5 Isotropie de la sonde

ISO – Variation de sensibilité de la sonde DAS due à sa rotation et à son inclinaison par rapport au vecteur de champ en cours de mesure. Elle est en général mentionnée dans le certificat d'étalonnage ou dans les spécifications du fabricant en tant qu'isotropie axiale (variation de sensibilité lorsque la sonde tourne autour de son axe) et en tant qu'isotropie hémisphérique (variation de sensibilité lorsque la sonde tourne autour de son axe et est inclinée par rapport au vecteur de champ). L'isotropie de la sonde doit être mesurée selon le protocole spécifié à l'Article E.4. Pendant les mesurages, l'axe de la sonde est maintenu dans les limites d'un angle spécifié par rapport à la perpendiculaire de la surface du fantôme, afin de limiter les erreurs d'isotropie (Tableau 3 et Tableau 4). Une approximation empirique de l'erreur d'isotropie totale pour ce cas est donnée par la Formule (28):

$$ISO = \sqrt{0{,}5\mu^2_{\text{axiale}} + 0{,}5\mu^2_{\text{hémisphérique}}} \tag{28}$$

et une distribution de probabilité rectangulaire doit être utilisée.

8.4.1.6 Autres erreurs de sonde et d'acquisition de données

DAE – Autres erreurs de sonde et d'acquisition de données, y compris la résolution spatiale (essai rapide de DAS), la distance de décalage de sonde, le temps d'intégration et le temps de réponse de la sonde (Article O.6), les effets de proximité de bord et les corrections (Article O.3) et les erreurs d'acquisition de données (Article O.4), qui sont données dans les spécifications du fabricant.

IECNORM.COM : Click to view the full PDF of IEC/IEEE 62209-1528:2020

8.4.1.7 Bruit ambiant RF et réflexions

AMB – Les effets du signal RF ambiant et des niveaux de bruit du système, ainsi que les réflexions, sont évalués en mesurant le DAS sans émission du DUT. Le présent document précise que les résultats doivent être inférieurs ou égaux à 0,012 W/kg (c'est-à-dire 3 % de 0,4 W/kg). Il n'est pas nécessaire de contrôler le bruit ambiant RF avant chaque essai de DAS, à condition que le laboratoire puisse démontrer l'absence de nouvelles sources RF. La procédure d'évaluation des contributions du bruit ambiant et des réflexions à l'incertitude est donnée à l'Article R.1.

8.4.1.8 Erreurs de positionnement de la sonde

Δ_{xyz} – Erreur de position de l'extrémité de la sonde par rapport à la surface de l'enveloppe du fantôme sur le volume utilisé pour le calcul du DAS à 1 g ou à 10 g. L'incertitude est obtenue à partir des spécifications du fabricant ou en mesurant la position de l'extrémité de la sonde et la séparation par rapport à l'enveloppe du fantôme en plusieurs points à l'intérieur du volume de balayage, puis en comparant ces éléments aux positions exigées. Dans le cas du fantôme plan, cette évaluation doit inclure l'effet d'affaissement du fond de la cuve. La tolérance de position doit être ≤ 0,2 mm. Étant donné que le DAS diminue avec la distance par rapport à la surface du fantôme avec $e^{-2x/\delta}$, le coefficient de sensibilité c_i est d'environ $2/\delta$, où δ est la profondeur de pénétration dans le fantôme, en mm. Des informations détaillées sont données à l'Article O.7. Étant donné que les positions de mesure $N \geq 96$ sont utilisées pour déterminer le DAS à 1 g ou à 10 g, les contributions de Type A associées à la répétabilité du système de balayage sont réduites de $\sqrt{N}$.

8.4.1.9 Erreur de traitement de données

DAT – Erreur résultant du calcul et des algorithmes de traitement des données utilisés dans le logiciel de mesure pour le DAS moyenné à 1 g ou à 10 g calculée à partir d'un nombre limité d'échantillons spatiaux. Les erreurs incluent celles dues à l'extrapolation et à l'interpolation. L'amplitude d'erreur est évaluée par le fabricant ou par le fournisseur du logiciel à l'aide d'un ensemble de fonctions d'essai. Des informations détaillées sont données à l'Article O.8.

8.4.2 Erreurs de fantôme et de dispositif (DUT ou antenne de validation)

8.4.2.1 Mesurage de la conductivité du fantôme

$LIQ(\sigma)$ – Erreur de mesure de la conductivité du fantôme à l'aide des techniques de mesure des propriétés diélectriques spécifiées à l'Annexe H, en principe obtenues auprès du fournisseur du système. La procédure est spécifiée et un exemple de tableau d'incertitudes est donné à l'Article O.9.

8.4.2.2 Effets de la température

$LIQ(T_c)$ – Erreur due à une variation de température ΔT du fantôme entre le mesurage des propriétés diélectriques et le mesurage de DAS.

Pour chaque formulation de fantôme, il convient d'estimer le coefficient de température T_c (°C) de ε' et σ à la fréquence considérée à partir des mesurages avec un milieu équivalent au tissu à des températures différentes comprises entre 18 °C et 25 °C, et mesurées selon une exactitude de 0,1 °C.

L'erreur due à la variation de température de ΔT est ensuite calculée par la Formule (29):

$$LIQ(T_c) = \Delta T \times \left\{0{,}25\left|T_c(\varepsilon')\right| + 0{,}75\left|T_c(\sigma)\right|\right\} \quad (29)$$

IECNORM.COM : Click to view the full PDF of IEC/IEEE 62209-1528:2020

où les facteurs de pondération sont obtenus en prenant en considération les formules de correction de O.9.6. La valeur de ΔT ne doit pas dépasser 2 °C.

8.4.2.3 Permittivité de l'enveloppe

EPS – La tolérance de la permittivité relative réelle par rapport à ε' = 4 est calculée par la Formule (30):

$$EPS = \frac{\Delta\varepsilon'}{\varepsilon'} = \frac{|\varepsilon' - 3{,}5|}{3{,}5} \tag{30}$$

La permittivité relative réelle doit être comprise entre 2 et 5 pour les fantômes de tête, et entre 3 et 5 pour les fantômes de corps. Dans les limites de cette plage, et pour des fréquences supérieures à 3 GHz, une variation de 25 % de ε' donne une variation d'environ 5 % du DAS moyenné à 1 g ou 10 g. Un coefficient de sensibilité c_i = 0,25 doit donc être utilisé. Pour les fréquences supérieures à 10 GHz, la variation de psDAS augmente à 10 %. Pour des fréquences inférieures ou égales à 3 GHz, l'erreur due à la permittivité de l'enveloppe est négligeable. Pour l'incertitude du psDAS due à la permittivité de l'enveloppe, le coefficient de sensibilité suivant c_i doit être appliqué comme cela est indiqué dans la Formule (31):

$$c_i = \begin{cases} 0 & f \le 3\ \text{GHz} \\ 0{,}25 & 3\ \text{GHz} < f \le 6\ \text{GHz} \\ 0{,}5 & 6\ \text{GHz} < f \le 10\ \text{GHz} \end{cases} \tag{31}$$

Des informations complémentaires peuvent être consultées en [36].

8.4.2.4 Distance entre le DUT et le milieu équivalent au tissu

DIS – L'incertitude dans la distance de séparation entre l'élément rayonnant à l'intérieur du DUT et le milieu équivalent au tissu. La séparation d de la source de courant par rapport au fantôme est égale à la somme de l'épaisseur d'entretoise, de l'épaisseur de l'enveloppe, de l'affaissement et de la distance par défaut de 5 mm entre l'élément rayonnant et la surface du DUT. Cette distance peut varier pour refléter la distance réelle, si disponible.

L'affaissement de la base du fantôme plan rempli de milieu équivalent au tissu jusqu'à la profondeur exigée (sag) peut être évalué en plaçant un bord rectiligne (une règle en métal, par exemple) sous l'enveloppe. Pour le fantôme de tête, l'affaissement est en général minime et peut être par hypothèse considéré comme étant nul.

L'erreur de distance qui en résulte, *DIS*, est alors calculée par la Formule (32):

$$DIS = \frac{\Delta d}{d} = \frac{1}{d}\sqrt{\left(\Delta_{\text{écarteur}}\right)^2 + \left(\Delta_{\text{épaisseur}}\right)^2 + \left(sag\right)^2} \tag{32}$$

où $\Delta_{\text{épaisseur}}$ est obtenu dans les spécifications du fabricant pour la tolérance de l'épaisseur de l'enveloppe et doit être inférieur à 0,2 mm. Étant donné que le DAS dans le fantôme diminue d'environ d^2,, un coefficient de sensibilité de 2 doit être appliqué.

IECNORM.COM : Click to view the full PDF of IEC/IEEE 62209-1528:2020

8.4.2.5 Répétabilité du positionnement

D_{xyz} – Erreur des mesurages de DAS due à l'écart de la position du DUT par rapport à la position nominale. Elle est évaluée en procédant à au moins cinq mesurages répétés de DAS à 1 g ou 10 g tout en repositionnant le DUT dans le support après chaque mesurage. Cette erreur peut être évaluée pour un groupe de DUT de formes (facteurs de formes), de dimensions et de distributions de DAS très semblables, à condition qu'au moins six dispositifs différents soient soumis à l'essai, chacun étant repositionné cinq fois et la moitié des mesurages étant réalisés en position "joue" et l'autre moitié en position "incliné". Si une base de données de ces essais est gérée pour un support de dispositif particulier, il est recommandé de la mettre à jour tous les ans afin de tenir compte des modifications de conception du DUT. Des informations détaillées sont données à l'Article R.2.

8.4.2.6 Effets du support de dispositif

H – Variation du DAS à 1 g ou à 10 g provoquée par le support de dispositif. Cela dépend du DUT. L'erreur doit être évaluée en mesurant le DAS à 1 g ou à 10 g avec le DUT en contact avec le fantôme: a) le DUT étant dans le support de dispositif, et b) le DUT étant posé sur un bloc de polystyrène. L'incertitude liée à un support de dispositif peut être attribuée à un type d'appareil générique, à condition d'évaluer la variabilité entre un échantillon d'au moins six de ces dispositifs et d'ajouter un terme d'incertitude de Type A supplémentaire pour tenir compte de cette variabilité. Des informations détaillées sont données à l'Article R.2.

8.4.2.7 Modulation du signal

MOD – Erreur de mesure de la sonde due au mode de fonctionnement du DUT. Cela se produit lorsque les détecteurs de sonde ne donnent pas la valeur efficace du signal modulé émis par le DUT. Si l'incertitude d'un schéma de modulation particulier n'est pas fournie par le fabricant de la sonde, elle doit être évaluée conformément à la procédure donnée à l'Article R.3.

8.4.2.8 DAS moyenné dans le temps

TAS – L'incertitude liée à l'évaluation du DAS moyenné sur une période est due au taux d'échantillonnage du mesurage. Un taux d'échantillonnage rapide permet au système de mesure du DAS de capturer avec exactitude les variations rapides d'amplitude du signal ou du cycle de service sur le temps d'intégration, ce qui permet de calculer avec exactitude le facteur TX (des informations détaillées sont données à l'Article R.4).

8.4.2.9 Variation du DAS due à la dérive

$RF_{\text{dérive}}$ – Variation du DAS en position fixe à l'intérieur du fantôme due à la dérive dans la sortie RF du DUT pendant la séquence de mesure de DAS (7.2.4). Si la dérive est supérieure à 5 %, des mesurages de stabilité supplémentaires du DUT doivent être réalisés (Article R.5) et des corrections peuvent être appliquées aux données de mesure de DAS pour compenser cette variation. Si ces corrections sont appliquées, $RF_{\text{dérive}}$ peut être ignoré dans l'analyse de l'incertitude.

8.4.2.10 Incertitude de l'antenne de validation

VAL – Erreur due à l'écart entre l'antenne de validation physique et celle utilisée pour déduire les valeurs de référence, y compris la puissance acceptée, les pertes de puissance et les dimensions (Annexe S).

8.4.2.11 Incertitude de la puissance acceptée

P_{in} – Erreur de puissance acceptée par l'antenne de validation.

IECNORM.COM : Click to view the full PDF of IEC/IEEE 62209-1528:2020

8.4.3 Corrections du résultat de DAS (si appliqué)

8.4.3.1 Écart du fantôme par rapport aux propriétés diélectriques cibles

$C(\varepsilon',\sigma)$ – La correction donnée en 7.8 est appliquée au DAS à 1 g ou à 10 g pour corriger les écarts des propriétés cibles du fantôme par rapport à celles spécifiées dans le présent document. La tolérance moyenne de cette correction, spécifiée comme étant égale à la racine carrée de la moyenne des différences au carré entre l'écart de DAS prévu par les formules et les écarts simulés, est indiquée dans le Tableau 10 pour le psDAS à 1 g et le psDAS à 10 g. Le Tableau 10 indique l'accroissement de l'incertitude à mesure qu'augmentent les valeurs maximales admissibles de $\Delta\varepsilon'$ et $\Delta\sigma$. Il a également été démontré que ces corrections sont valables pour des modèles de DUT réalistes [28], [29].

Tableau 10 – Incertitude de la Formule (8) (voir 7.8.2) en fonction de la variation maximale de permittivité et de conductivité

Tolérance max. pour ε ou σ	Incertitude-type du DAS à 1 g, %	Incertitude-type du DAS à 10 g, %
±5 %	1,2	0,97
±10 %	1,9	1,6

8.4.3.2 Mise à l'échelle du DAS

$C(R)$ – Erreur du rapport de puissance R utilisé pour déterminer le DAS d'un DUT en fonction des mesurages réalisés lorsque le dispositif émet un mode et/ou une puissance différent(e) (7.2.3.2). Si les enveloppes de signal des deux modes de fonctionnement sont identiques, cette erreur correspond à la linéarité du dispositif de mesure de puissance utilisé. Si les enveloppes sont différentes, les effets sur la sensibilité du wattmètre doivent également être inclus. Il convient que l'erreur ne dépasse pas 5 %.

L'incertitude peut être évaluée en mesurant le DAS du DUT à l'emplacement du psDAS dans les deux modes/niveaux de puissance, puis en comparant le rapport obtenu avec R. Dans ce cas, il convient d'utiliser une distribution de probabilité rectangulaire. Des informations détaillées sont spécifiées à l'Article R.6.

9 Rapport de mesure

9.1 Généralités

Tous les résultats d'essai doivent être consignés dans un rapport de mesure et doivent inclure toutes les informations nécessaires à l'interprétation des configurations de DUT soumises à l'essai, de l'étalonnage effectué, ainsi que toutes les informations exigées par la méthode et les instruments utilisés.

Un rapport de mesure, conforme à l'ISO/IEC 17025 [17] et contenant au moins les éléments ci-dessous, doit être utilisé pour démontrer que les exigences du présent document sont satisfaites.

9.2 Éléments à consigner dans le rapport de mesure

Toutes les informations nécessaires permettant d'effectuer des essais répétables, les calculs ou les mesures conduisant à des résultats dans l'étalonnage et les limites d'incertitude exigées doivent être consignées. Le rapport de mesure doit comprendre les éléments suivants.

IECNORM.COM : Click to view the full PDF of IEC/IEEE 62209-1528:2020

a) Introduction générale

1) Identification du laboratoire d'essai.

2) Identification du DUT, comprenant les numéros de révision du matériel et du logiciel, le numéro de série, par exemple IMEI (identité internationale de l'équipement mobile).

3) Exigences de conformité, par exemple normes d'essai, lignes directrices, recommandations, etc.

4) Limites d'exposition en vigueur, par exemple ICNIRP, IEEE/ICES, etc.

5) Une liste de toutes les accréditations délivrées par les organismes nationaux ou internationaux en vue de la réalisation des essais conformément aux normes indiquées en a) 3). La date d'expiration des accréditations doit être indiquée.

b) Système de mesure (pour le mesurage de DAS et l'essai rapide de DAS, le cas échéant)

1) Descriptions des principaux composants du système de mesure (milieu équivalent au tissu, lecture électronique, support de dispositif, fantôme(s) et tout autre composant pertinent, par exemple).

Pour les sondes utilisées, inclure les dimensions, l'isotropie, les résolutions spatiales, la plage dynamique et la linéarité.

2) Les données d'étalonnage des composants concernés, y compris les composants critiques du système d'essai rapide de DAS (les certificats d'étalonnage de la sonde, par exemple) doivent être fournies dans le rapport de mesure.

3) La description des algorithmes d'interpolation et d'extrapolation utilisés dans les balayages de surface et/ou les balayages-zooms doit être documentée dans le rapport de mesure.

4) Le milieu équivalent au tissu et les matériaux utilisés, ainsi que leurs caractéristiques.

Pour chaque milieu équivalent au tissu ou chaque matériau utilisé, inclure:

i) les propriétés diélectriques pour chaque bande de fréquences;

ii) l'écart par rapport à la valeur cible;

iii) la température du milieu équivalent au tissu;

iv) le récapitulatif de la composition des milieux équivalents aux tissus.

5) Résultats du contrôle du système:

i) résultats du mesurage pour chaque bande de fréquences;

ii) écart par rapport à la valeur de DAS cible;

iii) description de la source rayonnante.

c) Estimation de l'incertitude (contrôle du système pour la validation du système de mesure de DAS et essais rapides de DAS, le cas échéant)

1) Inclure les valeurs d'incertitude de mesure de l'Article 8 et de l'Annexe C.

2) Tout autre élément pertinent.

d) Informations détaillées relatives à l'appareil et à l'essai

1) Description du facteur de forme du DUT et une brève description de sa fonction prévue.

2) Description des positions et orientations soumises à l'essai, y compris des photos, et justification de toutes les réductions d'essai. En cas de décalage de la position du DUT (selon 6.5), cela doit également être documenté.

3) Description des antennes et accessoires disponibles et soumis à l'essai, y compris les batteries.

4) Description des modes de fonctionnement, niveaux de puissance et bandes de fréquences disponibles et soumis à l'essai, et justification de toutes les réductions d'essai.

5) Condition environnementale d'essai (la température, par exemple).

IECNORM.COM : Click to view the full PDF of IEC/IEEE 62209-1528:2020

6) Résultats de tous les essais effectués (valeur du psDAS pour chaque essai et représentation graphique des balayages à grosse maille par rapport au dispositif pour la valeur de DAS maximale de chaque mode de fonctionnement) et informations détaillées relatives à la mise à l'échelle des résultats.

e) Le rapport de mesure doit contenir les informations suivantes relatives à la validation de la méthode de mesure de DAS.

1) Description des procédures de validation.

2) Résultats des calculs, des mesurages et/ou d'autres évaluations réalisées par le développeur de la méthode (le fabricant du système, par exemple) afin de valider la méthode de mesure de DAS.

3) Analyses ou conditions supplémentaires imposées par le développeur de la méthode et appliquées par l'utilisateur afin de satisfaire à la méthode de mesure de DAS, selon le cas.

4) Description de la source rayonnante et distribution du DAS pour chaque bande de fréquences.

5) Fréquences de fonctionnement, modes de fonctionnement, configurations de fonctionnement du dispositif, position du DUT sur le fantôme et distributions de DAS pour chaque bande de fréquences spécifique à la méthode.

6) Incertitude de mesure des résultats du DAS.

7) En cas d'essai rapide de DAS, les informations détaillées relatives à toutes les modifications apportées aux algorithmes de post-traitement par rapport à ceux mis en œuvre pour l'essai complet du DAS.

f) Consignation de la réduction d'essai de DAS

Si les procédures de réduction d'essai sont appliquées pendant les mesurages de DAS d'un DUT, le rapport de mesure doit contenir des informations supplémentaires relatives aux alternatives de réduction d'essai suivantes.

1) Réduction d'essai pour différents modes de fonctionnement à la même fréquence (voir 7.9.3.2). Le rapport de mesure doit donner une description détaillée de la manière dont les conditions de 7.9.3.2 ont été satisfaites.

2) Réduction d'essai fondée sur les caractéristiques de conception du DUT (voir 7.9.3.3). Le rapport de mesure doit comprendre des dessins ou des photographies représentant la configuration et les emplacements d'antennes dans le DUT, et décrivant les modes de fonctionnement sans fil applicables à chaque antenne afin d'étayer la réduction d'essai et l'exclusion d'essai envisagées.

3) Réduction d'essai fondée sur l'analyse de niveau de DAS maximal (voir 7.9.3.4). Le rapport de mesure doit contenir une description systématique de la manière dont le protocole de réduction d'essai de 7.9.3.4 a été appliqué pour les mesurages du DUT.

4) Réduction d'essai fondée sur des considérations d'émission multibande simultanée (voir 7.9.3.5). Le rapport de mesure doit contenir la puissance de sortie moyennée dans le temps mesurée et la manière dont elle satisfait au niveau de puissance de seuil disponible, conformément à la Formule (18) et à la Formule (19).

g) Récapitulatif du rapport de mesure (pour toutes données d'essai rapide de DAS et 'essai complet de DAS)

1) Bandes de fréquences et configurations:

i) liste de tous les modes de fonctionnement soumis à l'essai;

ii) liste de toutes les configurations d'essai.

2) Valeurs de DAS tabulées sur les positions, bandes, modes de fonctionnement et configurations d'essai du dispositif.

3) Résultats tabulaires et graphiques pour la valeur d'essai rapide de DAS le plus élevé pour chaque mode de fonctionnement.

IECNORM.COM : Click to view the full PDF of IEC/IEEE 62209-1528:2020

4) Résultats de tous les essais complets de DAS réalisés dans le cadre de 7.4 et 7.5, qui incluent la valeur de psDAS pour chaque essai exigé et une représentation graphique des balayages par rapport au dispositif.

5) Les valeurs liées aux conditions de la Formule (13) à la Formule (19) doivent être documentées dans le rapport de mesure.

6) Une justification systématique fondée sur 7.9.2 et 7.9.3 pour l'exclusion de l'essai complet de DAS doit être fournie.

7) Référence aux limites d'exposition et à une déclaration de conformité ou une liste des limites d'exposition et une déclaration de conformité.

h) Consignation des capteurs de proximité

Pour un DUT exigeant un essai de DAS avec des capteurs de proximité actifs, le rapport de mesure doit inclure toutes les exigences relatives à la consignation de 7.7. De plus, le rapport de mesure doit comprendre les éléments suivants.

1) Description des capteurs de proximité, des emplacements dans le DUT, des milieux équivalents aux tissus utilisés dans les procédures de déclenchement, et toute autre information pertinente.

2) Description du montage d'essai pour les mesurages de la puissance conduite (ou de la puissance rayonnée, si applicable).

3) Photos du montage d'essai.

4) Résultats tabulés des distances de déclenchement, couverture et sensibilité du capteur (capacité/mm telle que spécifiée par le fabricant du capteur). Les points de déclenchement doivent également être documentés graphiquement, l'antenne et le capteur étant clairement identifiés, avec toutes les dimensions correspondantes.

5) Le montage d'essai qui établit le mouvement de 1 mm par rapport à la distance de déclenchement doit être expliqué dans le rapport de mesure (voir 7.7.4).

6) La puissance de sortie mesurée ou l'état du capteur déterminé par le logiciel d'essai, dans les limites de ±5 mm des points de déclenchement ou tant que le DUT ne touche pas le fantôme, pour des mouvements à destination et en provenance du fantôme, doit être indiqué dans un tableau inséré dans le rapport (voir 7.7.4). La puissance de sortie (ou l'état du capteur si un logiciel d'essai est utilisé) en fonction de l'espacement entre le DUT et le fantôme doit également être tracée.

7) Le niveau de puissance lié à la défaillance et au dysfonctionnement du capteur, y compris tous les problèmes de conformité, doit être totalement documenté dans le rapport.

8) Si les procédures de déclenchement appliquées ont changé par rapport à celles présentées en 7.7, le rapport de mesure doit contenir les procédures de déclenchement spécifiques au produit. Il doit également contenir une description des conditions de déclenchement du capteur de proximité en mode de fonctionnement normal du DUT, de l'emplacement de chaque capteur de proximité, du mode d'émission applicable et de la plage de fréquences des antennes couverte par chaque capteur de proximité, ainsi que toute autre information exigée pour l'approbation réglementaire ou considérée comme étant pertinente pour les essais du dispositif.

9) Si des essais de DAS supplémentaires ont été exigés parce que l'emplacement de DAS maximal mesuré pour l'antenne ne se trouvait pas à l'intérieur de la zone de couverture de déclenchement, les configurations des essais supplémentaires doivent être clairement décrites et justifiées dans le rapport de mesure.

i) DAS moyenné dans le temps

1) Description/spécifications de l'aptitude du système de mesure de DAS à mesurer et capturer les résultats de l'algorithme de moyennage dans le temps, y compris le temps de réponse minimal.

2) Description de la mise en œuvre du moyennage dans le temps, y compris l'exactitude des algorithmes de moyennage, et du temps de réponse minimal nécessaire pour évaluer correctement le facteur TX.

IECNORM.COM : Click to view the full PDF of IEC/IEEE 62209-1528:2020

3) Description détaillée du logiciel de mode d'essai applicable, y compris le numéro de version, exigé pour obtenir le facteur TX le plus défavorable, si cela est exigé.

4) Les caractéristiques du signal qui sont contrôlées/modifiées par l'algorithme de moyennage dans le temps (puissance de sortie, facteur d'utilisation, modulation, débit binaire, etc.).

5) Les bandes de fréquences et modes de fonctionnement applicables.

6) Les conditions d'exposition et positions d'essai applicables, ainsi que les distances de séparation d'essai associées.

7) Évaluation du psDAS maximal pour tous les modes de fonctionnement applicables.

8) Évaluation du facteur TX, y compris la puissance de sortie/les tracés de mesure du DAS utilisés pour déterminer le facteur TX.

9) Considérations relatives au DAS d'émetteur simultané.

10) Évaluation du facteur TX répété pour la condition d'essai la plus défavorable. Si plusieurs mises en œuvre d'algorithme de moyennage dans le temps sont utilisées par le dispositif pour différents jeux de puces (une pour WLAN et une pour WWAN, par exemple), l'évaluation du facteur TX doit être répétée pour chaque jeu de puces de la configuration soumise à l'essai la plus défavorable.

11) Les mécanismes en place pour éviter de modifier le ou les algorithmes de régulations de puissance ou de les rendre accessibles à l'utilisateur.

12) L'évaluation de l'incertitude de mesure des résultats du DAS moyenné dans le temps.

13) Les résultats des calculs et/ou les mesurages réalisés pour valider la capacité du système de mesure à évaluer le facteur TX.

IECNORM.COM : Click to view the full PDF of IEC/IEEE 62209-1528:2020

Annexe A
(normative)

Vérification du système de mesure de DAS

A.1 Vue d'ensemble

Les procédures sont spécifiées pour les deux niveaux de vérification du système de mesure de DAS:

– contrôle du système;

– validation du système.

Le contrôle du système constitue une méthode d'essai rapide et fiable qui peut être appliquée en routine pour vérifier l'exactitude de mesure du système DAS. L'objectif est d'assurer que le système DAS et les milieux équivalents aux tissus sont acceptables pour réaliser un essai aux fréquences de fonctionnement d'un DUT. Le contrôle du système exige un fantôme plan (voir A.2.2) et une antenne à rayonnement (voir A.2.3).

La validation du système constitue un moyen de validation au niveau du système par rapport aux spécifications du système DAS et ses composants. Le montage d'essai est constitué d'un fantôme plan et d'une antenne de validation du système (Annexe D). Cet essai est effectué tous les ans (par exemple après l'étalonnage de la sonde), avant les mesurages relatifs à une comparaison interlaboratoire (Annexe T) et chaque fois que des modifications sont apportées au système, telles que de nouvelles sondes, des changements de logiciel, l'ajout de lectures électroniques différentes ou de sondes différentes.

Étant donné qu'un fantôme plan est utilisé, un contrôle du système et une validation du système ne résolvent pas le problème d'incertitude de mesure associée au fantôme SAM anthropomorphe (si applicable) et à la variabilité de positionnement du dispositif d'essai.

NOTE Pour les mesurages réalisés à l'aide du fantôme SAM anthropomorphe, des comparaisons interlaboratoires (voir l'Annexe T) permettent de quantifier la reproductibilité de mesure de DAS en utilisant un DUT de référence. Les mesurages couvrent à la fois la diffusion des données due à l'incertitude de positionnement du fantôme SAM et celle due à l'incertitude du dispositif, qui ne sont pas incluses dans le contrôle du système et la validation du système. Les essais peuvent également être utilisés pour établir l'exactitude et l'incertitude de mesure prévues entre différents laboratoires.

A.2 Contrôle du système

A.2.1 Objet

Le contrôle du système a pour objet de vérifier que le système fonctionne dans les limites de ses spécifications aux fréquences d'essai du dispositif. Le contrôle du système vérifie l'exactitude et la répétabilité de mesure d'un système DAS avant l'essai de conformité et n'est pas une validation de toutes les spécifications du système. Cette dernière n'est pas exigée pour soumettre à l'essai un dispositif, mais est obligatoire avant le déploiement du système. Le contrôle du système détecte les dérives possibles à court terme et les incertitudes ou erreurs de mesure inacceptables dans le système, telles que:

a) paramètres de milieu équivalent au tissu incorrects ou modifications des paramètres du milieu;

b) défaillances de composant du système d'essai;

c) dérive de composant du système d'essai;

d) erreurs de l'opérateur dans le montage de mesure ou les paramètres du logiciel;

e) autres conditions indésirables possibles dans la configuration du système (un brouillage radioélectrique, par exemple).

IECNORM.COM : Click to view the full PDF of IEC/IEEE 62209-1528:2020

Le contrôle du système est un mesurage de psDAS à 1 g ou à 10 g psDAS réalisé dans un montage simplifié avec une antenne de contrôle (voir A.2.3). Les composants du système, les logiciels, les réglages et les autres procédures du contrôle du système doivent les mêmes que ceux utilisés pour les essais de conformité. Le contrôle du système doit être effectué en utilisant le même milieu équivalent au tissu et le même point de fréquence d'étalonnage de sonde que ceux des essais de conformité, et dans la plage de fréquences valide de l'étalonnage de sonde, les propriétés diélectriques du milieu équivalent au tissu et le facteur d'adaptation de l'antenne exigés pour les mesurages de DAS. Le contrôle du système doit être réalisé à une fréquence fixe choisie dans les limites de validité des facteurs de conversion d'étalonnage, et dans les limites de ±10 % ou ±100 MHz de la fréquence centrale de l'essai de conformité, selon la valeur la plus élevée. Au-dessus de 6 GHz, la fréquence d'essai du contrôle du système doit être dans les limites de ±1 GHz de la fréquence centrale de l'essai de conformité. Les exigences environnementales pour les essais de contrôle du système sont spécifiées en 6.1.

Le contrôle du système doit être effectué dans les 24 h qui précèdent l'évaluation de DAS du DUT et sur le même système de mesure de DAS qui est utilisé pour l'évaluation de DAS du DUT.

Les critères d'acceptation du contrôle du système sont donnés en A.2.6.

A.2.2 Montage du fantôme

Un fantôme plan doit être utilisé avec le milieu recommandé équivalent au tissu pour le contrôle du système et la validation du système. Les spécifications pour le fantôme plan sont données à l'Article G.3.

Pour les antennes doublets, le point d'alimentation doit être positionné au-dessous du centre du fantôme plan (dimensions données en 6.2.4) et les bras du doublet doivent être alignés sur l'axe principal ou l'axe long du fantôme (voir D.2.1 pour les spécifications du doublet). Pour les guides d'ondes, le côté le plus long doit être aligné sur l'axe principal du fantôme. Pour les antennes cadres confinées (CLA), le dispositif doit être centré sous le milieu du fantôme plan. Pour les antennes doublets en serpentin, le point d'alimentation doit être positionné sous le centre du fantôme plan. Pour les VPIFA, le point d'alimentation doit être positionné au-dessous du centre du fantôme plan et le plan de masse (voir la Figure D.5) doit être aligné sur l'axe principal ou l'axe long du fantôme.

A.2.3 Antenne de contrôle du système

Le fantôme doit être exposé en utilisant une antenne pour la fréquence exigée (un doublet demi-onde, une CLA, une VPIFA, un doublet en serpentin, une antenne dalle ou un guide d'ondes ouvert, par exemple). Les antennes de validation du système (voir l'Annexe D) sont en général, mais pas nécessairement, utilisées pour le contrôle du système. Une antenne de contrôle du système doit avoir une bonne reproductibilité de positionnement, une bonne stabilité mécanique et une bonne adaptation d'impédance. Dans les instructions de positionnement suivantes, le doublet demi-onde est pris comme exemple pour représenter les exigences de positionnement de l'antenne de contrôle du système. Des instructions similaires doivent être appliquées pour les autres antennes.

Un doublet demi-onde doit être positionné sous la base du fantôme et centré avec son axe parallèle à la plus grande dimension du fantôme, dans les limites de ±2°. La distance entre la surface interne du fantôme et le point d'alimentation du doublet, s, est spécifiée pour chaque fréquence d'essai.

Pour les doublets de référence spécifiés à l'Article D.2, un écarteur diélectrique est utilisé pour fournir la distance s et la tolérance mécanique de l'écarteur, donnés par:

a) s = 15 mm ± 0,2 mm, pour 150 MHz ≤ f ≤ 1 000 MHz

b) s = 10 mm ± 0,2 mm, pour 1 000 MHz < f ≤ 6 000 MHz

c) s = 5 mm ± 0,1 mm, pour 6 000 MHz < f ≤ 10 000 MHz

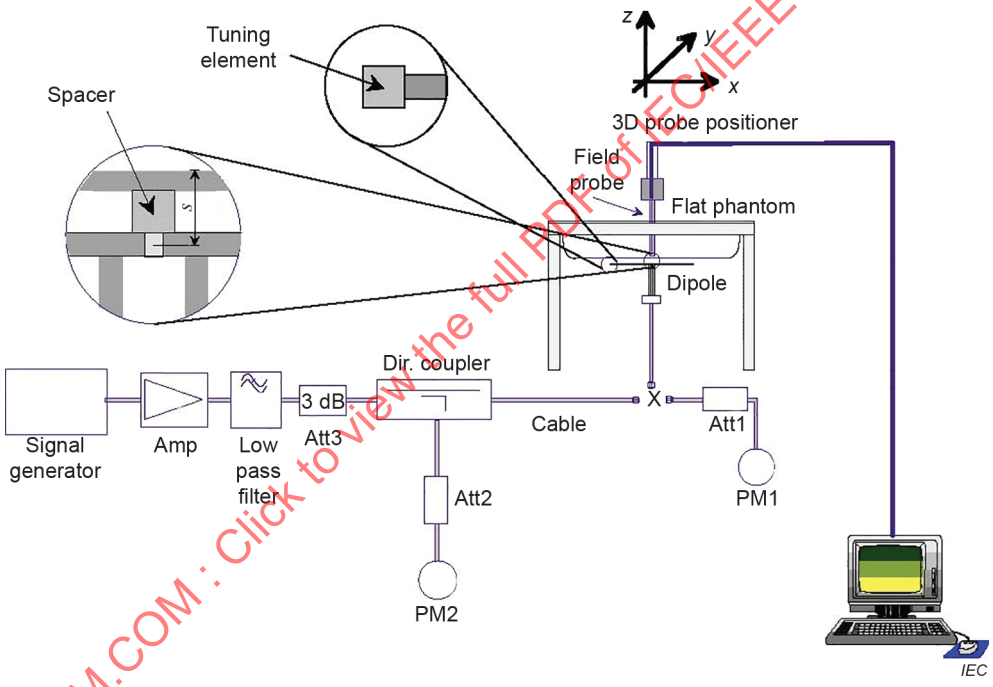
IECNORM.COM : Click to view the full PDF of IEC/IEEE 62209-1528:2020

Un écarteur de faible perte (tangente de perte < 0,05) et de faible permittivité (permittivité relative < 5) doit être utilisé pour établir la distance correcte entre le dessus de la surface du doublet et la surface de la base du fantôme. Sous 3 GHz, l'écarteur ne doit pas faire varier le psDAS à 1 g et à 10 g mesuré de plus de 1 %, comparé à l'état sans écarteur. Au-dessus de 3 GHz, l'écarteur peut affecter la valeur de DAS cible d'un doublet, et cela doit être pris en compte pour toute validation expérimentale supplémentaire (voir la NOTE 3 de D.2.2, Tableau D.2). Le facteur d'adaptation du doublet doit être supérieur à 20 dB à la fréquence d'essai de contrôle du système. Il doit être mesuré tous les ans pendant la validation du système en utilisant un analyseur de réseau, pour assurer que l'incertitude de mesure de DAS due à la réflexion de puissance reste faible.

A.2.4 Mesurage de la puissance d'entrée de la source de contrôle du système

L'incertitude de la puissance fournie à l'antenne doit être la plus faible possible. Le présent document exige l'utilisation d'un montage d'essai avec des coupleurs directifs et des wattmètres pendant le contrôle du système. Le montage recommandé est représenté à la Figure A.1 (qui utilise un doublet demi-onde en tant qu'exemple d'antenne de contrôle du système). Pour limiter la fluctuation de puissance lors du mesurage, un contrôle automatique du niveau de puissance d'entrée peut être mis en œuvre, comme cela est spécifié à l'Annexe V.

IECNORM.COM : Click to view the full PDF of IEC/IEEE 62209-1528:2020



Anglais	Français
Tuning element	Élément de réglage
Spacer	Écarteur
3D probe positioner	Positionneur de sonde 3D
Field probe	Sonde de champ
Flat phantom	Fantôme plan
Dipole	Doublet
Dir. Coupler	Coupleur directif
Signal generator	Générateur de signal
Low pass filter	Filtre passe-bas
Cable	Câble

NOTE Ce montage utilise une antenne doublet en tant qu'exemple pour représenter l'antenne de contrôle du système et les configurations de mesure. Un montage identique ou équivalent s'applique à d'autres antennes.

Figure A.1 – Montage d'essai pour le contrôle du système

Le facteur d'adaptation de l'antenne de contrôle du système doit être vérifié à l'aide d'un analyseur de réseau (pendant les intervalles annuels de caractérisation des performances, par exemple) afin d'assurer qu'il n'est pas supérieur à 20 dB. Si une antenne différente ou un guide d'ondes différent est utilisé lorsqu'une plus grande désadaptation est inhérente à la conception de l'antenne (par exemple, le guide d'ondes spécifié à l'Article D.3), un facteur d'adaptation plus faible est acceptable uniquement s'il a été totalement caractérisé comme étant stable. Le facteur d'adaptation spécifié doit être déterminé à la fréquence à laquelle le contrôle du système est effectué.

Les exigences relatives aux composants et à l'instrumentation sont les suivantes.

a) Le générateur de signal et les sorties de puissance de l'amplificateur doivent être stables à moins de 2 % (après préchauffage) de la valeur de sortie souhaitée. La puissance directe fournie à l'antenne de contrôle du système doit produire un psDAS d'au moins 0,4 W/kg. La plage de psDAS à 1 g ou à 10 g est comprise entre 0,4 W/kg et 10 W/kg. Si le générateur de signal peut délivrer au moins 15 dBm, un amplificateur n'est généralement pas nécessaire s'il est connecté à l'antenne de contrôle du système avec un câble à faible perte. Certains amplificateurs de forte puissance ne doivent pas fonctionner à un niveau très inférieur à leur puissance maximale de sortie. Par exemple, un amplificateur de puissance de 100 W fonctionnant avec une puissance de sortie de 250 mW peut générer trop de bruit. Un affaiblisseur placé entre le générateur de signal et l'amplificateur est recommandé pour protéger l'entrée de l'amplificateur.

b) Le filtre passe-bas inséré après l'amplificateur réduit l'effet des harmoniques et du bruit de l'amplificateur. Pour la plupart des amplificateurs dans les plages normales, le filtre n'est pas nécessaire.

c) L'affaiblisseur placé après l'amplificateur améliore l'adaptation et l'exactitude du capteur de puissance (consulter le manuel du wattmètre).

d) Le coupleur directif (facteur de couplage recommandé −20 dB) est utilisé pour contrôler la puissance directe et régler la sortie du générateur de signal pour une puissance directe constante à PM2. Le facteur d'adaptation du coupleur doit être supérieur à 25 dB aux accès d'entrée et de sortie. Un coupleur bidirectionnel est nécessaire lorsqu'une puissance directe et réfléchie doit être mesurée (lorsque des guides d'onde sont utilisés, par exemple).

e) Le wattmètre PM2 doit avoir une faible dérive et une résolution de 0,01 dB. Sinon, l'exactitude absolue a un impact négligeable sur le réglage de puissance au niveau de l'antenne de contrôle du système (aucun étalonnage absolu n'est exigé).

f) Le wattmètre PM1 et l'affaiblisseur Att1 doivent être des composants de haute qualité. Ils doivent être étalonnés, de préférence ensemble. L'affaiblisseur (−10 dB) améliore l'exactitude de la lecture de puissance (certaines têtes de haute puissance comportent un affaiblisseur incorporé étalonné). L'affaiblissement exact de l'affaiblisseur à la fréquence d'essai doit être connu. Pour certains affaiblisseurs, cette atténuation peut varier de ±0,2 dB par rapport à la valeur spécifiée sur la bande de fréquences de fonctionnement.

g) Un réglage de niveau de puissance fixe doit être utilisé pour PM1 et PM2 afin d'éviter les incertitudes de commutation de plage et de linéarité pour des mesurages de puissance. Si le niveau de puissance est ajusté, le même réglage de niveau de puissance doit être utilisé pour PM1 et PM2.

h) L'antenne de contrôle du système doit être raccordée directement au câble à la position X. Si le wattmètre comporte un type de connecteur différent, des adaptateurs de haute qualité doivent être utilisés.

i) La perte d'insertion des câbles, en particulier le câble qui relie le coupleur directif à l'antenne, doit être régulièrement contrôlée pour assurer que la perte d'insertion est stable entre les fréquences. Il convient de considérer qu'un câble qui fonctionne bien à une fréquence donnée (par exemple, 900 MHz) peut ne pas fonctionner de façon équivalente à une fréquence différente (par exemple, 5 GHz). Pendant des mesurages de contrôle du système, tous les mouvements du câble doivent être évités étant donné que cela peut modifier les caractéristiques de perte du câble et introduire des erreurs de DAS.

IECNORM.COM : Click to view the full PDF of IEC/IEEE 62209-1528:2020

A.2.5 Procédure de contrôle du système

Le contrôle du système est un mesurage complet de psDAS à 1 g et/ou 10 g réalisé conformément aux exigences de A.2.1 à A.2.4.

Les antennes de contrôle du système peuvent avoir deux paires de valeurs cibles:

a) Cibles numériques $DAS_{1g,num}$ et $DAS_{10g,num}$ – Si les antennes de l'Annexe D sont utilisées, les cibles numériques indiquées à l'Annexe D doivent être utilisées. Sinon, les cibles numériques doivent être déterminées selon les exigences de l'Article D.1.

b) Cibles expérimentales $DAS_{1g,sys}$ et $DAS_{10g,sys}$ – Il s'agit des valeurs de DAS mesurées des antennes de contrôle du système spécifiques. Elles sont déterminées à l'aide d'un montage d'essai de contrôle du système (voir A.2.4) avec un équipement étalonné. Les cibles expérimentales doivent être déterminées par le laboratoire d'étalonnage dans les deux semaines qui suivent l'étalonnage de l'antenne. $DAS_{1g,sys}$ et $DAS_{10g,sys}$ doivent être fournies par l'utilisateur. Les valeurs de $DAS_{1g,sys}$ et de $DAS_{10g,sys}$ ne doivent pas s'écarter des cibles numériques $DAS_{1g,num}$ et $DAS_{10g,num}$ de plus de ±10 %.

A.2.6 Critères d'acceptation du contrôle du système

Le psDAS à 1 g et/ou 10 g mesuré doit être normalisé à 1 W par la puissance d'entrée de l'antenne de contrôle du système (puissance directe des doublets, doublet en serpentin, VPIFA et CLA, et puissance nette pour les guides d'ondes). Les valeurs de DAS normalisées, $DAS_{1g,meas}$ et $DAS_{10g,meas}$, sont comparées aux cibles. Les exigences suivantes s'appliquent.

a) Les valeurs de psDAS mesurées ne doivent pas s'écarter des cibles numériques de plus de la valeur égale à l'incertitude de mesure élargie des antennes de contrôle du système, $2u_s$ ou ±15 %, selon la valeur la plus faible, comme cela est indiqué dans la Formule (A.1) et la Formule (A.2).

$$\left|DAS_{1g,meas} - DAS_{1g,num}\right| \Big/ DAS_{1g,num} \leq 2 \cdot u_{s,1g} \tag{A.1}$$

$$\left|DAS_{10g,meas} - DAS_{10g,num}\right| \Big/ DAS_{10g,num} \leq 2 \cdot u_{s,10g} \tag{A.2}$$

b) La valeur de psDAS mesurée ne doit pas s'écarter des cibles expérimentales de plus de ±10 %, comme cela est indiqué dans la Formule (A.3) et la Formule (A.4).

$$\left|DAS_{1g,meas} - DAS_{1g,sys}\right| \Big/ DAS_{1g,sys} \leq 10\ \% \tag{A.3}$$

$$\left|DAS_{10g,meas} - DAS_{10g,sys}\right| \Big/ DAS_{10g,sys} \leq 10\ \% \tag{A.4}$$

IECNORM.COM : Click to view the full PDF of IEC/IEEE 62209-1528:2020

A.3 Validation du système

A.3.1 Objet

La procédure de validation du système soumet à l'essai le système *DAS* en utilisant des antennes de validation du système afin de vérifier l'exactitude de mesure et les performances de la sonde, les lectures électroniques et le logiciel du système. C'est une validation du système par rapport à toutes les spécifications de performances. Ce montage utilise un fantôme plan et une antenne de validation du système définie à l'Annexe D. Par conséquent, ce processus de validation ne comprend pas l'incertitude de diffusion des données et de positionnement du dispositif. La validation du système doit être effectuée au moins une fois par an, lorsqu'un nouveau système est mis en service ou chaque fois que des modifications ont été apportées au système, par exemple une mise à jour de logiciel, l'utilisation d'une lecture électronique différente ou de types de sondes différents et après l'étalonnage de sonde. La validation du système doit être effectuée avec une sonde étalonnée.

L'objectif de l'Article A.3 est de présenter une méthodologie pour la validation du système de mesure de *DAS*. Étant donné que l'équipement de mesure de *DAS*, les techniques d'étalonnage, les fantômes et les milieux équivalents aux tissus peuvent varier d'un laboratoire à un autre, une méthodologie de validation est nécessaire pour assurer que des résultats uniformes sont obtenus dans les limites d'incertitude de mesure raisonnable. Les valeurs de DAS de référence calculées numériquement pour les antennes de validation du système définies en A.3.3 sont répertoriées dans le Tableau D.2, dans le Tableau D.4, dans le Tableau D.5, dans le Tableau D.7 et dans le Tableau D.10. Ces valeurs numériques ont également fait l'objet d'une validation expérimentale. Les exigences environnementales pour les essais de validation du système sont spécifiées en 6.1.

A.3.2 Montage du fantôme

Le montage du fantôme plan décrit pour le contrôle du système (voir A.2.2 et la Figure A.1) est également utilisé pour les essais de validation du système. La validation du système doit être effectuée en utilisant des milieux équivalents aux tissus ayant les propriétés diélectriques définies dans le Tableau 2 (voir 6.2.2).

A.3.3 Antennes de validation du système

Les antennes de validation du système sont spécifiées à l'Annexe D.

A.3.4 Mesurage de la puissance d'entrée

Le montage de mesure de la puissance d'entrée spécifié pour le contrôle du système (la A.2.4) est également utilisé pour les essais de validation du système.

A.3.5 Procédure de validation du système

La validation du système est utilisée pour vérifier l'exactitude de mesure d'un système DAS complet, y compris les algorithmes du logiciel. Les incertitudes de positionnement du dispositif d'essai et de la forme du fantôme ne sont pas prises en considération dans la validation du système. La puissance directe doit être limitée de sorte que les valeurs de DAS mesurées soient dans les limites de la plage dynamique de la sonde afin d'éviter d'endommager la sonde.

La procédure de validation du système comprend jusqu'à sept étapes, c'est-à-dire les étapes a) à g) suivantes. L'étape a) doit être effectuée pour chaque combinaison de sonde, lecture électronique et version du système de mesure et de post-traitement, chaque fois que la validation du système est exigée. Les essais b) à f) doivent être réalisés à chaque fois que les composants du système ont été modifiés (nouvelle version de logiciel, nouvelles lectures électroniques, nouvelle sonde ou nouveaux étalonnages, par exemple). L'étape g) peut être ignorée si des informations suffisantes sont fournies à l'utilisateur par le fabricant du système selon lesquelles le bilan d'incertitude est valable pour les sources à couplage capacitif. La procédure de validation du système est la suivante.

IECNORM.COM : Click to view the full PDF of IEC/IEEE 62209-1528:2020

a) Évaluation du DAS: Un mesurage complet du psDAS à 1 g et/ou 10 g est réalisé à l'aide d'une antenne de validation du système comme cela est spécifié à l'Annexe D. La puissance d'entrée de l'antenne de validation du système est ajustée de manière à produire une valeur de psDAS à 1 g et/ou 10 g dans les limites de la plage comprise entre 0,4 W/kg et 10 W/kg. Le psDAS à 1 g et/ou 10 g est mesuré aux fréquences indiquées dans le Tableau D.2, dans le Tableau D.4, dans le Tableau D.5, dans le Tableau D.7 et dans le Tableau D.10. Les résultats du psDAS sont normalisés tel que cela est spécifié dans le Tableau D.2 (antennes doublets), dans le Tableau D.4 (guides d'ondes), dans le Tableau D.5 (CLA), dans le Tableau D.7 (doublet en serpentin), ou dans le Tableau D.10 (VPIFAs) puis sont comparés aux valeurs de DAS numériques normalisées. Les différences entre les valeurs mesurées et les valeurs numériques cibles doivent être inférieures à l'incertitude élargie pour la validation du système en utilisant les procédures du Tableau 9, sans toutefois dépasser 10 %.

b) Routine d'extrapolation: Les valeurs locales de DAS sont mesurées le long d'un axe vertical directement au-dessus du centre de l'antenne de validation du système (c'est-à-dire, le point d'alimentation du doublet, de l'antenne en serpentin ou de la VIPFA, de la ligne centrale du guide d'ondes ou du centre de la CLA) en utilisant le même écartement des points de grille d'essai que lors du balayage-zoom dans les évaluations de DAS de DUT. Les valeurs mesurées sont extrapolées à la surface du fantôme et comparées à la valeur numérique cible appropriée indiquée dans le Tableau D.2 (colonne 5), dans le Tableau D.4 (colonne 5 avec d = 0), dans le Tableau D.5 (colonne 5), dans le Tableau D.7 (colonne 5) et dans le Tableau D.10 (colonne 5). Si l'antenne doublet, le doublet en serpentin ou la VPIFA est utilisé(e), ce mesurage est répété le long d'un autre axe vertical avec un décalage transversal de 2 cm (direction y de la Figure A.1) à partir du point d'alimentation. Les valeurs de DAS sont extrapolées à la surface du fantôme et comparées aux valeurs numériques normalisées indiquées dans la Colonne 6 du Tableau D.2, la colonne 6 du Tableau D.5 et la colonne 6 du Tableau D.10. La différence entre les valeurs extrapolées et les valeurs numériques cibles indiquées dans le Tableau D.2 (ou les valeurs pour l'antenne spécifique utilisée) doit être inférieure à l'incertitude élargie pour la validation du système en utilisant les procédures du Tableau 9 ou de 15 %, selon la valeur la moins élevée. Il est à noter que l'Étape b) peut être effectuée en même temps que l'Étape a) si un balayage-zoom agrandi est utilisé à l'Étape a) pour obtenir les valeurs de DAS extrapolées.

c) Linéarité de sonde pour CW – signaux équivalents: Les mesurages de l'Étape a) sont répétés en utilisant différents niveaux de puissance d'entrée. Les niveaux de puissance pour chaque fréquence sont sélectionnés afin de produire des valeurs de psDAS à 1 g ou 10 g d'environ 10 W/kg, 2 W/kg, 0,4 W/kg et 0,12 W/kg. Les valeurs de psDAS mesurées sont normalisées comme cela est indiqué dans les tableaux correspondants (voir l'étape a) et comparées aux résultats mesurés normalisés de l'Étape a). La différence entre ces valeurs doit être inférieure à l'incertitude élargie pour la composante de linéarité en utilisant les procédures du Tableau 9 et de 8.4.1.3 ou de 10 %, selon la valeur la moins élevée.

d) Linéarité de sonde pour des signaux pulsés périodiques: Cette étape doit être réalisée après avoir satisfait aux des exigences de l'Étape c). Les mesurages de l'étape a) sont répétés avec des signaux modulés par impulsions ayant un facteur d'utilisation de 0,1 et un régime de répétition des impulsions de 10 Hz. La puissance est réglée pour produire un psDAS à 1 g ou 10 g d'environ 8 W/kg avec le signal modulé par impulsions périodiques ou un DAS maximal d'environ 80 W/kg. Les valeurs de psDAS mesurées sont mises à l'échelle selon un facteur d'utilisation de 1, puis normalisées comme cela est indiqué dans les tableaux correspondants (voir l'étape a)) et comparées aux résultats mesurés normalisés de l'étape a). La différence entre ces valeurs doit être inférieure à l'incertitude élargie pour la validation du système en utilisant les procédures du Tableau 9 ou de 10 %, selon la valeur la moins élevée.

IECNORM.COM : Click to view the full PDF of IEC/IEEE 62209-1528:2020

e) Linéarité de la sonde pour les signaux non modulés en impulsions (signaux AMCR et OFDM, par exemple): Les mesurages de l'étape a) sont répétés avec les modes de fonctionnement spécifiques qui sont soumis à l'essai par le laboratoire. Cet essai peut être effectué à une seule fréquence par mode de fonctionnement. La puissance est réglée pour produire un psDAS à 1 g d'environ 8 W/kg. Si le rapport puissance de crête à puissance moyenne du mode de fonctionnement spécifique est suffisamment élevé de sorte que le DAS maximal local dépasse la plage dynamique du système, il convient de réduire la puissance d'entrée afin de produire un psDAS à 1 g inférieur à 8 W/kg, mais toujours aussi élevé que possible. Les valeurs de psDAS mesurées sont mises à l'échelle selon un facteur d'utilisation de 1, puis normalisées comme cela est indiqué dans les tableaux correspondants (voir l'étape a)) et comparées aux résultats mesurés normalisés de l'étape a). La différence entre ces valeurs doit être inférieure à l'incertitude élargie pour la validation du système en utilisant les procédures du Tableau 9 ou de 10 %, selon la valeur la moins élevée.

NOTE 1 Une procédure plus détaillée de validation du système pour tous les modes de fonctionnement est prévue dans une révision ultérieure du présent document par un amendement, une révision ou un Rapport technique d'accompagnement. La procédure permet d'assurer que la bande passante de la source est suffisante pour couvrir la bande passante de canal et tous les modes d'agrégation de porteuse.

f) Isotropie axiale de la sonde: Le centre géométrique des capteurs de la sonde est placé directement au-dessus du centre de l'antenne de validation du système à une distance de mesure d'environ 1 diamètre d'extrémité de sonde de la surface interne du fantôme. La sonde tourne autour de son axe ±180° par pas de 15° maximum. Les lectures maximale et minimale de DAS sont consignées. La différence entre ces valeurs doit être inférieure à l'incertitude élargie pour la composante d'isotropie axiale en utilisant les procédures du Tableau 9 et de 8.4.1.5 ou de 5 %, selon la valeur la moins élevée.

g) Évaluation du DAS pour la composante de champ E perpendiculaire à la surface du fantôme: Un mesurage complet du psDAS à 1 g et/ou 10 g est réalisé à l'aide des VPIFA spécifiées à l'Article D.5. Il convient d'utiliser le balayage-zoom pour des fréquences supérieures à 3 GHz spécifiées en 7.4.2, quelle que soit la fréquence de fonctionnement de la VPIFA. Les résultats sont normalisés à une puissance directe de 1 W, puis comparés aux valeurs de référence numérique de l'Article D.5. Cette validation a pour objet de soumettre à l'essai l'exactitude du système de mesure à l'aide d'antennes ayant une composante de champ E normale dominante. Cette étape soumet à l'essai la mise en œuvre du système et la conception de la sonde pour déterminer leur pertinence pour les champs à couplage capacitif. Ils peuvent être réalisés par le fabricant du système de mesure et ne nécessitent pas d'être répétés par le laboratoire d'essai tant que la documentation appropriée est disponible auprès du fabricant. Les différences entre les valeurs mesurées et les valeurs numériques cibles doivent être inférieures à l'incertitude élargie pour la validation du système, mais ne pas être supérieures à 10 %.

NOTE 2 La procédure du système de validation n'est ni une alternative à l'étalonnage de sonde ni une alternative à l'estimation de l'incertitude de l'Article 8. La sonde et la lecture électronique sont étalonnées régulièrement conformément aux procédures données à l'Annexe E. L'isotropie hémisphérique de la sonde n'est pas prise en considération dans le protocole pour la validation du système.

Pour les fréquences inférieures à 300 MHz, les antennes de validation appropriées spécifiées à l'Annexe D doivent être utilisées pour procéder à la validation du système.

A.4 Validation du système et contrôle du système d'essai rapide de DAS

A.4.1 Généralités

Les méthodes d'essai rapide de DAS de Classe 1 et de Classe 2 spécifiées en 7.9.2 reposent généralement sur des hypothèses ou des approximations qui sont typiques de chaque méthode rapide de DAS et s'écartent de la procédure de mesure normalisée. Pour un système de mesure de DAS donné, étant donné que les essais rapides de DAS reposent sur des simplifications et approximations spécifiques à chaque approche, les méthodes de contrôle du système et de validation du système exigées pour les essais complets de DAS ont été jugées insuffisantes pour mettre en œuvre les méthodes rapides de DAS de 7.9.2. Par conséquent, de nouvelles méthodes de contrôle du système et de validation du système sont introduites.

IECNORM.COM : Click to view the full PDF of IEC/IEEE 62209-1528:2020

Le A.4.2 décrit la validation du système qui doit être effectuée par le développeur de méthode. Il définit un ensemble d'exigences ou principes minimaux à appliquer par le développeur de méthode rapide de DAS pour valider que la méthode a été correctement mise en œuvre. Ces exigences sont également des exigences minimales applicables aux méthodes rapides de DAS décrites à l'Annexe C. Le développeur doit clairement documenter les calculs, les mesurages et autres évaluations effectués pour valider la méthode rapide de DAS pour que les utilisateurs déterminent comment appliquer la méthode spécifique pour l'évaluation de DAS. Toutes les analyses ou conditions supplémentaires auxquelles l'utilisateur doit satisfaire pour appliquer la méthode rapide de DAS doivent être clairement spécifiées.

Le A.4.3 décrit le contrôle du système de méthode rapide de DAS que l'utilisateur doit effectuer. Pour un système de mesure de DAS donné, une seule antenne de contrôle du système peut être utilisée pour les essais complets de DAS et les essais rapides de DAS en utilisant les procédures de l'Article A.2 et de A.4.3.

A.4.2 Validation du système d'essai rapide de DAS

La validation du système d'essai rapide de DAS est un moyen de quantifier la validité et la fiabilité de la méthode. Étant donné que la validation et l'incertitude de mesure sont toutes deux déterminées par le développeur de la méthode d'essai rapide de DAS, la validation du système permet également de confirmer la validité du bilan d'incertitude. Les principes suivants sont appliqués pour la validation du système d'une méthode rapide de DAS de Classe 2.

a) Plusieurs radiateurs avec des distributions de DAS adaptées pour valider la méthode doivent être utilisées. Les radiateurs peuvent être des DUT sans fil ou d'autres antennes ou guides d'ondes qui satisfont aux exigences de l'Article A.4. Plusieurs échantillons (un échantillon par bande, par exemple) peuvent être utilisés pour la validation du système d'essai rapide de DAS. Le développeur doit démontrer que la méthode d'essai rapide de DAS n'est pas biaisée par les radiateurs ou distributions de DAS sélectionné(e)s pour valider ou étalonner la méthode pour de tels radiateurs.

b) La validation du système doit être effectuée sur l'ensemble de la plage de fréquences de fonctionnement, des modes de fonctionnement, des niveaux de puissance (par exemple, psDAS à 10 g entre 0,1 W/kg et 10 W/kg), des configurations de fonctionnement du dispositif, des conditions d'exposition et des distributions de DAS qui sont spécifiés avec la méthode et utilisés pour l'évaluation du dispositif.

c) Les radiateurs choisis doivent couvrir la plage de distributions de DAS (par exemple, des distributions avec un DAS supérieur à −3 dB d'un maximum local dans un rayon allant de 5 mm à 50 mm, une polarisation dominante à la fois perpendiculaire et parallèle à la surface du fantôme, des emplacements à l'intérieur de la zone de mesure définis pour la méthode d'essai rapide de DAS et le nombre de DAS maximaux) prises en charge par la méthode d'essai rapide de DAS. Le développeur de méthode d'essai rapide de DAS doit spécifier les radiateurs utilisés pour valider la méthode d'essai rapide de DAS particulière et donner les informations détaillées nécessaires relatives à la validation afin de veiller à ce que les utilisateurs puissent appliquer correctement la méthode.

d) Les radiateurs doivent être choisis de sorte que l'incertitude de mesure lors de la validation du système ne dépende pas ou ne soit pas fortement dominée par le radiateur (le positionnement, l'incertitude ou l'antenne de validation, par exemple) et les configurations du fantôme

e) Un minimum de 10 configurations doit être soumis à l'essai, par bande de fréquences, de sorte que la confiance dans la validation du système soit élevée. Cela peut être obtenu, par exemple, en utilisant deux radiateurs à cinq distances ou orientations différentes.

Les protocoles et procédures de validation du système, ainsi que les antennes de validation, utilisés avec des systèmes reposant sur des mesurages vectoriels, sont donnés dans l'IEC 62209-3. Les recommandations en matière de validation de l'IEC 62209-3 doivent être appliquées pour les besoins de l'essai conformément à l'Annexe A.

IECNORM.COM : Click to view the full PDF of IEC/IEEE 62209-1528:2020

Une incertitude de DAS pour la validation du système d'essai rapide de DAS est déterminée en comparant le psDAS déterminé avec la méthode d'essai rapide de DAS, $DAS_{\text{rapide},i}$ au DAS cible de l'essai complet de DAS, $DAS_{\text{complet},i}$, pour la *i*-ème configuration d'essai (radiateur, fréquence, distribution de DAS). L'écart type de la différence entre les deux méthodes est déterminé selon la Formule (A.5), la Formule (A.6) et la Formule (A.7):

$$DAS_{\text{tol}}[\%] = \sqrt{\frac{1}{N}\sum_{i=1}^{N}(\Delta_i - \mu)^2} \tag{A.5}$$

$$\Delta_i[\%] = 100 \times \left(\frac{DAS_{\text{rapide},i} - DAS_{\text{complet},i}}{DAS_{\text{complet},i}} \right) \tag{A.6}$$

$$\mu = \frac{1}{N}\sum_{i=1}^{N}\Delta_i \tag{A.7}$$

La validation du système doit être appliquée séparément pour chaque bande de fréquences et mode de fonctionnement pris en charge par la méthode d'essai rapide de DAS et tel qu'utilisé pour l'évaluation du dispositif.

L'écart type de la Formule (A.6) doit être dans les limites de l'incertitude-type de la méthode d'essai rapide de DAS (Tableau 9 et Annexe C). Sinon, le développeur de la méthode d'essai rapide de DAS doit réviser l'incertitude composée de la méthode d'essai rapide de DAS en fonction des résultats de validation du système, ou déterminer si la méthode d'essai rapide de DAS est applicable.

La validation du système d'essai rapide de DAS doit être effectuée lorsque des modifications sont apportées aux algorithmes d'essai rapide de DAS ou de post-traitement. Un récapitulatif des méthodes et résultats de validation du système du développeur doit être décrit dans le rapport de DAS pour appuyer les résultats d'essai.

A.4.3 Contrôle du système d'essai rapide de DAS

A.4.3.1 Généralités

Le contrôle du système DAS est un moyen aisé pour les laboratoires de vérifier la fiabilité et la cohérence de l'essai rapide de DAS mis en œuvre dans un système DAS. Les exigences de contrôle du système d'essai rapide de DAS sont similaires au contrôle du système de l'essai complet de DAS, comme cela est décrit à l'Article A.2. Les principes suivants s'appliquent pour le contrôle du système DAS.

a) Il est appliqué séparément pour chaque bande de fréquences dans laquelle des composants du système (la sonde, le milieu équivalent au tissu, par exemple) sont différents.

b) Il doit être effectué dans les 24 h précédant l'essai rapide de DAS du DUT.

c) Il doit être effectué sur le même système de mesure que celui utilisé pour l'essai rapide de DAS du DUT.

d) Il est effectué en utilisant une seule antenne de contrôle du système (les antennes doublets ou les guides d'ondes et le montage décrits à l'Article A.2 ou un autre radiateur bien caractérisé). La valeur de référence d'essai rapide de DAS pour le radiateur doit être déterminée pour le montage de contrôle du système d'essai rapide de DAS, et un bilan d'incertitude de mesure pour le contrôle du système doit être fourni.

IECNORM.COM : Click to view the full PDF of IEC/IEEE 62209-1528:2020

A.4.3.2 Critères d'acceptation pour le contrôle du système d'essai rapide de DAS

Le résultat de mesure du contrôle du système d'essai rapide de DAS est comparé à la valeur de référence d'essai rapide de DAS pour le même radiateur et la même bande de fréquences. Les critères d'acceptation sont les mêmes que ceux du contrôle du système complet de DAS.

a) Les valeurs mesurées, $DAS_{1g,meas}$ et $DAS_{10g,meas}$, sont comparées aux cibles numériques $DAS_{1g,num}$ et/ou $DAS_{10g,num}$. La différence est dans les limites des écarts types de l'incertitude-type du système de méthode rapide de DAS u_s décrits dans la Formule (A.8) et la Formule (A.9):

$$\left|DAS_{1g,meas} - DAS_{1g,num}\right| \Big/ DAS_{1g,num} \leq 2 \cdot u_{s,1g} \tag{A.8}$$

$$\left|DAS_{10g,meas} - DAS_{10g,num}\right| \Big/ DAS_{10g,num} \leq 2 \cdot u_{s,10g} \tag{A.9}$$

b) Toutes les valeurs mesurées sont dans les limites de ±10 % des cibles relatives $DAS_{1g,sys}$ et $DAS_{10g,sys}$ pour ce système de mesure de la méthode d'essai rapide de DAS utilisant l'antenne de contrôle du système et le même système ou type de système que celui décrit dans la Formule (A.10) et dans la Formule (A.11):

$$\left|DAS_{1g,meas} - DAS_{1g,sys}\right| \Big/ DAS_{1g,sys} \leq 10\ \% \tag{A.10}$$

$$\left|DAS_{10g,meas} - DAS_{10g,sys}\right| \Big/ DAS_{10g,sys} \leq 10\ \% \tag{A.11}$$

Sinon, le système d'essai rapide de DAS ne doit pas être utilisé pour les besoins de l'essai de conformité.

IECNORM.COM : Click to view the full PDF of IEC/IEEE 62209-1528:2020

Annexe B
(informative)

Informations de support de réduction d'essai DAS

B.1 Généralités

L'Annexe B donne des informations de support utiles relatives aux procédures de réduction d'essai introduites en 7.9.3.

L'Article B.2 concerne la procédure de réduction d'essai fondée sur les caractéristiques de conception de DUT, tandis que l'Article B.4 concerne la procédure de réduction d'essai fondée sur l'analyse de niveau de DAS. Enfin, l'Article B.5 décrit d'autres approches statistiques possibles pour identifier des conditions d'essai de DAS élevées. L'Article B.5 donne des informations générales plutôt que des procédures détaillées. Pour cette raison, les approches décrites à l'Article B.5 exigent généralement une participation importante de l'utilisateur pour déterminer des configurations d'essai qui peuvent être effectivement exclues. En conclusion, il est fortement recommandé de ne pas utiliser les approches statistiques décrites à l'Article B.5 pour les besoins de l'essai de conformité. En principe, elles peuvent cependant être utilisées à des fins d'investigation initiales (par exemple, conformité préalable aux stades de recherche et de développement).

B.2 Réduction d'essai fondée sur les caractéristiques de conception du DUT

B.2.1 Généralités

Lorsque les premières éditions de l'IEEE 1528 et de l'IEC 62209 ont été initialement développées, de nombreux DUT comportaient des antennes rétractables. Il a été considéré que la position "incliné" peut induire un DAS plus élevé dans la tête comparée à la position de toucher ou la position "joue", étant donné que l'inclinaison du DUT peut diminuer la distance de séparation entre l'antenne rétractable et la tête. Cependant, la grande majorité des conceptions récentes de DUT contiennent des antennes internes. Au contraire, lorsque l'antenne est située à la base du DUT, la position "incliné" augmente la distance de séparation entre l'antenne et la tête. De plus, les contributions au DAS dans la tête dues aux courants RF qui circulent sur la surface du DUT diminuent lorsque le téléphone est dans la position "incliné", à nouveau en raison de la séparation augmentée.

B.2.2 Vue d'ensemble de l'analyse statistique

B.2.2.1 Objectifs et hypothèses

Après des années d'essai, l'expérience a démontré que pour des antennes internes, la valeur de DAS dans la position "incliné" est généralement plus faible que la valeur de DAS au niveau de la joue dans la même configuration d'essai. L'objectif était de procéder à une analyse de probabilité de la relation entre le DAS mesuré dans la position "incliné" et la position "joue" pour les mêmes configurations d'essai afin de déterminer si, et dans quelles conditions, l'essai dans la position "incliné" peut être éliminé.

L'hypothèse pour cette étude est qu'il existe une très faible probabilité que la valeur de DAS dans la position "incliné" puisse dépasser le DAS dans la position "joue" de plus d'un facteur de deux et, par conséquent, le DAS dans la position "incliné" ne peut pas dépasser la limite applicable de DAS, et il est attendu que le dispositif soit conforme à la réglementation relative au DAS si le DAS dans la position "joue" est 3 dB au-dessous de la limite applicable de DAS.

IECNORM.COM : Click to view the full PDF of IEC/IEEE 62209-1528:2020

B.2.2.2 DUT analysé

L'analyse est réalisée avec 139 DUT provenant de deux fabricants de DUT (qui sont principalement des modèles 2009). L'analyse inclut des DUT avec différentes positions d'antenne, différents types de dispositifs et plusieurs bandes de fréquences de fonctionnement. Dans la plupart des cas, des valeurs de psDAS à 1 g et 10 g sont mesurées et, par conséquent, le nombre total de mesurages de DAS utilisés pour l'analyse sont effectivement supérieurs au nombre de DUT (139). Le Tableau B.1 présente les caractéristiques de base des DUT utilisés pour l'étude.

Tableau B.1 – Nombre de DUT utilisés pour l'étude statistique

Type de DUT	Fabricant A	Fabricant B	Total
Total	112	27	139
Antenne en haut	30	14	44
Antenne en bas	82	13	95
Coulissant, ouvert	29	4	33
Coulissant, fermé	58	8	66
Coquille	23	4	27
Barre	60	19	79

B.2.3 Résultats d'analyse

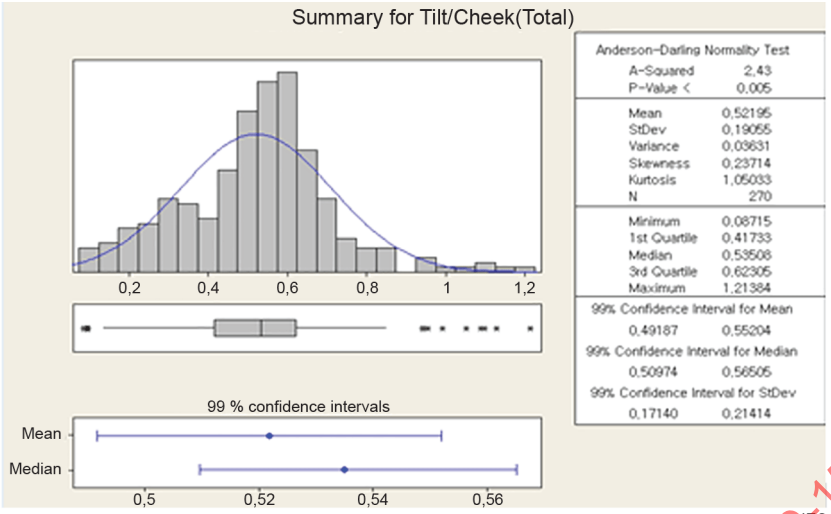
B.2.3.1 Résultats d'analyse totaux

Le B.2.3 décrit le résultat de l'analyse statistique avec 270 résultats d'essai comprenant des valeurs de psDAS à 1 g et 10 g de tous les dispositifs d'essai indépendamment des types de DUT, positions d'antenne et fabricants. La Figure B.1 représente la distribution de valeurs "Incliné/Joue" pour les dispositifs d'essai. Les valeurs moyennes et d'écart type sont de 0,52 et 0,19 respectivement.

Le Tableau B.2 indique la probabilité que le DAS dans la position "incliné" sur le DAS dans la position "joue" soit plus élevé que certaines valeurs (x) analysées en utilisant une loi normale et une analyse de probabilité cumulative fondée sur la moyenne et l'écart type identifiés avec les données d'échantillon représentées à la Figure B.1. Bien que la distribution réelle soit proche d'une distribution gamma, l'analyse a été réalisée en prenant pour hypothèse une loi normale étant donné que celle-ci donne une limite supérieure pour la fonction de probabilité et simplifie considérablement le calcul.

Le résultat d'analyse indique que la probabilité que le DAS dans la position "incliné" soit supérieur au double du DAS sur la joue est de $4{,}330 \times 10^{-15}$, ce qui peut être considéré comme une probabilité nulle. Même la probabilité que le DAS dans la position "incliné" soit supérieur au DAS sur la joue est de $6{,}057 \times 10^{-3}$, cette probabilité est toujours très faible.

IECNORM.COM : Click to view the full PDF of IEC/IEEE 62209-1528:2020



Anglais	Français
Summary for Tilt/Cheek	Récapitulatif pour Incliné/Joue
Mean	Moyen
Median	Médian
90 % confidence intervals	Intervalles de confiance de 90 %

Figure B.1 – Distribution de "Incliné/Joue"

Tableau B.2 – Résultats d'analyse statistique de P(Incliné/Joue > x) pour différentes valeurs de x

x	P(Incliné/Joue > x)
1,0	$6{,}057 \times 10^{-3}$
1,1	$1{,}208 \times 10^{-3}$
1,2	$1{,}866 \times 10^{-4}$
1,3	$2{,}221 \times 10^{-5}$
2,0	$4{,}330 \times 10^{-15}$

IECNORM.COM : Click to view the full PDF of IEC/IEEE 62209-1528:2020

B.2.3.2 Comparaison entre le psDAS à 10 g et 1 g

Le Tableau B.3 est le résultat d'analyse indiquant les différences entre le psDAS à 1 g et le DAS moyen à 10 g. Il indique la probabilité que le DAS en position "incliné" soit supérieur au double du DAS sur la joue est de $6{,}428 \times 10^{-14}$ même pour les bandes de fréquences élevées.

Tableau B.3 – Résultats d'analyse statistique de P(Incliné/Joue > x) pour un psDAS à 1 g et 10 g

x	P(Incliné/Joue > x)	
	psDAS à 10 g	psDAS à 1 g
1,0	$4{,}307 \times 10^{-3}$	$4{,}307 \times 10^{-3}$
1,1	$7{,}122 \times 10^{-4}$	$7{,}122 \times 10^{-4}$
1,2	$8{,}759 \times 10^{-5}$	$8{,}759 \times 10^{-5}$
1,3	$7{,}978 \times 10^{-6}$	$7{,}978 \times 10^{-6}$
2,0	$1{,}110 \times 10^{-16}$	$1{,}110 \times 10^{-16}$

B.2.3.3 Comparaison entre DUT avec antenne en bas et antenne en haut

Le Tableau B.4 est le résultat d'analyse indiquant les différences entre les DUT avec antenne en bas et antenne en haut. Il indique que la probabilité que le DAS en position "incliné" soit supérieur au double du DAS sur la joue est de $5{,}217 \times 10^{-9}$ même pour les dispositifs avec des antennes en haut, qui introduisent une valeur de DAS plus élevée en position "incliné" que sur la joue avec des antennes rétractables.

Tableau B.4 – Résultats d'analyse statistique de P(Incliné/Joue > x) pour différentes positions d'antenne

x	P(Incliné/Joue > x)	
	Antenne en bas	Antenne en haut
1,0	$1{,}718 \times 10^{-3}$	$3{,}725 \times 10^{-2}$
1,1	$2{,}095 \times 10^{-4}$	$1{,}472 \times 10^{-2}$
1,2	$1{,}815 \times 10^{-5}$	$5{,}062 \times 10^{-3}$
1,3	$1{,}112 \times 10^{-6}$	$1{,}511 \times 10^{-3}$
2,0	0,0 [a]	$5{,}217 \times 10^{-9}$

[a] Ce nombre est inférieur à la précision numérique de l'ordinateur utilisé pour procéder à l'analyse statistique.

IECNORM.COM : Click to view the full PDF of IEC/IEEE 62209-1528:2020

B.2.3.4 Comparaison entre bandes de fréquences

Le Tableau B.5 est le résultat d'analyse indiquant les différences entre les bandes de fréquences de fonctionnement. Il indique la probabilité que le DAS en position "incliné" soit supérieur au double du DAS sur la joue est de $3{,}492 \times 10^{-7}$ même pour les bandes de fréquences élevées.

Tableau B.5 – Résultats d'analyse statistique de P(Incliné/Joue > x) pour différentes bandes de fréquences

x	P(Incliné/Joue > x)			
	850 MHz	900 MHz	1 800 MHz	1 900 MHz
1,0	$7{,}638 \times 10^{-3}$	$4{,}578 \times 10^{-3}$	$6{,}536 \times 10^{-2}$	$1{,}920 \times 10^{-2}$
1,1	$1{,}526 \times 10^{-3}$	$6{,}350 \times 10^{-4}$	$3{,}170 \times 10^{-2}$	$7{,}076 \times 10^{-3}$
1,2	$2{,}334 \times 10^{-4}$	$6{,}172 \times 10^{-5}$	$1{,}385 \times 10^{-2}$	$2{,}283 \times 10^{-3}$
1,3	$2{,}721 \times 10^{-5}$	$4{,}180 \times 10^{-6}$	$5{,}442 \times 10^{-3}$	$6{,}435 \times 10^{-4}$
2,0	$3{,}331 \times 10^{-15}$	$0{,}000 \times 10^{0}$	$3{,}492 \times 10^{-7}$	$1{,}839 \times 10^{-9}$

B.2.3.5 Comparaison entre types de dispositifs

Le Tableau B.6 est le résultat d'analyse indiquant les différences entre types de dispositifs. Il indique que la probabilité que le DAS en position "incliné" soit supérieur au double du DAS sur la joue est très faible, quels que soient les types de dispositifs.

Tableau B.6 – Résultats d'analyse statistique de P(Incliné/Joue > x) pour différents types de dispositifs

x	P(Incliné/Joue > x)			
	Barre	Coquille	Coulissant (ouvert)	Coulissant (fermé)
1,0	$6{,}853 \times 10^{-3}$	$2{,}992 \times 10^{-8}$	$5{,}441 \times 10^{-4}$	$1{,}771 \times 10^{-3}$
1,1	$1{,}334 \times 10^{-3}$	$3{,}769 \times 10^{-10}$	$2{,}138 \times 10^{-5}$	$1{,}739 \times 10^{-4}$
1,2	$1{,}982 \times 10^{-4}$	$2{,}801 \times 10^{-12}$	$4{,}385 \times 10^{-7}$	$1{,}131 \times 10^{-5}$
1,3	$2{,}240 \times 10^{-5}$	$1{,}221 \times 10^{-14}$	$4{,}658 \times 10^{-9}$	$4{,}844 \times 10^{-7}$
2,0	$1{,}998 \times 10^{-15}$	$0{,}000 \times 10^{0}$	$0{,}000 \times 10^{0}$	$0{,}000 \times 10^{0}$

B.2.4 Conclusions

En conséquence de l'analyse statistique avec les dernières conceptions et derniers modèles de DUT (c'est-à-dire de 2009), la probabilité que le DAS en position "incliné" soit plus élevé que le DAS sur la joue est très faible, et très proche de zéro, ce qui signifie que le DAS en position "incliné" n'est très probablement jamais plus élevé que la limite applicable de DAS si le DAS sur la joue est de 3 dB inférieur à la limite de DAS. Cette approche garantit que les combinés sont dans les limites applicables de DAS, mais ne garantit pas que le DAS maximal est mesuré. Par conséquent, s'il s'agit principalement de respecter la limite de DAS respective, l'exigence pour l'essai de DUT dans la position "incliné" peut être exclue dans les conditions indiquées en 7.9.3.3.

IECNORM.COM : Click to view the full PDF of IEC/IEEE 62209-1528:2020

B.2.5 Extension à la transmission à plusieurs antennes

L'analyse dans cette étude a été réalisée sur des dispositifs tenus à la main comportant une seule antenne d'émission. Cependant, la conclusion peut également être appliquée à des dispositifs tenus à la main comportant plusieurs antennes d'émission. Les méthodes de mesure de DAS applicables aux DUT avec plusieurs antennes d'émission sont fondées sur la sommation des distributions de DAS de chaque antenne d'émission. Par conséquent, il peut être conclu que le DAS en position "incliné", même avec plusieurs antennes d'émission, n'est pas supérieur au double du DAS sur la joue avec les mêmes antennes, le DAS en position "incliné"/"joue" étant calculé par sommation des distributions de DAS de plusieurs antennes d'émission.

B.3 Réduction d'essai fondée sur l'analyse des résultats de DAS sur d'autres modulations de signal

B.3.1 Généralités

Lorsque les premières éditions de l'IEEE 1528 et de l'IEC 62209 ont été initialement développées, les DUT utilisaient généralement un seul mode de fonctionnement par bande de fréquences. La procédure d'essai normalisée exigeait de chaque mode de fonctionnement pour une bande de fréquences donnée qu'il soit entièrement soumis à l'essai. Les DUT de la génération actuelle ont maintenant plusieurs modes de fonctionnement utilisés pour une bande de fréquences donnée (GSM/GPRS, AMCR, AMRC à bande élargie (3G), LTE (4G) et 5 G NR, par exemple). Par conséquent, le nombre d'essais pour chaque bande de fréquences a considérablement augmenté. Il est prévu que cette tendance se poursuive pour les DUT futurs, à moins de pouvoir appliquer des procédures de réduction d'essai.

En général, la modulation de signal a peu d'effet sur la distribution de DAS si tous les signaux sont émis en utilisant la même antenne, le même point d'alimentation de l'antenne et le même circuit d'adaptation (voir la liste complète des exigences à la fin de B.3.1). Cela est également vrai en ce qui concerne les courants sur le corps du dispositif d'émission, puisque la même antenne excite les mêmes courants, quelle que soit la modulation de signal utilisée.

Il est généralement suffisant de mesurer totalement une modulation de signal, mod_X, dans toutes les positions/configurations et les autres modulations de signal mod_Y, mod_Z, etc., dans la position/configuration produisant le résultat de psDAS le plus élevé pour la modulation de signal mod_X. La précédente considération s'applique si les paramètres suivants sont les mêmes pour toutes les modulations de signaux émis:

- bande de fréquences;
- fréquences des canaux d'essai exigés;
- élément rayonnant de l'antenne;
- point d'alimentation de l'antenne;
- mise à la terre de l'antenne;
- circuit d'adaptation de l'antenne (le cas échéant);
- réglages du syntoniseur et du syntoniseur d'antenne (le cas échéant).

Si la conception du téléphone n'est pas suffisamment connue, c'est-à-dire, s'il est impossible de dire si les conditions ci-dessus sont remplies, les réductions d'essai ne peuvent pas être appliquées et il convient de réaliser des essais complets de DAS pour toutes les modulations de signal.

IECNORM.COM : Click to view the full PDF of IEC/IEEE 62209-1528:2020

B.3.2 Résultats d'analyse

Les études décrites en B.3.2 et [37] fournissent une justification pour effectuer le mesurage de DAS pour d'autres modulations de signal mod_Y, mod_Z, etc., à la même position/configuration qui donne le niveau de psDAS maximal pour la modulation de signal mod_X. Par exemple, si la position "joue gauche" donne la valeur de psDAS la plus élevée pour l'émission GSM, la position "joue gauche" génère généralement la valeur de psDAS la plus élevée pour d'autres modulations telles que AMRC à bande élargie et LTE fonctionnant dans la même bande de fréquences.

Des écarts mineurs par rapport à cette règle peuvent être expliqués par les incertitudes de mesure associées aux essais. Par exemple, un changement de la valeur de DAS maximal de la position "joue gauche" à la position "joue droite" lorsque la distribution de DAS est très symétrique le long de l'axe vertical du téléphone dépend de l'exactitude de positionnement. Les écarts sont souvent constatés lorsque les niveaux de DAS pour les deux positions "joue" et "incliné" sont très faibles (inférieurs à 0,4 W/kg). Cela est dû à la diminution de la sensibilité du système de mesure qui introduit du bruit dans les résultats de mesure.

Pour réduire les risques de ne pas obtenir la valeur de psDAS la plus élevée d'un DUT, une valeur-seuil de psDAS a été incluse dans la procédure de réduction d'essai (7.9.3.4) du présent document. En d'autres termes, si les valeurs de psDAS les plus élevées ont été obtenues pour les positions "joue" et si les valeurs de psDAS pour les positions "incliné" sont d'au moins 30 % en dessous de la limite applicable de DAS pour la modulation de signal mod_X, les mesurages pour les positions "incliné" ne sont pas exigés pour d'autres modulations de signal dans la même bande de fréquences.

Les données analysées sont constituées d'un total de 181 combinaisons de DUT et de bandes de fréquences. Les modèles de DUT avec plusieurs modes de fonctionnement dans la même bande de fréquences ont été sélectionnés chez différents fabricants. Les données portaient sur un total de 115 combinaisons de DUT et de bandes de fréquences fonctionnant au-dessous de 1 GHz, et 66 combinaisons fonctionnant au-dessus de 1 GHz, ce qui représente en tout un total de 181 cas.

Les données ont été divisées en deux catégories distinguant le fait que d'une part les combinés fonctionnant au-dessous de 1 GHz ont des champs électromagnétiques plus élevés dus aux courants RF circulant le long du châssis du dispositif, et que d'autre part pour les combinés fonctionnant au-dessus de 1 GHz, les courants sont concentrés à proximité de l'élément d'antenne et du châssis. Sur la base des tendances actuelles de conception d'antenne dans les combinés multimodes, les dispositifs ont été considérés par hypothèse avoir des antennes en bas (comme cela est décrit en 7.9.3.3 du présent document) répondant à toutes les conditions mentionnées en B.3.1. Les bandes de fréquences qui avaient au moins deux modes de fonctionnement différents ont été analysées. Chacune des bandes de fréquences avait généralement 2 ou 3 différents modes de fonctionnement. Les résultats pour les bandes de fréquences 850 MHz, 900 MHz, 1 700 MHz, 1 800 MHz, 1 900 MHz et 1 950 MHz ont été analysés.

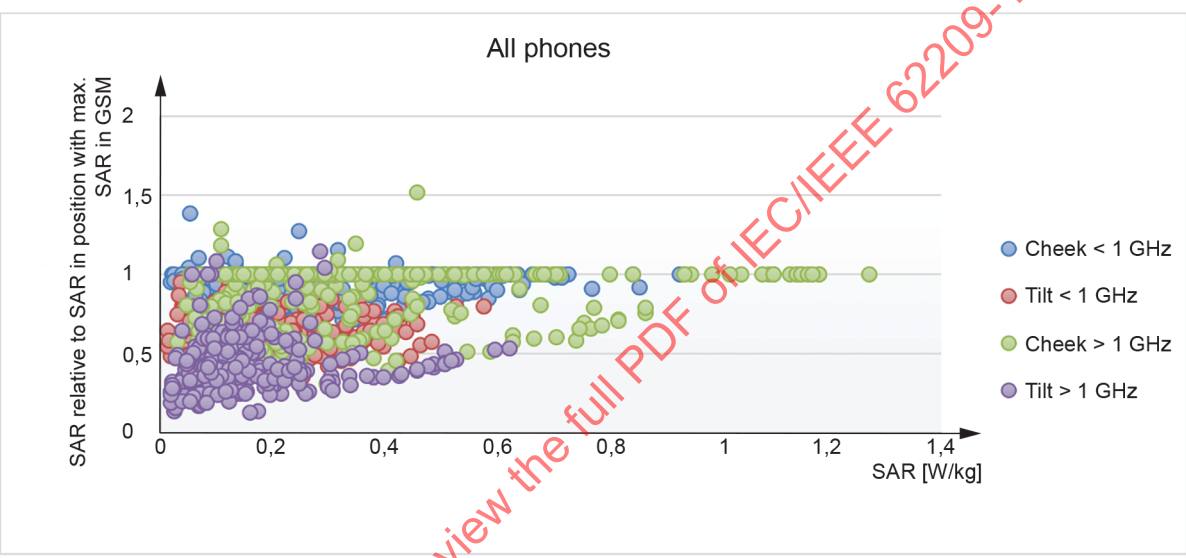
Les résultats du psDAS à 1 g ou 10 g pour toutes les positions d'essai (joue gauche, incliné à gauche, joue droite et incliné à droite) ont été recueillis. Le volume d'intégration a été le même pour chaque combinaison de téléphone et de bande de fréquences.

Pour chaque bande de fréquences et mode de fonctionnement, toutes les valeurs de psDAS ont été divisées par la valeur de psDAS maximal déterminée pour le mode GSM. Le mode GSM a été choisi comme référence, car il était disponible dans tous les cas d'essai analysés. Cela signifie que si des valeurs relatives de DAS pour d'autres modes de fonctionnement (AMRC à bande élargie ou LTE, par exemple) étaient supérieures à 1, le DAS maximal pour ce mode de fonctionnement a été mesuré dans une condition d'essai différente de celle de GSM.

IECNORM.COM : Click to view the full PDF of IEC/IEEE 62209-1528:2020

À la Figure B.2, l'axe des abscisses x représente tous les résultats avec la valeur absolue maximale de DAS de chaque mesurage, et l'axe des ordonnées *y* représente la valeur relative de DAS par rapport à la valeur maximale de DAS pour le mode GSM. Les résultats sont divisés par les positions "joue" et "incliné" au-dessous de 1 GHz et au-dessus de 1 GHz. La Figure B.2 indique que la majorité des résultats sont en dessous de 1, c'est-à-dire que le DAS maximal a été déterminé dans la même position, par exemple pour LTE, que lorsqu'il a été constaté pour le GSM.

Parmi les 181 cas d'essai, le psDAS maximal a été observé dans une position différente de celle pour GSM dans l'un des autres modes de fonctionnement dans seulement 19 cas. Dans l'ensemble des 19 cas, les valeurs de psDAS maximal étaient inférieures à 0,4 W/kg tant pour GSM que pour les autres modes de fonctionnement. Parmi ces 19 cas, seuls 3 cas sont survenus pour les positions "incliné", avec un rapport inférieur à 1,2. Dans les 162 cas restants où les valeurs de psDAS étaient supérieures à 0,4 W/kg, la condition d'essai de DAS maximal a été correctement identifiée sur la base des essais de GSM.



Anglais	Français
SAR relative to SAR in position with max. SAR in GSM	DAS par rapport au DAS en position avec DAS max. dans GSM
All phones	Tous les téléphones
Cheek	Joue
Tilt	Incliné
SAR	DAS

Figure B.2 – DAS par rapport au DAS en position avec le DAS maximal en mode GSM

IECNORM.COM : Click to view the full PDF of IEC/IEEE 62209-1528:2020

B.4 Réduction d'essai fondée sur l'analyse de niveau de DAS

B.4.1 Généralités

Dans la procédure de mesure de DAS décrite en 7.4, les résultats d'un seul balayage-zoom sont utilisés pour obtenir le psDAS à comparer à des restrictions de base. En conséquence, un nombre considérable de balayages-zooms peut être évité, ce qui permet de gagner du temps de mesure, s'il existe un critère permettant de prévoir que le psDAS pour une configuration d'essai est inférieur à la valeur la plus élevée du psDAS parmi toutes les configurations d'essai. En étendant ce concept à des dispositifs multibandes et multiconfigurations, le temps de mesure peut être réduit davantage en définissant une session de mesure de DAS non limitée par le mode de fonctionnement à bande unique, mais étendue à toutes les bandes et configurations de fonctionnement prises en charge par le dispositif et comprises dans le domaine d'application de la présente méthode de réduction d'essai. L'idée de base est d'éviter d'effectuer la session de balayage-zoom pour chaque essai unique (c'est-à-dire 7.4.2 d)) si la valeur de DAS maximal mesurée du balayage de surface est au-dessous d'un seuil. Le seuil est choisi de sorte que la valeur la plus élevée de psDAS soit:

- correctement évaluée et pas sous-estimée, en particulier si elle peut générer un psDAS proche de la limite de restriction de base;
- correctement identifiée, même si la session de balayage-zoom n'est pas exécutée.

Afin de définir la valeur du seuil satisfaisant à la première exigence, le psDAS issu du mesurage de balayage-zoom a été corrélé à la valeur de DAS maximal mesuré déterminée dans le balayage de surface correspondant [38]. Il a été observé que si la valeur de DAS maximal mesuré dans le balayage de surface est inférieure à un seuil, la limite de base pour le psDAS n'est jamais dépassée. En particulier, il existe une bonne corrélation entre le DAS maximal mesuré du balayage de surface et le psDAS à 1 g. En [38], le choix d'un seuil de 1,3 W/kg (80 % de la limite de base pour 1 g de 1,6 W/kg) donne une forte probabilité que la limite pour le psDAS ne soit jamais dépassée. Le même seuil peut également être utilisé pour l'évaluation du psDAS sur 10 g.

L'analyse statistique décrite en B.4.2 a été effectuée pour résoudre le problème d'identification correcte du DAS maximal moyenné le plus élevé [39].

B.4.2 Analyse statistique

L'analyse statistique présentée ici porte sur des DUT fonctionnant dans les bandes GSM 900 / DCS 1800 et UMTS I. Les paramètres d'espacement de grille de balayage de surface utilisés pour cette analyse (x et y) sont définis à 10 mm. Ils satisfont donc aux exigences du présent document, et des balayages de surface ont été effectués à une distance spécifiée fixe (espacement de 4 mm entre les capteurs et la surface de SAM dans ce cas) de la surface interne du SAM.

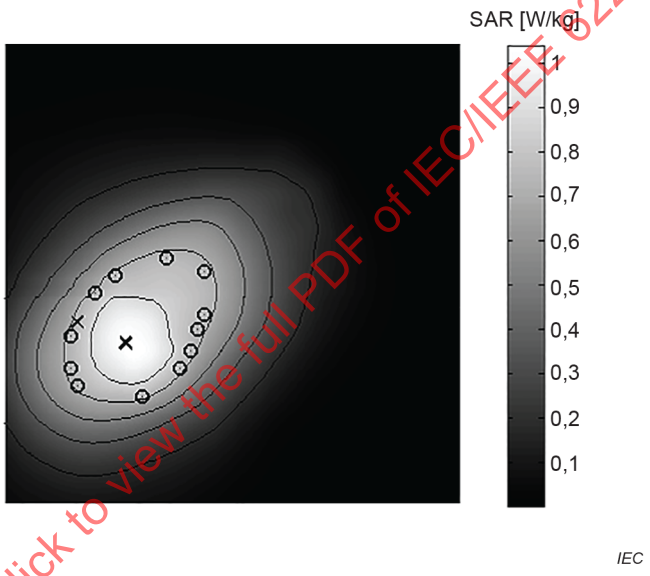
Étant donné que la valeur maximale de DAS n'a pas pu être exactement identifiée après le balayage de surface, en raison de son éventuelle position (en x et y) à l'intérieur d'une région carrée de 10 mm de côté, il est recommandé dans un premier temps d'évaluer par expérimentation le gradient spatial afin d'estimer l'amplitude de la valeur maximale de DAS qui peut être manquée en appliquant uniquement le balayage de surface. Pour ce faire, 420 distributions de DAS dans la bande GSM 900, 420 distributions dans la bande DCS 1800 et 300 distributions dans la bande UMTS I ont été prises en considération. Les distributions sont adaptées pour des téléphones mobiles commercialisés entre 2007 et 2010. Tous les facteurs de forme du combiné, comprenant des téléphones à coquille et coulissants, sont pris en considération dans cette étude. La première étape consistait à identifier "l'isoniveau" comme étant l'ensemble de points ayant une valeur fixe de DAS, puis à calculer la distance minimale D_{min} entre "l'isoniveau" à un niveau de DAS fixe et la position du DAS maximal interpolé (DAS_{max}, la distance entre les deux points représentés par un X à la Figure B.3).

IECNORM.COM : Click to view the full PDF of IEC/IEEE 62209-1528:2020

La Figure B.4 ci-dessous représente l'histogramme associé à la variable aléatoire D_{min} dans le cas de la bande GSM 900 et un niveau 0,6 × DAS_{max}. La courbe rouge représente une fonction de densité de probabilité (PDF) normale ajustée aux données en utilisant une procédure d'estimation de probabilité maximale.

Même si, dans certains cas, les données ne répondent pas à l'essai d'hypothèse de normalité (l'essai de normalité de Jarque-Bera, par exemple) et si les données peuvent être plus efficacement ajustées en utilisant une autre PDF (une PDF hyperbolique, par exemple), pour les besoins de cette analyse, seuls des ajustements normaux ont été pris en considération dans ces travaux. Compte tenu de la PDF normale, la valeur D^*_{min} représente la valeur pour laquelle la probabilité d'avoir D_{min} inférieure à D^*_{min} est de 5 %.

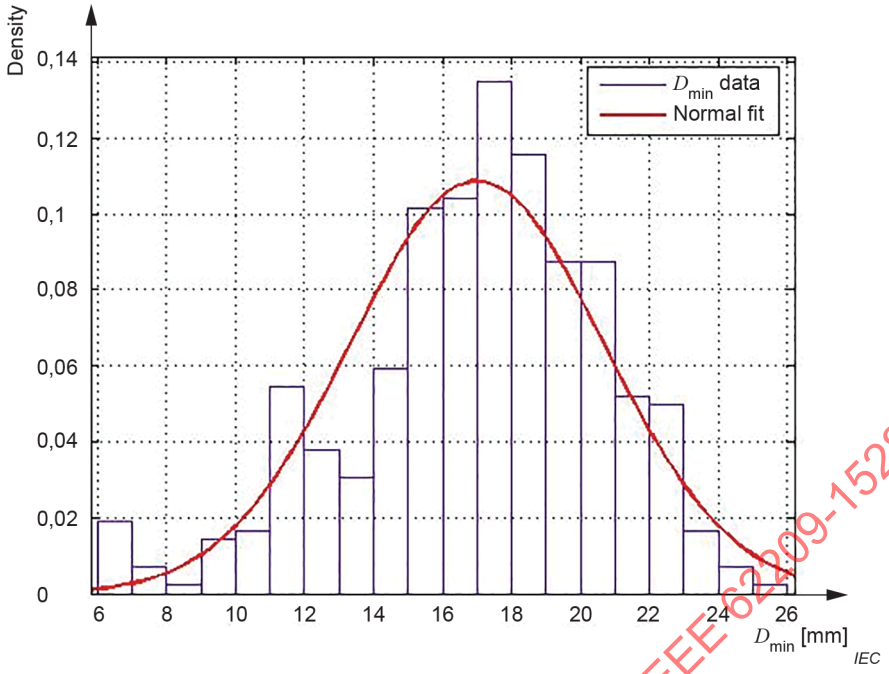
Le Tableau B.7 récapitule toutes les analyses effectuées pour chaque bande de fréquences considérée dans cette étude. Dans ce tableau, l'isoniveau est exprimé en pourcentage, de sorte qu'une valeur de 90 % signifie que l'isoniveau est à 0,9 × DAS_{max}.



Anglais	Français
SAR	DAS

Figure B.3 – Deux points identifiant la distance minimale entre la position du DAS maximal interpolé et les points à 0,6 × DAS_{max}

IECNORM.COM : Click to view the full PDF of IEC/IEEE 62209-1528:2020



Anglais	Français
Density	Masse volumique
D_{min} Data	Données D_{min}
Normal fit	Ajustement normal

Figure B.4 – Histogramme pour D_{min} dans le cas de GSM 900 et d'un isoniveau à 0,6 × DAS_{max}

Tableau B.7 – Distance D^{*}_{min} pour différentes valeurs de "l'isoniveau"

GSM 900		DCS 1800		UMTS I	
Isoniveau (%)	D^{*}_{min}	Isoniveau (%)	D^{*}_{min}	Isoniveau (%)	D^{*}_{min}
90	4,23	90	3,04	90	1,82
80	6,74	80	4,82	80	4,63
75	**7,86**	70	6,19	70	6,10
70	8,90	65	6,92	65	6,81
60	10,96	**60**	**7,54**	**60**	**7,48**
50	13,15	50	9,06	50	8,88

Pour récapituler les résultats de cette analyse, dans le cas, par exemple, de la bande GSM 900, il peut être conclu qu'il est improbable de déterminer des valeurs de DAS égales à 0,75 × DAS_{max} si une distance de 7,86 mm du point DAS_{max} est prise en considération. En particulier, les valeurs indiquées en gras dans le Tableau B.7 ont des D^{*}_{min} valeurs supérieures à 7 mm, ce qui est la valeur au milieu des grilles choisies de 10 mm. En d'autres termes, toujours pour l'exemple de GSM 900, il est improbable de manquer une valeur de DAS à l'intérieur d'une grille de balayage de surface de 10 mm qui est supérieure à 0,75 fois la valeur de DAS maximal mesurée au cours du balayage de surface.

IECNORM.COM : Click to view the full PDF of IEC/IEEE 62209-1528:2020

Pour conclure l'analyse statistique, la corrélation entre la valeur de DAS maximal mesurée au cours du balayage de surface et les valeurs de psDAS obtenues après les balayages-zooms a été examinée. Pour ce faire, une base de données de 100 combinés fonctionnant dans les bandes GSM 900 et DCS 1800 et 50 DUT fonctionnant dans la bande UMTS I a été prise en considération.

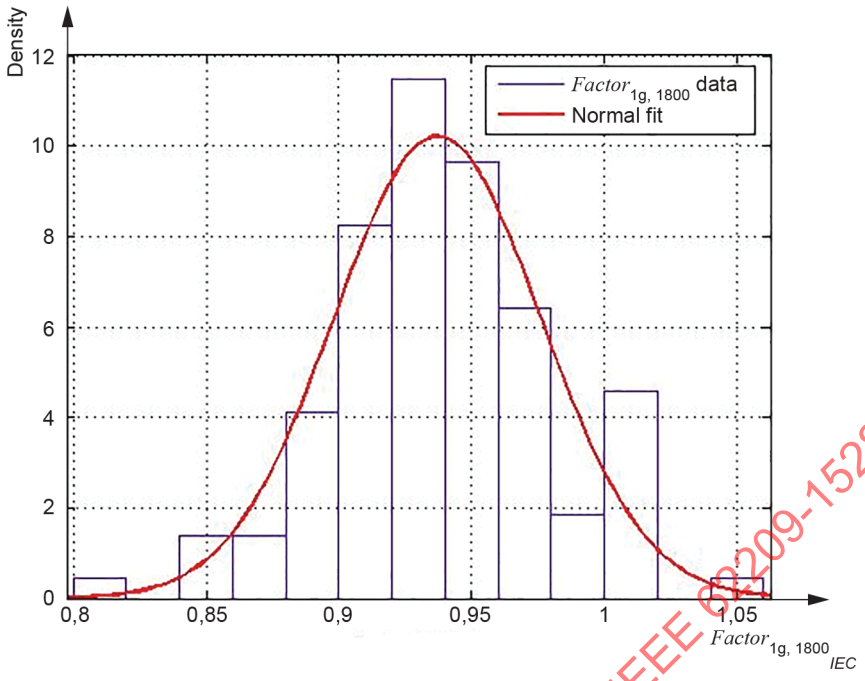
Pour chaque combiné, la valeur de DAS maximal mesurée du balayage de surface, le psDAS à 1 g et le psDAS à 10 g, mesurés après la procédure de mesure complète, ont été collectés. La Figure B.5 représente l'histogramme, ainsi que l'ajustement de PDF normal pour la variable aléatoire $Facteur_{1g,1800}$, définie comme étant le rapport entre le psDAS pour une masse de 1 g et la valeur de DAS maximal mesurée du balayage de surface dans le cas de la bande DCS 1800.

Dans ce cas particulier, il peut être démontré que la probabilité de 95 % est réalisée pour obtenir $Facteur_{1g,1800}$ dans l'intervalle [0,859, 1,015]. Dans ce cas particulier, il peut être conclu que s'il y a deux balayages de surface avec deux valeurs de DAS maximal mesurées différentes (pas celle interpolée) et si elles diffèrent d'un facteur de 0,859/1,015 = 0,84, il est alors improbable que la distribution ayant la valeur la plus élevée de DAS maximal mesurée lors du balayage de surface ait le psDAS à 1 g le plus faible. Dans ce cas particulier, 0,84 peut être retenu comme étant un seuil expérimental: si deux balayages de surface différents sont pris en considération et si les valeurs de DAS maximal mesurées pour chacun d'entre eux diffèrent d'un facteur inférieur au seuil, il existe alors une probabilité de 95 % que le balayage de surface avec le DAS le plus élevé produise le psDAS le plus élevé.

Des conclusions similaires peuvent être obtenues en analysant les autres bandes, ainsi que le psDAS à 10 g. Le Tableau B.8 récapitule l'ensemble des résultats.

En conclusion, les mêmes seuils obtenus dans le Tableau B.7 (75 % pour GSM 900, 60 % pour DCS 1800 et UMTS I) sont également suffisants pour déterminer (avec une valeur de probabilité de 95 %) que le psDAS est correctement identifié, même sans effectuer un balayage-zoom.

IECNORM.COM : Click to view the full PDF of IEC/IEEE 62209-1528:2020



Anglais	Français
Density	Masse volumique
D_{min} Data	Données D_{min}
Normal fit	Ajustement normal
$Factor_{1\ g,\ 1800}$ data	Données $Facteur_{1g,\ 1800}$
$Factor_{1\ g,\ 1800}$	$Facteur_{1g,\ 1800}$

Figure B.5 – Histogramme pour la variable aléatoire $Facteur_{1g,1800}$

Tableau B.8 – Seuils expérimentaux pour avoir une probabilité de 95 % que la valeur de DAS maximal mesurée à partir du balayage de surface ait également un psDAS

GSM 900		DCS 1800		UMTS I	
Seuil 1 g	Seuil 10 g	Seuil 1 g	Seuil 10 g	Seuil 1 g	Seuil 10 g
0,86	0,76	0,84	0,63	0,74	0,62

B.4.3 Exemple d'applicabilité de réduction d'essai

Deux exemples d'application des procédures présentées en B.4.2 sont donnés dans les alinéas suivants. Dans le premier, la méthode de réduction d'essai est appliquée à un seul mode de fonctionnement (c'est-à-dire GSM 900), tandis que dans le second, un DUT bimode (GSM 900/DCS 1800 et UMTS I) est pris en considération.

Le Tableau B.9 et le Tableau B.10 indiquent les valeurs de DAS consignées qui représentent la valeur de DAS maximal mesurée à partir du balayage de surface (bande GSM 900).

IECNORM.COM : Click to view the full PDF of IEC/IEEE 62209-1528:2020

Étant donné que cet exemple concerne GSM 900, il convient d'appliquer un seuil de 0,75. Pour la première position (joue gauche, fréquence de liaison montante centrale), le balayage-zoom est nécessaire étant donné que la valeur de DAS maximal est de 1,3 W/kg (80 % de 1,6 W/kg), tandis que pour position "incliné à gauche", 0,6 W/kg est inférieur à 0,75 × 1,3, de sorte que le balayage-zoom n'est pas nécessaire. Dans la position joue droite, le balayage-zoom est alors nécessaire et le nouveau DAS maximal absolu (APS) devient 1,5 W/kg. Ce nouvel APS permet de ne pas avoir besoin d'effectuer le balayage-zoom pour la position "incliné à droite" (fréquence centrale) et la position joue droite (fréquence inférieure), tandis qu'il n'est pas assez élevé pour exclure le dernier balayage-zoom (joue droite, fréquence supérieure).

Dans le second exemple, la bande GSM 900 est soumise à l'essai avant DCS 1800 et UMTS I, mais en règle générale, l'ordre dans lequel les bandes sont soumises à l'essai peut être différent.

Dans ce deuxième exemple, la procédure appliquée dans GSM 900 est répétée en prenant en considération tous les autres essais et l'APS précédemment obtenu. Pour chaque bande, il convient que l'utilisateur choisisse un seuil approprié (B.4.2). Pour le premier mesurage dans une bande différente, l'APS précédemment obtenu et le seuil associé à la nouvelle bande sont utilisés pour la comparaison avec la valeur de DAS maximal mesuré à partir du balayage de surface. Par exemple, le premier mesurage de balayage de surface de DCS 1800 a une valeur de crête de DAS maximal de 0,9 W/kg qui équivaut à 60 % (le seuil de DCS 1800) de 1,5 W/kg (l'APS précédent), par conséquent, dans ce cas, un balayage-zoom est nécessaire.

Comme il peut être observé dans cet exemple, neuf mesurages (50 %) n'exigent pas de réaliser un balayage-zoom (lignes en gras dans le Tableau B.10). Le nombre de balayages-zooms qui peuvent être évités dépend des valeurs de DAS maximal mesuré à partir des balayages de surface.

Tableau B.9 – Valeur de DAS à partir du balayage de surface (bande GSM 900): Exemple 1

Fréquence	Position	Valeur de DAS maximal [W/kg] [a]
Centrale	Joue gauche	1,3
Centrale	**Incliné à gauche**	**0,6**
Centrale	Joue droite	1,5
Centrale	**Incliné à droite**	**0,8**
Inférieure	**Joue droite**	**1,0**
Supérieure	Joue droite	1,3

[a] Pour les lignes en gras, selon la procédure de réduction d'essai proposée, un balayage-zoom n'est pas exigé.

IECNORM.COM : Click to view the full PDF of IEC/IEEE 62209-1528:2020

Tableau B.10 – Valeur de DAS à partir du balayage de surface (bande GSM 900): Exemple 2

Fréquence	Position	Valeur de DAS maximal [W/kg] [a]
Centrale (GSM 900)	Joue gauche	1,3
Centrale (GSM 900)	**Incliné à gauche**	**0,6**
Centrale (GSM 900)	Joue droite	1,5
Centrale (GSM 900)	**Incliné à droite**	**0,8**
Inférieure (GSM 900)	**Joue droite**	**1,0**
Supérieure (GSM 900)	Joue droite	1,3
Centrale (DCS 1800)	Joue gauche	0,9
Centrale (DCS 1800)	**Incliné à gauche**	**0,6**
Centrale (DCS 1800)	**Joue droite**	**0,8**
Centrale (DCS 1800)	**Incliné à droite**	**0,7**
Inférieure (DCS 1800)	Joue droite	1,1
Supérieure (DCS 1800)	**Joue droite**	**0,8**
Centrale (UMTS I)	Joue gauche	1,1
Centrale (UMTS I)	**Incliné à gauche**	**0,7**
Centrale (UMTS I)	Joue droite	1,4
Centrale (UMTS I)	**Incliné à droite**	**0,6**
Inférieure (UMTS I)	Joue droite	1,2
Supérieure (UMTS I)	Joue droite	1,4

[a] Pour les lignes en gras, selon la procédure de réduction d'essai proposée, un balayage-zoom n'est pas exigé.

B.5 Autres approches statistiques pour rechercher les configurations d'essai de DAS élevé

B.5.1 Généralités

Un dispositif peut être utilisé dans différentes modes d'émission et avec plusieurs options d'antenne, de batterie et autres accessoires, et le nombre de combinaisons possibles peut être très élevé. Des méthodes sont donc nécessaires pour rationaliser le processus de mesure, de sorte que les conditions d'essai de DAS le plus élevé puissent être rapidement identifiées. Par exemple, pour un dispositif avec deux configurations d'antenne (antenne déployée et rétractée) et quatre types de batteries, l'essai de toutes les combinaisons possibles conduit à un nombre important d'essais. Il n'est pas nécessaire de soumettre à l'essai toutes les combinaisons possibles. Des techniques statistiques peuvent être utilisées pour présenter des tendances à partir d'un ensemble de données plus petit et déterminer quelles combinaisons accessoire-dispositif conduisent à des valeurs plus élevées de DAS.

Trois méthodes traditionnelles d'expérimentation sont décrites en B.5.3 et B.5.4. Ces méthodes présentent des inconvénients par rapport à l'approche de plan d'expérience (DOE) décrite en B.5.2.

IECNORM.COM : Click to view the full PDF of IEC/IEEE 62209-1528:2020

B.5.2 Réductions d'essai fondées sur un plan d'expérience

L'analyse de données de DAS (l'analyse statistique fondée sur une approche de plan d'expérience, par exemple) peut être utilisée pour développer des justifications scientifiques ou techniques pour la réduction d'essai de certains essais de DAS. Par exemple, si des dispositifs sont disponibles avec des coques en option avec des revêtements de peinture facultatifs contenant différentes teneurs en métaux, l'analyse statistique de données de DAS peut être utilisée pour justifier l'exclusion de l'essai de coques ayant une teneur en métal inférieure à une certaine valeur. Il convient de limiter l'application de la réduction d'essai à des produits qui sont suffisamment semblables au produit original pour lequel la réduction d'essai est déterminée.

L'utilisation d'un plan d'expérience est la méthode statistique préférentielle pour obtenir ces réductions d'essai. Un plan d'expérience est une méthode organisée et structurée pour analyser l'influence de facteurs et les interactions entre facteurs sur le résultat d'un processus. L'approche de plan d'expérience est largement décrite dans l'ouvrage de référence [40].

B.5.3 Recherche "un facteur à la fois" (OFAT)

Avec cette méthode, l'expérimentateur commence par une condition d'essai de référence et fait varier successivement un facteur à la fois tout en maintenant tous les autres facteurs constants. Par exemple, cela peut être obtenu en modifiant d'abord les configurations d'antenne, puis les types de batteries, puis les types d'accessoires de transport, puis les types d'accessoires audio. À la fin de chaque étape, le facteur donnant le DAS le plus élevé est choisi pour les étapes suivantes. Le principal inconvénient de cette approche est qu'elle ne prend en considération aucune interaction entre les différents types d'accessoires (par exemple, l'interaction de la batterie et de l'antenne sur le DAS, qui n'est pas expliquée par les influences de chaque facteur indépendamment). S'il existe des interactions, l'approche OFAT peut ne pas permettre de trouver la solution optimale (c'est-à-dire, le DAS le plus élevé).

B.5.4 Analyse de données non structurées

Les données historiques sont une source courante de données non structurées. Ces données sont généralement collectées sans aucun objectif spécifique à l'esprit, ou bien elles peuvent avoir été collectées pour des applications différentes de l'objectif expérimental actuel. Ces données peuvent être utiles pour générer des tendances, mais il peut être très difficile d'avoir une confiance élevée dans ces observations.

Pour cette raison, il convient de vérifier tous les résultats de l'analyse de données non structurées (en utilisant un plan d'expérience, par exemple).

IECNORM.COM : Click to view the full PDF of IEC/IEEE 62209-1528:2020

Annexe C
(informative)

Incertitude de mesure des résultats obtenus à partir des méthodes d'essai rapide de DAS spécifiques

C.1 Généralités

Parmi les méthodes d'essai rapide de DAS existantes et connues, un grand nombre d'entre elles sont focalisées sur la réduction des mouvements de sonde, en particulier en utilisant des techniques de balayage ou un ensemble de sondes, et des techniques de reconstruction de champ afin de déterminer la distribution spatiale du DAS et du psDAS. Des sondes de différents types peuvent être utilisées (des sondes mesurant uniquement deux composantes de champ tangentiel, des sondes thermiques, par exemple). Certains systèmes utilisent également des technologies de sonde et une électronique permettant de mesurer de la phase du champ électrique dans un plan donné. Différents types d'algorithmes de post-traitement dédiés peuvent ensuite être utilisés pour reconstruire la distribution de DAS volumétrique à l'intérieur du fantôme.

NOTE Les techniques de reconstruction de champ sont décrites dans l'IEC 62209-3.

Il convient que les propriétés diélectriques du milieu équivalent au tissu utilisé pour l'essai rapide de DAS satisfassent aux exigences de l'Annexe G. Le milieu équivalent au tissu peut être liquide, solide ou sous forme de gel. Si le milieu équivalent au tissu du système d'essai rapide de DAS est accessible et remplaçable par l'utilisateur, il convient que les propriétés diélectriques soient caractérisées comme cela est spécifié en 7.2.1. Si le milieu équivalent au tissu est inaccessible ou non remplaçable par l'utilisateur, il convient que le fabricant du système démontre et documente la satisfaction des propriétés diélectriques aux exigences de l'Annexe G, y compris tout effet des variations spatiales des propriétés diélectriques (C.2.11) ou du vieillissement du matériau.

Les méthodes d'essai rapide de DAS qui sont décrites à l'Annexe C utilisent la procédure de mesure spécifiée en 7.9.2. Elles utilisent également la validation du système et le contrôle du système décrits à l'Article A.4. Il convient également de prendre en considération la plage complète de positions de capteur pour le type de systèmes d'essai rapide de DAS décrit à l'Annexe C. Il convient de fournir ces plages avec les résultats de validation du système. L'Annexe C est informative, car les exigences de validation du système n'ont pas encore été entièrement définies pour le type de système DAS rapide décrit ici.

Étant donné que cette classe de méthodes d'essai rapide de DAS utilise un matériel et un logiciel spécifiques qui ne sont pas conformes à ceux utilisés pour les systèmes complets de DAS exigés par le présent document, les informations de l'Article 8 peuvent ne pas être suffisantes pour déterminer l'incertitude de mesure. D'autres composantes d'incertitude qui sont spécifiques au système et à la méthode de mesure à l'étude peuvent être nécessaires. L'Article C.2 donne des recommandations générales pour déterminer l'incertitude de mesure des résultats obtenus à l'aide de cette classe de méthodes d'essai rapide de DAS.

C.2 Évaluation d'incertitude de mesure – paramètres de contribution

C.2.1 Généralités

Des recommandations générales sont fournies pour déterminer l'incertitude de mesure relative d'une méthode d'essai rapide de DAS de Classe 2. Pour les systèmes d'essai rapide de DAS de Classe 1, l'analyse de l'incertitude est la même que celle spécifiée à l'Article 8, si ce n'est qu'une incertitude supplémentaire liée à l'erreur d'échantillonnage est ajoutée comme cela est spécifié en C.2.7.

IECNORM.COM : Click to view the full PDF of IEC/IEEE 62209-1528:2020

Les méthodes d'évaluation de l'incertitude des résultats de DAS obtenus à l'aide des systèmes de mesure vectorielle sont données dans l'IEC 62209-3. Les recommandations en matière d'évaluation d'incertitude de l'IEC 62209-3 doivent être appliquées pour les besoins du présent document.

Pour une méthode d'essai rapide de DAS spécifique, il convient de procéder à une analyse d'incertitude rigoureuse pour tous les termes d'incertitude applicables, y compris ceux qui ne sont pas spécifiés à l'Article C.2. L'incertitude relative étant exigée, les contributions à l'incertitude qui représentent des décalages fixes pour un ensemble de configurations d'essai ne sont pas prises en considération dans le bilan d'incertitude. Cela comprend les décalages fixes dus à l'étalonnage du système, aux propriétés diélectriques qui ne varient pas de manière significative pendant les essais (les variations de température de milieu équivalent au tissu entre les configurations soumises à l'essai satisfont aux exigences de 6.1), aux incertitudes de construction du fantôme qui sont fixées pour un système donné, et d'autres décalages. Il convient que les termes d'incertitude qui conduisent à des variations des valeurs mesurées par rapport à leurs valeurs nominales pour un ensemble donné de mesurages soient pris en considération dans le bilan d'incertitude relative. Cela comprend le bruit de l'électronique, les variations dues au positionnement du dispositif et aux erreurs de mesure, et d'autres éléments.

Pour les essais rapides de DAS de Classe 2, deux bilans d'incertitude sont présentés à l'Annexe C.

a) Le Tableau C.1 (voir l'Article C.3) est le bilan d'incertitude à utiliser lorsqu'un essai rapide de DAS est appliqué pour plusieurs conditions d'essai dans la même bande de fréquences et modulation (par exemple, GSM dans la bande de fréquences 824 MHz à 849 MHz). Les décalages fixes qui s'appliquent lorsque des évaluations relatives sont réalisées ne sont pas inclus dans l'incertitude. De même, les décalages fixes qui sont spécifiques à la fréquence et au mode de fonctionnement (des décalages dus à l'incertitude d'étalonnage et à la modulation, par exemple) ne sont pas inclus.

b) Le Tableau C.2 (voir l'Article C.3) est le bilan d'incertitude pour le contrôle du système pour l'essai rapide de DAS de Classe 2. Ce bilan d'incertitude est très similaire au bilan d'incertitude de l'Article 8.

Il convient de calculer toutes les contributions à l'incertitude de façon rigoureuse, en utilisant les techniques statistiques appropriées. Il convient qu'une description des procédures utilisées pour les évaluations des contributions à l'incertitude, si elles sont différentes de celles indiquées dans le présent document, soit incluse dans le rapport de mesure.

C.2.2 Étalonnage de sonde et dérive d'étalonnage du système

Si la méthode d'essai rapide de DAS utilise une sonde, il convient d'utiliser la même méthode que celle décrite en 8.4.1.1, le cas échéant. Si la méthode d'essai rapide de DAS de Classe 2 utilise plusieurs sondes, il convient d'appliquer l'étalonnage sur le nombre de capteurs utilisés par le système, le cas échéant. Il convient que l'incertitude d'étalonnage du système soit documentée et appropriée à la méthode d'étalonnage appliquée.

La dérive de l'étalonnage de sonde dans le temps est une estimation de la modification des valeurs d'étalonnage du système sur l'intervalle d'étalonnage dans un laboratoire d'étalonnage spécifique, et repose sur l'historique d'étalonnage du système. Elle est déterminée par une évaluation de Type A (8.4.1.2). Par exemple, le laboratoire d'étalonnage peut avoir un système spécifique qu'il utilise pour un réétalonnage périodique. Dans ce cas, il convient de définir la dérive d'étalonnage comme étant l'écart type des réétalonnages, par rapport à la valeur moyenne. Il est recommandé d'effectuer les mesurages d'étalonnage du système utilisé pour déterminer cette incertitude sur une période plus longue que la période d'étalonnage de l'autre équipement (des wattmètres, par exemple) utilisé lors de l'étalonnage. Cela garantit que l'incertitude de dérive d'étalonnage comprend des variations dues au réétalonnage de cet équipement. Si un historique d'étalonnage n'est pas disponible, il convient d'utiliser l'estimation par le fabricant de la stabilité du système sur l'intervalle d'étalonnage. Il convient d'utiliser l'incertitude complète d'étalonnage si l'incertitude de dérive d'étalonnage n'est pas disponible.

IECNORM.COM : Click to view the full PDF of IEC/IEEE 62209-1528:2020

C.2.3 Isotropie

L'incertitude d'isotropie de la sonde décrite en 8.4.1.5 est applicable aux sondes qui peuvent être positionnées dans une plage d'angles par rapport à l'enveloppe du fantôme conformément aux spécifications du Tableau 3 et du Tableau 4 (voir 7.4.2).

Si les sondes du système d'essai rapide de DAS sont positionnées de façon similaire que pour l'essai rapide de DAS de Classe 1 convient d'utiliser la procédure de l'incertitude d'isotropie de sonde décrite en 8.4.1.5, le cas échant. Si les angles de sonde par rapport à l'enveloppe du fantôme ne satisfont pas aux angles de sonde spécifiés dans le Tableau 3 et dans le Tableau 4, alors une évaluation supplémentaire de l'incertitude peut être nécessaire. Si les angles de sonde sont limités à une plage plus étroite, l'incertitude d'isotropie peut être réalisée sur cette plage. Il convient que l'évaluation d'isotropie soit applicable au système de mesure utilisé. Si des algorithmes sont appliqués pour compenser l'écart par rapport à la réponse isotropique, alors l'incertitude de DAS doit être déterminée avec les mêmes matériel et logiciel d'évaluation que ceux utilisés pour effectuer les mesurages de DAS.

Pour l'essai rapide de DAS de Classe 2, des considérations spécifiques à la technologie doivent être prises en compte. Le fabricant doit évaluer cette contribution pendant l'étalonnage. Si des algorithmes sont appliqués pour compenser l'écart par rapport à la réponse isotropique, alors l'incertitude de DAS doit être déterminée avec les mêmes matériel et logiciel d'évaluation que ceux utilisés pour effectuer les mesurages de DAS. Pour évaluer l'isotropie, le système de mesure du DAS doit être exposé à des champs de référence contenant des ondes dont les angles d'incidence changent par rapport à la ligne perpendiculaire à la surface du fantôme. Les gradients de DAS dans la direction perpendiculaire à l'enveloppe du fantôme doivent être suffisamment bas pour que la tolérance de positionnement de la sonde n'ait pas d'impact significatif sur l'évaluation de l'isotropie. L'isotropie doit être caractérisée pour au moins une fréquence dans chaque bande de fréquences à l'étude du système de communication du DUT. Il est nécessaire de traduire en incertitude la tolérance évaluée valable à l'emplacement du capteur pour le psDAS et indiquée dans le Tableau C.1. La traduction dépend de la véritable reconstruction 3D mise en œuvre et peut uniquement être réalisée par le fabricant. Toutes les étapes doivent être documentées.

C.2.4 Positionnement de la sonde

Il existe une incertitude sur la position exacte de la ou des sondes utilisées par la méthode d'essai rapide de DAS. Si le système d'essai rapide de DAS utilise un ou plusieurs capteurs mobiles, l'incertitude est due aux incertitudes de positionnement des capteurs. Si le système d'essai rapide de DAS utilise un ou plusieurs capteurs fixes, l'incertitude est due aux incertitudes mécaniques du positionnement du capteur pendant la fabrication.

L'incertitude est évaluée en utilisant l'ensemble de distributions de référence de O.8.2. La procédure est la suivante.

a) Pour chaque distribution de référence, le champ est échantillonné aux points et dans les polarisations correspondant à la grille de mesure appliquée par le système physique.
b) À partir de ces données échantillonnées d'origine, le psDAS est calculé en utilisant le même processus que celui utilisé pour les mesurages avec ce système particulier. Dans ce processus, l'étape a) donne le DAS de référence, $DAS_{\mathrm{ref},i}$, pour chaque cas de distribution de champ i (plusieurs distributions i sont prises pour hypothèse par fréquence).
c) La tolérance connue sur le positionnement de la sonde est utilisée pour générer des grilles de balayage de mesure G_j (j = 1 à J) affectées par des erreurs mécaniques. Le fabricant doit créer un modèle pour représenter ce type d'erreurs mécaniques. Par exemple, chaque tolérance peut présenter une distribution rectangulaire ou triangulaire si le fabricant définit les écarts acceptables maximaux par rapport aux emplacements nominaux. Dans le cas des sondes mobiles, l'incertitude de répétabilité du positionnement de la sonde doit être incluse dans l'erreur mécanique. J distributions échantillonnées de chaque champ vectoriel de référence sont alors créées à l'aide des grilles d'échantillonnage G_j.

IECNORM.COM : Click to view the full PDF of IEC/IEEE 62209-1528:2020

d) Pour chaque distribution de référence i et chaque grille j, les algorithmes de reconstruction du système de mesure sont appliqués pour calculer le psDAS, $DAS_{i,j}$. Le logiciel doit prendre pour hypothèse des positions idéales des points dans la grille. Par conséquent, les algorithmes sont utilisés comme si les valeurs de champ échantillonnées étaient obtenues à partir d'une sonde ou d'un réseau de sondes dont la position est parfaitement connue, alors qu'en réalité, la sonde ou le réseau de sondes échantillonne le champ sur une grille qui s'écarte des emplacements ciblés.

e) Pour chaque paire (i, j), la différence relative $\Delta DAS_{i,j} = (DAS_{i,j} - DAS_{\text{ref},i}) / DAS_{\text{ref},i}$ est calculée.

U_i est alors calculé pour chaque configuration de champ de référence i en tant que 95e percentile de la valeur absolue de $\Delta DAS_{i,j}$ pour tous les emplacements de sonde ou de grille de réseau de sondes J. L'incertitude est alors estimée comme étant la valeur efficace de U_i dans la plage de fréquences applicable pour toutes les conditions d'exposition I. Cette valeur est calculée sur $I \times J$ cas avec $I \times J - 1$ degrés de liberté. Une distribution normale ($k = 2$) est prise pour hypothèse.

Il est nécessaire de traduire en incertitude la tolérance évaluée valable à l'emplacement du capteur pour le psDAS et indiquée dans le Tableau C.1. La traduction dépend de la véritable reconstruction 3D mise en œuvre et peut uniquement être réalisée par le fabricant. Toutes les étapes doivent être documentées.

C.2.5 Couplage mutuel de capteur

Pour les systèmes utilisant plusieurs sondes, il peut exister un couplage entre les capteurs de sonde en raison de l'imperfection de l'isolation des capteurs. Ce terme d'incertitude est provoqué par le couplage entre accès dans lequel la lecture au niveau d'un accès de capteur donné est influencée par la tension et/ou le courant au niveau d'un autre accès de capteur. Le couplage mutuel de capteur peut être évalué et compensé pendant l'étalonnage. Toutefois, ce couplage dépend en principe de la polarisation, de la distribution et de l'angle d'incidence du champ d'impact et est donc difficile à supprimer complètement pendant l'étalonnage.

Il est nécessaire de traduire en incertitude la tolérance évaluée valable à l'emplacement du capteur pour le psDAS et indiquée dans le Tableau C.1. La traduction dépend de la véritable reconstruction 3D mise en œuvre et peut uniquement être réalisée par le fabricant. Toutes les étapes doivent être documentées.

Pour isoler cette contribution à l'incertitude des autres composantes:

a) la sonde ou le réseau de sondes doit être plongé dans le milieu équivalent au tissu satisfaisant aux exigences du présent document;

b) la pureté de polarisation des antennes de référence utilisées doit être supérieure à 10 dB. La pureté de polarisation est le rapport de l'intensité de champ de la composante de champ dominant sur l'intensité de champ des deux composantes de champ orthogonal. Elle est spécifiée à l'emplacement du psDAS. Elle est évaluée à partir de simulations numériques de l'antenne de référence;

c) les antennes de référence doivent être suffisamment éloignées du fantôme pour que l'interaction avec la sonde ou le réseau de sondes puisse être négligée;

d) les niveaux de champs doivent être suffisamment supérieurs au bruit de fond.

IECNORM.COM : Click to view the full PDF of IEC/IEEE 62209-1528:2020

Dans le cas de réseaux de sondes dont les sondes sont étalonnées indépendamment avant l'assemblage ou de réseaux de sondes étalonnés ensemble dans leurs conditions de fonctionnement finales sans compensation pour le couplage mutuel, l'incertitude de couplage mutuel de capteur doit être évaluée en calculant la différence entre le DAS mesuré à un point en utilisant une sonde isolée et le DAS mesuré par la même sonde entourée par les autres sondes. Plusieurs antennes sources présentant différentes polarisations et différents angles d'incidence sont exigées. Les antennes sont déplacées vers les positions exigées de manière à exposer réellement chaque capteur à une intensité de champ compatible avec la plage dynamique du système de mesure. Pour chaque condition d'essai, les coefficients d'étalonnage et le post-traitement sont appliqués aux données mesurées afin d'évaluer la distribution de champ vectoriel sur la surface de mesure. La manière dont l'erreur se propage et dont l'incertitude est couplée à d'autres termes d'incertitude doit être documentée.

Pour les réseaux de sondes dont les sondes sont étalonnées ensemble dans leurs conditions de fonctionnement finales et dont le couplage mutuel entre les capteurs est caractérisé sous la forme d'une matrice de diffraction et est compensé (pendant l'étalonnage du réseau de sondes, par exemple), le couplage mutuel est réduit. Toutefois, l'erreur de couplage mutuel du capteur restante doit être évaluée. De même, l'incertitude de compensation est prise en compte comme une contribution supplémentaire à l'incertitude d'étalonnage du système de mesure. La manière dont l'erreur se propage et dont l'incertitude est couplée à d'autres termes d'incertitude doit être documentée.

C.2.6 Diffraction à l'intérieur du réseau de sondes

La diffraction des champs électromagnétiques dans le fantôme due à la présence du réseau de sondes est à l'origine de la distorsion de la distribution du champ d'impact capturé par les capteurs. Ces réflexions dépendent dans une large mesure de la distribution, de la polarisation et de l'angle d'incidence des champs incidents. Par conséquent, elles ne peuvent pas être totalement étalonnées. Ce terme d'incertitude est corrélé avec l'incertitude due au couplage mutuel entre les capteurs.

Il est également possible d'évaluer ensemble les composantes d'incertitude de l'isotropie (C.2.3), du couplage mutuel de capteur (C.2.5) et de la diffraction à l'intérieur du réseau (C.2.6).

C.2.7 Erreur d'échantillonnage

La distribution du DAS mesuré est estimée à partir de l'échantillonnage direct du champ à un niveau de points discrets. Si la résolution d'échantillonnage est grossière comparée aux gradients de la distribution du DAS induite, le résultat psDAS peut être inexact. L'incertitude est évaluée en utilisant l'ensemble de distributions de référence de O.8.2.

L'évaluation de cette incertitude peut être combinée à l'évaluation de l'incertitude des algorithmes de reconstruction.

C.2.8 Limites du réseau

Outre les incertitudes de DAS dues à la résolution spatiale et aux emplacements des capteurs, il existe des erreurs à la limite de la zone de mesure dues à la troncature du champ mesuré et à l'extrapolation de la distribution de champ mesuré au-delà de la zone de mesure.

Cette incertitude peut être évaluée avec l'incertitude des algorithmes de reconstruction.

L'incertitude est évaluée en utilisant les distributions de référence de O.8.2. Les distributions de référence sont appliquées à proximité de la limite de la zone de mesure. Si le système de mesure affiche des mises en garde ou des messages d'erreur adressés à l'utilisateur, concernant l'erreur de mesure aux emplacements proches de la limite, l'évaluation doit être réalisée à l'intérieur de ces emplacements. Comparer le psDAS à 1 g et le psDAS à 10 g obtenus aux valeurs cibles.

IECNORM.COM : Click to view the full PDF of IEC/IEEE 62209-1528:2020

C.2.9 Couplage de sonde ou de réseau de sonde avec le DUT

Outre le couplage spécifié en C.2.5, il peut exister un couplage entre les capteurs et le DUT qui cause également une incertitude de mesure. Afin d'évaluer l'incertitude, il convient d'évaluer plusieurs dispositifs rayonnants et positions d'essai de manière appropriée pour le système de mesure, en utilisant l'essai rapide de DAS et l'essai complet de DAS.

C.2.10 Immunité / réception secondaire du système de mesure

Comme pour les systèmes d'essai complet de DAS, il convient de concevoir les systèmes d'essai rapide de DAS de façon à atténuer tout bruit ou décalage des mesurages dû à la collecte de signal qui n'est pas mesuré au niveau du ou des capteurs. Les champs électriques incidents sur les lignes de transmission à impédance élevée peuvent être collectés par les lignes de qui cause une interférence (réception secondaire) avec le signal collecté par le ou les capteurs. Pour les essais complets de DAS, cet effet est réduit le plus possible en utilisant les lignes à impédance élevée le long de l'axe de sonde. Pour les systèmes d'essai rapide de DAS utilisant différents agencements de capteurs, il convient de mesurer l'immunité à ces signaux secondaires. Il convient de réaliser cela en effectuant un mesurage à point unique d'une sonde du système d'essai rapide de DAS en utilisant le montage de validation du système décrit à l'Annexe A et en comparant la valeur mesurée à la valeur obtenue en utilisant une sonde utilisée pour un essai complet du DAS. Afin d'assurer que le couplage potentiel entre les capteurs et le DUT (C.2.5 et C.2.9) n'est pas inclus, il convient de maintenir la source rayonnante éloignée du système d'essai rapide de DAS d'au moins un quart de longueur d'onde dans l'air.

NOTE Il est suffisant de soumettre à l'essai ce terme d'incertitude en utilisant l'espacement de sonde le plus dense du groupe de sondes si l'espacement de ce dernier est variable.

C.2.11 Écarts de forme de fantôme

Ce terme d'incertitude prend en compte les variations de mesure dues à la forme de fantôme, si la forme de fantôme s'écarte du fantôme normalisé décrit à l'Annexe G. Il convient de déterminer ce terme à partir de la différence entre le DAS pour la forme de fantôme utilisée pour la méthode d'essai rapide de DAS et le DAS pour le fantôme normalisé. Il est recommandé d'effectuer les mesurages sur les deux fantômes par un essai complet du DAS, de manière à ne pas inclure le couplage de capteur avec le DUT (C.2.9) dans l'analyse d'incertitude. Il convient d'appliquer les différentes sources et positions de source par rapport au fantôme, selon le cas, pour évaluer l'influence de la forme du fantôme sur différentes distributions de DAS.

C.2.12 Variation spatiale des propriétés diélectriques

Les propriétés diélectriques du milieu équivalent au tissu peuvent varier spatialement. La variation spatiale des propriétés diélectriques peut être évaluée sur un échantillon de production du matériau en mesurant les propriétés diélectriques dans plusieurs régions (au moins 10, y compris des différents emplacements dans les directions x, y et z dans le volume entourant les positions de capteurs) dans un échantillon diélectrique sur l'ensemble de la plage de fréquences d'intérêt. Si le milieu équivalent au tissu est inaccessible à l'utilisateur, il convient que ce mesurage soit effectué par le fabricant du système. Les méthodes de l'Annexe H peuvent être utilisées pour mesurer les propriétés diélectriques, le cas échéant. Il convient que les méthodes de mesure des propriétés diélectrique soient appropriées pour le matériau soumis à l'essai. Le terme d'incertitude est calculé à partir de la différence en pourcentage la plus élevée de chacune des valeurs de permittivité et de conductivité par rapport à la valeur moyenne, une loi rectangulaire étant prise pour hypothèse.

C.2.13 Reconstruction

La méthode d'évaluation de la contribution à l'incertitude due aux algorithmes de reconstruction, à l'exclusion du moyennage de psDAS, est la suivante.

a) Échantillonner les distributions de champ analytique de référence aux points de la grille et en utilisant les polarisations correspondant au balayage de mesure réalisé par le système réel.

IECNORM.COM : Click to view the full PDF of IEC/IEEE 62209-1528:2020

b) Traiter les données échantillonnées en utilisant la reconstruction du système et les algorithmes maximaux moyennés dans l'espace.

c) Pour chaque distribution, calculer la différence relative entre le psDAS obtenu à l'étape b) et les cibles de DAS de référence pour les fonctions analytiques fournies.

NOTE Les distributions de champ analytiques sont décrites dans l'IEC 62209-3.

C.3 Bilan d'incertitude

Le bilan d'incertitude spécifié dans le Tableau C.1 est l'incertitude de la valeur de DAS mesuré pour une configuration d'essai comparée au DAS mesuré des autres configurations d'essai qui ont été mesurées en utilisant le même système d'essai rapide de DAS aux mêmes bandes de fréquences et modulation.

Le bilan d'incertitude relatif pour le contrôle du système réalisé pour une méthode d'essai rapide de DAS est présenté dans le Tableau C.2. Ce bilan d'incertitude est similaire au bilan d'incertitude de répétabilité pour le contrôle du système. Les termes d'incertitude qui peuvent être négligés ont des coefficients de pondération de c_i = 0.

IECNORM.COM : Click to view the full PDF of IEC/IEEE 62209-1528:2020

Tableau C.1 – Bilan d'incertitude de mesure pour des mesurages de DAS relatifs à l'aide d'un essai rapide de DAS de Classe 2, pour les essais effectués dans une bande de fréquences et modulation

Grandeur d'entrée X_i (source d'incertitude)	Réf.	Prob. Dist. PDF_i	Unc. $a(x_i)$	Div. q_i	$u(x_i) = a(x_i)/q_i$	c_i (1 g, 10 g)	$u(y) = c_i \cdot u(x_i)$	v_i ou v_{eff}
Système de mesure								
Étalonnage du système	C.2.2	N		1		0		∞
Isotropie	C.2.3	R		√3		1		∞
Effet de proximité de bord	8.4.1.6	R		√3		1		∞
Linéarité	8.4.1.3	R		√3		1		∞
Limites de détection du système	8.4.1.3	R		√3		1		∞
Réponse en modulation	8.4.2.7	R		√3		1		∞
Lecture électronique	8.4.1.6	N		1		0		∞
Temps de réponse	8.4.1.6	R		√3		0		∞
Temps d'intégration	8.4.1.6	R		√3		1		∞
Conditions RF ambiantes – bruit	8.4.1.7	R		√3		1		∞
Conditions RF ambiantes – réflexions	8.4.1.7	R		√3		0		∞
Positionnement de la sonde	C.2.4	R		√3		1		∞
Couplage mutuel de capteur	C.2.5	R		√3		1		∞
Diffraction à l'intérieur du réseau	C.2.6	R		√3		1		∞
Erreur d'échantillonnage	C.2.7	R		√3		1		∞
Limites du réseau	C.2.8	R		√3		1		∞
Couplage de sonde ou de réseau de sonde avec le DUT	C.2.9	R		√3		1		∞
Immunité du système de mesure	C.2.10	R		√3		1		∞
Post-traitement de données de mesure	8.4.1.9	R		√3		1		$N-1$
Variation spatiale des propriétés diélectriques	C.2.12	R		√3		1		∞
Reconstruction	C.2.13	R		√3		1		∞
Échantillon d'essai								
Positionnement de l'échantillon d'essai	8.4.2.5	N		1		1		∞
Incertitude du support de dispositif	8.4.2.6	N		1		1		∞
Variation de la puissance de sortie – Mesure de la dérive de DAS	8.4.2.9	R		√3		1		∞
Mise à l'échelle du DAS	8.4.3.2	R		√3		0		∞
Paramètre de fantôme et de tissu								
Écarts de forme de fantôme	C.2.11	R		√3		1		∞
Incertitude de la correction de DAS pour des écarts de permittivité et de conductivité	8.4.3.1	N		1		0		∞
Mesure de la conductivité du milieu	8.4.2.1	N		1		0		M
Mesure de la permittivité du milieu	8.4.2.1	N		1		0		M
Conductivité du milieu – incertitude de température	8.4.2.2	R		√3		0		∞
Permittivité du milieu – incertitude de température	8.4.2.2	R		√3		0		∞
Incertitude-type composée, $u(\Delta DAS)$		RSS						v_{eff}
Incertitude élargie, U		k = 2						

IECNORM.COM : Click to view the full PDF of IEC/IEEE 62209-1528:2020

Tableau C.2 – Bilan d'incertitude de mesure pour le contrôle du système à l'aide d'un essai rapide de DAS de Classe 2

Grandeur d'entrée X_i (source d'incertitude)	Réf.	Prob. Dist. PDF_i	Unc. $a(x_i)$	Div. q_i	$u(x_i) = a(x_i)/q_i$	c_i (1 g; 10 g)	$u(y) = c_i \cdot u(x_i)$	v_i ou v_{eff}
Système de mesure								
Dérive de l'étalonnage du système	C.2.2	N		1		1		∞
Isotropie	C.2.3	R		√3		0		∞
Effet de proximité de bord	8.4.1.6	R		√3		0		∞
Linéarité	8.4.1.3	R		√3		0		∞
Limites de détection du système	8.4.1.3	R		√3		0		∞
Réponse en modulation	8.4.2.7	R		√3		0		∞
Lecture électronique	8.4.1.6	N		1		0		∞
Temps de réponse	8.4.1.6	R		√3		0		∞
Temps d'intégration	8.4.1.6	R		√3		0		∞
Conditions RF ambiantes – bruit	8.4.1.7	R		√3		0		∞
Conditions RF ambiantes – réflexions	8.4.1.7	R		√3		0		∞
Positionnement de la sonde	C.2.4	R		√3		1		∞
Couplage mutuel de capteur	C.2.5	R		√3		1		∞
Diffraction à l'intérieur du réseau	C.2.9	R		√3		0		∞
Erreur d'échantillonnage	C.2.7	R		√3		1		∞
Limites du réseau	C.2.8	R		√3		0		∞
Couplage de sonde ou de réseau de sonde avec le DUT	C.2.6	R		√3		0		∞
Immunité du système de mesure	C.2.10	R		√3		1		∞
Post-traitement de données de mesure	8.4.1.9	R		√3		0		$N-1$
Variation spatiale des propriétés diélectriques	C.2.12	R		√3		0		∞
Reconstruction	C.2.13	R		√3		1		∞
Échantillon d'essai								
Positionnement de l'échantillon d'essai	8.4.2.5	N		1		0		∞
Incertitude du support de dispositif	8.4.2.6	N		1		0		∞
Variation de la puissance de sortie – Mesure de la dérive de DAS	8.4.2.9	R		√3		0		∞
Mise à l'échelle du DAS	8.4.3.2	R		√3		0		∞
Paramètre de fantôme et de tissu								
Écarts de forme de fantôme	C.2.11	R		√3		1		∞
Incertitude de la correction de DAS pour des écarts de permittivité et de conductivité	8.4.3.1	N		1		*1;0,84*		∞
Mesure de la conductivité du milieu	8.4.2.1	N		1		*0,78;0,71*		M
Mesure de la permittivité du milieu	8.4.2.1	N		1		*0,23;0,26*		M
Conductivité du milieu – incertitude de température	8.4.2.2	R		√3		*0,78;0,71*		∞
Permittivité du milieu – incertitude de température	8.4.2.2	R		√3		*0,23;0,26*		∞
Incertitude-type composée		RSS						v_{eff}
Incertitude élargie, U		k = 2						

IECNORM.COM : Click to view the full PDF of IEC/IEEE 62209-1528:2020

Annexe D
(normative)

Antennes de validation du système DAS

D.1 Exigences générales relatives aux antennes

L'Annexe D décrit les antennes utilisées pour valider les systèmes de mesure de DAS satisfaisant aux exigences normatives du présent document. Les antennes autres que celles spécifiées dans les paragraphes de l'Annexe D peuvent être prises en considération pour la validation du système. Les exigences minimales spécifiées pour toute antenne de validation du système sont présentées ci-après.

a) La justification doit être fournie pour l'intégration d'une antenne et la mesure dans laquelle son utilisation renforce le protocole de validation.

b) Les configurations d'essai (les fréquences, les emplacements sur le fantôme, la distance, l'angle de rotation, par exemple) doivent être fournies.

c) Les dessins détaillés, y compris toutes les dimensions et tolérances, doivent être fournis. Les fichiers CAO des antennes doivent être mis à disposition avec des informations détaillées suffisantes relatives à la construction et des paramètres, de manière à pouvoir vérifier les cibles numériques indépendamment.

d) Les valeurs de DAS cibles numériques doivent être déterminées à partir de simulations numériques du fichier CAO de l'antenne. Les simulations numériques doivent satisfaire aux exigences de l'IEC/IEEE 62704-1 [41].

e) Les valeurs de DAS cibles numériques doivent être disponibles pour toutes les configurations d'essai spécifiées sur les fantômes.

f) Les antennes physiques doivent être mesurées à l'aide d'un système de mesure du DAS dont un étalonnage est agréé (ISO/IEC 17025 [17], par exemple) afin de valider les valeurs cibles numériques et générer un certificat de traçabilité.

NOTE L'acceptation réglementaire d'autres conceptions d'antenne peut impliquer des exigences supplémentaires autres que celles décrites ci-dessus.

Différentes antennes satisfaisant aux exigences précédentes sont spécifiées de l'Article D.2 à l'Article D.5.

D.2 Antenne doublet normalisée

D.2.1 Description mécanique

Les antennes doublets normalisées de la Figure D.1 avec les dimensions mécaniques indiquées dans le Tableau D.1 génèrent les valeurs DAS données dans le Tableau D.2 lorsque l'essai de validation du système de A.3.5 est réalisé. Si des antennes doublets dont les dimensions sont différentes de celles indiquées dans le Tableau D.1 sont utilisées ou si des antennes doublets sont utilisées à des fréquences autres que celles indiquées dans le Tableau D.1, les valeurs de DAS de référence pour ces antennes doivent être documentées et vérifiées indépendamment à l'aide de procédures en cohérence avec les méthodologies spécifiées dans le présent document.

IECNORM.COM : Click to view the full PDF of IEC/IEEE 62209-1528:2020

Le doublet de référence doit être positionné sous le fantôme plan et centré avec son axe parallèle au plus long côté du fantôme. Il convient d'utiliser un écarteur de faible perte (tangente de perte < 0,05) et de faible permittivité (permittivité relative < 5) pour établir la distance correcte entre le dessus de la surface du doublet de référence et la surface de la base du fantôme. Sous 3 GHz, l'écarteur ne doit pas faire varier les valeurs de psDAS à 1 g et à 10 g mesuré de plus de 1 %, comparé à l'état sans écarteur. Au-dessus de 3 GHz, l'écarteur peut avoir un impact sur le DAS mesuré et introduire des écarts par rapport aux valeurs numériques du Tableau D.2. Par conséquent, des valeurs numériques cibles de DAS validées de façon expérimentale avec des écarteurs spécifiques doivent être utilisées (voir le Tableau D.2). Le doublet de référence doit avoir un facteur d'adaptation supérieur à 20 dB à la fréquence d'essai afin de réduire la réflexion de puissance et l'incertitude de mesure de DAS.

Pour les doublets de référence, un écarteur diélectrique est utilisé pour fournir la distance s et la tolérance mécanique de l'écarteur, donnés par:

s = 15 mm ± 0,2 mm, pour 300 MHz ≤ f ≤ 1 000 MHz
s = 10 mm ± 0,2 mm, pour 1 000 MHz < f ≤ 6 000 MHz
s = 5 mm ± 0,1 mm, pour 6 000 MHz < f ≤ 10 000 MHz

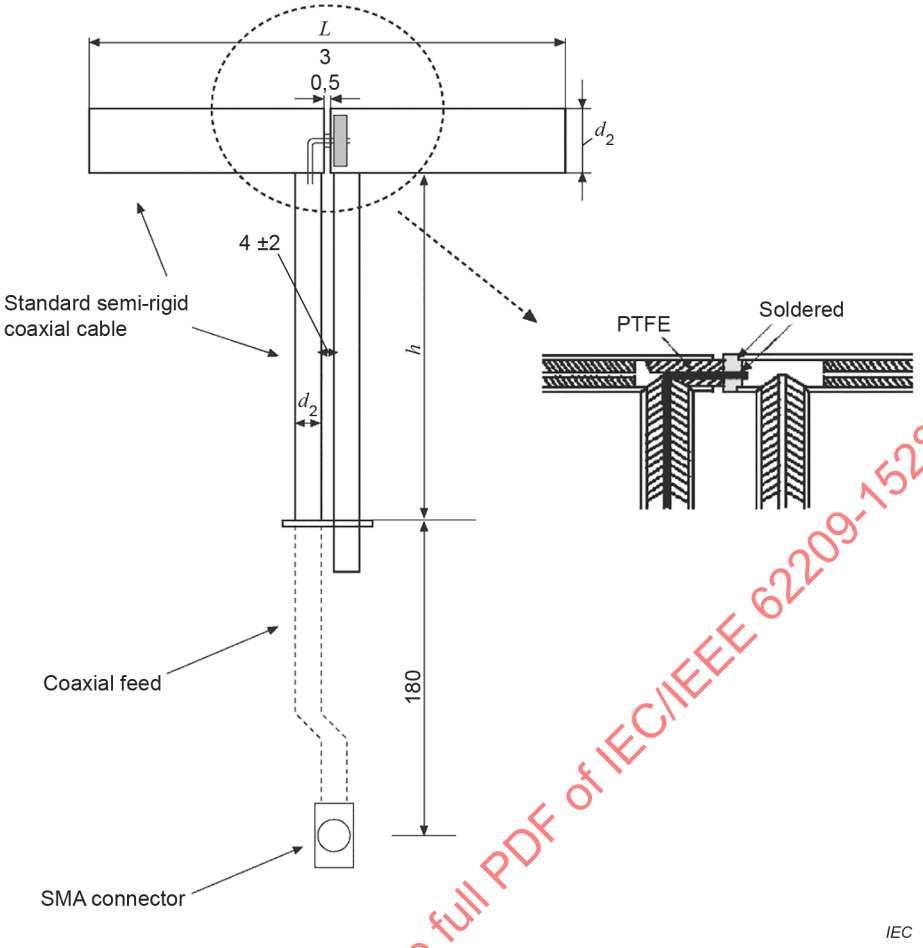
Le calcul des valeurs de référence du Tableau D.2 pour des fréquences supérieures à 5 000 MHz exige une considération particulière de la structure de construction des petits doublets (tant internes qu'externes), les valeurs numériques étant donc spécifiques à la conception de l'antenne doublet. L'écarteur diélectrique utilisé pour le doublet doit également être modélisé, étant donné qu'il peut avoir un impact sur la valeur de DAS déterminée de façon numérique.

Le doublet de référence doit avoir un facteur d'adaptation supérieur à 20 dB à la fréquence d'essai afin de réduire l'incertitude de mesure de puissance. Pour satisfaire à cette exigence, il est acceptable de régler finement les doublets de référence en utilisant des éléments de réglage en matériau diélectrique à faible perte ou métallique aux extrémités du doublet (Figure A.1).

Les bras du doublet de référence doivent être parallèles à la surface plane du fantôme avec une tolérance de ±2° ou moins (Figure D.1). Cela peut être assuré en positionnant avec précaution le fantôme vide et le doublet de référence dans le plan horizontal à l'aide d'un niveau à bulle.

Les valeurs numériques cibles au-dessus de 3 GHz ne peuvent pas être définies de façon universelle, car au-dessous de 3 GHz, en raison du plus grand effet de l'écarteur, de la base du fantôme et des incertitudes mécaniques. Par conséquent, les valeurs numériques cibles peuvent être différentes d'un doublet à un autre. Il est important que pour chaque doublet utilisé pour la validation du système, une analyse complètement documentée soit fournie, sur la base de simulations numériques et d'une validation expérimentale.

IECNORM.COM : Click to view the full PDF of IEC/IEEE 62209-1528:2020



Anglais	Français
Standard semi-rigid coaxial cable	Câble coaxial semi-rigide normalisé
Soldered	Soudé
Coaxial feed	Alimentation coaxiale
SMA connector	Connecteur SMA

Légende

L longueur du doublet

d_1 diamètre du doublet

d_2 diamètre du câble coaxial au niveau du symétriseur

h longueur du symétriseur

PTFE polytétrafluoroéthylène

Figure D.1 – Informations détaillées mécaniques relatives au doublet normalisé

IECNORM.COM : Click to view the full PDF of IEC/IEEE 62209-1528:2020

Tableau D.1 – Dimensions mécaniques des doublets de référence

Fréquence MHz	L mm	h mm	d_1 mm
300	420,0	250,0	6,35
450	290,0	166,7	6,35
750	176,0	100,0	6,35
835	161,0	89,8	3,6
900	149,0	83,3	3,6
1 450	89,1	51,7	3,6
1 500	86,2	50,0	3,6
1 640	79,0	45,7	3,6
1 750	75,2	42,9	3,6
1 800	72,0	41,7	3,6
1 900	68,0	39,5	3,6
1 950	66,3	38,5	3,6
2 000	64,5	37,5	3,6
2 100	61,0	35,7	3,6
2 300	55,5	32,6	3,6
2 450	51,5	30,4	3,6
2 600	48,5	28,8	3,6
3 000	41,5	25,0	3,6
3 500	37,0	26,4	3,6
3 700	34,7	26,4	3,6
5 000 à 6 000	20,6 [a]	40,3 [a]	3,6
6 000 à 8 000	14,5	35,1	2,2
8 000 à 10 000	12,2	25,0	2,2

NOTE Les dimensions L, h, et d_1 doivent être dans les limites de tolérance de ±2 %.

[a] Ces dimensions sont applicables pour un diamètre coaxial au niveau du symétriseur de d_2 = 2,1 mm (Figure D.1).

IECNORM.COM : Click to view the full PDF of IEC/IEEE 62209-1528:2020

D.2.2 Valeurs de DAS numériques cibles

Le Tableau D.2 présente les valeurs de DAS numériques cibles pour la validation du système (A.3.5), avec les doublets normalisés spécifiés en D.2.1. Les valeurs de DAS numériques cibles du Tableau D.2 ont été calculées à l'aide de la méthode des différences finies dans le domaine temporel (FDTD) en utilisant les exigences relatives au fantôme plan de l'Article G.3 et du Tableau G.3, et ont été validées par rapport aux résultats mesurés avec des montages d'essai équivalents de 300 MHz à 10 GHz. Les valeurs de DAS local de la colonne 5 et de la colonne 6 du Tableau D.2 ont été vérifiées de façon expérimentale pour chaque fréquence d'essai en utilisant une extrapolation polynomiale de 4e ordre. Les valeurs au-dessus de 3 GHz dépendent de l'écarteur de doublet utilisé et de la construction détaillée des doublets. Par conséquent, les cibles de doublets individuelles peuvent présenter un écart par rapport aux valeurs du Tableau D.2 allant jusqu'à ±10 %. Cela est dû au fait que les dimensions du doublet sont courtes par rapport à son diamètre et aux dimensions de l'écarteur, c'est-à-dire que les valeurs numériques cibles ne sont pas génériques, et il est nécessaire de les déterminer pour une configuration particulière. Les propriétés diélectriques utilisées pour le milieu équivalent au tissu sont spécifiées dans le Tableau 2 (voir 6.2.2), et les dimensions des doublets de

référence sont présentées dans le Tableau D.1. Une valeur de DAS de référence différente peut s'appliquer pour les doublets dont les dimensions mécaniques s'écartent de celles des doublets de référence données en D.2.1.

Tableau D.2 – Valeurs de DAS numériques cibles (W/kg) pour un doublet normalisé et un fantôme plan

Fréquence	Épaisseur de l'enveloppe du fantôme	DAS 1 g	DAS 10 g	DAS local à la surface (au-dessus du point d'alimentation)	DAS local à la surface (y = 2 cm de décalage par rapport au point d'alimentation)
MHz	mm	W/kg	W/kg	W/kg	W/kg
300	2,0	2,85	1,94	4,14	2,00
450	2,0	4,58	3,06	6,75	2,98
750	2,0	8,49	5,55	12,6	4,59
835	2,0	9,56	6,22	14,1	4,90
900	2,0	10,9	6,99	16,4	5,40
1 450	2,0	29,0	16,0	50,2	6,50
1 500	2,0	30,5	16,8	52,8	6,53
1 640	2,0	34,2	18,4	60,4	6,69
1 750	2,0	36,4	19,3	64,9	6,53
1 800	2,0	38,4	20,1	69,5	6,80
1 900	2,0	39,7	20,5	72,1	6,60
1 950	2,0	40,5	20,9	72,7	6,60
2 000	2,0	41,1	21,1	74,6	6,50
2 100	2,0	43,6	21,9	79,9	6,58
2 300	2,0	48,7	23,3	92,8	7,18
2 450	2,0	52,4	24,0	104	7,70
2 585	2,0	55,9	24,4	119	7,9
2 600	2,0	55,3	24,6	113	8,29
3 000	2,0	63,8	25,7	140	9,50
3 500	2,0	67,1	25,0	169	12,1
3 700	2,0	67,4	24,2	178	12,7
5 000	2,0	77,9	22,1	305	15,1
5 200	2,0	76,5	21,6	310	15,9
5 500	2,0	83,3	23,4	349	18,1
5 800	2,0	78,0	21,9	341	20,3
7 000	2,0	275,0	47,0	2 161,0	13,0
9 000	2,0	243,0	40,0	2 676,0	12,0

NOTE 1 Toutes les valeurs de DAS sont normalisées à une puissance directe de 1 W.

NOTE 2 Les valeurs de DAS cibles à 1 g et 10 g sont uniquement valables pour la validation du système spécifiée à l'Article A.1, à l'aide de doublets présentant les dimensions spécifiées en D.2.1.

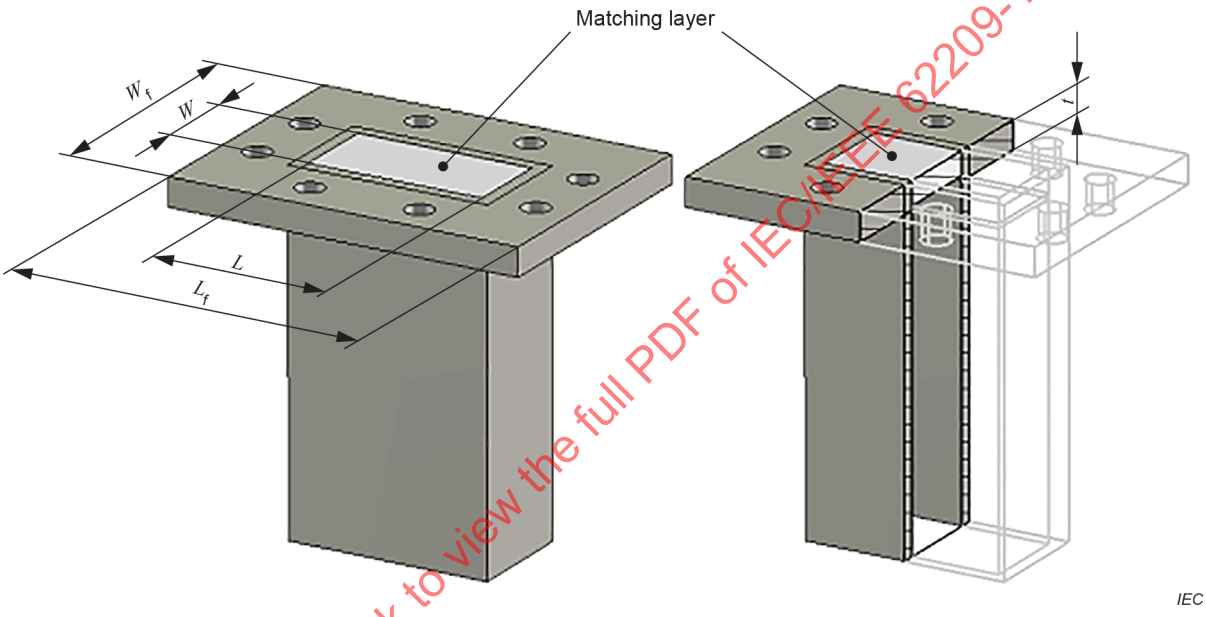
NOTE 3 Les valeurs de DAS au-dessus de 3 GHz sont sensibles à la géométrie du doublet et du fantôme (longueur du doublet, longueur et permittivité de l'écarteur, et permittivité de l'enveloppe du fantôme) et peuvent varier de ±10 % au maximum. Voir Onishi and Uebayashi [36] pour plus de détails.

IECNORM.COM : Click to view the full PDF of IEC/IEEE 62209-1528:2020

D.3 Guide d'ondes normalisé

D.3.1 Description mécanique

Le guide d'ondes normalisé de la Figure D.2 avec les dimensions mécaniques indiquées dans le Tableau D.3 (correspondant à WR159 ou UK WG-13 avec une bride IEC-UDR58 selon l'IEC 60154-2 [42]) donne les valeurs de DAS indiquées dans le Tableau D.4 lorsque l'essai de validation du système de A.3.5 est réalisé. L'alimentation du guide d'ondes doit être placée à au moins une longueur d'onde de la couche d'adaptation afin de veiller à ce que les modes d'ordre supérieur aient été atténués. La perte de transmission de guide d'ondes doit être caractérisée par un mesurage avec un analyseur de réseau. Si des guides d'onde sont utilisés et ont des paramètres différents de ceux indiqués dans le Tableau D.3 ou si des guides d'ondes sont utilisés à des fréquences autres que celles indiquées dans le Tableau D.3, les valeurs de référence de DAS pour ces guides d'ondes doivent être documentées et indépendamment vérifiées (en comparant des simulations numériques aux mesurages, par exemple).



Anglais	Français
Matching layer	Couche d'adaptation

Figure D.2 – Guide d'ondes normalisé (dimensions conformes au Tableau D.3)

IECNORM.COM : Click to view the full PDF of IEC/IEEE 62209-1528:2020

Tableau D.3 – Dimensions mécaniques du guide d'ondes normalisé

Fréquence MHz	Épaisseur de l'enveloppe du fantôme mm	L mm	W mm	L_f mm	W_f mm	t mm	ε_r
5 200	2	40,39	20,19	81,03	61,98	5,3	6
5 800	2	40,39	20,19	81,03	61,98	4,3	6

NOTE L et W sont la longueur et la largeur internes du guide d'ondes, L_f et W_f sont la longueur et la largeur de la bride du guide d'ondes, et t et ε_r sont l'épaisseur et la permittivité relative de la couche d'adaptation. La tolérance pour L et W est ±0,13 mm. La couche d'adaptation est une plaque de séparation diélectrique sans perte qui remplit la section transversale $L \cdot W$ du guide d'ondes. Le guide d'ondes et la couche d'adaptation sont en contact direct avec l'enveloppe du fantôme. La hauteur minimale du guide d'ondes (de l'alimentation à la bride) est une longueur d'onde d'espace libre. Cette configuration donne un facteur d'adaptation d'entrée d'au moins 8 dB. L'incertitude de la permittivité et l'épaisseur de la plaque de séparation diélectrique sont incluses dans le facteur d'adaptation. Par conséquent, il n'est pas nécessaire de les spécifier indépendamment.

D.3.2 Valeurs de DAS numériques cibles

Le Tableau D.4 présente les valeurs de DAS numériques cibles pour la validation du système avec les guides d'ondes normalisés spécifiés en D.3.1. Les valeurs cibles numériquement validées de DAS dépendent de la permittivité relative de l'enveloppe du fantôme. Par conséquent, les valeurs cibles sont données pour des permittivités relatives d'enveloppe du fantôme de 3, 4 et 5. Une interpolation linéaire doit être appliquée pour des valeurs de permittivité relatives d'enveloppe du fantôme comprises entre ces valeurs. Les valeurs numériques cibles de DAS du Tableau D.4 correspondent à une puissance nette mesurée de 1 W dans le guide d'ondes et ont été calculées en utilisant la méthode des différences finies dans le domaine temporel (FDTD) avec les exigences d'intégration volumique décrites dans l'IEEE C95.3-2002 [43] et vérifiées par des mesurages [44]. La puissance transmise au fantôme est égale à la puissance directe dans le guide d'ondes moins la puissance réfléchie et les pertes de transmission du guide d'ondes (comprenant les pertes dans l'adaptateur et les parois du guide d'ondes). La perte de transmission de l'adaptateur peut être déterminée en mesurant S_{11} à son accès coaxial avec trois terminaisons de guide d'ondes normalisées différentes raccordées à l'accès de guide d'ondes, par exemple un court-circuit plus deux courts-circuits de décalage différents (lignes de transmission court-circuitées à différentes longueurs de décalage). La perte de transmission de guide d'ondes doit être mesurée au moins une fois par an en utilisant un analyseur de réseau étalonné.

Le guide d'ondes utilisé dans les simulations a été modélisé comme un conducteur électrique parfait avec une fenêtre diélectrique d'adaptation ayant des dimensions telles que spécifiées en D.3.1. Le fantôme utilisé dans les simulations a une longueur de 216 mm, une largeur de 152 mm, une profondeur de 80 mm et une épaisseur d'enveloppe de 2 mm. Les propriétés diélectriques du milieu équivalent au tissu sont telles que définies dans le Tableau 2 (voir 6.2.2).

IECNORM.COM : Click to view the full PDF of IEC/IEEE 62209-1528:2020

Tableau D.4 – Valeurs numériques cibles de DAS pour les guides d'ondes

Fréquence MHz	Permittivité relative de l'enveloppe du fantôme	DAS 1 g W/kg	DAS 10 g W/kg	Point DAS en fonction de la distance, d [mm] dans le fantôme le long de sa ligne centrale
5 200	3	165	53,7	$667 \exp(-2d/6,2)$
	4	180	56,5	$733 \exp(-2d/6,2)$
	5	194	59,1	$796 \exp(-2d/6,2)$
5 800	3	165	49,3	$804 \exp(-2d/5,5)$
	4	184	52,5	$907 \exp(-2d/5,5)$
	5	200	55,2	$982 \exp(-2d/5,5)$
Si la puissance nette produit des valeurs de DAS mesuré qui sont supérieures à la plage dynamique de la sonde, des puissances plus faibles doivent être utilisées de manière à ne pas introduire une incertitude de mesure supplémentaire ou endommager la sonde. NOTE 1 La bride du guide d'ondes est en contact direct avec la surface extérieure de l'enveloppe du fantôme. NOTE 2 Toutes les valeurs de DAS sont normalisées à 1 W de puissance nette (c'est-à-dire, la puissance transmise au fantôme). NOTE 3 Les valeurs de DAS de référence de 1 g et 10 g sont valides uniquement pour la validation du système définie à l'Article A.1, en utilisant des guides d'ondes ayant les dimensions et la construction telles que définies en D.3.1.				

D.4 Antennes de validation du système au-dessous de 150 MHz

D.4.1 Généralités

À des fréquences de 150 MHz et au-dessous, les dimensions physiques des doublets et guides d'ondes normalisés deviennent trop importantes pour être pratiques. Par conséquent, d'autres antennes étalonnées pour un DAS à 1 g et 10 g peuvent être utilisées.

D.4.2 Antenne cadre confinée

D.4.2.1 Description mécanique

Un cadre résonant est un exemple d'antenne cadre confinée (CLA), comme cela est représenté à la Figure D.3. Les exigences relatives à ce type d'antennes sont les suivantes:

a) résonante à la fréquence cible: f_{cible} ± 1 MHz;

b) facteur d'adaptation à la fréquence de résonance: > 10 dB;

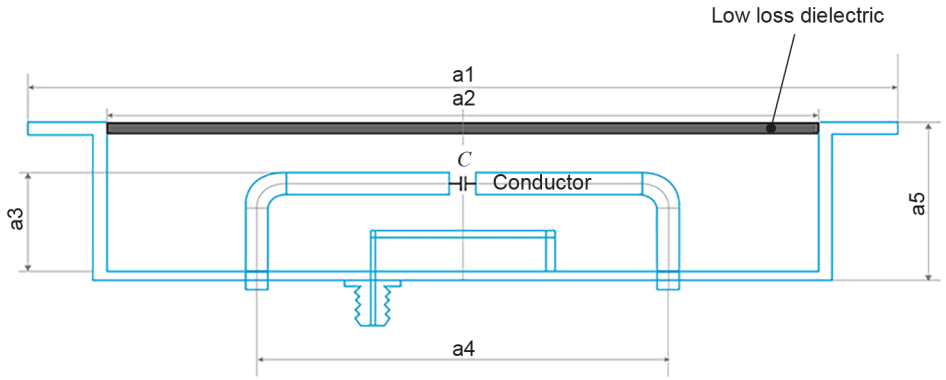
c) stabilité du psDAS à 1 g et 10 g (à la puissance d'entrée spécifiée maximale): < 2 % (> 60 min);

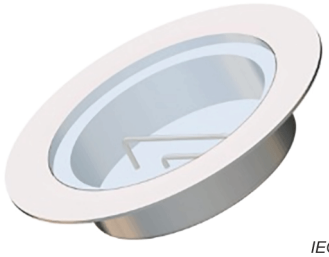
d) reproductibilité interlaboratoire du psDAS à 1 g et 10 g: < 10 %; < 10 %;

e) distorsion (en modifiant la réflectivité du sol ou la rotation de la structure sous le fantôme pour des configurations de validation classiques): < 3 %.

L'exigence de facteur d'adaptation est de 10 dB comparée à l'exigence de 20 dB pour les antennes doublets, car les dispositifs sont considérablement plus petits que la longueur d'onde. En règle générale, les antennes autres que les doublets et guides d'ondes décrits présentent des pertes plus élevées, et leur rendement peut varier à une puissance d'entrée élevée en raison des effets thermiques. De plus, les structures à facteur de qualité élevé sont sensibles aux petites variations par l'environnement de réflexion. Ces antennes doivent donc être conçues pour réduire le plus possible l'influence de l'environnement.

IECNORM.COM : Click to view the full PDF of IEC/IEEE 62209-1528:2020





Anglais	Français
Conductor	Conducteur
Low loss electric	Électrique faible perte

Légende

C capacité

NOTE Dimensions: a1 = 220 mm, a2 = 180 mm, a3 = 25 mm, a4 = 110 mm, a5 = 45 mm.

Figure D.3 – Dessin de la CLA correspondant à un cadre résonant intégré dans une structure métallique pour isoler la structure résonante de l'environnement

IECNORM.COM : Click to view the full PDF of IEC/IEEE 62209-1528:2020

D.4.2.2 Valeurs de DAS numériques cibles

Les valeurs cibles de la CLA ont été évaluées par modélisation FDTD de l'antenne sous le fantôme elliptique (600 × 400) mm avec une enveloppe diélectrique sans perte (ε_r = 3,7) de 2 mm d'épaisseur. L'antenne est alimentée par l'embase d'un câble coaxial terminé par une source de tension avec une résistance interne de 50 Ω. Le maillage maximal est limité à 3 mm dans le fantôme et à 15 mm dans l'espace libre. Pour les fréquences inférieures et mailles supérieures, le maillage maximal est relâché, mais est toujours maintenu sous λ/10. Les conditions limites d'absorption terminent le domaine de calcul à environ 200 mm de l'antenne. Aux fréquences de 64 MHz et en dessous, cette distance augmente à environ λ/4. Dans toutes les simulations, les antennes sont excitées avec une impulsion à large bande. Compte tenu de leur facteur de qualité élevé (Q), les simulations sont exécutées pendant 50 périodes de fréquences de fonctionnement. En particulier, à l'extrémité inférieure de la plage de fréquences étudiée, l'impédance d'entrée devient très réactive pour de petits écarts par rapport à la fréquence de résonance, ce qui gêne l'évaluation du bilan de puissance des simulations. Étant donné que les écarts observés par rapport à la fréquence de résonance nominale sont petits (< 5 %), le DAS est évalué à la résonance réelle du modèle numérique. Pour obtenir des valeurs cibles fiables, les valeurs de psDAS sont normalisées à la crête des champs H dans le plan à 5 mm du centre de la base à l'intérieur du fantôme. Le Tableau D.5 répertorie les résultats de psDAS à 1 g et 10 g normalisés par rapport au champ H. La normalisation de champ H fournit les valeurs cibles de DAS indépendantes des pertes d'antenne internes, ces dernières pouvant être importantes et varier d'une mise en œuvre à l'autre. Pour le même type de CLA, un laboratoire d'étalonnage peut convertir la valeur de champ H primaire en valeur de puissance d'entrée secondaire, plus pratique à utiliser que les valeurs de champ H primaires et sans perte de répétabilité, à condition de ne pas ouvrir et ne pas modifier la CLA.

L'incertitude numérique est évaluée à 150 MHz, qui est considérée comme étant représentative de la plupart des configurations. La contribution à l'incertitude du bilan de puissance est évaluée pour la simulation la plus défavorable à 30 MHz. Pour l'évaluation de l'incertitude de résolution de la grille, la maille a été affinée à 1,5 mm au maximum dans le fantôme et à 7 mm dans l'espace libre. Dans le rectangle englobant de l'antenne, le maillage maximal était de 1 mm. L'incertitude élargie des paramètres numériques a été évaluée à 0,5 dB (k = 2).

Tableau D.5 – Valeurs numériques cibles de DAS pour les CLA

	f	psDAS à 1 g	psDAS à 10 g	DAS local à la surface (au-dessus du point d'alimentation)	DAS local à la surface (décalage de 20 mm)	Incertitude
	MHz	W/kg/(A/m)^2	W/kg/(A/m)^2	W/kg/(A/m)^2	W/kg/(A/m)^2	dB, k = 2
CLA-6	6	0,000 84	0,000 54	0,001 33	0,000 390	0,5
CLA-13	13	0,004 04	0,002 59	0,006 36	0,001 96	0,5
CLA-30	30	0,022 3	0,014 3	0,035 5	0,010 3	0,5
CLA-64	64	0,106	0,068 1	0,168	0,047 4	0,5
CLA-128	128	0,607	0,417	0,904	0,032 6	0,5
CLA-150	150	0,842	0,586	1,24	0,489	0,5
CLA-220	220	1,20	0,818	1,82	0,686	0,5

NOTE 1 Le boîtier de la CLA est en contact direct avec la surface extérieure de l'enveloppe du fantôme plan.

NOTE 2 Toutes les valeurs de DAS sont normalisées à un champ H de crête de 1 A/m mesuré à une distance de 5 mm à partir de la base centrale à l'intérieur du fantôme.

IECNORM.COM : Click to view the full PDF of IEC/IEEE 62209-1528:2020

D.4.3 Antenne doublet en serpentin

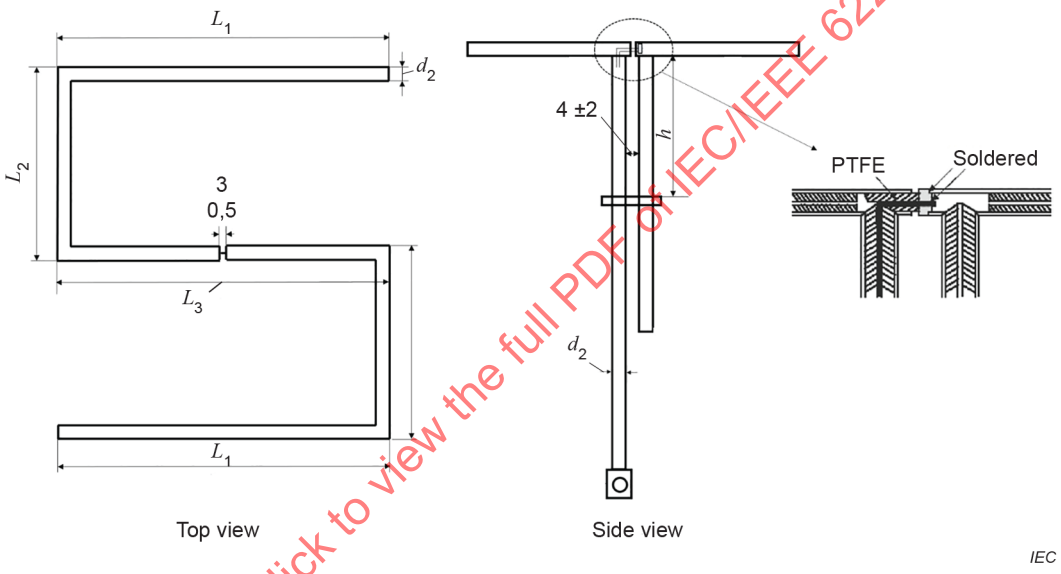
D.4.3.1 Description mécanique

Le D.4.3 décrit une antenne de 150 MHz modifiée, appelée antenne en serpentin, qui peut être installée sous le fantôme elliptique normalisé [45], [46]. Les dimensions mécaniques du doublet en serpentin sont données à la Figure D.4 et dans le Tableau D.6. Pour les doublets en serpentin, un écarteur diélectrique est utilisé pour assurer la distance de 15 mm ± 0,2 mm [47].

Tableau D.6 – Dimensions mécaniques du doublet en serpentin de référence

Fréquence	L_1	L_2	L_3	h	d_1	d_2
MHz	mm	mm	mm	mm	mm	mm
150	197,35	129,35	197,0	165,0	6,35	6,35

Dimensions en millimètres



Anglais	Français
Top view	Vue de dessus
Side view	Vue de côté
Soldered	Soudé

Légende

L_1 longueur partielle du doublet
L_2 longueur partielle du doublet
L_3 longueur partielle du doublet
h longueur du symétriseur
d_1 diamètre des bras du doublet
d_2 diamètre de l'embase
PTFE polytétrafluoroéthylène

Figure D.4 – Informations détaillées mécaniques relatives aux doublets en serpentin pour 150 MHz

IECNORM.COM : Click to view the full PDF of IEC/IEEE 62209-1528:2020

D.4.3.2 Valeurs de DAS numériques cibles

Les valeurs cibles pour l'antenne doublet en serpentin sont présentées dans le Tableau D.7 [45].

Tableau D.7 – Valeurs numériques cibles de DAS (W/kg) pour les antennes en serpentin

Fréquence	DAS 1 g	DAS 10 g	DAS local à la surface (au-dessus du point d'alimentation)	DAS local à la surface (y = 2 cm de décalage par rapport au point d'alimentation)	Incertitude (dB, k = 2)
MHz	W/kg	W/kg	W/kg	W/kg	
150	1,71	1,23	2,16	1,22	0,2
NOTE 1 Toutes les valeurs de DAS sont normalisées à une puissance directe de 1 W. NOTE 2 L'antenne en serpentin est placée parallèle à la surface du fantôme plan à une distance de 15 mm à l'aide d'un écarteur diélectrique.					

D.5 Source de champ E orthogonal – VPIFA

D.5.1 Description mécanique

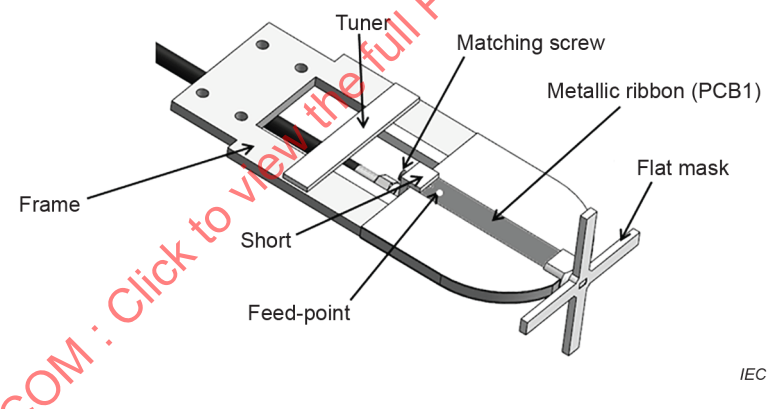
Ces antennes monobandes sont conçues pour être positionnées en de nombreux emplacements, sur la surface courbe de la tête SAM ou sur un fantôme plan. La conception est choisie pour fournir un couplage essentiellement de champ E, comme dans un certain nombre de structures d'antennes dans lesquelles la métallisation d'antenne s'étend au-delà du plan de masse. La structure est celle d'une antenne PIFA. Le principal ruban métallique résonant est perpendiculaire à la surface du fantôme. Il est court-circuité sur un côté et sans terminaison sur le côté proche du fantôme, un couplage capacitif étant généré. La distance entre le conducteur et le fantôme, et sa position, sont fixées à l'aide d'un séparateur en plastique, qui fait partie intégrante de l'antenne. Il convient de maintenir le dispositif perpendiculaire à la surface. Le schéma de DAS est localisé avec une composante de champ orthogonal dominante. Quatre versions de fréquence pour VPIFA-750, VPIFA-835, VPIFA-1950 et VPIFA-3700 sont spécifiées. À des fréquences plus élevées, les composantes normales dominent pour $d \geq 2$ mm. La Figure D.5 a) représente la structure de base de l'antenne, vue du côté PCB1. La Figure D.5 b) représente l'antenne telle qu'elle est vue du côté PCB2, le masque plan ayant été ici retiré afin de voir plus facilement l'écarteur intégré. Les dimensions critiques sont représentées à la Figure D.5 c). Deux substrats PCB sont utilisés pour graver le ruban métallique et le plan de masse, respectivement, et présentent une épaisseur de 0,508 mm chacun. Les deux substrats sont séparés mécaniquement par un châssis FR4. Une extrémité de ce châssis permet de fixer l'antenne à un support. L'antenne est conçue pour être associée à une connexion coaxiale de 50 Ω. Les dimensions pour chaque fréquence et les propriétés matérielles sont indiquées dans le Tableau D.8 et dans le Tableau D.9, respectivement. Pour compenser les erreurs de fabrication, l'antenne comporte une structure de syntonisation et une vis d'adaptation. Pour la syntonisation, une barre diélectrique est ajustée pour accorder la fréquence de résonance, alors que pour l'adaptation, une vis en laiton intégrée dans le court-circuit peut être ajustée pour faire varier la distance entre le point d'alimentation et le court-circuit, et donc, améliorer l'adaptation. La mise en œuvre de la vis exige un prisme de 0,3 mm avec un orifice afin de positionner et fixer mécaniquement la vis. De plus, un contre-écrou est utilisé pour sécuriser la position de la vis. Après affinage du réglage de l'antenne, il convient de fixer les deux éléments. Le connecteur SMA exige une section coudée pour placer le câble de connexion parallèlement à l'axe de l'antenne. Pour réduire la force de torsion (couple), qui peut casser le connecteur, il est recommandé en premier lieu de raccorder le coude au câble, puis de raccorder l'autre côté du coude au connecteur.

IECNORM.COM : Click to view the full PDF of IEC/IEEE 62209-1528:2020

La Figure D.6 représente le masque plan utilisé avec les VPIFA (voir également la Figure D.5 a)). La tolérance de positionnement utilisant ces masques est dominée par l'incertitude de masque, et l'incertitude de DAS correspondante est déjà prise en considération dans l'incertitude des valeurs cibles.

Tableau D.8 – Dimensions des antennes VPIFA à différentes fréquences

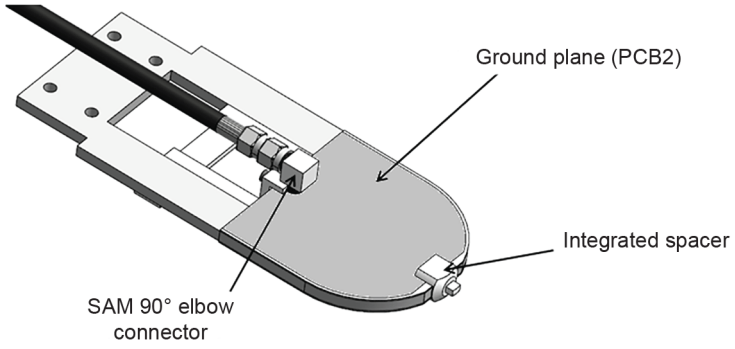
Fréq. (MHz)	**Largeur de ruban et de pliure** W (mm)	**Longueur de la largeur de pliure** l_b (mm)	**Épaisseur du châssis,** l_f **/ épaisseur de l'émetteur,** l_t (mm)	**Largeur du châssis,** W_f (mm)	**Diamètre / longueur de la vis d'adaptation** (mm)	**Largeur du syntoniseur** W_t (mm)	$d_{b\text{-}f}$ (mm)	$d_{b\text{-}s}$ (mm)	l_{gr} (mm)	g (mm)
750	10,00 ± 0,05	1,50 ± 0,10	4,00 ± 0,05 /5,35 ± 0,05	5,00 ± 0,05	4,00 ± 0,05 / 12,00 ± 0,10	10,00 ± 0,10	58,00 ± 0,10	5,50 ± 0,10	59,90 ± 0,10	2,50 ± 0,05
835	10,00 ± 0,05	1,50 ± 0,10	4,00 ± 0,05 /5,35 ± 0,05	5,00 ± 0,05	4,00 ± 0,05 / 12,00 ± 0,10	3,50 ± 0,10	51,70 ± 0,10	5,55 ± 0,10	53,70 ± 0,10	2,50 ± 0,05
1 950	10,00 ± 0,05	1,50 ± 0,10	4,00 ± 0,05 /5,35 ± 0,05	5,00 ± 0,05	4,00 ± 0,05 / 12,00 ± 0,10	3,00 ± 0,10	77,70 ± 0,10	4,55 ± 0,10	78,45 ± 0,10	2,50 ± 0,05
3 700	3,00 ± 0,05	1,50 ± 0,10	4,00 ± 0,05 /5,35 ± 0,05	5,00 ± 0,05	4,00 ± 0,05 / 12,00 ± 0,10	2,00 ± 0,10	36,7 ± 0,10	5,77 ± 0,10	38,75 ± 0,10	2,50 ± 0,05



Anglais	Français
Tuner	Syntoniseur
Matching screw	Vis d'adaptation
Metallic ribbon	Ruban métallique
Flat mask	Masque plan
Feed-point	Point d'alimentation
Short	Court-circuit
Frame	Châssis

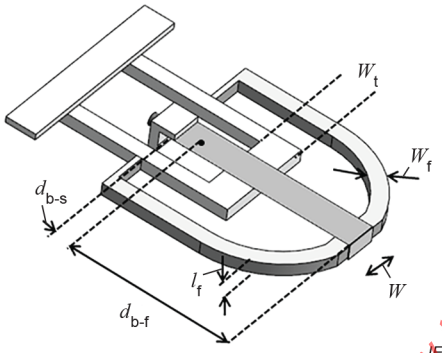
a) Vue schématique générale du côté ruban métallique

IECNORM.COM : Click to view the full PDF of IEC/IEEE 62209-1528:2020

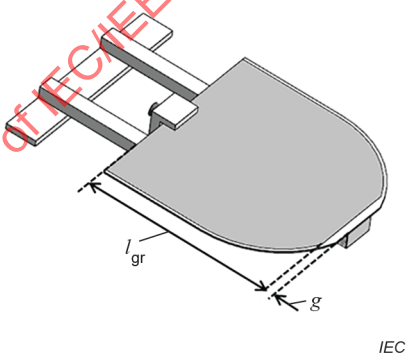


Anglais	Français
Ground plane	Plan de masse
SAM 90° elbow connector	Connecteur coudé à 90° du SAM
Integrated spacer	Écarteur intégré

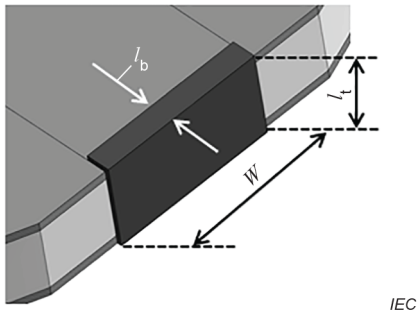
b) Vue schématique générale du côté plan de masse



c) Dimensions critiques – Vue avant

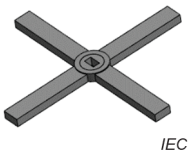


d) Dimensions critiques – Vue arrière



e) Vue détaillée du segment plié

Figure D.5 – Antenne de validation VPIFA



Les tolérances recommandées pour les masques plans imprimés en 3D sont ±0,10 mm.

Figure D.6 – Masque de positionnement des VPIFA

IECNORM.COM : Click to view the full PDF of IEC/IEEE 62209-1528:2020

Tableau D.9 – Propriétés diélectriques des couches diélectriques des antennes VPIFA

Couche	750 MHz		835 MHz		1 950 MHz		3 700 MHz	
	ε_r	σ [S/m]	ε_r	σ [S/m]	ε_r	σ [S/m]	ε_r	σ [S/m]
Châssis (FR4)	4,38	$3{,}49 \times 10^{-3}$	4,38	$3{,}84 \times 10^{-3}$	4,37	$8{,}45 \times 10^{-3}$	4,34	$15{,}7 \times 10^{-3}$
Masque (impression 3D)	2,22	$1{,}74 \times 10^{-3}$	2,22	$1{,}83 \times 10^{-3}$	2,22	$3{,}09 \times 10^{-3}$	2,22	$5{,}06 \times 10^{-3}$
PCB_1 (RO4350B)	3,75	463×10^{-6}	3,75	517×10^{-6}	3,75	$1{,}24 \times 10^{-3}$	3,74	$2{,}46 \times 10^{-3}$
PCB_2 (RO4350B)	3,75	463×10^{-6}	3,75	517×10^{-6}	3,75	$1{,}24 \times 10^{-3}$	3,74	$2{,}46 \times 10^{-3}$
Écarteur (PET)	2,97	$7{,}52 \times 10^{-3}$	2,96	$8{,}05 \times 10^{-3}$	2,90	$14{,}5 \times 10^{-3}$	2,84	$22{,}6 \times 10^{-3}$
Syntoniseur (FR4)	4,38	$3{,}49 \times 10^{-3}$	4,38	$3{,}84 \times 10^{-3}$	4,37	$8{,}45 \times 10^{-3}$	4,34	$15{,}7 \times 10^{-3}$

D.5.2 Valeurs de DAS numériques cibles

Le Tableau D.10 donne les valeurs cibles pour l'antenne VPIFA lorsque l'écarteur spécifié est placé directement contre le fantôme plan à l'emplacement central.

Tableau D.10 – Valeurs de DAS numériques cibles pour les VPIFA sur le fantôme plan

Antenne	Fréquence [MHz]	DAS_{1g} [W/kg]	DAS_{10g} [W/kg]	DAS local à la surface (au-dessus du point d'alimentation) [W/kg]	DAS local à la surface (y = 2 cm de décalage par rapport au point d'alimentation) [W/kg]	u_c (k = 1) dB
VPIFA-750	750	12,94	3,86	66,06	0,81	0,3
VPIFA-835	835	13,22	3,82	57,02	0,729	0,3
VPIFA-1950	1 950	8,68	3,58	31,84	1,005	0,3
VPIFA-3700	3 700	9,87	4,14	27,22	0,54	0,3
NOTE Toutes les valeurs de DAS sont normalisées à une puissance directe de 1 W.						

IECNORM.COM : Click to view the full PDF of IEC/IEEE 62209-1528:2020

Annexe E
(normative)

Étalonnage et caractérisation de sondes dosimétriques (DAS)

E.1 Remarques introductives

Les sondes de DAS actuellement disponibles sont fondées sur des détecteurs à diode Schottky. Le signal mesuré à la sortie de chaque capteur est une tension proportionnelle à E ou E^2, suivant l'amplitude de champ électrique incident sur la sonde.

La plupart des sondes isotropes sont constituées de trois petits capteurs dipôles avec des détecteurs à diode dans leurs fentes centrales. Les diagrammes de directivité de tels capteurs sont orthogonaux, et l'amplitude totale de champ E est proportionnelle à la somme quadratique (RSS) des trois composantes de champ orthogonales. Dans la région quadratique de la caractéristique de diode, la tension de sortie du capteur est proportionnelle à la moyenne quadratique de la composante de champ correspondante. Au-delà de cette plage, la tension de sortie est comprimée et exige donc une linéarisation dans la plage dynamique. Les différences dues aux tolérances de fabrication produisent des sensibilités quelque peu différentes pour chaque capteur, qui doivent être prises en compte pendant l'étalonnage et compensées pendant le mesurage.

L'étalonnage de sonde pour les essais de DAS dans un milieu équivalent au tissu produit un facteur de conversion de DAS ou de champ E. Étant donné que le DAS est proportionnel à la conductivité du milieu équivalent au tissu, un étalonnage direct en matière de DAS est valable seulement pour des milieux ayant exactement la même conductivité. La sensibilité du champ E dépend plus de la permittivité complexe du liquide et est moins sensible à la seule conductivité. L'étalonnage en matière de champ E plutôt qu'en matière de DAS a une plus grande plage de validité et est donc préférentiel pour les essais de DAS individuels de série dans lesquels les propriétés du milieu équivalent au tissu varient légèrement au fil du temps.

L'étalonnage de sonde est généralement réalisé à l'aide des méthodes en une étape ou en deux étapes. Dans la méthode en deux étapes, le champ total est donné par la Formule (E.1):

$$|E|^2 = \sum_{i=1}^{3} |E_i|^2 = \sum_{i=1}^{3} \frac{f_i(V_i)}{\eta_i \psi_i} \tag{E.1}$$

Ici, E_i (i = 1, 2, 3) sont les composantes résultant de la projection du vecteur de champ E sur les trois capteurs orthogonaux, $f_i(V_i)$ est la fonction de linéarisation du signal de capteur rectifié V_i, η_i [in µV/(V/m)^2] est la sensibilité du capteur-dipôle i dans l'air, et ψ_i est le rapport de la réponse du capteur dans l'air à la réponse dans les milieux diélectriques (parfois désigné sous le nom de facteur de conversion). Cette méthode en deux étapes est également appelée méthode en trois étapes (Meier et al. [48]), où la troisième étape implique la fonction de linéarisation $f_i(V_i)$.

La fonction de linéarisation $f_i(V_i)$ est non seulement une fonction de la valeur efficace de V_i, mais est également dépendante de l'enveloppe de signal. Nadakuduti et al. [20] a démontré que les signaux CW et les signaux modulés par impulsions périodiques avec une amplitude constante (par exemple GSM) peuvent être plus facilement corrigés pour la linéarité que pour les protocoles de communication utilisant des modulations complexes avec des enveloppes de signal stochastique. Une linéarisation acceptable des modulations complexes peut être obtenue sur une large plage dynamique avec une incertitude de linéarité inférieure à 0,4 dB.

IECNORM.COM : Click to view the full PDF of IEC/IEEE 62209-1528:2020

Dans les méthodes en une étape décrites en E.3.3, le champ total est donné par la Formule (E.2):

$$|E|^2 = \sum_{i=1}^{3} |E_i|^2 = \sum_{i=1}^{3} \frac{f_i(V_i)}{\gamma_i} \tag{E.2}$$

Ici, les facteurs η_i sont inclus dans la sensibilité γ_i totale dans un tissu. Une autre procédure en une étape fondée sur une méthode d'antenne normalisée est décrite dans Person et al. [49].

Les étalonnages de sonde ne sont valides que lorsque les capteurs sont suffisamment éloignés (au moins un diamètre d'extrémité de sonde) de toutes les limites du milieu. Lorsque la sonde est proche de ces limites et que la compensation n'est pas appliquée, la sensibilité peut changer. L'effet de proximité de bord, ainsi que la réponse isotrope de la sonde, doivent être évalués au moyen d'essais séparés, comme cela est décrit en 8.4.1.5, en 8.4.1.6, à l'Article E.4 et à l'Article E.6.

E.2 Linéarité

La linéarité de sonde est présentée et expliquée en 8.4.1.3. L'incertitude associée peut être déterminée selon les méthodes indiquées en 8.4.1.3 pour les signaux CW et en 8.4.2.7 pour les signaux modulés. L'Article E.2 décrit une méthodologie générale pour l'évaluation de la linéarité de sonde de tout signal.

La fonction de linéarisation $f_i(V_i)$ doit être déterminée et appliquée avant d'évaluer la sensibilité (voir l'Article E.1). Cette opération est améliorée en utilisant une amplitude ou un balayage de puissance avec un champ incident bien défini ayant les caractéristiques de signal correspondantes. L'une quelconque des configurations suivantes peut être utilisée à condition que la plage dynamique concernée soit évaluée par pas de 3 dB ou moins. Il convient d'utiliser un wattmètre efficace vrai ou une sonde de champ étalonnée de façon appropriée comme référence. Les paramètres de linéarisation sont déterminés pour le i-ème capteur en évaluant et en supprimant l'erreur de linéarisation entre la réponse mesurée $E_{\text{inc,meas}}$ et le champ incident E_{inc} comme cela est présenté dans la Formule (E.3):

$$erreur_{\text{linéarisation}} = 20\lg\frac{E_{\text{inc,meas}}}{E_{\text{inc}}} \tag{E.3}$$

Une approche est décrite par Nadakaduti et al. [20] pour appliquer l'ajustement de courbe afin de supprimer l'erreur de linéarisation des signaux ayant des enveloppes de signal complexes.

E.3 Évaluation de la sensibilité des capteurs-dipôles

E.3.1 Généralités

Les facteurs de sensibilité peuvent être déterminés en appliquant des procédures d'étalonnage en une étape ou en deux étapes. Par ailleurs, l'étalonnage de transfert peut être appliqué.

E.3.2 Procédures d'étalonnage en deux étapes

E.3.2.1 Généralités

Le champ total doit être évalué selon la Formule (E.2). La séparation de la sensibilité de la sonde en deux facteurs (η_i et γ_i) permet l'utilisation de certaines procédures normalisées d'étalonnage de sonde en espace libre et permet une validation supplémentaire des performances de la sonde et du montage d'étalonnage.

IECNORM.COM : Click to view the full PDF of IEC/IEEE 62209-1528:2020

E.3.2.2 Sensibilité dans l'air (première étape)

Les montages les plus exacts utilisés pour la génération de champs bien définis afin de simuler des conditions d'espace libre, destinés à l'étalonnage des sondes, sont les guides d'ondes. Les raisons en sont les suivantes:

- les montages à guide d'ondes exigent une puissance modérée et moins d'espace que les montages d'étalonnage de champs lointains;
- la génération de champs plus exacts permettant de remonter aux relevés de puissance est possible;
- l'incertitude produite par la perturbation du champ due à l'insertion de la sonde est négligeable pour de petites sondes de champ proche, lorsque les dimensions du guide d'ondes sont beaucoup plus grandes que celles de la sonde;
- les montages permettent un accès facile pour orienter l'axe de la sonde perpendiculairement ou parallèlement à la polarisation du champ à l'intérieur du montage;
- en outre, la validation croisée des intensités de champ est en général possible en utilisant un jeu de guides d'ondes avec des plages de fréquences se recouvrant.

Tant que la ligne d'alimentation résistive ne charge pas la diode/dipôle du capteur et que la sonde est petite comparée à la longueur d'onde, la sensibilité dans l'espace libre est indépendante de la fréquence. Cela permet une validation supplémentaire des montages d'étalonnage et le contrôle d'éventuelles perturbations du champ par la sonde. Les effets dus à l'insertion de la sonde sont généralement négligeables si des coupleurs de guide d'ondes de bonne qualité et des sources adaptées sont utilisés. Une source supplémentaire d'incertitude dans les montages de guide d'ondes provient des réflexions sur la charge de terminaison, qui peut avoir comme conséquence une configuration d'ondes stationnaires dans le montage. Les réflexions peuvent être maintenues au-dessous de 1 % si des charges de guide d'ondes de bonne qualité sont utilisées. De plus, l'incertitude peut être compensée en effectuant des mesurages supplémentaires avec une charge décalée de $\lambda/4$ et en faisant la moyenne des deux relevés.

Aux basses fréquences (par exemple en dessous de 750 MHz), des cellules TEM peuvent être utilisées à la place des guides d'ondes. Toutefois, le champ à l'intérieur d'une cellule TEM est moins bien défini, c'est-à-dire qu'il y a un écart assez important de la distribution homogène du champ par rapport à celle prévue [20]. La sonde est généralement insérée dans les petits trous dans les parois de la cellule TEM et positionnée au centre (au-dessus ou au-dessous du septum), là où le champ est la plupart du temps homogène par rapport aux dimensions de la sonde. Chaque capteur est évalué par rapport à la composante de champ parallèle à ce dernier.

E.3.2.3 Sensibilité dans le milieu (deuxième étape)

E.3.2.3.1 Généralités

La sensibilité dans le milieu équivalent au tissu est déterminée en générant des valeurs d'intensité de champ localement connues à l'intérieur des milieux. Deux méthodes peuvent être utilisées:

a) étalonnage de transfert avec la sonde de température;

b) étalonnage avec des champs analytiques.

E.3.2.3.2 Étalonnage de transfert avec les sondes de température

Dans des milieux avec pertes, le DAS est lié à la fois au champ électrique (E) et à la vitesse d'échauffement ($\mathrm{d}T/\mathrm{d}t$) dans le milieu ayant une capacité thermique massique c_h. Par conséquent, en se fondant sur la Formule (E.4)

$$DAS = \sigma \frac{E^2}{\rho} = c_\mathrm{h} \left. \frac{\mathrm{d}T}{\mathrm{d}t} \right|_{t=0}, \tag{E.4}$$

IECNORM.COM : Click to view the full PDF of IEC/IEEE 62209-1528:2020

le champ électrique dans le milieu avec pertes peut être mesuré indirectement en mesurant la vitesse d'échauffement dans le milieu. Des sondes ne perturbant pas la température (sondes optiques ou sondes à thermistance à fils résistifs) avec des capteurs de petite taille (< 2 mm) et un temps de réponse court (< 1 s) sont disponibles et peuvent être facilement étalonnées avec une grande précision [50]. Le montage et la source d'excitation n'ont aucune influence sur l'étalonnage. Seules les incertitudes de positionnement relatif de la sonde de température et de la sonde de champ E à étalonner doivent être prises en considération. Cependant, plusieurs problèmes limitent l'exactitude effective des étalonnages de sondes de température.

a) La vitesse d'échauffement n'est pas directement mesurable, mais doit être évaluée à partir de mesurages de température effectués sur une courte période. Des précautions particulières sont nécessaires pour éviter des incertitudes de mesure provoquées par des gradients de température dus aux effets de répartition d'énergie ou de courants de convection dans le milieu. De tels effets ne peuvent pas être complètement évités. Avec un montage soigneusement réalisé, ces incertitudes peuvent être réduites au minimum.

b) Le volume mesuré autour de la sonde de température n'est pas bien défini. Il est difficile de calculer le transfert d'énergie dans la sonde à partir du champ de gradient de température environnant dans la sonde (les sondes de température sont généralement étalonnées dans le milieu avec des températures homogènes). Il n'existe pas de norme identifiable pour les mesurages des augmentations de température.

c) L'étalonnage dépend de l'évaluation de la masse volumique, de la capacité thermique massique et de la conductivité électrique du milieu. Alors que la masse volumique et la capacité thermique massique peuvent être mesurées avec exactitude avec des procédures normalisées (de l'ordre de ±2 % pour c_h, beaucoup mieux pour ρ), il n'existe aucune norme pour le mesurage de la conductivité électrique. Suivant la méthode et le milieu, l'incertitude peut être de ±5 %.

d) Un échauffement suffisant est exigé pour produire des échauffements mesurables. Par conséquent, l'étalonnage est souvent effectué à un niveau de puissance plus élevé que celui utilisé par les méthodes de champ E. Les non-linéarités dans le système (par exemple, mesurages de puissance, différentes composantes de champ, etc.) doivent être compensées.

Compte tenu de ces problèmes, l'exactitude d'étalonnage des sondes de champ E utilisant une technique d'échauffement dans un montage soigneusement conçu est d'environ ±10 % (incertitude-type composée) [48]. Un montage utilisant une combinaison des techniques de guide d'ondes et d'échauffement a été présenté en [51]. L'incertitude-type composée estimée de ce montage est de ±5 % quand le même milieu est utilisé à la fois pour l'étalonnage et pour les mesurages réels, et sinon de ±7 % à ±9 %, ce qui est en bon accord avec les estimations indiquées en [48].

E.3.2.3.3 Analyse de l'incertitude de l'étalonnage du transfert avec des sondes de température

Lors de l'exécution d'une analyse d'incertitude de l'étalonnage de transfert au moyen d'une technique d'échauffement, les paramètres indiqués dans le Tableau E.1 doivent au moins être pris en considération.

IECNORM.COM : Click to view the full PDF of IEC/IEEE 62209-1528:2020

Tableau E.1 – Analyse de l'incertitude de l'étalonnage du transfert avec des sondes de température

Grandeur d'entrée X_i (source d'incertitude)	Loi de probabilité	Incertitude ± %	Diviseur	c_i	Incertitude-type u_i ± %	v_i ou v_{eff}
Positionnement de la sonde de champ E	R		√3	1		∞
Positionnement de la sonde de température	R		√3	1		∞
Linéarité de la sonde de champ E	R		√3	1		∞
Dérive et bruit de la sonde de température	R		√3	1		∞
Linéarité de la sonde de température	R		√3	1		∞
Conductivité du milieu	R		√3	1		∞
Chaleur massique du liquide	R		√3	1		∞
Masse volumique du milieu	R		√3	1		∞
Exactitude de la sonde de température	R		√3	1		∞
Incertitude-type composée	RSS					
NOTE c_i est le coefficient de sensibilité.						

IECNORM.COM : Click to view the full PDF of IEC/IEEE 62209-1528:2020

Les tolérances des composantes du Tableau E.1 doivent être déterminées comme suit:

a) Les tolérances de positionnement des sondes de température et de champ E sont évaluées selon O.7.1 en utilisant la profondeur de pénétration réelle déterminée à partir des propriétés diélectriques du milieu équivalent au tissu mesurées à la fréquence d'étalonnage. Étant donné que les variations de DAS aux emplacements du maximum sont beaucoup plus petites dans les directions parallèles à la surface du fantôme que dans les directions perpendiculaires, les procédures de O.7.1 sont applicables lorsque les mouvements de la sonde de température et de champ E sont limités à des directions parallèles uniquement.

b) L'incertitude de linéarité de la sonde de champ est évaluée selon l'Article O.1 et l'incertitude d'étalonnage ne doit pas dépasser 0,1 dB à l'intensité de champ d'étalonnage.

c) Les dérives et le bruit de la sonde de température sont évalués par des mesurages de température à des intervalles de 1 s pendant 1 h, avec un temps d'intégration de moins de 0,5 s dans des conditions de température constantes. La tolérance de température est calculée selon la formule $100 \times [(T_{max} - T_{min})/\Delta T_{min}]$, où ΔT_{min} est l'échauffement minimal pour les différents niveaux de puissance utilisés pour l'étalonnage.

d) Il convient de déterminer la tolérance de linéarité de la sonde de température à l'aide des procédures suivantes. L'exactitude et la linéarité des résultats de la sonde de température sont comparées à une température de référence identifiable à 10 paliers de température dans une plage supérieure ou égale à celle utilisée pendant l'étalonnage. La tolérance de est calculée selon la formule $100 \times [(T_{max} - T_{min})/\Delta T_{min}]$, où ΔT_{min} est la valeur la plus élevée de l'échauffement minimal pour les différents niveaux de puissance utilisés pour l'étalonnage et de la tolérance pour la température de référence.

e) La tolérance de mesure de la conductivité du milieu pendant l'étalonnage de la température est déterminée en utilisant les mêmes procédures que celles indiquées en O.9.3.

f) La tolérance de chaleur massique des milieux équivalents aux tissus doit être déterminée en utilisant des procédures calorimétriques ([51], [52]).

g) La tolérance de mesure de la masse volumique du milieu doit être calculée en fonction de la somme quadratique (RSS) des tolérances de volume et de poids obtenues au moyen de méthodes de mesure normalisées pour le volume et le poids.

h) La sonde de température doit avoir un temps de réponse à un échelon de 1 s ou moins, qui est déterminé à partir du temps exigé par l'équipement de mesure, la sonde de température et la lecture électronique pour atteindre 90 % de la valeur de température finale prévue après l'application d'une variation d'échelon d'au moins 5 °C sur la sonde de température.

E.3.2.3.4 Étalonnage avec des champs analytiques (guides d'ondes)

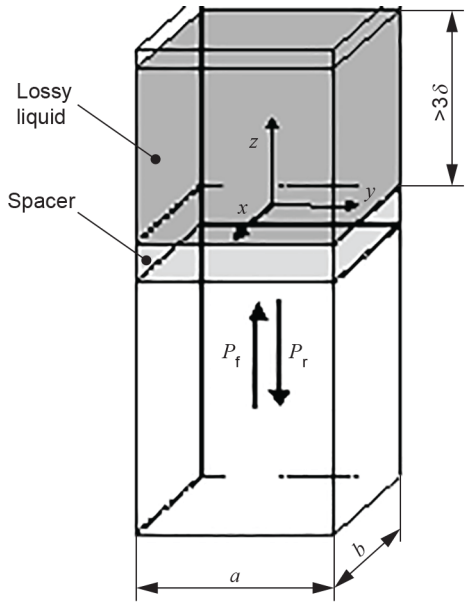
Dans cette méthode, un montage d'essai dans lequel le champ peut être calculé de manière analytique à partir des mesurages d'autres grandeurs physiques (la puissance d'entrée, par exemple) est utilisé. Cela correspond à la méthode du champ normalisé pour l'étalonnage de la sonde dans l'air. Cependant, aucune norme n'est définie pour des champs dans des milieux avec pertes.

Lorsque les champs calculés dans des milieux avec pertes sont utilisés pour l'étalonnage de la sonde, plusieurs points doivent être pris en considération dans l'estimation de l'incertitude.

- La puissance nette RF dissipée dans le guide d'ondes doit être mesurée avec exactitude. Cette exigence implique des mesurages précis de deux des trois grandeurs suivantes: la puissance incidente, la puissance réfléchie et le coefficient de réflexion au niveau de l'accès d'entrée du guide d'ondes.
- L'exactitude de l'intensité de champ calculée dépend de l'évaluation des propriétés diélectriques du milieu.
- Du fait de la faible longueur d'onde dans les milieux de forte permittivité, des modes d'un ordre plus élevé peuvent être excités. La distribution des champs dans le montage doit être soigneusement vérifiée afin d'assurer la conformité à la distribution de champ théorique.

Les guides d'ondes peuvent être utilisés pour générer un champ connu d'un point de vue analytique à l'intérieur des milieux équivalents aux tissus, par exemple, le montage présenté en [53]. Dans ce montage (Figure E.1), la partie supérieure d'un guide d'ondes ouvert et vertical est remplie de liquide. Une plaque de séparation diélectrique à une distance > λ (λ fait référence à la longueur d'onde dans la section d'air du guide d'ondes) du coupleur d'alimentation permet une adaptation d'impédance (facteur d'adaptation > 10 dB) entre l'air et le liquide. La symétrie de la construction et des pertes élevées dans le liquide garantit que la distribution de champ à l'intérieur du milieu équivalent au tissu suit le mode de guide d'ondes TE_{10}, bien que des modes d'ordre plus élevé puissent en théorie exister. En [53], l'absence de modes d'ordre plus élevé a été soigneusement validée par un mesurage de la distribution du champ électrique dans le volume du liquide, et celle-ci s'est révélée être dans les limites de ±2 % du mode théorique TE_{10}.

IECNORM.COM : Click to view the full PDF of IEC/IEEE 62209-1528:2020



Anglais	Français
Lossy liquid	Liquide avec pertes
Spacer	Écarteur

Légende

x, y, z axes dans le système cartésien de coordonnées

3δ profondeur de liquide (> 3 fois la profondeur de pénétration)

a largeur de la section du guide d'ondes

b hauteur de la section du guide d'ondes

P_f puissance incidente

P_r puissance réfléchie

Figure E.1 – Montage expérimental pour l'évaluation de la sensibilité (facteur de conversion) utilisant un guide d'ondes rectangulaire vertical

IECNORM.COM : Click to view the full PDF of IEC/IEEE 62209-1528:2020

À l'intérieur du liquide, le champ se propage presque comme une onde TEM, en raison de la fréquence de coupure basse. La profondeur de liquide (> 3 fois la profondeur de pénétration) a été choisie de sorte que les réflexions à la surface supérieure du liquide soient négligeables. La Formule (E.5) représente la relation entre le DAS au centre de la section (x = y = 0) du guide d'ondes avec pertes et la distance longitudinale (z) du séparateur diélectrique:

$$DAS(z) = \frac{4(P_f - P_r)}{\rho ab\delta} e^{-2z/\delta} \quad \text{(E.5)}$$

où

ab est la section transversale du guide d'ondes;

P_f est la puissance directe à l'intérieur de la section remplie d'air du guide d'ondes;

P_r est la puissance réfléchie à l'intérieur de la section remplie d'air du guide d'ondes;

z est la distance au-dessus de la surface supérieure de la séparation diélectrique;

ρ est la masse volumique du liquide;

δ est la profondeur de pénétration à l'intérieur du liquide avec pertes.

NOTE Pour les besoins de la présente norme, la masse volumique ρ est par hypothèse de 1 000 kg/m^3.

La profondeur de pénétration δ, qui est l'inverse du coefficient d'atténuation du guide d'ondes α, est déterminée à partir d'un balayage le long de l'axe z et comparée à la valeur théorique déterminée à partir de la Formule (E.6) en utilisant les propriétés diélectriques mesurées du liquide avec pertes.

$$\delta = \alpha^{-1} = \Re\left\{\sqrt{(\pi/a)^2 + j\omega\mu_0(\sigma + j\omega\varepsilon_0\varepsilon_r')}\right\}^{-1} \quad \text{(E.6)}$$

Le Tableau E.2 donne des lignes directrices de conception pour des guides d'onde d'étalonnage ayant un facteur d'adaptation au moins égal à 10 dB aux fréquences les plus importantes utilisées pour les communications personnelles sans fil. Les valeurs de profondeur de pénétration pour ces dispositifs et propriétés diélectriques du milieu équivalent au tissu spécifiques sont également répertoriées dans le Tableau E.2.

Tableau E.2 – Lignes directrices de conception de guides d'ondes d'étalonnage

Fréquence MHz	**Dimension du guide d'ondes**	**Séparateur diélectrique**[a]	
	a mm	ε_r'	**Épaisseur** mm
300	584,2	5,5	106,0
450	457,2	6,0	66,1
900	247,6	5,6	34,8
1 450	129,5	4,7	24,8
1 800 à 2 000	109,2	4,8	19,4
2 450	109,2	5,7	12,6
3 000	86,4	5,7	10,3
3 500	58,2	4,9	9,76
3 900	58,2	4,9	9,76
4 200	58,2	4,9	9,76
4 600	47,5	3,5	9,50
4 900	47,5	3,5	9,50
5 400	47,5	5,6	5,73
6 000	40,4	5,4	5,25
7 000	35,0	3,1	20,0
9 000	23,0	3,1	16,0

[a] La permittivité et l'épaisseur du séparateur diélectrique peuvent s'écarter des valeurs indiquées afin de s'adapter à des matériaux commercialisés. Si la permittivité du séparateur diélectrique varie par rapport à la valeur indiquée de plus de 2 %, il est recommandé d'optimiser à nouveau l'épaisseur de l'écarteur pour identifier la plus adaptée (facteur d'adaptation généralement supérieur à 10 dB).

NOTE 1 Les guides d'ondes sont remplis de milieu équivalent au tissu ayant les propriétés diélectriques indiquées dans le Tableau 2.

NOTE 2 Par convention, la longueur du bord court de section transversale est la moitié du bord long, c'est-à-dire b = a/2.

NOTE 3 Les dimensions du guide d'ondes sont conformes à l'EIA RS-261-B: 1979 [54].

NOTE 4 Ces dimensions dépendent également des largeurs de bande des fréquences d'intérêt.

IECNORM.COM : Click to view the full PDF of IEC/IEEE 62209-1528:2020

Cette technique donne une excellente exactitude avec une incertitude-type composée < ±3,6 % suivant la fréquence et le milieu. L'étalonnage proprement dit est réduit aux mesurages de puissance identifiables par rapport à une procédure d'étalonnage normalisée. La limitation pratique causée par la taille du guide d'ondes pour la plage de fréquences entre 750 MHz et 6 000 MHz n'est pas gênante dans le contexte des essais de conformité, puisque la plupart des fréquences de fonctionnement pour les systèmes de communications mobiles sont couvertes dans cette plage. Pour les fréquences au-dessous de 750 MHz, l'étalonnage de transfert avec des sondes de température demeure la méthode la plus pratique pour réaliser l'étalonnage avec les plus faibles incertitudes.

E.3.2.3.5 Analyse d'incertitude pour l'étalonnage avec des champs analytiques (guides d'ondes)

Lors de l'exécution d'une analyse d'incertitude de l'étalonnage de sonde avec des champs analytiques dans un guide d'ondes, les paramètres indiqués dans le Tableau E.3 doivent au moins être pris en considération.

Tableau E.3 – Analyse d'incertitude de l'étalonnage de sonde dans le guide d'ondes

Grandeur d'entrée X_i (source d'incertitude)	Loi de probabilité PDF_i	Incertitude $a(x_i)$ ± %	Diviseur q_i	$u(x_i) = a(x_i)/q_i$	c_i (1 g, 10 g)	$u(y) = c_i \cdot u(x_i)$ ± %	v_i ou v_{eff}
Puissance incidente ou directe	R		√3		1		∞
Puissance réfléchie	R		√3		1		∞
Mesurage de la conductivité du liquide	R		√3		1		∞
Mesurage de la permittivité du liquide	R		√3		1		∞
Écart de conductivité du liquide	R		√3		1		∞
Écart de permittivité du liquide	R		√3		1		∞
Écart de fréquence	R		√3		1		∞
Homogénéité du champ	R		√3		1		∞
Positionnement de la sonde de champ	R		√3		1		∞
Linéarité de la sonde de champ	R		√3		1		∞
Incertitude-type composée	RSS						

IECNORM.COM : Click to view the full PDF of IEC/IEEE 62209-1528:2020

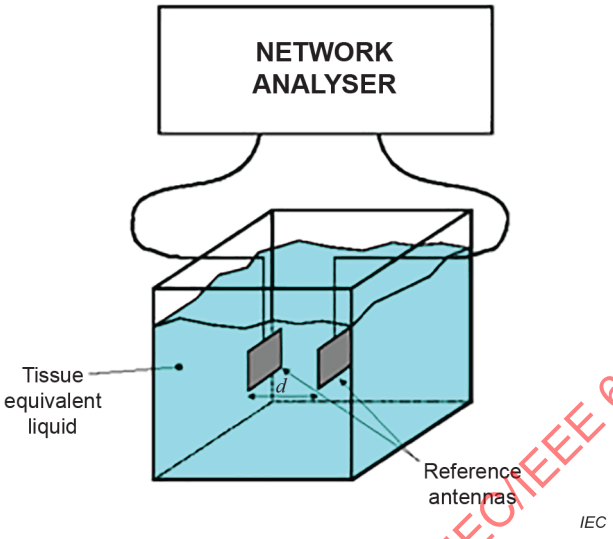
E.3.3 Procédures d'étalonnage en une étape – méthode de l'antenne de référence

E.3.3.1 Généralités

La procédure de E.3.2 peut être combinée en une procédure en une étape en utilisant des antennes de référence. Le champ total doit être évalué selon la Formule (E.2). Les antennes de référence sont de petites antennes conçues pour fonctionner avec le milieu équivalent au tissu approprié. Des exemples d'antennes développées à 900 MHz et 1 800 MHz ont été décrits en [49], [55]. Au moins deux antennes identiques sont nécessaires pour évaluer le gain dans le lobe principal pour utilisation dans l'étalonnage de sonde.

Les méthodes en une étape indiquées en E.3.3 et en E.3.4 évaluent l'isotropie par rapport à la rotation de la sonde et la polarisation du champ incident. La méthode indiquée en E.3.4 prend également en considération l'angle d'incidence.

Les antennes typiques utilisées ici comprennent des antennes dalles simples avec un gain de 5 dBi ou mieux (voir la Figure E.2 pour le montage). Dans la mesure où des lobes latéraux dus à des réflexions multiples au niveau de la paroi du réservoir peuvent gêner l'étalonnage, il faut vérifier que ceux-ci sont suffisamment atténués par le milieu équivalent au tissu avant qu'ils n'atteignent l'extrémité de la sonde.



Anglais	Français
NETWORK ANALYSER	ANALYSEUR DE RÉSEAU
Tissue equivalent liquid	Liquide équivalent au tissu
Reference antennas	Antennes de référence

Figure E.2 – Représentation graphique du montage d'évaluation du gain de l'antenne

E.3.3.2 Mesurage du gain de l'antenne de référence

Le gain de l'antenne de référence est évalué selon le protocole suivant:

a) Positionner les antennes dans le milieu équivalent au tissu de sorte que les axes de leurs faisceaux principaux soient alignés et à une distance bien définie d, où $d \geq 2D^2/\lambda_{\text{liquid}}$, D est la plus grande dimension de l'antenne de référence, et λ_{liquide} est la longueur d'onde dans le milieu. Les antennes doivent être à au moins 10 cm de toute paroi du récipient.

b) Mesurer les coefficients de réflexion ρ_1 et ρ_2 aux accès d'entrée de chaque antenne.

c) Mesurer le coefficient de transmission S_{21} entre les deux antennes au niveau des mêmes accès.

d) Le gain est décrit dans la Formule (E.7):

$$G = |S_{21}(d)| \times e^{\alpha d} \left(\frac{4\pi d}{\lambda_{\text{liquide}}} \right) \times \frac{1}{\sqrt{\left(1-|\rho_1|^2\right)\left(1-|\rho_2|^2\right)}} \quad \text{(E.7)}$$

où le coefficient d'atténuation est décrit dans la Formule (E.8):

$$\alpha = \frac{2\pi f}{c} \times \left(\varepsilon_r'^2 + \varepsilon_r''^2\right)^{1/4} \times \sin\left[\frac{1}{2}\arctan\left(\frac{\varepsilon_r''}{\varepsilon_r'}\right)\right] \quad \text{(E.8)}$$

IECNORM.COM : Click to view the full PDF of IEC/IEEE 62209-1528:2020

E.3.3.3 Analyse de l'incertitude pour le mesurage du gain de l'antenne de référence

Lorsqu'une analyse de l'incertitude du gain mesuré de l'antenne de référence est effectuée, les paramètres inclus dans le Tableau E.4 doivent au moins être pris en considération. Des méthodes complémentaires pour le calcul du gain d'antenne peuvent être consultées en E.3.3.6.

Tableau E.4 – Modèle d'incertitude pour l'évaluation du gain de l'antenne de référence

Grandeur d'entrée X_i (source d'incertitude)	Loi de probabilité PDF_i	Incertitude $a(x_i)$ ± %	Diviseur q_i	$u(x_i) = a(x_i)/q_i$	c_i	$u(y) = c_i \cdot u(x_i)$ ± %	v_i ou v_{eff}
Puissance incidente	R		√3		1		∞
Coefficients de réflexion	R		√3		1		∞
Distance	R		√3		1		∞
Conductivité du milieu	R		√3		1		∞
Permittivité du milieu	R		√3		1		∞
Incertitude-type composée	RSS		√3				

E.3.3.4 Procédure d'étalonnage de sonde par la méthode de l'antenne de référence

Le protocole suivant doit être utilisé pour évaluer les coefficients de sensibilité de la sonde.

a) Placer une antenne dans le milieu équivalent au tissu. L'antenne doit être à au moins 10 cm des parois du récipient.

b) Relier une source d'alimentation à l'accès d'entrée de l'antenne de référence. Le champ électrique théorique E_{th} à une distance d_a de l'antenne est donné par la Formule (E.9):

$$E_{th} = \left(\frac{P_{in}\left(1-|\Gamma|^2\right) G e^{-2\alpha d_a}}{4\pi d_a^2} \times \frac{120\pi}{\Re\left\{\sqrt{\varepsilon_r}\right\}} \right)^{\frac{1}{2}} \quad \text{(E.9)}$$

où

d_a est la distance entre l'antenne et le centre géométrique des capteurs lorsque $d \geq 2D^2/\lambda_{liquid}$;

D est la plus grande dimension de l'antenne de référence;

$\lambda_{liquide}$ est la longueur d'onde dans le milieu;

G est le gain d'antenne;

P_{in} est la puissance d'entrée;

Γ est le coefficient de réflexion de l'antenne.

Il est recommandé de connecter un coupleur bidirectionnel pour commander la puissance d'entrée. Régler la puissance d'entrée de sorte que E_{th} ~ 30 V/m.

c) Positionner la sonde dans le milieu équivalent au tissu de sorte que le centre des détecteurs soit à une distance d de l'antenne.

d) Orienter la sonde afin d'aligner la direction du capteur sur la polarisation de l'antenne de référence.

e) Mesurer la tension $V_{1,meas}$ au niveau de l'accès de l'antenne d'émission.

IECNORM.COM : Click to view the full PDF of IEC/IEEE 62209-1528:2020

f) Le coefficient de sensibilité K_1 pour cette antenne est $K_1 = V_{1,\text{meas}} / E_{\text{th}}^2$

g) Répéter les étapes d) à f) pour les deux autres capteurs afin d'évaluer K_2 et K_3.

h) En utilisant les coefficients de sensibilité de la sonde, le DAS est déterminé par la Formule (E.10):

$$DAS = \frac{\sigma}{\rho}\left(\frac{V_{1,\text{meas}}}{K_1} + \frac{V_{2,\text{meas}}}{K_2} + \frac{V_{3,\text{meas}}}{K_3}\right) \quad \text{(E.10)}$$

où ρ est la masse volumique (1 000 kg/m^3).

E.3.3.5 Analyse de l'incertitude pour l'étalonnage de sonde par la méthode de l'antenne de référence

Lorsqu'une analyse de l'incertitude de l'étalonnage avec des antennes de référence est effectuée, les paramètres inclus dans le Tableau E.5 doivent au moins être pris en considération.

Tableau E.5 – Modèle d'incertitude pour l'étalonnage à l'aide de l'antenne de référence

Grandeur d'entrée X_i (source d'incertitude)	Loi de probabilité PDF_i	Incertitude $a(x_i)$ ± %	Diviseur q_i	$u(x_i) = a(x_i)/q_i$	c_i	$u(y) = c_i \cdot u(x_i)$ ± %	v_i ou v_{eff}
Puissance incidente	R		√3		1		∞
Coefficients de réflexion	R		√3		1		∞
Gain d'antenne	N		1 ou k		1		∞
Conductivité du milieu	R		√3		1		∞
Permittivité du milieu	R		√3		1		∞
Positionnement de la sonde	R		√3		1		∞
Incertitude-type composée	RSS						

E.3.3.6 Formules étendues pour le gain d'antenne dans le mesurage en champ proche

Le gain d'antenne G calculé dans la Formule (E.7) et l'intensité de champ électrique théorique E_{th} sont fondés sur le mesurage en champ lointain dans le milieu équivalent au tissu. Cependant, il est souvent difficile de mesurer S_{21} dans la région de champ lointain en raison d'une forte atténuation du champ dans le milieu équivalent au tissu. Dans un tel cas, une extension de la formule de transmission de Friis dans le milieu avec pertes peut être introduite pour définir le gain en champ proche de l'antenne de référence $G_{\text{proche}}(d)$, et E_{th} dans la région de champ proche peut alors être estimé [56]. Le gain en champ proche $G_{\text{proche}}(d)$ est une fonction de la distance par rapport à l'antenne d, et peut être exprimé par la série de puissance de l'inverse de d. La procédure pour déterminer le gain d'antenne de référence G en E.3.3.1 a) est alors modifiée comme suit.

a) Positionner les antennes dans le milieu de sorte que les axes de leurs faisceaux principaux soient alignés et à une distance bien définie d, et λ_{liquide} est la longueur d'onde dans le milieu. Les antennes doivent être à au moins 10 cm de toute paroi du récipient.

b) Mesurer les coefficients de réflexion ρ_1 et ρ_2 aux accès d'entrée de chaque antenne.

c) Mesurer le coefficient de transmission $S_{21}(d)$ entre les deux antennes au niveau des mêmes accès et à la même distance en modifiant d.

d) Le gain en champ proche $G_{\text{proche}}(d)$ peut être exprimé par la Formule (E.11):

IECNORM.COM : Click to view the full PDF of IEC/IEEE 62209-1528:2020

$$G_{\text{proche}}(d) = \frac{|S_{21}(d)|\exp(\alpha d)\cdot(2\beta d)}{\sqrt{(1-|\rho_1|^2)\cdot(1-|\rho_2|^2)}} = G \times \exp\left(\frac{a_1}{d} + \frac{a_2}{d^2} + \ldots\right) \quad \text{(E.11)}$$

où

d est la distance depuis l'antenne;

$S_{21}(d)$ est le coefficient de transmission entre les deux antennes;

P_{in} est la puissance d'entrée;

ρ_1 est le coefficient de réflexion de l'antenne 1;

ρ_2 est le coefficient de réflexion de l'antenne 2;

α est donné par la Formule (E.8);

β est $2\pi/\lambda_{\text{liquide}}$;

G est le gain d'antenne, exprimé en dB, donné dans la Formule (E.12):

$$G_{\text{procheddB}}(d) = G_{\text{dB}}\left[1 + \frac{1}{A \times d} + \frac{1}{B \times d^2}\right] \quad \text{(E.12)}$$

où

d est la distance depuis l'antenne;

G_{dB} est le gain d'antenne.

La constante A, B ou a_1, a_2,... peut être déterminée par ajustement de courbe. Par conséquent, le choix d'un ajustement de courbe approprié pour la plage de d est important. Les constantes d'atténuation et de phase α et β dans le liquide sont obtenues à partir des propriétés diélectriques du milieu.

e) $E_{\text{th}}(d)$ dans la région des champs proches est alors obtenu par la Formule (E.13):

$$|E_{\text{th}}(d)|^2 = \frac{30 P_{\text{in}}\left(1-|\Gamma|^2\right) G_{\text{proche}}(d) e^{-2\alpha d}}{\Re\left\{\sqrt{\varepsilon_r}\right\} d^2} \quad \text{(E.13)}$$

où

α est donné par la Formule (E.8);

d est la distance depuis l'antenne;

ε_r est la permittivité relative complexe;

$G_{\text{proche}}(d)$ est le gain en champ proche;

P_{in} est la puissance d'entrée;

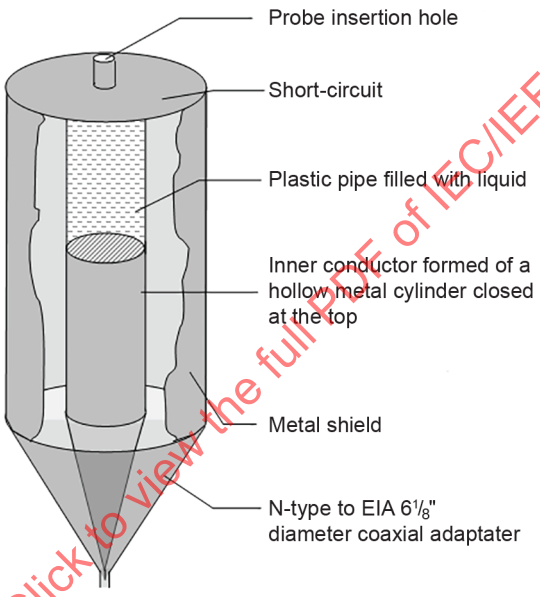
Γ est le coefficient de réflexion de l'antenne.

IECNORM.COM : Click to view the full PDF of IEC/IEEE 62209-1528:2020

E.3.4 Procédures d'étalonnage en une étape – méthode du calorimètre coaxial

E.3.4.1 Généralités

La Figure E.3 décrit un système de calorimètre coaxial pour étalonner des sondes de DAS par la méthode de l'échauffement à des fréquences inférieures à 450 MHz, selon [57]. Il est constitué d'une ligne coaxiale avec un diélectrique d'air, ayant un diamètre de blindage extérieur égal à 2,3 fois le diamètre du conducteur interne, qui produit une impédance caractéristique de 50 Ω. À proximité de l'extrémité de court-circuit de la ligne, le conducteur interne est remplacé par un tuyau en plastique contenant le milieu équivalent au tissu, qui est en contact direct avec l'extrémité métallique du conducteur central ainsi que la plaque de court-circuit au sommet du système. La sonde est insérée par l'intermédiaire d'une ouverture au centre de la plaque de court-circuit. Le diamètre du liquide dans le tuyau doit être le même que celui du conducteur métallique interne, et doit être suffisamment grand pour empêcher que les erreurs à proximité de la sonde ne deviennent significatives. La puissance appliquée à l'accès d'entrée conduit à un champ polarisé axialement dans le liquide avec une distribution relativement uniforme au-dessous de 150 MHz.



Anglais	Français
Probe insertion hole	Orifice d'insertion de la sonde
Short-circuit	Court-circuit
Plastic pipe filled with liquid	Tuyau en plastique rempli de liquide
Inner conductor formed of a hollow metal cylinder closed at the top	Conducteur interne formé d'un cylindre de métal creux fermé au sommet
Metal shield	Blindage métallique
N-type to EIA 6 ⅛" diameter coaxial adaptor	Adaptateur coaxial de type N selon l'EIA de 6⅛ pouces de diamètre

Figure E.3 – Schéma du système de calorimètre coaxial

IECNORM.COM : Click to view the full PDF of IEC/IEEE 62209-1528:2020

La sonde de DAS est utilisée pour mesurer le champ électrique dans le liquide au point de référence pour une puissance d'entrée d'environ 1 W. Une sonde de température est ensuite utilisée pour mesurer la vitesse d'échauffement dans le liquide à la même position, en utilisant une puissance d'environ 30 W. À des fins d'exactitude, il est important que l'échauffement réel soit limité à 1 °C, étant donné que la conductivité du milieu varie de 3 % à 5 % par degré Celsius. Le rapport de la puissance pour le mesurage de sonde de DAS et de l'échauffement doit être déterminé en utilisant un capteur de puissance directionnel ou un coupleur directif et un capteur de puissance, bien que la puissance absolue ne soit pas exigée. L'étalonnage est effectué en comparant les tensions de sortie linéaires provenant des capteurs de sonde de DAS au champ électrique dans le liquide qui est calculé par la Formule (E.14):

$$E^2_{\text{sonde}} = \frac{\rho \times c_{\text{h}}}{\sigma} \frac{\mathrm{d}T}{\mathrm{d}t} \frac{P_{\text{capteur}}}{P_{\text{température}}} \tag{E.14}$$

où

E^2_{sonde} est le champ électrique quadratique aux capteurs de sonde;

ρ est la masse volumique du liquide fantôme;

σ est la conductivité;

c_{h} est la chaleur massique;

P_{capteur} est la puissance utilisée dans le mesurage de sonde de DAS;

$P_{\text{température}}$ est la puissance utilisée dans le mesurage de température;

$\mathrm{d}T/\mathrm{d}t$ est le taux d'augmentation de température dans le liquide.

Ce système permet des étalonnages exacts sur la plage de fréquences de 30 MHz à 450 MHz, avec une incertitude-type d'environ ±5 %.

E.3.4.2 Analyse de l'incertitude pour l'étalonnage de sonde du calorimètre coaxial

Lorsque l'étalonnage est réalisé avec cette méthode, les paramètres inclus dans le Tableau E.6 doivent au moins être pris en considération.

IECNORM.COM : Click to view the full PDF of IEC/IEEE 62209-1528:2020

Tableau E.6 – Composantes d'incertitude pour l'étalonnage de sonde en utilisant des méthodes thermiques

Grandeur d'entrée X_i (source d'incertitude)	Loi de probabilité PDF_i	Incertitude $a(x_i)$ ± %	Diviseur q_i	$u(x_i) = a(x_i)/q_i$	c_i	$u(y) = c_i \cdot u(x_i)$ ± %	v_i ou v_{eff}
Coefficient de température du liquide	R		√3		1		∞
Capacité thermique du liquide	R		√3		1		∞
Masse volumique du liquide	R		√3		1		∞
Conductivité du liquide	R		√3		1		∞
Linéarité et dérive du capteur de puissance	R		√3		1		∞
Linéarité de la sonde de température	R		√3		1		∞
Effets thermiques conduisant à un échauffement non linéaire	R		√3		1		∞
Erreurs de position	N		1		1		∞
Incertitude-type composée	RSS						

E.4 Isotropie

E.4.1 Isotropie axiale

La sonde doit être exposée à une onde de référence avec des angles d'incidence variables par rapport au plan perpendiculaire à l'axe de la sonde. Tourner la sonde autour de son axe principal de 0° jusqu'à 360° avec des incréments inférieurs ou égaux à 15°.

E.4.2 Isotropie hémisphérique

E.4.2.1 Généralités

La sonde doit être exposée à une onde de référence avec des angles d'incidence qui changent par rapport au plan perpendiculaire à l'axe de la sonde. L'évaluation de l'isotropie sphérique doit être effectuée dans un emplacement où les gradients de DAS sont inférieurs à 3 % par millimètre. Cela peut être réalisé à l'aide d'ondes stationnaires. L'isotropie hémisphérique doit être déterminée en inclinant la sonde ou en modifiant la polarisation de l'onde de référence. Les angles d'incidence doivent varier de 90° (axial) à 0° (normal), avec des incréments inférieurs ou égaux à 30°. Pour chaque angle d'incidence, la sonde doit être tournée sur 360°, par incréments inférieurs ou égaux à 15°.

Les quatre méthodes suivantes, qui donnent des résultats similaires, peuvent être utilisées pour l'isotropie hémisphérique:

a) fantôme plan avec doublet sur le côté (voir E.4.2.2);

b) fantôme plan avec doublet au-dessous (voir E.4.2.3);

c) fantôme sphérique avec doublet (voir E.4.2.4);

d) méthode de l'antenne de référence (voir E.4.2.5).

IECNORM.COM : Click to view the full PDF of IEC/IEEE 62209-1528:2020

E.4.2.2 Isotropie avec fantôme plan et doublet sur le côté

Le montage est constitué d'une boîte en plastique aux fines parois remplie de milieu équivalent au tissu, exposé à un doublet résonnant en demi-onde et fonctionnant à la fréquence d'essai. Le protocole suivant doit être utilisé pour évaluer l'isotropie sphérique de la sonde.

a) Monter l'antenne doublet horizontalement sur un dispositif de montage et la positionner parallèlement au fantôme plan (voir la Figure E.4). L'antenne doit être placée à une distance maximale de $e = \lambda/10$ de la paroi adjacente du récipient de milieu.

b) Insérer la sonde verticalement dans le liquide de sorte que le centre des trois capteurs de la sonde soit positionné face au point d'alimentation du doublet à la hauteur de l'axe du doublet.

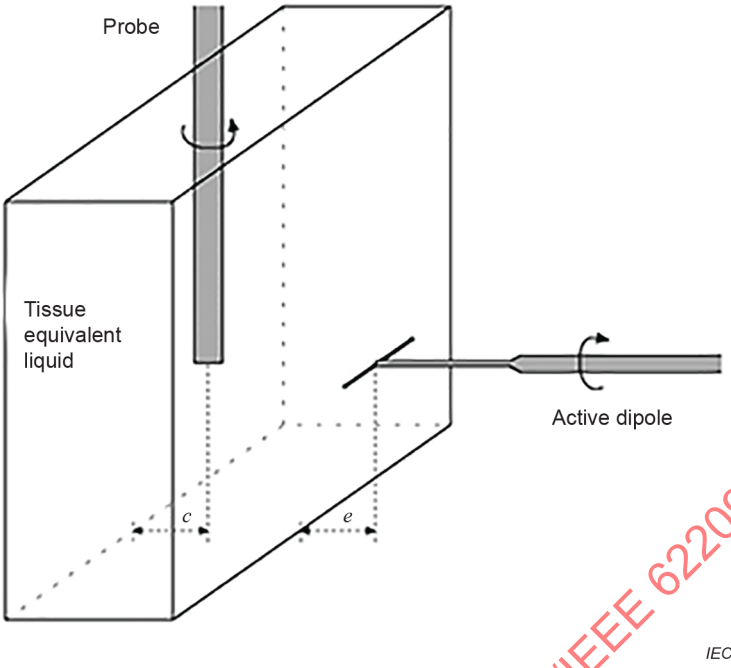
c) La position horizontale de la sonde doit être, autant que possible, au maximum de l'onde stationnaire, à proximité du côté arrière de la boîte, à une distance c de l'interface fantôme/liquide, où le champ E est partiellement homogène et le champ H est à un minimum.

d) Le doublet doit pivoter autour de l'axe de son dispositif de montage d'au moins 0° à 180° par incréments inférieurs ou égaux à 30°.

e) À chaque incrément, la sonde est tournée sur son axe de 0° à 360° par le positionneur de sonde et les données de mesure sont enregistrées, avec des incréments inférieurs ou égaux à 15°.

L'écart de l'isotropie sphérique est alors exprimé comme étant une composante d'incertitude avec une loi de probabilité rectangulaire limitée par les maxima de réponse mesurés. Des informations détaillées peuvent être consultées en [22].

IECNORM.COM : Click to view the full PDF of IEC/IEEE 62209-1528:2020



Anglais	Français
Probe	Sonde
Tissue equivalent liquid	Liquide équivalent au tissu
Active dipole	Doublet actif

Légende

c Distance entre la sonde et la paroi arrière

e Distance maximale par rapport à la paroi avant du récipient de liquide

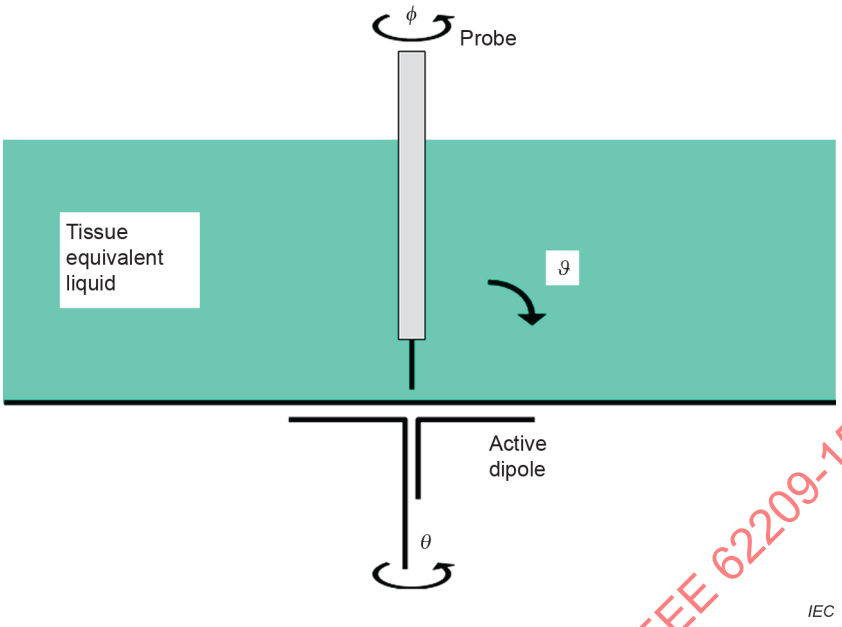
NOTE L'évaluation est effectuée de préférence à la position c des gradients de champ minimal résultant de l'onde stationnaire. La dimension e est la distance entre le point d'alimentation du doublet et l'interface de la paroi avant et du liquide.

Figure E.4 – Montage utilisé pour évaluer l'écart de l'isotropie hémisphérique dans le milieu équivalent au tissu

E.4.2.3 Isotropie avec fantôme plan et doublet au-dessous

Un autre montage pour l'évaluation de l'isotropie est représenté à la Figure E.5. Un doublet demi-onde monté sur un support est positionné avec ses bras parallèles à et situés sous un fantôme plan rempli de milieu équivalent au tissu. Une sonde est positionnée à un point directement au-dessus du point d'alimentation du doublet. Toutes les rotations de la sonde sont effectuées et commandées par un positionneur de haute exactitude. La rotation de la sonde sur son axe (rotation ϕ de 0° à 360°), de même que la rotation du doublet (rotation θ de 0° à 180°) et les variations de l'angle d'inclinaison ϑ de la sonde (de 0° à 75°) produisent une évaluation 3D d'une part significative de l'hémisphère recevant le signal.

IECNORM.COM : Click to view the full PDF of IEC/IEEE 62209-1528:2020



Anglais	Français
Probe	Sonde
Tissue equivalent liquid	Liquide équivalent au tissu
Active dipole	Doublet actif

Légende

ϑ angle d'inclinaison de l'axe de la sonde

θ angle de rotation de l'axe du dispositif de montage du doublet

ϕ angle de rotation de la sonde sur son axe

Figure E.5 – Autre montage utilisé pour évaluer l'écart de l'isotropie hémisphérique dans le milieu équivalent au tissu

E.4.2.4 Isotropie avec le doublet et le fantôme sphérique

L'isotropie hémisphérique de la sonde recevant le signal peut être évaluée en utilisant un montage comprenant un flacon sphérique rempli d'un milieu équivalent au tissu et un doublet [58] (voir la Figure E.6). Les capteurs de la sonde sont positionnés au centre géométrique du flacon et la sonde est tournée sur son axe pour différentes conditions d'excitation. La sonde est maintenue dans son orientation verticale pendant la procédure.

Les conditions d'excitation sont assurées par l'antenne doublet extérieure au flacon et déplacée en différents emplacements afin de fournir les angles d'incidence et les polarisations. L'axe du doublet est aligné sur le plan tangent de la surface de la sphère au-dessus du point d'alimentation du doublet. L'impédance de l'antenne est adaptée pour cette condition à la fréquence de fonctionnement.

NOTE Des flacons plus petits peuvent être préférentiels, car l'augmentation de la conductivité du milieu ou de la fréquence de fonctionnement implique une perte de trajet plus grande pour les ondes transmises à la sonde. Des flacons plus grands possèdent des surfaces localement plus planes (rayon de courbure plus grand) qui produisent localement un front d'onde plus plat sur l'extrémité de la sonde et augmentent la tolérance sur le positionnement du doublet.

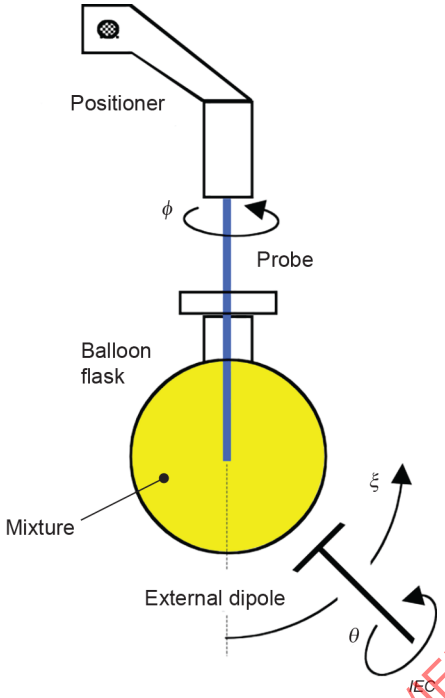
IECNORM.COM : Click to view the full PDF of IEC/IEEE 62209-1528:2020

La Figure E.7 [58] représente les conventions utilisées pour décrire la position et la polarisation de l'antenne. Un mesurage 3D du signal reçu par la sonde sur un hémisphère est accompli par la rotation sur 360° de la sonde autour de son axe (ϕ) en positionnant le doublet externe selon des angles 0° ≤ ξ ≤ 360°. Chaque polarisation souhaitée de l'onde incidente est obtenue par une rotation 0° ≤ θ ≤ 180° du doublet autour de son axe. Plusieurs positions θ ne sont pas nécessaires lorsque ξ = 0°. Bien qu'un grand nombre de points de mesure soit possible avec ce montage, généralement des incréments de 30° pour ξ et de 15° pour θ sont suffisants pour la caractérisation.

Les mesurages consistent en des rotations complètes de 360° de la sonde pour chaque position du doublet et pour chaque polarisation (ξ, θ). La puissance rayonnée pendant chaque rotation doit être contrôlée et enregistrée pour chaque position ϕ de la sonde, et les échantillons de DAS doivent être normalisés à une valeur nominale. Bien que cela ne puisse pas être exclu a priori, il n'y a pas de raison particulière pour que des positions et des polarisations du doublet externe autres que celles envisagées ici produisent des résultats d'isotropie significativement plus défavorables. Cependant, la matrice d'essais peut être étendue pour inclure n'importe quel cas d'intérêt particulier, par exemple des conditions de polarisation qui coïncident avec l'orientation du capteur de certaines sondes.

Comme pour l'essai d'isotropie du fantôme plan, l'hypothèse est faite d'une loi rectangulaire de l'incertitude. Cependant, l'incertitude peut être réduite considérablement quand l'étalonnage de la sonde est effectué sous une polarisation spécifique et sous une direction de l'onde incidente particulière, et que les mêmes conditions sont maintenues pendant les mesurages de DAS.

IECNORM.COM : Click to view the full PDF of IEC/IEEE 62209-1528:2020



Anglais	Français
Positioner	Positionneur
Probe	Sonde
Baloon flask	Fiole ballon
Mixture	Mélange
External dipole	Doublet externe

Légende

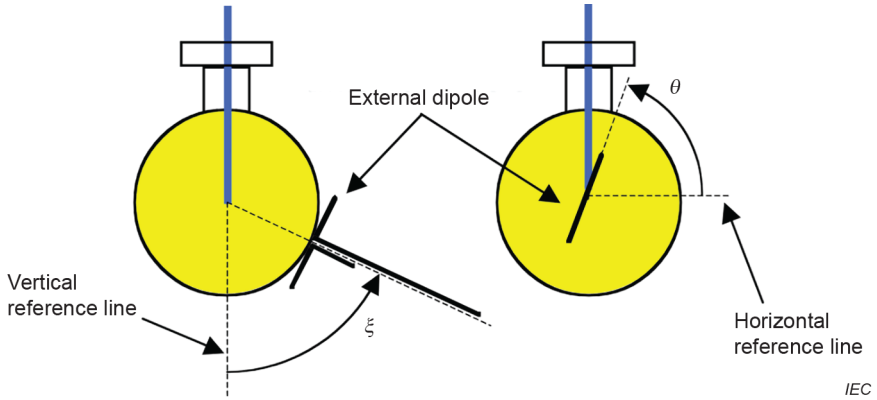
ξ angle d'élévation de l'axe du doublet

θ angle de rotation du doublet

ϕ angle de rotation de l'axe de la sonde

Figure E.6 – Montage expérimental pour l'évaluation de l'isotropie hémisphérique

IECNORM.COM : Click to view the full PDF of IEC/IEEE 62209-1528:2020



Anglais	Français
Vertical reference line	Ligne de référence verticale
Horizontal reference line	Ligne de référence horizontale
External dipole	Doublet externe

Légende

ξ angle d'élévation de l'axe du doublet

θ angle de rotation du doublet

NOTE ξ est l'angle entre l'axe de la sonde et l'axe du support de doublet, θ est l'angle entre l'axe de la sonde et l'axe du doublet.

Figure E.7 – Conventions pour la position (ξ) du doublet et la polarisation (θ)

E.4.2.5 Isotropie avec des antennes de référence

Le protocole suivant doit être adopté pour évaluer l'isotropie de la sonde en utilisant le montage de l'antenne de référence représenté à la Figure E.8.

a) Placer une antenne dans le milieu équivalent au tissu. L'antenne doit être à une distance minimale de 10 cm des parois du récipient du liquide et avec des dimensions telles qu'elle peut être placée dans la position indiquée à la Figure E.8.

b) Placer la sonde dans le liquide de sorte que le centre géométrique des capteurs soit à une distance d de l'antenne, où $d \geq 2D^2/\lambda_{\text{liquid}}$, D est la plus grande dimension de l'antenne de référence et λ_{liquide} est la longueur d'onde dans le liquide. Il est recommandé que, dans cette position, la valeur de DAS soit comprise entre 0,5 W/kg et 1 W/kg.

c) Orienter l'axe de la sonde de sorte que son axe principal soit orthogonal à la direction de propagation de l'antenne (voir la Figure E.8).

d) Tourner la sonde autour de son axe principal de 0° jusqu'à 360° avec des incréments inférieurs ou égaux à 15°. Consigner les valeurs de DAS. L'isotropie axiale est exprimée comme étant une composante d'incertitude avec une loi de probabilité rectangulaire reposant sur les maxima de réponse mesurés.

e) Modifier l'incidence du champ de référence en inclinant l'antenne de référence ou l'axe de la sonde (voir la Figure E.8) de 0° à 90° avec des incréments de 15° ou 30°.

f) Pour chaque angle d'incidence, tourner la sonde autour de son axe principal de 0° jusqu'à 360° avec des incréments inférieurs ou égaux à 15°. Consigner les valeurs de DAS.

g) L'isotropie hémisphérique est exprimée comme étant une composante d'incertitude avec une loi de probabilité rectangulaire limitée par les maxima de réponse mesurés.

IECNORM.COM : Click to view the full PDF of IEC/IEEE 62209-1528:2020